

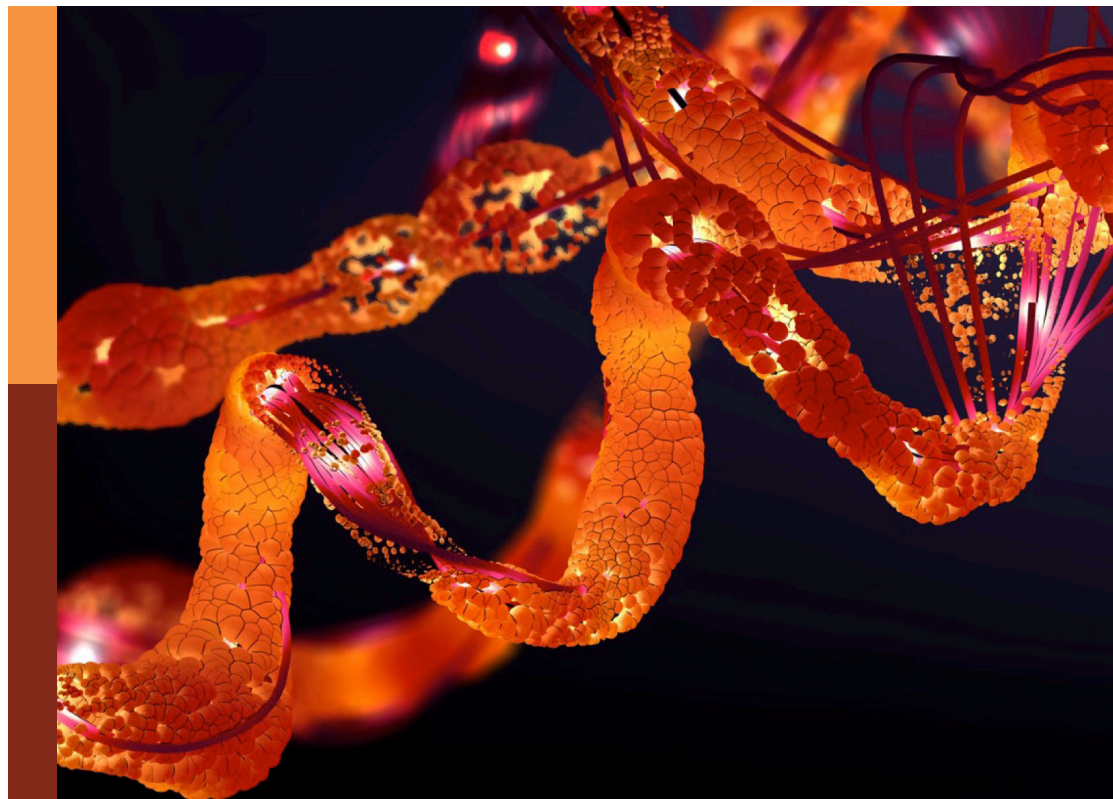
# Molecular chaperones and human disease

**Edited by**

Graham Chakafana, Stanley Makumire and Xolani Henry Makhoba

**Published in**

Frontiers in Molecular Biosciences



## FRONTIERS EBOOK COPYRIGHT STATEMENT

The copyright in the text of individual articles in this ebook is the property of their respective authors or their respective institutions or funders. The copyright in graphics and images within each article may be subject to copyright of other parties. In both cases this is subject to a license granted to Frontiers.

The compilation of articles constituting this ebook is the property of Frontiers.

Each article within this ebook, and the ebook itself, are published under the most recent version of the Creative Commons CC-BY licence. The version current at the date of publication of this ebook is CC-BY 4.0. If the CC-BY licence is updated, the licence granted by Frontiers is automatically updated to the new version.

When exercising any right under the CC-BY licence, Frontiers must be attributed as the original publisher of the article or ebook, as applicable.

Authors have the responsibility of ensuring that any graphics or other materials which are the property of others may be included in the CC-BY licence, but this should be checked before relying on the CC-BY licence to reproduce those materials. Any copyright notices relating to those materials must be complied with.

Copyright and source acknowledgement notices may not be removed and must be displayed in any copy, derivative work or partial copy which includes the elements in question.

All copyright, and all rights therein, are protected by national and international copyright laws. The above represents a summary only. For further information please read Frontiers' Conditions for Website Use and Copyright Statement, and the applicable CC-BY licence.

ISSN 1664-8714  
ISBN 978-2-83250-918-0  
DOI 10.3389/978-2-83250-918-0

## About Frontiers

Frontiers is more than just an open access publisher of scholarly articles: it is a pioneering approach to the world of academia, radically improving the way scholarly research is managed. The grand vision of Frontiers is a world where all people have an equal opportunity to seek, share and generate knowledge. Frontiers provides immediate and permanent online open access to all its publications, but this alone is not enough to realize our grand goals.

## Frontiers journal series

The Frontiers journal series is a multi-tier and interdisciplinary set of open-access, online journals, promising a paradigm shift from the current review, selection and dissemination processes in academic publishing. All Frontiers journals are driven by researchers for researchers; therefore, they constitute a service to the scholarly community. At the same time, the *Frontiers journal series* operates on a revolutionary invention, the tiered publishing system, initially addressing specific communities of scholars, and gradually climbing up to broader public understanding, thus serving the interests of the lay society, too.

## Dedication to quality

Each Frontiers article is a landmark of the highest quality, thanks to genuinely collaborative interactions between authors and review editors, who include some of the world's best academicians. Research must be certified by peers before entering a stream of knowledge that may eventually reach the public - and shape society; therefore, Frontiers only applies the most rigorous and unbiased reviews. Frontiers revolutionizes research publishing by freely delivering the most outstanding research, evaluated with no bias from both the academic and social point of view. By applying the most advanced information technologies, Frontiers is catapulting scholarly publishing into a new generation.

## What are Frontiers Research Topics?

Frontiers Research Topics are very popular trademarks of the *Frontiers journals series*: they are collections of at least ten articles, all centered on a particular subject. With their unique mix of varied contributions from Original Research to Review Articles, Frontiers Research Topics unify the most influential researchers, the latest key findings and historical advances in a hot research area.

Find out more on how to host your own Frontiers Research Topic or contribute to one as an author by contacting the Frontiers editorial office: [frontiersin.org/about/contact](https://frontiersin.org/about/contact)

# Molecular chaperones and human disease

## Topic editors

Graham Chakafana — Stanford University, United States

Stanley Makumire — University of Cape Town, South Africa

Xolani Henry Makhoba — University of Limpopo, South Africa

## Citation

Chakafana, G., Makumire, S., Makhoba, X. H., eds. (2022). *Molecular chaperones and human disease*. Lausanne: Frontiers Media SA.

doi: 10.3389/978-2-83250-918-0

## Table of contents

- 05 **Editorial: Molecular chaperones and human disease**  
Graham Chakafana, Stanley Makumire and Xolani Henry Makhoba
- 07 **Muscle Histopathological Abnormalities in a Patient With a CCT5 Mutation Predicted to Affect the Apical Domain of the Chaperonin Subunit**  
Federica Scalia, Rosario Barone, Francesca Rappa, Antonella Marino Gammazza, Fabrizio Lo Celso, Giosuè Lo Bosco, Giampaolo Barone, Vincenzo Antona, Maria Vadalà, Alessandra Maria Vitale, Giuseppe Donato Mangano, Domenico Amato, Giusy Sentiero, Filippo Macaluso, Kathryn H. Myburgh, Everly Conway de Macario, Alberto J. L. Macario, Mario Giuffrè and Francesco Cappello
- 21 **High Expression of Plasma Extracellular HSP90 $\alpha$  is Associated With the Poor Efficacy of Chemotherapy and Prognosis in Small Cell Lung Cancer**  
Baoyue Huang, Jinmiao Pan, Haizhou Liu, Yamei Tang, Shirong Li, Yingzhen Bian, Shufang Ning, Jilin Li and Litu Zhang
- 33 **HSP70 and their co-chaperones in the human malaria parasite *P. falciparum* and their potential as drug targets**  
Julian Barth, Tim Schach and Jude M. Przyborski
- 42 **Host cell stress response as a predictor of COVID-19 infectivity and disease progression**  
Celine Caillet, Melissa Louise Stofberg, Victor Muleya, Addmore Shonhai and Tawanda Zininga
- 66 **Neurotransmitters and molecular chaperones interactions in cerebral malaria: Is there a missing link?**  
Michael Oluwatoyin Daniyan, Funmilola Adesodun Fisusi and Olufunso Bayo Adeoye
- 84 **Exported J domain proteins of the human malaria parasite**  
Shaikha Y. Almaazmi, Harpreet Singh, Tanima Dutta and Gregory L. Blatch
- 93 **Inhibition of *Plasmodium falciparum* Hsp70-Hop partnership by 2-phenylthynesulfonamide**  
Tshifhiwa Muthelo, Vhahangwele Mulaudzi, Munei Netshishivhe, Tendamudzimu Harmfree Dongola, Michelle Kok, Stanley Makumire, Marianne de Villiers, Adéle Burger, Tawanda Zininga and Addmore Shonhai
- 108 ***In silico* analysis of the HSP90 chaperone system from the African trypanosome, *Trypanosoma brucei***  
Miebaka Jamabo, Stephen John Bentley, Paula Macucule-Tinga, Praise Tembo, Adrienne Lesley Edkins and Aileen Boshoff



- 130 **Nucleosome proteostasis and histone turnover**  
Adrian Arrieta and Thomas M. Vondriska
- 141 **A non-traditional crystal-based compound screening method targeting the ATP binding site of *Plasmodium falciparum* GRP78 for identification of novel nucleoside analogues**  
Alexander Mrozek, Tetyana Antoshchenko, Yun Chen, Carlos Zepeda-Velázquez, David Smil, Nirbhay Kumar, Hua Lu and Hee-Won Park



## OPEN ACCESS

## EDITED AND REVIEWED BY

Benoit Coulombe,  
Montreal Clinical Research Institute  
(IRCM), Canada

## \*CORRESPONDENCE

Graham Chakafana,  
graham.chakafana@hamptonu.edu

## SPECIALTY SECTION

This article was submitted to Molecular  
Diagnostics and Therapeutics,  
a section of the journal  
Frontiers in Molecular Biosciences

RECEIVED 12 October 2022

ACCEPTED 02 November 2022

PUBLISHED 17 November 2022

## CITATION

Chakafana G, Makumire S and  
Makhoba XH (2022), Editorial: Molecular  
chaperones and human disease.  
*Front. Mol. Biosci.* 9:1068238.  
doi: 10.3389/fmolb.2022.1068238

## COPYRIGHT

© 2022 Chakafana, Makumire and  
Makhoba. This is an open-access article  
distributed under the terms of the  
[Creative Commons Attribution License  
\(CC BY\)](#). The use, distribution or  
reproduction in other forums is  
permitted, provided the original  
author(s) and the copyright owner(s) are  
credited and that the original  
publication in this journal is cited, in  
accordance with accepted academic  
practice. No use, distribution or  
reproduction is permitted which does  
not comply with these terms.

# Editorial: Molecular chaperones and human disease

Graham Chakafana<sup>1\*</sup>, Stanley Makumire<sup>2</sup> and  
Xolani Henry Makhoba<sup>3</sup>

<sup>1</sup>Department of Chemistry and Biochemistry, Hampton University, Hampton, VA, United States,

<sup>2</sup>Structural Biology Research Unit, Department of Integrative Biomedical Sciences, University of Cape  
Town, Cape Town, South Africa, <sup>3</sup>Department of Biochemistry, Microbiology, and Biotechnology,  
School of Molecular and Life Sciences, University of Limpopo, Sovange, South Africa

## KEYWORDS

molecular chaperone, HSP (heat shock protein), disease, proteostasis, protein

## Editorial on the Research Topic

### Molecular chaperones and human disease

Protein dysregulation is a hallmark of several human diseases. As such, molecular chaperones (being custodians of cellular proteostasis) are largely implicated in several diseases, including cancers and neurodegenerative disorders. The goal of this topic was to provide an update on the recent progress made in understanding the roles of molecular chaperones in the progression of model diseases with the prospects of targeting molecular chaperones toward the identification of novel drug therapies.

Heat shock proteins (Hsps) are some of the most studied molecular chaperones that are associated with several chaperonopathies. They particularly play an important role in the pathogenesis of malaria, which is caused by the parasite *Plasmodium falciparum*. *P. falciparum* exhibits a very complex life cycle where its development partly occurs in a poikilothermic mosquito and a homeothermic human host. Hsps, therefore, play an integral role in ensuring that proteostasis is maintained throughout the parasite's life cycle and may thus be exciting antimalarial drug targets. Despite several efforts in the development of novel antimalarial therapies, drug resistance to front-line malarial treatments presents an urgent need for the development of novel therapies that are more reliable as highlighted by (Mrozek et al.). Using *in vitro* and cell-based assays, Muthelo et al. reported that the anti-cancer drug 2-Phenylthynylsulfonamide (PES) exhibits antiplasmodial activity and capability to inhibit the functions of the *P. falciparum* cytosol-localized chaperones PfHsp70-1 and PfHop (Muthelo et al.). Barth et al. reviewed the current state of knowledge about the Hsp70 family of chaperones focusing on the suitability of these proteins and interactions for drug development (Barth et al.). Together with the Hsp90s, Hsp70 proteins have been widely studied in several disease models though, to date, there have not been many FDA-approved Hsp70 drugs. A review by Daniyan et al. looked into the roles of the exported parasite chaperone PfHsp70-x in the pathophysiology of cerebral malaria. The article also explored the possible links between host-parasite chaperones, and neurotransmitters, in relation to other molecular signalling components in the development of cerebral malaria (Daniyan et al.). This

signalling pathway may provide further insights in antimalarial drug discovery. Collectively, the findings from these studies may contribute to the ongoing efforts in identifying novel antimalarial therapies, especially in the wake of growing parasite resistance against currently used drugs.

Chaperone/co-chaperone inhibition is being explored as a potential therapeutic target for several diseases. A review by [Cailliet et al.](#) looks into the potential roles of molecular chaperones in mediating cell and systemic stress in COVID-19. The article discusses the roles of the host stress response as a convergent point for COVID-19 and several non-communicable diseases while further assessing the merits of targeting the host stress response to manage the clinical outcomes of COVID-19. It sets an interesting argument on the possible roles Hsps might play in COVID-19 and the potential of targeting Hsps in novel COVID-19 therapy. Using an *in silico* approach, [Jamabo et al.](#) conducted a structural analysis of the *Trypanosoma brucei* (*T. brucei*) Hsp90 variants in relation to human and other trypanosomal species. *T. brucei* is responsible for African trypanosomiasis which is a neglected tropical disease mostly endemic to sub-Saharan Africa. The parasite is spread by insects (tsetse fly). Similar to *P. falciparum*, the trypanosome relies on heat shock proteins for survival in the insect vector and mammalian host. In their analysis, [Jamabo et al.](#) identified a total of eighteen putative *T. brucei* Hsp90 co-chaperones with one notable absence being cell division cycle 37 (Cdc37) ([Jamabo et al.](#)). Their findings provide an updated framework for approaching Hsp90 and its interactions as drug targets in the African trypanosome ([Jamabo et al.](#)).

Hsp90 has previously attracted a lot of attention in drug discovery research and several Hsp90-targeting drugs have gone through various stages of clinical trials in the development of treatments for cancers and cardiovascular diseases. A study by [Scalia et al.](#) reported the reduced Hsp90 expression levels observed in a mutant version of the CCT5 subunit from a patient with distal motor neuropathy. This indicates that the imbalance of the chaperone has a negative impact which potentially triggers the development of distal motor neuropathy. Follow-up studies could provide further information on how Hsp-dysregulation triggers neurophysiological disorders. The role of Hsp90 in tumor progression and prognosis was also

investigated in the development of small cell lung cancer ([Huang et al.](#)). Upon analyzing the relationship between eHSP90 $\alpha$  expression and clinicopathological features, eHSP90 $\alpha$  and NSE were found to be positively correlated in patients with small cell lung cancer ([Huang et al.](#)). This study provided new evidence for the efficacy response and prognostic assessment of SCLC with eHSP90 $\alpha$  being suggested to be a potential SCLC biomarker.

Altogether, the articles included in this topic highlight the new advances that have been made in the application of molecular chaperones in translational medicine. The section also reported on the successes and potential use of Hsps in novel drug therapies and biomarkers for several disease models. As there has been rapid development in the field of chaperone biology, we envision that novel, groundbreaking findings will further contribute to the development of applicable solutions in drug and biomarker discovery.

## Author contributions

All authors listed have made a substantial, direct, and intellectual contribution to the work and approved it for publication.

## Conflict of interest

The authors declare that the research was conducted in the absence of any commercial or financial relationships that could be construed as a potential conflict of interest.

## Publisher's note

All claims expressed in this article are solely those of the authors and do not necessarily represent those of their affiliated organizations, or those of the publisher, the editors and the reviewers. Any product that may be evaluated in this article, or claim that may be made by its manufacturer, is not guaranteed or endorsed by the publisher.



# Muscle Histopathological Abnormalities in a Patient With a CCT5 Mutation Predicted to Affect the Apical Domain of the Chaperonin Subunit

Federica Scalia<sup>1,2</sup>, Rosario Barone<sup>1</sup>, Francesca Rappa<sup>1</sup>, Antonella Marino Gammazza<sup>1</sup>, Fabrizio Lo Celso<sup>3,4</sup>, Giosuè Lo Bosco<sup>2,5</sup>, Giampaolo Barone<sup>6</sup>, Vincenzo Antona<sup>7</sup>, Maria Vadalà<sup>1,2</sup>, Alessandra Maria Vitale<sup>1,2</sup>, Giuseppe Donato Mangano<sup>1</sup>, Domenico Amato<sup>5</sup>, Giusy Sentiero<sup>1,2</sup>, Filippo Macaluso<sup>8</sup>, Kathryn H. Myburgh<sup>9</sup>, Everly Conway de Macario<sup>10</sup>, Alberto J. L. Macario<sup>2,10</sup>, Mario Giuffrè<sup>7</sup> and Francesco Cappello<sup>1,2\*</sup>

## OPEN ACCESS

### Edited by:

Xolani Henry Makhoba,  
University of Fort Hare, South Africa

### Reviewed by:

Olga S. Sokolova,  
Lomonosov Moscow State University,  
Russia  
Dario Coletti,  
Sapienza University of Rome, Italy

### \*Correspondence:

Francesco Cappello  
francesco.cappello@unipa.it  
francapp@hotmail.com

### Specialty section:

This article was submitted to  
Molecular Diagnostics and  
Therapeutics,  
a section of the journal  
Frontiers in Molecular Biosciences

**Received:** 01 March 2022

**Accepted:** 29 April 2022

**Published:** 02 June 2022

### Citation:

Scalia F, Barone R, Rappa F,  
Marino Gammazza A, Lo Celso F,  
Lo Bosco G, Barone G, Antona V,  
Vadalà M, Vitale AM,  
Donato Mangano G, Amato D,  
Sentiero G, Macaluso F, Myburgh KH,  
Conway de Macario E, Macario AJ,  
Giuffrè M and Cappello F (2022)  
Muscle Histopathological  
Abnormalities in a Patient With a CCT5  
Mutation Predicted to Affect the Apical  
Domain of the Chaperonin Subunit.  
Front. Mol. Biosci. 9:887336.  
doi: 10.3389/fmolb.2022.887336

<sup>1</sup>Department of Biomedicine, Neuroscience and Advanced Diagnostics (BIND), University of Palermo, Palermo, Italy, <sup>2</sup>Euro-Mediterranean Institute of Science and Technology (IEMEST), Palermo, Italy, <sup>3</sup>Department of Physics and Chemistry - Emilio Segrè, University of Palermo, Palermo, Italy, <sup>4</sup>Ionic Liquids Laboratory, Institute of Structure of Matter, Italian National Research Council (ISM-CNR), Rome, Italy, <sup>5</sup>Department of Mathematics and Computer Science, University of Palermo, Palermo, Italy, <sup>6</sup>Department of Biological, Chemical and Pharmaceutical Sciences and Technologies, University of Palermo, Palermo, Italy, <sup>7</sup>Department of Health Promotion, Mother and Child Care, Internal Medicine and Medical Specialties, University of Palermo, Palermo, Italy, <sup>8</sup>SMART Engineering Solutions & Technologies (SMARTEST) Research Center, eCampus University, Palermo, Italy, <sup>9</sup>Department of Physiological Sciences, Stellenbosch University, Stellenbosch, South Africa, <sup>10</sup>Department of Microbiology and Immunology, School of Medicine, University of Maryland at Baltimore-Institute of Marine and Environmental Technology (IMET), Baltimore, MD, United States

Recognition of diseases associated with mutations of the chaperone system genes, e.g., chaperonopathies, is on the rise. Hereditary and clinical aspects are established, but the impact of the mutation on the chaperone molecule and the mechanisms underpinning the tissue abnormalities are not. Here, histological features of skeletal muscle from a patient with a severe, early onset, distal motor neuropathy, carrying a mutation on the CCT5 subunit (MUT) were examined in comparison with normal muscle (CTR). The MUT muscle was considerably modified; atrophy of fibers and disruption of the tissue architecture were prominent, with many fibers in apoptosis. CCT5 was diversely present in the sarcolemma, cytoplasm, and nuclei in MUT and in CTR and was also in the extracellular space; it colocalized with CCT1. In MUT, the signal of myosin appeared slightly increased, and actin slightly decreased as compared with CTR. Desmin was considerably delocalized in MUT, appearing with abnormal patterns and in precipitates. Alpha-B-crystallin and Hsp90 occurred at lower signals in MUT than in CTR muscle, appearing also in precipitates with desmin. The abnormal features in MUT may be the consequence of inactivity, malnutrition, denervation, and failure of protein homeostasis. The latter could be at least in part caused by malfunction of the CCT complex with the mutant CCT5 subunit. This is suggested by the results of the *in silico* analyses of the mutant CCT5 molecule, which revealed various abnormalities when compared with the wild-type counterpart, mostly affecting the apical domain and potentially impairing chaperoning functions. Thus, analysis of mutated CCT5 *in vitro* and *in vivo* is anticipated to provide additional insights on subunit involvement in neuromuscular disorders.

**Keywords:** CCT5, neurochaperonopathies, chaperonin, neurodegenerative diseases, neuropathies, chaperone system, muscle histopathology, CCT5 apical domain

## 1 INTRODUCTION

Neuromyopathies constitute a large group of diverse diseases typically associated with genetic variants that have a pathogenic impact on nerves and muscles (Morrison 2016; collection of articles in Front Mol Biosci, 2018- Pathologic Conditions of the Human Nervous and Muscular Systems Associated with Mutant Chaperones: Molecular and Mechanistic Aspects). In many of these diseases there is a mutant gene that encodes a component of the chaperone system (CS), e.g., a chaperone gene such as those that code for the chaperonins Hsp60 (Heat shock protein 60) and CCT (Chaperonin Containing TCP1; also called TRiC, TCP1 Ring Complex), and these disorders are classified as neurochaperonopathies (Scalia et al., 2021). An illustrative example of neurochaperonopathy is the distal sensory mutilating neuropathy associated with a point mutation on the CCT5 subunit described earlier (Bouhouché et al., 2006a; Bouhouché et al., 2006b). More recently, we reported a different genetic variant of CCT5 that was associated with a severe distal motor neuropathy (Antona et al., 2020), which is the object of this article.

The hereditary and clinical aspects of chaperonopathies in general, including the neurochaperonopathies, are well established for the most part (Macario and Conway de Macario, 2005; Rubin et al., 2012; Macario et al., 2013). However, the impact of the pathogenic mutation on the properties and functions of the chaperone molecule has been characterized for only very few chaperonopathies, and still less is known on the associated histopathology and the molecular mechanisms responsible for the tissue abnormalities (Macario and Conway de Macario 2020). The scarcity of data on the histopathological manifestations of chaperonopathies impedes advances in the elucidation of the molecular mechanisms underpinning the severe muscular deficiency observed in patients and this, in turn, stands in the way for developing specific treatments. To remedy this lack of necessary knowledge, we studied the available muscle sample from the patient reported earlier, who suffered from a severe motor disorder and carried a point mutation on the CCT5 subunit (Antona et al., 2020). Here, we define histological abnormalities occurring in striated skeletal muscle from this patient. In our *ex vivo* investigation, we asked the few questions that seemed most relevant under the circumstances, pertaining to the status of 1) the muscle tissue; 2) the CCT5 subunit and other pertinent components of the CS; and 3) other molecules involved in the maintenance of the muscle structure and function. Consequently, we performed experiments to reveal the general architecture of the muscle and to determine if it presented signs of atrophy and apoptosis. We also ran tests to determine whether the presence and distribution of the CCT5 subunit were altered in comparison with normal muscle. Likewise, we tested for the presence and location of other components of the CS known to play key roles in skeletal muscle, i.e., alpha-B-crystallin and Hsp90. These are in normal muscle predominantly localized to the Z discs and we looked to see if the muscle from the patient showed this characteristic. We

also ran experiments to determine if CCT5 colocalized with another member of the CCT complex, CCT1, which would indicate that the mutant subunit is competent to integrate the chaperoning complex and does form it. We investigated levels of proteins that are known (e.g., actin) or suspected substrates for CCT because any abnormality of these proteins would be an indicator of deficient chaperoning by the chaperonin. Lastly, we tested for the presence and distribution of desmin, the muscle molecule with key functions in the maintenance of overall structure and connections between the main components of the muscle fiber, essential for the coordinated functioning of all of them. The impact of the mutation on the molecular properties of the mutant CCT5 protein were investigated *in silico* by modelling and molecular dynamics simulation.

## 2 MATERIAL AND METHODS

### 2.1 Muscle Tissues and Microscopy

A lateral gastrocnemius skeletal muscle biopsy from the patient, and a corresponding specimen from a healthy individual, were used. The study was approved by the Ethics Committee of University Hospital AUOP Paolo Giaccone of Palermo. Skeletal muscle tissue samples were fixed in 10% buffered formalin and embedded in paraffin. Thin sections (5 µm), obtained from paraffin blocks by microtome, were stained with haematoxylin-eosin and Alcian Blue Pas for histological evaluation. Examination of the sections was performed by two expert pathologists (F. C. and F. R.) with an optical microscope (Microscope Axioscope 5/7 KMAT, Carl Zeiss, Milan, Italy) connected to a digital camera (Microscopy Camera AxioCam 208 color, Carl Zeiss, Milan, Italy).

### 2.2 Immunohistochemistry for Desmin

Sections were obtained from the paraffin blocks of skeletal muscle tissue and dewaxed in xylene for 30 min at 60°C and, after being passed through a descending scale of alcohol concentrations, they were rehydrated in distilled water at 22°C. Subsequently, antigen unmasking was performed with sodium citrate buffer (pH 6) at 75°C for 8 min and then immersion in acetone at -20 °C for 8 min. Then, the sections were immunostained using a Histostain®-Plus third Gen IHC Detection Kit (Life Technologies, Cat. No. 85-9,073). The primary antibody used was anti-desmin mouse monoclonal diluted 1:50 (Table 1). Appropriate negative controls were run concurrently for each reaction. Nuclear counterstaining was performed using hematoxylin (Hematoxylin aqueous formula, REF 05-06012/LN. Cat. No. S2020, Bio-Optica, Milan, Italy). Finally, the sections were examined with an optical microscope as described in the previous Section by two independent observers (F. C. and F. R.), who evaluated the reactions and the immunolocalization on two separate occasions.

### 2.3 Immunofluorescence

Deparaffinized sections were incubated in the antigen-unmasking solution (10 mM tri-sodium citrate, 0.05%

Tween-20) for 10 min at 75 °C, and treated with blocking solution (3% BSA in PBS) for 30 min. Next, the primary antibody (**Table 1**), was applied, and the sections were incubated in a humidified chamber overnight at 4 °C. Then, the sections were incubated for 1 h at 22°C with a conjugated secondary antibody (anti-rabbit IgG–FITC antibody produced in goat, F0382, Sigma-Aldrich; anti-mouse IgG-TRITC antibody produced in goat, T5393, Sigma-Aldrich). Nuclei were stained with Hoescht Stain Solution (1:1,000, Hoechst 33258, Sigma-Aldrich). The slices on the slides were treated with Perma Fluor Mountant (Thermo Fisher Scientific, Inc. Waltham, MA, United States) and covered with a coverslip. The images were captured using a Leica Confocal Microscope TCS SP8 (Leica Microsystems).

## 2.4 Double Immunofluorescence

Double immunofluorescence was performed as previously described (Marino Gammazza et al., 2014). Briefly, slices of the muscle tissues were deparaffinized, incubated in the antigen unmasking solution for 10 min at 75°C, and treated with blocking solution for 30 min. The sections were then incubated with the first primary antibody (**Table 1**) overnight at 4°C. The day after, the sections were incubated with the second primary antibody (**Table 1**) overnight in a humidified chamber at 4°C. Afterwards, the tissue slices were incubated with fluorescent secondary mouse IgG antibody TRITC conjugated (Sigma-Aldrich), diluted 1:250, for 1 h at 22°C, and with FITC conjugated rabbit IgG secondary antibody (Sigma-Aldrich), diluted 1:250, for 1 h at 22°C in a moist chamber. The nuclei were counterstained with Hoechst 33342 for 15 min at 22°C. Finally, the slices were covered with two drops of PBS and mounted with coverslips, using a drop of Vectashield. Imaging was immediately performed with a Leica Confocal Microscope TCS SP8 and the fibers' positivity for both markers ("merge") was assessed using the Leica application suite advanced fluorescences software.

## 2.5 In Silico Analyses

We used the structure of crystallized protein deposited in the Protein Data Bank with accession codes 5UYZ (Pereira et al., 2017) to compare the structure of wild type and mutant CCT5 subunit. Study and alignment of CCT5 wild type and mutant linear amino acid sequences was conducted using Clustal Omega multiple sequence alignment program.

## 2.6 Molecular Modelling and Dynamic Simulations

The molecular modelling of the mutant CCT5 subunit was obtained by replacing the amino acid residue Leucine in position 224 with a Valine, using the package Maestro Schrödinger LLC, New York, NY, 2018, version 11.6.010] and compared with the model of the wild type molecule. Molecular Dynamics simulations were performed for 150 ns (in some cases were extended to 200 ns), using the GROMACS 5.1.1 package (Van Der Spoel et al., 2005; Hess et al., 2008). Interactions were described using an all-atoms CHARMM27 force field (Foloppe and MacKerell, 2000; MacKerell and Banavali, 2000). All the simulations for the various systems, and radius of gyration and RMSD analyses were performed as previously described (Antona et al., 2020).

## 3 RESULTS

### 3.1 Atrophy of Muscle Fibers and Disruption of the Tissue Architecture

Histological analysis showed changes in muscle from the patient (henceforth designated MUT muscle) compared to muscle from the healthy control (henceforth designated CTR muscle). MUT muscle showed widespread atrophy, hyper eosinophilia, and disruption of the tissue architecture (**Figures 1A–C; Supplementary Figures S1**). The MUT muscle fibers were different in shape and size from those in CTR muscle being predominantly small and rounded in cross section (**Figures 1A, B**). The same features were revealed with Alcian-Pas staining (**Supplementary Figures S1**). In longitudinal sections the MUT muscle fibers had a wavy shape (**Figure 1C**). In MUT muscle, nuclei were swelled and in contact with the sarcolemma but in some fibers the nuclei were internal, paracentric.

### 3.2 Apoptosis of Muscle Fibers

MUT muscle showed many more apoptotic fibers than CTR muscle by the TUNEL assay (**Figure 2**).

### 3.3 CCT5 Presence, Distribution, and Colocalization With CCT1

In the CTR muscle, CCT5 was present in the sarcolemma, cytoplasm, and within the nuclei (**Figure 3**, CTR panels) but its signal was slighter in the cytoplasm, nuclei, and, but not as much, in the sarcolemma of MUT muscle fibers

**TABLE 1** | Primary antibodies used for immunohistochemistry (IH), and immunofluorescence and double immunofluorescence (IF).

Method	Antigen	Antibody	Supplier	Catalogue Number	Dilution
IF	CCT5	Rabbit polyclonal	Origene	TA308298	1:50
	CCT1 TCP1α (B-3)	Mouse monoclonal	Santa Cruz Biotechnology	SC-374088	
	α-actin	Rabbit polyclonal	Sigma A2066	A2066	
	Myosin heavy chain Type IIX	Mouse monoclonal	DSHB	AB_2266724	
	Alpha-B-crystallin	Rabbit polyclonal	Abcam	AB 5577	
	Hsp90	Rabbit polyclonal	Abcam	AB 13495	
IH-IF	Desmin	Mouse monoclonal	Biocaremedical	CM 036A	



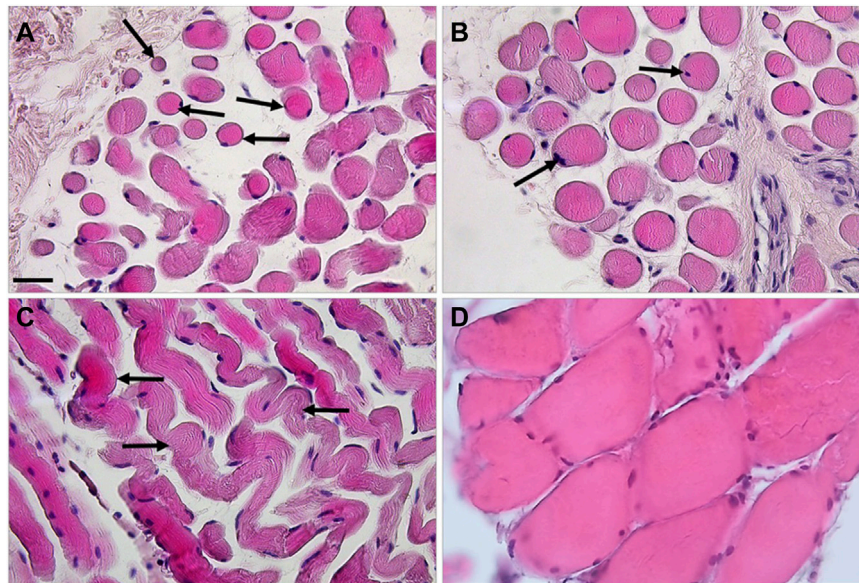


**FIGURE 1** | Haematoxylin-eosin staining revealed striking differences between the MUT (panels **A–C**) and CTR (panel **D**) muscles. In cross-section the MUT muscle fibers appeared rounded, of diverse sizes, with swelled nuclei in contact with the sarcolemma or near it (examples shown by arrows on panels **A,B**). These fibers in longitudinal section showed a wavy shape with a striated pattern inside (examples shown by arrows on panel **C**). The inter-fiber space is considerably wider in the MUT than in the CTR muscle. Bar = 100  $\mu$ m.

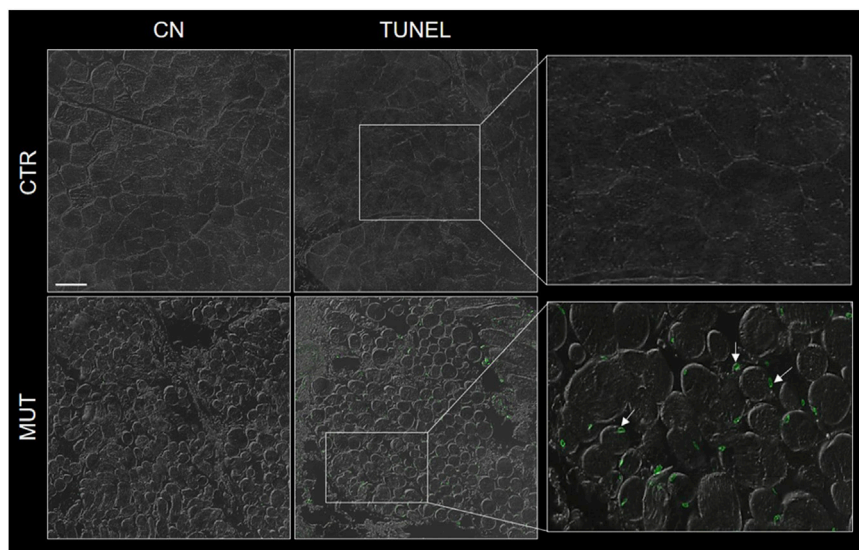


**FIGURE 2** | Representative image of TUNEL assay of MUT and CTR muscles. DNA-strand breaks (green spots) were more abundant in the MUT (white arrows in the panel with enlargement to the far right, bottom) than in the CTR muscle. CN, negative control for MUT and CTR muscles without TdT enzyme. Bar = 100  $\mu$ m.

(**Figure 3**, MUT panels). In the MUT muscle, CCT5 was detected in the extracellular space (intercellular matrix) (**Figure 3**, MUT panels).

To determine if the CCT5 subunit in the MUT muscle was associated to other components of its chaperoning team, i.e., the CCT oligomer, colocalization experiments were performed, using

double immunofluorescence with antibodies against CCT5 and CCT1. The two subunits colocalized in the MUT and CTR muscles (**Figure 4**). The results for CCT5 confirm the localization shown in **Figure 3**: it appears, here together with CCT1, in the sarcolemma, cytoplasm and nuclei of CTR muscle, whereas in the MUT muscle the two subunits appear mostly in



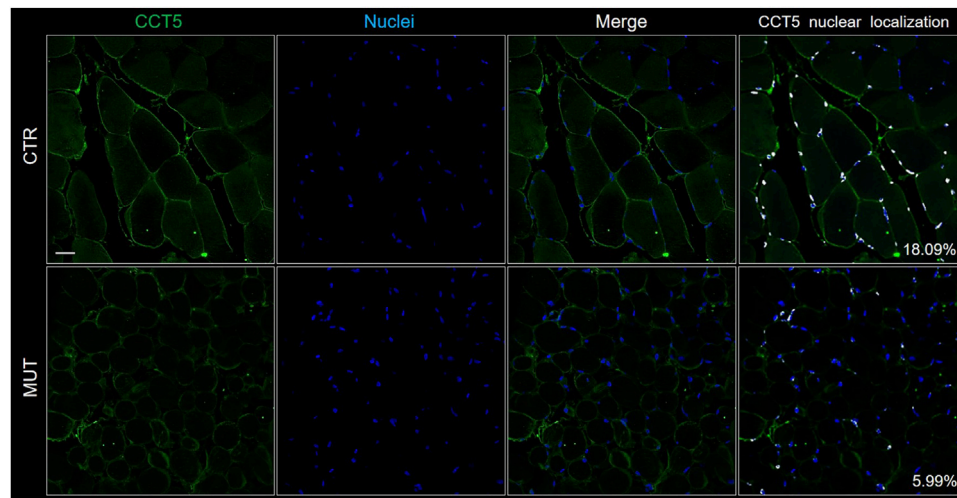


**FIGURE 3** | Localization of CCT5 on CTR and MUT muscles. Immunofluorescence was done with FITC conjugated anti-CCT5 antibody (green); nuclei were stained with the Hoechst (blue). Nuclear localization of CCT5 (white spots) in CTR muscle (18.09%) was more frequent than in MUT muscle (5.99%). Bar = 25  $\mu$ m.

sarcolemma and the extracellular matrix (**Figure 4**). The lower signal of CCT1 in nuclei of MUT muscle closely parallel the low signal of CCT5, suggesting these subunits tend to associate with each other in MUT muscle as well.

### 3.4 Actin and Myosin

Actin and myosin distribution patterns in MUT and CTR muscles were similar, but myosin signal was slightly increased, and that of actin was decreased in MUT as compared with CTR muscle (**Figure 5**).

### 3.5 Desmin

Desmin (muscle-specific type III intermediate filament) is a muscle-specific protein, normally localized in the sarcolemma, Z-disc, and nuclear membrane, that maintains the sarcomere structure, linking the sarcolemma, mitochondria, lysosomes, and nucleus. In CTR muscle, desmin was visible in the sarcolemma and cytoplasm with the expected banding pattern in longitudinal sections (**Figures 6A–C** panels). In MUT muscle the presence of desmin appeared lower than in CTR muscle and its distribution pattern was different (**Figures 6D–F** panels). The desmin banding pattern was absent in MUT muscle, and aggregates containing this protein were present at paracentral and peripheral locations within the muscle fibers (**Figure 6E**).

### 3.6 CCT5, Alpha-B-Crystallin, Hsp90, and Desmin

The CS components CCT5, alpha-B-crystallin, and Hsp90, the latter two normally associated at the level of the Z-discs, and desmin were assessed to determine presence and distribution. We performed double immunofluorescence for: 1) desmin and CCT5 subunit (**Figure 7B**); desmin and alpha-B-crystallin (**Figure 8C**) desmin and Hsp90 (**Figure 9**). Desmin was homogeneously distributed in CTR muscle along the Z-discs, seen as

horizontal striations and with a striated pattern in cross- and longitudinal sections, respectively (green fluorescence in CTR panels of **Figures 7–9**). In MUT muscle, signal of desmin appeared slighter than in CTR muscle and appeared as irregular or trabecular patterns, and as dots (green fluorescence in MUT panels of **Figures 7–9**). In some fibers the desmin-labelled sarcolemma was not visible.

The cytoplasm of MUT muscle fibers showed little if any signal for CCT5 subunit, but this signal was present in the sarcolemma and the intercellular matrix, as also illustrated in **Figure 3**. Almost no colocalization of CCT5 with desmin was observed in the extracellular matrix of affected tissue (**Figure 7**, rightmost MUT panel).

Alpha-B-crystallin was uniformly distributed in CTR muscle showing a striated pattern in longitudinal and cross sections (**Figure 8**). In contrast, in MUT muscle, alpha-B-crystallin signal was milder, appearing as a light band in longitudinal sections and as precipitates with desmin in the sarcoplasm (white arrows in MUT merge panel of **Figure 8**). Likewise, colocalization of alpha-B-crystallin and desmin was reduced in half in MUT muscle as compared with CTR muscle.

Hsp90 was distributed throughout the cytosol of the CTR muscle fibers in a well-organized pattern in longitudinal and cross sections (**Figure 9**, CTR panels). In the MUT muscle, Hsp90 was present but appeared in an irregular pattern somewhat like that of desmin (**Figure 9**, MUT panels). Hsp90 and desmin colocalization was reduced in the MUT muscle as compared with the CTR muscle.

### 3.7 In Silico Analysis of the CCT5 Mutant Protein

The histopathological abnormalities found in the MUT muscle suggested poor protein homeostasis, which can, as a working hypothesis, be attributed to a defective CCT complex carrying the mutant CCT5 subunit. Therefore, we investigated the impact of the mutation on the CCT5 protein molecule. We used bioinformatics as

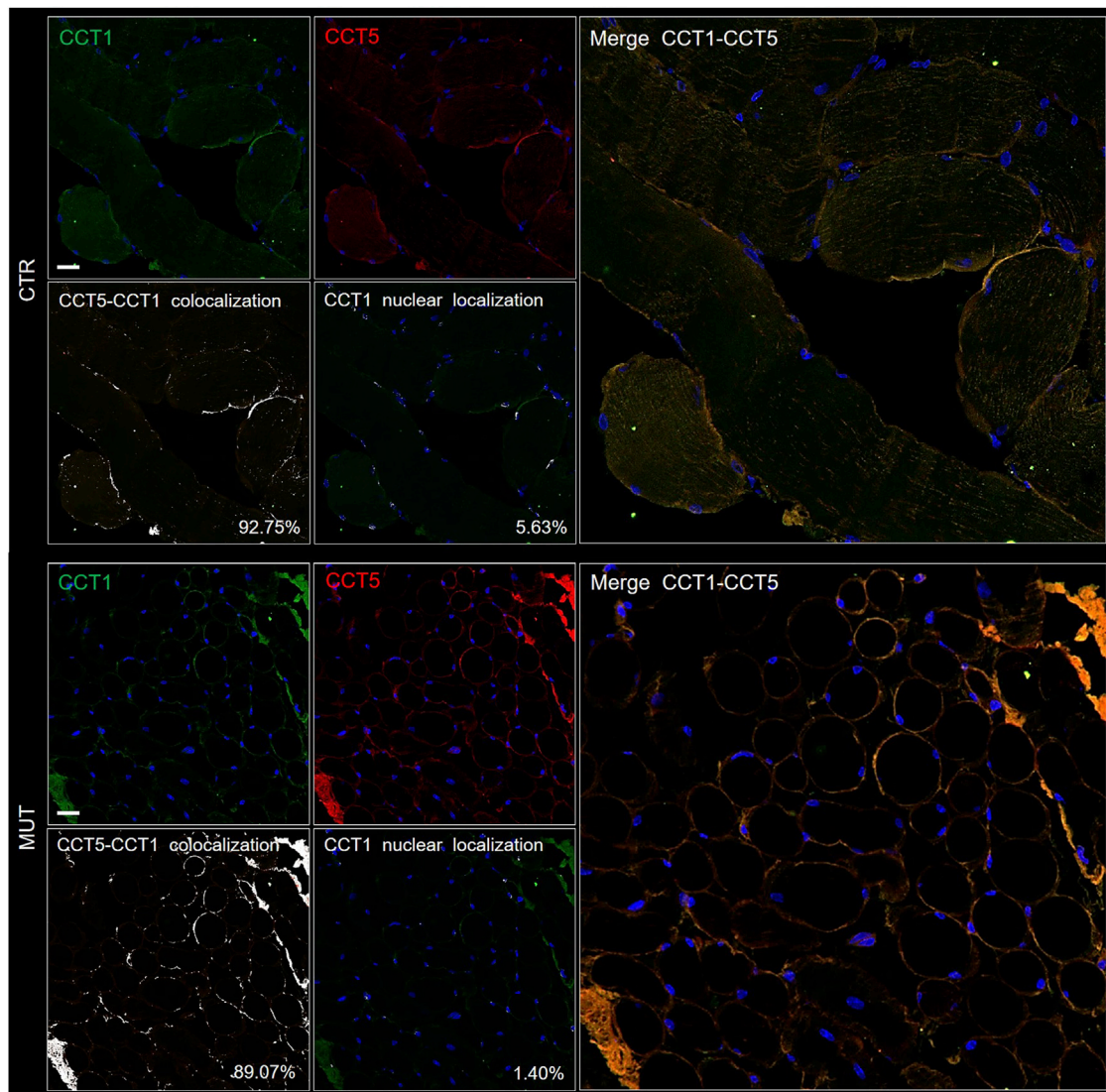


**FIGURE 4 |** Double immunofluorescence for CCT5 and CCT1 subunits on CTR (top set of five panels) and MUT (bottom set of five panels) muscles. CTR and MUT muscles were stained with FITC conjugated anti-CCT1 antibody (green) and with TRITC conjugated anti-CCT5 antibody (red). Nuclei were stained with probe Hoechst (blue). Colocalization of CCT5 and CCT1 in CTR muscle (92.75%) and in MUT (89.07%) muscle appeared as white spots (see the two panels at the bottom left corner of the CTR and MUT sets of panels). Bar = 25  $\mu$ m. Nuclear localization of CCT1 in CTR (5.63%) and in MUT (1.40%) muscles appeared as white spots (see the two middle panels at the bottom of the CTR and MUT series of panels with the legend “CCT1 nuclear colocalization”). Bar = 25  $\mu$ m.

we did in a previous work with another mutant of CCT5 because, in that work, we detected molecular abnormalities caused by the mutation that accurately predicted the abnormalities of the CCT5 subunit molecular properties and functions that were also demonstrated by wet lab experiments (Min et al., 2014; Spigolon et al., 2017; Macario and Conway de Macario, 2020).

### 3.7.1 CCT5 Structure

The properties and functions of the CCT5 subunit and its mutant can be visualized better by looking at the alignment of the amino acid sequences of the wild type and mutant molecules, showing the structural domains named equatorial, intermediate, and apical, and the subdivision of

the former two into N-terminal and C-terminal segments, **Supplementary Figure S2**. Other comparative analyses of the two molecules are facilitated by keeping in mind the details shown in the alignment figure.

### 3.7.2 Comparison of Molecular Models

To learn about the impact of the mutation on the CCT5 apical domain configuration previously reported for the Leu224Val mutant (Antona et al., 2020), we superposed wild type and mutant molecular models under three conditions, nucleotide free, ATP bound, and ADP bound, **Figure 10**. It was confirmed that the mutant protein differs from the wild type, particularly at the level of the apical domain.



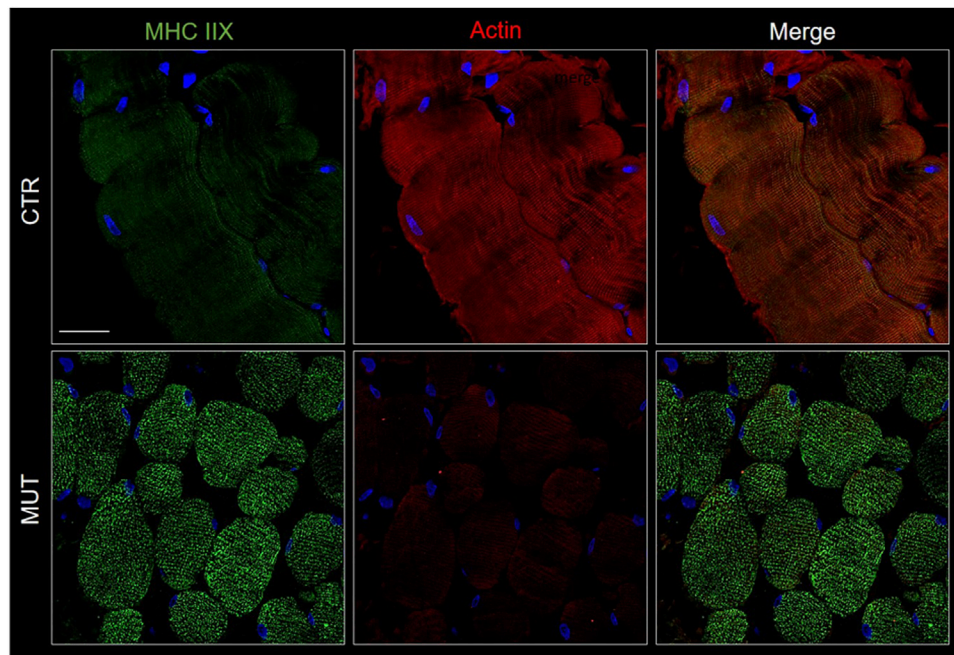


**FIGURE 5** | Detection of myosin (MHC IIX) with FITC-conjugated antibody (green) and actin with TRITC-conjugated antibody (red) in CTR and MUT muscles. Myosin positivity was higher in the MUT than in the CTR muscle whereas actin positivity showed the reverse pattern being higher in the CTR muscle. Also, the distribution patterns of the two proteins differed in the CTR and MUT muscles and colocalization was absent. Nuclei were stained with probe Hoechst 33342 (blue). Bar = 25  $\mu$ m.

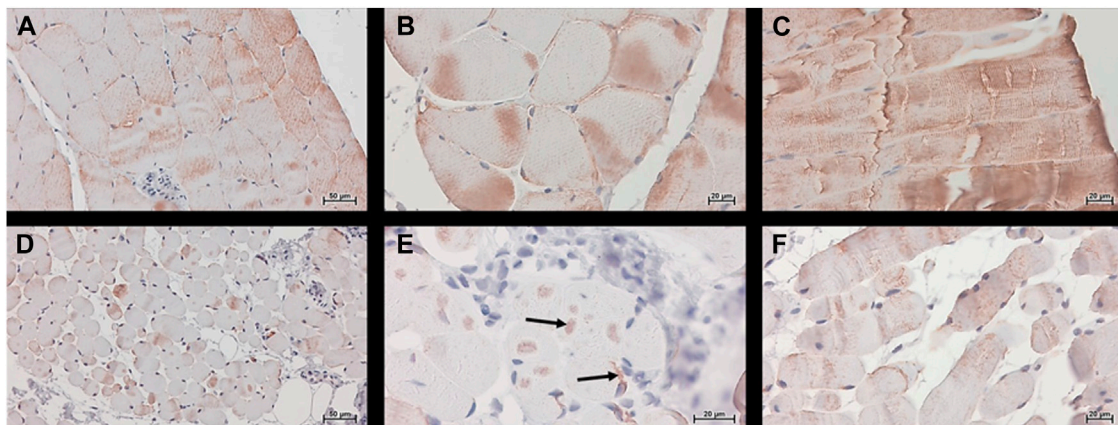


**FIGURE 6** | Desmin was detected histochemically, using the Histostain®-Plus third Gen IHC Detection Kit, which revealed desmin (brown color) in CTR (panels A–C) and MUT (panels D–F) muscles. (A,D) Magnification  $\times 200$ ; scale bar 50  $\mu$ m; (B,C,E,F) magnification  $\times 400$ ; scale bar 20  $\mu$ m. Desmin was present in the cytoplasm and in the sarcoplasmic membrane of the CTR muscle. In MUT muscle, desmin appeared at lower levels than in the CTR muscle in the sarcoplasm and as aggregates in paracentral and peripheral locations (examples indicated by arrows on panel E). The banding pattern typical of normal muscle in longitudinal section (panel C) was absent in the muscle from the patient (panel F).

### 3.7.3 Radius of Gyration

We used the radius of gyration (RG) versus time method to determine if the distribution of atomic masses in the mutant was different from that of the wild-type protein under three conditions: nucleotide free, ATP bound, and ADP bound (Figure 11). All trends of the mutant protein showed different

RG values than the wild-type counterparts. For instance, the nucleotide-free mutant (Figure 11, right panel, black) had a trend opposite to that of the wild-type nucleotide-free protein, with increasing values, 2.9–3.2 RG for the mutant and decreasing values, 2.9–2.7 RG, for the wild-type molecule (Figure 11, left panel, black).

### 3.7.4 Root Mean Square Deviation (RMSD)

The CCT5 molecule, like the other CCT subunits consists of three domains, apical, equatorial, and intermediate and while the latter two are composed of two separate segments of the protein's amino sequence, the apical domain consists of single segment (**Supplementary Figure S2**). Molecular dynamics simulations were carried out to determine if there were differences between the domain segments of the mutant and the wild type proteins nucleotide free, and ATP- or ADP bound. The RMSD analysis showed substantial differences between the two molecules, particularly at the level of the apical domain (**Figure 12**).

### 3.7.5 Heat Maps

To identify the amino acids within each domain involved in the molecular conformational changes observed by molecular dynamics simulations, we resorted to heat maps. The heat maps show the RMSD value in Angström unit (Å, in *y*-axis) of each individual amino acid residue during simulations (frame in ns, in *x*-axis). Collectively, these analyses revealed instability of the apical domain of the mutant nucleotide-free protein (**Figure 13**).

## 4 DISCUSSION

Many diseases of the central and peripheral nervous systems and of skeletal muscle are proteinopathies, namely, the central pathogenic-diagnostic molecule is a defective protein, which in most instances is the product of a mutant gene, thus the diseases are by definition genetic, and for the most part hereditary

(Jameson et al., 2018). When the abnormal protein belongs to the chaperone system (CS), the disease can be classified as a chaperonopathy (Macario and Conway de Macario, 2005). In this report, we deal with a disease that according to clinical signs and symptoms is a genetic, early onset, distal motor neuropathy, associated to a mutation in a chaperone gene, the subunit CCT5 of the chaperone complex CCT (Antona et al., 2020). We report the histopathological characteristics of the skeletal muscle of the patient, focusing on details that in principle might be the result of deficient protein homeostasis caused by inadequate chaperoning.

Information on the tissue abnormalities found in chaperonopathies and the molecular mechanisms underpinning these abnormalities, including the role of the defective chaperones, is scarce and badly needed (Macario and Conway de Macario, 2020). There is some information on the histopathological manifestations of myopathies, including one associated to a chaperonopathy, but little is available on specific aspects of protein homeostasis that might be affected by faulty chaperoning (Ruggieri et al., 2015; Cassandrini et al., 2017).

It is noteworthy that, in our patient, there is considerable disruption of the skeletal muscle architecture coinciding with abnormalities of desmin in the absence of cardiac manifestations of disease. Desmin is essential to maintain the structure of not only the skeletal but also the cardiac muscle. Diverse mutants of the desmin gene are associated with myopathy and cardiopathy (Brodehl et al., 2018). Alterations of desmin expression have been described in conditions of muscle atrophy induced by disuse and aging (Marzuca-Nassr et al., 2017). Also, the size of nuclei in muscle tissue may increase when desmin is functionally impaired (Heffler et al., 2020). If the desmin abnormalities in our patient are the result of deficient chaperoning by CCT, one may ask why

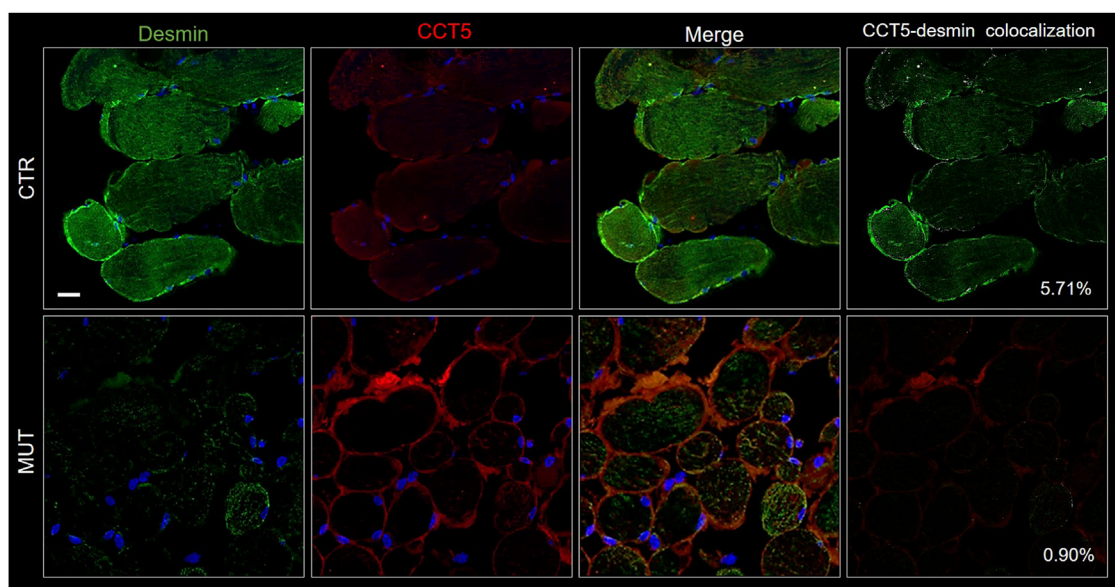


**FIGURE 7 |** Double immunofluorescence with FITC-conjugated antibody for desmin (green) and with TRITC conjugated anti-CCT5 antibody (red) in CTR and MUT muscles. Solid desmin positivity at the costamer level occurred in CTR muscle while it appeared as disorganized dots in the MUT muscle. CCT5 and desmin colocalization was reduced in MUT muscle (0.90%) as compared with the CTR muscle (5.71%). Nuclei were stained with probe Hoechst 33342 (blue). Bar = 25  $\mu$ m.



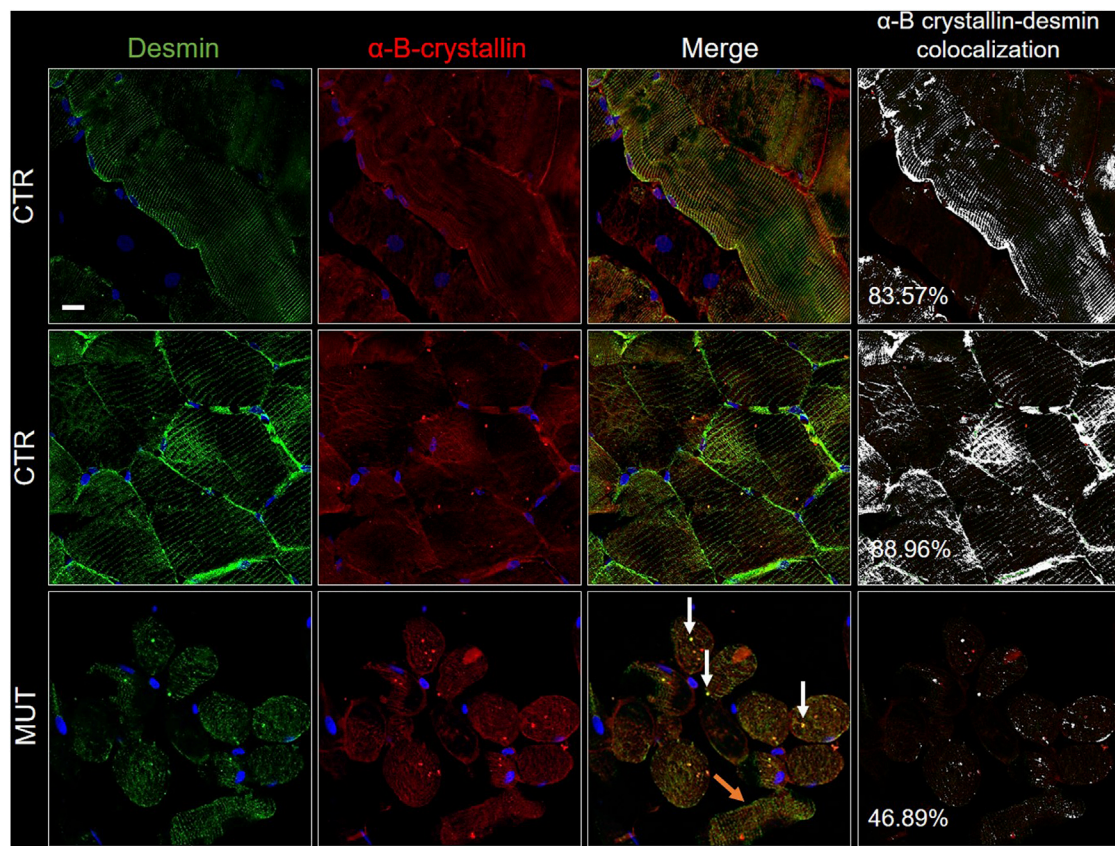


**FIGURE 8 |** Double immunofluorescence with FITC-conjugated antibody for desmin (green) and with TRITC conjugated anti- $\alpha$ -B-crystallin antibody (red) in CTR and MUT muscles.  $\alpha$ -B-crystallin positivity in the sarcolemma and sarcoplasm of CTR muscle fibers appeared in the longitudinal (top row of CTR panels) and the transversal sections (middle row of CTR panels); this positivity was weaker in the MUT muscle fibers (bottom row, MUT panels). Fiber disorganization was evident (orange arrows on the MUT panel to the right, one before the last or “merge” panel). On this same “merge” panel, white arrows point to examples of  $\alpha$ -B-crystallin and desmin aggregates.  $\alpha$ -B-crystallin and desmin colocalization was higher in CTR muscle (longitudinal section, 83.57%; transversal section, 88.96%) than in MUT muscle (for example, only 46.89% in MUT muscle transversal section, as shown in this figure). Nuclei were stained with probe Hoechst 33342 (blue). Bar = 25  $\mu$ m.

the myocardium does not seem to be affected. An explanation could be derived from understanding the CS physiology. The CS components are distributed in all cells and tissues but assembled in groups of interacting molecules that are distinctive for each cell and tissue type, thus while the CCT chaperoning team may be present in the cytosol of all cell and tissue types its interacting partners (i.e., other teams to form networks, co-chaperones, chaperone co-factors, and chaperone interactors and receptors (Macario and Conway de Macario, 2020) are not the same in all locations. Therefore, a defective CCT team bearing a pathogenic mutant may show a range of capabilities depending on the cell type. This may explain the observation that desmin is considerably affected in the skeletal muscle while it is not in the cardiac muscle since the patient does not show clinical manifestations of heart disease. Another explanation could be that CCT does not participate directly in the folding of desmin, or in any of the steps leading to its maturation to become a functional protein in the appropriate cell locale but plays an indirect role. For example, CCT could be key for the folding and maturation of a protein, e.g., an enzyme, required by desmin

production and migration to its physiological locations in skeletal but not in the cardiac muscle. If the CCT complex with the mutant CCT5 subunit fails in its chaperoning functions regarding that protein, desmin would be altered.

In the last few years, it has been found that, differently from other subunits, CCT5 (and in a less competent manner also the CCT4 subunit) has the ability to form homo-oligomeric complexes (micro-complex and single ring), supporting the hypothesis that single CCT5 homo-oligomeric rings may be the base assembly units for the formation of the functional hetero-oligomeric CCT hexadecamer (Sergeeva et al., 2019; Liu et al., 2021). A certain functional ability of the mutant CCT5 in our patient is suggested by its ability to form part of the CCT team, i.e., the CCT hexadecamer. This is suggested by the finding that CCT5 colocalized with CCT1, another component of the CCT team, in which these two subunits are not in direct contact (Leitner et al., 2012). Thus, one may conclude that if the mutant CCT5 colocalizes with CCT1 it must do so indirectly, through contact with the other subunits; and this would indicate that the mutant subunit must be competent to join the other subunits,

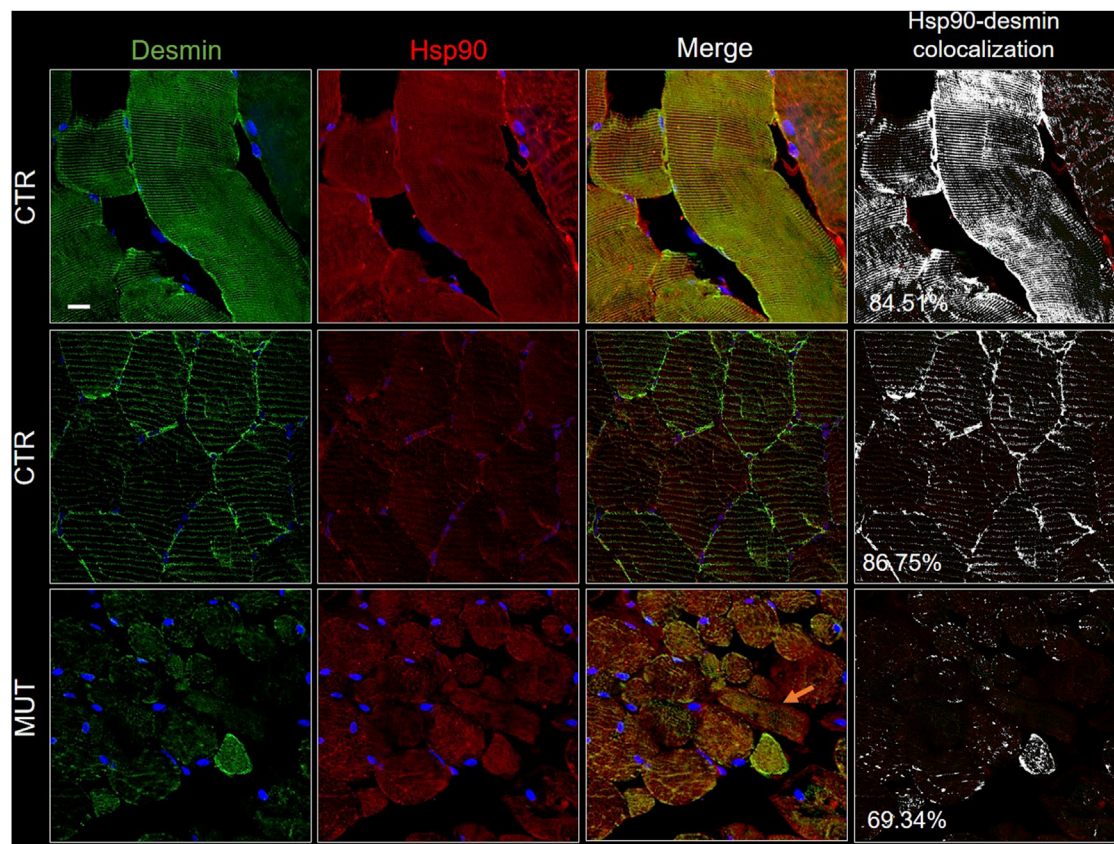


**FIGURE 9 |** Double immunofluorescence with FITC-conjugated antibody for desmin (green) and with TRITC conjugated anti-Hsp90 antibody (red) in CTR and MUT muscles. Hsp90 positivity was well organized in longitudinal and transversal sections of the CTR muscle, but in contrast, it was disrupted and weaker in the MUT muscle (see for example the MUT muscle longitudinal fiber indicated by the orange arrow on the MUT “Merge” panel). Hsp90 and desmin colocalization was high in CTR muscle (longitudinal section, 84.51%; transversal section, 86.75%) by comparison with the MUT muscle (for example, it was 69.34% in MUT muscle transversal section, as shown in this figure). Nuclei were stained with probe Hoechst 33342 (blue). Bar = 25  $\mu$ m.

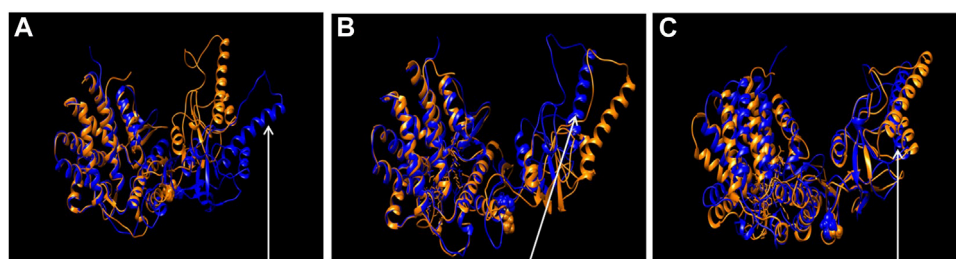


**FIGURE 10 |** Comparison of wild type and the mutant CCT5 using molecular models. Superposition of the most probable conformations obtained by molecular dynamics simulations of wild type CCT5 (orange) and the mutant Leu224Val CCT5 (blue), nucleotide free **(A)**, ATP-bound **(B)**, and ADP-bound **(C)**. Spheres in the intermediate domain correspond to Leucine (orange, wild type) and Valine (blue, mutation) at position 224. Noteworthy in panel **(A)** is the greater opening of the mutant protein, especially at the level of the  $\alpha$ 9 helix, compared to the wild-type protein (arrow). In panel **(B)**, the  $\alpha$ 9 helix of the mutant CCT5 is more closed than in the wild type (arrow), in contrast with the situation in the nucleotide-free conditions, shown in panel **(A)**. In panel **(C)**, under the ADP-bound conditions, the mutant protein shows the lid still more closed than in the wild type (arrow).

form the octameric ring, and the full hexadecameric chaperoning machine. This is in line with the fact that the mutation affects primarily the apical domain of CCT5, namely, the domain involved in substrate recognition and chaperoning chamber

closing and opening, but not in the formation of rings and hexadecamers (Lopez et al., 2015). Thus, one can expect a certain level of chaperoning ability from the CCT complex, only curtailed by insufficient capability for substrate



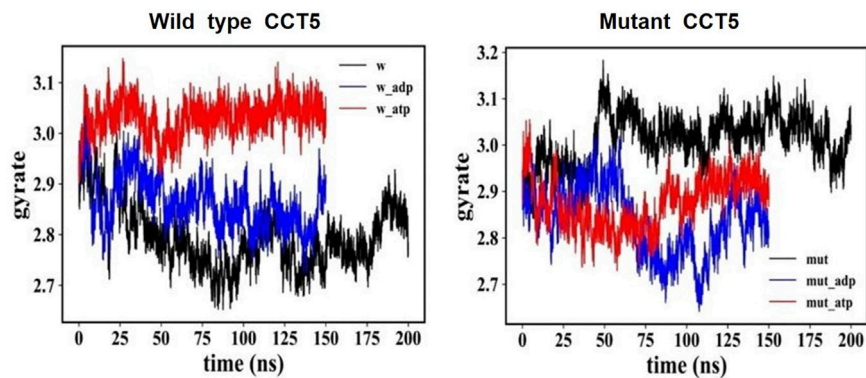


**FIGURE 11 |** Distribution of atomic masses in the wild type and mutant CCT5 by radius of gyration analysis. Comparison of the radius of gyration of wild type (left panel) and mutant (right panel) CCT5 subunits as a function of time was done under the three conditions studied: nucleotide free (black), ATP bound (red), and ADP bound (blue).

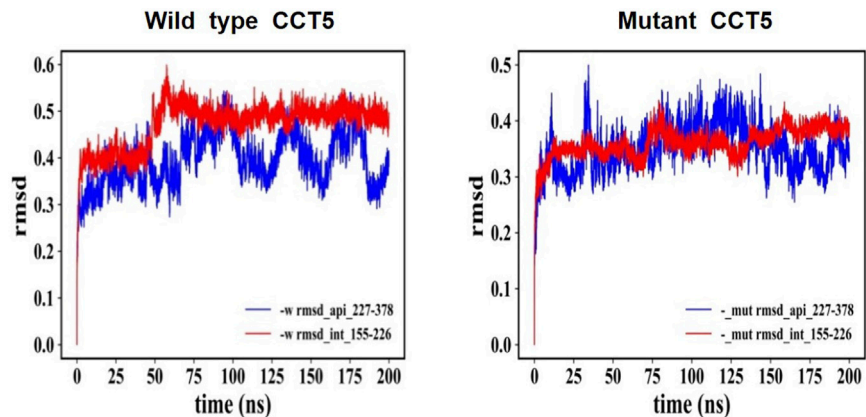


**FIGURE 12 |** RMSD: Comparison of nucleotide-free CCT5, wild type vs. mutant. RMSD of the entire molecules, wild type and mutant CCT5, were determined, and the outputs were examined in various ways. Here, we present the comparison of the parts of the outputs pertaining to the N-terminal segment of the intermediate domain and to the apical domain, which illustrates the difference between the wild type and the mutant molecules. Left panel: Wild type molecule apical domain, blue; N-terminal segment of intermediate domain, red. Right panel: Mutant molecule apical domain, blue; N-terminal segment of intermediate domain, red. The RMSD values reveal differences between the two molecules and instability of the apical domain of the mutant. Similar trends were shown when ADP and ATP bound molecules were examined, although in the ATP-bound molecules the differences in instability of the mutant with regard to the wild-type molecule were less marked (data not shown).

recognition and handling and depending on the cell type's proteome, which is different for each cell type. Consequently, one can expect diverse kinds and levels of failure of protein homeostasis in different cell and tissue types. To further complicate the landscape of deficient protein homeostasis in the whole organism stands the diversity of possible substrates for CCT, which include a variety of proteins: structural (Yam et al., 2008), regulatory of cell cycle and apoptosis (Willison, 2018a; 2018b), and others involved in neural tissue development and degeneration (Chávez-Cárdenas and Vázquez-Contreras, 2012). Substrate selection and binding depend on specific amino acid sequences on the client protein (Willison, 2018a; 2018b) and on the translational context (Yam et al., 2008). In different tissue types (with distinct proteomes), and under

different conditions (e.g., normal vs stress condition), CCT can bind different substrates. This adds to the diversity of effects that a defective CCT complex may cause in various tissues, for example, striated skeletal and cardiac muscles, and nervous tissue and skeletal muscle.

Another finding that also indicates that the chaperonin complex with the mutant CCT5 subunit can function, at least to some extent and for a reduced range of substrates, is that the signal for actin, a canonical substrate for CCT (Berger et al., 2018; Willison, 2018a, 2018b), was only slightly affected in the patient's muscle. It can therefore be inferred that while actin, normally the substrate for which CCT has high avidity, is still recognized by the defective chaperone, whereas other less preferred substrates are not.



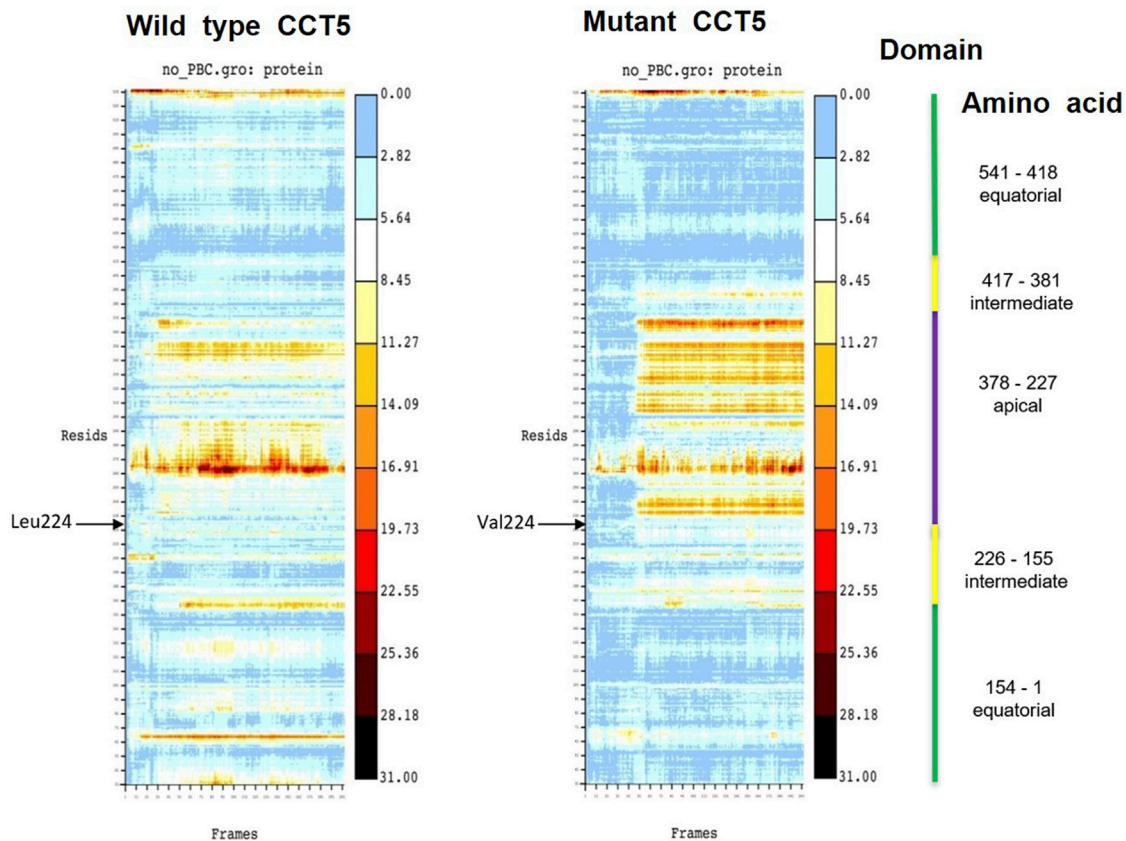


**FIGURE 13 |** Heat maps of wild type and mutant nucleotide-free CCT5 subunits. In the heat map of the wild type subunit a wider area of heat is observed in the region between the amino acids (Resids) 260 and 270 (at 11.27 Å) and between amino acids 230 and 250 (at 16.91 Å). These two regions are within the apical domain (indicated by a violet vertical line on far the right). In the mutant subunit a wider heat area is observed in a region between amino acids 230 and 370 (between 19.73 and 16.91 Å), which is in the intermediate domain, beginning very close to position 224 in the N-terminal segment of the intermediate domain, where the point mutation occurs (indicated by the black arrow Val224), and it spans the entire apical domain.

The CCT complex, and the Hsp90 and alpha-B-crystallin chaperones are at the Z-disc of healthy skeletal muscle and are believed to play key roles in the development and maintenance of this structure (Roh et al., 2015; Unger et al., 2017; Berger et al., 2018). Our experiments demonstrate that all three components are affected in MUT muscle, which would impair the functionality of the Z-disc; Z-lines would not anchor the contractile filaments and, in turn, desmin would not transmit the force of contraction to sarcolemma, hampering the shortening of muscle fibers. Alpha-B-crystallin is a desmin chaperone but which of the two proteins is primarily damaged is to be investigated. Hsp90 and alpha-B-crystallin genetic variants are related to hereditary myopathies (Reilich et al., 2010; Unger et al., 2017). Many fibers of skeletal muscle tissue from the patient were in apoptosis, but TUNEL assay does not allow us to differentiate the classical apoptosis, from denervation and necrosis, and further investigations are required. However, a skeletal muscle histomorphology due to inactivity and comparable to the one described here is not reported in literature, whereas protein aggregation and reduction of

myofibrils in zebrafish *cct5*-mutant model was accompanied by severe decrease of skeletal muscle-dependent force generation (Berger et al., 2018). Therefore, it is highly likely that failure of CCT entails defects involving alpha-B crystallin and Hsp90, which is not surprising considering the physiological interactions known to occur between different members of the CS.

The *in silico* analyses of the mutant CCT5 in comparison with the wild type counterpart, demonstrated changes in the mutant, most evident in the apical domain, which suggest that the chaperonin is defective and could be the cause of some of the abnormalities observed in our patient.

The CCT complex fold diverse substrates, typically actin and tubulin, which differ in structure. This suggests that substrates for CCT do not have to have a specific amino acid signature for recognition and binding by the chaperonin but must show other features for the purpose. For instance, matching tridimensional conformations in the chaperone and the substrate could be involved with participation of multiple weak interactions. In this regard, the radius of gyration and RMSD analyses revealed in the

mutant molecule an energy disturbance, suggesting altered folding with opposite masses distribution and a different molecular equilibrium as compared with the wild type CCT5 subunit. The apical domain of the mutant subunit showed a major deviation of atoms in comparison with the wild-type counterpart, most notably under nucleotide-free conditions but also appreciable under ATP-bound conditions. Helix-10 of the apical domain (amino acids <sup>309</sup>EANHLLQ<sup>316</sup>) and the proximal loop region (amino acids <sup>234</sup>FSHPQMPK<sup>241</sup>) are involved in substrate-binding (Pereira et al., 2017). Beyond the substrate-binding region, the extended  $\alpha$ -helix (helix-9) of the apical domain functions as a built-in lid to close the CCT hexadecamer's cavity and is linked to an apical loop (amino acids <sup>259</sup>KPKTKHK<sup>265</sup>), which creates a highly charged region probably involved in substrate interaction (Pereira et al., 2017). Heat maps of the mutant CCT5 subunit confirmed the instability of the apical domain affecting helix-10, proximal loop, and helix-9 position in absence of nucleotide. It is, therefore, possible that the chaperoning functions of the CCT hexadecamer with the mutant CCT subunit are deficient with compromise of substrate recognition, binding, and conveyance. Thus, it is likely that at least some of the abnormalities observed in the striated muscle of the patient are the consequence of deficient chaperoning.

Here we report for the first time the histomorphology of a genetic chaperonopathy in the skeletal muscle tissue. We believe that, taking into account the difficulty to reproduce the complexity of a tissue *in vitro*, our results provide the indispensable platform for designing and launching the experiments necessary for elucidating the molecular mechanisms underpinning the reported tissue abnormalities.

## REFERENCES

- Antona, V., Scalia, F., Giorgio, E., Radio, F. C., Brusco, A., Oliveri, M., et al. (2020). A Novel Cct5 Missense Variant Associated with Early Onset Motor Neuropathy. *Int. J. Mol. Sci.* 21, 1–12. doi:10.3390/ijms21207631
- Berger, J., Berger, S., Li, M., Jacoby, A. S., Arner, A., Bavi, N., et al. (2018). *In Vivo* Function of the Chaperonin TRiC in  $\alpha$ -Actin Folding during Sarcomere Assembly. *Cell Rep.* 22, 313–322. doi:10.1016/j.celrep.2017.12.069
- Bouhouche, A., Benomar, A., Bouslam, N., Chkili, T., and Yahyaoui, M. (2006a). Mutation in the Epsilon Subunit of the Cytosolic Chaperonin-Containing T-Complex Peptide-1 (Cct5) Gene Causes Autosomal Recessive Mutilating Sensory Neuropathy with Spastic Paraplegia. *J. Med. Genet.* 43, 441–443. doi:10.1136/jmg.2005.039230
- Bouhouche, A., Benomar, A., Bouslam, N., Ouazzani, R., Chkili, T., and Yahyaoui, M. (2006b). Autosomal Recessive Mutilating Sensory Neuropathy with Spastic Paraplegia Maps to Chromosome 5p15.31-14.1. *Eur. J. Hum. Genet.* 14, 249–252. doi:10.1038/sj.ejhg.5201537
- Brodehl, A., Gaertner-Rommel, A., and Milting, H. (2018). Molecular Insights into Cardiomyopathies Associated with Desmin (DES) Mutations. *Biophys. Rev.* 10, 983–1006. doi:10.1007/s12551-018-0429-0
- Cassandrini, D., Trovato, R., Trovato, R., Rubegni, A., Lenzi, S., Fiorillo, C., et al. (2017). Congenital Myopathies: Clinical Phenotypes and New Diagnostic Tools. *Ital. J. Pediatr.* 43, 101. doi:10.1186/s13052-017-0419-z
- Chávez-Cárdenas, M. E., and Vázquez-Contreras, E. (2012). The Aggregation of Huntingtin and  $\alpha$ -Synuclein. *J. Biophys.* 2012, 606172.
- Foloppe, N., and MacKerell, A. D., Jr. (2000). All-atom Empirical Force Field for Nucleic Acids: I. Parameter Optimization Based on Small Molecule and Condensed Phase Macromolecular Target Data. *J. Comput. Chem.* 21, 86–104. doi:10.1002/(sici)1096-987x(20000130)21:2<86::aid-jcc2>3.0.co;2-g
- Heffler, J., Shah, P. P., Robison, P., Phyto, S., Veliz, K., Uchida, K., et al. (2020). A Balance between Intermediate Filaments and Microtubules Maintains Nuclear Architecture in the Cardiomyocyte. *Circ. Res.* 126, E10–E26. doi:10.1161/CIRCRESAHA.119.315582
- Hess, B., Kutzner, C., Van Der Spoel, D., and Lindahl, E. (2008). GROMACS 4: Algorithms for Highly Efficient, Load-Balanced, and Scalable Molecular Simulation. *J. Chem. Theory Comput.* 4, 435–447. doi:10.1021/ct700301q
- Jameson, L., Kasper, D. L., Longo, D. L., Fauci, A. S., Hauser, S. L., and Loscalzo, J. (2018). “Neurologic Disorders,” in *Harrison's Principles of Internal Medicine*. 20th Ed. (New York: McGraw-Hill Education), 3026–3295.
- Leitner, A., Joachimiak, L. A., Bracher, A., Mönkemeyer, L., Walzthoeni, T., Chen, B., et al. (2012). The Molecular Architecture of the Eukaryotic Chaperonin TRiC/CCT. *Structure* 20, 814–825. doi:10.1016/j.str.2012.03.007
- Liu, C., Wang, H., Jin, M., Han, W., Wang, S., Wang, Y., et al. (2021). *Cryo-EM Study on the Homo-Oligomeric Ring Formation of Yeast TRiC/CCT Subunits Reveals TRiC Ring Assembly Mechanism*. bioRxiv. doi:10.1101/2021.02.24.432666
- Lopez, T., Dalton, K., and Frydman, J. (2015). The Mechanism and Function of Group II Chaperonins. *J. Mol. Biol.* 427, 2919–2930. doi:10.1016/j.jmb.2015.04.013
- Macario, A. J. L., Conway de Macario, E., and Cappello, F. (2013). *The Chaperonopathies - Diseases with Defective Molecular Chaperones*. Dordrecht, Netherlands: SpringerBriefs Biochem Mol Biol.
- Macario, A. J. L., and Conway de Macario, E. (2005). Sick Chaperones, Cellular Stress, and Disease. *N. Engl. J. Med.* 353, 1489–1501. doi:10.1056/nejmra050111
- Macario, A. J. L., and Conway de Macario, E. (2020). Molecular Mechanisms in Chaperonopathies: Clues to Understanding the Histopathological Abnormalities and Developing Novel Therapies. *J. Pathol.* 250, 9–18. doi:10.1002/path.5349
- MacKerell, A. D., and Banavali, N. (2000). *All-atom Empirical Force Field for Nucleic Acids: II. Application to Molecular Dynamics Simulations of DNA and*

## DATA AVAILABILITY STATEMENT

The original contributions presented in the study are included in the article/**Supplementary Material**, further inquiries can be directed to the corresponding author.

## AUTHOR CONTRIBUTIONS

FS, AMV, RB, FR, AMG, GLB, GB, MV, DA, ECdeM, and AJLM formal analysis; FM and KHM have provided the healthy sample; FS, AMV, GDM, GS, and FLC investigation; FC, MG, VA, ECdeM, and AJLM project administration; FS, AMV, ECdeM, and AJLM writing, critical review, and editing. All authors have read and agreed to the published version of the manuscript.

## FUNDING

AJLM and ECdeM. were partially supported by IMET and IEMEST. This is IMET contribution number IMET 22-103.

## SUPPLEMENTARY MATERIAL

The Supplementary Material for this article can be found online at: <https://www.frontiersin.org/articles/10.3389/fmolb.2022.887336/full#supplementary-material>

- RNA in Solution, 2. doi:10.1002/(SICI)1096-987X(20000130)21:2<105:AID-JCC3>3.0.CO
- Marino Gammazza, A., Rizzo, M., Citarrella, R., Rappa, F., Campanella, C., Bucchieri, F., et al. (2014). Elevated Blood Hsp60, its Structural Similarities and Cross-Reactivity with Thyroid Molecules, and its Presence on the Plasma Membrane of Oncocytes Point to the Chaperonin as an Immunopathogenic Factor in Hashimoto's Thyroiditis. *Cell Stress Chaperones* 19, 343–353. doi:10.1007/s12192-013-0460-9
- Marzuca-Nassr, G. N., Droguett-Cervela, R., Córdova-Sáez, M., Ibarra-Fuentealba, I., Donoso-Torres, W., López-Suárez, A., et al. (2017). Acute Electrical Stimulation Modifies Cross-Sectional Area and Desmin Protein in the Skeletal Muscle of Old Rats Submitted to Hindlimb Suspension. *Indian J. Physiology Pharmacol.* 61, 219.
- Min, W., Angileri, F., Luo, H., Lauria, A., Shanmugasundaram, M., Almerico, A. M., et al. (2014). A Human CCT5 Gene Mutation Causing Distal Neuropathy Impairs Hexadecamer Assembly in an Archaeal Model. *Sci. Rep.* 4, 6688–6689. doi:10.1038/srep06688
- Morrison, B. (2016). Neuromuscular Diseases. *Semin. Neurol.* 36, 409–418. doi:10.1055/s-0036-1586263
- Pereira, J. H., McAndrew, R. P., Sergeeva, O. A., Ralston, C. Y., King, J. A., and Adams, P. D. (2017). Structure of the Human TRiC/CCT Subunit 5 Associated with Hereditary Sensory Neuropathy. *Sci. Rep.* 7, 3673. doi:10.1038/s41598-017-03825-3
- Reilich, P., Schoser, B., Schramm, N., Krause, S., Schessl, J., Kress, W., et al. (2010). The p.G154S Mutation of the Alpha-B Crystallin Gene (CRYAB) Causes Late-Onset Distal Myopathy. *Neuromuscul. Disord.* 20, 255–259. doi:10.1016/j.nmd.2010.01.012
- Roh, S.-H., Kasembeli, M., Bakthavatsalam, D., Chiu, W., and Tweardy, D. (2015). Contribution of the Type II Chaperonin, TRiC/CCT, to Oncogenesis. *Ijms* 16, 26706–26720. doi:10.3390/ijms161125975
- Rubin, R., Strayer, D. S., and Rubin, E. (2012). "Cell Adaptation, Cell Injury and Cell Death," in *Rubin's Pathology: Clinicopathologic Foundations of Medicine*. 6th Ed. (Philadelphia: Wolters Kluwer Health/Lippincott Williams & Wilkins).
- Ruggieri, A., Brancati, F., Zanotti, S., Maggi, L., Pasanisi, M. B., Saredi, S., et al. (2015). Complete Loss of the DNAJB6 G/F Domain and Novel Missense Mutations Cause Distal-Onset DNAJB6 Myopathy. *Acta Neuropathol. Commun.* 3, 44. doi:10.1186/s40478-015-0224-0
- Scalia, F., Vitale, A. M., Santonocito, R., Conway de Macario, E., Macario, A. J. L., and Cappello, F. (2021). The Neurochaperonopathies: Anomalies of the Chaperone System with Pathogenic Effects in Neurodegenerative and Neuromuscular Disorders. *Appl. Sci.* 11, 1–22. doi:10.3390/app11030898
- Sergeeva, O. A., Haase-Pettingell, C., and King, J. A. (2019). Co-expression of CCT Subunits Hints at TRiC Assembly. *Cell Stress Chaperones* 24 (6), 1055–1065. doi:10.1007/s12192-019-01028-5
- Spigolon, D., Gallagher, D. T., Velazquez-Campoy, A., Bulone, D., Narang, J., San Biagio, P. L., et al. (2017). Quantitative Analysis of the Impact of a Human Pathogenic Mutation on the CCT5 Chaperonin Subunit Using a Proxy Archaeal Ortholog. *Biochem. Biophys. Rep.* 12, 66–71. doi:10.1016/j.bbrep.2017.07.011
- Unger, A., Beckendorf, L., Böhme, P., Kley, R., von Frieling-Salewsky, M., Lochmüller, H., et al. (2017). Translocation of Molecular Chaperones to the Titin Springs Is Common in Skeletal Myopathy Patients and Affects Sarcomere Function. *Acta Neuropathol. Commun.* 5, 72. doi:10.1186/s40478-017-0474-0
- Van Der Spoel, D., Lindahl, E., Hess, B., Groenhof, G., Mark, A. E., and Berendsen, H. J. C. (2005). GROMACS: Fast, Flexible, and Free. *J. Comput. Chem.* 26, 1701–1718. doi:10.1002/jcc.20291
- Willison, K. R. (2018a). The Structure and Evolution of Eukaryotic Chaperonin-Containing TCP-1 and its Mechanism that Folds Actin into a Protein Spring. *Biochem. J.* 475, 3009–3034. doi:10.1042/bcj20170378
- Willison, K. R. (2018b). The Substrate Specificity of Eukaryotic Cytosolic Chaperonin CCT. *Phil. Trans. R. Soc. B* 373, 20170192. doi:10.1098/rstb.2017.0192
- Yam, A. Y., Xia, Y., Lin, H.-T. J., Burlingame, A., Gerstein, M., and Frydman, J. (2008). Defining the TRiC/CCT Interactome Links Chaperonin Function to Stabilization of Newly Made Proteins with Complex Topologies. *Nat. Struct. Mol. Biol.* 15, 1255–1262. doi:10.1038/nsmb.1515

**Conflict of Interest:** The authors declare that the research was conducted in the absence of any commercial or financial relationships that could be construed as a potential conflict of interest.

**Publisher's Note:** All claims expressed in this article are solely those of the authors and do not necessarily represent those of their affiliated organizations, or those of the publisher, the editors and the reviewers. Any product that may be evaluated in this article, or claim that may be made by its manufacturer, is not guaranteed or endorsed by the publisher.

Copyright © 2022 Scalia, Barone, Rappa, Marino Gammazza, Lo Celso, Lo Bosco, Barone, Antona, Vadalà, Vitale, Donato Mangano, Amato, Sentiero, Macaluso, Myburgh, Conway de Macario, Macario, Giuffrè and Cappello. This is an open-access article distributed under the terms of the Creative Commons Attribution License (CC BY). The use, distribution or reproduction in other forums is permitted, provided the original author(s) and the copyright owner(s) are credited and that the original publication in this journal is cited, in accordance with accepted academic practice. No use, distribution or reproduction is permitted which does not comply with these terms.



# High Expression of Plasma Extracellular HSP90 $\alpha$ is Associated With the Poor Efficacy of Chemotherapy and Prognosis in Small Cell Lung Cancer

## OPEN ACCESS

### Edited by:

Xolani Henry Makhoba,  
University of Fort Hare, South Africa

### Reviewed by:

Tze-Sing Huang,  
National Health Research Institutes  
(Taiwan), Taiwan  
Tawanda Zininga,  
Stellenbosch University, South Africa

### \*Correspondence:

Jilin Li  
lijilingxmu@outlook.com  
Litu Zhang  
zhanglitu@gmail.com

<sup>†</sup>These authors have contributed  
equally to this work

### Specialty section:

This article was submitted to  
Molecular Diagnostics and  
Therapeutics,  
a section of the journal  
Frontiers in Molecular Biosciences

**Received:** 05 April 2022

**Accepted:** 06 June 2022

**Published:** 11 July 2022

### Citation:

Huang B, Pan J, Liu H, Tang Y, Li S,  
Bian Y, Ning S, Li J and Zhang L (2022)  
High Expression of Plasma  
Extracellular HSP90 $\alpha$  is Associated  
With the Poor Efficacy of  
Chemotherapy and Prognosis in Small  
Cell Lung Cancer.  
Front. Mol. Biosci. 9:913043.  
doi: 10.3389/fmolb.2022.913043

Baoyue Huang<sup>1†</sup>, Jinmiao Pan<sup>1†</sup>, Haizhou Liu<sup>1,2†</sup>, Yamei Tang<sup>1</sup>, Shirong Li<sup>1</sup>, Yingzhen Bian<sup>1</sup>,  
Shufang Ning<sup>1,2</sup>, Jilin Li<sup>1,2\*</sup> and Litu Zhang<sup>1,2\*</sup>

<sup>1</sup>Department of Research, Guangxi Medical University Cancer Hospital, Guangxi Medical University, Nanning, China,

<sup>2</sup>Department of Research, Guangxi Cancer Molecular Medicine Engineering Research Center, Nanning, China

**Purpose:** eHSP90 $\alpha$  is closely related to tumor progression and prognosis. This study aimed to investigate the significance of eHSP90 $\alpha$  in the response evaluation and prediction of small cell lung cancer.

**Methods:** We analyzed the relationship between eHSP90 $\alpha$  expression and clinicopathological features in 105 patients with small cell lung cancer. Univariate and multivariate analyses were used to determine the association of parameters and ratios with response assessment, progression-free survival (PFS), and overall survival (OS).

**Results:** In SCLC patients, eHSP90 $\alpha$  and NSE were positively correlated. The cutoff values of eHSP90 $\alpha$  in OS, PFS, and response evaluation were 61.2 ng/ml, 48.7 ng/ml, and 48.7 ng/ml, respectively. eHSP90 $\alpha$  could better predict OS, PFS, and response evaluation (AUC OS 0.791, PFS 0.662, 0.685). Radiotherapy and eHSP90 $\alpha$  were independent variables for effective chemotherapy through univariate and multivariate analysis. In contrast, radiotherapy, eHSP90 $\alpha$ , NSE, and M stage were independent variables for OS. eHSP90 $\alpha$ , and M stage were independent variables for PFS. Kaplan-Meier analysis showed that higher eHSP90 $\alpha$  expression predicted poorer OS and earlier progression in patients.

**Conclusions:** This study aims to provide new evidence for the efficacy response and prognostic assessment of SCLC. eHSP90 $\alpha$  may be a better biomarker for SCLC.

**Keywords:** SCLC-small cell lung cancer, eHSP90 $\alpha$ , prognosis, response evaluation criteria in solid tumor, NSE

**Abbreviations:** eHSP90 $\alpha$ , extracellular heat shock protein 90 aa1; SCLC, Small cell lung cancer; NSCLC, non-small cell lung cancer; OS, overall survival; PFS, progression-free survival; AUC, area under the curve; NSE, neuron-specific enolase; CT, computed tomography; CEA, carcinoembryonic antigen; ELISA, Enzyme-linked immunosorbent assay; RPM, Round per minute; DI water, Deionized water.



## INTRODUCTION

By 2021 and for the foreseeable future, it is commonly acknowledged in the academic and medical field that lung cancer is the most lethal type of cancer globally, and small cell lung cancer (SCLC) is a malignant tumor with a relatively poor prognosis (Mai et al., 2021). Most patients tend to be in a metastatic stage at the early diagnosis stage rather than a less aggressive stage (Pedersen et al., 2021). 30,000 to 35,000 new cases of SCLC, also known as oat cell carcinoma, is a neuroendocrine tumor derived from bronchial epithelial cells, which accounts for 13–15% of all lung cancers that appear in the US per year (Oronsky et al., 2017). Currently, techniques for diagnosis and response assessment of lung cancer involve image scanning, bronchoscopy, transbronchial needle aspiration, CT-guided puncture of lung tumor, etc. While comparatively low diagnostic sensitivity shows in image scanning, the level of invasiveness and undesirable effects also seem too apparent in the regular histological diagnostic procedure-bronchial biopsy. Subsequently, with possible early detection, accurate subtyping, and intensive monitoring being essential for an optimal result of SCLC therapy, the issue of SCLC being diagnosed at a later stage and drastically reducing curing rates of this aggressive malignancy will be at ease (Cummings et al., 2008; Fang et al., 2021). There are several potential markers carcinoembryonic antigen (CEA), Neuron-specific enolase (NSE), Progastrin releasing peptide (ProGRP), Creatine kinase BB (CK-BB), Chromogranin A (CgA), Neural cell adhesion molecule (NCAM) and several cytokeratins (Harmsma et al., 2013). NSE, also known as enolase- $\gamma$ , is a neuro- and neuroendocrine

specific isoenzyme of enolase which is frequently reported to show an elevation in SCLC at the time of diagnosis (Massabki et al., 2003; Tian et al., 2020). Notwithstanding, its levels are repeatedly tested to be correlated to tumor mass extension, for which it is considered to be a reliable marker while patients undergo chemotherapy, and it has proven to be a suitable biomarker for follow-up and a noteworthy predictor of SCLC patients (Zhou et al., 2017; Tian et al., 2020).

Heat shock protein 90 (HSP90) is a ubiquitously expressed molecular chaperone that plays an essential part in various biological processes with two isoforms in the cytosol, HSP90 $\alpha$  (also known as HSP90AA1) and HSP90 $\beta$  (also known as HSP90AB1) (Li et al., 2013; Tian et al., 2019). HSP90 $\alpha$  is an essential intracellular molecular chaperone for hundreds of diverse and important protein clients, making HSP90 a central regulator of cellular processes ranging from protein folding to DNA repair, development, immune response, and many other important functions (Hou et al., 2021). Previous studies showed that plasma Hsp90 levels are positively correlated with tumor malignancy, which may be a potential clinical diagnostic and prognostic marker (Wang et al., 2009). Moreover, extracellular HSP90 $\alpha$  has recently been tested as an excellent biomarker for liver and lung cancer in clinical practices (Fu et al., 2017; Zhou et al., 2021). According to recent demonstrations, the area under the diagnosis curve of eHSP90 $\alpha$  against lung cancers appears to be 0.857, with outstanding sensitivity and specificity. Thus, eHSP90 $\alpha$  is well anticipated to be a game-changer in tumor biomarkers for lung cancer diagnosis and prognostic assessment (Zhou et al., 2021).

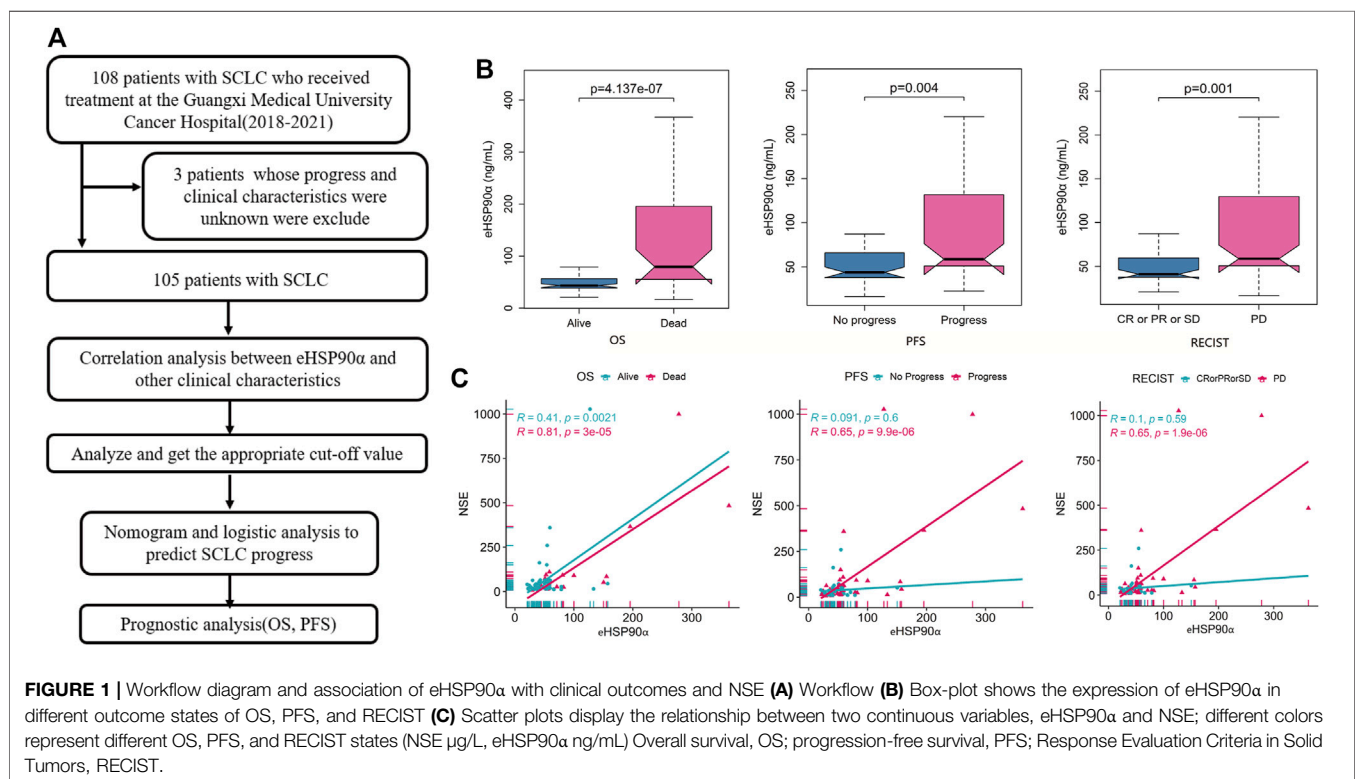


**TABLE 1 |** Patient characteristics and hematologic parameters.

Features	SCLC
Total	105
Gender	
Male (%)	87 (82.9%)
Female (%)	18 (17.1%)
Age (years)	
<55 (%)	23 (21.9%)
$\geq 55$ (%)	82 (78.1%)
Location	
Left (%)	40 (38.1%)
Right (%)	60 (57.1%)
Mediastinal (%)	5 (4.8%)
Diameter(cm)	
$\leq 3$ (%)	26 (24.8%)
>3 (%)	79 (75.2%)
TNM stage	
Stage I (%)	3 (2.9%)
Stage II (%)	2 (1.9%)
Stage III (%)	22 (21.0%)
Stage IV (%)	78 (74.3%)
VALG stage	
LD-SCLC (%)	27 (25.7%)
ED-SCLC (%)	78 (74.3%)
T stage	
T1 (%)	14 (13.3%)
T2 (%)	17 (16.2%)
T3 (%)	19 (18.1%)
T4 (%)	55 (52.4%)
N stage	
0 (%)	6 (5.71%)
1 (%)	16 (15.24%)
2 (%)	37 (35.24%)
3 (%)	46 (43.81%)
M	
0 (%)	27 (25.7%)
1 (%)	78 (74.3%)
Chemotherapy	
Yes (%)	94 (89.52%)
No (%)	11 (10.48%)
Radiotherapy	
Yes (%)	33 (31.43%)
No (%)	72 (68.57%)
eHSP90 $\alpha$ [median (IQR)]	54.90 (39.10.80.90)
Ki-67 [median (IQR)]	80 (70.90)
T lymphocytes [median (IQR)]	66.17 (60.20.72.30)
T helper cells [median (IQR)]	38.80 (33.20.45.90)
T suppressor cells [median (IQR)]	18.20 (15.60.23.40)
T helper cells/T suppressor cells [median (IQR)]	2.10 (1.60.2.90)
Natural killer cells [median (IQR)]	12.20 (9.20.18.60)
B lymphocytes [median (IQR)]	11.60 (8.10.15.80)
Carcinoembryonic antigen [median (IQR)]	4.38 (2.22.14.62)
Carbohydrate antigen 19–9 [median (IQR)]	10.50 (3.83.34.98)
Thymidine kinase1 [median (IQR)]	0.78 (0.41.1.54)
Neuron-specific enolase [median (IQR)]	30.81 (15.84.61.97)

Limited disease small cell lung cancer, LD-SCLC; extension disease small cell lung cancer, ED-SCLC.

A nomogram is a graphical representation of a mathematical model involving several factors to predict a particular endpoint with statistical methods applied (Balachandran et al., 2015). Nomograms have been considered reliable tools to predict the clinical outcomes in several types of cancer and have proven to be more precise than the currently available staging systems (Iasonos et al., 2008). It is of

certain urgency and great importance to developing a non-invasive methodology for observing small cell lung cancer prognosis. To allow improved monitoring of efficacy in therapeutic modalities and further accuracy in subtyping, we employed said the strategy to investigate the predictive value of various clinical variables and established a nomogram by analyzing SCLC patients.

## METHODS AND MATERIALS

### Patients and Data Selection

105 patients diagnosed with small cell lung cancer (SCLC) were enrolled at the Department of Medical Oncology of Respiratory in Guangxi Medical University Cancer Hospital from January 2018 to April 2021. Ethics approval number: LW2022044.

SCLC patients were qualified for inclusion if they met the following criteria: 1. They have pathologically diagnosed SCLC; 2. Obtained blood samples; 3. Response assessments were done with a computed tomography scan (CT scan) of the chest and abdomen every two treatment cycles according to Response Evaluation Criteria in Solid Tumors (RECIST version 1.1). Each patient's response was classified into one of the following categories: responders, including cases of complete response (CR), partial response (PR), and stable disease (SD), and non-responders, including issues of disease progression (PD). The exclusion criteria were as follows: incomplete demographic statistical information such as age, sex, or race; incomplete clinicopathology information such as tumor size (defined as the most accurate measurement of a solid primary tumor), tumor-node-metastasis (TNM) stage, tumor grade; incomplete therapeutic information in chemotherapy and radiotherapy (defined as the method performed as part of the first course of treatment); missing survival status and follow-up data. According to the National Comprehensive Cancer Network (NCCN) combined with the Veterans Administration Lung Study Group (VALG) approach for SCLC staging, limited disease (LD)-SCLC is specified as stage I to III (T any, N any, M0), and extension disease (ED)-SCLC is defined as stage IV (T any, N any, M1a/b). All subjects involved had received treatment using etoposide plus platinum antineoplastic agent in the first place. For general methods, see Figure 1A.

In this retrospective study, the data on the peripheral blood of the patients diagnosed with SCLC were collected which included T lymphocytes, T helper cells, T suppressor cells, T helper cells/T suppressor cells, natural killer cells, B lymphocytes, carcinoembryonic antigen, carbohydrate antigen 19–9, thymidine kinase1, neuron-specific enolase and Ki-67. All blood samples were collected before subjects had received any treatment.

### Specimen Collection and Measurement of Tumor Markers

Heat shock protein 90 $\alpha$  (Yantai Protgen Biotechnology Development Co., Ltd., Shandong, China): Collect blood from patients with EDTA-K2 anticoagulation tube in the morning and apply it in a centrifuge 3000RPM for 15 min. Incubate the kit in water at 37°C for 30 min. The liquid in the kit gets thoroughly mixed to a point where no air bubbles are visible. Add  $4.75 \times 10^5$   $\mu$ L of deionized water to the

**TABLE 2 |** Correlation of eHSP90 $\alpha$  and Other Index in SCLC Patients.

Parameter	Total		LD-SCLC		ED-SCLC	
	r	p	r	p	r	p
Sex	-0.090	0.363	-0.146	0.402	-0.110	0.366
Age	-0.087	0.378	0.145	0.407	-0.216	0.073
Diameter(cm)	0.213	0.029	0.165	0.342	0.223	0.064
T lymphocytes	-0.200	0.041	-0.404	0.016	-0.095	0.435
T helper cells	-0.199	0.042	-0.300	0.080	-0.148	0.222
T suppressor cells	-0.045	0.648	-0.262	0.128	0.048	0.691
T helper cells/T suppressor cells	-0.066	0.502	0.049	0.778	-0.102	0.399
Natural killer cells	0.129	0.191	0.273	0.112	0.050	0.682
B lymphocytes	-0.060	0.542	0.074	0.672	-0.054	0.660
Ki-67	0.021	0.831	0.286	0.096	-0.104	0.389
CEA	0.067	0.496	0.163	0.350	-0.020	0.867
CA19-9	0.146	0.138	0.196	0.260	0.112	0.359
TK1	-0.086	0.385	-0.147	0.401	-0.046	0.705
NSE	0.376	<b>0.001</b>	0.068	0.771	0.441	<b>0.001</b>

Spearman correlation, bold font indicates statistical. Carcinoembryonic antigen, CEA; Carbohydrate antigen 19–9, CA19-9; Thymidine kinase1, TK1; Neuron-specific enolase, NSE.

concentrated washing solution and mix well. Add calibrator to 400  $\mu$ L of analyte diluent to dissolve and mix. Plasma samples need to be diluted 20-fold with diluent. Take 50  $\mu$ L each of the calibrator and the diluted plasma sample, add them to the calibration well and sample the microplate. Add 50  $\mu$ L of heat shock protein 90 $\alpha$  marker solution to the wells and mix gently. Subsequent incubation happens in warm water at 37°C for 60 min after being sealed. Shake off the reactant solution, add a 300  $\mu$ L washing solution/washing machine, wash the plate six times, and dry on absorbent paper. Add 50  $\mu$ L of chromogenic reagent A to the wells above, then add 50  $\mu$ L of chromogenic reagent B and incubate with warm water at 37°C for 20 min after mixing. Add 50  $\mu$ L of stopping solution to the above wells to stop color development. Read the OD value immediately at 450 nm/620 (630) nm wavelength. Calculate the content of HSP90 $\alpha$  in plasma samples based on the software algorithm.

## Nomogram for OS, PFS, and Response Evaluation

The least absolute shrinkage and selection operator (LASSO) regression model selected the relevant factors for response

evaluation and prognosis of small cell lung cancer. Logistic regression analysis was then used to build a convincing model for predicting chemotherapy efficacy and prognostic outcomes for small cell lung cancer by incorporating features selected in the LASSO approach. Clinicopathological features and biomarkers with *p*-values less than 0.05 in peripheral blood were included in the model. All selected predictors were used to develop a nomogram model to predict small cell lung cancer.

## Cell Culture

NCI-H146 and A549 lung cancer cells were purchased from the Institute of Cell Biology, Chinese Academy of Sciences (Shanghai, China). Cells were grown in Roswell Park Memorial Institute 1,640 medium containing 10% fetal bovine serum and 1% penicillin/streptomycin at 37°C in a humidified atmosphere with 5% CO<sub>2</sub>.

## Statistical Analysis

The data were expressed as median and quartile. The Spearman correlation analysis evaluated the association between eHSP90 $\alpha$  and other indexes. Receiver operating characteristic (ROC)

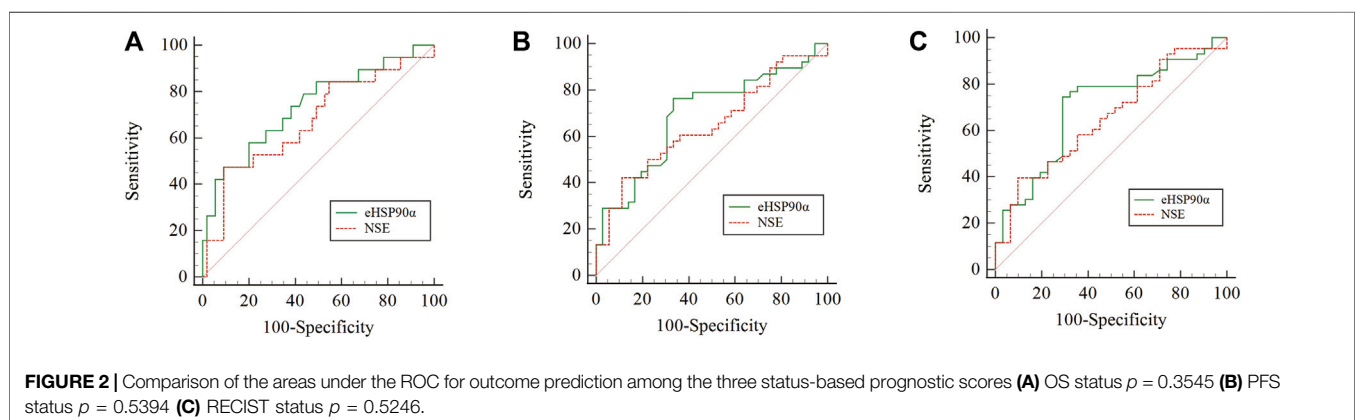




TABLE 3 | Receiver operating characteristic curve of parameters.

Characteristics	OS				PFS				Response Evaluation						
	AUC (95% CI)	Threshold	specificity	Sensitivity	Youden	AUC (95% CI)	Threshold	specificity	Sensitivity	Youden	AUC (95% CI)	Threshold	specificity	sensitivity	Youden
B lymphocytes	0.53 (0.416–0.644)	8.265	0.787	0.341	0.128	0.526 (0.413–0.638)	7.93	0.865	0.302	0.167	0.504 (0.393–0.615)	13.45	0.714	0.429	0.143
CA199	0.523 (0.409–0.637)	4.25	0.311	0.791	0.102	0.552 (0.44–0.664)	6.55	0.431	0.717	0.148	0.629 (0.518–0.74)	6.55	0.524	0.758	0.282
CEA	0.553 (0.44–0.667)	9.355	0.721	0.442	0.163	0.607 (0.496–0.718)	3.86	0.725	0.585	0.31	0.538 (0.424–0.651)	3.855	0.667	0.5	0.167
eHSP90α	<b>0.791 (0.699–0.884)</b>	61.2	0.852	0.682	<b>0.534</b>	<b>0.682 (0.556–0.768)</b>	48.7	0.558	<b>0.792</b>	0.35	<b>0.685 (0.58–0.79)</b>	48.7	0.619	<b>0.778</b>	<b>0.397</b>
Natural killer cells	0.631 (0.521–0.741)	11.75	0.541	0.705	0.246	0.512 (0.4–0.624)	11.23	0.442	0.66	0.103	0.585 (0.452–0.678)	11.225	0.5	0.683	0.183
NSE	0.673 (0.521–0.825)	68.55	0.909	0.474	0.383	0.646 (0.519–0.773)	57.33	<b>0.889</b>	0.421	0.31	0.65 (0.524–0.777)	57.325	<b>0.903</b>	0.395	0.299
T lymphocytes	0.61 (0.501–0.72)	70.35	0.443	<b>0.841</b>	0.284	0.555 (0.444–0.666)	72.10	0.346	<b>0.792</b>	0.139	0.626 (0.513–0.738)	68.82	0.595	0.687	0.262
T helper cells	0.577 (0.464–0.689)	30.95	0.918	0.25	0.168	0.59 (0.48–0.699)	32.2	0.885	0.302	<b>0.187</b>	0.616 (0.506–0.726)	42	0.571	0.635	0.206
T helper cells/T suppressor cells	0.496 (0.384–0.614)	3.8	<b>0.984</b>	0.091	0.075	0.577 (0.467–0.688)	2.05	0.635	0.528	0.163	0.565 (0.454–0.677)	2.05	0.643	0.508	0.151
TK1	0.565 (0.45–0.68)	0.46	0.77	0.386	0.157	0.487 (0.375–0.599)	0.54	0.692	0.358	0.051	0.525 (0.411–0.64)	0.615	0.69	0.429	0.119
T suppressor cells	0.456 (0.339–0.573)	23.765	0.787	0.295	0.082	0.527 (0.415–0.639)	18.15	0.538	0.586	0.104	0.496 (0.381–0.61)	18.15	0.548	0.556	0.103

*Bold font indicates maximum value. Carcinoembryonic antigen, CEA; Carbohydrate antigen 19–9, CA19–9; Thymidine kinase1, TK1; Neuron-specific enolase, NSE.*

curves were used to identify optimal cutoff values of variables in overall survival, progression-free survival, and response to treatment. Grouped according to cutoff value, Least Absolute Shrinkage and Selection Operator (LASSO) was used to analyze eHSP90α and efficacy. R 4.03 software was used to draw Kaplan-Meier curves of OS and PFS. The univariate and multivariate Cox regression was performed to investigate the relationship between eHSP90α and OS and PFS. A *p-value* less than 0.05 was considered statistically significant. Statistical analyses were performed using the SPSS computer program (SPSS 22.0).

RESULTS

SCLC Patients' Characteristics and Hematologic Baseline

In total, 105 patients with SCLC were enrolled in our analysis. All patients were with an average age of 62.00 ± 8.55 years at the time of diagnosis. Of the 105 patients, 33 (31.43%) underwent radiotherapy and 94 (89.52%) underwent chemotherapy. 27 (25.7%) were classified with limited disease small cell lung cancer and 78 (74.3%) were extension disease small cell lung cancer. The other parameters clinicopathological data are shown in Table 1. Next, we analyzed the differences and progressive groups of all peripheral blood indicators in Table 1 Alive and DEAD groups in OS, progress and no progressive group in PFS and the differences between the CR \ PR \ SD and PD groups in Response Evaluation. We found that eHSP90α has different expressions in these groups, as shown in Figure 1B. The expression of other peripheral blood indicators in these groups, see Supplementary Figure S1.

Correlations of eHSP90α and Clinical Index

NSE is currently a commonly used marker for SCLC, and eHSP90α is a new biomarker. The correlation between these two biomarkers and other clinical indicators is analyzed here. Correlation analysis revealed that eHSP90α was positively correlated to the diameter of the tumor and neuron-specific enolase (NSE) in SCLC patients. This analysis shows that eHSP90α was negatively related to T lymphocytes and T helper cells in SCLC patients. There is no significant relationship between eHSP90α and another clinical index in LD-SCLC patients. NSE and eHSP90α had the same trend in ED-SCLC patients (Table 2). NSE was positively correlated with eHSP90α in total SCLC and ED patients, indicating that eHSP90α is likely to have excellent diagnostic and prognostic efficacy. We next use the scattered dot diagram to show the relationship between the two continuous variables eHSP90α and NSE. We found that NSE and eHSP90α in the OS group, PFS progress group and PD groups in the Response Evaluation have significant correlations. See Figure 1C. Other correlation analysis results show in Supplementary Figures S1,S2.

The Cut-Off Value of eHSP90α Outcome Prediction Among SCLC Patients' Index and Their Combined Prognostic Value

ROC curves were used to analyze the diagnostic effect of eHSP90α in dichotomous variables such as overall survival

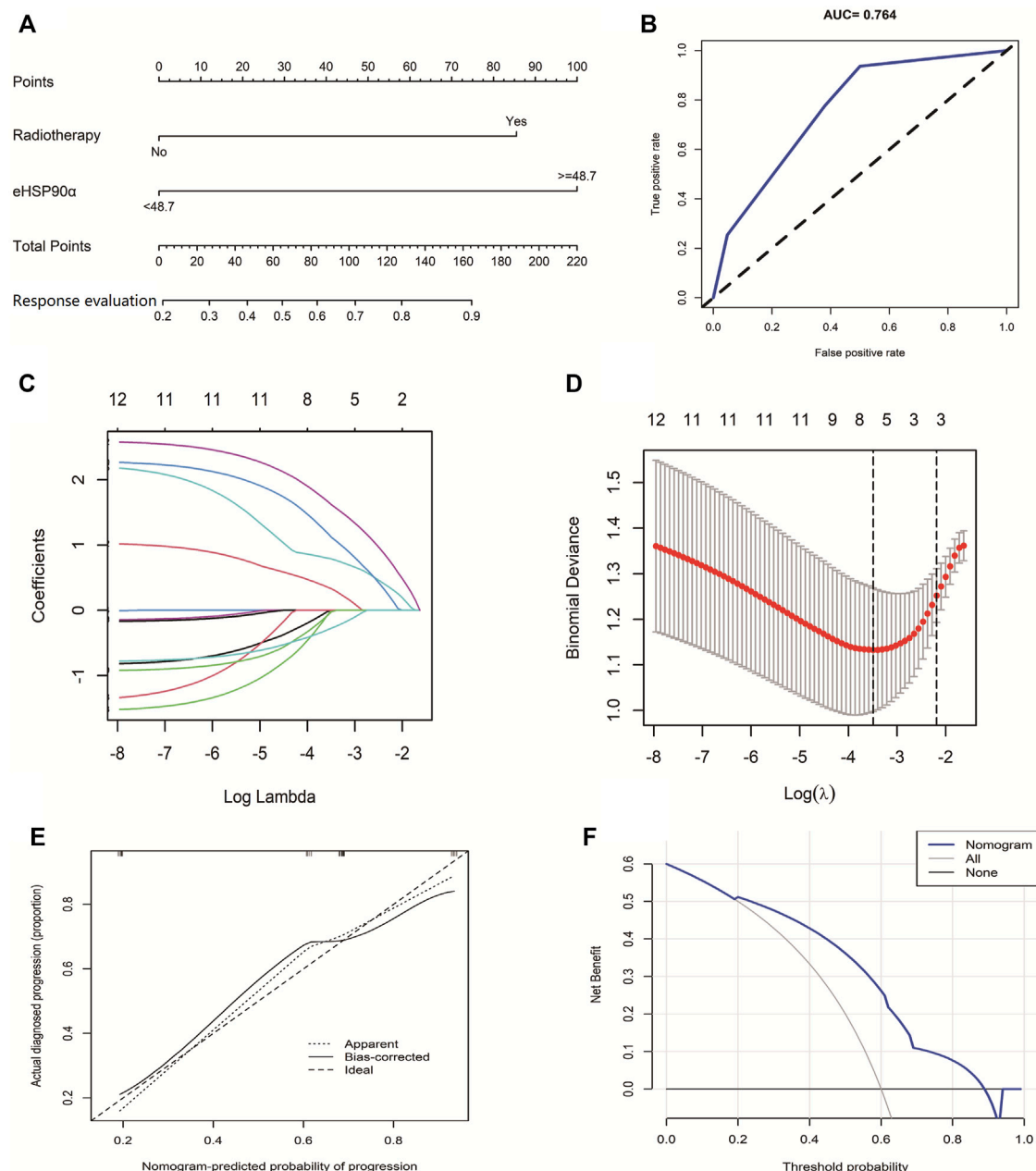


**FIGURE 3 |** The Predictive Value of eHSP90 $\alpha$  for SCLC effective chemotherapy **(A)** Established small cell lung cancer response evaluation nomogram with eHSP90 $\alpha$  **(B)** Receiver operating characteristic curve of the model **(C)** LASSO coefficient profiles of the 12 features **(D)** A coefficient profile plot was produced against the log $\lambda$  sequence **(E)** Calibration curves of the nomogram. Notes: The x-axis represents the predicted probability of progression. The y-axis represents the actual progression of small cell lung cancer. The diagonal dotted line represents a perfect prediction by an ideal model. The solid line represents the performance of the nomogram, of which a closer fit to the diagonal dotted line means a better prognosis **(F)** Decision curve analysis of our model showed that response evaluation nomogram. The x-axis is the risk threshold probability that changes from 0 to 1, and the y-axis is the calculated net profit for a given threshold probability.

status (alive/dead), progression-free survival status (whether progress or recurrence) and response evaluation (RECIST version 1.1), see **Table 3** eHSP90 $\alpha$  had the highest AUC value (OS 0.791, PFS 0.662, response evaluation 0.685) in all three ROC curves. T helper cells/T suppressor cells had the highest specificity (0.984) in the OS ROC curve, and NSE had the highest specificity in the PFS ROC curve (AUC 0.889) and response evaluation ROC

curve (AUC 0.903). T lymphocytes had the highest specificity (0.903) in the response evaluation ROC curve and the highest sensitivity (0.841) in the OS ROC curve. eHSP90 $\alpha$  and T lymphocytes had the same highest sensitivity (0.792) in the PFS ROC curve. eHSP90 $\alpha$  had the highest sensitivity (0.778) in the response evaluation ROC curve. eHSP90 $\alpha$  had the highest Youden in the OS ROC curve (0.534) and response evaluation

**TABLE 4 |** Multivariate logistic regression analysis of influencing results of SCLC chemotherapy.

Variables	Multivariate Analysis		
	Odds Ratio	95% CI	p-value
Diameter (>3 cm)	0.606	5.321e-01–6.358e+00	0.333
Stage II	0.141	1.882e-30–5.250e+29	1.000
Stage III	16.417	6.130e-113-NA	0.994
Stage IV	17.368	7.726e-114-NA	0.994
Chemotherapy	–0.813	6.216e-02–2.630e+00	0.389
Radiotherapy	2.110	2.353e+00–3.692e+01	<b>0.002</b>
Right tumor	–0.662	1.587e-01–1.546e+00	0.249
Mediastinal tumor	–1.609	1.409e-02–2.533e+00	0.213
eHSP90 $\alpha$ ( $\geq 48.7$ )	2.268	2.931e+00–3.997e+01	<b>0.001</b>

*bold font indicates statistical.*

ROC curve (0.397), while T helper cells had the highest Youden (0.187) in the PFS ROC curve. Taken together, eHSP90 $\alpha$  has better sensitivity and specificity than NSE, and similar diagnostic effectiveness as NSE in ROC curves of OS (**Figure 2A**), PFS (**Figure 2B**) and response evaluation (**Figure 2C**).

## The Predictive Value of ehsp90 $\alpha$ for the Effect of Chemotherapy in SCLC

Compared with OS and PFS, response evaluation (RECIST version1.1) does not contain information on survival time. Therefore, eHSP90 $\alpha$  was used to explore the diagnostic significance of response status. We used two indicators, including eHSP90 $\alpha$ , to establish a nomogram to evaluate the response of SCLC (**Figure 3A**). The receiver operating characteristic curve of the model had a higher AUC (0.764) than eHSP90 $\alpha$  (AUC = 0.564) (**Figure 3B**). First, based on 105 SCLC patients, we used LASSO and 10-fold cross-validation to screen out six indicators (**Figures 3C,D**), including diameter, staging, chemotherapy, radiotherapy, location, eHSP90 $\alpha$  (**Figure 3C** lambda. min = 0.03050932). To further select independent variables for effective chemotherapy from LASSO results, multivariate logistic regression analysis among these above features is shown in **Table 4**. The model finally contains radiotherapy (OR = 2.1103,  $p$  = 0.002276), eHSP90 $\alpha$  (OR = 2.2677,  $p$  = 0.000524). The model was verified by bootstrapping (**Figure 3E**, C-index = 0.764). In this study, the threshold is from 20 to 88% (probability of patients and doctors); the decision curve analysis of our model showed that the response evaluation nomogram would profit more than of threshold (**Figure 3F**).

## Clinical Prognostic Evaluation of eHSP90 $\alpha$ in SCLC

The ROC curve of the PFS was performed to determine the cutoff points of the index. The result is shown in **Table 5**. The threshold values of eHSP90 $\alpha$  for OS, and PFS were 61.2 and 48.7, respectively. To determine which parameters were the independent prognostic factors of SCLC, univariate and multivariate analyses were conducted to explore the

relationship between multiple variables, OS and PFS. In the multivariate analysis, high eHSP90 $\alpha$  was an independent prognostic factor of a poor evolution in SCLC (OS,  $p$  < 0.001 and PFS,  $p$  = 0.024), whereas receiving radiotherapy was a good prognostic factor in SCLC (OS,  $p$  = 0.010 and PFS,  $p$  = 0.016). High NSE and M1 stage were significantly associated with shorter OS (NSE,  $p$  < 0.001 and M1 stage,  $p$  = 0.009). High CA-199 and M1 stage predicts earlier progression (CA-199,  $p$  = 0.018 and M1 stage,  $p$  < 0.001). We constructed a nomogram with four factors, including eHSP90 $\alpha$ , to predict overall survival in SCLC patients (**Figure 4A**). The receiver operating characteristic curve of this model shows that AUC is 0.788. A nomogram for predicting progression-free survival was established with two indexes (**Figure 4B**). AUC is 0.671 in the receiver operating characteristic curve of this model. We analyzed the distribution of risk levels, survival status, and survival time patterns in SCLC patients divided into two groups with 61.2 ng/mL as the eHSP90 $\alpha$  cut-off value. Kaplan-Meier survival analysis revealed that SCLC patients with higher eHSP90 $\alpha$  expression had worse OS than those with lower eHSP90 $\alpha$  expression (**Figure 5A**). Patients with high eHSP90 $\alpha$  expression levels died more and survived shorter, as seen by survival time patterns (**Figure 5B**). The distribution of the eHSP90 $\alpha$  risk score distribution suggests that higher expression of eHSP90 $\alpha$  implies higher risk (**Figure 5C**). We analyzed the progression of SCLC patients and divided them into two groups with an eHSP90 $\alpha$  cut-off value of 48.7 ng/mL. Kaplan-Meier survival analysis showed that the low expression group was more likely to be free of progression (**Figure 6A**). We made a scatterplot to assess progression risk, suggesting that more progression and higher mortality rates appear in the high-expression group. In contrast, patients' conditions in the low-expression group were mostly non-progressive (**Figure 6B**). By sorting the patients according to the risk value from low to high, we obtained the progression risk curve graph, which shows the high expression of eHSP90 $\alpha$  corresponds to a greater risk of progression (**Figure 6C**). eHSP90 $\alpha$  above was significantly associated with NSE in ED-SCLC patients, but not in LD-SCLC patients. The occurrence of distant metastases is the main cause of poor PFS and OS in SCLC. But only eHSP90 $\alpha$  but not NSE was significantly associated with poorer PFS in SCLC. We performed based on distant metastasis status for NSE and eHSP90 $\alpha$  as we made a prediction that NSE might be associated with distant metastasis (**Supplementary Tables S1,S2**). The results showed that NSE was an independent factor affecting the distant metastasis of SCLC.

## Validation of eHSP90 $\alpha$ Expression in Supernatants of Two Lung Cancer Cell Lines

To further explore the expression of eHSP90 $\alpha$  in SCLC and NSCLC, we detected eHSP90 $\alpha$  in different cell supernatants from six dishes (**Supplementary Figure S3**). The eHSP90 $\alpha$  in SCLC cell supernatant is higher than in NSCLC (**Figure 7**). Consistent with our clinical results.

**TABLE 5 |** Univariate and multivariate cox proportional regression analysis of OS and PFS in SCLC.

Variables	Univariate				Multivariate			
	OS		PFS		OS		PFS	
	HR (95%CI)	p Value	HR (95%CI)	p Value	HR (95%CI)	p Value	HR (95%CI)	p Value
Age (≤55 vs. >55)	1.610 (0.743–3.487)	0.227	1.022 (0.540–1.934)	0.948				
Chemotherapy (Yes vs. No)	0.431 (0.189–983)	0.045	2.321 (0.562–9.584)	0.244				
Diameter (≤3 cm vs. >3 cm)	1.610 (0.743–3.487)	0.227	1.957 (0.970–3.947)	0.061				
Ki-67 (≤50% vs. >50%)	2.572e+07 (0-Inf)	0.997	0.413 (0.099–1.717)	0.224				
M (M0 vs. M1)	2.562 (1.261–5.205)	<b>0.009</b>	5.326 (2.356–12.040)	<b>5.830e-05</b>	2.716 (1.323–5.573)	<b>0.006</b>	4.044 (1.777–9.204)	<b>0.001</b>
Mediastinal tumor	1.522 (0.348–6.661)	0.577	1.243 (0.290–5.332)	0.770				
N (N0 vs. N1-3)	3.159 (0.433–23.050)	0.257	N1-3 8.299e+07 (0-Inf)	0.996				
Radiotherapy (Yes vs. No)	0.398 (0.198–0.799)	<b>0.010</b>	0.467 (1.135–3.389)	<b>0.016</b>	0.403 (0.227–0.962)	<b>0.039</b>		
Right tumor	1.108 (0.591–2.077)	0.750	1.004 (0.5754–1.751)	0.990				
Stage (I-II vs. III-IV)	5.118e+07 (0-Inf)	0.997	8.433e-07 (0-Inf)	0.996				
T (T1-2 vs. T3-4)	0.881 (0.462–1.678)	0.699	1.422 (0.769–2.628)	0.262				
B lymphocytes (OS: < 8.27 vs. ≥8.27, PFS: < 7.93 vs. ≥7.93)	0.639 (0.341–1.201)	0.164	0.718 (0.398–1.295)	0.271				
CA-199 (OS: < 4.25 vs. ≥4.25, PFS: < 6.55 vs. ≥6.55)	1.650 (0.808–3.367)	0.169	2.268 (1.152–4.466)	<b>0.018</b>				
CEA (OS: < 9.36 vs. ≥9.36, PFS: < 3.86 vs. ≥3.86)	2.586 (1.406–4.758)	0.002	1.230 (0.6735–2.246)	0.501				
eHSP90α (OS: < 65.80 vs. ≥65.80, PFS: < 48.70 vs. ≥48.70)	3.410 (1.808–6.430)	<b>0.000</b>	2.155 (1.106–4.200)	<b>0.024</b>	2.271 (1.122–4.595)	<b>0.023</b>	2.056 (1.037–4.077)	<b>0.039</b>
Natural killer cells (OS: < 11.75 vs. ≥11.75, PFS: < 11.23 vs. ≥11.23)	1.785 (0.927–3.435)	0.083	1.130 (0.652–1.957)	0.664				
NSE (OS: < 68.55 vs. ≥68.55, PFS: < 57.33 vs. ≥57.33)	3.811 (1.872–7.758)	<b>0.000</b>	1.133 (0.659–1.949)	0.651	2.580 (1.200–5.546)	<b>0.015</b>		
T helper cells (OS: < 30.95 vs. ≥30.95, PFS: < 32.20 vs. ≥32.20)	1.010 (0.500–2.042)	0.977	0.852 (0.445–1.633)	0.630				
T helper cells/T suppressor cells (OS: < 3.80 vs. ≥3.80, PFS: < 2.05 vs. ≥2.05)	2.569 (0.914–7.221)	0.074	1.952 (0.700–5.441)	0.201				
T lymphocytes (OS: < 70.35 vs. ≥70.35, PFS: < 72.10 vs. ≥72.10)	0.489 (0.217–1.103)	0.085	0.874 (0.472–1.618)	0.668				
T suppressor cells (OS: < 23.77 vs. ≥23.77, PFS: < 18.15 vs. ≥18.15)	1.033 (0.538–1.986)	0.922	0.925 (0.502–1.706)	0.803				
TK1 (OS: < 0.46 vs. ≥0.46, PFS: < 0.54 vs. ≥0.54)	0.649 (0.351–1.198)	0.167	0.787 (0.435–1.424)	0.429				

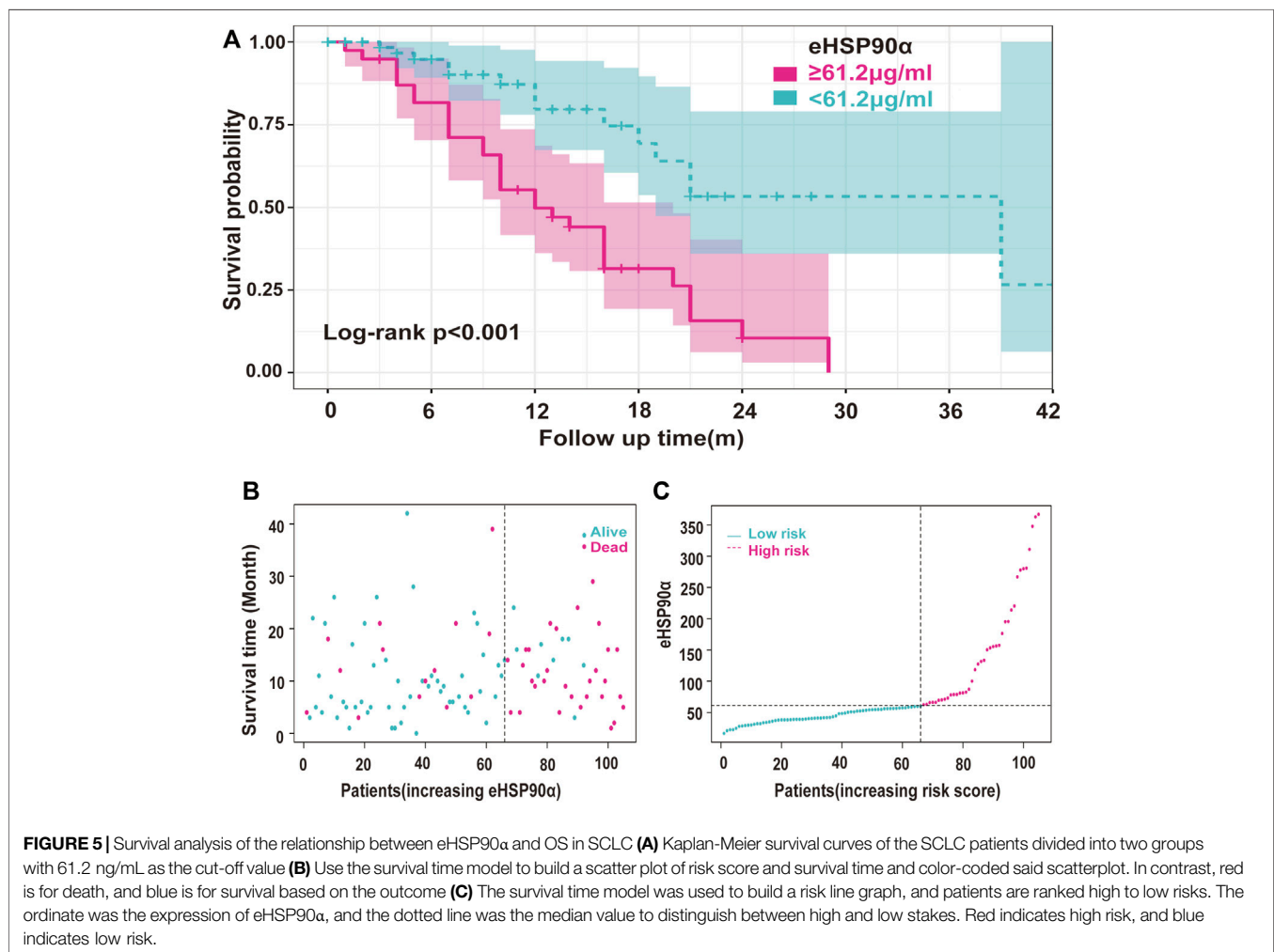
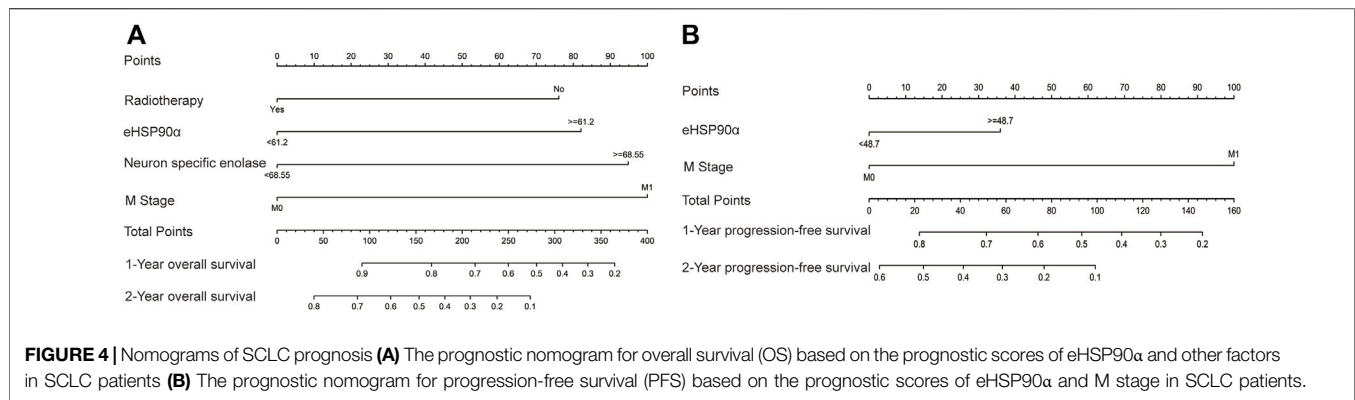
*bold font indicates statistical. Carcinoembryonic antigen, CEA; Carbohydrate antigen 19–9, CA19-9; Thymidine kinase1, TK1; Neuron-specific enolase, NSE.*

## DISCUSSION

Small cell lung cancer prognosis has been challenging, especially in patients diagnosed during the ED (Wang et al., 2020). Some tumor markers have been used for the response assessment and prognosis monitoring, but they lack the level of sensitivity or specificity. In this study, the clinical index and the follow-up information of one hundred and five SCLC patients were analyzed to determine better markers.

Treatment of small cell lung cancer is very limited. In terms of response assessment, it has been shown that the neutrophil/

lymphocyte ratio (NLR) value 6 weeks after anti-PD-1/PD-L1 antibody therapy appears to be a promising predictor of response in patients with small-cell lung cancer (Xiong et al., 2021). A study suggests that serum NSE and lactate dehydrogenase (LDH) may serve as biomarkers for predicting efficacy and survival in patients with small-cell lung cancer receiving first-line platinum-based chemotherapy (Liu et al., 2017). The ROC curve showed that the areas under the curve of NSE, ProGRP, and LDH expression on CR + PR were 0.683, 0.610, and 0.639, respectively, all of which were lower than those of eHSP90α.



In most studies' prognosis of small cell lung cancer, NSE is a relevant tumor marker (Shibayama et al., 2001). NSE is often elevated in extensive-stage disease, and patients with high levels of NSE may suggest distant metastases, and higher NSE tends to predict shorter OS (Wang et al., 2021). The role of radiotherapy in SCLC has been controversial in the past, and the brain is SCLC's most common metastatic site. Brain metastases occur in more

than 50% of SCLC patients, and the prognosis is extremely poor, with an OS of only about 1–3 months. In the present study, eHSP90 $\alpha$  exhibited similar diagnostic efficacy and prognostic value as NSE in patients with small-cell lung cancer. Prophylactic cranial irradiation (PCI) can reduce the occurrence of brain metastases. Several studies have confirmed that PCI can reduce the occurrence of brain metastases and improve overall



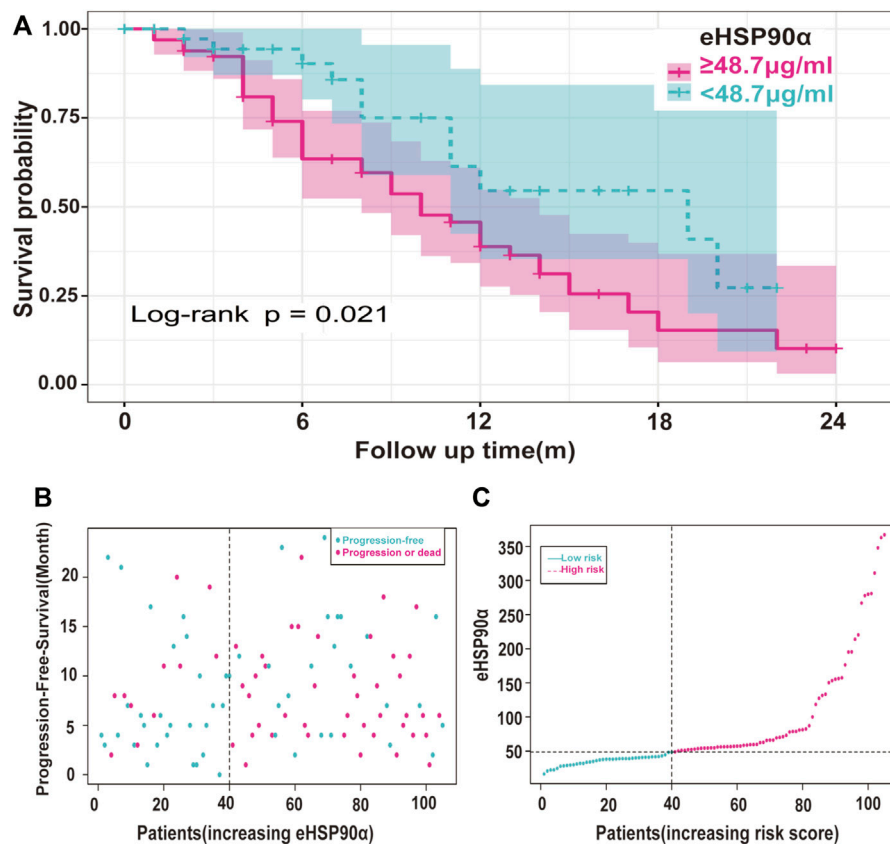


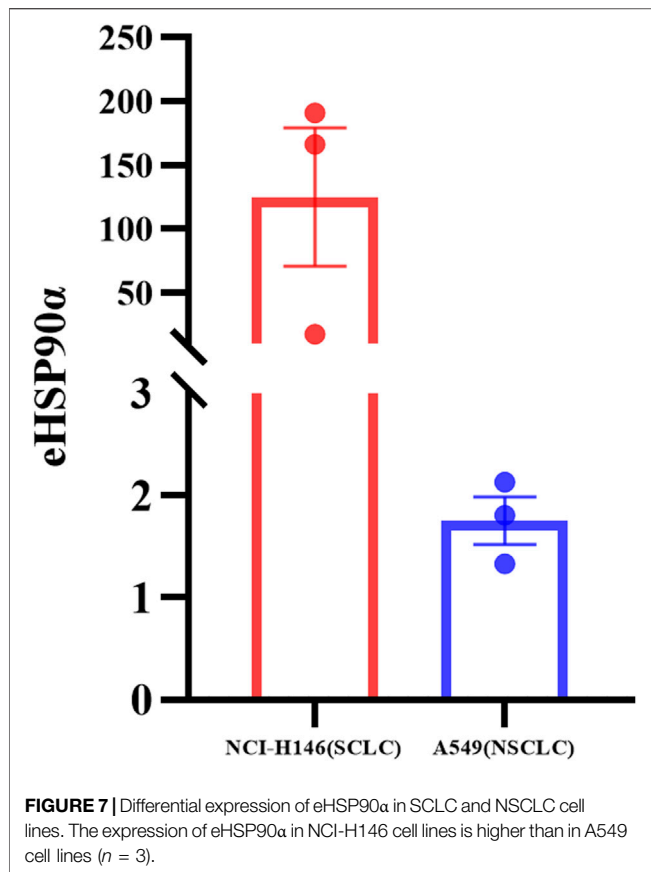
**FIGURE 6 |** Risk Analysis of eHSP90 $\alpha$  and progression in SCLC **(A)** Kaplan-Meier curves of the SCLC patients were divided into two groups with 48.7 ng/mL as the cut-off value **(B)** Scatter plots of risk score and time to progression were constructed using the survival time model and divided according to the results shown red for progression and blue for survival **(C)** A risk profile was created using a survival time model to rank patients from low to high risk. The ordinate is the expression of eHSP90 $\alpha$ , and the dotted line is the median value, distinguishing high and low risks: red means high risk, and blue means low risk.

survival in limited-stage patients with complete remission and extensive-stage patients with effective induction chemotherapy (Weaver and Coonar, 2017). However, a recent prospective clinical trial (Takahashi et al., 2017) from Japan showed that the incidence of brain metastases in the PCI group was 48 and 69% in the observation group,  $p < 0.001$ , but the 1-year OS did not improve ( $p = 0.094$ ). Patients in our study who received radiotherapy at any site had longer OS. A study's findings suggest that women have an advantage in survival compared to men (Cai et al., 2016). There were no statistically significant differences in the gender factor in our study, as the number of males was significantly higher than that of females in both studies. Therefore, the relationship between gender and prognosis is inconclusive. In addition, some studies suggest that the ratio of radiation dose to tumor diameter is related to the prognosis of limited-stage SCLC. Still, there is a lack of data on radiation dose in this study (Komatsu et al., 2010).

Studies have shown that NSE is an independent predictor of response and follow-up in SCLC, LD-SCLC, and ED-SCLC (Zhou et al., 2017). In our study, NSE and eHSP90 $\alpha$  showed the same trend in all SCLC and a significant positive correlation in ED-SCLC. Serum NSE can also be present in platelets and red blood cells, and the results

can be false-positive once the specimen has hemolysis or if the blood has been stagnant for a certain period (Massabki et al., 2003). Previous studies have found that the level of HSP90 $\alpha$  in the serum of non-small cell lung cancer is significantly increased and it gradually increases with the clinical stage (Xu et al., 2007). The detection of a single tumor marker often has certain limitations, often cannot fully reflect the tumor, and has limited value for diagnosis and prognosis; therefore, the combined diagnosis of tumor markers can reduce the missed diagnosis rate of a single test and increase the accuracy of disease diagnosis.

Initially, 108 SCLC patients were included in the study while their medical records were being reviewed for information. Three patients were excluded due to missing data. In predicting OS, PFS, and response evaluation, eHSP90 $\alpha$  had good AUC, sensitivity, and specificity. We built a nomogram from independent variables obtained from LASSO and multivariate logistic regression analysis. The AUC of this model is 0.764. Of the 105 SCLC patients who were finally included in the study, 39 patients had elevated eHSP90 $\alpha$  expression ( $>61.2$  ng/ml), and 66 patients had eHSP90 $\alpha$  below 61.2 ng/ml. Through survival analysis, we found that patients with elevated eHSP90 $\alpha$  expression had a higher risk of death than those with low expression. This is consistent with previous studies. We found that the expression of eHSP90 $\alpha$  in SCLC cells was higher than



that in NSCLC cells, which more experiments should confirm. We still need to investigate the mechanism further.

Due to the low proportion of small cell lung cancer in lung cancer, the sample size of this study is limited. The next step will be to expand the validation trial with a more rigorous sample size and conduct a long-term follow-up to determine the rigid prognosis. eHSP90 $\alpha$  is a novel biomarker. Currently, there are few commercial kits to choose from. When more detection methods are available in the future, we will carry out strict verification through other detection methods.

In conclusion, this study found that SCLC patients with eHSP90 $\alpha$  overexpression had a worse response and survival times. Diameter, staging, chemotherapy, radiotherapy, location, and eHSP90 $\alpha$  have significant effects on patient response evaluation. eHSP90 $\alpha$  and radiotherapy were independent factors in response evaluation in SCLC patients. eHSP90 $\alpha$ , NSE, M staging, radiotherapy, and CEA had significant effects on OS in SCLC. Among them, eHSP90 $\alpha$ , NSE, M stage, and

radiotherapy were the independent prognostic factors affecting the survival of patients. This study aims to provide new evidence for the efficacy response and prognostic assessment of SCLC. eHSP90 $\alpha$  may be a better biomarker for SCLC.

## DATA AVAILABILITY STATEMENT

The original contributions presented in the study are included in the article/Supplementary Material, further inquiries can be directed to the corresponding authors.

## ETHICS STATEMENT

The studies involving human participants were reviewed and approved by the Guangxi Medical University Cancer Hospital Ethics Committee. The patients/participants provided their written informed consent to participate in this study.

## AUTHOR CONTRIBUTIONS

Study design: LZ and HL; Data acquisition: BH, JP, SL, YB, and SN; Quality control of data and algorithms: SL and YB; Data analysis and interpretation: HL; Statistical analysis: JL; Manuscript preparation: BH; Manuscript editing: LZ. All authors reviewed and approved the final manuscript.

## FUNDING

This study was supported by the grants from the Key R&D Program of Scientific Research and Technology Development Project of Nanning, Guangxi (Grant No. ZC20213009), and a Self-funded scientific research project of Guangxi Zhuang Autonomous Region Health Committee (Grant No. 20191022) and the Key R&D Program of Scientific Research and Technical Development Project of Qingxiu District, Nanning, Guangxi (Grant No. 2021015).

## SUPPLEMENTARY MATERIAL

The Supplementary Material for this article can be found online at: <https://www.frontiersin.org/articles/10.3389/fmolb.2022.913043/full#supplementary-material>

## REFERENCES

- Balachandran, V. P., Gonen, M., Smith, J. J., and DeMatteo, R. P. (2015). Nomograms in Oncology: More Than Meets the Eye. *Lancet Oncol.* 16, e173–e180. doi:10.1016/S1470-2045(14)71116-7
- Cai, Q., Luo, H.-l., Gao, X.-c., Xiong, C.-j., Tong, F., Zhang, R.-g., et al. (2016). Clinical Features and Prognostic Factors of Small Cell Lung Cancer: A Retrospective Study in 148 Patients. *J. Huazhong Univ. Sci. Technol. Med. Sci.* 36, 916–922. doi:10.1007/s11596-016-1684-6
- Cummings, J., Ward, T. H., Greystoke, A., Ranson, M., and Dive, C. (2008). Biomarker Method Validation in Anticancer Drug Development. *Br. J. Pharmacol.* 153, 646–656. doi:10.1038/sj.bjp.0707441
- Fang, X., Li, S., Fu, Q., Wang, P., Wu, X., and Zhang, Y. (2021). Label-free Identification of Lung Cancer Cells from Blood Cells Based on Surface-



- Enhanced Raman Scattering and Support Vector Machine. *Optik* 248, 168157. doi:10.1016/j.ijleo.2021.168157
- Fu, Y., Xu, X., Huang, D., Cui, D., Liu, L., Liu, J., et al. (2017). Plasma Heat Shock Protein 90 $\alpha$  as a Biomarker for the Diagnosis of Liver Cancer: An Official, Large-Scale, and Multicenter Clinical Trial. *EBioMedicine* 24, 56–63. doi:10.1016/j.ebiom.2017.09.007
- Harmsma, M., Schutte, B., and Ramaekers, F. C. (2013). Serum Markers in Small Cell Lung Cancer: Opportunities for Improvement. *Biochim. Biophys. Acta* 1836, 255–272. doi:10.1016/j.bbcan.2013.06.002
- Hou, Q., Chen, S., An, Q., Li, B., Fu, Y., and Luo, Y. (2021). Extracellular Hsp90 $\alpha$  Promotes Tumor Lymphangiogenesis and Lymph Node Metastasis in Breast Cancer. *Int. J. Mol. Sci.* 22, 7747. doi:10.3390/ijms22147747
- Iasonos, A., Schrag, D., Raj, G. v., and Panageas, K. S. (2008). How to Build and Interpret a Nomogram for Cancer Prognosis. *J. Clin. Oncol.* 26, 1364–1370. doi:10.1200/JCO.2007.12.9791
- Komatsu, T., Oizumi, Y., Kunieda, E., Tamai, Y., Akiba, T., and Kogawa, A. (2010). Definitive Chemoradiotherapy of Limited-Disease Small Cell Lung Cancer: Retrospective Analysis of New Predictive Factors Affecting the Treatment Results. *Int. J. Radiat. Oncology\*Biophysics* 78, S532–S533. doi:10.1016/J.IJROBP.2010.07.1243
- Li, W., Tsen, F., Sahu, D., Bhatia, A., Chen, M., Multhoff, G., et al. (2013). “Extracellular Hsp90 (eHsp90) as the Actual Target in Clinical Trials. Intentionally or Unintentionally,” in *International Review of Cell and Molecular Biology* (Elsevier), 203–235. doi:10.1016/B978-0-12-407697-6.00005-2
- Liu, X., Zhang, W., Yin, W., Xiao, Y., Zhou, C., Hu, Y., et al. (2017). The Prognostic Value of the Serum Neuron Specific Enolase and Lactate Dehydrogenase in Small Cell Lung Cancer Patients Receiving First-Line Platinum-Based Chemotherapy. *Med. (United States)* 96, e8258. doi:10.1097/MD.00000000000008258
- Mai, V., Trahan, S., Pagé, S., Simon, M., and Labbé, C. (2021). Severe Hyponatremia Due to Paraneoplastic Syndrome of Inappropriate Antidiuretic Hormone Secretion in Non-small Cell Lung Carcinoma Transforming to Small Cell Lung Carcinoma during Treatment with Immune Checkpoint Inhibitor. *Curr. Problems Cancer Case Rep.* 4, 100125. doi:10.1016/j.cpcr.2021.100125
- Massabki, P. S., Silva, N. P., Lourenço, D. M., and Andrade, L. E. (2003). Neuron Specific Enolase Concentration Is Increased in Serum and Decreased in Platelets of Patients with Active Systemic Sclerosis. *J. Rheumatol.* 30, 2606–2612.
- Oronsky, B., Reid, T. R., Oronskey, A., and Carter, C. A. (2017). What’s New in SCLC? A Review. *Neoplasia* 19, 842–847. doi:10.1016/j.neo.2017.07.007
- Pedersen, S., Hansen, J. B., Maltesen, R. G., Szejniuk, W. M., Andreassen, T., Falkmer, U., et al. (2021). Identifying Metabolic Alterations in Newly Diagnosed Small Cell Lung Cancer Patients. *Metab. Open* 12, 100127. doi:10.1016/j.metop.2021.100127
- Shibayama, T., Ueoka, H., Nishii, K., Kiura, K., Tabata, M., Miyatake, K., et al. (2001). Complementary Roles of Pro-gastrin-releasing Peptide (ProGRP) and Neuron Specific Enolase (NSE) in Diagnosis and Prognosis of Small-Cell Lung Cancer (SCLC). *Lung Cancer* 32, 61–69. doi:10.1016/S0169-5002(00)00205-1
- Takahashi, T., Yamanaka, T., Seto, T., Harada, H., Nokihara, H., Saka, H., et al. (2017). Prophylactic Cranial Irradiation versus Observation in Patients with Extensive-Disease Small-Cell Lung Cancer: a Multicentre, Randomised, Open-Label, Phase 3 Trial. *Lancet Oncol.* 18, 663–671. doi:10.1016/S1470-2045(17)30230-9
- Tian, Y., Wang, C., Chen, S., Liu, J., Fu, Y., and Luo, Y. (2019). Extracellular Hsp90 $\alpha$  and Clusterin Synergistically Promote Breast Cancer Epithelial-To-Mesenchymal Transition and Metastasis via LRP1. *J. Cell Sci.* 132. doi:10.1242/JCS.228213
- Tian, Z., Liang, C., Zhang, Z., Wen, H., Feng, H., Ma, Q., et al. (2020). Prognostic Value of Neuron-specific Enolase for Small Cell Lung Cancer: A Systematic Review and Meta-Analysis. *World J. Surg. Onc.* 18, 116. doi:10.1186/s12957-020-01894-9
- Wang, C., Jin, S., Xu, S., and Cao, S. (2021). The Combination of Pretreatment Prognostic Nutritional Index and Neuron-specific Enolase Enhances Prognosis Predicting Value of Small Cell Lung Cancer. *Clin. Respir. J.* 15, 264–271. doi:10.1111/crj.13291
- Wang, X., Song, X., Zhuo, W., Fu, Y., Shi, H., Liang, Y., et al. (2009). The Regulatory Mechanism of Hsp90 Secretion and its Function in Tumor Malignancy. *Proc. Natl. Acad. Sci. U.S.A.* 106 (50), 21288–21293. doi:10.1073/pnas.0908151106
- Wang, Y., Zou, S., Zhao, Z., Liu, P., Ke, C., and Xu, S. (2020). New Insights into Small-cell Lung Cancer Development and Therapy. *Cell Biol. Int.* 44, 1564–1576. doi:10.1002/cbin.11359
- Weaver, H., and Coonar, A. S. (2017). Lung Cancer: Diagnosis, Staging and Treatment. *Surg. Oxf.* 35, 247–254. doi:10.1016/J.MPSUR.2017.02.007
- Xiong, Q., Huang, Z., Xin, L., Qin, B., Zhao, X., Zhang, J., et al. (2021). Post-treatment Neutrophil-To-Lymphocyte Ratio (NLR) Predicts Response to Anti-PD-1/pd-L1 Antibody in SCLC Patients at Early Phase. *Cancer Immunol. Immunother.* 70, 713–720. doi:10.1007/s00262-020-02706-5
- Xu, A., Tian, T., Hao, J., Liu, J., Zhang, Z., Hao, J., et al. (2007). Elevation of Serum HSP90 $\alpha$  Correlated with the Clinical Stage of Non-small Cell Lung Cancer. Available at: <http://www.mupnet.com>.
- Zhou, M., Wang, Z., Yao, Y., Zhou, H., Liu, M., and Sun, J. (2017). Neuron-specific Enolase and Response to Initial Therapy Are Important Prognostic Factors in Patients with Small Cell Lung Cancer. *Clin. Transl. Oncol.* 19, 865–873. doi:10.1007/s12094-017-1617-2
- Zhou, W., Yang, Y., Wang, Z., Liu, Y., and Lari Najafi, M. (2021). Impact of HSP90  $\alpha$ , CEA, NSE, SCC, and CYFRA21-1 on Lung Cancer Patients. *J. Healthc. Eng.* 2021, 1–6. doi:10.1155/2021/6929971

**Conflict of Interest:** The authors declare that the research was conducted in the absence of any commercial or financial relationships that could be construed as a potential conflict of interest.

**Publisher’s Note:** All claims expressed in this article are solely those of the authors and do not necessarily represent those of their affiliated organizations, or those of the publisher, the editors and the reviewers. Any product that may be evaluated in this article, or claim that may be made by its manufacturer, is not guaranteed or endorsed by the publisher.

Copyright © 2022 Huang, Pan, Liu, Tang, Li, Bian, Ning, Li and Zhang. This is an open-access article distributed under the terms of the Creative Commons Attribution License (CC BY). The use, distribution or reproduction in other forums is permitted, provided the original author(s) and the copyright owner(s) are credited and that the original publication in this journal is cited, in accordance with accepted academic practice. No use, distribution or reproduction is permitted which does not comply with these terms.



## OPEN ACCESS

## EDITED BY

Xolani Henry Makhoba,  
University of Fort Hare, South Africa

## REVIEWED BY

Nitika,  
University of North Carolina at  
Charlotte, United States

## \*CORRESPONDENCE

Jude M. Przyborski,  
Jude.Przyborski@ernaehrung.uni-  
giessen.de

## SPECIALTY SECTION

This article was submitted to Molecular  
Diagnostics and Therapeutics,  
a section of the journal  
Frontiers in Molecular Biosciences

RECEIVED 13 June 2022

ACCEPTED 04 July 2022

PUBLISHED 05 August 2022

## CITATION

Barth J, Schach T and Przyborski JM  
(2022), HSP70 and their co-chaperones  
in the human malaria parasite  
*P. falciparum* and their potential as  
drug targets.  
*Front. Mol. Biosci.* 9:968248.  
doi: 10.3389/fmolb.2022.968248

## COPYRIGHT

© 2022 Barth, Schach and Przyborski.  
This is an open-access article  
distributed under the terms of the  
[Creative Commons Attribution License  
\(CC BY\)](#). The use, distribution or  
reproduction in other forums is  
permitted, provided the original  
author(s) and the copyright owner(s) are  
credited and that the original  
publication in this journal is cited, in  
accordance with accepted academic  
practice. No use, distribution or  
reproduction is permitted which does  
not comply with these terms.

# HSP70 and their co-chaperones in the human malaria parasite *P. falciparum* and their potential as drug targets

Julian Barth, Tim Schach and Jude M. Przyborski\*

Biochemistry and Molecular Biology, Justus-Liebig University Giessen, Giessen, Germany

As part of their life-cycle, malaria parasites undergo rapid cell multiplication and division, with one parasite giving rise to over 20 new parasites within the course of 48 h. To support this, the parasite has an extremely high metabolic rate and level of protein biosynthesis. Underpinning these activities, the parasite encodes a number of chaperone/heat shock proteins, belonging to various families. Research over the past decade has revealed that these proteins are involved in a number of essential processes within the parasite, or within the infected host cell. Due to this, these proteins are now being viewed as potential targets for drug development, and we have begun to characterize their properties in more detail. In this article we summarize the current state of knowledge about one particular chaperone family, that of the HSP70, and highlight their importance, function, and potential co-chaperone interactions. This is then discussed with regard to the suitability of these proteins and interactions for drug development.

## KEYWORDS

chaperones, malaria, *Plasmodium falciparum*, Hsp40, Hsp70, protein-protein interaction, small molecule inhibitors, heat shock proteins

## Introduction

Malaria is one of the leading infectious diseases worldwide. The most lethal form is caused by *Plasmodium falciparum* (*P. falciparum*) which caused 241 million cases in 2020. The African continent accounted for up to 95% of these cases. Children under 5 years of age represent the most vulnerable group to the disease and account for 80% of the 627,000 deaths reported in 2020 (WHO, 2021).

Similar to other organisms, *Plasmodium* encodes a wide variety of HSP and other chaperones/co-chaperones which are involved in many essential cellular processes. These proteins play (or are predicted to play) a major role in the survival, virulence and pathogenicity of the parasite. As they lie at the heart of proteostasis, they assist in protecting parasite proteins in several situations of proteotoxic stress, including the temperature spikes caused by febrile episodes of the human host, temperature transitions taking place during transmission from the mosquito vector to the human host and *vice-versa*, and exposure to cytotoxic drugs. Due to their central role in such a diverse number of essential biological processes, these proteins have gained interest as potential targets for

development of small molecule inhibitors. Several HSP have been shown to be upregulated in response to various drug treatments, and may play a role in helping parasites survive these stress situations (Akide-Ndunge et al., 2009; Cheeseman et al., 2012; Shahinas et al., 2013). Thus, as well as potentially being direct targets for drug development, any inhibitors identified may allow some measure of reversal of drug resistance.

Special interest has been paid to members of the HSP70 family, and their interactions with co-chaperones (HSP40, also known as J-domain proteins, JDP). The focus of this mini-review is to collate what is currently known about the biology of PfHSP70 and PfJDP, their interactions, and what progress has so far been made in developing specific inhibitors of this important parasite Achilles Heel.

## The HSP70 family

Chaperones of the HSP70-class are crucial elements of the cellular protein surveillance network. They are a highly conserved family of proteins that share a very similar structure. In general, they comprise an N-terminal nucleotide-binding domain (NBD) that is able to bind ATP. Following this is a protease-sensitive linker domain leading to a substrate-binding domain to which the corresponding substrate polypeptides bind (Flaherty et al., 1990). HSP70 are involved in diverse cellular processes such as protection from thermal insult, folding of nascent proteins, refolding of misfolded proteins, targeting terminally misfolded proteins for degradation and protein translocation.

## J-domain proteins

J-domain proteins (JDP, also referred to as HSP40, DNAJ) are generally co-chaperones for HSP70. They perform several tasks including recruitment of substrates to HSP70 and then stimulating the ATPase activity of HSP70. They can thus be viewed as adapters which allow a limited number of HSP70 to work on highly diverse substrates, and JDP are one of the most diverse co-chaperone families. In agreement with this, most organisms encode a higher number of JDP than HSP70 (Kamppinga et al., 2019).

## The ATPase cycle and JDP-HSP70 interaction

HSP70 act as molecular chaperones. As such, they are able to bind and hold exposed hydrophobic peptide-sequences of other, aggregation-prone proteins. Beyond this “holdase” function, HSP70 are able to refold denatured proteins. A catalytic ATP-dependent interaction cycle enables the folding or refolding of

substrate proteins. This essential cycle couples the ATPase activity of HSP70 to its affinity for substrate proteins (Figure 1A). In the ATP-bound state, the affinity to peptide substrates is low. In this context, a JDP binds first to a hydrophobic peptide-segment of any substrate protein and subsequently transfers it to HSP70 (Laufen et al., 1999; Mayer et al., 2000; Kityk et al., 2018). The simultaneous binding of a substrate to the SBD of HSP70 and a J-domain stimulate the ATPase activity of HSP70 synergistically (Figure 1A). Upon ATP-hydrolysis, the substrate-bound chaperone state is stabilized (Wittung-Stafshede et al., 2003). In the high-affinity HSP70-substrate-complex, the rate of ADP dissociation is the rate-determining step for the remainder of the cycle (Figure 1A). Nucleotide exchange factors (NEFs) facilitate ADP release and initiate ATP binding again with subsequent substrate release.

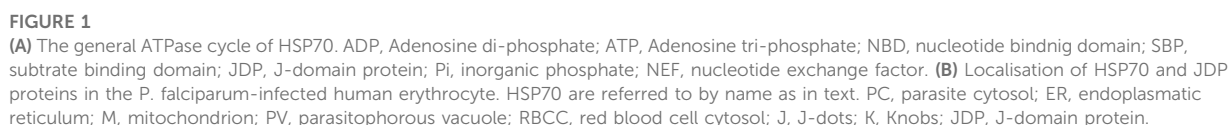
The enzymatic ability to hydrolyze ATP is essential for functional HSP70-substrate interaction (Mayer et al., 2000). Based on this mechanism, HSP70 are able to bind and protect virtually every protein from further denaturation and aggregation (Boorstein et al., 1994).

## The *P. falciparum* HSP70 and JDP families

Based on their structure and localisation, several PfHSP70 can be assigned functions by comparison to homologues in other systems (Figure 1B). Some members of the family have been more extensively studied and we now have some insight into their specialised function. Limited reverse genetic work has been carried out, however it is likely that the HSP70 (and some JDP) involved in core processes within the parasite will be essential for parasite survival, whereas those involved in (for example) host cell modification are not required in *in vitro* cell culture but may be important in an infection situation (Przyborski et al., 2015).

**PfHSP70-1:** PfHSP70-1 is likely to be the only canonical cytosolic HSP70. It contains a C-terminal -EEVD motif which is used for interaction with PfHOP (Zininga et al., 2015b). Although no definitive experimental evidence exists, inhibitor studies suggest that PfHSP70-1 has essential functions in the blood stages. Biochemical characterisation of recombinant PfHSP70-1 reveals that the protein has a slightly higher ATPase rate than that of the human homologue, but has a dramatically lower affinity for ATP (Matambo et al., 2004). PfHSP70-1 appears to be upregulated upon thermal stress (Kumar et al., 1991). PfHSP70-1 has been shown to associate with its putative NEF PfHSP70-Z in a nucleotide dependent manner (Zininga et al., 2015a; Zininga et al., 2016).

**PfHSP70-2:** PfHSP70-2 is localised in the ER, contains an N-terminal ER-type signal sequence and a C-terminal -SDEL ER retrieval sequence. PfHSP70-2 is likely to be a homologue of BiP/



*PfHSP70-X*: PfHSP70-X is only encoded by Plasmodium parasites belonging to the laverian subgenus. These parasites infected humans, chimpanzees, and gorillas. PfHSP70-X locates to the lumen of the parasitophous vacuole and is also exported to the host cell (Kölzer et al., 2012). In the host cell, this protein is

found in structures referred to as J-dots, which also contain a number of parasite encoded JDP (Külzer et al., 2010; Külzer et al., 2012). Although partially exported to the host cell, the protein lacks a PEXEL export motif, and its transport appears to be directed by an atypical export signal found following an N-terminal ER-type signal sequence (Rhiel et al., 2016). Although not essential for parasite growth under normal conditions in culture, knockout experiments suggest that PfHSP70 is involved in a number of host cell modification processes including cytoadherence, antigenic variation and

regulating the stiffness of the infected host cell (Charnaud et al., 2017). Knockdown experiments hint that PfHSP70-X may be involved in protecting the parasite from heat stress during fever periods (Cobb et al., 2017). Immunoprecipitation allowed the identification of a number of proteins interacting with PfHSP70-X, including both exported parasite proteins, a PV resident chaperone PfHSP101, human HSP70 and an exported parasite JDP (Zhang et al., 2017). The significance of this result is so far not known.

**PfHSP70-Y:** Also now known as PfGRP170, PfHSP70-Y belongs to the HSP110 protein family. These proteins are generally known to be NEFs for other members of the HSP70 family. PfGRP170 contains an N-terminal ER-type signal sequence and a C-terminal -KDEL ER retrieval sequence, and localises to the lumen of the ER. Earlier studies suggested that this protein may localise to the parasite's apicoplast due to a predicted apicoplast transit peptide, however later work determined that the C-terminal -KDEL signal was dominant and retained the protein in the ER (Heiny et al., 2012). It is likely that PfHSP70-Y acts as a NEF for PfHSP70-2. The protein appears to be essential for parasite development and is linked to parasite stress responses (Kudyba et al., 2019).

**PfHSP70-Z:** PfHSP70-Z, also known as PfHSP110, belongs to the HSP110 protein family, and is likely to be the NEF for the cytosolic PfHSP70-1. Indeed, PfHSP70-Z has been shown to associate with PfHSP70-1 in a nucleotide dependent manner (Zininga et al., 2016). Recombinant PfHSP70-Z forms higher order oligomers and has been reported to have endogenous ATPase activity (Zininga et al., 2015a; Zininga et al., 2016). Functional inactivation of PfHSP70-Z is lethal, likely due to its role in preventing aggregation of a number of asparagine-rich proteins, especially under heat stress condition (Muralidharan et al., 2012). In agreement with this, expression of PfHSP70-Z is increased in response to heat stress (Zininga et al., 2015a).

***P. falciparum* JDP:** *P. falciparum* encodes 43 proteins which can be assigned to the JDP family (Botha et al., 2007). Of these, 17 are predicted to be exported to the host cell, many of which are *P. falciparum* specific [not found in other non-laverania species (Botha et al., 2007)]. Based on the presence or absence of specific domains, the 43 JDP have been further assigned to a number of sub families, HSP40 Type I-Type IV. The 12 Type IV proteins are of particular interest as, although they contain a recognisable J-domain, the classical catalytic triad HPD has been replaced by HPE (Botha et al., 2007). This does not exclude a functional interaction with a HSP70, but implies that such interactions may be more specific and specialised. The function of the parasite-localised JDP has not been analysed in any great detail, but it is suggested that they likely act in concert with PfHSP70-1, PfHSP70-2 or PfHSP70-3. It is unknown why the parasite exports so many JDP. As JDP generally function in concert with a HSP70, it is supposed that these JDP functionally interact with either the exported PfHSP70-X, or potentially residual human HSP70/HSC70. A number of the exported JDP proteins have been knocked out, and many of these parasite lines show aberrations in host cell modification (Maier et al., 2008; Diehl et al., 2021). Of particular note, a knockout of the Type II

exported JDP PFA66 shows dramatic changes in the morphology of the knobs (Diehl et al., 2021). Interestingly, further analysis suggested that this JDP functions in concert with residual human HSP70/HSC70. A model is emerging in which the parasite exports JDP to act as “adapter” molecules between parasite-encoded and residual host cell proteins (Diehl et al., 2021).

## The search for specific inhibitors of PfHSP70

A meaningful inhibitor would be specific for only Plasmodium PfHSP70, and its target and mode of action would be clear. A number of studies (detailed below) have reported inhibitors of PfHSP70 (Table 1). Some of these studies were carried out on recombinant protein, however the assays used are not always directly comparable, as they assay different sub-functions of HSP function. *In vitro* screening on parasite cell cultures has also been carried out, however it is not always clear what protein is being targeted. For inhibitors which have been assayed using both methods, there are often striking disparities between the effects on recombinant protein and in cell cultures. This suggests either off-target effects, or possibly limited bioavailability.

## Rational drug design

Modern drug discovery is moving more and more towards a rational design strategy based on knowledge of the target structure(s) and or interfaces. In infectious disease research, this often involves finding differences between proteins found in host and pathogen. Recent research findings focused on crystallographic elucidation of the functional domains of PfHSP70 and JDP (Day et al., 2019; Schmidt and Vakonakis, 2020; Mohamad et al., 2021). A study of the PfHSP70-X substrate-binding domain (SBD) reveals that the SBD-structure is conserved and extremely similar to both the human HSP70 (HsHSP70) and *E. coli* DnaK structure (Schmidt and Vakonakis, 2020). The NBD also shows a high conservation and similarity to that of the NBD of HsHSP70 (Mohamad et al., 2021).

While these results might lead to the conclusion that it is not viable to design inhibitors which specifically target PfHSP70-X while not affecting HsHSP70, the authors indicate that the NBD of PfHSP70-X does indeed contain potential binding sites for small-molecule activity-modulation which are structurally different in the human homologue. It is worth noting that crystallography can merely outline fixed protein structures whereas in the cell proteins (especially chaperones) are often conformationally dynamic. This flexibility influences their binding affinity to small molecules, allosteric modulators or other proteins (Johansson and Lindorff-Larsen, 2018). Thus, the use of structural information for the identification of specific small molecule inhibitors is complicated but a success is nonetheless possible.



TABLE 1 Inhibitors so far tested against PfHSP70.

Substance		Biological effect			References
Classes	Compounds	<i>P. falciparum</i> IC <sub>50</sub> , effect on human cells	HSP70 effect	HSP70/JDP effect	
Pyrimidinones	MAL3-39	PfIC <sub>50</sub> = 0.8 $\mu$ M, HsIC <sub>50</sub> = N/A	Weak inhibition of PfHSP70-1 and HSPA1A steady-state ATPase activity at 300 $\mu$ M	Inhibitory effect on HSPA1A/Hdj2	Chiang et al., (2009) Botha et al., (2011)
	DMT-2264	PfIC <sub>50</sub> = 1.1 $\mu$ M, HsIC <sub>50</sub> = N/A		Inhibitory effect on HSPA1A/Hdj2 and PfHSP70-1/PfHSP40	
Malonganenones	Malonganenone A	PfIC <sub>50</sub> = 0.8 $\mu$ M, Hs (MCF12A, MDA-231-MB, 50 $\mu$ M) No effect	No inhibitory effect on basal ATPase activities of PfHSP70-X, PfHSP70-1 and HSPA1A	Strong inhibitory effect on PfHSP70-1/PfHSP40	Cockburn et al., (2011) Cockburn et al., (2014)
	Malonganenone B	PfIC <sub>50</sub> > 50 $\mu$ M, HsIC <sub>50</sub> = N/A		All three compounds have a small significant inhibitory effect on PfHSP70-X/Hsj1a but no effect on HSPA1A/Hsj1a or PfHSP70-1/Hsj1a ATPase activity	
	Malonganenone C	PfIC <sub>50</sub> = 5.2 $\mu$ M, Hs (MCF12A, MDA-231-MB, 250 $\mu$ M) No effect			
Napthaquinones	Bromo- $\beta$ -lapachona	PfIC <sub>50</sub> = 17.3 $\mu$ M, Hs (MCF12A, MDA-231-MB, 20 $\mu$ M) 80% cell growth decrease	Strong basal PfHSP70-X ATPase activity inhibition, small inhibitory effect on HSPA1A, no effect on PfHSP70-1	Strong inhibitory effect on ATPase activity of PfHSP70-X/Hsj1a and PfHSP70-1/PfHSP40, no effect on HSPA1A/Hsj1a and PfHSP70-X/PFA066w <sub>j</sub>	Cockburn et al., (2011) Cockburn et al., (2014) Day et al., (2019)
	Lapachol	PfIC <sub>50</sub> = 18.6 $\mu$ M, Hs (MDA-231-MB, 200 $\mu$ M) ~ 50% cell growth decrease	Medium PfHSP70-X ATPase activity inhibition, no effect on PfHSP70-1 and HSPA1A	Medium inhibitory effect on PfHSP70-X/Hsj1a and PfHSP70-1/PfHSP40, no effect on HSPA1A/Hsj1a	Cockburn et al., (2011) Cockburn et al., (2014)
Chalcones	C86	PfIC <sub>50</sub> = N/A, Hs (22Rv1, 5 $\mu$ M) 55% cell viability decrease	No effect on basal PfHSP70-X ATPase activity. HsHSP70: N/A	Pre-incubation of PFE0055c with C86 results in inhibition of PfHSP70-X ATPase activity	Moses et al., (2018) Dutta et al., (2021)
(Benzothiazole)-Rhodacyanines	MKT-077	PfEC <sub>50</sub> = 0.07 $\mu$ M (3D7), HsEC <sub>50</sub> = 0.98 $\mu$ M (HCT-116)	Minimal PfHSP70-X ATPase activity inhibition under 100 $\mu$ M HsHSP70: N/A	Small concentration-dependent inhibitory effect detected for PfHSP70-X/PFA066w <sub>j</sub> and PfHSP70-X/PFE0055c <sub>j</sub>	Chen et al., (2018) Day et al., (2019) Dutta et al., (2021)
	YM-01	N/A		Concentration-dependent inhibitory effect on PfHSP70-X/PFA066w <sub>j</sub> and PfHSP70-X/PFE0055c <sub>j</sub>	Day et al. (2019)
	JG98	PfIC <sub>50</sub> N/A, HsIC <sub>50</sub> ~ 500 nM (22Rv1)	Significant PfHSP70-X ATPase activity inhibition at 10 $\mu$ M HsHSP70: N/A	Significant inhibitory effect on PfHSP70-X/PFE0055c ATPase activity at 10 $\mu$ M	Dutta et al. (2021)
Lipopeptides	Polymyxin B	PfIC <sub>50</sub> = N/A, HsIC <sub>50</sub> = varying, 1.05 mM (NRK-52E), 350 $\mu$ M (HK-2)	Inhibition of basal ATPase and aggregation suppression activity of PfHSP70-1 and PfHSP70-z. HsHSP70: N/A	N/A	Azad et al. 2013) Zininga et al., (2017a)
Catechin	EGCG	PfIC <sub>50</sub> = 2.9 $\mu$ M, HsIC <sub>50</sub> = varying, 22 $\mu$ M (H661, H1299), 65 $\mu$ M (HT-29)			Yang et al. 1998) Zininga et al., (2017b)
Bis-Indole	Violacein	PfEC <sub>50</sub> = 400 nm (3D7), HsIC <sub>50</sub> = 1.4 $\mu$ M (HepG2)	Inhibition of basal ATPase and aggregation suppression activity of PfHSP70-1. HsHSP70: N/A		Bilsland et al. 2018 Tavella et al. 2021)

## Characterised inhibitors of PHSP70

The search for small molecule inhibitors of the Plasmodium HSP70 chaperones has identified several suitable compounds. Amongst others, these compounds are pyrimidinones, malonganenones, napthaquinones, lipopeptides, and a catechin from green tea extract (Chiang et al., 2009; Cockburn et al., 2011; Cockburn et al., 2014; Zininga et al., 2017a; Zininga et al., 2017b; Day et al., 2019). The activity-modulating effects towards several PfHSP70 chaperones are summarized in the following section.

### PfHSP70-1

As the main cytosolic chaperone of *P. falciparum*, PfHSP70-1 is heavily associated with maintaining viability and proteostasis and is thus a prominent target of molecular inhibitory research.

Members of the class of pyrimidinones exhibited varying effects on the intrinsic ATPase activity of PfHSP70-1 in single turnover assays. While they generally stimulated the ATPase activity at concentrations of 100  $\mu$ M, the compounds DMT2264 and MAL3-39 inhibited the ATPase activity at higher concentrations of 300  $\mu$ M (Chiang et al., 2009). First data regarding the malonganenones A-C, lapachol and bromo- $\beta$ -lapachona (BBL) showed a concentration dependent inhibition of the aggregation suppression activity of PfHSP70-1 (Cockburn et al., 2011). However, the ATPase activity of PfHSP70-1 was not modulated by any of these compounds (Cockburn et al., 2014).

Studies with a focus on SPR analyses aim for the elucidation of binding affinities of potential small molecule inhibitors to several PfHSP70 chaperones. In this context, a screening of quinoline-pyrimidine hybrid molecules revealed varying binding affinities of these small molecules to PfHSP70-1 (Kayamba et al., 2021). Thus, the authors suppose that PfHSP70-1 is a target of these compounds as they exhibit moderate to high anti-plasmodial activity *in vitro*. Binding affinities for the green-tea polyphenol epigallocatechin-3-gallate (EGCG) and the lipopeptide polymyxin B (PMB) were defined in the same way (Zininga et al., 2017a; Zininga et al., 2017b). Additionally, both compounds inhibited the basal ATPase activity of PfHSP70-1 *in vitro*.

Furthermore, the phytocompounds iso-mukaadial acetate (IMA) and ursolic acid (UAA) feature anti-Plasmodium activity *in vitro* and *in vivo* (Nyaba et al., 2018; Salomane et al., 2021). Both compounds were able to abrogate the aggregation suppression activity of PfHSP70-1 in a concentration dependent manner. The basal ATPase activity of PfHSP70-1 was inhibited by IMA similarly. UAA, however, did not modulate the ATPase activity in the highest tested concentrations significantly (Salomane et al., 2021).

Recently, the bis-indole violacein was tested for anti-malarial properties and possible inhibitory effects on PfHSP70-1. A significant

and concentration dependent inhibition of the chaperone's ATPase and aggregation suppression activity by violacein was observed (Tavella et al., 2021). Thus, the small molecule is predicted to compromise the ATP hydrolysis of PfHSP70-1 by interacting with the SBD or the SBD-NBD-interface (Tavella et al., 2021). However, as violacein exhibits broad biological activity, it also shows low selectivity for Plasmodium.

### PfHSP70-2

Data on small molecule inhibitors of PfHSP70-2 is limited. Four commercially available GRP78 inhibitors, namely Gilvocarcin V, Apoptozole, MKT-077 and VER-155008, have been reported to exhibit broad specificity to members of the HSP70-family (Matsumoto and Hanawalt, 2000; Rousaki et al., 2011; Kim et al., 2014; Park et al., 2017). They were confirmed to interact with PfHSP70-2 in *in vitro* binding assays, recently (Chen et al., 2018). However, the binding affinities of the compounds to PfGRP78 and HsGRP78 showed little difference across the species. An exception was VER-155008 that stood out due to a three-fold lower affinity to PfGRP78 than HsGRP78. The authors propose that the higher protein rigidity of PfGRP78 leads to lower affinities for this inhibitor. The marginally different properties of PfHSP70-2 possibly enable researchers to design compound derivatives with specific inhibitory effects.

### PfHSP70-X

PfHSP70-X is of high interest in inhibitor research, as it is believed to assist the correct folding of exported proteins and thereby supporting parasite virulence. Similar to PfHSP70-1, the malonganenone-compounds did not modulate the basal ATPase activity of PfHSP70-X. However, napthaquinones, especially BBL, inhibited its ATPase and aggregation suppression activity in a concentration dependent manner (Cockburn et al., 2014). Regarding the ATPase activity, these findings were recently confirmed (Day et al., 2019). Additionally, the broad-spectrum HSP70 inhibitor MKT-077 attenuates the ATPase activity of PfHSP70-X only at concentrations above 100  $\mu$ M. Its derivative YM-01 exhibits similar inhibitory properties at slightly lower concentrations (Day et al., 2019).

In contrary to the benzothiazole rhodacyanines JG98 and JG231, the chalcone C86 did not inhibit the basal PfHSP70-X ATPase activity significantly (Dutta et al., 2021). The authors evaluate their findings to be in accordance to the functional interaction of the compounds with PfHSP70-X. JG98 and JG231 are considered to prevent nucleotide exchange of an HSP70 and thus locking it in its ADP-bound form (Shao et al., 2018).

Comparing the varying results of studies with multiple small molecules and particularly PfHSP70-1 and PfHSP70-X, a striking distinction regarding their susceptibility to these compounds is observable. Thus, and according to [Mohamad et al., 2021](#), it may be possible to design small molecule inhibitors to target specific PfHSP70s ([Mohamad et al., 2021](#)).

## PfHSP70-Z

Because PfHSP70-Z acts as a NEF for PfHSP70-1, inhibitors of the chaperones' interaction have become a research target. The binding of the small molecules EGCG and PMB to PfHSP70-Z has been confirmed *via* SPR and *in vitro* activity assays showed an inhibitory effect of both compounds for the basal PfHSP70-Z ATPase activity. Additionally, EGCG and PMB interfere with the capability of PfHSP70-Z to suppress the aggregation of heat stress-prone proteins ([Zininga et al., 2017a](#); [Zininga et al., 2017b](#)). Alternatively, a SPR screening of quinoline-pyrimidine hybrids suggested high binding affinities to PfHSP70-Z within the nanomolar and micromolar range for some compounds ([Kayamba et al., 2021](#)).

## Inhibitors of PfHSP70/PfJDP interaction

The explicated chaperone/co-chaperone interaction offers the possibility to inhibit a single part of the network and thereby achieving a loss of function in associated metabolic pathways ([Daniyan et al., 2019](#)). Especially the HSP70/JDP interface might be a viable target for controlling the PfHSP70's ATPase activity *via* small molecule inhibitors ([Day et al., 2019](#)). The fact that small molecule compounds are able to modify the PfJDP-stimulated ATPase activity of their corresponding PfHSP70 is described in the literature for over a decade ([Chiang et al., 2009](#); [Botha et al., 2011](#); [Cockburn et al., 2014](#)). A number of compounds which have been shown to modulate intrinsic PfHSP70 activity have also been shown to modulate PfHSP70/PfJDP activities ([Chiang et al., 2009](#); [Cockburn et al., 2014](#); [Day et al., 2019](#); [Dutta et al., 2021](#)). Similar strategies have been suggested in cancer research, in which HSP70/JDP activities have been associated with cancer cell progression ([Nitika et al., 2020](#); [Knighton et al., 2021](#)).

First promising results were achieved by examining the human, Plasmodium and yeast HSP70 in combination with the human and yeast HSP40 co-chaperones Hlj1 and Ydj1, respectively ([Chiang et al., 2009](#)). Distinct and species-specific modulations of the HSP70 ATPase activity by a selection of nine pyrimidinones were reported. The capabilities of some particular compounds (MAL3-39 and DMT2264) were further assessed in a

PfHSP70-1/PfHSP40 system ([Botha et al., 2011](#)). As a result, only DMT2264 was found to inhibit the PfHSP40 stimulated ATPase activity of PfHSP70-1.

Since the export of PfHSP70-X into the RBC has been shown, this particular chaperone gained further attention in small molecule compounds and JDP-interaction research ([Külzer et al., 2012](#); [Cockburn et al., 2014](#)). Changes in PfHSP40-stimulated ATPase activity of PfHSP70-X and pfHSP70-1 in combination with lapachol, BBL and the malonganenones A (MA), B and C were monitored. The effects of the compounds were highly diverse. While BBL modulated the ATPase activities of PfHSP40/PfHSP70-1 and Hsj1a/PfHSP70-X, it also inhibited the ones of the Hsj1a/HSPA1A controls. Interestingly, MA provided selectivity of the HSP70' modulation. The ATPase activity of the PfHSP40/PfHSP70-1 and Hsj1a/PfHSP70-X was significantly inhibited. The human controls, however, were not affected ([Cockburn et al., 2014](#)).

As more details on the interaction of PfHSP70 with specific PfHSP40 partners emerged, new experimental data on their inhibition was obtained ([Daniyan et al., 2016](#); [Day et al., 2019](#)). Upon the simultaneous stimulation of PfHSP70-X by the J-domains of its supposed cognate co-chaperones PFA0660w<sub>1</sub> or PFE0055c<sub>1</sub>, BBL did not decrease the ATPase activity of PfHSP70-X. Even broad-spectrum HSP70 inhibitors like methylene blue and MKT-077 showed little potency against PfHSP70-X that was stimulated by its *in vivo* co-chaperones ([Day et al., 2019](#)).

The chalcone C86 and the benzothiazole-rhodacyanines JG98 and JG231 were already identified as small molecule inhibitors of the human JDP/HSP70 system. Recently, they have been used on plasmodium proteins ([Dutta et al., 2021](#)). A significant inhibition of the stimulated ATPase activity of PfHSP70-X was observed when the JDP PFE055c was pre-incubated with C86 prior to its addition. This result fits the proposed function of C86 as a JDP pan-inhibitor ([Moses et al., 2018](#)). Additionally, JG98 and JG231 provided inhibitory effects on the PFE055c-stimulated ATPase activity of PfHSP70-X ([Dutta et al., 2021](#)).

These results imply that the development of parasite-specific chaperone/co-chaperone-based small molecule inhibitors is a complex task, but success can be achieved ([Daniyan and Blatch, 2017](#)).

## Conclusion

This mini-review summarizes the current findings of the search for Plasmodium HSP70 and HSP40 small molecule inhibitors. As these molecular chaperones are involved in multiple important molecular-biological processes of *P. falciparum*, they represent a promising new and sustainable drug target. Several studies successfully targeted and inhibited

the PfHSP70's and PfHSP40's molecular chaperone activity in *in vitro* assays with small molecule inhibitors. However, the specificity of potential inhibitors is a critical point in research as human and Plasmodium chaperone counterparts share high structural similarity. Recent studies suggest that it may be possible to design specific small molecule inhibitors for PfHSP. Results of high-throughput screenings with derivatives of already identified small molecule activity modulators and entirely new compounds are expected in the near future.

## Author contributions

JB: Writing, editing and generation of Table 1, Figure 1A. TS: Writing and editing. JP: Writing, editing and generation of figure 1B.

## Funding

JB is financed through the LOEWE-DRUID centre (Project A7, PI Jude Przyborski).

## References

- Akide-Ndunge, O. B., Tambini, E., Giribaldi, G., McMillan, P. J., Muller, S., Arese, P., et al. (2009). Co-ordinated stage-dependent enhancement of Plasmodium falciparum antioxidant enzymes and heat shock protein expression in parasites growing in oxidatively stressed or G6PD-deficient red blood cells. *Malar. J.* 8, 113. doi:10.1186/1475-2875-8-113
- Azad, M. A., Finnin, B. A., Poudyal, A., Davis, K., Li, J., Hill, P. A., et al. (2013). Polymyxin B induces apoptosis in kidney proximal tubular cells. *Antimicrob. Agents Chemother.* 57, 4329–4335. doi:10.1128/AAC.02587-12
- Boorstein, W. R., Ziegelhoffer, T., and Craig, E. A. (1994). Molecular evolution of the HSP70 multigene family. *J. Mol. Evol.* 38, 1–17. doi:10.1007/BF00175490
- Botha, M., Chiang, A. N., Needham, P. G., Stephens, L. L., Hoppe, H. C., Kulzer, S., et al. (2011). Plasmodium falciparum encodes a single cytosolic type I Hsp40 that functionally interacts with Hsp70 and is upregulated by heat shock. *Cell. Stress Chaperones* 16, 389–401. doi:10.1007/s12192-010-0250-6
- Botha, M., Pesce, E. R., and Blatch, G. L. (2007). The Hsp40 proteins of plasmodium falciparum and other apicomplexa: Regulating chaperone power in the parasite and the host. *Int. J. Biochem. Cell. Biol.* 39, 1781–1803. doi:10.1016/j.biocel.2007.02.011
- Charnaud, S. C., Dixon, M. W. A., Nie, C. Q., Chappell, L., Sanders, P. R., Nebl, T., et al. (2017). The exported chaperone Hsp70-x supports virulence functions for Plasmodium falciparum blood stage parasites. *PLoS One* 12, e0181656. doi:10.1371/journal.pone.0181656
- Cheeseman, I. H., Miller, B. A., Nair, S., Nkhoma, S., Tan, A., Tan, J. C., et al. (2012). A major genome region underlying artemisinin resistance in malaria. *Science* 336, 79–82. doi:10.1126/science.1215966
- Chen, Y., Murillo-Solano, C., Kirkpatrick, M. G., Antoshchenko, T., Park, H. W., Pizarro, J. C., et al. (2018). Repurposing drugs to target the malaria parasite unfolding protein response. *Sci. Rep.* 8, 10333. doi:10.1038/s41598-018-28608-2
- Chiang, A. N., Valderramos, J. C., Balachandran, R., Chovatiya, R. J., Mead, B. P., Schneider, C., et al. (2009). Select pyrimidinones inhibit the propagation of the malarial parasite, Plasmodium falciparum. *Bioorg. Med. Chem.* 17, 1527–1533. doi:10.1016/j.bmc.2009.01.024
- Cobb, D. W., Florentin, A., Fierro, M. A., Krakowiak, M., Moore, J. M., Muralidharan, V., et al. (2017). The exported chaperone PfHsp70x is dispensable for the plasmodium falciparum intraerythrocytic life cycle. *mSphere* 2, 63. doi:10.1128/mSphere.00363-17
- Cockburn, I. L., Boshoff, A., Pesce, E. R., and Blatch, G. L. (2014). Selective modulation of plasmodial Hsp70s by small molecules with antimalarial activity. *Biol. Chem.* 395, 1353–1362. doi:10.1515/hsz-2014-0138
- Cockburn, I. L., Pesce, E. R., Przyborski, J. M., Davies-Coleman, M. T., Clark, P. G. K., Keyzers, R. A., et al. (2011). Screening for small molecule modulators of Hsp70 chaperone activity using protein aggregation suppression assays: Inhibition of the plasmodial chaperone PfHsp70-1. *Biol. Chem.* 392, 431–438. doi:10.1515/BC.2011.040
- Daniyan, M. O., and Blatch, G. L. (2017). Plasmodial Hsp40s: New avenues for antimalarial drug discovery. *Curr. Pharm. Des.* 23, 4555–4570. doi:10.2174/1381612823666170124142439
- Daniyan, M. O., Boshoff, A., Prinsloo, E., Pesce, E. R., and Blatch, G. L. (2016). The malarial exported PFA0660w is an Hsp40 Co-chaperone of PfHsp70-x. *PLoS One* 11, e0148517. doi:10.1371/journal.pone.0148517
- Daniyan, M. O., Przyborski, J. M., and Shonhai, A. (2019). Partners in mischief: Functional networks of heat shock proteins of plasmodium falciparum and their influence on parasite virulence. *Biomolecules* 9, E295. doi:10.3390/biom9070295
- Day, J., Passecker, A., Beck, H. P., and Vakonakis, I. (2019). The Plasmodium falciparum Hsp70-x chaperone assists the heat stress response of the malaria parasite. *FASEB J.* 33, 14611–14624. doi:10.1096/fj.201901741R
- Diehl, M., Roling, L., Rohland, L., Weber, S., Cyrklaff, M., Sanchez, C. P., et al. (2021). Co-chaperone involvement in knob biogenesis implicates host-derived chaperones in malaria virulence. *PLoS Pathog.* 17, e1009969. doi:10.1371/journal.ppat.1009969
- Dutta, T., Singh, H., Gestwicki, J. E., and Blatch, G. L. (2021). Exported plasmodial J domain protein, PFE0055c, and PfHsp70-x form a specific co-chaperone-chaperone partnership. *Cell. Stress Chaperones* 26, 355–366. doi:10.1007/s12192-020-01181-2
- Flaherty, K. M., DeLuca-Flaherty, C., and McKay, D. B. (1990). Three-dimensional structure of the ATPase fragment of a 70K heat-shock cognate protein. *Nature* 346, 623–628. doi:10.1038/346623a0
- Heiny, S., Spork, S., and Przyborski, J. M. (2012). The apicoplast of the human malaria parasite *P. falciparum*. *J. Endocytobiosis Cell. Res.* 23, 91–95.
- Johansson, K. E., and Lindorff-Larsen, K. (2018). Structural heterogeneity and dynamics in protein evolution and design. *Curr. Opin. Struct. Biol.* 48, 157–163. doi:10.1016/j.sbi.2018.01.010

## Acknowledgments

We acknowledge the kind financial support of the LOEWE Center DRUID and the Justus-Liebig University. We apologise in advance to colleagues we were unable to cite due to length restrictions.

## Conflict of interest

The authors declare that the research was conducted in the absence of any commercial or financial relationships that could be construed as a potential conflict of interest.

## Publisher's note

All claims expressed in this article are solely those of the authors and do not necessarily represent those of their affiliated organizations, or those of the publisher, the editors and the reviewers. Any product that may be evaluated in this article, or claim that may be made by its manufacturer, is not guaranteed or endorsed by the publisher.



- Kampinga, H. H., Andreasson, C., Barducci, A., Cheetham, M. E., Cyr, D., Emanuelsson, C., et al. (2019). Function, evolution, and structure of J-domain proteins. *Cell. Stress Chaperones* 24, 7–15. doi:10.1007/s12192-018-0948-4
- Kayamba, F., Malimabe, T., Ademola, I. K., Poole, O. J., Kushwaha, N. D., Mahlalela, M., et al. (2021). Design and synthesis of quinoline-pyrimidine inspired hybrids as potential plasmodial inhibitors. *Eur. J. Med. Chem.* 217, 113330. doi:10.1016/j.ejmech.2021.113330
- Kim, S. H., Kang, J. G., Kim, C. S., Ihm, S. H., Choi, M. G., Yoo, H. J., et al. (2014). The hsp70 inhibitor VER155008 induces paraptosis requiring de novo protein synthesis in anaplastic thyroid carcinoma cells. *Biochem. Biophys. Res. Commun.* 454, 36–41. doi:10.1016/j.bbrc.2014.10.060
- Kityk, R., Kopp, J., and Mayer, M. P. (2018). Molecular mechanism of J-domain-triggered ATP hydrolysis by Hsp70 chaperones. *Mol. Cell.* 69, 227–237. e4. doi:10.1016/j.molcel.2017.12.003
- Knighton, L. E., Nitika, Wani, T. H., and Truman, A. W. (2021). Chemogenomic and bioinformatic profiling of ERdj paralogs underpins their unique roles in cancer. *Cell. Stress Chaperones* 27, 135–147. doi:10.1007/s12192-022-01256-2
- Kudyba, H. M., Cobb, D. W., Fierro, M. A., Florentin, A., Ljolje, D., Singh, B., et al. (2019). The endoplasmic reticulum chaperone PfGRP170 is essential for asexual development and is linked to stress response in malaria parasites. *Cell. Microbiol.* 21, e13042. doi:10.1111/cmi.13042
- Külzer, S., Charnaud, S., Dagan, T., Riedel, J., Mandal, P., Pesce, E. R., et al. (2012). Plasmodium falciparum-encoded exported hsp70/hsp40 chaperone/co-chaperone complexes within the host erythrocyte. *Cell. Microbiol.* 14, 1784–1795. doi:10.1111/j.1462-5822.2012.01840.x
- Külzer, S., Rug, M., Brinkmann, K., Cannon, P., Cowman, A., Lingelbach, K., et al. (2010). Parasite-encoded Hsp40 proteins define novel mobile structures in the cytosol of the P. falciparum-infected erythrocyte. *Cell. Microbiol.* 12, 1398–1420. doi:10.1111/j.1462-5822.2010.01477.x
- Kumar, N., Koski, G., Harada, M., Aikawa, M., and Zheng, H. (1991). Induction and localization of Plasmodium falciparum stress proteins related to the heat shock protein 70 family. *Mol. Biochem. Parasitol.* 48, 47–58. doi:10.1016/0166-6851(91)90163-z
- Laufen, T., Mayer, M. P., Beisel, C., Klostermeier, D., Mogk, A., Reinstein, J., et al. (1999). Mechanism of regulation of hsp70 chaperones by DnaJ cochaperones. *Proc. Natl. Acad. Sci. U. S. A.* 96, 5452–5457. doi:10.1073/pnas.96.10.5452
- Maier, A. G., Rug, M., O'Neill, M. T., Brown, M., Chakravorty, S., Szeftak, T., et al. (2008). Exported proteins required for virulence and rigidity of Plasmodium falciparum-infected human erythrocytes. *Cell.* 134, 48–61. doi:10.1016/j.cell.2008.04.051
- Matambo, T. S., Odunuga, O. O., Boshoff, A., and Blatch, G. L. (2004). Overproduction, purification, and characterization of the Plasmodium falciparum heat shock protein 70. *Protein Expr. Purif.* 33, 214–222. doi:10.1016/j.pep.2003.09.010
- Matsumoto, A., and Hanawalt, P. C. (2000). Histone H3 and heat shock protein GRP78 are selectively cross-linked to DNA by photoactivated givocarcin V in human fibroblasts. *Cancer Res.* 60, 3921–3926.
- Mayer, M. P., Schröder, H., Rüdiger, S., Paal, K., Laufen, T., Bukau, B., et al. (2000). Multistep mechanism of substrate binding determines chaperone activity of Hsp70. *Nat. Struct. Biol.* 7, 586–593. doi:10.1038/76819
- Mohamad, N., O'Donoghue, A., Kantsadi, A. L., and Vakonakis, I. (2021). Structures of the Plasmodium falciparum heat-shock protein 70-x ATPase domain in complex with chemical fragments identify conserved and unique binding sites. *Acta Crystallogr. F. Struct. Biol. Commun.* 77, 262–268. doi:10.1107/S2053230X21007378
- Moses, M. A., Kim, Y. S., Rivera-Marquez, G. M., Oshima, N., Watson, M. J., Beebe, K. E., et al. (2018). Targeting the hsp40/hsp70 chaperone Axis as a novel strategy to treat castration-resistant prostate cancer. *Cancer Res.* 78, 4022–4035. doi:10.1158/0008-5472.CAN-17-3728
- Muralidharan, V., Oksman, A., Pal, P., Lindquist, S., and Goldberg, D. E. (2012). Plasmodium falciparum heat shock protein 110 stabilizes the asparagine repeat-rich parasite proteome during malarial fevers. *Nat. Commun.* 3, 1310. doi:10.1038/ncomms2306
- Nitika, Blackman, J. S., Knighton, L. E., Takakuwa, J. E., Calderwood, S. K., and Truman, A. W. (2020). Chemogenomic screening identifies the Hsp70 co-chaperone DNAJA1 as a hub for anticancer drug resistance. *Sci. Rep.* 10, 13831. doi:10.38/s41598-020-70764-x
- Nyaba, Z. N., Murambiwa, P., Opoku, A. R., Mukaratirwa, S., Shode, F. O., Simelane, M. B. C., et al. (2018). Isolation, characterization, and biological evaluation of a potent anti-malarial drimane sesquiterpene from Warburgia salutaris stem bark. *Malar. J.* 17, 296. doi:10.1186/s12936-018-2439-6
- Park, S. H., Kim, W. J., Li, H., Seo, W., Kim, H., Shin, S. C., et al. (2017). Anti-leukemia activity of a Hsp70 inhibitor and its hybrid molecules. *Sci. Rep.* 7, 3537. doi:10.1038/s41598-017-03814-6
- Przyborski, J. M., Diehl, M., and Blatch, G. L. (2015). Plasmodial HSP70s are functionally adapted to the malaria parasite life cycle. *Front. Mol. Biosci.* 2, 34. doi:10.3389/fmolb.2015.00034
- Rhiel, M., Bittl, V., Tribensky, A., Charnaud, S. C., Strecker, M., Muller, S., et al. (2016). Trafficking of the exported P. falciparum chaperone PfHsp70x. *Sci. Rep.* 6, 36174. doi:10.1038/srep36174
- Rousaki, A., Miyata, Y., Jinwal, U. K., Dickey, C. A., Gestwicki, J. E., Zuiderweg, E. R., et al. (2011). Allosteric drugs: The interaction of antitumor compound MKT-077 with human Hsp70 chaperones. *J. Mol. Biol.* 411, 614–632. doi:10.1016/j.jmb.2011.06.003
- Salomane, N., Poole, O. J., and Simelane, M. B. C. (2021). Iso-mukaadial acetate and ursolic acid acetate inhibit the chaperone activity of Plasmodium falciparum heat shock protein 70-1. *Cell. Stress Chaperones* 26, 685–693. doi:10.1007/s12192-021-01212-6
- Schmidt, J., and Vakonakis, I. (2020). Structure of the substrate-binding domain of Plasmodium falciparum heat-shock protein 70-x. *Acta Crystallogr. F. Struct. Biol. Commun.* 76, 495–500. doi:10.1107/S2053230X2001208X
- Shahinas, D., Folefoc, A., and Pillai, D. R. (2013). Targeting plasmodium falciparum Hsp90: Towards reversing antimalarial resistance. *Pathogens* 2, 33–54. doi:10.3390/pathogens2010033
- Shao, H., Li, X., Moses, M. A., Gilbert, L. A., Kalyanaraman, C., Young, Z. T., et al. (2018). Exploration of benzothiazole rhodacyanines as allosteric inhibitors of protein-protein interactions with heat shock protein 70 (Hsp70). *J. Med. Chem.* 61, 6163–6177. doi:10.1021/acs.jmedchem.8b00583
- Tavella, T. A., da Silva, N. S. M., Spillman, N., Kayano, A. C. A. V., Cassiano, G. C., Vasconcelos, A. A., et al. (2021). Violacein-induced chaperone system collapse underlies multistage antiparasmodial activity. *ACS Infect. Dis.* 7, 759–776. doi:10.1021/acsinfecdis.0c00454
- WHO (2021). *World malaria report 2021*. Geneva, Switzerland: WHO.
- Wittung-Stafshede, P., Guidry, J., Horne, B. E., and Landry, S. J. (2003). The J-domain of Hsp40 couples ATP hydrolysis to substrate capture in Hsp70. *Biochemistry* 42, 4937–4944. doi:10.1021/bi027333o
- Yang, G. Y., Liao, J., Kim, K., Yurkow, E. J., and Yang, C. S. (1998). Inhibition of growth and induction of apoptosis in human cancer cell lines by tea polyphenols. *Carcinogenesis* 19, 611–616. doi:10.1093/carcin/19.4.611
- Zhang, Q., Ma, C., Oberli, A., Zinz, A., Engels, S., Przyborski, J. M., et al. (2017). Proteomic analysis of exported chaperone/co-chaperone complexes of P. falciparum reveals an array of complex protein-protein interactions. *Sci. Rep.* 7, 42188. doi:10.1038/srep42188
- Zininga, T., Achilonu, I., Hoppe, H., Prinsloo, E., Dirr, H. W., Shonhai, A., et al. (2015a). Overexpression, purification and characterisation of the plasmodium falciparum hsp70-z (PfHsp70-z) protein. *PLoS One* 10, e0129445. doi:10.1371/journal.pone.0129445
- Zininga, T., Achilonu, I., Hoppe, H., Prinsloo, E., Dirr, H. W., Shonhai, A., et al. (2016). Plasmodium falciparum Hsp70-z, an Hsp110 homologue, exhibits independent chaperone activity and interacts with Hsp70-1 in a nucleotide-dependent fashion. *Cell. Stress Chaperones* 21, 499–513. doi:10.1007/s12192-016-0678-4
- Zininga, T., Makumire, S., Gitau, G. W., Njunge, J. M., Poole, O. J., Klimek, H., et al. (2015b). Plasmodium falciparum hop (PfHop) interacts with the Hsp70 chaperone in a nucleotide-dependent fashion and exhibits ligand selectivity. *PLoS One* 10, e0135326. doi:10.1371/journal.pone.0135326
- Zininga, T., Poole, O. J., Makhado, P. B., Ramatsui, L., Prinsloo, E., Achilonu, I., et al. (2017a). Polymyxin B inhibits the chaperone activity of Plasmodium falciparum Hsp70. *Cell. Stress Chaperones* 22, 707–715. doi:10.1007/s12192-017-0797-6
- Zininga, T., Ramatsui, L., Makhado, P. B., Makumire, S., Achilonu, I., Hoppe, H., et al. (2017b). (-)-Epigallocatechin-3-Gallate inhibits the chaperone activity of plasmodium falciparum Hsp70 chaperones and abrogates their association with functional partners. *Molecules* 22, E2139. doi:10.3390/molecules22122139





## OPEN ACCESS

## EDITED BY

Xolani Henry Makhoba,  
University of Fort Hare, South Africa

## REVIEWED BY

Ofentse Jacob Poee,  
University of KwaZulu-Natal, South  
Africa  
Jefferson Leandro Jimenez Restrepo,  
University of São Paulo, Brazil

## \*CORRESPONDENCE

Tawanda Zininga,  
tzininga@sun.ac.za

## SPECIALTY SECTION

This article was submitted to Molecular  
Diagnostics and Therapeutics,  
a section of the journal  
Frontiers in Molecular Biosciences

RECEIVED 06 May 2022

ACCEPTED 15 July 2022

PUBLISHED 11 August 2022

## CITATION

Caillet C, Stofberg ML, Muleya V,  
Shonhai A and Zininga T (2022), Host  
cell stress response as a predictor of  
COVID-19 infectivity and  
disease progression.  
*Front. Mol. Biosci.* 9:938099.  
doi: 10.3389/fmolb.2022.938099

## COPYRIGHT

© 2022 Caillet, Stofberg, Muleya,  
Shonhai and Zininga. This is an open-  
access article distributed under the  
terms of the [Creative Commons  
Attribution License \(CC BY\)](#). The use,  
distribution or reproduction in other  
forums is permitted, provided the  
original author(s) and the copyright  
owner(s) are credited and that the  
original publication in this journal is  
cited, in accordance with accepted  
academic practice. No use, distribution  
or reproduction is permitted which does  
not comply with these terms.

# Host cell stress response as a predictor of COVID-19 infectivity and disease progression

Celine Caillet<sup>1</sup>, Melissa Louise Stofberg<sup>1</sup>, Victor Muleya<sup>2</sup>,  
Addmore Shonhai<sup>3</sup> and Tawanda Zininga<sup>1\*</sup>

<sup>1</sup>Department of Biochemistry, Stellenbosch University, Stellenbosch, South Africa, <sup>2</sup>Department of Biochemistry, Midlands State University, Gweru, Zimbabwe, <sup>3</sup>Department of Biochemistry and Microbiology, University of Venda, Thohoyandou, South Africa

The coronavirus disease (COVID-19) caused by a coronavirus identified in December 2019 has caused a global pandemic. COVID-19 was declared a pandemic in March 2020 and has led to more than 6.3 million deaths. The pandemic has disrupted world travel, economies, and lifestyles worldwide. Although vaccination has been an effective tool to reduce the severity and spread of the disease there is a need for more concerted approaches to fighting the disease. COVID-19 is characterised as a severe acute respiratory syndrome. The severity of the disease is associated with a battery of comorbidities such as cardiovascular diseases, cancer, chronic lung disease, and renal disease. These underlying diseases are associated with general cellular stress. Thus, COVID-19 exacerbates outcomes of the underlying conditions. Consequently, coronavirus infection and the various underlying conditions converge to present a combined strain on the cellular response. While the host response to the stress is primarily intended to be of benefit, the outcomes are occasionally unpredictable because the cellular stress response is a function of complex factors. This review discusses the role of the host stress response as a convergent point for COVID-19 and several non-communicable diseases. We further discuss the merits of targeting the host stress response to manage the clinical outcomes of COVID-19.

## KEYWORDS

SARS-CoV-2, COVID-19, cell stress responses, heat shock proteins, stress proteins, drug target

## 1 Introduction

In December 2019, a novel Severe Acute Respiratory Syndrome Corona Virus 2 (SARS-CoV2) was found to be the cause of the Coronavirus disease (COVID-19) outbreak. SARS-CoV2 spread rapidly worldwide, resulting in a pandemic that started in March of 2020 ([World Health Organization, 2020](#)). To date, it has infected over 556 million people and caused more than 6.3 million deaths globally (<https://www.worldometers.info/coronavirus/>). The pandemic has also negatively impacted international travel, trade, education and social interactions across the globe. Coronaviruses (CoVs) have caused three 21st century outbreaks of SARS-related

## Mechanisms of viral entry

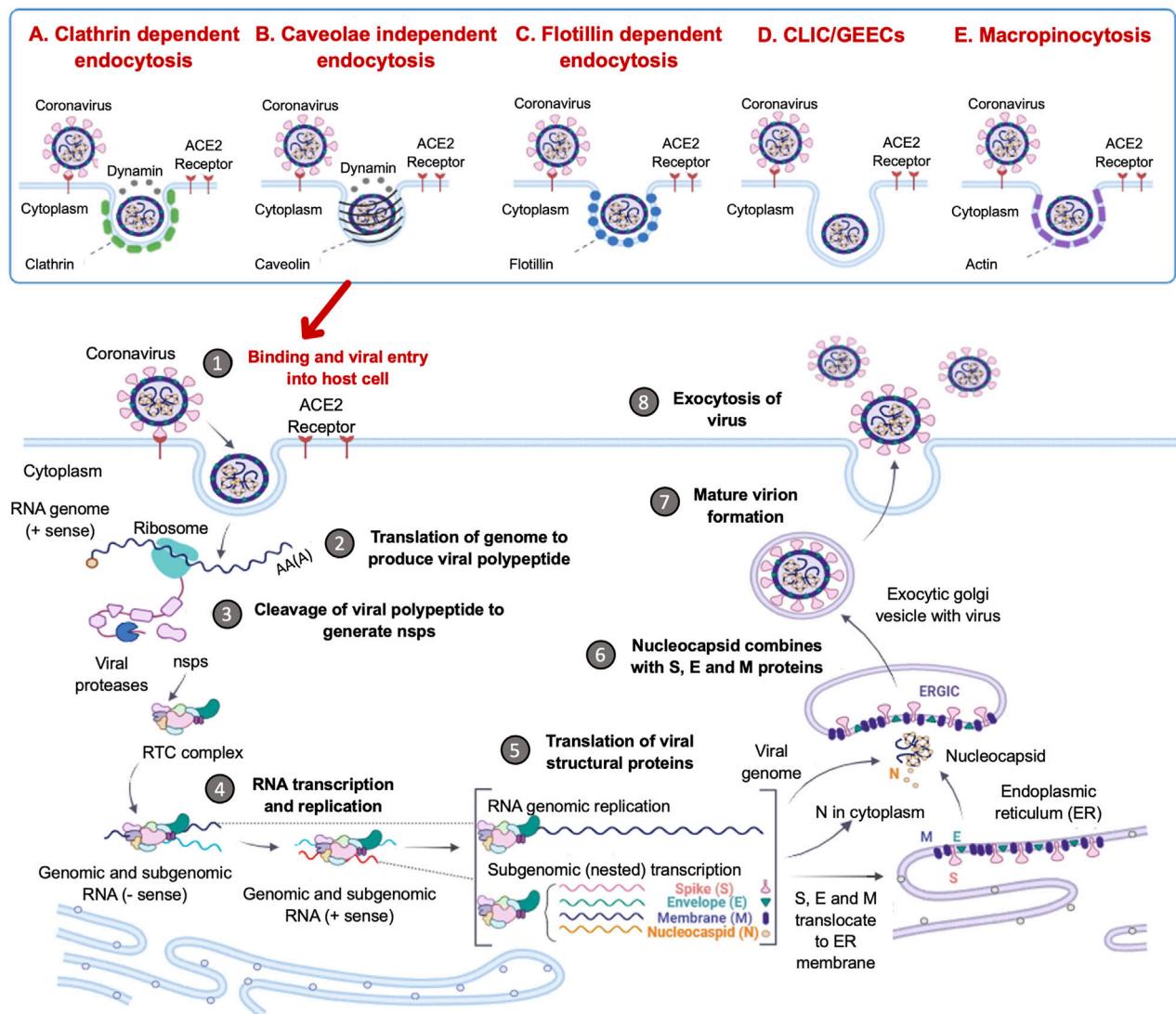


**FIGURE 1**

Coronavirus Life Cycle in the Host Cell. The potential mechanisms of viral entry into the host cell include canonical Clathrin-dependent endocytosis and non-canonical pathways such as: Caveolae-independent endocytosis, Flotillin-dependent endocytosis, CLIC/GEEC endocytosis and Macropinocytosis. After viral entry, the replication of the coronavirus in the target cell is initiated. The RNA genome is uncoated, which allows for the initiation of translation using host ribosomes to produce viral polypeptides. These polypeptides are cleaved by proteases to produce non-structural proteins (NSPs), which are responsible for the formation of the replication-transcription complex (RTC). The RTC facilitates the production of genomic and sub-genomic RNA (-sense and + sense) copies. Following the sub-genomic (nested) transcription, viral structural proteins are produced: spike (S), small envelope (E), membrane (M) and nucleocapsid (N) proteins. The ER facilitates the translation of these viral structural proteins and subsequent embedding on the ER membrane. The nucleocapsids assemble in the cytoplasm and bud off to the Endoplasmic Reticulum-Golgi Intermediate Compartment (ERGIC), where they combine with the structural proteins. The accumulation of viral material causes swelling of the Golgi-apparatus, which results in the formation of smooth structures of virions budding off as enveloped smooth vesicles containing the newly acquired envelopes. These mature virions are released through exocytosis. (Figure created using <https://biorender.com/>).

diseases in humans, namely: SARS-CoV of 2004, Middle East Respiratory Syndrome (MERS-CoV) of 2012 and the current SARS-CoV2 of 2019 (Zhang T. et al., 2020; Zhu et al., 2020). SARS-CoV2 is part of the  $\beta$ -coronavirus genus which shares 79% sequence identity with SARS-CoV and 50% with MERS-CoV

(Wang Y. et al., 2020). The clinical features of COVID-19 are flu-like symptoms, including nasal congestion, sore throat and dry cough, which can lead to severe pneumonia (Zhu et al., 2020). Severe cases of COVID-19 infection have been reported to be associated with comorbidities such as chronic respiratory and

cardiovascular diseases, diabetes, hypertension, and cancer. In these cases, the main causes of death are shock, respiratory and multiple organ failures. This review will mainly focus on the host stress response process to SARS-CoV2 infection and discuss the roles of host cell stress pathways in regulating the progression of the various comorbidities associated with the infection. We further discuss the therapeutic potential of targeting these processes.

## 2 SARS-CoV2 as a cellular stressor

SARS-CoV2 entry into host cells is an important step in viral infectivity and pathogenesis. To facilitate entry, the viral surface-exposed spike glycoprotein (S) attaches to the host cell receptors. The S protein has a receptor-binding domain (RBD), which contains a cleavage site where it is first preactivated with a proprotein convertase furin. Once it is processed, the RBD binds to the human angiotensin-converting enzyme 2 (ACE2) receptor on the host cells (Zhang H. et al., 2020). Studies have shown that SARS-CoV2 utilises the same ACE2 receptor as SARS-CoV to enter the host cell via its S protein (Hoffmann et al., 2020). The RBD is generally believed to facilitate receptor-mediated endocytosis for viral entry into the host cells (Petersen et al., 2020). However, several other mechanisms of viral entry have been proposed (Figure 1). These mechanisms include: A. The canonical clathrin-mediated endocytosis pathway, which is thought to be ACE2 receptor-dependent and pH-sensitive (Milewska et al., 2018; Yang and Shen, 2020); B. The non-canonical caveolae independent endocytosis pathway (Szczepanski et al., 2018), which involves anchored lipid rafts and micropinocytosis (Glebov, 2020); C. Flotillin-1-associated endocytosis; D. Clathrin-independent carrier (CLIC)/glycosylphosphatidylinositol-anchored protein-enriched endosomal compartment (GEEC) endocytosis and E. Macropinocytosis (Glebov, 2020). These various entry pathways are thought to be utilised by the virus depending on the target cell types. It has been reported that more than one mechanism of host entry could be employed by SARS-CoV2 (Yang and Shen, 2020).

Following the entry of the virus into the host cell via an endosome, lysosomal proteases facilitate viral uncoating to release the RNA genome in the cytoplasm. When the released positive-sense RNA genome is translated at the ribosome to produce viral polypeptides and structural proteins. This is followed by the transcription of the viral genes with subsequent packaging in the nucleocapsids (Figure 1). In the first event, the positive-sense RNA genome is translated into two large viral polyproteins, namely: PP1a and PP1b, that are encoded from approximately two-thirds of the viral genome (Chen et al., 2020; Hidalgo et al., 2021). These viral polyproteins are cleaved by viral encoded chymotrypsin-like

proteases (3CLpro) and papain-like proteases, to yield 16 non-structural proteins (NSP1-16) (Andersen et al., 2020; Uddin et al., 2020). The second event is facilitated by NSPs that form the replication-transcription complex (RTC) which facilitates the transcription and replication of the remaining one-third of sub-genomic mRNAs encoding for the four main structural proteins, namely: spike (S) receptor binding, envelope (E), membrane (M) and nucleocapsid (N) (Gordon et al., 2020; Kim et al., 2020). Thereafter, the structural proteins are embedded onto the Endoplasmic Reticulum-Golgi Intermediate Compartment (ERGIC) or on the Endoplasmic Reticulum (ER). These newly synthesised genomic RNA molecules and proteins accumulate to form the nucleocapsid. The modified ERGIC containing the viral structural proteins, buds off the ER and encloses the nucleocapsid to form a mature virion (Klumpperman et al., 1994). The new virions are prepared for secretion through exocytosis via the Golgi apparatus. During this process, the ER membranes are depleted and the cell protein folding machinery is hijacked to process these viral proteins. These events exert stress upon the infected cell. Interestingly, it has previously been established that the stress-induced expression of heat shock proteins (Hsps) in *Drosophila* restricts viral infectivity (Merkling et al., 2015).

## 3 Overview of stress proteins

Stress proteins (SPs) are a set of molecular chaperones, whose expression is upregulated in response to cellular stress. These SPs are involved in cytoprotection by facilitating protein folding and unfolding, protein activation and the assembly of protein complexes. Cellular stress response modulates pathways that stimulate cell survival or cell death and the dysregulation thereof. For this reason, cell stress response is implicated in various human diseases including cardiovascular diseases, neurodegenerative diseases, cancer and some other infectious diseases. Hsps, along with the predominantly ER localised Protein Disulphide Isomerases (PDI) (Wan et al., 2020), constitute key components of the cellular stress response machinery. Hsps are generally classified into several different families based on their average molecular sizes in kDa as well as sequence conservation. They fall within the following key groupings: Hsp110, Hsp100, Hsp90, Hsp70, Hsp60, Hsp40 (also known as J domain proteins; JDP) and lastly, small Hsps (sHsps) (Figure 2). Due to their central role, Hsps are implicated in several cellular pathways and are inherently linked to various pathologies (Favatier et al., 1997; Edkins et al., 2018).

### 3.1 The Hsp100 protein family

In humans, there are six Hsp100 members with diverse functions. Two members exhibit protein disaggregation

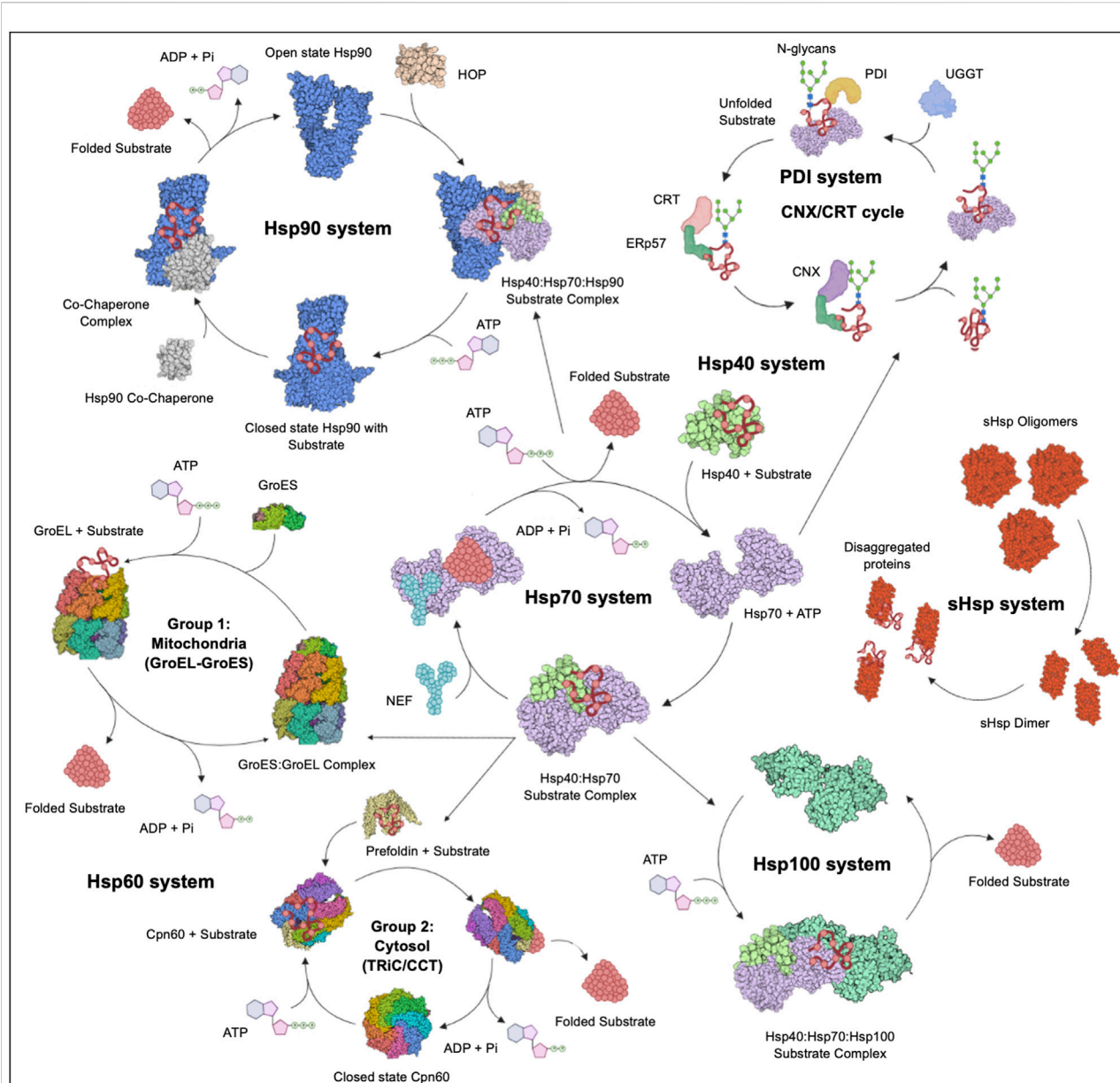


FIGURE 2

The Hsp chaperone system. The Hsp40 chaperone system recruits nascent substrate proteins and transports them to the Hsp70 folding system. Thereafter, the folded clients are transferred over to the Hsp90 system for activation or assistance to form multiple protein complexes. The more complex substrates are brought to the Hsp60 (GroEL) and TRiC systems. Unfolded proteins are transferred to the Hsp100 system for disaggregation in cooperation with the sHsp system. The CRT and CNX recruit Hsp folded glycoproteins to PDIs for further folding and disulphide bond stabilisation. Figure adapted from the HSP information resource database (<http://pdslab.biochem.iisc.ernet.in/hspir/index.php>).

capabilities, while the other four members are proteases (represented by caseinolytic protease (Clp)). Structurally, Hsp100s are grouped into two groups, type 1 and type 2. Type 1 refers to members with two AAA+ ATPases domains, namely the NBD 1 and NBD2. These domains are characterised by the presence of two walker motifs (1 and 2) and a middle domain between the NBDs (Zolkiewski et al., 2012). Hsp104/

ClpB, ClpA, ClpC and Hsp78 constitute the type I cluster. The type 2 members of the Hsp100 members, ClpP and Hsv, possess a single NBD2 but lack the middle domain. Hsp100 proteins have been implicated in neurodegenerative diseases and other protein-folding-related diseases. Their implication in these pathologies is based on their role in suppressing and reversing protein aggregation (Ferrari et al., 2018). As a disaggregase,



Hsp100 occurs in complex with Hsp70, Hsp110 and Hsp40 (Kaimal et al., 2017; Lin et al., 2022). This highlights that while the functions of the various Hsps are unique, they also cooperate to manage cellular stress.

### 3.2 The Hsp90 protein family

Five human Hsp90s are localised within the cytosol, ER and mitochondria. The three cytosolic paralogs include: the stress-inducible  $\alpha$ -Hsp90 (HSP90AA2/HSPC2), the truncated chimeric Hsp90 (HSP90AAA1/HSPC1) and the housekeeping  $\beta$ -isoform (HSPB1/HSPC3) (Chen et al., 2005). The ER and mitochondria host the 94 kDa glucose-regulated protein (Grp94/HSPC4) and the tumour necrosis factor receptor-associated protein-1 (TRAP 1/HSPC5) respectively (Kampinga et al., 2009). Structurally, these proteins share a conserved domain architecture that comprises the N-terminal ATPase domain, the middle domain with substrate binding capability and the C-terminal dimerization domain (Jackson, 2012). Hsp90s are ATP-dependent molecular chaperones that play a central role in protein homeostasis (Obermann et al., 1998; Chakraborty and Edkins, 2021). The function of Hsp90 is regulated by several co-chaperones (Bachman et al., 2018). In the ADP-bound state, the clients/substrates are recruited into an early complex consisting of the Hsp70/Hsp40/Hsp-interacting protein (HIP) and the Hsp90/Hsp70-organising protein (Hop) (Luengo et al., 2019). ATP hydrolysis is activated by the Hsp90 ATPase activator 1 (AHA1; Oroz et al., 2019). Following nucleotide exchange, the Hsp90 forms a mature complex with co-chaperones p23, p50, cell division cycle 37 (cdc37) and immunophilins (Biebl et al., 2020). Furthermore, post-translational modification of Hsp90 through phosphorylation (Xu et al., 2019) and acetylation (Mollapour and Neckers, 2012), regulates its functional specificity (Prodromou, 2016). Host Hsp90 substrates that are associated with the possible uptake of viruses include those responsible for transcription, translation, mitochondrial function, kinetochore assembly, centrosome function and maintenance of the cell cycle (Lubkowska et al., 2021). Hsp90 also facilitates membrane trafficking and membrane deformability during the release of exosomes (Lauwers et al., 2018). There is a wide array of Hsp90 clients, most of which are molecules involved in signal transduction. Hsp90 facilitates the conformational maturation of several of its client. In addition, Hsp90 is also involved in the ordered assembly and stabilisation of subunits of multiprotein complexes (Makhnevych and Houry, 2012). This highlights a possible central role of this chaperone in viral replication within the host. To this end, inhibitors of Hsp90 are of interest as possible therapies against COVID-19 (Ramos and Ayinde, 2021; Wyler et al., 2021; Biancatelli et al., 2022).

### 3.3 The Hsp70 family

At least seventeen members of the Hsp70 family of chaperones are found in humans. Hsp70s are grouped into two subfamilies: canonical members (Hsp70) and non-canonical members (Hsp110) subgroup. There are 13 canonical Hsp70s which resemble the prokaryotic Hsp70, represented by *E. coli* DnaK. They include the cytosolic Hsp70-1/Hsp72/HSPA1A, HSPA1B/Hsp70-2, HSPA1L/Hum70t, HSPA2, Hsp70B/HSPA6, HspA7/Hsp70-7, Hcs70/HSPA8, HSPA12A/FLJ13874, HSP112B/RP23-32L15.1, HSPA13/Stch and HspA14/Hsp70-4; the ER localised Grp78/Bip/HSPA5 and the mitochondrial localised mortalin/GRP75/HSPA9. Hsp110 members include, the cytosolic Hsp105/HSPH1, Apg-2/Hsp110/HSPH2, Apg-1/HSPH3 and the ER localised Grp170/HSPH4 (Easton et al., 2000; Kampinga et al., 2009; Chakafana and Shonhai, 2021). Structurally, Hsp70s are composed of an N-terminal nucleotide-binding domain (NBD) that exhibits ATPase activity and a C-terminal substrate-binding domain (SBD). The Hsp110 subfamily displays a similar domain architecture, however, they have a long acidic insertion in the SBD, making them larger members (Oh et al., 1999; Chakafana et al., 2019). Hsp110 functions as a chaperone, whilst also facilitating nucleotide exchange for its canonical Hsp70 counterparts (Dragovic et al., 2006; Andreasson et al., 2008). The Hsp70 chaperone plays a central role in the folding of nascent polypeptides released from the ribosomes. It also refolds misfolded proteins and as well as facilitates the assembly of multiprotein complexes (Figure 2). In addition, Hsp70 also cooperates with Hsp90 and Hsp60 to facilitate the maturation of some of its clients (Luengo et al., 2019; Wang et al., 2022).

The primary co-chaperone of Hsp70s are the Hsp40 proteins (JDP). Hsp40s are composed of a conserved J domain that facilitates the interaction with Hsp70, activating ATP hydrolysis by the latter (Cintron and Toft, 2006; Kampinga et al., 2009). Hsp40s are also known to recruit substrates to Hsp70 and are therefore called substrate scanners (Fan et al., 2003). Hsp70 has a high affinity for substrates in the ADP-bound state. To facilitate substrate release, the nucleotide exchange factors (NEFs), such as Hsp110, exchange ADP for ATP (Dragovic et al., 2006; Alderson et al., 2016). These functions contrast with HIP, which locks Hsp70 in the ADP-bound state (Nollen et al., 2001). Therefore, the action of NEFs and HIP determines the substrate residency time on Hsp70, which influences substrate fate. Hsp70 was found to be one of the distinct biomarkers circulating in COVID-19 ICU cases (Fraser et al., 2020). Considering the cytoprotective role of Hsp70, it has been proposed that the periodic fever conditions associated with COVID-19 infections, may benefit the host by stimulating the expression of this chaperone (Guihur et al., 2020).

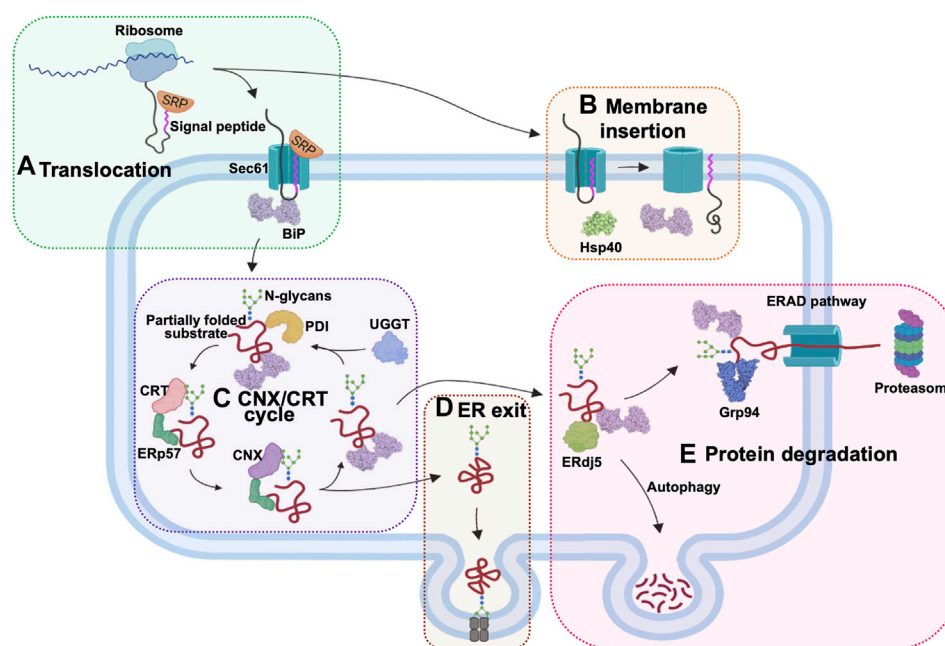


FIGURE 3

The role of ER chaperones in proteostasis. The ER-localised chaperones have numerous roles in this cellular organelle. (A) ER chaperones enable the translocation of proteins into the ER. Newly synthesized proteins are targeted by the signal recognition particle (SRP) as they emerge from the ribosomes. The SRP-bound protein enters the ER through the Sec61 translocon protein channel and is bound by Hsp70 (Grp78/BiP) inside the ER lumen for active import. (B) Chaperones also facilitate post-translational ER membrane insertion of proteins. (C) The CNX/CRT chaperone system facilitates proper glycosylation of proteins targeted for various cellular compartments. (D) ER chaperones are involved in processing the exit of the proteins via the ERGIC pathway. (E) Proteins that are not properly folded are bound by ERdj5, BiP, and Grp94 in the ER and channelled for degradation by autophagy or through the ERAD pathway in the cytosol.

The ER-based chaperones have widespread functions in nearly every stage of protein processing (Figure 3). During protein import into the ER lumen, newly synthesised polypeptides that emerge from the ribosomes, are recognized by the signal recognition particle (SRP), which transports these proteins to the ER membrane for translocation via the Sec61 channel (Haßdenteufel et al., 2018; Jomaa et al., 2022). The ER-resident Hsp70 (Grp78/BiP), binds incoming peptides and actively threads them into the ER lumen (Craig, 2018; Haßdenteufel et al., 2018). BiP and the ER-resident Hsp40 (ERdj5), play a role in the post-translational insertion of proteins into the ER membrane (Araki and Nagata, 2012). They also facilitate the processing of aggregated membrane proteins, by earmarking them for degradation. Additionally, ER chaperones also facilitate the export of proteins from the ER through their involvement in the ERGIC pathway (Ito and Nagata, 2019). Irreparably misfolded proteins are destroyed by autophagy or redirected to the ER-associated degradation (ERAD) pathway for destruction in the proteasomes located in the cytosol (Oikonomou and Hendershot, 2020; Braakman and Hebert, 2021). This pathway involves the ER-resident chaperones such as ERdj5, BiP and Grp94, which bind and target substrates for degradation (Adams et al., 2019).

### 3.4 The Hsp60 chaperonins

Hsp60 proteins are ATP-dependent chaperonins and are classified into two main groups, namely, type 1 and type 2 (Okamoto et al., 2017; Ishida et al., 2018). Type 1 chaperonins are mainly found in the mitochondria of eukaryotes and in the cytoplasm of prokaryotes (GroEL in *E. coli*). This class of chaperonins form a 7-member ring back-to-back complex with a central core, which then requires Hsp10 (GroES in *E. coli*) to close the core, functioning as a lid (Enriquez et al., 2017). The type 2 chaperonins, which include the cytosolic TCP1-ring complex (TRiC), are not well studied but are found in the archaeal chromosome and eukaryotic cytosol. They form a similar dimerization of the 8-9 protomer complexes to make 16–18 subunits joined end to end, forming a barrel structure with a central core (Ishida et al., 2018). Similar to type 1 chaperonins, the central core is closed by the Hsp10 protein. Some Hsp60s escape the mitochondria and translocate to the circulatory system, where they are known to induce proinflammatory cytokines. For this reason, Hsp60 is implicated in hypertension and is therefore thought to aggravate COVID-19 related complications (Jakovac, 2020).

### 3.5 Small heat shock proteins

In humans, there are eleven members of the small heat shock protein (sHsp) family of chaperones. They include HSPB1/Hsp25, HSPB2/Hsp27, HSPB3/Hspl27, HSPB4/crystallin  $\alpha$ -A, HSPB5/crystallin  $\alpha$ -B, HSPB6/Hsp20, HSPB7/cvHsp, HSPB8/Hsp22, HSPB9/FLJ27437, HSPB10/ODF1 and HSPB11/Hsp16.2 (Kampinga et al., 2009). Structurally, sHsps have a conserved  $\alpha$ -crystallin domain, sandwiched with a variable N-terminal region and the C-terminal regions. These sHsps exhibit holdase chaperone activity which is ATP-independent. They function in complexes to minimise protein unfolding and serve as holdases (Haslbeck et al., 2019). The most studied sHsps are the Hsp27, crystallin  $\alpha$ -A and crystallin  $\alpha$ -B. Of these, only Hsp27 has been implicated in COVID-19 pathology (Wendt et al., 2021).

### 3.6 Protein disulphide isomerases

Protein Disulphide Isomerases (PDIs) are oxidoreductases that catalyse the enzymatic reduction and isomerization of disulphide bridge formation (Appenzeller-Herzog and Ellgaard, 2008). In eukaryotes, almost a third of the cellular proteome contains disulphide bonds (Mahmood et al., 2021). In the ER, the PDIs stabilise and promote the folding of client proteins into three-dimensional structures (Kranz et al., 2017). In humans, there are 19 PDIs localised in the ER (Ellgaard and Ruddock, 2005). Generally, the PDIs are characterised by the CXXC active site motif, where the cysteine residues take part in the exchange of disulphide bond formation to stabilise client proteins. PDIs are also involved in ER protein degradation (ERAD) and calcium level regulation (Kramer et al., 2001; Riemer et al., 2011). The most studied PDI is PDIA3 (Erp57/Grp58), which is comprised of the canonical four thioredoxin domain structure of the **a-b-b-a** domain organisation. In general, the **a**-domains of PDIs contain the catalytic CXXC active site motif, which can exhibit thiol-sulphate reductase, oxidase or isomerase activity (Darby and Creighton, 1995; Chichiarelli et al., 2022). The **b**-domains bind substrates with high affinity to facilitate isomerization (Klappa et al., 1998). The PDIA3 **b**-domains do not directly interact with substrate proteins but rather indirectly through their association with lectins, calreticulin (CRT) and calnexin (CNX) (Oliver et al., 1999; Molinari et al., 2004). The CRT and CNX recruit glycoproteins to PDIA3 for correct folding and disulphide bond stabilisation. If the PDI fails to achieve a competent fold, the substrate protein undergoes re-glycosylation by the glucose:glycoprotein:glucosyl transferase (UGGT) to repeat the cycle (Kozlov and Gehring, 2020; Mahmood et al., 2021). Therefore, PDIs play an essential role in protein disulphide bond formation and protein glycosylation quality control mechanisms that are thought to be essential for SARS-CoV2

protein maturation (Fu et al., 2020). Abnormalities in these protein quality control systems in all cell organelles, have severe consequences for the cell and have been implicated in several diseases (Parakh and Atkin, 2015; Chamberlain and Anathy, 2020). Protein folding aberrances are at the centre of diseases such as cancer, neurodegenerative disorders, metabolic diseases, and infections (Gómez et al., 2018).

## 4 COVID-19 susceptibility profiles

SARS-CoV2 pathogenesis is mainly exacerbated by underlying cellular stress, which is more pronounced in patients with comorbidities such as diabetes, cardiovascular disease, hypertension and obesity among others (Sanyaolu et al., 2020). Generally, viral infections are associated with inflammation, a hallmark of COVID-19 pathology (Varga et al., 2020), which further puts strain on the protein folding system (Kuppalli and Rasmussen, 2020; McGonagle et al., 2020). The role of Hsps in immunomodulation is well established and appears to be a function of their circulating levels (Zininga et al., 2018). Thus, the expression profiles of these proteins in various disease conditions could serve as biomarkers of disease severity and patient outcomes (Table 1).

### 4.1 Chronic lung diseases

Chronic lung diseases include a wide array of diseases such as asthma, Chronic Obstructive Pulmonary Diseases (COPD), Interstitial Lung Diseases (ILD), cystic fibrosis, lung cancer and chronic pneumonia to name a few (Cottin, 2013; Celli and Wedzicha, 2019). Chronic lung diseases cause excessive inflammation, immune dysregulation, and impaired repair processes, which ultimately leads to tissue damage and diminished organ function (Meikle et al., 2021). Chronic inflammation is a prominent symptom of chronic lung diseases and causes elevated levels of reactive oxygen species (ROS) in cells, resulting in oxidative stress (Hulgan et al., 2003; Sharif-Askari et al., 2021). Excessive ROS may stimulate prolonged inflammatory responses and signalling cascades that damage cells, which may lead to apoptosis (Chatterjee, 2016; Ivanov et al., 2017).

Hsp70 is variably expressed depending on the nature of the conditions affecting the lungs. The elevated expression of Hsp70 associated with asthma may trigger either pro- or anti-inflammatory pathways, due to its diverse immunomodulating effects (Shevchenko et al., 2020). Hsp70 and Hsp27 expression levels were elevated in lung tissues of patients with COPD, when compared to healthy controls, and were correlated to disease severity (Dong et al., 2013; Zimmermann et al., 2020). In Idiopathic Pulmonary Fibrosis (IPF), one of the common interstitial lung diseases, Hsp70s were observed to be

TABLE 1 The role of Hsp expression levels in diseases.

Disease (COVID-19 co-morbidity state)	Implicated Hsp	Implication on inflammation/disease severity	References
<b>Chronic lung diseases</b>			
•Asthma	Hsp70↑	Triggers both pro- and anti- inflammatory responses	Choi et al. (2021) Shevchenko et al. (2020)
•Chronic obstructive pulmonary diseases (COPD)	Hsp27↑; Hsp70↑	Elevated serum concentrations of Hsp27 and Hsp70 is a strong predictor of mortality	Gerayeli et al. (2021) Celli and Wedzicha, (2019) Zimmermann et al. (2020) Dong et al. (2013)
•Interstitial lung diseases (ILD)	Hsp70↓; Hsp90↑	Reduced Hsp70 and increased Hsp90 trigger pro-inflammatory responses	Skolnik and Ryerson, (2016) Cottin, (2013) Sellaes et al. (2019) Chen et al. (2018) Storkanova et al. (2018)
<b>Chronic kidney diseases</b>			
	Hsp27↑; Hsp72↑ Hsp90↑	Reduced Hsp27 and Hs72 triggers pro-inflammatory responses and protects cells Increased Hsp90 enhances oxidative stress and inflammation	Marzec et al. (2009) Musial et al. (2010) Musial and Zwolińska, (2011)
<b>Obesity</b>			
	Hsp60↑; Hsp72↑; Hsp90↑; Hsp70↑; Grp94↑; Hsp40↓	Increased expression of Hsps is linked to increased inflammation Decreased Hsp40 may be implicated in regulation of insulin resistance	Sell et al. (2017) Märker et al. (2012) Tiss et al. (2014)
<b>Diabetes</b>			
	Hsp60↓; Hsp70↓; Hsp72↓; Hsp90↑	Reduced expression of Hsp 60 and Hsp70 is associated with increased inflammation  Decreased Hsp72 expression is linked to insulin resistance  Upregulated Hsp90 contributes to inflammation and vascular complications	Bijur et al. (2000) Archer et al. (2018) Khadir et al. (2018) Lee et al. (2013) Zilae and Shirali, 2016 Amawi et al. (2019)
<b>Cardiovascular diseases</b>			
	Hsp27↓; Hsp60↑; Hsp90↑; Hsp70↑	Low Hsp27 associated with cardiac disease and death  Increased Hsp60, Hsp70 and Hsp90 associated with atherosclerosis and cardiac failure	Jaroszyński et al. (2018) Duan et al. (2020) Ranek Mark et al. (2018) Rodriguez-Iturbe and Johnson, (2018)
<b>Cancers</b>			
•Neuroblastoma	Hsp27↓; Hsp60↑	Increased levels of Hsps in cancer cells lead to cancer cell proliferation, metastasis, immunomodulation, and prevention of apoptosis	Wu et al. (2017a)
•Renal	Hsp70↓		
•Pancreatic	Hsp90↑; Hsp110↑		
•Ovarian	Hsp40↑; Hsp90↑		
•Breast	Hsp27↑; Hsp40↑; Hsp60↑; Hsp70↑; Hsp90↑; Hsp110↑		
•Colon	Hsp40↑; Hsp70↑		
•Lung	Hsp27↑; Hsp40↑; Hsp60↓; Hsp70↑; Hsp90↑		
•Liver	Hsp27↑; Hsp60↑; Hsp70↑; Hsp90↑; Hsp110↑		
			Luo et al. (2020) Mittal and Rajala, (2020) Cedrés et al. (2018) Sun et al. (2018) Jiang and Shen, (2020) Wu et al. (2017a)

The level of expression of Hsps present in each disease state is indicated with the arrow direction for upregulated (↑) and downregulated (↓) expression levels.



downregulated in response to an increase in the profibrotic molecules, IGFBP5 (insulin-like growth factor-binding protein 5) or (TGF  $\beta$ 1) transforming growth factor- $\beta$ 1 (Sellares et al., 2019). Thus, Hsp70 suppression perpetuates fibrosis development in the human fibroblasts. Hsps alleviate oxidative stress through their active roles in the refolding of damaged proteins and PDIs are important for maintaining a redox balance inside the cells suppressing the development of pulmonary fibrosis (Parakh and Atkin, 2015; Marinova et al., 2020; Tanguy et al., 2021).

One of the major complications of COVID-19 is the development of acute respiratory distress syndrome (ARDS), a condition that tremendously impairs the ability of the lungs to absorb oxygen (Meikle et al., 2021). In a 2007 study, lung injury was induced in rats, whereafter the rats were administered with adenoviral vectors expressing Hsp70 proteins (Weiss et al., 2007). It was observed that Hsp70 limited NF- $\kappa$ B activation, which in turn limited the proteasomal degradation of I $\kappa$ B $\alpha$ . Indeed, Hsp70 expression is reportedly elevated in ARDS (Alreshidi et al., 2021), and is known to inhibit intracellular proteasomal degradation (Ryu and Ha, 2020). It was observed that Hsp70 limited NF- $\kappa$ B activation, which in turn limited the proteasomal degradation of I $\kappa$ B kinase signalosome, thereby suppressing inflammation (Weiss et al., 2007). Thus, by suppressing inflammation, Hsp70 expression may indirectly regulate COVID-19 pathology (Sharif-Askari et al., 2021). Additionally, it was reported that several oxidative stress genes are upregulated during Coronavirus infection and expression of these genes is thus likely induced by SARS-CoV2 (Sharif-Askari et al., 2021). Hsp70 being a central player in preventing the accumulation of oxidative stress, might be similarly affected by SARS-CoV2. Although not yet experimentally confirmed, there might be a link between the dysregulation of Hsp70 and other stress proteins and the severity of SARS-CoV2 infection.

## 4.2 Chronic kidney disease

Chronic Kidney Disease (CKD) is a condition characterised by glomerulosclerosis and interstitial fibrosis (Musiał and Zwolińska, 2011). CKD is commonly a result of stress inflicted on hepatocytes from various sources such as, uremic toxins, pro-inflammatory molecules, reactive oxygen species, pro-apoptotic molecules, infectious agents, and dialysis (Nayak Rao, 2016). Several studies reported that the level of Hsp72 expression was upregulated in patients with CKD (Musiał and Zwolińska, 2011; Leberherz-Eichinger et al., 2012; Morales-Buenrostro et al., 2014). The presence of uremic toxic may cause increased expression of Hsp72, which has been shown to inhibit the proliferation and apoptosis of renal tubular cells, resulting in reduced renal fibrosis (Pan et al., 2020). Chronic kidney damage is also thought to be associated with noxious

conditions where upregulated Hsp72 suppresses apoptosis (Rao, 2016). Although research regarding the role of Hsps in CKD is limited, more work on the role of these proteins in renal dialysis has been conducted. It has been observed that renal ischemia-reperfusion injury (IRI), incurred during renal dialysis, resulted in an induction of Hsp72 (43-fold increase) and Hsp27 (12-fold increase) (Nayak Rao, 2016). Additionally, Hsp70 offers protective properties from renal IRI that include, cytoskeletal stabilization, anti-inflammatory effects, anti-apoptotic properties, and influence over the stimulation of regulatory T-cells (Nayak Rao, 2016). These functions of Hsp70 and sHsp are potentially important in reducing further complications upon the onset of SARS-CoV2 (ERA-EDTA Council et al., 2021). Furthermore, elevated levels of Hsp90 observed in CKD patients are associated with increased oxidative stress and inflammation (Musiał and Zwolińska, 2011).

## 4.3 Obesity

Obesity is a metabolic syndrome generally linked to the increased severity of several non-communicable diseases such as, type 2 diabetes mellitus (T2DM), cardiovascular diseases (CVD) and certain cancers (Blüher, 2019). The accumulation of adipose tissue and the increases in energy inputs associated with obesity often triggers chronic inflammation in the fatty tissues (Sell et al., 2017). This inflammation results in an increase in proinflammatory cytokines, both locally and systemically (Lehr et al., 2012; Sell et al., 2012; Tiss et al., 2014). The role of Hsps in inflammation in obese individuals is not well established, as conflicting results have been reported. For example, increased levels of Hsp60, Hsp72, Hsp90, Hsp70 and Grp94 released from adipocytes under stressful conditions have been shown to act as adipokines, linking their expression to obesity and chronic inflammation (Märker et al., 2012; Tiss et al., 2014; Sell et al., 2017). Conversely, individuals with obesity and insulin resistance were reported to exhibit suppressed heat shock response (HSR) activity which by extension results in reduced Hsps expression, as insulin signalling is essential to HSR activity (Di Naso et al., 2015; de Lemos Muller et al., 2018; Bruxel et al., 2019). This contrasts with normal inflammatory conditions where the HSR upregulates Hsp production, which counteracts the inflammatory response (Singh and Hasday, 2013; Zininga et al., 2018; Krause et al., 2020). The decreased HSR activity in obese individuals could be responsible for the dysregulated inflammation and negative prognosis in individuals infected with SARS-CoV-2 (Krause et al., 2020). Unlike the other Hsps, Hsp40 expression is decreased in obese individuals. A study reported that normal levels of Hsp40 were restored upon exercise, suggesting a possible role for this protein in the regulation of insulin resistance and thus mitigating against obesity (Tiss et al., 2014).

## 4.4 Diabetes

The metabolic disorder, T2DM, is characterised by the dysregulation of insulin production and activity, leading to chronically elevated levels of sugar in the blood. The disruption of insulin production associated with diabetes, in turn, disrupts the insulin signalling pathway which is a crucial part of the HSR system. Insulin inhibits the activity of the glycogen synthase kinase-3 $\beta$  (GSK-3), which suppresses the activation of HSF-1, abrogating its interaction with heat shock elements, an important step in regulating transcription of HSP genes (Bijur et al., 2000). Without insulin to inhibit the activity of GSK-3, HSR activity is downregulated and so is the expression of Hsps. Therefore, patients with diabetes are more susceptible to severe infections as they are unable to regulate the resulting inflammation, culminating in further complications (Krause et al., 2020). This partially explains the increased case fatality in individuals infected with COVID-19 when compared to non-diabetic patients (Xue et al., 2020). T2DM patients display dysregulated levels of Hsp60, Hsp70 and Hsp72, which contribute to inflammation and insulin resistance and vascular complications (Khadir et al., 2018; Zilae and Shirali, 2016; Amawi et al., 2019).

## 4.5 Cardiovascular diseases

Cardiovascular diseases (CVD) are characterised by cellular stress, in which a collection of cardioprotective Hsps are released in the heart (Henderson and Pockley, 2012; Ranek Mark et al., 2018). Several Hsps including Hsp27, Hsp60, Hsp70 and Hsp90, are secreted and released at different rates during coronary stress (Jaroszyński et al., 2018; Duan et al., 2020; Krishnan-Sivadoss et al., 2021). A high secretion of Hsp27 has been shown to offer some cardioprotection, whilst low Hsp27 serum levels, especially in older patients, has been associated with carotid atherosclerosis and oxidative stress. This leads to an increased risk of cardiovascular disease and sudden cardiovascular death (Jaroszyński et al., 2018). Upon cardiac injury, Hsp60 is released into the extracellular fluid, where it activates the body's innate immunity through the induction of a proinflammatory state in the heart. The subsequent increase in the production of the tumour necrosis factor, TNF- $\alpha$ , facilitates apoptosis and thus attributes to the progression of heart failure (Duan et al., 2020).

Upregulated Hsp60 expression has been found in atherosclerotic lesions and has increased the risk of atherosclerosis (Grundtman et al., 2011). In addition, the cross-reactivity of the immune system with autologous Hsp60 and Hsp70 results in T-cell adhesion to endothelial cells and the initial inflammatory response of atherosclerosis (Rodriguez-Iturbe et al., 2019; Duan et al., 2020). Consequently, autoantibodies produced against either Hsp60 or Hsp70 were

reported to exacerbate atherosclerosis (Schett et al., 1997; Stocker and Keaney, 2004; Wick et al., 2014) and hypertension (Rodriguez-Iturbe et al., 2019; Romagnoli et al., 2020). Therefore, Hsp60 and Hsp70 are intricately involved in the development and progression of atherosclerosis and subsequent complications in other diseases. Notably, there are increasing reports linking the induction of Hsp70, Hsp90 and co-chaperones to heart failure (Ranek Mark et al., 2018; Rodriguez-Iturbe and Johnson, 2018).

Patients who become infected with SARS-CoV2, whilst having underlying cardiovascular conditions, have a higher risk of developing a severe infection, myocarditis, and blood clots, which increases the chance of death (Huang et al., 2020; Srivastava, 2020). This is due to a combination of the effects of a viral infection, coupled with the stress caused by the underlying cardiovascular conditions (Srivastava, 2020). Consequently, the intricate involvement of Hsps in several cardiovascular diseases most likely influences the severity of COVID-19 in these patients. Hsp60 appears to be the most studied Hsp implicated in cardiovascular diseases and COVID-19 (Jakovac, 2020). For example, one study hypothesized that the high levels of Hsp60 present in the plasma of hypertensive patients contribute to the cytokine release syndrome (Song et al., 2020). This is the main mechanism responsible for the third hyperinflammatory phase of COVID-19, which often leads to heart failure (Romagnoli et al., 2020). SARS-CoV2 also causes substantial tissue damage, which can result in the release of intracellular Hsp60 into the plasma. Subsequently, this causes an increase in pre-existing Hsp60 levels and could result in systemic hyper inflammation, causing damage to multiple organs (Romagnoli et al., 2020). It was also found that Hsp60 levels in the plasma positively correlate to acute lung injury and systemic inflammatory responses in patients with no prior pulmonary trauma (Pespeni et al., 2005). Although more research is required to fully understand the role of Hsps in heart failure, there is a common consensus that these proteins have important therapeutic and diagnostic considerations in COVID-19.

## 4.6 Cancer

Cancer is a disease state during which abnormal cells grow rapidly and uncontrollably, such that they have harmful effects on tissues and organs. Cancerous cell propagation is highly dependent on stress proteins to assist in the folding of improperly folded and mutated proteins, for their continued dysregulated growth and development (Wu et al., 2017a; reviewed in Chakafana and Shonhai, 2021). The underlying causes and mechanisms involved in Hsp expression are not fully understood. For example, Hsp27 and Hsp70 expression is downregulated in neuroblastoma and renal cancer respectively (Wu P. et al., 2017). Conversely, in hepatocellular carcinoma

(HCC), the upregulation of Hsp27 plays a cytoprotective role in preventing cancerous cell apoptosis by interfering with the proteins in the apoptotic pathways (Guo et al., 2009; Wang et al., 2015). Cancer cells exploit the cytoprotective function of Hsp70 to sustain themselves (Giri et al., 2017). In HCC and lung cancer, it was observed that both Hsp90 and Hsp70 expression levels were upregulated, leading to proliferation and metastasis of cancerous cells (Leng et al., 2012; Cedrés et al., 2018; Sun et al., 2018; Jiang and Shen, 2020). Cell survival was facilitated through cytochrome c inhibition, regulation of extracellular signal-regulated kinase (ERK), phosphorylation of protein kinase B (Akt) and degradation of apoptotic components (Guo et al., 2009; Wang et al., 2015). Therefore, the upregulated expression levels of Hsp27, Hsp70 and Hsp90, increase the invasion and metastasis of some cancerous cells (Katsogiannou et al., 2014; Zhou et al., 2015; Saha and Anirvan, 2020; Wan et al., 2020). Furthermore, the Hsp70 and Hsp60 proteins present on the surface of cancer cells are implicated in immunomodulation, as they bind and activate immune cells and antibodies (Burgio et al., 2021). Thus, this could explain the possible link between cancer and COVID-19 susceptibility. This association is thought to be due to the dysregulated immune system in both cancer and COVID-19 patients (Zong et al., 2021).

## 5 Cellular stress drives heat shock protein expression

Cells that are exposed to stress respond by upregulating some of their Hsp stress proteins (Samali and Orrenius, 1998; Richter et al., 2010). The levels of upregulation are dependent on the type of stress, as the first response for cells is to facilitate post-translational modification (PTM). PTMs on Hsps modulate the chaperone efficiency and enable it to deal with increased demand due to increased protein unfolding. For example, Hsp90 phosphorylation and Hsp70 acetylation have been shown to increase their chaperone activities (Xu et al., 2012; Park et al., 2017). Continued stress stimuli activate the HSR, which is mainly modulated by HSF1 (Sarkar and Roy, 2017). In its inactive state, the HSF is bound to an HSP (Figure 4A). When an HSF is activated, it dissociates from the Hsp and undergoes phosphorylation and oligomerization in the cytosol, after which it translocates into the nucleus (Xu, 2012). The HSF binds to the HSE, located in the promoter regions of HSP genes, which in turn activates the increased expression of the Hsps (Kmieciak and Mayer, 2022).

The ER is also an important organelle in cell stress response as it houses a protein folding machinery. In the wake of external stress sources, the ER-resident Hsps are known to transverse and dissociate from their substrates to become available for the suppression of protein aggregation. Grp78 and Grp94 are central players in the ER protein refolding machinery, and

they often cooperate to achieve their chaperone goals (Zhu and Lee, 2015). However, if these proteins are overwhelmed, the unfolded protein response (UPR) is activated. During this event, Hsp expression is upregulated, and cytosolic protein translation is halted to limit the peptide load in the ER (Marzec et al., 2012; Hetz and Papa, 2018). Terminally misfolded proteins that cannot be rescued are channelled to the ERAD pathway for degradation (Oikonomou and Hendershot, 2020; Ninagawa et al., 2021). It should be noted that the PDIs and their associated systems are also responsive to stress as they control proper disulphide bond formation and can also catalyse reverse reactions. In addition, they also distinguish properly and erroneously glycosylated proteins, towards channelling the latter to the ERAD for degradation.

The UPR stress response is activated and regulated via three distinct pathways which enable the expression of UPR related genes (Figure 4B). These three pathways are initiated by the dissociation of Grp78 from the client protein, in response to elevated levels of unfolded proteins in the ER lumen (Lukas et al., 2019). In the Inositol requiring enzyme 1 $\alpha$  (IRE1 $\alpha$ ) pathway, IRE1 $\alpha$  undergoes autophosphorylation, followed by oligomerization which facilitates its association with downstream signalling molecules (Hetz et al., 2006; Sano and Reed 2013). Thus, IRE1 $\alpha$  interacts with c-Jun N-terminal kinase (JNK) to activate autophagy and with the nuclear factor NF $\kappa$ B, to activate inflammatory signalling pathways that regulate the release of cytokines and chemokines (Sano and Reed, 2013). IRE1 $\alpha$  also has endoribonuclease activity, which is utilized to alternatively splice the X-box binding protein 1 (XBP-1) mRNA, yielding the XBP-1 transcription factor. XBP-1 translocates to the cell nucleus where it activates the transcription of Grp78 and other proteins that are inherent to the ERAD pathway (Kitamura, 2008). The second pathway involves the protein kinase, RNA-like endoplasmic reticulum kinase (PERK). When PERK is released from Grp78, autophosphorylation of PERK is triggered, which in turn phosphorylates the translation elongation initiation factor 2 $\alpha$  (eIF2 $\alpha$ ) (Schönthal, 2012). The subsequent inactivation of eIF2 $\alpha$ , relieves ER stress by preventing additional protein synthesis and thereby decreasing the number of proteins that require folding. Transcription factor 4 (ATF4) is translocated to the nucleus, where it activates the expression of numerous stress regulating and pro-apoptotic genes (Lukas et al., 2019). The third pathway involves activating transcription factor 6 (ATF6). Upon dissociation from Grp78, this protein is transported to the Golgi apparatus, where it is proteolytically cleaved. The mature ATF6 protein enters the nucleus where it activates the expression of various UPR and ERAD pathway proteins (Sano and Reed, 2013; Lukas et al., 2019). These events are implicated in the viral life cycle as the coronavirus replication cycle induces ER stress (Sureda et al., 2020). As such, the patient's UPR/ER stress response may be a predictor of the SARS-CoV2 antiviral response.

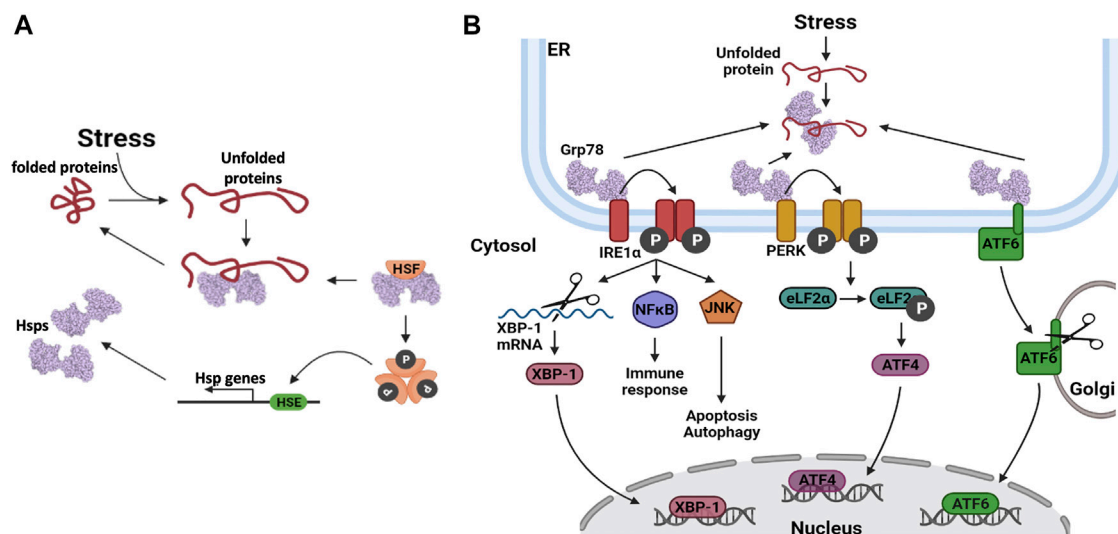


FIGURE 4

Heat shock protein expression regulation. **(A)** Upregulation of Hsp gene transcription. When unfolded proteins accumulate in the cell, Hsps dissociate from their bound heat shock factors (HSF). This frees up the Hsps to assist in protein folding and it also activates the HSF. The HSFs are phosphorylated, after which they oligomerize. The HSFs bind to heat shock elements (HSE) in the promoter regions of Hsp genes, thereby enhancing their transcription. **(B)** Hsp gene transcription is upregulated via three distinct pathways involving three distinct transcription factors (TFs); Inositol requiring enzyme 1α (IRE1α), protein kinase RNA-like endoplasmic reticulum kinase (PERK) protein and activating transcription factor 6 (ATF6).

## 6 Heat shock protein upregulation could facilitate both viral cellular uptake and replication

Viral proteins, like human proteins, require host chaperones for the folding and assembly of complex viral core particles (Xiao et al., 2010). The upregulation of these host molecular chaperones thus facilitates viral replication (Table 2). Hsps are important in the replication of virtually all viruses including, DNA viruses, both positive and negative sense RNA genomes and double-stranded RNA viruses (Song et al., 2010; Wan et al., 2020). Due to limited data on the role of Hsps on SARS-CoV2 infection, we highlight some of the important pathways from other unrelated viruses that may use unique protein folding systems to draw similarities in COVID-19 pathogenesis. Generally, viral protein homeostasis presents a distinct set of clients for cellular protein folding machinery. As such, viral replication is subject to the folding capacity of the host cell due to three main factors. Firstly, the limited genomes of viruses entail that the viral proteins are multifunctional, and as such, require structurally complex proteins that are solely dependent on chaperones for folding (McBride et al., 2014). Secondly, many cytopathic viruses produce copious amounts of viral proteins within a short time (Oualikene et al., 2000), which places a huge protein folding burden on the host cell. Thirdly, viral capsid precursors are more prone to aggregation and misfolding due to their complexity as they are made of at least a thousand identical

subunits (Rossmann, 1984; Geller et al., 2012; Cheng and Brooks, 2013). Several RNA viruses replicate with minimal proofreading and produce several mutant viral proteins during infection, which require a robust host chaperone system to fold into functional forms. In general, CoV manipulate the host chaperone system to render the cells more conducive for their replication. For example, the SARS CoVs E-protein has been implicated in suppressing the stress response in host cells upon infection (DeDiego et al., 2007). It has also been reported that SARS-CoVs structural proteins S, 6, 3a and 8a, induce ER stress response (Ye et al., 2008; Fung et al., 2014; Shi et al., 2019).

### 6.1 Viral entry

Several viruses interact with Hsps as auxiliary receptors to enter host cells through the clathrin-mediated endocytosis pathway. Hsp70 is commonly implicated as an auxiliary receptor (Figure 5), as is observed in the host cell entry of zika virus; a process that is facilitated by extracellular Hsp70 (Pujhari et al., 2019). The ER Hsp70 homology, Grp78, has been reported to facilitate the invasion of host cells by several viruses, amongst them, the Japanese encephalitis virus (Nain et al., 2017) and SARS-CoV2 (Ha et al., 2020; Carlos et al., 2021). The SBD of Grp78 positioned on the surface of African green monkey kidney epithelial Vero cells, was reported to recognize the S protein RBD of the SARS CoV2 to facilitate viral entry into these cells. In



TABLE 2 The functions of Hsps in RNA virus infections.

Chaperone family	Selected members	Function in RNA viral infection	Related RNA viruses	References
Hsp90	Hsp90 $\alpha$ ; Hsp90 $\beta$	Virus entry into host cell	Enterovirus A71, Dengue, Japanese encephalitis virus	Tsou et al. (2013) Reyes-del Valle et al. (2005) Cabrera-Hernandez et al. (2007)
		Virus replication	Influenza, Paramyxoviruses: vesicular stomatitis virus, Human parainfluenza virus type 2 and 3, Simian Virus 41 or Chikungunya, Hepatitis C virus	Momose et al. (2002) Connor et al. (2007) Geller et al. (2013) Rathore et al. (2014) Ujino et al. (2009)
		Virus protein maturation and assembly	Hepatitis C virus, Influenza, Picornaviruses, Poliovirus, Rhinovirus, Coxsackievirus, Noroviruses	Waxman et al. (2001) Geller et al. (2007) Vashist et al. (2015) Kumar et al. (2019)
Hsp70	Grp78; Hsc70; Hsp70; Hsp72	Cellular transformation	Human T-lymphotropic virus	Ikebe et al. (2014)
		Virus entry into host cell	Chicken Anaemia virus-9, Enterovirus A71, Dengue, Japanese encephalitis virus, Zika virus, Human T-lymphotropic virus, human immunodeficiency virus -1	Triantafilou et al., 2002, Xu et al., 2019 Vega-Almeida et al. (2013) Das et al. (2009) Taguwa et al. (2019) Pujhari et al. (2019) Sagara et al. (1998) Fang et al. (1999) Agostini et al. (2000) Reyes-del Valle et al. (2005)
		Virus replication	Mumps virus, Canine distemper virus, Hepatitis C virus, Respiratory syncytial virus, Ebola virus, Influenza, SARS-CoV2	Katoh et al. (2015) Vasconcelos et al. (1998) Oglesbee et al. (1993) Chen et al. (2010) Oliveira et al. (2013) García-Dorival et al. (2016) Nelson et al. (2017) Manzoor et al. (2014)
		Virus gene expression	Coxsackievirus B3, Enterovirus A71, Influenza A	Wang et al. (2017) Dong et al. (2018) Lee et al. (1994) Melville et al. (1999)
		Virus assembly	Reovirus, Poliovirus, Coxsackievirus B1, Influenza	Leone et al. (1996) Macejak and Sarnow, (1992) Hirayama et al. (2004)
		Virus release	Hepatitis C virus	Khachatoorian et al. (2014) Khachatoorian et al. (2015)
Hsp60	Hsp60; TRiC; GroEL; Hsp58; yHsp60	Immunomodulation	Japanese encephalitis virus, Influenza, Dengue	Swaroop et al. (2018) Graef et al. (2010) Fislová et al. (2010) Karlas et al. (2010) Padwad et al. (2009)
		Apoptosis regulation	Hepatitis C virus, Rotavirus	Kang et al. (2009) Chattopadhyay et al. (2017)
		Genome integration	Human immunodeficiency virus	Bartz et al. (1994) Parissi et al. (2001)

(Continued on following page)

TABLE 2 (Continued) The functions of Hsps in RNA virus infections.

Chaperone family	Selected members	Function in RNA viral infection	Related RNA viruses	References
Hsp40	Hdj2; DnaJB1; DnaJA1; DnaJA1; DnaJC14; DnaJA3; Hdj1; hTid1; DnaJB6; ERdj5	Virus entry into host cell	Human immunodeficiency virus	Chiang et al. (2014) Ko et al. (2019)
		Virus replication	Japanese encephalitis virus, Influenza	Wang et al. (2011) Batra et al. (2016) Cao et al. (2014)
		Virus gene expression	Influenza, Human immunodeficiency virus	Melville et al. (1997) Sharma et al. (2011) Saksela, (1997) Simmons et al. (2001) Doms and Trono, (2000)
		Virus protein maturation	Yellow fever virus	Yi et al. (2012)
		Immunomodulation	Hand foot and mouth disease virus	Zhang et al. (2019)
Small Hsps	Hsp27	Virus replication	Enterovirus A71, Classical swine fever virus	Ling et al. (2018) Sun et al. (2017)
PDIs	PDI; ERp57	Virus entry into host cell and uncoating	Dengue, Human immunodeficiency virus	Gallina et al. (2002) Bi et al. (2011) Diwaker et al. (2015)
		Virus translation	Enterovirus A71	Wang et al. (2016)
		Oxidative stress and ER stress	Influenza, Hepatitis C virus, Encephalomyocarditis virus, Respiratory syncytia virus, Japanese encephalitis virus, Human immunodeficiency virus	Knobil et al. (1998) Korenaga et al. (2005) Ano et al. (2010) Olagner et al. (2014) Liao et al. (2002) Dobmeyer et al. (1997)

addition, the upregulated expression of Grp78 was associated with the surface expression of the ACE2 receptors in SARS-CoV2 patients (Sabirli et al., 2021). The interaction of the ACE2 receptors with Grp78 required both the NBD and SBD (Carlos et al., 2021). These findings suggest that the full-length human Grp78 protein and possibly its functional partners Grp94, Hsp40 and PDIs could be targeted to reduce SARS-CoV2 entry into host cells and to combat the ensuing viral infection.

## 6.2 Virus replication

The central role of Hsp90 in protein complex formation is thought to function as a catalyst for the replication of invading viruses (Wan et al., 2020). Hsp90 acts as a buffer, preventing deleterious folding outcomes of mutated viral proteins (Blagosklonny et al., 1996; Jaeger and Whitesell, 2019). As such, its role in facilitating fold of mutation prone viral proteins is apparent. Both Hsp40 and Hsp70 are virtually involved in virtually all the stages of viral infection in the host cell, as they modulate viral entry, replication, gene expression, and virion assembly and release (Table 2). In addition, the Hsp40 protein, DnaJB6 is also involved in immunomodulation of the foot-and-mouth-disease

virus (FDV) infection (Zhang et al., 2019), and it is therefore plausible that these Hsps play a role in viral replication.

## 6.3 Viral protein maturation and viral assembly

Hsp70/Hsp90 proteins are the main drivers of protein folding within host cells and, inadvertently, they also facilitate the folding of invader viral proteins, enabling them to attain functional states. Protein folding occurs mainly in the cytosol of the infected cell and the Hsp40 chaperones are involved in the recruitment of the viral proteins from the ribosomes. Several of the replication steps of the Coronavirus, such as translation, takes place on the ER membranes (Knoops et al., 2008). Some of the viral proteins are thus, translocated across the ER membrane during translation, while others remain in the cytosol for folding, after which they are recruited to the ER for virion assembly. A distinct set of chaperones control the folding processes of the proteins within the ER lumen. The SARS-CoV2 structural proteins S, 6, 3a and 8a, require folding inside the ER lumen. The increased load of viral proteins in the ER disrupts the ER protein folding machinery, which induces ER stress (Fung et al., 2014; Shi et al., 2019). SARS-COV2 viruses are

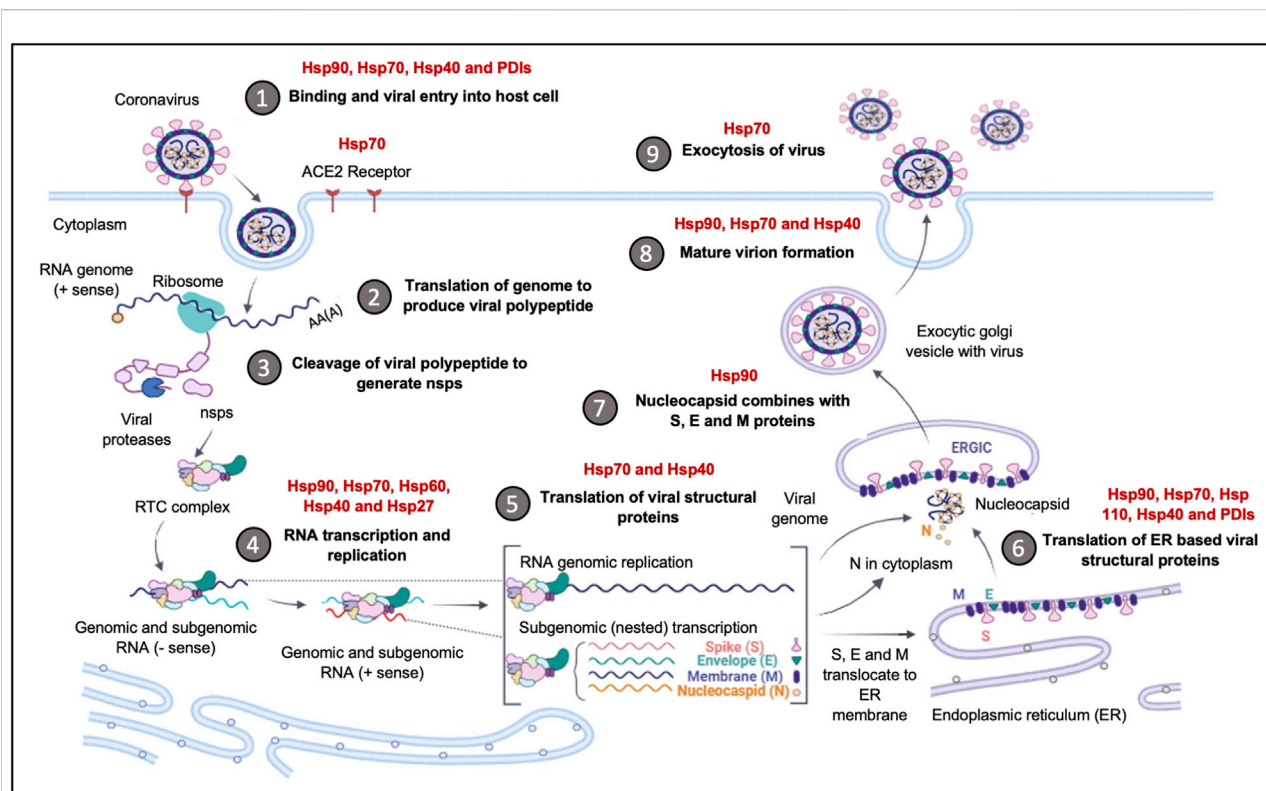


FIGURE 5

The upregulation of Hsps facilitates Coronavirus invasion and replication. The Hsps implicated in the Coronavirus replication cycle are highlighted. The binding and entry of the viral particle is achieved through the ACE-2 receptor, with Hsp90, Hsp70, Hsp40 and PDI, acting as auxiliary receptors. Upon viral entry and initial translation and transcription, Hsp40, Hsp70, Hsp60 and Hsp27, are recruited to facilitate in viral protein maturation. The folding of structural proteins is assisted by Hsp70 and Hsp90. The ER-resident chaperones, Grp94, Grp78, ERDnaJ and PDIs, facilitate the folding and insertion of viral proteins onto the ERGIC membrane. The formation of the nucleocapsid complex is overseen by Hsp90, while viral exocytosis requires the cooperation of Hsp90, Hsp70 and Hsp40. Image created with Biorender.

so dependent on the integrity of the ER folding machinery for their own replication, the virus inhibits the ER stress cascade mechanisms by the activation of the XBP-1 mediated pathway of the UPR, thereby preventing apoptosis. This is potentially mediated by the E protein; a 76 amino acid protein that oligomerises to form an ion conductive pore in the ER membranes, which restores the  $\text{Ca}^{2+}$  imbalance generated during ER stress (Torres et al., 2006). Viral proteins heavily depend on Hsp90 for their folding, assembly, and maturation, which partly accounts for the induction of Hsp90 expression (Ha et al., 2020).

## 7 Role of heat shock proteins in inflammation

SARS-CoVs cause ARDS (Reizine et al., 2021), hemophagocytic syndrome (Yang et al., 2021), lymphoid depletion (Silverstein et al., 2022) and skeletal muscle fibre necrosis (Suh et al., 2021), which are all consequences of elevated levels of pro-inflammatory cytokines.

Although predominantly expressed and found intracellularly, Hsp90 and Hsp70 were reportedly found in the extracellular space surrounding both stressed and non-stressed cells (Tsutsumi and Neckers, 2007). Surface exposed Hsp90 is thought to be involved in immunomodulation and facilitates the internalisation of viruses such as dengue virus (DENV), infectious bursal disease virus (IBDV) and influenza A virus (Reyes-del Valle et al., 2005; Cabrera-Hernandez et al., 2007; Wang X. et al., 2020). In line with recent evidence, SARS-CoV2 has been linked to the stimulation of stress proteins (Gadotti et al., 2021) which may potentially facilitate virus internalisation and immunomodulation. SARS-CoV2 infection potentially utilises molecular mimicry to imitate host cell surface receptors facilitating entry and evading the host immune response (Angileri et al., 2020; Cappello, 2020; Cappello et al., 2020; Hightower and Santoro, 2020; Kasperkiewicz, 2021). The molecular mimicry of human cell surface-expressed molecules could result in the expression of antibodies that cross-react with human proteins. This culminates in an autoimmune response from the host (Burgio et al., 2021). Hsps are some of the

molecules that share epitopes with microbial counterparts and are often the targets for molecular mimicry (Burgio et al., 2021). It was reported that some Hsps share both immunogenic and antigenic epitopes with SARS-CoV2 viral proteins (Marino Gammazza et al., 2020). This partly explains the cause of an increase in autoimmunity cases in SARS-CoV2 patients.

The cytokine storm that results from a SARS-CoV2 infection is the major cause of lung damage resulting in mortality (Song et al., 2020). A cytokine storm refers to the excessive production of proinflammatory cytokines such as interleukins 1 and 6 (IL-1 and IL-6), tumour necrosis factor  $\alpha$  (TNF- $\alpha$ ) and interferon  $\gamma$  (Huang et al., 2005; Copaesu et al., 2020). The release of these cytokines triggers a flood of immune cells to the infection site, including T cells, macrophages, and neutrophils, among others. This excessive immune response results in tissue and organ damage, which may ultimately lead to organ failure and, by extension, untimely death (Ragab et al., 2020).

Hsps facilitate the presentation of antigens by the major histocompatibility complex (MHC-1) on the surface of coronavirus infected cells, for clearance by the NK and CD8+T cell subsets (Moseley, 2000; Furuta and Eguchi, 2020; Neukirch et al., 2020). Hsp90 was shown to not only function as chaperone, but also as an antigen-presenting molecule during lymphocytic choriomeningitis viral infection (Basta et al., 2005). In addition, Hsp90 immunomodulates the host response to Sendai virus infection by regulating the activation of interferon regulatory factor 3 and TBK-1 stabilization of Sendai virus (Yang et al., 2009). Generally, Hsps are upregulated to assist in the assembly and folding of numerous immune system antigen-recognition proteins. These include molecules such as immunoglobulins, T-cell receptors and components of the MHC (Zugel and Kaufmann, 1999). Furthermore, the ER-resident Grp94, BiP and calnexin, are involved in the assembly of antibody light and heavy chains in the ER lumen (Zugel and Kaufmann, 1999). It has also been suggested that Hsps may take part in antigen delivery to MHC proteins, due to their promiscuity in binding a wide range of similar peptides (Zininga et al., 2018). These diverse roles Hsps make them important immune modulators that promote viral infection.

## 8 Conclusion and future perspectives

Hsp90 plays a central role in cellular protein quality control. Inhibition of the Hsp90 system affects various signalling pathways, making it an attractive drug target in viral infections. Additionally, the high mutation rates of RNA viruses further support targeting Hsp90 as an antiviral candidate. In many viral infections, Hsp90 was shown to be an important chaperone that functions in facilitating viral protein folding, replication, transport, and assembly (Geller et al., 2013; Geller et al., 2018; Wyler et al., 2021). Most Hsp90 inhibitors were initially identified as anticancer

agents and some of these are being repurposed for use against viral infections (Ramos and Ayinde, 2021; Zhao et al., 2022). Hsp90 inhibitors are potential broad action antivirals, as they act on several viruses by blocking their replication and stimulating apoptosis in infected host cells. It was recently reported that Hsp90 inhibitors prevented endothelial barrier damage in lung tissues and reduced SARS-CoV2 replication (Kubra et al., 2020; Lubkowska et al., 2021; Wyler et al., 2021). Another study hypothesised that Hsp70 and Hsp90 proteins potentially bind to the ACE2 receptors, masking the receptors and inhibiting binding to SARS-CoV2 viruses, resulting in reduced viral host cell entry (Alreshidi et al., 2021). These Hsp90 inhibitors exhibiting potent antiviral activity were reportedly effective at lower concentrations compared to the dosages required in cancer treatments. Therefore, there is merit in targeting the Hsp system, as the shorter acute nature of viral infection implies the use of much less total dosage compared to that required to treat cancer. Taken together, the use of Hsp inhibitors offers promising prospects as combinational treatments in controlling COVID-19.

## Author contributions

Conceptualization, TZ; writing-original draft preparation, CC, MS and TZ; writing-review and editing, CC, MS, VM, AS, and TZ; supervision, TZ; funding acquisition, TZ. All authors have read and agreed to the published version of the manuscript.

## Funding

This work is based on the research supported in part by the Department of Science and Technology/National Research Foundation (NRF) of South Africa (Grant numbers 129401 and 145,405) awarded to TZ, (Grant number 131724) awarded to MLS and (Grant number 140943) awarded to CC.

## Acknowledgments

The authors would like to acknowledge Stellenbosch University Sub-Committee B and the ECAD for support to TZ. We thank Thomas Tipih and Jared Reece Prinsloo for their critical reading of this manuscript.

## Conflict of interest

The authors declare that the research was conducted in the absence of any commercial or financial relationships that could be construed as a potential conflict of interest.



## Publisher's note

All claims expressed in this article are solely those of the authors and do not necessarily represent those of their affiliated

## References

- Adams, B. M., Oster, M. E., and Hebert, D. N. (2019). Protein quality control in the endoplasmic reticulum. *Protein J.* 38, 317–329. doi:10.1007/s10930-019-09831-w
- Agostini, I., Popov, S., Li, J., Dubrovsky, L., Hao, T., and Bukrinsky, M. (2000). Heat-shock protein 70 can replace viral protein R of HIV-1 during nuclear import of the viral preintegration complex. *Exp. Cell Res.* 259 (2), 398–403. doi:10.1006/excr.2000.4992
- Alderson, T. R., Kim, J. H., and Markley, J. L. (2016). Dynamical structures of Hsp70 and hsp70-hsp40 complexes. *Structure* 24 (7), 1014–1030. doi:10.1016/j.str.2016.05.011
- Alreshidi, F. S., Ginawi, I. A., Hussain, M. A., and Arif, J. M. (2021). Piperazine and aspirin-mediated protective role of Hsp70 and Hsp90 as modes to strengthen the natural immunity against potent SARS-CoV-2. *Biointerface Res. Appl. Chem.* 11, 12364–12379. doi:10.33263/BRIAC114.1236412379
- Amawi, K. F., Al-Mazari, I. S., Alsarhan, A., Alhamad, H. Q. M., and Alkhatib, A. J. (2019). Diabetes upregulates the expression of HSP90 and downregulates HSP70 in the liver of diabetic rats. *Comp. Clin. Path.* 28 (2), 473–478. doi:10.1007/s00580-019-02902-5
- Andersen, K. G., Rambaut, A., Lipkin, W. I., Holmes, E. C., and Garry, R. F. (2020). The proximal origin of SARS-CoV-2. *Nat. Med.* 26 (4), 450–452. doi:10.1038/s41591-020-0820-9
- Andreasson, C., Fiaux, J., Rampelt, H., Mayer, M. P., and Bukau, B. (2008). Hsp110 is a nucleotide-activated exchange factor for Hsp70. *J. Biol. Chem.* 283 (14), 8877–8884. doi:10.1074/jbc.M710063200
- Angileri, F., Angileri, F., L  gar  , S., Gammazza, A. M., de Macario, E. C., Macario, A. J., et al. (2020). Is molecular mimicry the culprit in the autoimmune haemolytic anaemia affecting patients with COVID-19? *Br. J. Haematol.* 190, e92–e93. doi:10.1111/bjh.16883
- Ano, Y., Sakudo, A., Kimata, T., Uraki, R., Sugiura, K., and Onodera, T. (2010). Oxidative damage to neurons caused by the induction of microglial NADPH oxidase in encephalomyocarditis virus infection. *Neurosci. Lett.* 469 (1), 39–43. doi:10.1016/j.neulet.2009.11.040
- Appenzeller-Herzog, C., and Ellgaard, L. (2008). The human PDI family: Versatility packed into a single fold. *Biochim. Biophys. Acta* 1783 (4), 535–548. doi:10.1016/j.bbamcr.2007.11.010
- Araki, K., and Nagata, K. (2012). Protein folding and quality control in the ER. *Cold Spring Harb. Perspect. Biol.* 4, a015438. doi:10.1101/cshperspect.a015438
- Archer, A. E., Von Schulze, A. T., and Geiger, P. C. (2018). Exercise, heat shock proteins and insulin resistance. *Philos. Trans. R. Soc. Lond. B Biol. Sci.* 373 (1738), 20160529. doi:10.1098/rstb.2016.0529
- Bachman, A. B., Keramisanou, D., Xu, W., Beebe, K., Moses, M. A., Vasantha Kumar, M. V., et al. (2018). Phosphorylation induced cochaperone unfolding promotes kinase recruitment and client class-specific Hsp90 phosphorylation. *Nat. Commun.* 9 (1), 265. doi:10.1038/s41467-017-02711-w
- Bartz, S. R., Pauza, C. D., Ivanyi, J., Jindal, S., Welch, W. J., and Malkovsky, M. (1994). An Hsp60 related protein is associated with purified HIV and SIV. *J. Med. Primatol.* 23 (2-3), 151–154. doi:10.1111/j.1600-0684.1994.tb00116.x
- Basta, S., Stoessel, R., Basler, M., van den Broek, M., and Groettrup, M. (2005). Cross-presentation of the long-lived lymphocytic choriomeningitis virus nucleoprotein does not require neosynthesis and is enhanced via heat shock proteins. *J. Immunol.* 175 (2), 796–805. doi:10.4049/jimmunol.175.2.796
- Batra, J., Tripathi, S., Kumar, A., Katz, J. M., Cox, N. J., Lal, R. B., et al. (2016). Human Heat shock protein 40 (Hsp40/DnaJB1) promotes influenza A virus replication by assisting nuclear import of viral ribonucleoproteins. *Sci. Rep.* 6 (1), 19063. doi:10.1038/srep19063
- Bi, S., Hong, P. W., Lee, B., and Baum, L. G. (2011). Galectin-9 binding to cell surface protein disulfide isomerase regulates the redox environment to enhance T-cell migration and HIV entry. *Proc. Natl. Acad. Sci. U. S. A.* 108 (26), 10650–10655. doi:10.1073/pnas.1017954108
- Biancatelli, R. M. L. C., Solopov, P. A., Gregory, B., Khodour, Y., and Catravas, J. D. (2022). HSP90 inhibitors modulate SARS-CoV-2 spike protein subunit 1-induced human pulmonary microvascular endothelial activation and barrier dysfunction. *Front. Physiol.* 13, 812199. doi:10.3389/fphys.2022.812199
- Biebl, M. M., Riedl, M., and Buchner, J. (2020). Hsp90 Co-chaperones form plastic genetic networks adapted to client maturation. *Cell Rep.* 32 (8), 108063. doi:10.1016/j.celrep.2020.108063
- Bijur, G. N., De Sarno, P., and Jope, R. S. (2000). Glycogen synthase kinase-3 $\beta$  facilitates staurosporine- and heat shock-induced apoptosis protection by lithium. *J. Biol. Chem.* 275 (11), 7583–7590. doi:10.1074/jbc.275.11.7583
- Blagosklonny, M. V., Toretsky, J., Bohlen, S., and Neckers, L. (1996). Mutant conformation of p53 translated *in vitro* or *in vivo* requires functional HSP90. *Proc. Natl. Acad. Sci. U. S. A.* 93 (16), 8379–8383. doi:10.1073/pnas.93.16.8379
- Bl  her, M. (2019). Obesity: Global epidemiology and pathogenesis. *Nat. Rev. Endocrinol.* 15 (5), 288–298. doi:10.1038/s41574-019-0176-8
- Braakman, I., and Hebert, D. N. (2021). Protein folding in the endoplasmic reticulum. *Cold Spring Harb. Perspect. Biol.* 2013, a013201–18. doi:10.1101/cshperspect.a013201
- Bruxel, M. A., Tavares, A. M. V., Neto, L. D. Z., de Souza Borges, V., Schroeder, H. T., Bock, P. M., et al. (2019). Chronic whole-body heat treatment relieves atherosclerotic lesions, cardiovascular and metabolic abnormalities, and enhances survival time restoring the anti-inflammatory and anti-senescent heat shock response in mice. *Biochimie* 156, 33–46. doi:10.1016/j.biochi.2018.09.011
- Burgio, S., Conway de Macario, E., Macario, A. J., and Cappello, F. (2021). SARS-CoV-2 in patients with cancer: Possible role of mimicry of human molecules by viral proteins and the resulting anti-cancer immunity. *Cell Stress Chaperones* 26 (4), 611–616. doi:10.1007/s12192-021-01211-7
- Cabrera-Hernandez, A., Thepparit, C., Suksanpaisan, L., and Smith, D. R. (2007). Dengue virus entry into liver (HepG2) cells is independent of hsp90 and hsp70. *J. Med. Virol.* 79 (4), 386–392. doi:10.1002/jmv.20786
- Cao, M., Wei, C., Zhao, L., Wang, J., Jia, Q., Wang, X., et al. (2014). DnaJ1/Hsp40 is co-opted by influenza A virus to enhance its viral RNA polymerase activity. *J. Virol.* 88 (24), 14078–14089. doi:10.1128/JVI.02475-14
- Cappello, F., Cappello, F., Marino Gammazza, A., Dieli, F., Conway de Macario, E., and Macario, A. J. (2020). Does SARS-CoV-2 trigger stress-induced autoimmunity by molecular mimicry? A hypothesis. *J. Clin. Med.* 9 (7), E2038. doi:10.3390/jcm9072038
- Cappello, F. (2020). COVID-19 and molecular mimicry: The Columbus' egg? *J. Clin. Neurosci.* 77, 246. doi:10.1016/j.jocn.2020.05.015
- Carlos, A. J., Ha, D. P., Yeh, D. W., Van Krieken, R., Tseng, C. C., Zhang, P., et al. (2021). The chaperone GRP78 is a host auxiliary factor for SARS-CoV-2 and GRP78 depleting antibody blocks viral entry and infection. *J. Biol. Chem.* 296, 100759. doi:10.1016/j.jbc.2021.100759
- Ced  s, S., Felip, E., Cruz, C., Mart  nez de Castro, A., Pardo, N., Navarro, A., et al. (2018). Activity of HSP90 inhibitor in a metastatic lung cancer patient with a germline BRCA1 mutation. *J. Natl. Cancer Inst.* 110 (8), 914–917. doi:10.1093/jnci/djy012
- Celli, B. R., and Wedzicha, J. A. (2019). Update on clinical aspects of chronic obstructive pulmonary disease. *N. Engl. J. Med.* 381, 1257–1266. doi:10.1056/NEJMr1900500
- Chakafana, G., and Shonhai, A. (2021). The role of non-canonical Hsp70s (Hsp110/Grp170) in cancer. *Cells* 10 (2), 254. doi:10.3390/cells10020254
- Chakafana, G., Zininga, T., and Shonhai, A. (2019). Comparative structure-function features of Hsp70s of *Plasmodium falciparum* and human origins. *Biophys. Rev.* 11 (4), 591–602. doi:10.1007/s12551-019-00563-w

- Chakraborty, A., and Edkins, A. L. (2021). HSP90 as a regulator of extracellular matrix dynamics. *Biochem. Soc. Trans.* 49 (6), 2611–2625. doi:10.1042/BST20210374
- Chamberlain, N., and Anathy, V. (2020). Pathological consequences of the unfolded protein response and downstream protein disulphide isomerases in pulmonary viral infection and disease. *J. Biochem.* 167 (2), 173–184. doi:10.1093/jb/mvz101
- Chatterjee, S. (2016). “Chapter two - oxidative stress, inflammation, and disease,” in *Oxidative stress and biomaterials*. Editors T. Dziubla and D. A. Butterfield (Academic Press), 35–58.
- Chattopadhyay, S., Mukherjee, A., Patra, U., Bhowmick, R., Basak, T., Sengupta, S., et al. (2017). Tyrosine phosphorylation modulates mitochondrial chaperonin Hsp60 and delays rotavirus NSP4-mediated apoptotic signaling in host cells. *Cell. Microbiol.* 19 (3), e12670. doi:10.1111/cmi.12670
- Chen, B., Piel, W. H., Gui, L., Bruford, E., and Monteiro, A. (2005). The HSP90 family of genes in the human genome: Insights into their divergence and evolution. *Genomics* 86 (6), 627–637. doi:10.1016/j.ygeno.2005.08.012
- Chen, J., Song, S., Liu, Y., Liu, D., Lin, Y., Ge, S., et al. (2018). Autoreactive T cells to citrullinated HSP90 are associated with interstitial lung disease in rheumatoid arthritis. *Int. J. Rheum. Dis.* 21 (7), 1398–1405. doi:10.1111/1756-185X.13316
- Chen, Y.-J., Chen, Y.-H., Chow, L.-P., Tsai, Y.-H., Chen, P.-H., Huang, C.-Y. F., et al. (2010). Heat shock protein 72 is associated with the hepatitis C virus replicase complex and enhances viral RNA replication. *J. Biol. Chem.* 285 (36), 28183–28190. doi:10.1074/jbc.M110.118323
- Chen, Y., Liu, Q., and Guo, D. (2020). Emerging coronaviruses: Genome structure, replication, and pathogenesis. *J. Med. Virol.* 92 (4), 418–423. doi:10.1002/jmv.25681
- Cheng, S., and Brooks, C. L., III (2013). Viral capsid proteins are segregated in structural fold space. *PLoS Comput. Biol.* 9 (2), e1002905. doi:10.1371/journal.pcbi.1002905
- Chiang, Y., Sheng, W.-H., Shao, P.-L., Chi, Y.-H., Chen, Y.-M., Huang, S.-W., et al. (2014). Large isoform of mammalian relative of dnaj is a major determinant of human susceptibility to HIV-1 infection. *EBioMedicine* 284, 126–132. doi:10.1016/j.ebiom.2014.10.002
- Chichiarelli, S., Altieri, F., Paglia, G., Rubini, E., Minacori, M., and Eufemi, M. (2022). ERp57/PDIA3: New insight. *Cell. Mol. Biol. Lett.* 27, 12. doi:10.1186/s11658-022-00315-x
- Choi, Y. J., Park, J. Y., Lee, H. S., Suh, J., Song, J. Y., Byun, M. K., et al. (2021). Effect of asthma and asthma medication on the prognosis of patients with COVID-19. *Eur. Respir. J.* 57 (3), 2002226. doi:10.1183/13993003.02226-2020
- Cintron, N. S., and Toft, D. (2006). Defining the requirements for Hsp40 and Hsp70 in the Hsp90 chaperone pathway. *J. Biol. Chem.* 281 (36), 26235–26244. doi:10.1074/jbc.M605417200
- Connor, J. H., McKenzie, M. O., Parks, G. D., and Lyles, D. S. (2007). Antiviral activity and RNA polymerase degradation following Hsp90 inhibition in a range of negative strand viruses. *Virology* 362 (1), 109–119. doi:10.1016/j.virol.2006.12.026
- Copaescu, A., Smibert, O., Gibson, A., Phillips, E. J., and Trubiano, J. A. (2020). The role of IL-6 and other mediators in the cytokine storm associated with SARS-CoV-2 infection. *J. Allergy Clin. Immunol.* 146 (3), 518–534. doi:10.1016/j.jaci.2020.07.001
- Cottin, V. (2013). Interstitial lung disease. *Eur. Respir. Rev.* 22, 26–32. doi:10.1183/09059180.00006812
- Craig, E. A. (2018). Hsp70 at the membrane: Driving protein translocation. *BMC Biol.* 16, 11. doi:10.1186/s12915-017-0474-3
- Darby, N. J., and Creighton, T. E. (1995). Functional properties of the individual thioredoxin-like domains of protein disulfide isomerase. *Biochemistry* 34 (37), 11725–11735. doi:10.1021/bi00037a009
- Das, S., Laxminarayana, S. V., Chandra, N., Ravi, V., and Desai, A. (2009). Heat shock protein 70 on Neuro2a cells is a putative receptor for Japanese encephalitis virus. *Virology* 385 (1), 47–57. doi:10.1016/j.virol.2008.10.025
- de Lemos Muller, C. H., Rech, A., Botton, C. E., Schroeder, H. T., Bock, P. M., Farinha, J. B., et al. (2018). Heat-induced extracellular HSP72 release is blunted in elderly diabetic people compared with healthy middle-aged and older adults, but it is partially restored by resistance training. *Exp. Gerontol.* 111, 180–187. doi:10.1016/j.exger.2018.07.014
- DeDiego, M. L., Alvarez, E., Almazán, F., Rejas, M. T., Lamirande, E., Roberts, A., et al. (2007). A severe acute respiratory syndrome coronavirus that lacks the E gene is attenuated *in vitro* and *in vivo*. *J. Virol.* 81 (4), 1701–1713. doi:10.1128/JVI.01467-06
- Di Naso, F. C., Rosa Porto, R., Sarubbi Fillmann, H., Maggioni, L., Vontobel Padoin, A., Jacques Ramos, R., et al. (2015). Obesity depresses the anti-inflammatory HSP70 pathway, contributing to NAFLD progression. *Obesity* 23 (1), 120–129. doi:10.1002/oby.20919
- Diwaker, D., Mishra, K. P., Ganju, L., and Singh, S. B. (2015). Protein disulfide isomerase mediates dengue virus entry in association with lipid rafts. *Viral Immunol.* 28 (3), 153–160. doi:10.1089/vim.2014.0095
- Dobmeyer, T. S., Findhammer, S., Dobmeyer, J. M., Klein, S. A., Raffel, B., Hoelzer, D., et al. (1997). *Ex vivo* induction of apoptosis in lymphocytes is mediated by oxidative stress: Role for lymphocyte loss in HIV infection. *Free Radic. Biol. Med.* 22 (5), 775–785. doi:10.1016/s0891-5849(96)00403-0
- Doms, R. W., and Trono, D. (2000). The plasma membrane as a combat zone in the HIV battlefield. *Genes Dev.* 14 (21), 2677–2688. doi:10.1101/gad.833300
- Dong, J., Guo, L., Liao, Z., Zhang, M., Zhang, M., Wang, T., et al. (2013). Increased expression of heat shock protein 70 in chronic obstructive pulmonary disease. *Int. Immunopharmacol.* 17 (3), 885–893. doi:10.1016/j.intimp.2013.09.003
- Dong, Q., Men, R., Dan, X., Chen, Y., Li, H., Chen, G., et al. (2018). Hsc70 regulates the IRES activity and serves as an antiviral target of enterovirus A71 infection. *Antivir. Res.* 150, 39–46. doi:10.1016/j.antiviral.2017.11.020
- Dragovic, Z., Broadley, S. A., Shomura, Y., Bracher, A., and Hartl, F. U. (2006). Molecular chaperones of the Hsp110 family act as nucleotide exchange factors of Hsp70s. *EMBO J.* 25 (11), 2519–2528. doi:10.1038/sj.emboj.7601138
- Duan, Y., Tang, H., Mitchell-Silbaugh, K., Fang, X., Han, Z., and Ouyang, K. (2020). Heat shock protein 60 in cardiovascular physiology and diseases. *Front. Mol. Biosci.* 7, 73. doi:10.3389/fmolb.2020.00073
- Easton, D. P., Kaneko, Y., and Subjeck, J. R. (2000). The Hsp110 and Grp170 stress proteins: Newly recognized relatives of the Hsp70s, *Cell stress and chaperones*. *Cell Stress Chaperones* 5 (4), 276–290. doi:10.1379/1466-1268(2000)005<0276:thasp>2.0.co;2
- Edkins, A. L., Price, J. T., Pockley, A. G., and Blatch, G. L. (2018). Heat shock proteins as modulators and therapeutic targets of chronic disease: An integrated perspective. *Philos. Trans. R. Soc. Lond. B Biol. Sci.* 373 (1738), 20160521. doi:10.1098/rstb.2016.0521
- Ellgaard, L., and Ruddock, L. W. (2005). The human protein disulfide isomerase family: Substrate interactions and functional properties. *EMBO Rep.* 6 (1), 28–32. doi:10.1038/sj.embo.7400311
- Enriquez, A. S., Rojo, H. M., Bhatt, J. M., Molugu, S. K., Hildenbrand, Z. L., and Bernal, R. A. (2017). The human mitochondrial Hsp60 in the APO conformation forms a stable tetradecameric complex. *Cell Cycle* 16 (13), 1309–1319. doi:10.1080/15384101.2017.1321180
- ERA-EDTA Council; ERACODA Working GroupFliser, D., Fouque, D., Goumenos, D., Massy, Z. A., et al. (2021). Chronic kidney disease is a key risk factor for severe COVID-19: A call to action by the ERA-EDTA. *Nephrol. Dial. Transpl.* 36 (1), 87–94. PMID: PMC7771976. doi:10.1093/ndt/gfaa314
- Fan, C.-Y., Lee, S., and Cyr, D. M. (2003). Mechanisms for regulation of Hsp70 function by Hsp40. *Cell Stress Chaperones* 8 (4), 309–316. doi:10.1379/1466-1268(2003)008<0309:mfrh>2.0.co;2
- Fang, D., Haraguchi, Y., Jinno, A., Soda, Y., Shimizu, N., and Hoshino, H. (1999). Heat shock cognate protein 70 is a cell fusion-enhancing factor but not an entry factor for human T-cell lymphotropic virus type I. *Biochem. Biophys. Res. Commun.* 261 (2), 357–363. doi:10.1006/bbrc.1999.1028
- Favati, F., Bornman, L., Hightower, L. E., Günther, E., and Polla, B. S. (1997). Variation in hsp gene expression and hsp polymorphism: Do they contribute to differential disease susceptibility and stress tolerance. *Cell Stress Chaperones* 2 (3), 141–155. doi:10.1379/1466-1268(1997)002<0141:vihea>2.3.co;2
- Ferrari, L., Geerts, W. J., van Wezel, M., Kos, R., Konstantoule, A., van Bezouwen, L. S., et al. (2018). *Human chaperones untangle fibrils of the Alzheimer protein Tau*. *Biorxiv*, 426650. doi:10.1101/426650
- Fislová, T., Thomas, B., Graef, K. M., and Fodor, E. (2010). Association of the influenza virus RNA polymerase subunit PB2 with the host chaperonin CCT. *J. Virol.* 84 (17), 8691–8699. doi:10.1128/JVI.00813-10
- Fraser, D. D., Cepinskas, G., Slessarev, M., Martin, C., Daley, M., Miller, M. R., et al. (2020). Novel outcome biomarkers identified with targeted proteomic analyses of plasma from critically ill coronavirus disease 2019 patients. *Crit. Care Explor.* 2 (6), e0189. doi:10.1097/CCE.0000000000000189
- Fu, J., Gao, J., Liang, Z., and Yang, D. (2020). PDI-regulated disulfide bond formation in protein folding and biomolecular assembly. *Molecules* 26 (1), 171. doi:10.3390/molecules26010171
- Fung, T. S., Huang, M., and Liu, D. X. (2014). Coronavirus-induced ER stress response and its involvement in regulation of coronavirus–host interactions. *Virus Res.* 194, 110–123. doi:10.1016/j.virusres.2014.09.016
- Furuta, K., and Eguchi, T. (2020). “Roles of HSP on antigen presentation,” in *Heat shock proteins in human diseases* (Cham: Springer), 275–280.
- Gadotti, A. C., Lipinski, A. L., Vasconcellos, F. T., Marqueze, L. F., Cunha, E. B., Campos, A. C., et al. (2021). Susceptibility of the patients infected with Sars-Cov2 to

oxidative stress and possible interplay with severity of the disease. *Free Radic. Biol. Med.* 165, 184–190. doi:10.1016/j.freeradbiomed.2021.01.044

Gallina, A., Hanley, T. M., Mandel, R., Trahey, M., Broder, C. C., Viglianti, G. A., et al. (2002). Inhibitors of protein-disulfide isomerase prevent cleavage of disulfide bonds in receptor-bound glycoprotein 120 and prevent HIV-1 entry. *J. Biol. Chem.* 277 (52), 50579–50588. doi:10.1074/jbc.M204547200

Gámez, A., Yuste-Checa, P., Brasil, S., Briso-Montiano, Á., Desviat, L. R., Ugarte, M., et al. (2018). Protein misfolding diseases: Prospects of pharmacological treatment. *Clin. Genet.* 93 (3), 450–458. doi:10.1111/cge.13088

García-Dorival, I., Wu, W., Armstrong, S. D., Barr, J. N., Carroll, M. W., Hewson, R., et al. (2016). Elucidation of the cellular interactome of Ebola virus nucleoprotein and identification of therapeutic targets. *J. Proteome Res.* 15 (12), 4290–4303. doi:10.1021/acs.jproteome.6b00337

Geller, R., Andino, R., and Frydman, J. (2013). Hsp90 inhibitors exhibit resistance-free antiviral activity against respiratory syncytial virus. *PLoS One* 8 (2), e56762. doi:10.1371/journal.pone.0056762

Geller, R., Pechmann, S., Acevedo, A., Andino, R., and Frydman, J. (2018). Hsp90 shapes protein and RNA evolution to balance trade-offs between protein stability and aggregation. *Nat. Commun.* 9 (1), 1781. doi:10.1038/s41467-018-04203-x

Geller, R., Taguwa, S., and Frydman, J. (2012). Broad action of Hsp90 as a host chaperone required for viral replication. *Biochim. Biophys. Acta* 1823 (3), 698–706. doi:10.1016/j.bbamcr.2011.11.007

Geller, R., Vignuzzi, M., Andino, R., and Frydman, J. (2007). Evolutionary constraints on chaperone-mediated folding provide an antiviral approach refractory to development of drug resistance. *Genes Dev.* 21 (2), 195–205. doi:10.1101/gad.1505307

Gerayeli, F. V., Milne, S., Cheung, C., Li, X., Yang, C. W. T., Tam, A., et al. (2021). COPD and the risk of poor outcomes in COVID-19: A systematic review and meta-analysis. *EclinicalMedicine* 33, 100789. doi:10.1016/j.eclinm.2021.100789

Giri, B., Sethi, V., Modi, S., Garg, B., Banerjee, S., Saluja, A., et al. (2017). Heat shock protein 70 in pancreatic diseases: Friend or foe. *J. Surg. Oncol.* 116 (1), 114–122. doi:10.1002/jso.24653

Glebov, O. O. (2020). Understanding SARS-CoV-2 endocytosis for COVID-19 drug repurposing. *FEBS J.* 287 (17), 3664–3671. doi:10.1111/febs.15369

Gordon, D. E., Jang, G. M., Bouhaddou, M., Xu, J., Obernier, K., White, K. M., et al. (2020). A SARS-CoV-2 protein interaction map reveals targets for drug repurposing. *Nature* 583 (7816), 459–468. doi:10.1038/s41586-020-2286-9

Graef, K. M., Vreede, F. T., Lau, Y. F., McCall, A. W., Carr, S. M., Subbarao, K., et al. (2010). The PB2 subunit of the influenza virus RNA polymerase affects virulence by interacting with the mitochondrial antiviral signaling protein and inhibiting expression of beta interferon. *J. Virol.* 84 (17), 8433–8445. doi:10.1128/JVI.00879-10

Grundtman, C., Kreutmayer, S. B., Almanzar, G., Wick, M. C., and Wick, G. (2011). Heat shock protein 60 and immune inflammatory responses in atherosclerosis. *Arterioscler. Thromb. Vasc. Biol.* 31 (5), 960–968. doi:10.1161/ATVBAHA.110.217877

Guihur, A., Rebeaud, M. E., Fauvet, B., Tiwari, S., Weiss, Y. G., and Goloubinoff, P. (2020). Moderate fever cycles as a potential mechanism to protect the respiratory system in COVID-19 patients. *Front. Med.* 7, 564170. doi:10.3389/fmed.2020.564170

Guo, K., Kang, N. X., Li, Y., Sun, L., Gan, L., Cui, F. J., et al. (2009). Regulation of HSP27 on NF- $\kappa$ B pathway activation may be involved in metastatic hepatocellular carcinoma cells apoptosis. *BMC Cancer* 9 (1), 100–110. doi:10.1186/1471-2407-9-100

Ha, D. P., Van Krieken, R., Carlos, A. J., and Lee, A. S. (2020). The stress-inducible molecular chaperone GRP78 as potential therapeutic target for coronavirus infection. *J. Infect.* 81 (3), 452–482. doi:10.1016/j.jinf.2020.06.017

Haslbeck, M., Weinkauff, S., and Buchner, J. (2019). Small heat shock proteins: Simplicity meets complexity. *J. Biol. Chem.* 294 (6), 2121–2132. doi:10.1074/jbc.REV118.002809

Haßdenteufel, S., Johnson, N., Paton, A. W., Paton, J. C., High, S., and Zimmermann, R. (2018). Chaperone-mediated Sec61 channel gating during ER import of small precursor proteins overcomes Sec61 inhibitor-reinforced energy barrier. *Cell Rep.* 23, 1373–1386. doi:10.1016/j.celrep.2018.03.122

Henderson, B., and Pockley, A. G. (2012). Proteotoxic stress and circulating cell stress proteins in the cardiovascular diseases. *Cell Stress Chaperones* 17 (3), 303–311. doi:10.1007/s12192-011-0318-y

Hetz, C., Bernasconi, P., Fisher, J., Lee, A. H., Bassik, M. C., Antonsson, B., et al. (2006). Proapoptotic BAX and BAK modulate the unfolded protein response by a

direct interaction with IRE1 $\alpha$ . *Science* 312 (5773), 572–576. doi:10.1126/science.1123480

Hetz, C., and Papa, F. R. (2018). The unfolded protein response and cell fate control. *Mol. Cell* 69, 169–181. doi:10.1016/j.molcel.2017.06.017

Hidalgo, P., Valdés, M., and González, R. A. (2021). Molecular biology of coronaviruses: An overview of virus-host interactions and pathogenesis. *Bol. Med. Hosp. Infant. Mex.* 78 (1), 41–58. doi:10.24875/BMHIM.20000249

Hightower, L. E., and Santoro, M. G. (2020). Coronaviruses and stress: From cellular to global. *Cell Stress Chaperones* 25 (5), 701–705. doi:10.1007/s12192-020-01155-4

Hirayama, E., Atagi, H., Hiraki, A., and Kim, J. (2004). Heat shock protein 70 is related to thermal inhibition of nuclear export of the influenza virus ribonucleoprotein complex. *J. Virol.* 78 (3), 1263–1270. doi:10.1128/jvi.78.3.1263-1270.2004

Hoffmann, M., Kleine-Weber, H., Schroeder, S., Krüger, N., Herrler, T., Erichsen, S., et al. (2020). SARS-CoV-2 cell entry depends on ACE2 and TMPRSS2 and is blocked by a clinically proven protease inhibitor. *Cell* 181 (2), 271–280. e8. doi:10.1016/j.cell.2020.02.052

Huang, C., Wang, Y., Li, X., Ren, L., Zhao, J., Hu, Y., et al. (2020). Clinical features of patients infected with 2019 novel coronavirus in Wuhan, China. *Lancet* 395 (10223), 497–506. doi:10.1016/S0140-6736(20)30183-5

Huang, K. J., Su, I. J., Theron, M., Wu, Y. C., Lai, S. K., Liu, C. C., et al. (2005). An interferon- $\gamma$ -related cytokine storm in SARS patients. *J. Med. Virol.* 75 (2), 185–194. doi:10.1002/jmv.20255

Hulgan, T., Morrow, J., D'Aquila, R. T., Raffanti, S., Morgan, M., Rebeiro, P., et al. (2003). Oxidant stress is increased during treatment of human immunodeficiency virus infection. *Clin. Infect. Dis.* 37, 1711–1717. doi:10.1086/379776

Ikebe, E., Kawaguchi, A., Tezuka, K., Taguchi, S., Hirose, S., Matsumoto, T., et al. (2014). A novel HSP90 inhibitor, 17-DMAG, induces Tax down-regulation and its oral administration to ATL-model mice intervenes against the infiltration property of the ATL-like lymphocytes and provides extended survival period. *Retrovirology* 11 (1), P44. doi:10.1186/1742-4690-11-S1-P44

Ishida, R., Okamoto, T., Motojima, F., Kubota, H., Takahashi, H., Tanabe, M., et al. (2018). Physicochemical properties of the mammalian molecular chaperone HSP60. *Int. J. Mol. Sci.* 19 (2), 489. doi:10.3390/ijms19020489

Ito, S., and Nagata, K. (2019). Roles of the endoplasmic reticulum-resident, collagen-specific molecular chaperone Hsp47 in vertebrate cells and human disease. *J. Biol. Chem.* 294 (6), 2133–2141. doi:10.1074/jbc.TM118.002812

Ivanov, A. V., Bartosch, B., and Isagulyants, M. G. (2017). Oxidative stress in infection and consequent disease. *Oxid. Med. Cell. Longev.* 2017, 3496043. doi:10.1155/2017/3496043

Jackson, S. E. (2012). “Hsp90: Structure and function,” in *Molecular chaperones* (Springer), 155–240.

Jaeger, A. M., and Whitesell, L. (2019). HSP90: Enabler of cancer adaptation. *Annu. Rev. Cancer Biol.* 3, 275–297. doi:10.1146/annurev-cancerbio-030518-055533

Jakovac, H. (2020). COVID-19 and hypertension: Is the HSP60 culprit for the severe course and worse outcome? *Am. J. Physiol. Heart Circ. Physiol.* 319 (4), H793–H796. doi:10.1152/ajpheart.00506.2020

Jaroszyński, A., Jaroszyńska, A., Zaborowski, T., Drelich-Zbroja, A., Zapolski, T., and Dabrowski, W. (2018). Serum heat shock protein 27 levels predict cardiac mortality in hemodialysis patients. *BMC Nephrol.* 19, 359. doi:10.1186/s12882-018-1157-1

Jiang, Q., and Shen, X. (2020). Research progress of heat shock protein 90 and hepatocellular carcinoma. *Int. J. Clin. Med.* 11 (2), 43–52. doi:10.4236/ijcm.2020.112005

Jomaa, A., Gämderinger, M., Hsieh, H. H., Wallisch, A., Chandrasekaran, V., Ulusoy, Z., et al. (2022). Mechanism of signal sequence handover from NAC to SRP on ribosomes during ER-protein targeting. *Science* 375 (6583), 839–844. doi:10.1126/science.abl6459

Kaimal, J. M., Kandasamy, G., Gasser, F., and Andréasson, C. (2017). Coordinated Hsp110 and Hsp104 activities power protein disaggregation in *Saccharomyces cerevisiae*. *Mol. Cell. Biol.* 37 (11), e00027–17. doi:10.1128/MCB.00027-17

Kampinga, H. H., Hageman, J., Vos, M. J., Kubota, H., Tanguay, R. M., Bruford, E. A., et al. (2009). Guidelines for the nomenclature of the human heat shock proteins. *Cell Stress Chaperones* 14 (1), 105–111. doi:10.1007/s12192-008-0068-7

Kang, S. M., Kim, J.-H., Lee, W., Kim, G.-W., Lee, K.-H., Choi, K.-Y., et al. (2009). Interaction of hepatitis C virus core protein with Hsp60 triggers the production of reactive oxygen species and enhances TNF- $\alpha$ -mediated apoptosis. *Cancer Lett.* 279 (2), 230–237. doi:10.1016/j.canlet.2009.02.003



- Karlas, A., Machuy, N., Shin, Y., Pleissner, K.-P., Artarini, A., Heuer, D., et al. (2010). Genome-wide RNAi screen identifies human host factors crucial for influenza virus replication. *Nature* 463 (7282), 818–822. doi:10.1038/nature08760
- Kasperkiewicz, M. (2021). Covid-19, heat shock proteins, and autoimmune bullous diseases: A potential link deserving further attention. *Cell Stress Chaperones* 26 (1), 1–2. doi:10.1007/s12192-020-01180-3
- Katoh, H., Kubota, T., Kita, S., Nakatsu, Y., Aoki, N., Mori, Y., et al. (2015). Heat shock protein 70 regulates degradation of the mumps virus phosphoprotein via the ubiquitin-proteasome pathway. *J. Virol.* 89 (6), 3188–3199. doi:10.1128/JVI.03343-14
- Katsogiannou, M., Andrieu, C., and Rocchi, P. (2014). Heat shock protein 27 phosphorylation state is associated with cancer progression. *Front. Genet.* 5, 346. doi:10.3389/fgene.2014.00346
- Khachatourian, R., Ganapathy, E., Ahmadi, Y., Wheatley, N., Sundberg, C., Jung, C. L., et al. (2014). The NS5A-binding heat shock proteins HSC70 and HSP70 play distinct roles in the hepatitis C viral life cycle. *Virology* 454, 118–127. doi:10.1016/j.virol.2014.02.016
- Khachatourian, R., Ruchala, P., Waring, A., Jung, C. L., Ganapathy, E., Wheatley, N., et al. (2015). Structural characterization of the HSP70 interaction domain of the hepatitis C viral protein NS5A. *Virology* 475, 46–55. doi:10.1016/j.virol.2014.10.011
- Khadir, A., Kavalakatt, S., Cherian, P., Warsame, S., Abubaker, J. A., Dehbi, M., et al. (2018). Physical exercise enhanced heat shock protein 60 expression and attenuated inflammation in the adipose tissue of human diabetic obese. *Front. Endocrinol.* 9, 16. doi:10.3389/fendo.2018.00016
- Kim, D., Lee, J. Y., Yang, J. S., Kim, J. W., Kim, V. N., and Chang, H. (2020). The architecture of SARS-CoV-2 transcriptome. *Cell* 181 (4), 914–921. doi:10.1016/j.cell.2020.04.011
- Kitamura, M. (2008). Endoplasmic reticulum stress in the kidney. *Clin. Exp. Nephrol.* 12, 317–325. doi:10.1007/s10157-008-0060-7
- Klappa, P., Uddock, L. W., Darby, N. J., and Freedman, R. B. (1998). The b' domain provides the principal peptide-binding site of protein disulfide isomerase but all domains contribute to binding of misfolded proteins. *EMBO J.* 17 (4), 927–935. doi:10.1093/emboj/17.4.927
- Klumperman, J., Locker, J. K., Meijer, A., Horzinek, M. C., Geuze, H. J., and Rottier, P. J. (1994). Coronavirus M proteins accumulate in the Golgi complex beyond the site of virion budding. *J. Virol.* 68 (10), 6523–6534. doi:10.1128/JVI.68.10.6523-6534.1994
- Kmicik, S. W., and Mayer, M. P. (2022). Molecular mechanisms of heat shock factor 1 regulation. *Trends biochem. Sci.* 47, 218–234. doi:10.1016/j.tbs.2021.10.004
- Knobil, K., Choi, A. M., Weigand, G. W., and Jacoby, D. B. (1998). Role of oxidants in influenza virus-induced gene expression. *Am. J. Physiol.* 274 (1), L134–L142. doi:10.1152/ajplung.1998.274.1.L134
- Knoops, K., Kikkert, M., Van Den Wormsjoerd, H. E., van der Meer, Y., Koster, A. J., et al. (2008). SARS-coronavirus replication is supported by a reticulovesicular network of modified endoplasmic reticulum. *PLoS Biol.* 6 (9), e226. doi:10.1371/journal.pbio.0060226
- Ko, S. H., Liao, Y. J., Chi, Y. H., Lai, M. J., Chiang, Y. P., Lu, C. Y., et al. (2019). Interference of DNAJB6/MR1 isoform switch by morpholino inhibits replication of HIV-1 and RSV. *Mol. Ther. Nucleic Acids* 14, 251–261. doi:10.1016/j.omtn.2018.12.001
- Korenaga, M., Wang, T., Li, Y., Showalter, L. A., Chan, T., Sun, J., et al. (2005). Hepatitis C virus core protein inhibits mitochondrial electron transport and increases reactive oxygen species (ROS) production. *J. Biol. Chem.* 280 (45), 37481–37488. doi:10.1074/jbc.M506412200
- Kozlov, G., and Gehring, K. (2020). Calnexin cycle—structural features of the ER chaperone system. *FEBS J.* 287 (20), 4322–4340. doi:10.1111/febs.15330
- Kramer, B., Ferrari, D. M., Klappa, P., Pohlmann, N., and Soling, H. D. (2001). Functional roles and efficiencies of the thioredoxin boxes of calcium-binding proteins 1 and 2 in protein folding. *Biochem. J.* 357 (1), 83–95. doi:10.1042/0264-6021:3570083
- Kranz, P., Neumann, F., Wolf, A., Classen, F., Pompsch, M., Ocklenburg, T., et al. (2017). PDI is an essential redox-sensitive activator of PERK during the unfolded protein response (UPR). *Cell Death Dis.* 8 (8), e2986e2986. doi:10.1038/cddis.2017.369
- Krause, M., Gerchman, F., and Friedman, R. (2020). Coronavirus infection (SARS-CoV-2) in obesity and diabetes comorbidities: Is heat shock response determinant for the disease complications? *Diabetol. Metab. Syndr.* 12 (1), 63. doi:10.1186/s13098-020-00572-w
- Krishnan-Sivadoss, I., Mijares-Rojas, I. A., Villarreal-Leal, R. A., Torre-Amione, G., Knowlton, A. A., and Guerrero-Beltrán, C. E. (2021). Heat shock protein 60 and cardiovascular diseases: An intricate love-hate story. *Med. Res. Rev.* 41, 29–71. doi:10.1002/med.21723
- Kubra, K.-T., Uddin, M. A., Akhter, M. S., and Barabutis, N. (2020). Hsp90 inhibitors induce the unfolded protein response in bovine and mice lung cells. *Cell. Signal.* 67, 109500. doi:10.1016/j.cellsig.2019.109500
- Kumar, P., Gaur, P., Kumari, R., and Lal, S. K. (2019). Influenza A virus neuraminidase protein interacts with Hsp90, to stabilize itself and enhance cell survival. *J. Cell. Biochem.* 120 (4), 6449–6458. doi:10.1002/jcb.27935
- Kuppalli, K., and Rasmussen, A. L. (2020). A glimpse into the eye of the COVID-19 cytokine storm. *EBioMedicine* 55, 102789. doi:10.1016/j.ebiom.2020.102789
- Lauwers, E., Wang, Y. C., Gallardo, R., Van der Kant, R., Michiels, E., Swerts, J., et al. (2018). Hsp90 mediates membrane deformation and exosome release. *Mol. Cell* 71 (5), 689–702. doi:10.1016/j.molcel.2018.07.016
- Leberher-Eichinger, D., Ankersmit, H. J., Hacker, S., Hetz, H., Kimberger, O., Schmidt, E. M., et al. (2012). HSP27 and HSP70 serum and urine levels in patients suffering from chronic kidney disease. *Clin. Chim. Acta* 413 (1–2), 282–286. doi:10.1016/j.cca.2011.10.010
- Lee, J. H., Gao, J., Kosinski, P. A., Elliman, S. J., Hughes, T. E., Gromada, J., et al. (2013). Heat shock protein 90 (HSP90) inhibitors activate the heat shock factor 1 (HSF1) stress response pathway and improve glucose regulation in diabetic mice. *Biochem. Biophys. Res. Commun.* 430 (3), 1109–1113. doi:10.1016/j.bbrc.2012.12.029
- Lee, T. G., Tang, N., Thompson, S., Miller, J., and Katze, M. G. (1994). The 58,000-dalton cellular inhibitor of the interferon-induced double-stranded RNA-activated protein kinase (PKR) is a member of the tetratricopeptide repeat family of proteins. *Mol. Cell. Biol.* 14 (4), 2331–2342. doi:10.1128/mcb.14.4.2331
- Lehr, S., Hartwig, S., and Sell, H. (2012). Adipokines: A treasure trove for the discovery of biomarkers for metabolic disorders. *Proteomics. Clin. Appl.* 6 (1–2), 91–101. doi:10.1002/prca.201100052
- Leng, A. M., Liu, T., Yang, J., Cui, J. F., Li, X. H., Zhu, Y. N., et al. (2012). The apoptotic effect and associated signalling of HSP90 inhibitor 17-DMAG in hepatocellular carcinoma cells. *Cell Biol. Int.* 36 (10), 893–899. doi:10.1042/CBI20110473
- Leone, G., Coffey, M. C., Gilmore, R., Duncan, R., Maybaum, L., and Lee, P. W. (1996). C-terminal trimerization, but not N-terminal trimerization, of the reovirus cell attachment protein is a posttranslational and Hsp70/ATP-dependent process. *J. Biol. Chem.* 271 (14), 8466–8471. doi:10.1074/jbc.271.14.8466
- Liao, J. B. (2006). Viruses and human cancer. *Yale J. Biol. Med.* 79, 115–122.
- Liao, S. L., Raung SI Fau - Chen, C.-J., and Chen, C. J. (2002). Japanese encephalitis virus stimulates superoxide dismutase activity in rat glial cultures. *Neurosci. Lett.* 324 (2), 133–136. doi:10.1016/s0304-3940(02)00236-7
- Lin, J., Shorter, J., and Lucius, A. L. (2022). AAA+ proteins: One motor, multiple ways to work. *Biochem. Soc. Trans.* 50 (2), 895–906. doi:10.1042/BST20200350
- Ling, S., Luo, M., Jiang, S., Liu, J., Ding, C., Zhang, Q., et al. (2018). Cellular Hsp27 interacts with classical swine fever virus NS5A protein and negatively regulates viral replication by the NF-κB signaling pathway. *Virology* 518, 202–209. doi:10.1016/j.virol.2018.02.020
- Lubkowska, A., Pluta, W., Strońska, A., and Lalko, A. (2021). Role of heat shock proteins (HSP70 and HSP90) in viral infection. *Int. J. Mol. Sci.* 22 (17), 9366. doi:10.3390/ijms22179366
- Luengo, T. M., Mayer, M. P., and Rüdiger, S. G. D. (2019). The Hsp70–Hsp90 chaperone cascade in protein folding. *Trends Cell Biol.* 29 (2), 164–177. doi:10.1016/j.tcb.2018.10.004
- Lukas, J., Pospech, J., Oppermann, C., Hund, C., Iwanov, K., Pantoom, S., et al. (2019). Role of endoplasmic reticulum stress and protein misfolding in disorders of the liver and pancreas. *Adv. Med. Sci.* 64, 315–323. doi:10.1016/j.advms.2019.03.004
- Luo, J., Rizvi, H., Preeshagul, I. R., Egger, J. V., Hoyos, D., Bandlamudi, C., et al. (2020). COVID-19 in patients with lung cancer. *Ann. Oncol.* 31 (10), 1386–1396. doi:10.1016/j.annonc.2020.06.007
- Macejak, D. G., and Sarnow, P. (1992). Association of heat shock protein 70 with enterovirus capsid precursor P1 in infected human cells. *J. Virol.* 66 (3), 1520–1527. doi:10.1128/JVI.66.3.1520-1527.1992
- Mahmood, F., Xu, R., Awan, M. U. N., Song, Y., Han, Q., Xia, X., et al. (2021). PDIA3: Structure, functions and its potential role in viral infections. *Biomed. Pharmacother.* 143, 112110. doi:10.1016/j.biopha.2021.112110
- Makhnevych, T., and Houry, W. A. (2012). The role of Hsp90 in protein complex assembly. *Biochim. Biophys. Acta* 1823 (3), 674–682. doi:10.1016/j.bbamer.2011.09.001
- Manzoor, R., Kuroda, K., Yoshida, R., Tsuda, Y., Fujikura, D., Miyamoto, H., et al. (2014). Heat shock protein 70 modulates influenza A virus polymerase activity. *J. Biol. Chem.* 289 (11), 7599–7614. doi:10.1074/jbc.M113.507798



- Marino Gammazza, A., Légaré, S., Lo Bosco, G., Fucarino, A., Angileri, F., Conway de Macario, E., et al. (2020). Human molecular chaperones share with SARS-CoV-2 antigenic epitopes potentially capable of eliciting autoimmunity against endothelial cells: Possible role of molecular mimicry in COVID-19. *Cell Stress Chaperones* 25 (5), 737–741. doi:10.1007/s12192-020-01148-3
- Marinova, M., Solopov, P., Dimitropoulou, C., Colunga Biancatelli, R. M., and Catravas, J. D. (2020). Post-treatment with a heat shock protein 90 inhibitor prevents chronic lung injury and pulmonary fibrosis, following acute exposure of mice to HCl. *Exp. Lung Res.* 46 (6), 203–216. doi:10.1080/01902148.2020.1764148
- Märker, T., Sell, H., Zilleßen, P., Glöde, A., Kriebel, J., Ouwens, D. M., et al. (2012). Heat shock protein 60 as a mediator of adipose tissue inflammation and insulin resistance. *Diabetes* 61 (3), 615–625. doi:10.2337/db10-1574
- Marzec, L., Zdrojewski, Z., Liberek, T., Bryl, E., Chmielewski, M., Witkowski, J. M., et al. (2009). Expression of Hsp72 protein in chronic kidney disease patients. *Scand. J. Urol. Nephrol.* 43 (5), 400–408. doi:10.3109/00365590903089489
- Marzec, M., Eletto, D., and Argon, Y. (2012). GRP94: An HSP90-like protein specialized for protein folding and quality control in the endoplasmic reticulum. *Biochim. Biophys. Acta* 1823, 774–787. doi:10.1016/j.bbamcr.2011.10.013
- McBride, R., Van Zyl, M., and Fielding, B. C. (2014). The coronavirus nucleocapsid is a multifunctional protein. *Viruses* 6 (8), 2991–3018. doi:10.3390/v6082991
- McGonagle, D., O'Donnell, J. S., Sharif, K., Emery, P., and Bridgewood, C. (2020). Immune mechanisms of pulmonary intravascular coagulopathy in COVID-19 pneumonia. *Lancet Rheumatol.* 2 (7), e437–e445. doi:10.1016/S2665-9913(20)30121-1
- Meikle, C. K. S., Creeden, J. F., McCullumsmith, C., and Worth, R. G. (2021). SSRIs: Applications in inflammatory lung disease and implications for COVID-19. *Neuropsychopharmacol. Rep.* 41, 325–335. doi:10.1002/npr2.12194
- Melville, M. W., Hansen, W. J., Freeman, B. C., Welch, W. J., and Katze, M. G. (1997). The molecular chaperone hsp40 regulates the activity of P58IPK, the cellular inhibitor of PKR. *Proc. Natl. Acad. Sci. U. S. A.* 94 (1), 97–102. doi:10.1073/pnas.94.1.97
- Merkling, S. H., Overheul, G. J., van Mierlo, J. T., Arends, D., Gilissen, C., and van Rij, R. P. (2015). The heat shock response restricts virus infection in *Drosophila*. *Sci. Rep.* 5 (1), 12758. doi:10.1038/srep12758
- Milewska, A., Nowak, P., Owczarek, K., Szczepanski, A., Zarebski, M., Hoang, A., et al. (2018). Entry of human coronavirus NL63 into the cell. *J. Virol.* 92 (3), e01933–17. doi:10.1128/JVI.01933-17
- Mittal, S., and Rajala, M. S. (2020). Heat shock proteins as biomarkers of lung cancer. *Cancer Biol. Ther.* 21 (6), 477–485. doi:10.1080/15384047.2020.1736482
- Molinari, M., Eriksson, K. K., Calanca, V., Galli, C., Cresswell, P., Michalak, M., et al. (2004). Contrasting functions of calreticulin and calnexin in glycoprotein folding and ER quality control. *Mol. Cell* 13 (1), 125–135. doi:10.1016/s1097-2765(03)00494-5
- Mollapour, M., and Neckers, L. (2012). Post-translational modifications of Hsp90 and their contributions to chaperone regulation. *Biochim. Biophys. Acta* 1823 (3), 648–655. doi:10.1016/j.bbamcr.2011.07.018
- Momose, F., Naito, T., Yano, K., Sugimoto, S., Morikawa, Y., and Nagata, K. (2002). Identification of Hsp90 as a stimulatory host factor involved in influenza virus RNA synthesis. *J. Biol. Chem.* 277 (47), 45306–45314. doi:10.1074/jbc.M206822200
- Morales-Buenrostro, L. E., Salas-Nolasco, O. I., Barrera-Chimal, J., Casas-Aparicio, G., Irizar-Santana, S., Perez-Villalva, R., et al. (2014). Hsp72 is a novel biomarker to predict acute kidney injury in critically ill patients. *PLoS one* 9 (10), e109407. doi:10.1371/journal.pone.0109407
- Moseley, P. (2000). Stress proteins and the immune response. *Immunopharmacology* 48 (3), 299–302. doi:10.1016/s0162-3109(00)00227-7
- Musiał, K., Szprynger, K., Szczepańska, M., and Zwolińska, D. (2010). The heat shock protein profile in children with chronic kidney disease. *Perit. Dial. Int.* 30 (2), 227–232. doi:10.3747/pdi.2008.00153
- Musiał, K., and Zwolińska, D. (2011). Heat shock proteins in chronic kidney disease. *Pediatr. Nephrol.* 26, 1031–1037. doi:10.1007/s00467-010-1709-5
- Nain, M., Mukherjee, S., Karmakar, S. P., Paton, A. W., Paton, J. C., Abidin, M. Z., et al. (2017). GRP78 is an important host factor for Japanese encephalitis virus entry and replication in mammalian cells. *J. Virol.* 91 (6), e02274–16. doi:10.1128/JVI.02274-16
- Nayak Rao, S. (2016). The role of heat shock proteins in kidney disease. *J. Transl. Int. Med.* 4, 114–117. doi:10.1515/jtım-2016-0034
- Nelson, E. V., Pacheco, J. R., Hume, A. J., Cressey, T. N., Deflubé, L. R., Ruedas, J. B., et al. (2017). An RNA polymerase II-driven Ebola virus minigenome system as an advanced tool for antiviral drug screening. *Antivir. Res.* 146, 21–27. doi:10.1016/j.antiviral.2017.08.005
- Neukirch, L., Fougeroux, C., Andersson, A. M. C., and Holst, P. J. (2020). The potential of adenoviral vaccine vectors with altered antigen presentation capabilities. *Expert Rev. Vaccines* 19 (1), 25–41. doi:10.1080/14760584.2020.1711054
- Ninagawa, S., George, G., and Mori, K. (2021). Mechanisms of productive folding and endoplasmic reticulum-associated degradation of glycoproteins and non-glycoproteins. *Biochim. Biophys. Acta. Gen. Subj.* 1865, 129812–129820. doi:10.1016/j.bbagen.2020.129812
- Nollen, E. A. A., Kabakov, A. E., Brunsting, J. F., Kanon, B., Höhfeld, J., and Kamping, H. H. (2001). Modulation of *in vivo* HSP70 chaperone activity by hip and bag-1. *J. Biol. Chem.* 276 (7), 4677–4682. doi:10.1074/jbc.M009745200
- Obermann, W. M. J., Sondermann, H., Russo, A. A., Pavletich, N. P., and Hartl, F. U. (1998). *In vivo* function of Hsp90 is dependent on ATP binding and ATP hydrolysis. *J. Cell Biol.* 143 (4), 901–910. doi:10.1083/jcb.143.4.901
- Oglesbee, M. J., Kenney, H., Kenney, T., and Krakowka, S. (1993). Enhanced production of morbillivirus gene-specific RNAs following induction of the cellular stress response in stable persistent infection. *Virology* 192 (2), 556–567. doi:10.1006/viro.1993.1072
- Oh, H. J., Easton, D., Murawski, M., Kaneko, Y., and Subjeck, J. R. (1999). The chaperoning activity of hsp110 identification of functional domains by use of targeted deletions. *J. Biol. Chem.* 274 (22), 15712–15718. doi:10.1074/jbc.274.22.15712
- Oikonomou, C., and Hendershot, L. M. (2020). Disposing of misfolded ER proteins: A troubled substrate's way out of the ER. *Mol. Cell. Endocrinol.* 500, 110630–30. doi:10.1016/j.mce.2019.110630
- Okamoto, T., Yamamoto, H., Kudo, I., Matsumoto, K., Odaka, M., Grave, E., et al. (2017). HSP60 possesses a GTPase activity and mediates protein folding with HSP10. *Sci. Rep.* 7 (1), 16931. doi:10.1038/s41598-017-17167-7
- Olagnier, D., Peri, S., Steel, C., van Montfort, N., Chiang, C., Beljanski, V., et al. (2014). Cellular oxidative stress response controls the antiviral and apoptotic programs in dengue virus-infected dendritic cells. *PLoS Pathog.* 10 (12), e1004566. doi:10.1371/journal.ppat.1004566
- Oliveira, A. P., Simabuco, F. M., Tamura, R. E., Guerrero, M. C., Ribeiro, P. G., Libermann, T. A., et al. (2013). Human respiratory syncytial virus N, P and M protein interactions in HEK-293T cells. *Virus Res.* 177 (1), 108–112. doi:10.1016/j.virusres.2013.07.010
- Oliver, J. D., Roderick, H. L., Llewellyn, D. H., and High, S. (1999). ERp57 functions as a subunit of specific complexes formed with the ER lectins calreticulin and calnexin. *Mol. Biol. Cell* 10 (8), 2573–2582. doi:10.1091/mbc.10.8.2573
- Oroz, J., Blair, L. J., and Zweckstetter, M. (2019). Dynamic Aha1 co-chaperone binding to human Hsp90. *Protein Sci.* 28 (9), 1545–1551. doi:10.1002/pro.3678
- Oualikene, W., Lamoureux, L., Weber, J. M., and Massie, B. (2000). Protease-deleted adenovirus vectors and complementing cell lines: Potential applications of single-round replication mutants for vaccination and gene therapy. *Hum. Gene Ther.* 11 (9), 1341–1353. doi:10.1089/10430340050032438
- Padwad, Y. S., Mishra, K. P., Jain, M., Chanda, S., Karan, D., and Ganju, L. (2009). RNA interference mediated silencing of Hsp60 gene in human monocytic myeloma cell line U937 revealed decreased dengue virus multiplication. *Immunobiology* 214 (6), 422–429. doi:10.1016/j.imbio.2008.11.010
- Pan, Z., Wu, Q., Xie, Z., Wu, Q., Tan, X., and Wang, X. (2020). Upregulation of HSP72 attenuates tendon adhesion by regulating fibroblast proliferation and collagen production via blockade of the STAT3 signaling pathway. *Cell. Signal.* 71, 109606. doi:10.1016/j.cellsig.2020.109606
- Parakh, S., and Atkin, J. D. (2015). Novel roles for protein disulphide isomerase in disease states: A double edged sword? *Front. Cell Dev. Biol.* 3, 30. doi:10.3389/fcell.2015.00030
- Parissi, V., Calmels, C., De Soultrait, V. R., Caumont, A., Fournier, M., Chaignepain, S., et al. (2001). Functional interactions of human immunodeficiency virus type 1 integrase with human and yeast HSP60. *J. Virol.* 75 (23), 11344–11353. doi:10.1128/JVI.75.23.11344-11353.2001
- Park, Y. H., Seo, J. H., Park, J., Lee, H. S., and Kim, K. (2017). Hsp70 acetylation prevents caspase-dependent/independent apoptosis and autophagic cell death in cancer cells. *Int. J. Oncol.* 51, 573–578. doi:10.3892/ijo.2017.4039
- Pespeni, M., Mackersie, R. C., Lee, H., Morabito, D., Hodnett, M., Howard, M., et al. (2005). Serum levels of Hsp60 correlate with the development of acute lung injury after trauma. *J. Surg. Res.* 126 (1), 41–47. doi:10.1016/j.jss.2005.01.012
- Petersen, O. H., Gerasimenko, O. V., and Gerasimenko, J. V. (2020). Endocytic uptake of SARS-CoV-2: the critical roles of pH, Ca<sup>2+</sup>, and NAADP. *Function* 1 (1), zqaa003. doi:10.1093/function/zqaa003

- Prodromou, C. (2016). Mechanisms of Hsp90 regulation. *Biochem. J.* 473 (16), 2439–2452. doi:10.1042/BCJ20160005
- Pujhari, S., Brustolin, M., Macias, V. M., Nissly, R. H., Nomura, M., Kuchipudi, S. V., et al. (2019). Heat shock protein 70 (Hsp70) mediates Zika virus entry, replication, and egress from host cells. *Emerg. Microbes Infect.* 8 (1), 8–16. doi:10.1080/22221751.2018.1557988
- Ragab, D., Salah Eldin, H., Taeimah, M., Khattab, R., and Salem, R. (2020). The COVID-19 cytokine storm; what we know so far. *Front. Immunol.* 11, 1446. doi:10.3389/fimmu.2020.01446
- Ramos, C. H., and Ayinde, K. S. (2021). Are Hsp90 inhibitors good candidates against Covid-19? *Curr. Protein Pept. Sci.* 22 (3), 192–200. doi:10.2174/138920372166620111160925
- Ranek Mark, J., Stachowski Marisa, J., Kirk Jonathan, A., and Willis Monte, S. (2018). The role of heat shock proteins and co-chaperones in heart failure. *Philos. Trans. R. Soc. Lond. B Biol. Sci.* 373 (1738), 20160530. doi:10.1098/rstb.2016.0530
- Rao, S. N. (2016). The role of heat shock proteins in kidney disease. *J. Transl. Int. Med.* 4 (3), 114–117. doi:10.1515/jtim-2016-0034
- Rathore, A. P., Haystead, T., Das, P. K., Merits, A., Ng, M. L., and Vasudevan, S. G. (2014). Chikungunya virus nsP3 & nsP4 interacts with HSP-90 to promote virus replication: HSP-90 inhibitors reduce CHIKV infection and inflammation *in vivo*. *Antivir. Res.* 103, 7–16. doi:10.1016/j.antiviral.2013.12.010
- Reizine, F., Lesouhaitier, M., Gregoire, M., Pinceaux, K., Gacouin, A., Maamar, A., et al. (2021). SARS-CoV-2-induced ARDS associates with MDSC expansion, lymphocyte dysfunction, and arginine shortage. *J. Clin. Immunol.* 41 (3), 515–525. doi:10.1007/s10875-020-00920-5
- Reyes-del Valle, J., Chávez-Salinas, S., Medina, F., and Del Angel, R. M. (2005). Heat shock protein 90 and heat shock protein 70 are components of dengue virus receptor complex in human cells. *J. Virol.* 79 (8), 4557–4567. doi:10.1128/JVI.79.8.4557-4567.2005
- Richter, K., Haslbeck, M., and Buchner, J. (2010). The heat shock response: Life on the verge of death. *Mol. Cell* 40, 253–266. doi:10.1016/j.molcel.2010.10.006
- Riemer, J., Hansen, H. G., Appenzeller-Herzog, C., Johansson, L., and Ellgaard, L. (2011). Identification of the PDI-family member ERp90 as an interaction partner of ERFAD. *PLoS One* 6 (2), e17037. doi:10.1371/journal.pone.0017037
- Rodriguez-Iturbe, B., and Johnson, R. J. (2018). Heat shock proteins and cardiovascular disease. *Physiol. Int.* 105 (1), 19–37. doi:10.1556/2060.105.2018.1.4
- Rodriguez-Iturbe, B., Lanaspas, M. A., and Johnson, R. J. (2019). The role of autoimmune reactivity induced by heat shock protein 70 in the pathogenesis of essential hypertension. *Br. J. Pharmacol.* 176 (12), 1829–1838. doi:10.1111/bph.14334
- Romagnoli, S., Peris, A., De Gaudio, A. R., and Geppetti, P. (2020). SARS-CoV-2 and COVID-19: From the bench to the bedside. *Physiol. Rev.* 100 (4), 1455–1466. doi:10.1152/physrev.00020.2020
- Rossmann, M. G. (1984). Constraints on the assembly of spherical virus particles. *Virology* 134 (1), 1–11. doi:10.1016/0042-6822(84)90267-8
- Ryu, H. H., and Ha, S. H. (2020). HSP70 interacts with Rheb, inhibiting mTORC1 signaling. *Biochem. Biophys. Res. Commun.* 533 (4), 1198–1203. doi:10.1016/j.bbrc.2020.07.053
- Sabirli, R., Koseler, A., Goren, T., Turkcu, I., and Kurt, O. (2021). High GRP78 levels in covid-19 infection: A case-control study. *Life Sci.* 265, 118781. doi:10.1016/j.lfs.2020.118781
- Sagara, Y., Ishida, C., Inoue, Y., Shiraki, H., and Maeda, Y. (1998). 71-kilodalton heat shock cognate protein acts as a cellular receptor for syncytium formation induced by human T-cell lymphotropic virus type 1. *J. Virol.* 72 (1), 535–541. doi:10.1128/JVI.72.1.535-541.1998
- Saha, A., and Anirvan, P. (2020). Cancer progression in COVID-19: Integrating the roles of renin angiotensin aldosterone system, angiotensin-2, heat shock protein-27 and epithelial mesenchymal transition. *Ecancermedicalscience* 14, 1099. doi:10.3332/ecancer.2020.1099
- Saksela, K. (1997). HIV-1 Nef and host cell protein kinases. *Front. Biosci.* 2 (4), 606–618. doi:10.2741/a217
- Samali, A., and Orrenius, S. (1998). Heat shock proteins: Regulators of stress response and apoptosis. *Cell Stress Chaperones* 3, 228–236. doi:10.1379/1466-1268(1998)003<0228:hspros>2.3.co;2
- Sano, R., and Reed, J. C. (2013). ER stress-induced cell death mechanisms. *Biochim. Biophys. Acta* 1833, 3460–3470. doi:10.1016/j.bbamcr.2013.06.028
- Sanyaolu, A., Okorie, C., Marinkovic, A., Patidar, R., Younis, K., Desai, P., et al. (2020). Comorbidity and its impact on patients with COVID-19. *SN Compr. Clin. Med.* 2, 1069–1076. doi:10.1007/s42399-020-00363-4
- Sarkar, S., and Roy, S. (2017). A mini review on heat shock proteins (hsps): Special emphasis on heat shock protein70 (hsp70). *BN Seal. J. Sci.* 9, 129–138.
- Schett, G., Metzler, B., Kleindienst, R., Moschén, I., Hattmannsdorfer, R., Wolf, H., et al. (1997). Salivary anti-hsp65 antibodies as a diagnostic marker for gingivitis and a possible link to atherosclerosis. *Int. Arch. Allergy Immunol.* 114 (3), 246–250. doi:10.1159/000237675
- Schönthal, A. H. (2012). Endoplasmic reticulum stress: its role in disease and novel prospects for therapy. *Scientifica* 2012, 857516. doi:10.6064/2012/857516
- Sell, H., Habich, C., and Eckel, J. (2012). Adaptive immunity in obesity and insulin resistance. *Nat. Rev. Endocrinol.* 8 (12), 709–716. doi:10.1038/nrendo.2012.114
- Sell, H., Poitou, C., Habich, C., Bouillot, J. L., Eckel, J., and Clément, K. (2017). Heat shock protein 60 in obesity: Effect of bariatric surgery and its relation to inflammation and cardiovascular risk. *Obesity* 25 (12), 2108–2114. doi:10.1002/oby.22014
- Sellares, J., Veraldi, K. L., Thiel, K. J., Cárdenas, N., Alvarez, D., Schneider, F., et al. (2019). Intracellular heat shock protein 70 deficiency in pulmonary fibrosis. *Am. J. Respir. Cell Mol. Biol.* 60 (6), 629–636. doi:10.1165/rcmb.2017-0268OC
- Sharif-Askari, N. S., Sharif-Askari, F. S., Mdkhana, B., Alsayed, H. A. H., Alsafar, H., Alrais, Z. F., et al. (2021). Upregulation of oxidative stress gene markers during SARS-CoV-2 viral infection. *Free Radic. Biol. Med.* 172, 688–698. doi:10.1016/j.freeradbiomed.2021.06.018
- Sharma, K., Tripathi, S., Ranjan, P., Kumar, P., Garten, R., Dey, V., et al. (2011). Influenza A virus nucleoprotein exploits Hsp40 to inhibit PKR activation. *PLoS One* 6 (6), e20215. doi:10.1371/journal.pone.0020215
- Shevchenko, M., Servuli, E., Albakova, Z., Kanevskiy, L., and Sapozhnikov, A. (2020). The role of heat shock protein 70 kDa in asthma. *J. Asthma Allergy* 13, 757–772. doi:10.2147/JAA.S288886
- Shi, C.-S., Nabar, N. R., Huang, N. N., and Kehrl, J. H. (2019). SARS-Coronavirus Open Reading Frame-8b triggers intracellular stress pathways and activates NLRP3 inflammasomes. *Cell Death Discov.* 5 (1), 101. doi:10.1038/s41420-019-0181-7
- Simmons, A., Aluvihare, V., and McMichael, A. (2001). Nef triggers a transcriptional program in T cells imitating single-signal T cell activation and inducing HIV virulence mediators. *Immunity* 14 (6), 763–777. doi:10.1016/s1074-7613(01)00158-3
- Singh, I. S., and Hasday, J. D. (2013). Fever, hyperthermia and the heat shock response. *Int. J. Hyperth.* 29 (5), 423–435. doi:10.3109/02656736.2013.808766
- Silverstein, N. J., Wang, Y., Manickas-Hill, Z., Carbone, C., Dauphin, A., Boribong, B. P., et al. (2022). Innate lymphoid cells and COVID-19 severity in SARS-CoV-2 infection. *elife* 11, e74681. doi:10.7554/eLife.74681
- Skolnik, K., and Ryerson, C. J. (2016). Unclassifiable interstitial lung disease: A review. *Respirology* 21 (1), 51–56. doi:10.1111/resp.12568
- Song, H., Moseley, P. L., Lowe, S. L., and Ozbun, M. A. (2010). Inducible heat shock protein 70 enhances HPV31 viral genome replication and virion production during the differentiation-dependent life cycle in human keratinocytes. *Virus Res.* 147 (1), 113–122. doi:10.1016/j.virusres.2009.10.019
- Song, P., Li, W., Xie, J., Hou, Y., and You, C. (2020). Cytokine storm induced by SARS-CoV-2. *Clin. Chim. Acta.* 509, 280–287. doi:10.1016/j.cca.2020.06.017
- Srivastava, K. (2020). Association between COVID-19 and cardiovascular disease. *Int. J. Cardiol. Heart Vasc.* 29, 100583. doi:10.1016/j.ijcha.2020.100583
- Stocker, R., and Keaney, J. F. (2004). Role of oxidative modifications in Atherosclerosis. *Physiol. Rev.* 84 (4), 1381–1478. doi:10.1152/physrev.00047.2003
- Storkanova, H., Oreska, S., Spiritovic, M., Hermankova, B., Pavelka, K., Vencovsky, J., et al. (2018). SAT0493 Plasma levels of hsp90 are increased in interstitial lung disease and skin fibrosis in patients with systemic sclerosis. *Ann. Rheum. Dis.* 73 (6), 1215–1222.
- Suh, J., Mukerji, S. S., Collens, S. I., Padera, R. F., Pinkus, G. S., Amato, A. A., et al. (2021). Skeletal muscle and peripheral nerve histopathology in COVID-19. *Neurology* 97 (8), e849–e858. doi:10.1212/WNL.0000000000012344
- Sun, M., Yu, Z., Ma, J., Pan, Z., Lu, C., and Yao, H. (2017). Down-regulating heat shock protein 27 is involved in porcine epidemic diarrhea virus escaping from host antiviral mechanism. *Vet. Microbiol.* 205, 6–13. doi:10.1016/j.vetmic.2017.04.031
- Sun, Y., Huang, Y.-H., Huang, F.-Y., Mei, W.-L., Liu, Q., Wang, C.-C., et al. (2018). 3'-epi-12 $\beta$ -hydroxyfroside, a new cardenolide, induces cytoprotective autophagy via blocking the Hsp90/Akt/mTOR axis in lung cancer cells. *Theranostics* 8, 2044–2060. doi:10.7150/thno.23304
- Sureda, A., Alizadeh, J., Nabavi, S. F., Berindan-Neagoe, I., Cismaru, C. A., Jeandet, P., et al. (2020). Endoplasmic reticulum as a potential therapeutic target for Covid-19 infection management? *Eur. J. Pharmacol.* 882, 173288. doi:10.1016/j.ejphar.2020.173288
- Swaroop, S., Mahadevan, A., Shankar, S. K., Adlakhia, Y. K., and Basu, A. (2018). HSP60 critically regulates endogenous IL-1 $\beta$  production in activated microglia by

- stimulating NLRP3 inflammasome pathway. *J. Neuroinflammation* 15 (1), 177. doi:10.1186/s12974-018-1214-5
- Szczepanski, A., Owczarek, K., Milewska, A., Baster, Z., Rajfur, Z., Mitchell, J. A., et al. (2018). Canine respiratory coronavirus employs caveolin-1-mediated pathway for internalization to HRT-18G cells. *Vet. Res.* 49 (1), 55. doi:10.1186/s13567-018-0551-9
- Tagawa, S., Yeh, M. T., Rainbolt, T. K., Nayak, A., Shao, H., Gestwicki, J. E., et al. (2019). Zika virus dependence on host Hsp70 provides a protective strategy against infection and disease. *Cell Rep.* 26 (4), 906–920. doi:10.1016/j.celrep.2018.12.095
- Tanguy, J., Pommerolle, L., Garrido, C., Kolb, M., Bonniaud, P., Goirand, F., et al. (2021). Extracellular heat shock proteins as therapeutic targets and biomarkers in fibrosing interstitial lung diseases. *Int. J. Mol. Sci.* 22 (17), 9316. doi:10.3390/ijms22179316
- Tiss, A., Khadir, A., Abubaker, J., Abu-Farha, M., Al-Khairi, I., Cherian, P., et al. (2014). Immunohistochemical profiling of the heat shock response in obese non-diabetic subjects revealed impaired expression of heat shock proteins in the adipose tissue. *Lipids Health Dis.* 13, 106. doi:10.1186/1476-511X-13-106
- Torres, J., Parthasarathy, K., Lin, X., Saravanan, R., Kukol, A., and Liu, D. X. (2006). Model of a putative pore: the pentameric  $\alpha$ -helical bundle of SARS coronavirus E protein in lipid bilayers. *Biophys. J.* 91 (3), 938–947. doi:10.1529/biophysj.105.080119
- Triantafyllou, K., Fradelizi, D., Wilson, K., and Triantafyllou, M. (2002). GRP78, a coreceptor for coxsackievirus A9, interacts with major histocompatibility complex class I molecules which mediate virus internalization. *J. Virol.* 76 (2), 633–643. doi:10.1128/jvi.76.2.633-643.2002
- Tsou, Y. L., Lin, Y. W., Chang, H. W., Lin, H. Y., Shao, H. Y., Yu, S. L., et al. (2013). Heat shock protein 90: Role in enterovirus 71 entry and assembly and potential target for therapy. *PLoS One* 8 (10), e77133. doi:10.1371/journal.pone.0077133
- Tsutsumi, S., and Neckers, L. (2007). Extracellular heat shock protein 90: A role for a molecular chaperone in cell motility and cancer metastasis. *Cancer Sci.* 98 (10), 1536–1539. doi:10.1111/j.1349-7006.2007.00561.x
- Uddin, M., Mustafa, F., Rizvi, T. A., Loney, T., Al Suwaidi, H., Al-Marzouqi, A. H., et al. (2020). SARS-CoV-2/COVID-19: Viral genomics, epidemiology, vaccines, and therapeutic interventions. *Viruses* 12 (5), 526. doi:10.3390/v12050526
- Ujino, S., Yamaguchi, S., Shimotohno, K., and Takaku, H. (2009). Heat-shock protein 90 is essential for stabilization of the hepatitis C virus nonstructural protein NS3. *J. Biol. Chem.* 284 (11), 6841–6846. doi:10.1074/jbc.M806452200
- Varga, Z., Flammer, A. J., Steiger, P., Haberecker, M., Andermatt, R., Zinkernagel, A. S., et al. (2020). Endothelial cell infection and endotheliitis in COVID-19. *Lancet* 395 (10234), 1417–1418. doi:10.1016/S0140-6736(20)30937-5
- Vasconcelos, D. Y., Cai, X. H., and Oglesbee, M. J. (1998). Constitutive overexpression of the major inducible 70 kDa heat shock protein mediates large plaque formation by measles virus. *J. Gen. Virol.* 79 (9), 2239–2247. doi:10.1099/0022-1317-79-9-2239
- Vashist, S., Urena, L., Gonzalez-Hernandez, M. B., Choi, J., de Rougemont, A., Rocha-Pereira, J., et al. (2015). Molecular chaperone Hsp90 is a therapeutic target for noroviruses. *J. Virol.* 89 (12), 6352–6363. doi:10.1128/JVI.00315-15
- Vega-Almeida, T. O., Salas-Benito, M., Nova-Ocampo, D., Ascensión, M., del Angel, R. M., and Salas-Benito, J. S. (2013). Surface proteins of C6/36 cells involved in dengue virus 4 binding and entry. *Arch. Virol.* 158 (6), 1189–1207. doi:10.1007/s00705-012-1596-0
- Wan, Q., Song, D., Li, H., and He, M. L. (2020). Stress proteins: The biological functions in virus infection, present and challenges for target-based antiviral drug development. *Signal Transduct. Target. Ther.* 5 (1), 125–140. doi:10.1038/s41392-020-00233-4
- Wang, C., Zhang, Y., Guo, K., Wang, N., Jin, H., Liu, Y., et al. (2015). Heat shock proteins in hepatocellular carcinoma: Molecular mechanism and therapeutic potential. *Int. J. Cancer* 138 (8), 1824–1834. doi:10.1002/ijc.29723
- Wang, F., Qiu, Y., Zhang, H. M., Hanson, P., Ye, X., Zhao, G., et al. (2017). Heat shock protein 70 promotes coxsackievirus B3 translation initiation and elongation via Akt-mTORC1 pathway depending on activation of p70S6K and Cdc2. *Cell. Microbiol.* 19 (7), e12725. doi:10.1111/cmi.12725
- Wang, M., Dong, Q., Wang, H., He, Y., Chen, Y., Zhang, H., et al. (2016). Oblongifolin M, an active compound isolated from a Chinese medical herb *Garcinia oblongifolia*, potentially inhibits enterovirus 71 reproduction through downregulation of ERp57. *Oncotarget* 7 (8), 8797–8808. doi:10.18632/oncotarget.7122
- Wang, R. Y. L., Huang, Y. R., Chong, K. M., Hung, C. Y., Ke, Z. L., and Chang, R. Y. (2011). DnaJ homolog Hdj2 facilitates Japanese encephalitis virus replication. *Virol. J.* 8 (1), 471–477. doi:10.1186/1743-422X-8-471
- Wang, R. Y. R., Noddings, C. M., Kirschke, E., Myasnikov, A. G., Johnson, J. L., and Agard, D. A. (2022). Structure of hsp90–hsp70–hop–GR reveals the Hsp90 client-loading mechanism. *Nature* 601 (7893), 460–464. doi:10.1038/s41586-021-04252-1
- Wang, X., Zheng, T., Lin, L., Zhang, Y., Peng, X., Yan, Y., et al. (2020b). Influenza A virus induces autophagy by its hemagglutinin binding to cell surface heat shock protein 90AA1. *Front. Microbiol.* 11, 566348. doi:10.3389/fmicb.2020.566348
- Wang, Y., Grunewald, M., and Perlman, S. (2020a). Coronaviruses: An updated overview of their replication and pathogenesis. *Methods Mol. Biol.* 2203, 1–29. doi:10.1007/978-1-0716-0900-2\_1
- Waxman, L., Whitney, M., Pollok, B. A., Kuo, L. C., and Darke, P. L. (2001). Host cell factor requirement for hepatitis C virus enzyme maturation. *Proc. Natl. Acad. Sci. U. S. A.* 98 (24), 13931–13935. doi:10.1073/pnas.241510898
- Weiss, Y. G., Bromberg, Z., Raj, N., Raphael, J., Goloubinoff, P., Ben-Neriah, Y., et al. (2007). Enhanced heat shock protein 70 expression alters proteasomal degradation of I $\kappa$ B kinase in experimental acute respiratory distress syndrome. *Crit. Care Med.* 35 (9), 2128–2138. doi:10.1097/01.ccm.00000278915.78030.74
- Wendt, R., Lingitz, M. T., Laggner, M., Mildner, M., Traxler, D., Graf, A., et al. (2021). Clinical relevance of elevated soluble ST2, HSP27 and 20S proteasome at hospital admission in patients with COVID-19. *Biology* 10 (11), 1186. doi:10.3390/biology10111186
- Wick, G., Jakic, B., Buszko, M., Wick, M. C., and Grundtman, C. (2014). The role of heat shock proteins in atherosclerosis. *Nat. Rev. Cardiol.* 11 (9), 516–529. doi:10.1038/nrcardio.2014.91
- World Health Organization (2020). Novel coronavirus (2019-nCoV): Situation report, 3. Available at: <https://reliefweb.int/report/china/novel-coronavirus-2019-ncov-situation-report-3-23-january-2020>.
- Wu, J., Liu, T., Rios, Z., Mei, Q., Lin, X., and Cao, S. (2017a). Heat shock proteins and cancer. *Trends Pharmacol. Sci.* 38 (3), 226–256. doi:10.1016/j.tips.2016.11.009
- Wu, P., Chang, Y., and Pan, C. (2017b). High expression of heat shock proteins and heat shock factor-1 distinguishes an aggressive subset of clear cell renal cell carcinoma. *Histopathology* 71 (5), 711–718. doi:10.1111/his.13284
- Wyler, E., Mösbauer, K., Franke, V., Diag, A., Gottula, L. T., Arsiè, R., et al. (2021). Transcriptomic profiling of SARS-CoV-2 infected human cell lines identifies HSP90 as target for COVID-19 therapy. *Iscience* 24 (3), 102151. doi:10.1016/j.isci.2021.102151
- Xiao, A., Wong, J., and Luo, H. (2010). Viral interaction with molecular chaperones: Role in regulating viral infection. *Arch. Virol.* 155 (7), 1021–1031. doi:10.1007/s00705-010-0691-3
- Xu, T., Lin, Z., Wang, C., Li, Y., Xia, Y., Zhao, M., et al. (2019). Heat shock protein 70 as a supplementary receptor facilitates enterovirus 71 infections *in vitro*. *Microb. Pathog.* 128, 106–111. doi:10.1016/j.micpath.2018.12.032
- Xu, W., Mollapour, M., Prodromou, C., Wang, S., Scroggins, B. T., Palchick, Z., et al. (2012). Dynamic tyrosine phosphorylation modulates cycling of the Hsp90-P50CDC37-AHA1 chaperone machine. *Mol. Cell* 47, 434–443. doi:10.1016/j.molcel.2012.05.015
- Xue, T., Li, Q., Zhang, Q., Lin, W., Weng, J., Li, L., et al. (2020). Blood glucose levels in elderly subjects with type 2 diabetes during Covid-19 outbreak: A retrospective study in a single center (3/31/2020). Available at SSRN: <https://ssrn.com/abstract=3566198>.
- Yang, D., de la Rosa, G., Tewary, P., and Oppenheim, J. J. (2009). Alarmins link neutrophils and dendritic cells. *Trends Immunol.* 30 (11), 531–537. doi:10.1016/j.it.2009.07.004
- Yang, K., Xing, M. Y., Jiang, L. Y., Cai, Y. P., Yang, L. L., Xie, N. N., et al. (2021). Infection-associated hemophagocytic syndrome in critically ill patients with COVID-19. *Curr. Med. Sci.* 41 (1), 39–45. doi:10.1007/s11596-021-2315-4
- Yang, N., and Shen, H. M. (2020). Targeting the endocytic pathway and autophagy process as a novel therapeutic strategy in COVID-19. *Int. J. Biol. Sci.* 16 (10), 1724–1731. doi:10.7150/ijbs.45498
- Ye, Z., Wong, C. K., Li, P., and Xie, Y. (2008). A SARS-CoV protein, ORF-6, induces caspase-3 mediated, ER stress and JNK-dependent apoptosis. *Biochim. Biophys. Acta* 1780 (12), 1383–1387. doi:10.1016/j.bbagen.2008.07.009

- Yi, Z., Yuan, Z., Rice, C. M., and MacDonald, M. R. (2012). Flavivirus replication complex assembly revealed by DNAJC14 functional mapping. *J. Virol.* 86 (21), 11815–11832. doi:10.1128/JVI.01022-12
- Zhang, H., Penninger, J. M., Li, Y., Zhong, N., and Slutsky, A. S. (2020b). Angiotensin-converting enzyme 2 (ACE2) as a SARS-CoV-2 receptor: Molecular mechanisms and potential therapeutic target. *Intensive Care Med.* 46 (4), 586–590. doi:10.1007/s00134-020-05985-9
- Zhang, T., Wu, Q., and Zhang, Z. (2020a). Probable pangolin origin of SARS-CoV-2 associated with the COVID-19 outbreak. *Curr. Biol.* 30 (7), 1346–1351. doi:10.1016/j.cub.2020.03.022
- Zhang, W., Yang, F., Zhu, Z., Yang, Y., Wang, Z., Cao, W., et al. (2019). Cellular DNAJA3, a novel VP1-interacting protein, inhibits foot-and-mouth disease virus replication by inducing lysosomal degradation of VP1 and attenuating its antagonistic role in the beta interferon signaling pathway. *J. Virol.* 93 (13), e00588–19. doi:10.1128/JVI.00588-19
- Zhao, Y., Xiao, D., Zhang, L., Song, D., Chen, R., Li, S., et al. (2022). HSP90 inhibitors 17-AAG and VER-82576 inhibit porcine deltacoronavirus replication *in vitro*. *Vet. Microbiol.* 265, 109316. doi:10.1016/j.vetmic.2021.109316
- Zilae, M., and Shirali, S. (2016). Heat shock proteins and diabetes. *Can. J. Diabetes* 40 (6), 594–602. doi:10.1016/j.cjcd.2016.05.016
- Zhou, X., Zhang, C. Z., Lu, S. X., Chen, G. G., Li, L. Z., Liu, L. L., et al. (2015). miR-625 suppresses tumour migration and invasion by targeting IGF2BP1 in hepatocellular carcinoma. *Oncogene* 34 (8), 965–977. doi:10.1038/ncr.2014.35
- Zhu, G., and Lee, A. S. (2015). Role of the unfolded protein response, GRP78 and GRP94 in organ homeostasis. *J. Cell. Physiol.* 230, 1413–1420. doi:10.1002/jcp.24923
- Zhu, N., Zhang, D., Wang, W., Li, X., Yang, B., Song, J., et al. (2020). A novel coronavirus from patients with pneumonia in China, 2019. *N. Engl. J. Med.* 382, 727–733. doi:10.1056/NEJMoa2001017
- Zimmermann, M., Traxler, D., Bekos, C., Simader, E., Mueller, T., Graf, A., et al. (2020). Heat shock protein 27 as a predictor of prognosis in patients admitted to hospital with acute COPD exacerbation. *Cell Stress Chaperones* 25 (1), 141–149. doi:10.1007/s12192-019-01057-0
- Zininga, T., Ramatsui, L., and Shonhai, A. (2018). Heat shock proteins as immunomodulators. *Molecules* 23 (11), 2846. doi:10.3390/molecules23112846
- Zolkiewski, M., Zhang, T., and Nagy, M. (2012). Aggregate reactivation mediated by the Hsp100 chaperones. *Arch. Biochem. Biophys.* 520 (1), 1–6. doi:10.1016/j.abb.2012.01.012
- Zong, Z., Wei, Y., Ren, J., Zhang, L., and Zhou, F. (2021). The intersection of COVID-19 and cancer: Signaling pathways and treatment implications. *Mol. Cancer* 20 (1), 76–19. doi:10.1186/s12943-021-01363-1
- Zugel, U., and Kaufmann, S. H. (1999). Role of heat shock proteins in protection from and pathogenesis of infectious diseases. *Clin. Microbiol. Rev.* 12 (1), 19–39. doi:10.1128/CMR.12.1.19





## OPEN ACCESS

## EDITED BY

Stanley Makumire,  
University of Cape Town, South Africa

## REVIEWED BY

Prakash Chandra Mishra,  
Guru Nanak Dev University, India  
Victor Muleya,  
Midlands State University, Zimbabwe  
Ikechukwu Achilonu,  
University of the Witwatersrand, South Africa

## \*CORRESPONDENCE

Michael Oluwatoyin Daniyan,  
mdaniyan@oauife.edu.ng,  
toyinpharm@gmail.com

## SPECIALTY SECTION

This article was submitted to Molecular Diagnostics and Therapeutics, a section of the journal Frontiers in Molecular Biosciences

RECEIVED 09 June 2022

ACCEPTED 28 July 2022

PUBLISHED 24 August 2022

## CITATION

Daniyan MO, Fisusi FA and Adeoye OB (2022), Neurotransmitters and molecular chaperones interactions in cerebral malaria: Is there a missing link? *Front. Mol. Biosci.* 9:965569. doi: 10.3389/fmolb.2022.965569

## COPYRIGHT

© 2022 Daniyan, Fisusi and Adeoye. This is an open-access article distributed under the terms of the [Creative Commons Attribution License \(CC BY\)](#). The use, distribution or reproduction in other forums is permitted, provided the original author(s) and the copyright owner(s) are credited and that the original publication in this journal is cited, in accordance with accepted academic practice. No use, distribution or reproduction is permitted which does not comply with these terms.

# Neurotransmitters and molecular chaperones interactions in cerebral malaria: Is there a missing link?

Michael Oluwatoyin Daniyan<sup>1\*</sup>, Funmilola Adesodun Fisusi<sup>2</sup> and Olufunso Bayo Adeoye<sup>3</sup>

<sup>1</sup>Department of Pharmacology, Faculty of Pharmacy, Obafemi Awolowo University, Ile-Ife, Osun State, Nigeria, <sup>2</sup>Drug Research and Production Unit, Faculty of Pharmacy, Obafemi Awolowo University, Ile-Ife, Osun State, Nigeria, <sup>3</sup>Department of Biochemistry, Benjamin S. Carson (Snr.) College of Medicine, Babcock University, Ilishan-Remo, Ogun State, Nigeria

*Plasmodium falciparum* is responsible for the most severe and deadliest human malaria infection. The most serious complication of this infection is cerebral malaria. Among the proposed hypotheses that seek to explain the manifestation of the neurological syndrome in cerebral malaria is the vascular occlusion/sequestration/mechanic hypothesis, the cytokine storm or inflammatory theory, or a combination of both. Unfortunately, despite the increasing volume of scientific information on cerebral malaria, our understanding of its pathophysiologic mechanism(s) is still very limited. In a bid to maintain its survival and development, *P. falciparum* exports a large number of proteins into the cytosol of the infected host red blood cell. Prominent among these are the *P. falciparum* erythrocytes membrane protein 1 (PfEMP1), *P. falciparum* histidine-rich protein II (PfHRP2), and *P. falciparum* heat shock proteins 70-x (PfHsp70-x). Functional activities and interaction of these proteins with one another and with recruited host resident proteins are critical factors in the pathology of malaria in general and cerebral malaria in particular. Furthermore, several neurological impairments, including cognitive, behavioral, and motor dysfunctions, are known to be associated with cerebral malaria. Also, the available evidence has implicated glutamate and glutamatergic pathways, coupled with a resultant alteration in serotonin, dopamine, norepinephrine, and histamine production. While seeking to improve our understanding of the pathophysiology of cerebral malaria, this article seeks to explore the possible links between host/parasite chaperones, and neurotransmitters, in relation to other molecular players in the pathology of cerebral malaria, to explore such links in antimalarial drug discovery.

## KEYWORDS

neurotransmitters, molecular chaperones, cerebral malaria, *P. falciparum*, cytoadherence, sequestration, inflammation

## Introduction

Malaria remains one of the disturbing public health challenges and a major vector-borne transmitted infection worldwide (Goldberg and Cowman, 2010; Boel et al., 2012; Khanam, 2017; WHO, 2021). The causative pathogen is *Plasmodium* species, five of which are known to infect human, namely, *Plasmodium falciparum*, *P. vivax*, *P. ovale*, *P. malariae*, and *P. knowlesi*, with *P. vivax* and *P. falciparum* known to cause the most lethal infection (Schiess et al., 2020; WHO, 2021). Its complex life cycle, spanning two hosts, human, and female *Anopheles* mosquito, and unabated transmission, has resulted in the high rate of infections, morbidity, and mortality (Nkumama et al., 2016; Khanam, 2017; WHO, 2021). Malaria is most common in rural, indigenous, and impoverished zones of Africa, Asia, and the tropics of America (Monteiro et al., 2014; Talapko et al., 2019). Prior to the advent of the COVID-19 pandemic, the fight against malaria infection appears to have been gaining success with noticeable decreases in the number of reported infections and deaths when compared to the previous year (Daniyan, 2021). However, the disruption in all malaria intervention areas, including prevention, diagnosis, treatment, elimination, and surveillance, occasioned by the pandemic, has led to marked increases in reported cases and associated mortality (Daniyan, 2021; WHO, 2021). The year 2021 world malaria reports estimated 241 million malaria cases and 627,000 deaths, representing 14 million more cases and 69,000 more deaths in 2020, with about 7.5% of these deaths linked to COVID-19 associated disruption (WHO, 2021). Therefore, the dynamics of malaria disease management has been altered by COVID-19 pandemic, and without a more concerted effort, and new strategies to arrest the upsurge, the gains of yesteryears may soon be completely wiped out.

Cerebral malaria (CM) is a deadly complicating manifestation of severe *P. falciparum* malaria with fast-rising fatal neurological syndromes and a high rate of mortality among children from sub-Saharan Africa (Desruisseaux et al., 2010; Grau and Craig, 2012; Shikani et al., 2012). Cerebral malaria occurs in about 1% of all *P. falciparum* infections and has a high mortality rate of 15%–25% (Shikani et al., 2012; WHO, 2021) leaving its surviving subjects with acute or long-term physical disability and neurological syndrome even post-treatment of the infection (Kihara et al., 2006; Grau and Craig, 2012; Hora et al., 2016). These manifestations differ in children and adults and vary depending on the onset of severe symptoms, including coma and status epilepticus, which could propel focal sequelae, impaired movement, hyperactivity, and inappropriate speech or vision (MacCormick et al., 2014). For instance, CM is not common in adults in sub-Saharan Africa due to acquired immunity during childhood attributable to high malaria transmission rates. In Southeast Asia on the other hand, where the transmission rate is lower and consequently not enough to lead to the development of immunity, CM is more

common in adults and older children (Sahu et al., 2015; Sierro and Grau, 2019a). There are differences in CM-related organ dysfunction between adults and children (Sahu et al., 2015; Sierro and Grau, 2019a). While dysfunction in children is almost exclusively neurological, adults experience other organ dysfunctions, such as renal and respiratory dysfunction, in addition to neurological dysfunction (Sahu et al., 2015). Months or years after CM, neuropsychiatric manifestations and disabilities can set in (Monteiro et al., 2014). Meanwhile, despite the undeniable role of increased parasitemia, the levels of parasitemia are not necessarily the determinant for developing the disease, as there is no clear association between particular parasite features and CM (Storm and Craig, 2014a). However, CM is likely to occur in the absence of adequate antimalarials, and to a greater extent among the non-immune people (Bruneel, 2019), necessitating the need for adequate, affordable and accessible health facilities with approved medicine. Unfortunately, the extremely complex aetiology of CM has not been fully elucidated, and thus limiting our understanding of the pathologic mechanisms of CM (Bruneel, 2019; Sierro and Grau, 2019b). Nevertheless, there is a prevailing asymptomatic parasitaemia and certain non-specific pathological features among CM patients presenting with coma (Hora et al., 2016; Idro et al., 2016). In addition, lack of accurate and early diagnosis may have also contributed greatly to limited specificity and knowledge of the infection. Moreover, the available but limited post-mortem histological studies have not vividly explained the processes in the brain, identified the key players, nor shed light on how to ameliorate the aftermath effect of CM, necessitating the need for new and improve approaches to study CM (Sierro and Grau, 2019b). Therefore, despite increasing volume of scientific information on CM, our understanding of the pathophysiologic mechanism(s) of CM is still very limited.

Meanwhile, in a bid to maintain its survival and development, *P. falciparum* exports a large number of proteins into the cytosol of the infected host red blood cell (iRBC) (Acharya et al., 2007; Liu and Houry, 2014). Prominent among these are the molecular chaperones of the heat shock proteins family. Functional activities and interaction of these proteins with one another and with recruited host resident proteins are critical factors in the pathology of malaria infection (Banumathy et al., 2002; Pavithra et al., 2007; Daniyan et al., 2019b). Detailed reviews on the activities of these chaperones and their potential as drug targets have been presented (Shonhai, 2010; Daniyan and Blatch, 2017; Daniyan et al., 2019b; Shonhai et al., 2021). Furthermore, several neurological impairments, including cognitive, behavioral, and motor dysfunctions, are known to be associated with CM (Oluwayemi et al., 2013; Monteiro et al., 2014). Available evidence has implicated glutamate and glutamatergic pathways in CM, coupled with a resultant possible alteration in nitric oxide (NO), serotonin (5-HT), dopamine, norepinephrine, and histamine production (Roy et al., 1993; Enwonwu et al., 1999;

Rubach et al., 2015; Yeo et al., 2015; Kempaiah et al., 2016; Oliveira et al., 2017). While seeking to improve our understanding of the pathophysiology of CM, this article seeks to explore the possible links or interactions between host/parasite chaperones, and neurotransmitters, in relation to other molecular players in the pathology of CM, with a view to exploring possible functional relationships in antimalarial drug discovery.

## Pathogenesis of cerebral malaria

There is currently no complete understanding of the pathogenesis of CM. Although some hypotheses, such as that of mechanical obstruction of microvessels (sequestration of parasitized erythrocytes), and that of the release of copious amounts of pro-inflammatory cytokines, have been put forward for the pathogenesis of CM, they do not fully account for disease progression, prognosis, and outcome (van der Heyde et al., 2006; Storm and Craig, 2014a; Dunst et al., 2017; Schiess et al., 2020). The vascular occlusion or sequestration hypothesis is based on the sequestration of iRBCs into the brain capillary endothelia, resulting in microvascular blockage, loss of blood, tissue hypoxia, blood-brain barrier (BBB) compromise, and finally, CM (Storm et al., 2019; Schiess et al., 2020). Sequestration of the parasitized cells is seen as a survival strategy *via* immune evasion used by the parasites to avoid the removal of the cells by the spleen (Amante et al., 2010; Sierro and Grau, 2019a). Moreover, the somewhat hypoxic environment of venous blood is ideal for the growth of the parasites while protecting them from being destroyed by the spleen (Newton et al., 2000). Human CM post-mortem is characterized by swelling of cerebral capillaries and venules containing parasitized and non-parasitized erythrocytes (Newton et al., 2000; Sierro and Grau, 2019a), and platelets (Sierro and Grau, 2019a). Sequestration occurs to different extents in the various vital organs and the severity and prognosis of the disease have been linked to the size of the sequestered biomass (Newton et al., 2000; Ponsford et al., 2012), which cannot be deduced from peripheral parasite counts (Newton et al., 2000). Meanwhile, the binding of sequestered iRBCs to the endothelium is made possible by the *P. falciparum* erythrocytes membrane protein I (PfEMP1), ensuring an increased affinity of iRBCs to various receptors, notably, cytokine-activated endothelial protein C receptor (EPCR) and intercellular adhesion molecule-1 (ICAM-1) on the brain endothelial cells (Storm and Craig, 2014b; Nishanth and Schlüter, 2019; Storm et al., 2019). This is followed by the activation of thrombocytes to stimulate adhesion of iRBCs to one another, forming clots and inducing the non-iRBCs rosettes, hence, restraining blood flow, aggravating microvascular obstruction and tissue hypoxia (Storm and Craig, 2014b; Nishanth and Schlüter, 2019; Schiess et al., 2020), and

eventual compromise of the BBB integrity (Ponsford et al., 2012; Rosenberg, 2012; Shimizu et al., 2018).

The inflammatory hypothesis is based on the release of toxic products by *P. falciparum*, causing an imbalance in systemic inflammatory responses, which are exacerbated due to sequestration and cytoadherence of iRBC (Storm and Craig, 2014b; Plewes et al., 2018). The resultant surge in the release of pro-inflammatory cytokines by macrophages, such as tumor necrosis factor- $\alpha$  (TNF- $\alpha$ ), interleukin-B1 (IL-B1), and interleukin 10 (IL-10), amplify inflammation and BBB breakage by producing reactive oxygen species (ROS) and nitric oxide (NO) into the circulation (Bruneel, 2019; Schiess et al., 2020), resulting in impaired erythropoiesis and fever (Milner et al., 2014; Milner, 2018; Sierro and Grau, 2019b). On the other hand, these macrophages can as well release interferon- $\gamma$  which aids the expression of surface proteins such as PfEMP-1, histidine-rich proteins (HRPs), ring erythrocyte surface antigen (RESA) in iRBCs and increase the formulation of adhesion molecules on endothelial cells to aid binding of surface proteins, thereby proliferating vascular permeability in several organs (Sierro and Grau, 2019b). These organs express several adhesion molecules, including cytokine-activated endothelial protein C receptor (EPCR), intercellular adhesion molecule-1 (ICAM-1), thrombospondin, and vascular cell adhesion molecule-1 (V-CAM-1) (Storm and Craig, 2014b; Storm et al., 2019), which further propels the endothelial cell to express several chemokines (Dunst et al., 2017; Nishanth and Schlüter, 2019). Also, *P. falciparum*-induced platelets are capable of binding to iRBCs, endothelial cells, and rosettes to promote immune activation by binding parasite-derived molecules *via* their toll-like receptors to further induce cytokines and chemokines (Bruneel, 2019). A detailed review of the roles of cytokines and chemokines in the pathogenesis of CM has been presented (Dunst et al., 2017). Following the multifunctional involvement of platelets in sequestration, humoral response, and endothelial dysfunction in both hypotheses, further investigation of their roles might pave way for more robust drug intervention.

## The roles of chaperones in cerebral malaria

The life cycle of the *Plasmodium* parasite spans two hosts, mosquito and human. The malaria parasite especially requires a robust adaptation system to cope with the stress of existence in two thermally different hosts, viz: the cold-blooded mosquito vector and warm-blooded humans. This coupled with intermittent febrile events in infected humans predisposes the parasite to experience thermal variations that would be stressful to the organism's continued survival and growth. To easily adapt to varying physiological changes within these hosts, the malaria parasite expresses a large number of proteins, including

molecular chaperones, some of which are exported to aid hosts invasion, facilitate cytoadherence, promote pathogenicity, and establishment of clinical malaria infection (Bozdech et al., 2003; Maier et al., 2008, 2009; Pallavi et al., 2010; Spielmann and Gilberger, 2010; Montagna et al., 2012; Liu and Houry, 2014). Molecular chaperones play critical roles in ensuring that newly synthesized proteins are functional, through proper folding, and where applicable, facilitate their subsequent trafficking to desired destinations and refolded to their native three-dimensional conformations (Hartl, 1996; Smith et al., 1998; Hartl and Hayer-Hartl, 2002; Pallavi et al., 2010). Furthermore, they facilitate the assembly of multi-protein complexes, maintain surveillance on cellular protein quality, and ensure that irreparably damaged proteins are timely handed over for degradation (Hartl, 1996; Hartl and Hayer-Hartl, 2002; Pallavi et al., 2010). They are known to function independently or in association with one another, forming a multi-functional network (Acharya et al., 2007; Pavithra et al., 2007). Generally, molecular chaperones of the heat shock protein (Hsp) superfamily, including Hsp90, Hsp70, Hsp60, Hsp40, and small Hsp, are important in this regard. Among the well-known functional networks involve the functional relationship between Hsp90 and Hsp70 and between these and their counterpart Hsp40 co-chaperones (Chua et al., 2014; Pesce and Blatch, 2014). The functional features of these plasmodial heat shock proteins, functional interplay, and networks of interactions, as well as their potential application in antimalarial drug discoveries, have been presented (Pavithra et al., 2007; Shonhai, 2010; Daniyan and Blatch, 2017; Daniyan et al., 2019b; Shonhai et al., 2021).

Meanwhile, the analysis of potential host-parasite protein-protein interactions has shown that the expression of heat shock proteins is important for efficient PfEMP1 presentation, and thus cytoadherence and sequestration (Rao et al., 2010). The PfEMP1 is a virulence factor encoded by *var* genes and available evidence has shown that the expression of DC8 and DC13 *var* genes is associated with cerebral malaria (Avril et al., 2013). Its trafficking to the surface of infected erythrocytes involves a network of proteins complex (Wickert et al., 2003; Acharya et al., 2007; Pavithra et al., 2007; Spycher et al., 2008). The PfEMP1 plays a critical role in malaria pathogenesis, cytoadherence, and immune evasion and has been presented as a potential drug target (Pasternak and Dzikowski, 2009; Hviid and Jensen, 2015; Bull and Abdi, 2016). Another virulence factor of importance to the establishment of CM is *P. falciparum* histidine-rich protein II (PfHRP2). The PfHRP2 is known to be transported into the cytosol of infected erythrocytes (Howard et al., 1986), compromised the brain endothelial barrier, promote CM pathogenesis (Pal et al., 2016), caused vascular leakage, and exacerbate CM (Pal et al., 2017). PfHRP2 is also involved in the protection of *P. falciparum* parasite from the toxic effects of heme by aiding neutralization of heme (Huy et al., 2003). Therefore, the combined activities of PfEMP1 and PfHRP2 are critical for the

establishment of CM. Also, it has been demonstrated that the ability of human Hsp70 (HSPA1A) to regulate nuclear factor- $\kappa$ B (NF- $\kappa$ B) signaling and production of proinflammatory cytokines (such as IL-1 $\beta$ , IL-6, and TNF- $\alpha$ ), can be suppressed by intraleukocytic hemozoin (PfHz). Interestingly, this suppression can be reversed in the presence of glutamine, which upregulates human Hsp70, thereby promoting the activation of NF- $\kappa$ B, and attenuation of overexpression of proinflammatory cytokines (Kempaiah et al., 2016). These findings suggest that suppression of functional activities of human Hsp70 is critical for the establishment of cerebral malaria. However, with their ubiquitous nature and multifunctional activities, as well as the involvements of human heat shock proteins, which are often recruited into the cytosol of iRBC (Banumathy et al., 2002), in nervous system activities (including neurotransmission and neuroprotection), and in modulation of the activities of NF- $\kappa$ B (a critical factor in CM pathology) (Stetler et al., 2010; Fusella et al., 2020), these findings show that more are still yet to be unraveled on the importance of host and plasmodial heat shock proteins in the pathogenesis of cerebral malaria.

## The roles of neurotransmitters in cerebral malaria

Neurotransmitters are critical components of central and peripheral nervous systems. They are signaling molecules that are key players in the abilities of nerve cell, or neuron, to efficiently conveys information both electrically and chemically (Rangel-Gomez and Meeter, 2016). Functionally, neurotransmitters can be classified as excitatory and inhibitory neurotransmitters, neuromodulators, and neurohormones. The excitatory neurotransmitters, such as glutamate, acetylcholine, histamine, dopamine, and norepinephrine, induce or motivate target cells to take action by promoting the generation of the action potential. The inhibitory neurotransmitters function to decrease the chances of target cells initiating actions. Examples are dopamine, serotonin, and gamma-Aminobutyric acid (GABA). The neuromodulators, such as dopamine, acetylcholine, serotonin, norepinephrine, and histamine, can send messages to several neurons simultaneously. Finally, neurohormones, such as oxytocin and vasopressin, induce hormonal activities (Hyman, 2005; Rangel-Gomez and Meeter, 2016; Sheffler et al., 2022). Neurotransmitters can also be classified based on their chemical and molecular properties. They are monoamines (dopamine and norepinephrine); peptides (somatostatin and opioids); purines (adenosine triphosphate); and amino acids (glutamate and glycine). Also, some gaseous substances, such as nitric oxide, and endogenous substances, such as tryptamine and phenethylamines, have been shown to function as neurotransmitters (Rangel-Gomez and Meeter, 2016; Sheffler et al., 2022).



The neurodegenerative abnormalities that are consistent with the progression of cerebral malaria are likely to result from the interplay between specific neurotransmitters at various nerve terminals and their receptors. Available reports have shown that these baseline biochemical changes may lead to deteriorations in the histoarchitectural integrity of localized areas of the brain, especially those concerned with the coordination of cognitive, motor, and neurobehavioural activities (Roy et al., 1993; Cha et al., 1998; Suda et al., 2008; Jamwal and Kumar, 2019). In addition, the interplay between neurotransmitters with specific receptor molecules and associated protein expressions has been implicated in the complex cascade mechanisms of cerebral malaria. For instance, dopamine is known to play a central role in modulating cognitive functions, which may be linked to specific dopamine receptor signaling (Cropley et al., 2006). Specifically, the expressions of dopamine D2 receptor within the striatal medium spiny neurons (MSNs) are involved in the flexibility of human cognitive functions (van Holstein et al., 2011), and its defective signaling may alter metabolic activities within the brain while also taking a deregulatory toll on certain neural functions (Bhatia et al., 2022). Interestingly, the progression of cerebral malaria has been shown to trigger overexpression of dopamine D1 and D2 receptors (Kumar and Babu, 2020). The pathological consequence associated with defective signaling of dopamine receptors is the alteration of the structural and functional histoarchitecture of striatal MSNs (Rangel-Barajas et al., 2015). In addition, while excessive dopamine utilization within the prefrontal cortex was found to be consistent with the decline in cognitive functions among experimental animals (Murphy et al., 1996), the neuronal degenerations in the nigrostriatal dopamine signaling pathway can be very detrimental to motor coordination (Krashia et al., 2019). This evidence suggests that dopamine receptors may play an intermediary role between the induction of CM and associated neurodegenerative changes. Therefore, the defective interaction of dopamine with specific dopamine receptors may likely be having a significant implication on the neuropathogenesis of cognitive decline among CM subjects. Moreover, the interference of estrogen with dopaminergic pathways has been used to establish the memory deficits associated with certain neurodegenerative symptoms (Quinlan et al., 2008; Almey et al., 2015; Tozzi et al., 2015; McEwen and Milner, 2017). However, the relationship between sex hormone levels and the molecular pathway of dopamine-dependent neuromodulation in cerebral malaria is unclear. Consequently, the elucidation of these biochemical mechanisms may explain gender-related susceptibility to cerebral malaria. Also, it is possible that the chronic level of oxidative imbalance, occasioned by the presence of highly reactive metabolic by-products of dopamine, such as 3, 4-dihydroxyphenylacetaldehyde, may be involved in the neuroinflammatory pathologic mechanism of cerebral malaria (Miyazaki and Asanuma, 2009; Juárez Olguín et al., 2015; Monzani et al., 2019; Chen et al., 2020).

Furthermore, glutamate signaling is commonly associated with excitatory neurotransmission (Dauvermann et al., 2017). The interaction of glutamate with several receptors at the presynaptic and postsynaptic terminal is known to play important roles in normal brain functioning (Yamaguchi et al., 2011). Of all the L - glutamate receptors, the dense expressions of the N-methyl-D-aspartate (NMDA) receptor within the hippocampus and the cerebral cortex makes it highly critical for mediating learning and memory, or spatial memory activities within the central nervous system (Kumar, 2015). As ionotropic glutamate receptors, the NMDA receptors also confer synaptic plasticity as well as excitotoxic neuronal dysfunctions (Reiner and Levitz, 2018). Apart from the individual functional roles of glutamate and NMDA—glutamate receptors under physiological conditions, their overexpressions have been implicated in the neuropathogenesis of debilitating degenerative conditions (Singh et al., 2019). As a result, potential agents which can function as a specific antagonist of NMDA receptor signaling are currently being explored as ideal drug candidates for the improvement of cognitive decline and other comorbidities associated with cerebral malaria (de Miranda et al., 2017). Also, the metabolic products of glutamate and their baseline interactions with several important biomolecules have been found to play pivotal roles in the initiation and progression of cerebral malaria, and similar to dopamine, metabolic by-products of glutamate oxidation can also worsen the prognosis of cerebral malaria (Kelly and Stanley, 2001; Walker and van der Donk, 2016; Simões et al., 2018). The overstimulation of glutamate release is known to be excitotoxic (Simões et al., 2018), resulting in epileptic seizures commonly manifested in cerebral malaria (Lewerenz and Maher, 2015). Although the exact pathophysiology is unclear, oxidative stress and upregulated mitochondrial dysfunction have been implicated (Atlante et al., 2001). Also, there is an increasing interest in exploring glutamate receptor antagonist as potential neuroprotective agent (de Miranda et al., 2017).

Apart from dopamine and glutamate, available evidence revealed possible alteration in nitric oxide (NO), norepinephrine, histamine, and serotonin (5-HT) (Roy et al., 1993; Enwonwu et al., 1999; Beghdadi et al., 2009a; Miller et al., 2013; Rubach et al., 2015; Yeo et al., 2015; Kempaiah et al., 2016; Oliveira et al., 2017). For instance, the proinflammatory cytokines induce nitric oxide synthase, guanidine triphosphate (GTP) cyclohydrolase I, and indoleamine-pyrrole-2,3-dioxygenase pathways (Busse and Mülsch, 1990; Sakai et al., 1995; Katusic et al., 1998; Dunst et al., 2017). The induction of GTP cyclohydrolase I lead to the generation of tetrahydrobiopterin, a cofactor for nitric oxide synthase and tryptophan hydroxylase (Sakai et al., 1995; Higgins and Gross, 2010), with subsequent generation of nitric oxide and serotonin respectively. Similarly, the induction of indoleamine-pyrrole-2,3-dioxygenase, a regulatory enzyme in the kynurenine pathway,

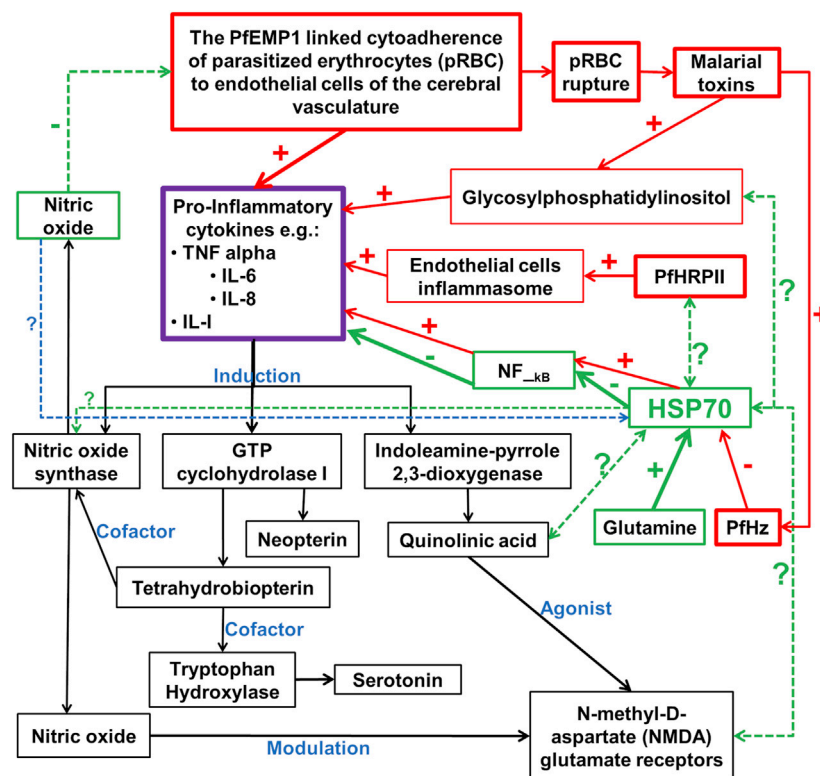


**FIGURE 1**

Potential chaperones linked neurotransmitter pathways of the inflammation pathophysiologic mechanism of cerebral malaria. PfEMP1 is *P. falciparum* erythrocyte membrane protein 1; PfHz is hemozoin; PfHRP II is *P. falciparum* histidine-rich protein II; In red boxes are the pro-inflammatory cytokines inducers; In green boxes are the potentially major players in the inhibition of pro-inflammatory cytokines; In black boxes are downstream biochemical cascade potentially linked to the neurological syndrome in cerebral malaria; - and + signs indicate inhibition and induction respectively; ? With dotted double or single-faced arrows are potential functional relationships that are yet to be or partially investigated respectively; - and + signs with arrows are reported functional relationships with HSPA1A, but not for plasmodial Hsp70 chaperones.

leads to the generation of quinolinic acid, a potent agonist of N-methyl-D-aspartate (NMDA) glutamate receptor (Guillemin et al., 2005; Lugo-Huitrón et al., 2013). Furthermore, enhanced synthesis of histamine has been linked to cerebral malaria-associated pathogenetic processes, including the disruption of BBB, and sequestration of T lymphocytes to cerebral vascular endothelium in mice (Enwonwu et al., 2000; Beghdadi et al., 2009a, 2009b). Also, an increased level of norepinephrine may lead to the potential aggravation of cerebral vasospasm (Zeiler et al., 2014). Therefore, the understanding of the roles of neurotransmitters, and their functional interplay are important not only to better understand pathogenic processes in CM but also for effective drug intervention and drug discovery.

## Possible links among molecular players in CM pathology

The ability of iRBC to induce NF-κB-regulated inflammatory pathways in human cerebral endothelium has been demonstrated

(Tripathi et al., 2009), indicating that NF-κB signaling has an important role to play in the pathology of CM (Figure 1). The NF-κB transcription factors have been implicated in many key physiological and pathophysiological processes, such as regulation of expression of genes needed for inflammation and immune responses, as well as cell proliferation, and apoptosis. In the central nervous system, the NF-κB is involved in diverse functions, including neuroinflammation. It is constitutively expressed in glutamatergic neurons, such as the cerebral cortex and hippocampus, serves neuroprotective roles, and is implicated in learning and memory. Both canonical and non-canonical NF-κB pathways are involved and serve to regulate gene transcription, including those involved in inflammatory processes, such as cytokines, chemokines, adhesion molecules, and proinflammatory enzymes and transcription factors. NF-κB is also found in glial cells, where its induction leads to the regulation of inflammatory processes that exacerbate neurodegenerating diseases, such as Alzheimer's disease [reviewed here (Kaltschmidt and Kaltschmidt, 2009; Shih et al., 2015)]. These findings underscore the importance of NF-κB

in immune responses to malaria infection (Baska and Norbury, 2022) and may therefore serve as a critical link between the proposed vascular and inflammation hypotheses of CM pathology (Figure 1). Interestingly, chaperones are known to play functional roles in many processes regulated by NF- $\kappa$ B pathways (Fusella et al., 2020). Such roles depend on the regulated processes as well as on whether these chaperones are constitutively expressed or inducible. For instance, several lines of evidence have validated the inhibitory effects of upregulation of human Hsp70 on the induced expression of TNF- $\alpha$  and IL-6, and the activation of NF- $\kappa$ B (Senf et al., 2008; Wang C.-H. et al., 2017; Lyu et al., 2020) (Figure 1). However, the inhibition of Hsc70 by deoxyspergualin and the siRNA knocked down variant of Hsc70, significantly decreased nuclear translocation and neuronal activity of NF- $\kappa$ B p65. This suggests that Hsc70 may likely be involved in the activation, rather than inhibition of NF- $\kappa$ B (Klenke et al., 2013, 65). In addition, beyond the protein folding and chaperoning, available evidence has also implicated chaperones of the heat shock proteins as critical regulator of normal neuronal physiological functions, including neurotransmission. Essentially, chaperones, especially Hsc70 and human Hsp70 (HSPA1A), and their counterpart DNAJ have been implicated in the vesicular storage of neurotransmitters, release into the synaptic cleft, reforming and recycling of the vesicular membrane, postsynaptic interaction, and G-protein signaling [reviewed here (Stetler et al., 2010)]. For instance, recent evidence has shown that in response to dopamine-induced oxidative assaults on other proteins concerned with neurodegeneration, molecular chaperones are commonly expressed as endogenous mechanisms for curtailing protein aggregation (Webster et al., 2019). These chaperones, including Hsp27 and  $\alpha$ B—crystallin (Hayashi et al., 2021), as well as Hsp 40 and Hsp70 (Hu et al., 2021), were able to prevent the aggregation of certain proteins that are associated with the progression of parkinsonism (Hayashi et al., 2021). Interestingly, the induction of Hsp70 molecular chaperone in the dopaminergic neurons has been associated with neurodegeneration (Pastukhov et al., 2013; Smith et al., 2015; Zhang et al., 2018). Nevertheless, the effects of dopamine oxidation on the structural and functional integrities of human and plasmodial Hsp70 and its implication on the pathogenesis of cerebral malaria, remain unclear. However, it is clear that for any CM-mediated neurotransmitter alteration to take place, the malaria parasite needs molecular chaperones for continuous survival and development. Indeed, the presence of Hsp70 in dopaminergic neuron suggest a potential functional relationship. Furthermore, the induction of pro-inflammatory cytokines following cytoadherence and rupturing of pRBC to release malaria toxins (PfHz and glycosylphosphatidylinositol) is linked to the induction of cascade of biochemical pathways that are critical for the establishment of CM (Storm and Craig, 2014b; Storm et al., 2019) (Figure 1). While the induction of nitric oxide synthase and GTP cyclohydrolase I lead to the increased

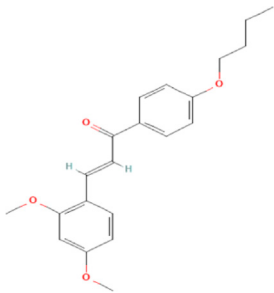
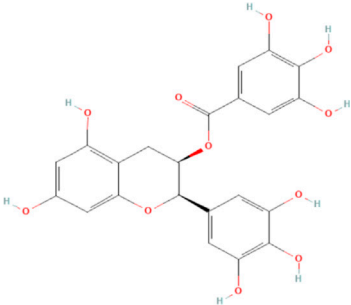
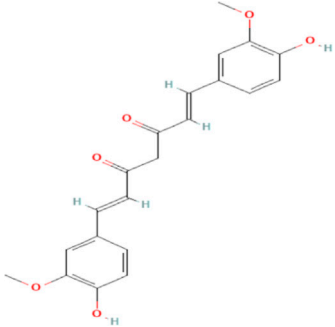
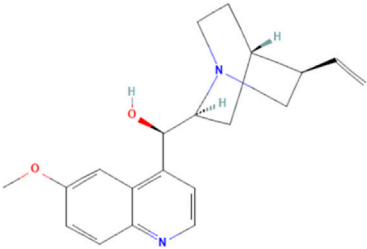
production of serotonin (Katusic et al., 1998), induction of indoleamine-pyrole-2,3-dioxygenase leads to the generation of quinolinic acid, a potent agonist of NMDA receptor (Guillemin et al., 2005; Liu et al., 2015) (Figure 1). Interestingly, nitric oxide is also known to modulate NMDA receptor and may inhibit cytoadherence of pRBC (Hopper et al., 2004). However, the inhibitory effect of PfHz on human Hsp70 can be reversed in the presence of glutamine (Kempaiah et al., 2016) (Figure 1). Therefore, chaperones may be the important link among the many molecular players in the pathophysiology of cerebral malaria (Figure 1). The interrelationship between chaperones and other associated molecular indices (Figure 1) may likely be a promising target for the development of novel drug candidates for the effective treatment of cerebral malaria.

## Potential usefulness of known chaperones targeted small molecule inhibitors in CM

Several reports have shown that heat shock proteins are promising antimalarial drug targets (Pesce et al., 2010; Shonhai, 2010; Shrestha et al., 2016; Daniyan and Blatch, 2017; Daniyan et al., 2019b; Daniyan, 2021). Despite the potential for compensatory upregulation of some heat shock proteins when one is inhibited (e.g., Hsp90 and Hsp70) (Posfai et al., 2018), the essentiality of some members of the heat shock proteins family, their unique functional features, and their ability to form functional networks, not only make their inhibition lethal but that such inhibition could cause a wave of deleterious consequences on the down-stream biochemical processes that these functional networks influence (Pavithra et al., 2007; Daniyan et al., 2019a; Daniyan and Ojo, 2019). Today, small molecule inhibition of plasmodial heat shock proteins has shown promise in reversing *P. falciparum* - induced drug resistance, while also synergizing with traditional antimalarial drugs (Shahinas et al., 2013b; Cockburn et al., 2014; Posfai et al., 2018). Chalcones, polyphenols, terpenoids, alkaloids, and peptides are among the well-tested classes of small molecule inhibitors of heat shock proteins Table 1 [reviewed here (Anokwuru et al., 2021; Daniyan, 2021)]. While there are evidence that some may help in preventing the breakdown of the blood-brain barrier (BBB) (Kam et al., 2012), their potential usefulness in cerebral malaria is largely unexplored.

Chalcones possess several biological activities and have shown promise in antimalarial drug discovery (Singh et al., 2014; Murwih Alidmat et al., 2021; Salehi et al., 2021). The reported potent antimalarial activity of a novel oxygenated chalcone, 2,4-Dimethoxy-4'-Butoxychalcone, against *Plasmodium falciparum* *in vitro*, and *Plasmodium berghei* and *Plasmodium yoelii* *in vivo* (Chen et al., 1997), suggest a possible role for chalcone in the management of cerebral malarial. However, an important limitation is their low bioavailability

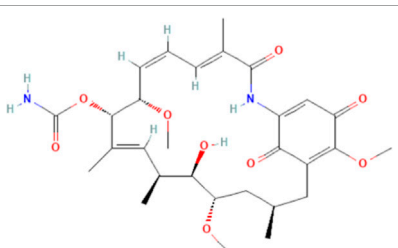
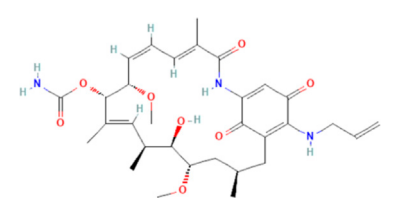
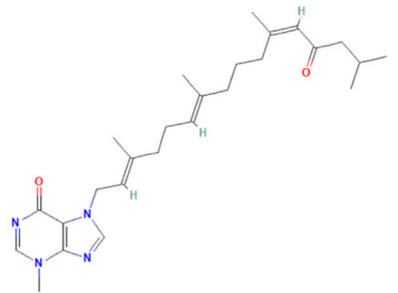
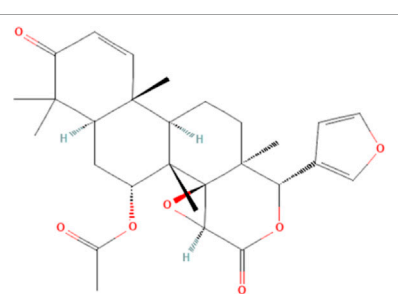
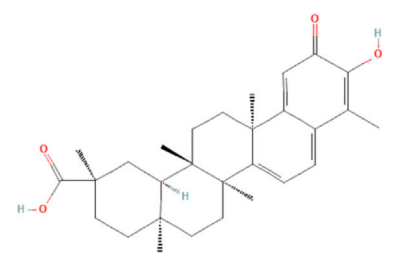
TABLE 1 Features of selected small molecule inhibitors of molecular chaperones with antimalarial/antiplasmodial activities.

Class	Selected member	Biological activities/ Mechanisms	Structural formula	References
Chalcones	2,4-Dimethoxy-4'-Butoxychalcone	Acts against <i>P. falciparum</i> <i>in vitro</i> , and <i>P. berghei</i> and <i>P. yoelii</i> <i>in vivo</i>		Chen et al. (1997), Salehi et al. (2021)
Polyphenols	Epigallocatechin-3-gallate	Possess antiplasmodial activity, possibly by inhibiting Hsp90 and Hsp70 chaperone and ATPase activities. Neuroprotective		Tran et al. (2010), Zininga et al. (2017b), Youn et al. (2022)
	Curcumin	Modulates NMDA receptors and protects against NMDA and glutamate-induced toxicity. Used as adjuvant in cerebral Malaria		Matteucci et al. (2011), Jain et al. (2013), Wang et al. (2017b), Martí Coma-Cros et al. (2018)
Alkaloids	Quinine	Modulate the expression of some plasmodial proteins, and decrease serotonin production		Pussard et al. (2007), Islahudin et al. (2014)
	Geldanamycin	#1C1D1E Prevent focal ischemia in the brain, possibly by stimulating heat shock gene transcription		Lu et al. (2002)

(Continued on following page)

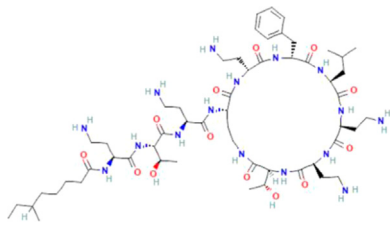
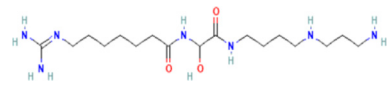


TABLE 1 (Continued) Features of selected small molecule inhibitors of molecular chaperones with antimalarial/antiplasmodial activities.

Class	Selected member	Biological activities/ Mechanisms	Structural formula	References
				
	<sup>a</sup> 17-AAG	Hsp90 inhibitory activities		Wu et al. (2010), Shahinas et al. (2013a), Posfai et al. (2018)
	Malonganenone A	Selectively inhibit plasmodial Hsp70		Cockburn et al. (2011), (2014)
Terpenoids	Gedunin	Inhibit Hsp90 and/or induced degradation of Hsp90-dependent client proteins		Mackinnon et al. (1997), Brandt et al. (2008), Patwardhan et al. (2013)
	Celastrol	Protects motor neurons from excitotoxicity, possibly by induction of increased Hsp70 expression		Westerheide et al. (2004), Petrović et al. (2019)
Peptide antibiotic	Polymyxin B	Immunosuppressant, and inhibition of activities of PfHsp70-1		Zininga et al. (2017a)

(Continued on following page)

TABLE 1 (Continued) Features of selected small molecule inhibitors of molecular chaperones with antimalarial/antiplasmodial activities.

Class	Selected member	Biological activities/ Mechanisms	Structural formula	References
				
	Deoxyspergualin	Immuno-suppressant. Modulate Hsc70 activity, primarily targeting trafficking of apicoplast protein in <i>P. falciparum</i>		Midorikawa and Haque (1997), Brodsky (1999), Ramya et al. (2007)

<sup>a</sup>17-AAG, is 17-allylamino-17-demethoxygeldanamycin.

(Mathew et al., 2016; Sinha et al., 2021), necessitating the need for improvement in the design of chalcone derivatives. Polyphenols, on the other hand, can suppress neuroinflammation, as well as promote memory, learning, and cognitive function (Vauzour, 2012; Figueira et al., 2019). They are neuroprotective, possibly *via* neuronal protection against oxidative stress and inflammatory injury (Filosa et al., 2018). While some polyphenols, such as epigallocatechin, daidzein, genistein, equol, and nobiletin, are reported to show high BBB permeability, others like apigenin, and kaempferol, as well as epicatechin, and curcumin showed medium to no permeability (Figueira et al., 2017, 2019; Shimazu et al., 2021). Interestingly, epigallocatechin-3-gallate, an essential polyphenol in green tea, has demonstrated antiplasmodial activity and inhibited both the chaperone and ATPase activity of Hsp90 and plasmodial Hsp70 (Tran et al., 2010; Moses et al., 2015; Zininga et al., 2017b). These reported dual inhibitory activities on Hsp90 and Hsp70 chaperones, coupled with the ability to cross the BBB, and protect neurons (Youn et al., 2022), suggest that epigallocatechin-3-gallate may be a promising candidate in the management of cerebral malaria. In addition, curcumin, another neuroprotective polyphenol (Chin et al., 2013; Wang X.-S. et al., 2017; Subedi and Gaire, 2021), has severally been shown to have potential as adjuvant therapy in ameliorating neurological syndrome in cerebral malarial despite its poor bioavailability (Jain et al., 2013). However, recent evidence has shown that the use of nano-formulated and liposome-incorporated curcumin has the potential to improve the bioavailability and biological activity of curcumin (Dende et al., 2017; Martí Coma-Cros et al., 2018). Moreover, curcumin modulates NMDA receptors and protects against NMDA and glutamate-induced toxicity (Matteucci et al., 2011; Mallozzi et al., 2018; Simões et al., 2018). Therefore, polyphenols are a promising class of small molecules in the management of cerebral malarial.

Meanwhile, alkaloids remain one of the oldest and most popular classes of compounds whose members have found usefulness for decades as antimalarial agents. The most popular member of this group is quinine (Kaur et al., 2009). Quinine, given within the recommended doses, is safe, and at higher doses with proper monitoring, the benefits often outweigh the exaggerated toxicity (White et al., 1982; Pussard et al., 2003). Moreso, quinine, though an old friend, still has a comparable level of effectiveness with newer artesunate despite the reported superiority of parenteral artesunate (Dondorp et al., 2010; Eltahir et al., 2010; Sinclair et al., 2012; Abdallah et al., 2014). However, though available evidence suggests that quinine does not freely cross the BBB (Silamut et al., 1985), quinine uptake into the brain can be increased by inhibition of P-glycoprotein (Pussard et al., 2007). Thus, inhibition of P-glycoprotein may improve the effectiveness of quinine in cerebral malaria through enhanced uptake into the brain. Also, quinine could modulate the expression of some plasmodial proteins, including enolase (PF3D7\_1015900), endoplasmic reticulum-resident calcium-binding protein (PF3D7\_1108600), chaperonin (PF3D7\_1213500), the host cell invasion protein (PF3D7\_1027300) and proteins related to redox processes (PF3D7\_0827900) (Segura et al., 2014). In addition, quinine has been shown to decrease serotonin production *via* competitive inhibition of tryptophan hydroxylase in the presence of tryptophan (Islahudin et al., 2014), suggesting a potential mechanism of quinine action in cerebral malaria. Other members of the alkaloid class of compounds that have shown antimalarial properties and demonstrated Hsp90 inhibitory activities include ganetespib, harmine, PU-H71, geldanamycin (GA), and its analogs, 17-dimethylaminoethylamino-17-demethoxygeldanamycin (17-DMAG) and 17-allylamino-17-demethoxygeldanamycin

TABLE 2 Some medicinal plants' derived compounds with neuroprotective and/or antimalarial properties.

Compounds	Related biological effects	References
Ginsenoside and ginseng	Antimalarial, anti-inflammatory, antioxidant, antiparasitic	Han et al. (2011), Huang et al. (2019)
Bacopasaponin	Antioxidative, increased cerebral blood flow, neuromodulatory	Aguir and Borowski (2013), Velaga et al. (2014)
Betulnic Acid	Curtails neuroinflammation by modulating NF- $\kappa$ B and inhibition of Interleukin -6; Antimalarial	Vijayan et al. (2010)
6-Gingerol	Reduced IL-6, TNF- $\alpha$ , nitric oxide, cerebral cortex lesion; Reversed memory deficit and cognitive impairment	Farombi et al. (2018), Kim et al. (2018), Huang et al. (2019)
Zingerone	Prevents lipid peroxidation and neuroinflammation; Antimalarial	Alam (2018), Ounjaijean and Somsak (2020)
Chrysin	Reduced neuroinflammation; Antimalarial	Nabavi et al. (2015)
L-3- <i>n</i> -butylphthalide	Increases expression of glutamic acid decarboxylase, anticonvulsant, antioxidative, and anti-inflammation. Attenuate cognitive decline	Bhatt et al. (2017), Liao et al. (2018), Ye et al. (2018)
Quercetin	Antioxidant, improved motor activity, anti-inflammation; Antiplasmodial	Ganesh et al. (2012), Ezenyi et al. (2014), Singh et al. (2017)
Rutin	Antioxidative, anti-inflammatory, antiapoptotic; Antimalarial	Budzynska et al. (2019), Bhatt et al. (2022)
Baicalein	Modulation of NMDA receptor, ameliorates neuroinflammation, anti-apoptotic, antiexcitotoxic, antipyretic	Hung et al. (2016), Sowndhararajan et al. (2018)
Caffeic acid	Antioxidative, anti-inflammation, decreases neuronal apoptosis, boosts memory; Antimalarial	Fu et al. (2017), Alson et al. (2018), Morroni et al. (2018)
Magnolol	Free radical scavenging, prevents brain infarction and cognitive deficits, anti-inflammation, reduces neuronal apoptosis	Chen et al. (2011), Santos et al. (2021)
kavalactone	Curtails oxidative stress and neuroinflammation, anticonvulsant, anti-anxiolytic, sedative, modulation of GABA receptors	Tzeng and Lee (2015), Alves et al. (2021)
kolaviron	Anti-inflammatory, antioxidative, improved motor and cognitive decline, antiapoptotic, antimalarial	Oluwatosin et al. (2014), Farombi et al. (2019)
Riboflavin	Mitigates oxidative stress, neuroinflammation, and glutamate neurotoxicity; Inhibited hemozoin production, decreases food vacuole size in <i>P. falciparum</i>	Akompong et al. (2000), Tripathi et al. (2014), Huang et al. (2022)
Huperzine A	NMDA receptor antagonist inhibits acetylcholine esterase and improves cognition	Zhang (2012), Gul et al. (2019)
Berberine	Prevents learning and memory impairment, heavy metal chelation	Hussien et al. (2018), Wang et al. (2018)
Andrographolide	Inhibit NF- $\kappa$ B activation. Prevent inflammation. Antimalarial	Mishra et al. (2011), Raghavan et al. (2012), Chang et al. (2014)

(Shahinas et al., 2013a, 2013b; Posfai et al., 2018). The available report shows that geldanamycin could prevent focal ischemia in the brain, possibly by stimulating heat shock gene transcription (Lu et al., 2002). The synergistic ability of PU-H71 with chloroquine (Shahinas et al., 2013b), suggests that these compounds can be combined with existing antimalarial agents to improve treatment outcomes and reduce resistance. Also, a marine prenylated alkaloid, malonganenone A was shown to possess the antimalarial activity and selectively inhibit plasmodial Hsp70 (Cockburn et al., 2014).

Furthermore, terpenoids, which are the most abundant and structurally diverse secondary metabolites, possess a wide range of pharmacological activities, including antimalarial effects and heat shock protein inhibitory activities (Wang et al., 2005; Gabriel et al., 2018; Anokwuru et al., 2021). For instance, gedunin, kotschyins D, celastrol, and fusicoccane have been shown to inhibit Plasmodial Hsp90 and/or induced degradation of Hsp90-dependent client proteins (Westerheide et al., 2004; Brandt et al., 2008; Zhang et al., 2008; Piaz et al., 2012; Patwardhan et al., 2013; D'Ambola et al., 2019). Interestingly,

celastrol also induces increased expression of human Hsp70 and protects motor neurons from excitotoxicity (Westerheide et al., 2004; Petrović et al., 2019). It is tempting to postulate that celastrol may find usefulness in cerebral malarial as evidence has shown that increased expression of Hsp70 prevents the production of inflammatory mediators *via* inhibition of NF- $\kappa$ B (Kempaiah et al., 2016). In addition, a peptide antibiotic, polymyxin B, and an immunosuppressant, deoxyspergualin, have also demonstrated antimalarial activities (Anokwuru et al., 2021). Polymyxin B showed inhibitory activities on PfHsp70-1 (PF3D7\_0818900) and PfHsp70-z (PF3D7\_0708800) (Zininga et al., 2017a).

Therefore, while there are limitations, such as limited or inability to cross the blood-brain barrier, and limited to lack of information on the effects of these small molecules on brain neurotransmitters, there is more than enough evidence to propel further research into their potential usefulness in the treatment or as adjuvant therapy to mitigate the deleterious effects of the associated neurological syndrome in cerebral malaria.

## Searching for new drug candidates from natural products

Plants and other natural sources have been the bedrock of drug discovery over the years (Balunas and Kinghorn, 2005; Ahmad et al., 2006; Gurib-Fakim, 2006; Dzoyem et al., 2013). They are not just serving as sources of drug candidates, they have and still are been used in traditional medicine as worthy alternatives to orthodox drugs (Ahmad et al., 2006; Amoateng et al., 2018). Many of the tested small molecules are from these natural sources [reviewed here (Anokwuru et al., 2021; Daniyan, 2021)]. Many medicinal plant products have shown antimalarial, and/or neuroprotective abilities (Kaur et al., 2009; Mahomoodally, 2013; Amoateng et al., 2018; Erhirhie et al., 2021), and may therefore find usefulness in the management of cerebral malarial. Apart from those already mentioned and discussed, Table 2 provided a list of some medicinal plants' derived compounds with neuroprotective and/or antimalarial activities which may find usefulness in cerebral malarial.

## Conclusion

Cerebral malaria is a deadly complication of severe *P. falciparum* malaria, with many survivors left to cope with long-term neurological deficits. A thorough understanding of the functional interplay among major molecular players, including molecular chaperones, neurotransmitters, and NF- $\kappa$ B signaling, in the pathology of CM, is critical for the development of a new treatment approach, and a new focus on antimalarial drug discovery. With their ubiquitous nature, multi-functional activities in the central nervous systems, and

NF- $\kappa$ B signaling pathways, host heat shock protein chaperones, maybe the critical link amidst these molecular players. However, while functional interactions between host and parasite proteins are well established, the functional interplay between plasmodial heat shock proteins, especially the exported chaperones, and other molecular players (neurotransmitters, NF- $\kappa$ B, etc), requires further investigations.

## Author contributions

MD: Conceptualization, Validation, and Project Administration. MD, FF, and OA: Contributed equally to writing, reviewing, and editing of the manuscript.

## Conflict of interest

The authors declare that the research was conducted in the absence of any commercial or financial relationships that could be construed as a potential conflict of interest.

## Publisher's note

All claims expressed in this article are solely those of the authors and do not necessarily represent those of their affiliated organizations, or those of the publisher, the editors and the reviewers. Any product that may be evaluated in this article, or claim that may be made by its manufacturer, is not guaranteed or endorsed by the publisher.

## References

- Abdallah, T. M., Elmardi, K. A., Elhassan, A. H., Omer, M. B., Elhag, M. S., Desogi, M. A., et al. (2014). Comparison of artesunate and quinine in the treatment of severe *Plasmodium falciparum* malaria at Kassala hospital, Sudan. *J. Infect. Dev. Ctries.* 8, 611–615. doi:10.3855/jidc.3813
- Acharya, P., Kumar, R., and Tatu, U. (2007). Chaperoning a cellular upheaval in malaria: Heat shock proteins in *Plasmodium falciparum*. *Mol. Biochem. Parasitol.* 153, 85–94. doi:10.1016/j.molbiopara.2007.01.009
- Aguiar, S., and Borowski, T. (2013). Neuropharmacological review of the nootropic herb bacopa monnieri. *Rejuvenation Res.* 16, 313–326. doi:10.1089/rej.2013.1431
- Ahmad, I. A., Farrukh, F., and Owais, M. (2006). "Herbal medicines: Prospects and constraints," in *Aqil and M. Owais, modern phytomedicine: Turning medicinal plants into drugs*. Editor I. F. Ahmad (Germany: VCH Verlag GmbH & Co.), 59–78.
- Akompong, T., Ghori, N., and Haldar, K. (2000). *In vitro* activity of riboflavin against the human malaria parasite *Plasmodium falciparum*. *Antimicrob. Agents Chemother.* 44, 88–96. doi:10.1128/AAC.44.1.88-96.2000
- Alam, Dr. M. (2018). Neuroprotective effects of Zingerone against carbon tetrachloride (CCl<sub>4</sub>) induced brain mitochondrial toxicity in Swiss albino mice. *J. Appl. Nat. Sci.* 10, 548–552. doi:10.31018/jans.v10i2.1734
- Almey, A., Milner, T. A., and Brake, W. G. (2015). Estrogen receptors in the central nervous system and their implication for dopamine-dependent cognition in females. *Horm. Behav.* 74, 125–138. doi:10.1016/j.yhbeh.2015.06.010
- Alson, S. G., Jansen, O., Ciekiewicz, E., Rakotoarimanana, H., Rafatro, H., Degotte, G., et al. (2018). *In-vitro* and *in-vivo* antimalarial activity of caffeic acid and some of its derivatives. *J. Pharm. Pharmacol.* 70, 1349–1356. doi:10.1111/jphp.12982
- Alves, P. e. S., Santos, F. P. da S., Rodrigues, A. P., Dias, L. S., Silva, G. C. da, Araújo, L. da S., et al. (2021). Piper methysticum G. Forst (piperaceae) in the central nervous system: Phytochemistry, pharmacology and mechanism of action. *Res. Soc. Dev.* 10, e216101220479. doi:10.33448/rsd-v10i12.20479
- Amante, F. H., Haque, A., Stanley, A. C., Rivera, F. de L., Randall, L. M., Wilson, Y. A., et al. (2010). Immune-mediated mechanisms of parasite tissue sequestration during experimental cerebral malaria. *J. Immunol.* 185, 3632–3642. doi:10.4049/jimmunol.1000944
- Amoateng, P., Quansah, E., Karikari, T. K., Asase, A., Osei-Safo, D., Kukuia, K. K. E., et al. (2018). Medicinal plants used in the treatment of mental and neurological disorders in Ghana. *Evid. Based. Complement. Altern. Med.* 2018, 8590381. doi:10.1155/2018/8590381
- Anokwuru, C., Makumire, S., and Shonhai, A. (2021). "Bioprospecting for novel heat shock protein modulators: The new frontier for antimalarial drug discovery?" in *Heat shock Proteins of malaria advances in experimental medicine and biology*. Editors A. Shonhai, D. Picard, and G. L. Blatch (Cham: Springer International Publishing), 187–203. doi:10.1007/978-3-030-78397-6\_8
- Atlante, A., Calissano, P., Bobba, A., Giannattasio, S., Marra, E., and Passarella, S. (2001). Glutamate neurotoxicity, oxidative stress and mitochondria. *FEBS Lett.* 497, 1–5. doi:10.1016/S0014-5793(01)02437-1



- Avril, M., Brazier, A. J., Melcher, M., Sampath, S., and Smith, J. D. (2013). DC8 and DC13 var genes associated with severe malaria bind avidly to diverse endothelial cells. *PLoS Pathog.* 9, e1003430. doi:10.1371/journal.ppat.1003430
- Balunas, M. J., and Kinghorn, A. D. (2005). Drug discovery from medicinal plants. *Life Sci.* 78, 431–441. doi:10.1016/j.lfs.2005.09.012
- Banumathy, G., Singh, V., and Tatu, U. (2002). Host chaperones are recruited in membrane-bound complexes by Plasmodium falciparum. *J. Biol. Chem.* 277, 3902–3912. doi:10.1074/jbc.M110513200
- Başka, P., and Norbury, L. J. (2022). The role of nuclear factor kappa B (NF-κB) in the immune response against parasites. *Pathogens* 11, 310. doi:10.3390/pathogens11030310
- Beghdadi, W., Porcherie, A., Schneider, B. S., Dubayle, D., Peronet, R., Huerre, M., et al. (2009a). Role of histamine and histamine receptors in the pathogenesis of malaria. *Med. Sci.* 25, 377–381. doi:10.1051/medsci/2009254377
- Beghdadi, W., Porcherie, A., Schneider, B. S., Morisset, S., Dubayle, D., Peronet, R., et al. (2009b). Histamine H3 receptor-mediated signaling protects mice from cerebral malaria. *PLOS ONE* 4, e6004. doi:10.1371/journal.pone.0006004
- Bhatia, A., Lenchner, J. R., and Saadabadi, A. (2022). *StatPearls*. Treasure Island (FL): StatPearls Publishing. Available at: <http://www.ncbi.nlm.nih.gov/books/NBK538242/> (Accessed May 8, 2022). Biochemistry, dopamine receptors.
- Bhatt, D., Kumar, S., Kumar, P., Bisht, S., Kumar, A., Maurya, A. K., et al. (2022). Rutin ameliorates malaria pathogenesis by modulating inflammatory mechanism: An *in vitro* and *in vivo* study. *Inflammopharmacology* 30, 159–171. doi:10.1007/s10787-021-00920-w
- Bhatt, P. C., Pandey, P., Panda, B. P., Anwar, F., and Kumar, V. (2017). Commentary: L-3-n-butylphthalide rescues hippocampal synaptic failure and attenuates neuropathology in aged APP/PS1 mouse model of alzheimer's disease. *Front. Aging Neurosci.* 9, 4. doi:10.3389/fnagi.2017.00004
- Boel, M. E., Rijken, M. J., Brabin, B. J., Nosten, F., and McGready, R. (2012). The epidemiology of postpartum malaria: A systematic review. *Malar. J.* 11, 114. doi:10.1186/1475-2875-11-114
- Bozdech, Z., Llinás, M., Pulliam, B. L., Wong, E. D., Zhu, J., DeRisi, J. L., et al. (2003). The transcriptome of the intraerythrocytic developmental cycle of Plasmodium falciparum. *PLoS Biol.* 1, 85–100. doi:10.1371/journal.pbio.0000005
- Brandt, G. E. L., Schmidt, M. D., Prisinzano, T. E., and Blagg, B. S. J. (2008). Gedunin, a novel hsp90 inhibitor: Semisynthesis of derivatives and preliminary structure-activity relationships. *J. Med. Chem.* 51, 6495–6502. doi:10.1021/jm8007486
- Brodsky, J. L. (1999). Selectivity of the molecular chaperone-specific immunosuppressive agent 15-deoxyspergualin: Modulation of Hsc70 ATPase activity without compromising DnaJ chaperone interactions. *Biochem. Pharmacol.* 57, 877–880. doi:10.1016/s0006-2952(98)00376-1
- Brunel, F. (2019). Human cerebral malaria: 2019 mini review. *Rev. Neurol. Paris.* 175, 445–450. doi:10.1016/j.neurol.2019.07.008
- Budzynska, B., Faggio, C., Kruk-Slomka, M., Samec, D., Nabavi, S. F., Sureda, A., et al. (2019). Rutin as neuroprotective agent: From bench to bedside. *Curr. Med. Chem.* 26, 5152–5164. doi:10.2174/0929867324666171003114154
- Bull, P. C., and Abdi, A. I. (2016). The role of PfEMP1 as targets of naturally acquired immunity to childhood malaria: Prospects for a vaccine. *Parasitology* 143, 171–186. doi:10.1017/S0031182015001274
- Busse, R., Mülsch, A., and Mülsch, A. (1990). Induction of nitric oxide synthase by cytokines in vascular smooth muscle cells. *FEBS Lett.* 275, 87–90. doi:10.1016/0014-5793(90)81445-T
- Cha, J.-H. J., Kosinski, C. M., Kerner, J. A., Alsdorf, S. A., Mangiarini, L., Davies, S. W., et al. (1998). Altered brain neurotransmitter receptors in transgenic mice expressing a portion of an abnormal human Huntington disease gene. *Proc. Natl. Acad. Sci. U. S. A.* 95, 6480–6485. doi:10.1073/pnas.95.11.6480
- Chang, C.-C., Duann, Y.-F., Yen, T.-L., Chen, Y.-Y., Jayakumar, T., Ong, E.-T., et al. (2014). Andrographolide, a novel NF-κB inhibitor, inhibits vascular smooth muscle cell proliferation and cerebral endothelial cell inflammation. *Acta Cardiol. Sin.* 30, 308–315.
- Chen, H.-H., Lin, S.-C., and Chan, M.-H. (2011). Protective and restorative effects of magnolol on neurotoxicity in mice with 6-hydroxydopamine-induced hemiparkinsonism. *Neurodegener. Dis.* 8, 364–374. doi:10.1159/000323872
- Chen, M., Christensen, S. B., Zhai, L., Rasmussen, M. H., Theander, T. G., Frøkjær, S., et al. (1997). The novel oxygenated chalcone, 2, 4-dimethoxy-4'-butoxychalcone, exhibits potent activity against human malaria parasite Plasmodium falciparum *in vitro* and rodent parasites Plasmodium berghei and Plasmodium yoelii *in vivo*. *J. Infect. Dis.* 176, 1327–1333. doi:10.1086/514129
- Chen, S.-H., Kuo, C.-W., Lin, T.-K., Tsai, M.-H., and Liou, C.-W. (2020). Dopamine therapy and the regulation of oxidative stress and mitochondrial DNA copy number in patients with Parkinson's disease. *Antioxidants* 9, 1159. doi:10.3390/antiox9111159
- Chin, D., Huebbe, P., Pallauf, K., and Rimbach, G. (2013). Neuroprotective properties of curcumin in Alzheimer's disease—merits and limitations. *Curr. Med. Chem.* 20, 3955–3985. doi:10.2174/09298673113209990210
- Chua, C.-S., Low, H., and Sim, T.-S. (2014). Co-chaperones of Hsp90 in Plasmodium falciparum and their concerted roles in cellular regulation. *Parasitology* 141, 1177–1191. doi:10.1017/S0031182013002084
- Cockburn, I. L., Boshoff, A., Pesce, E., and Blatch, G. L. (2014). Selective modulation of plasmodial Hsp70s by small molecules with antimalarial activity. *Biol. Chem.* 395, 1353–1362. doi:10.1515/hsz-2014-0138
- Cockburn, I. L., Pesce, E. R., Pryzborski, J. M. M., Davies-Coleman, M. T. T., Clark, P. G. G., Keyzers, R. A. A., et al. (2011). Screening for small molecule modulators of Hsp70 chaperone activity using protein aggregation suppression assays: Inhibition of the plasmodial chaperone PfHsp70-1. *Biol. Chem.* 392, 431–438. doi:10.1515/BC.2011.040
- Cropley, V. L., Fujita, M., Innis, R. B., and Nathan, P. J. (2006). Molecular imaging of the dopaminergic system and its association with human cognitive function. *Biol. Psychiatry* 59, 898–907. doi:10.1016/j.biopsych.2006.03.004
- D'Ambola, M., Fiengo, L., Chini, M. G., Cotugno, R., Bader, A., Bifulco, G., et al. (2019). Fusicoccane diterpenes from Hypoestes forsskaolii as heat shock protein 90 (Hsp90) modulators. *J. Nat. Prod.* 82, 539–549. doi:10.1021/acs.jnatprod.8b00924
- Daniyan, M. O., and Blatch, G. L. (2017). Plasmodial Hsp40s: New avenues for antimalarial drug discovery. *Curr. Pharm. Des.* 23, 4555–4570. doi:10.2174/1381612823666170124142439
- Daniyan, M. O. (2021). Heat shock proteins as targets for novel antimalarial drug discovery. *Adv. Exp. Med. Biol.* 1340, 205–236. doi:10.1007/978-3-030-78397-6\_9
- Daniyan, M. O., and Ojo, O. T. (2019). *In silico* identification and evaluation of potential interaction of Azadirachta indica phytochemicals with Plasmodium falciparum heat shock protein 90. *J. Mol. Graph. Model.* 87, 144–164. doi:10.1016/j.jmgm.2018.11.017
- Daniyan, M. O., Przyborski, J. M., Shonhai, A., Daniyan, M. O., Przyborski, J. M., and Shonhai, A. (2019b). Partners in mischief: Functional networks of heat shock proteins of Plasmodium falciparum and their influence on parasite virulence. *Biomolecules* 9, 295. doi:10.3390/biom9070295
- Daniyan, M. O., Przyborski, J. M., and Shonhai, A. (2019a). Partners in mischief: Functional networks of heat shock proteins of Plasmodium falciparum and their influence on parasite virulence. *Biomolecules* 9 (7), 285(1–17). doi:10.3390/biom9070295
- Dauvermann, M. R., Lee, G., and Dawson, N. (2017). Glutamatergic regulation of cognition and functional brain connectivity: Insights from pharmacological, genetic and translational schizophrenia research. *Br. J. Pharmacol.* 174, 3136–3160. doi:10.1111/bph.13919
- de Miranda, A. S., Brant, F., Vieira, L. B., Rocha, N. P., Vieira, É. L. M., Rezende, G. H. S., et al. (2017). A neuroprotective effect of the glutamate receptor antagonist MK801 on long-term cognitive and behavioral outcomes secondary to experimental cerebral malaria. *Mol. Neurobiol.* 54, 7063–7082. doi:10.1007/s12035-016-0226-3
- Dende, C., Meena, J., Nagarajan, P., Nagaraj, V. A., Panda, A. K., and Padmanaban, G. (2017). Nanocurcumin is superior to native curcumin in preventing degenerative changes in Experimental Cerebral Malaria. *Sci. Rep.* 7, 10062. doi:10.1038/s41598-017-10672-9
- Desruisseaux, M. S., Machado, F. S., Weiss, L. M., Tanowitz, H. B., and Golightly, L. M. (2010). Cerebral malaria: A vasculopathy. *Am. J. Pathol.* 176, 1075–1078. doi:10.2353/ajpath.2010.091090
- Dondorp, A. M., Fanello, C. I., Hendriksen, I. C., Gomes, E., Seni, A., Chhaganlal, K. D., et al. (2010). Artesunate versus quinine in the treatment of severe falciparum malaria in african children (AQUAMAT): An open-label, randomised trial. *Lancet* 376, 1647–1657. doi:10.1016/S0140-6736(10)61924-1
- Dunst, J., Kamena, F., and Matuschewski, K. (2017). Cytokines and chemokines in cerebral malaria pathogenesis. *Front. Cell. Infect. Microbiol.* 7, 324(1–16). doi:10.3389/fcimb.2017.00324
- Dzoyem, J. P., Tshikalange, E., and Kuete, V. (2013). “Medicinal plants market and industry in Africa,” in *Medicinal plant research in Africa*. Editor V. Kuete (Oxford: Elsevier), 859–890. doi:10.1016/B978-0-12-405927-6.00024-2
- Eltahir, H. G., Omer, A. A., Mohamed, A. A., and Adam, I. (2010). Comparison of artesunate and quinine in the treatment of Sudanese children with severe Plasmodium falciparum malaria. *Trans. R. Soc. Trop. Med. Hyg.* 104, 684–686. doi:10.1016/j.trstmh.2010.05.009
- Enwonwu, C. O., Afolabi, B. M., Salako, L. A., Idigbe, E. O., al-Hassan, H., and Rabi, R. A. (1999). Hyperphenylalaninaemia in children with falciparum malaria. *QJM Mon. J. Assoc. Physicians* 92, 495–503. doi:10.1093/qjmed/92.9.495

- Enwonwu, C. O., Afolabi, B. M., Salako, L. O., Idigbe, E. O., and Bashirelah, N. (2000). Increased plasma levels of histidine and histamine in falciparum malaria: Relevance to severity of infection. *J. Neural Transm.* 107, 1273–1287. doi:10.1007/s007020070017
- Ehrhlich, E. O., Ikegbun, C., Okeke, A. I., Onwuzuligbo, C. C., Madubuogwu, N. U., Chukwudulue, U. M., et al. (2021). Antimalarial herbal drugs: A review of their interactions with conventional antimalarial drugs. *Clin. Phytosci.* 7, 4–10. doi:10.1186/s40816-020-00242-4
- Ezenyi, I. C., Salawu, O. A., Kulkarni, R., and Emeje, M. (2014). Antiplasmodial activity-aided isolation and identification of quercetin-4'-methyl ether in *Chromolaena odorata* leaf fraction with high activity against chloroquine-resistant *Plasmodium falciparum*. *Parasitol. Res.* 113, 4415–4422. doi:10.1007/s00436-014-4119-y
- Farombi, E. O., Abolaji, A. O., Adetuyi, B. O., Awosanya, O., and Fabusoro, M. (2018). Neuroprotective role of 6-Gingerol-rich fraction of *Zingiber officinale* (Ginger) against acrylonitrile-induced neurotoxicity in male Wistar rats. *J. Basic Clin. Physiol. Pharmacol.* 30 (3), 1–11. doi:10.1515/jbcp-2018-0114
- Farombi, E. O., Awogbindin, I. O., Farombi, T. H., Oladele, J. O., Izomoh, E. R., Aladelokun, O. B., et al. (2019). Neuroprotective role of kolaviron in striatal redox-inflammation associated with rotenone model of Parkinson's disease. *Neurotoxicology* 73, 132–141. doi:10.1016/j.neuro.2019.03.005
- Figueira, I., Garcia, G., Pimpão, R. C., Terraso, A. P., Costa, I., Almeida, A. F., et al. (2017). Polyphenols journey through blood-brain barrier towards neuronal protection. *Sci. Rep.* 7, 11456. doi:10.1038/s41598-017-11512-6
- Figueira, I., Tavares, L., Jardim, C., Costa, I., Terraso, A. P., Almeida, A. F., et al. (2019). Blood-brain barrier transport and neuroprotective potential of blackberry-digested polyphenols: An *in vitro* study. *Eur. J. Nutr.* 58, 113–130. doi:10.1007/s00394-017-1576-y
- Filosa, S., Di Meo, F., and Crispi, S. (2018). Polyphenols-gut microbiota interplay and brain neuromodulation. *Neural Regen. Res.* 13, 2055–2059. doi:10.4103/1673-5374.241429
- Fu, W., Wang, H., Ren, X., Yu, H., Lei, Y., and Chen, Q. (2017). Neuroprotective effect of three caffeic acid derivatives via ameliorate oxidative stress and enhance PKA/CREB signaling pathway. *Behav. Brain Res.* 328, 81–86. doi:10.1016/j.bbr.2017.04.012
- Fusella, F., Secl, L., Cannata, C., and Brancaccio, M. (2020). The one thousand and one chaperones of the NF- $\kappa$ B pathway. *Cell. Mol. Life Sci.* 77, 2275–2288. doi:10.1007/s00018-019-03402-z
- Gabriel, H. B., Sussmann, R. A., Kimura, E. A., Rodriguez, A. A. M., Verdager, I. B., Leite, G. C. F., et al. (2018). "Terpenes as potential antimalarial drugs," in *Terpenes and Terpenoids*. 1<sup>st</sup> Editors S. Perveen and A. Al-Taweel (IntechOpen) Chapter 3, 39–57. doi:10.5772/intechopen.75108
- Ganesh, D., Fuehrer, H.-P., Starzengruber, P., Swoboda, P., Khan, W. A., Reismann, J. A. B., et al. (2012). Antiplasmodial activity of flavonol quercetin and its analogues in *Plasmodium falciparum*: Evidence from clinical isolates in Bangladesh and standardized parasite clones. *Parasitol. Res.* 110, 2289–2295. doi:10.1007/s00436-011-2763-z
- Goldberg, D. E., and Cowman, A. F. (2010). Moving in and renovating: Exporting proteins from *Plasmodium* into host erythrocytes. *Nat. Rev. Microbiol.* 8, 617–621. doi:10.1038/nrmicro2420
- Grau, G. E. R., and Craig, A. G. (2012). Cerebral malaria pathogenesis: Revisiting parasite and host contributions. *Future Microbiol.* 7, 291–302. doi:10.2217/fmb.11.155
- Guillemin, G. J., Smythe, G., Takikawa, O., and Brew, B. J. (2005). Expression of indoleamine 2, 3-dioxygenase and production of quinolinic acid by human microglia, astrocytes, and neurons. *Glia* 49, 15–23. doi:10.1002/glia.20090
- Gul, A., Bakht, J., and Mehmood, F. (2019). Huperzine-A response to cognitive impairment and task switching deficits in patients with Alzheimer's disease. *J. Chin. Med. Assoc.* 82, 40–43. doi:10.1016/j.jcma.2018.07.004
- Gurib-Fakim, A. (2006). Medicinal plants: Traditions of yesterday and drugs of tomorrow. *Mol. Asp. Med.* 27, 1–93. doi:10.1016/j.mam.2005.07.008
- Han, H., Chen, Y., Bi, H., Yu, L., Sun, C., Li, S., et al. (2011). *In vivo* antimalarial activity of ginseng extracts. *Pharm. Biol.* 49, 283–289. doi:10.3109/13880209.2010.511235
- Hartl, F. U., and Hayer-Hartl, M. (2002). Molecular chaperones in the cytosol: From nascent chain to folded protein. *Science* 295, 1852–1858. doi:10.1126/science.1068408
- Hartl, F. U. (1996). Molecular chaperones in cellular protein folding. *Nature* 381, 571–579. doi:10.1038/381571a0
- Hayashi, J., Ton, J., Negi, S., Stephens, D. E. K. M., Pountney, D. L., Preiss, T., et al. (2021). The effect of oxidized dopamine on the structure and molecular chaperone function of the small heat-shock proteins,  $\alpha$ -crystallin and Hsp27. *Int. J. Mol. Sci.* 22, 3700. doi:10.3390/ijms22073700
- Higgins, C. E., and Gross, S. S. (2010). "Chapter 6 - tetrahydrobiopterin: An essential cofactor for nitric oxide synthases and amino acid hydroxylases," in *Nitric oxide*. Editor L. J. Ignarro. 2nd Edition (San Diego: Academic Press), 169–209. doi:10.1016/B978-0-12-373866-0.00006-X
- Hopper, R., Lancaster, B., and Garthwaite, J. (2004). On the regulation of NMDA receptors by nitric oxide. *Eur. J. Neurosci.* 19, 1675–1682. doi:10.1111/j.1460-9568.2004.03306.x
- Hora, R., Kapoor, P., Thind, K. K., and Mishra, P. C. (2016). Cerebral malaria – clinical manifestations and pathogenesis. *Metab. Brain Dis.* 31, 225–237. doi:10.1007/s11011-015-9787-5
- Howard, R. J., Uni, S., Aikawa, M., Aley, S. B., Leech, J. H., Lew, A. M., et al. (1986). Secretion of a malarial histidine-rich protein (Pf HRP II) from *Plasmodium falciparum*-infected erythrocytes. *J. Cell Biol.* 103, 1269–1277. doi:10.1083/jcb.103.4.1269
- Hu, S., Tan, J., Qin, L., Lv, L., Yan, W., Zhang, H., et al. (2021). Molecular chaperones and Parkinson's disease. *Neurobiol. Dis.* 160, 105527. doi:10.1016/j.nbd.2021.105527
- Huang, S.-K., Lu, C.-W., Lin, T.-Y., and Wang, S.-J. (2022). Neuroprotective role of the B vitamins in the modulation of the central glutamatergic neurotransmission. *CNS Neurol. Disord. Drug Targets* 21, 292–301. doi:10.2174/1871527320666210902165739
- Huang, X., Li, N., Pu, Y., Zhang, T., and Wang, B. (2019). Neuroprotective effects of ginseng phytochemicals: Recent perspectives. *Molecules* 24, 2939. doi:10.3390/molecules24162939
- Hung, K.-C., Huang, H.-J., Wang, Y.-T., and Lin, A. M.-Y. (2016). Baicalein attenuates  $\alpha$ -synuclein aggregation, inflammasome activation and autophagy in the MPP<sup>+</sup>-treated nigrostriatal dopaminergic system *in vivo*. *J. Ethnopharmacol.* 194, 522–529. doi:10.1016/j.jep.2016.10.040
- Hussien, H. M., Abd-Elmegied, A., Ghareeb, D. A., Hafez, H. S., Ahmed, H. E. A., and El-moneam, N. A. (2018). Neuroprotective effect of berberine against environmental heavy metals-induced neurotoxicity and Alzheimer's-like disease in rats. *Food Chem. Toxicol.* 111, 432–444. doi:10.1016/j.fct.2017.11.025
- Huy, N. T., Serada, S., Thi, D., Trang, X., Takano, R., Kondo, Y., et al. (2003). Neutralization of toxic heme by *Plasmodium falciparum* histidine-rich protein 2. *J. Biochem. (Tokyo)* 133, 693–698. doi:10.1093/jb/mvg089
- Hviid, L., and Jensen, A. T. R. (2015). "PfEMP1 – a parasite protein family of key importance in *Plasmodium falciparum* malaria immunity and pathogenesis," in *Advances in parasitology*. Editors D. Rollinson, and J. R. Stothard (San Diego: Academic Press), 51–84. doi:10.1016/bs.apar.2015.02.004
- Hyman, S. E. (2005). Neurotransmitters. *Curr. Biol.* 15, R154–R158. doi:10.1016/j.cub.2005.02.037
- Idro, R., Kakooza-Mwesige, A., Asea, B., Ssebunya, K., Bangirana, P., Opoka, R. O., et al. (2016). Cerebral malaria is associated with long-term mental health disorders: A cross sectional survey of a long-term cohort. *Malar. J.* 15, 184. doi:10.1186/s12936-016-1233-6
- Islahudin, F., Tindall, S. M., Mellor, I. R., Swift, K., Christensen, H. E. M., Fone, K. C. F., et al. (2014). The antimalarial drug quinine interferes with serotonin biosynthesis and action. *Sci. Rep.* 4, 3618. doi:10.1038/srep03618
- Jain, K., Sood, S., and Gowthamarajan, K. (2013). Modulation of cerebral malaria by curcumin as an adjunctive therapy. *Braz. J. Infect. Dis.* 17, 579–591. doi:10.1016/j.bjid.2013.03.004
- Jamwal, S., and Kumar, P. (2019). Insight into the emerging role of striatal neurotransmitters in the pathophysiology of Parkinson's disease and huntington's disease: A review. *Curr. Neuropharmacol.* 17, 165–175. doi:10.2174/1570159X16666180302115032
- Juárez Olguín, H., Calderón Guzmán, D., Hernández García, E., and Barragán Mejía, G. (2015). The role of dopamine and its dysfunction as a consequence of oxidative stress. *Oxid. Med. Cell. Longev.* 2016, e9730467. doi:10.1155/2016/9730467
- Kaltschmidt, B., and Kaltschmidt, C. (2009). NF- $\kappa$ B in the nervous system. *Cold Spring Harb. Perspect. Biol.* 1, a001271. doi:10.1101/cshperspect.a001271
- Kam, A., Li, K. M., Razmovski-Naumovski, V., Nammi, S., Chan, K., Li, Y., et al. (2012). The protective effects of natural products on blood-brain barrier breakdown. *Curr. Med. Chem.* 19, 1830–1845. doi:10.2174/092986712800099794
- Katusic, Z. S., Stelter, A., and Milstien, S. (1998). Cytokines stimulate GTP cyclohydrolase I gene expression in cultured human umbilical vein endothelial cells. *Arterioscler. Thromb. Vasc. Biol.* 18, 27–32. doi:10.1161/01.atv.18.1.27
- Kaur, K., Jain, M., Kaur, T., and Jain, R. (2009). Antimalarials from nature. *Bioorg. Med. Chem.* 17, 3229–3256. doi:10.1016/j.bmc.2009.02.050

- Kelly, A., and Stanley, C. A. (2001). Disorders of glutamate metabolism. *Ment. Retard. Dev. Disabil. Res. Rev.* 7, 287–295. doi:10.1002/mrdd.1040
- Kempaiah, P., Dokladny, K., Karim, Z., Raballah, E., Ong'echa, J. M., Moseley, P. L., et al. (2016). Reduced Hsp70 and glutamine in pediatric severe malaria anemia: Role of hemozoin in suppressing Hsp70 and NF- $\kappa$ B activation. *Mol. Med.* 22, 570–584. doi:10.2119/molmed.2016.00130
- Khanam, S. (2017). Prevalence and epidemiology of malaria in Nigeria: A review. *Int. J. Res. Pharm. Biosci.* 4, 10–12.
- Kihara, M., Carter, J. A., and Newton, C. R. J. C. (2006). The effect of *Plasmodium falciparum* on cognition: A systematic review. *Trop. Med. Int. Health* 11, 386–397. doi:10.1111/j.1365-3156.2006.01579.x
- Kim, C.-Y., Seo, Y., Lee, C., Park, G. H., and Jang, J.-H. (2018). Neuroprotective effect and molecular mechanism of [6]-Gingerol against scopolamine-induced amnesia in C57bl/6 mice. *Evid. Based. Complement. Altern. Med.* 2018, e8941564. doi:10.1155/2018/8941564
- Klenke, C., Widera, D., Engelen, T., Müller, J., Noll, T., Niehaus, K., et al. (2013). Hsc70 is a novel interactor of NF-kappaB p65 in living hippocampal neurons. *PLoS ONE* 8, e65280. doi:10.1371/journal.pone.0065280
- Krashia, P., Nobili, A., and D'Amelio, M. (2019). Unifying hypothesis of dopamine neuron loss in neurodegenerative diseases: Focusing on Alzheimer's disease. *Front. Mol. Neurosci.* 12, 123. doi:10.3389/fnmol.2019.00123
- Kumar, A. (2015). NMDA receptor function during senescence: Implication on cognitive performance. *Front. Neurosci.* 9, 473. doi:10.3389/fnins.2015.00473
- Kumar, S. P., and Babu, P. P. (2020). Aberrant dopamine receptor signaling plays critical role in the impairment of striatal neurons in experimental cerebral malaria. *Mol. Neurobiol.* 57, 5069–5083. doi:10.1007/s12035-020-02076-0
- Lewerenz, J., and Maher, P. (2015). Chronic glutamate toxicity in neurodegenerative diseases—what is the evidence? *Front. Neurosci.* 9, 469. doi:10.3389/fnins.2015.00469
- Liao, D., Xiang, D., Dang, R., Xu, P., Wang, J., Han, W., et al. (2018). Neuroprotective effects of dl-3-n-Butylphthalide against doxorubicin-induced neuroinflammation, oxidative stress, endoplasmic reticulum stress, and behavioral changes. *Oxid. Med. Cell. Longev.* 2018, e125601. doi:10.1155/2018/9125601
- Liu, K., and Houry, W. A. (2014). “Chaperones and proteases of *Plasmodium falciparum*,” in *Heat shock proteins of malaria*. Editors A. Shonhai, and G. L. Blatch (Dordrecht: Springer), 161–187. doi:10.1007/978-94-007-7438-4\_9
- Liu, Y.-N., Peng, Y.-L., -Liu, L., Wu, T.-Y., Zhang, Y., Lian, Y.-J., et al. (2015). TNF $\alpha$  mediates stress-induced depression by upregulating indoleamine 2, 3-dioxygenase in a mouse model of unpredictable chronic mild stress. *Eur. Cytokine Netw.* 26, 15–25. doi:10.1684/ecn.2015.0362
- Lu, A., Ran, R., Parmentier-Batteur, S., Nee, A., and Sharp, F. R. (2002). Geldanamycin induces heat shock proteins in brain and protects against focal cerebral ischemia. *J. Neurochem.* 81, 355–364. doi:10.1046/j.1471-4159.2002.00835.x
- Lugo-Huitrón, R., Ugalde Muñiz, P., Pineda, B., Pedraza-Chaverri, J., Ríos, C., and Pérez-de la Cruz, V. (2013). Quinolinic acid: An endogenous neurotoxin with multiple targets. *Oxid. Med. Cell. Longev.* 2013, e104024. doi:10.1155/2013/104024
- Lyu, Q., Wawrzyniuk, M., Rutten, V. P. M. G., van Eden, W., Sijts, A. J. A. M., and Broere, F. (2020). Hsp70 and NF- $\kappa$ B mediated control of innate inflammatory responses in a canine macrophage cell line. *Int. J. Mol. Sci.* 21, E6464. doi:10.3390/ijms21186464
- MacCormick, I. J. C., Beare, N. A. V., Taylor, T. E., Barrera, V., White, V. A., Hiscott, P., et al. (2014). Cerebral malaria in children: Using the retina to study the brain. *Brain* 137, 2119–2142. doi:10.1093/brain/awu001
- Mackinnon, S., Durst, T., Arnason, J. T., Angerhofer, C., Pezzuto, J., Sanchez-Vindas, P. E., et al. (1997). Antimalarial activity of tropical meliaceae extracts and gedunin derivatives. *J. Nat. Prod.* 3864, 336–341. doi:10.1021/np9605394
- Mahomoodally, M. F. (2013). Traditional medicines in Africa: An appraisal of ten potent african medicinal plants. *Evid. Based. Complement. Altern. Med.* 2013, 617459. doi:10.1155/2013/617459
- Maier, A. G., Cooke, B. M., Cowman, A. F., and Tilley, L. (2009). Malaria parasite proteins that remodel the host erythrocyte. *Nat. Rev. Microbiol.* 7, 341–354. doi:10.1038/nrmicro2110
- Maier, A. G., Rug, M., O'Neill, M. T., Brown, M., Chakravorty, S., Szestak, T., et al. (2008). Exported proteins required for virulence and rigidity of *Plasmodium falciparum*-infected human erythrocytes. *Cell* 134, 48–61. doi:10.1016/j.cell.2008.04.051
- Mallozzi, C., Parravano, M., Gaddini, L., Villa, M., Pricci, F., Malchiodi-Albedi, F., et al. (2018). Curcumin modulates the NMDA receptor subunit composition through a mechanism involving CaMKII and ser/thr protein phosphatases. *Cell. Mol. Neurobiol.* 38, 1315–1320. doi:10.1007/s10571-018-0595-4
- Martí Coma-Cros, E., Biosca, A., Lantero, E., Manca, M. L., Caddeo, C., Gutiérrez, L., et al. (2018). Antimalarial activity of orally administered curcumin incorporated in eudragit®-containing liposomes. *Int. J. Mol. Sci.* 19, 1361. doi:10.3390/ijms19051361
- Mathew, B., Suresh, J., Elizabeth Mathew, G., Haridas, A., Suresh, G., and Sabreena, P. (2016). Synthesis, ADME studies, toxicity estimation, and exploration of molecular recognition of thiophene based chalcones towards monoamine oxidase-A and B. *Beni. Suef. Univ. J. Basic Appl. Sci.* 5, 396–401. doi:10.1016/j.bjbas.2015.06.003
- Matteucci, A., Cammarota, R., Paradisi, S., Varano, M., Balduzzi, M., Leo, L., et al. (2011). Curcumin protects against NMDA-induced toxicity: A possible role for NR2A subunit. *Invest. Ophthalmol. Vis. Sci.* 52, 1070–1077. doi:10.1167/iops.10-5966
- McEwen, B. S., and Milner, T. A. (2017). Understanding the broad influence of sex hormones and sex differences in the brain. *J. Neurosci. Res.* 95, 24–39. doi:10.1002/jnr.23809
- Midorikawa, Y., and Haque, Q. M. (1997). 15-Deoxyspergualin, an immunosuppressive agent, used in organ transplantation showed suppressive effects on malarial parasites. *Chemotherapy* 43, 31–35. doi:10.1159/000239532
- Miller, A. H., Haroon, E., Raison, C. L., and Felger, J. C. (2013). Cytokine targets in the brain: Impact on neurotransmitters and neurocircuits. *Depress. Anxiety* 30, 297–306. doi:10.1002/da.22084
- Milner, D. A. (2018). Malaria pathogenesis. *Cold Spring Harb. Perspect. Med.* 8, a025569–12. doi:10.1101/cshperspect.a025569
- Milner, D. A., Whitten, R. O., Kamiza, S., Carr, R., Liomba, G., Dzamalala, C., et al. (2014). The systemic pathology of cerebral malaria in African children. *Front. Cell. Infect. Microbiol.* 4, 104–113. doi:10.3389/fcimb.2014.00104
- Mishra, K., Dash, A. P., and Dey, N. (2011). Andrographolide: A novel antimalarial diterpene lactone compound from andrographis paniculata and its interaction with curcumin and artesunate. *J. Trop. Med.* 2011, 579518. doi:10.1155/2011/579518
- Miyazaki, I., and Asanuma, M. (2009). Approaches to prevent dopamine quinone-induced neurotoxicity. *Neurochem. Res.* 34, 698–706. doi:10.1007/s11064-008-9843-1
- Montagna, G. N., Matuschewski, K., and Buscaglia, C. A. (2012). Small heat shock proteins in cellular adhesion and migration: Evidence from *Plasmodium* genetics. *Cell Adh. Migr.* 6, 78–84. doi:10.4161/cam.20101
- Monteiro, M. C., Oliveira, F. R., Oliveira, G. B., Romão, P. R. T., and Maia, C. S. F. (2014). Neurological and behavioral manifestations of cerebral malaria: An update. *World J. Transl. Med.* 3, 9–16. doi:10.5528/wjtm.v3.i1.9
- Monzani, E., Nicolis, S., Dell'Acqua, S., Capucciati, A., Bacchella, C., Zucca, F. A., et al. (2019). Dopamine, oxidative stress and protein–quinone modifications in Parkinson's and other neurodegenerative diseases. *Angew. Chem. Int. Ed. Engl.* 58, 6512–6527. doi:10.1002/anie.201811122
- Morrioni, F., Sita, G., Graziosi, A., Turrini, E., Fimognari, C., Tarozzi, A., et al. (2018). Neuroprotective effect of caffeic acid phenethyl ester in A mouse model of Alzheimer's disease involves Nrf2/HO-1 pathway. *Aging Dis.* 9, 605–622. doi:10.14339/AD.2017.0903
- Moses, M. A., Henry, E. C., Ricke, W. A., and Gasiewicz, T. A. (2015). The heat shock protein 90 inhibitor, (-)-epigallocatechin gallate, has anticancer activity in a novel human prostate cancer progression model. *Cancer Prev. Res. Phila. Pa.* 8, 249–257. doi:10.1158/1940-6207.CAPR-14-0224
- Murphy, B. L., Arnsten, A. F., Goldman-Rakic, P. S., and Roth, R. H. (1996). Increased dopamine turnover in the prefrontal cortex impairs spatial working memory performance in rats and monkeys. *Proc. Natl. Acad. Sci. U. S. A.* 93, 1325–1329. doi:10.1073/pnas.93.3.1325
- Murwih Alidmat, M., Khairuddean, M., Mohammad Norman, N., Mohamed Asri, A. N., Mohd Suhaimi, M. H., and Sharma, G. (2021). Synthesis, characterization, docking study and biological evaluation of new chalcone, pyrazoline, and pyrimidine derivatives as potent antimalarial compounds. *Arab. J. Chem.* 14, 103304. doi:10.1016/j.arabjc.2021.103304
- Nabavi, S. F., Braid, N., Habtemariam, S., Orhan, I. E., Daglia, M., Manayi, A., et al. (2015). Neuroprotective effects of chrysin: From chemistry to medicine. *Neurochem. Int.* 90, 224–231. doi:10.1016/j.neuint.2015.09.006
- Newton, C. R. J. C., Hien, T. T., and White, N. (2000). Cerebral malaria. *J. Neurol. Neurosurg. Psychiatry* 69, 433–441. doi:10.1136/jnnp.69.4.433
- Nishanth, G., and Schlüter, D. (2019). Blood–brain barrier in cerebral malaria: Pathogenesis and therapeutic intervention. *Trends Parasitol.* 35, 516–528. doi:10.1016/j.pt.2019.04.010
- Nkumama, I. N., Meara, W. P. O., and Osier, F. H. A. (2016). Changes in malaria epidemiology in Africa and new challenges for elimination. *Trends Parasitol.* 33, 128–140. doi:10.1016/j.pt.2016.11.006



- Oliveira, K. R. H. M., Kauffmann, N., Leão, L. K. R., Passos, A. C. F., Rocha, F. A. F., Herculanio, A. M., et al. (2017). Cerebral malaria induces electrophysiological and neurochemical impairment in mice retinal tissue: Possible effect on glutathione and glutamatergic system. *Malar. J.* 16, 440. doi:10.1186/s12936-017-2083-6
- Oluwatosin, A., Tolulope, A., Ayokulehin, K., Patricia, O., Aderemi, K., Catherine, F., et al. (2014). Antimalarial potential of kolaviron, a biflavonoid from *Garcinia kola* seeds, against *Plasmodium berghei* infection in Swiss albino mice. *Asian pac. J. Trop. Med.* 7, 97–104. doi:10.1016/S1995-7645(14)60003-1
- Oluwayemi, I. O., Brown, B. J., Oyediji, O. A., and Oluwayemi, M. A. (2013). Neurological sequelae in survivors of cerebral malaria. *Pan Afr. Med. J.* 15, 88–89. doi:10.11604/pamj.2013.15.88.1897
- Ounjaijean, S., and Somsak, V. (2020). Combination of zingerone and dihydroartemisinin presented synergistic antimalarial activity against *Plasmodium berghei* infection in BALB/c mice as *in vivo* model. *Parasitol. Int.* 76, 102088. doi:10.1016/j.parint.2020.102088
- Pal, P., Balaban, A. E., Diamond, M. S., Sinnis, P., Klein, R. S., and Goldberg, D. E. (2017). *Plasmodium falciparum* histidine-rich protein II causes vascular leakage and exacerbates experimental cerebral malaria in mice. *PLoS ONE* 12, e0177142. doi:10.1371/journal.pone.0177142
- Pal, P., Daniels, B. P., Oskman, A., Diamond, M. S., Klein, R. S., and Goldberg, D. E. (2016). *Plasmodium falciparum* histidine-rich protein II compromises brain endothelial barriers and may promote cerebral malaria pathogenesis. *mBio* 7, e00617–16. doi:10.1128/mBio.00617-16
- Pallavi, R., Acharya, P., Chandran, S., Daily, J. P., and Tatu, U. (2010). Chaperone expression profiles correlate with distinct physiological states of *Plasmodium falciparum* in malaria patients. *Malar. J.* 9, 236. doi:10.1186/1475-2875-9-236
- Pasternak, N. D., and Dzikowski, R. (2009). PfEMP1: An antigen that plays a key role in the pathogenicity and immune evasion of the malaria parasite *Plasmodium falciparum*. *Int. J. Biochem. Cell Biol.* 41, 1463–1466. doi:10.1016/j.biocel.2008.12.012
- Pastukhov, Yu. F., Ekimova, I. V., Guzlova, I. V., Romanova, I. V., and Artyukhina, Z. E. (2013). Chaperone Hsp70 content in dopaminergic neurons of the substantia nigra increases in proteasome dysfunction. *Neurosci. Behav. Physiol.* 43, 380–387. doi:10.1007/s11055-013-9744-x
- Patwardhan, C. A., Fauq, A., Peterson, L. B., Miller, C., Blagg, B. S. J., and Chadli, A. (2013). Gedunin inactivates the co-chaperone p23 protein causing cancer cell death by apoptosis. *J. Biol. Chem.* 288, 7313–7325. doi:10.1074/jbc.M112.427328
- Pavithra, S. R., Kumar, R., and Tatu, U. (2007). Systems analysis of chaperone networks in the malarial parasite *Plasmodium falciparum*. *PLoS Comput. Biol.* 3, 1701–1715. doi:10.1371/journal.pcbi.0030168
- Pesce, E.-R., Cockburn, I. L., Goble, J. L., Stephens, L. L., and Blatch, G. L. (2010). Malaria heat shock proteins: Drug targets that chaperone other drug targets. *Infect. Disord. Drug Targets* 10, 147–157. doi:10.2174/187152610791163417
- Pesce, E., and Blatch, G. L. (2014). Plasmodial Hsp40 and Hsp70 chaperones: Current and future perspectives. *Parasitology* 141, 1167–1176. doi:10.1017/S003118201300228X
- Petrović, A., Kaur, J., Tomljanović, I., Nistri, A., and Mladinic, M. (2019). Pharmacological induction of Heat Shock Protein 70 by celastrol protects motoneurons from excitotoxicity in rat spinal cord *in vitro*. *Eur. J. Neurosci.* 49, 215–231. doi:10.1111/ejn.14218
- Piaz, F. D., Malafronte, N., Romano, A., Gallotta, D., Belisario, M. A., Bifulco, G., et al. (2012). Structural characterization of tetranortriterpenes from *Pseudocedrela kotschy* and *Trichilia emetica* and study of their activity towards the chaperone Hsp90. *Phytochemistry* 75, 78–89. doi:10.1016/j.phytochem.2011.12.002
- Plewes, K., Turner, G. D. H., and Dondorp, A. M. (2018). Pathophysiology, clinical presentation, and treatment of coma and acute kidney injury complicating falciparum malaria. *Curr. Opin. Infect. Dis.* 31, 69–77. doi:10.1097/QCO.0000000000000419
- Ponsford, M. J., Medana, I. M., Prapansilp, P., Hien, T. T., Lee, S. J., Dondorp, A. M., et al. (2012). Sequestration and microvascular congestion are associated with coma in human cerebral malaria. *J. Infect. Dis.* 205, 663–671. doi:10.1093/infdis/jir812
- Posfai, D., Eubanks, A. L., Keim, A. I., Lu, K. Y., Wang, G. Z., Hughes, P. F., et al. (2018). Identification of Hsp90 inhibitors with anti-plasmodium activity. *Antimicrob. Agents Chemother.* 62, e01799–17. doi:10.1128/AAC.01799-17
- Pussard, E., Bernier, A., Fouquet, E., and Bouree, P. (2003). Quinine distribution in mice with plasmodium berghei malaria. *Eur. J. Drug Metab. Pharmacokinet.* 28, 11–20. doi:10.1007/BF03190862
- Pussard, E., Merzouk, M., and Barennes, H. (2007). Increased uptake of quinine into the brain by inhibition of P-glycoprotein. *Eur. J. Pharm. Sci.* 32, 123–127. doi:10.1016/j.ejps.2007.06.007
- Quinlan, M. G., Hussain, D., and Brake, W. G. (2008). Use of cognitive strategies in rats: The role of estradiol and its interaction with dopamine. *Horm. Behav.* 53, 185–191. doi:10.1016/j.yhbeh.2007.09.015
- Raghavan, R., Cheriyaundath, S., and Madassery, J. (2012). Andrographolide, a new potential NF- $\kappa$ B inhibitor: Docking simulation and evaluation of drug-likeness. *Mol. Simul.* 38, 582–588. doi:10.1080/08927022.2011.651138
- Ramya, T. N. C., Karmodiya, K., Surolia, A., and Surolia, N. (2007). 15-Deoxyspergualin primarily targets the trafficking of apicoplast proteins in *Plasmodium falciparum*. *J. Biol. Chem.* 282, 6388–6397. doi:10.1074/jbc.M610251200
- Rangel-Barajas, C., Coronel, I., and Florán, B. (2015). Dopamine receptors and neurodegeneration. *Aging Dis.* 6, 349–368. doi:10.14336/AD.2015.0330
- Rangel-Gomez, M., and Meeter, M. (2016). Neurotransmitters and novelty: A systematic review. *J. Psychopharmacol.* 30, 3–12. doi:10.1177/0269881115612238
- Rao, A., Kumar, M. K., Joseph, T., and Bulusu, G. (2010). Cerebral malaria: Insights from host-parasite protein-protein interactions. *Malar. J.* 9, 155. doi:10.1186/1475-2875-9-155
- Reiner, A., and Levitz, J. (2018). Glutamatergic signaling in the central nervous system: Ionotropic and metabotropic receptors in concert. *Neuron* 98, 1080–1098. doi:10.1016/j.neuron.2018.05.018
- Rosenberg, G. A. (2012). Neurological diseases in relation to the blood – brain barrier. *J. Cereb. Blood Flow. Metab.* 32, 1139–1151. doi:10.1038/jcbfm.2011.197
- Roy, S., Chattopadhyay, R. N., and Maitra, S. K. (1993). Changes in brain neurotransmitters in rodent malaria. *Indian J. Malariol.* 30, 183–185.
- Rubach, M. P., Mukemba, J., Florence, S., Lopansri, B. K., Hyland, K., Volkheimer, A. D., et al. (2015). Impaired systemic tetrahydrobiopterin bioavailability and increased oxidized bipterins in pediatric falciparum malaria: Association with disease severity. *PLoS Pathog.* 11, e1004655. doi:10.1371/journal.ppat.1004655
- Sahu, P. K., Satpathi, S., Behera, P. K., Mishra, S. K., Mohanty, S., and Wassmer, S. C. (2015). Pathogenesis of cerebral malaria: New diagnostic tools, biomarkers, and therapeutic approaches. *Front. Cell. Infect. Microbiol.* 5, 75. doi:10.3389/fcimb.2015.00075
- Sakai, N., Kaufman, S., and Miltien, S. (1995). Parallel induction of nitric oxide and tetrahydrobiopterin synthesis by cytokines in rat glial cells. *J. Neurochem.* 65, 895–902. doi:10.1046/j.1471-4159.1995.65020895.x
- Salehi, B., Qusie, C., Chamkhi, I., El Omari, N., Balahbib, A., Sharifi-Rad, J., et al. (2021). Pharmacological properties of chalcones: A review of preclinical including molecular mechanisms and clinical evidence. *Front. Pharmacol.* 11, 592654. doi:10.3389/fphar.2020.592654
- Santos, J., Quimque, M. T., Liman, R. A., Agbay, J. C., Macabeo, A. P. G., Corpuz, M. J.-A., et al. (2021). Computational and experimental assessments of magnolol as a neuroprotective agent and utilization of UiO-66(Zr) as its drug delivery system. *ACS Omega* 6, 24382–24396. doi:10.1021/acsomega.1c02555
- Schiess, N., Villabona-Rueda, A., Cottier, K. E., Huether, K., Chipeta, J., and Stins, M. F. (2020). Pathophysiology and neurologic sequelae of cerebral malaria. *Malar. J.* 19, 266(1–12). doi:10.1186/s12936-020-03336-z
- Segura, C., Cuesta-Astroz, Y., Nunes-Batista, C., Zalis, M., von Krüger, W. M. de A., and Mascarello Bisch, P. (2014). Partial characterization of *Plasmodium falciparum* trophozoite proteome under treatment with quinine, mefloquine and the natural antiplasmodial diosgenone. *Biomedica* 34, 237–249. doi:10.1590/S0120-41572014000200010
- Senf, S. M., Dodd, S. L., McClung, J. M., and Judge, A. R. (2008). Hsp70 overexpression inhibits NF- $\kappa$ B and Foxo3a transcriptional activities and prevents skeletal muscle atrophy. *FASEB J.* 22, 3836–3845. doi:10.1096/fj.08-110163
- Shahinas, D., Folefoc, A., and Pillai, D. R. (2013a). Targeting *Plasmodium falciparum* Hsp90: Towards reversing antimalarial resistance. *Pathogens* 2, 33–54. doi:10.3390/pathogens2010033
- Shahinas, D., Folefoc, A., Taldone, T., Chiosis, G., Crandall, I., and Pillai, D. R. (2013b). A purine analog synergizes with chloroquine (CQ) by targeting *Plasmodium falciparum* Hsp90 (PfHsp90). *PLoS One* 8 (1–13), e75446. doi:10.1371/journal.pone.0075446
- Sheffler, Z. M., Reddy, V., and Pillarisetty, L. S. (2022). *In StatPearls*. Treasure Island (FL): StatPearls Publishing. Physiology, neurotransmitters.
- Shih, R.-H., Wang, C.-Y., and Yang, C.-M. (2015). NF- $\kappa$ B signaling pathways in neurological inflammation: A mini review. *Front. Mol. Neurosci.* 8, 77. doi:10.3389/fnmol.2015.00077
- Shikani, H. J., Freeman, B. D., Lisanti, M. P., Weiss, L. M., Tanowitz, H. B., and Desruisseaux, M. S. (2012). Cerebral malaria: We have come a long way. *Am. J. Pathol.* 181, 1484–1492. doi:10.1016/j.ajpath.2012.08.010



- Shimazu, R., Anada, M., Miyaguchi, A., Nomi, Y., and Matsumoto, H. (2021). Evaluation of blood-brain barrier permeability of polyphenols, anthocyanins, and their metabolites. *J. Agric. Food Chem.* 69, 11676–11686. doi:10.1021/acs.jafc.1c02898
- Shimizu, F., Nishihara, H., and Kanda, T. (2018). Blood – brain barrier dysfunction in immuno- mediated neurological diseases. *Immunol. Med.* 41, 120–128. doi:10.1080/25785826.2018.1531190
- Shonhai, A., Picard, D., and Blatch, G. L. (Editors) (2021). *Heat shock proteins of malaria*. 2nd Edition (Germany: Springer Nature Switzerland AG).
- Shonhai, A. (2010). Plasmodial heat shock proteins: Targets for chemotherapy. *FEMS Immunol. Med. Microbiol.* 58, 61–74. doi:10.1111/j.1574-695X.2009.00639.x
- Shrestha, L., Bolaender, A., Patel, H. J., and Taldone, T. (2016). Heat shock protein (HSP) drug discovery and development: Targeting heat shock proteins in disease. *Curr. Top. Med. Chem.* 16, 2753–2764. doi:10.2174/1568026616666160413141911
- Sierro, F., and Grau, G. E. R. (2019a). The ins and outs of cerebral malaria pathogenesis: Immunopathology, extracellular vesicles, immunometabolism, and trained immunity. *Front. Immunol.* 10, 830. doi:10.3389/fimmu.2019.00830
- Sierro, F., and Grau, G. E. R. (2019b). The ins and outs of cerebral malaria pathogenesis: Immunopathology, extracellular vesicles, immunometabolism, and trained immunity. *Front. Immunol.* 10, 830(1–11). doi:10.3389/fimmu.2019.00830
- Silamut, K., White, N. J., Looareesuwan, S., and Warrell, D. A. (1985). Binding of quinine to plasma proteins in falciparum malaria. *Am. J. Trop. Med. Hyg.* 34, 681–686. doi:10.4269/ajtmh.1985.34.681
- Simões, A. P., Silva, C. G., Marques, J. M., Pochmann, D., Porciúncula, L. O., Ferreira, S., et al. (2018). Glutamate-induced and NMDA receptor-mediated neurodegeneration entails P2Y1 receptor activation. *Cell Death Dis.* 2012 (6), 1–50. doi:10.1038/s41419-018-0351-1
- Sinclair, D., Donegan, S., Isba, R., and Lalloo, D. G. (2012). Artesunate versus quinine for treating severe malaria. *Cochrane Database Syst. Rev.* 2012, CD005967. doi:10.1002/14651858.CD005967.pub4
- Singh, P., Anand, A., and Kumar, V. (2014). Recent developments in biological activities of chalcones: A mini review. *Eur. J. Med. Chem.* 85, 758–777. doi:10.1016/j.ejmech.2014.08.033
- Singh, S., Jamwal, S., and Kumar, P. (2017). Neuroprotective potential of Quercetin in combination with piperine against 1-methyl-4-phenyl-1, 2, 3, 6-tetrahydropyridine-induced neurotoxicity. *Neural Regen. Res.* 12, 1137–1144. doi:10.4103/1673-5374.211194
- Singh, S. K., Dwivedi, H., Gunjan, S., Chauhan, B. S., Pandey, S. K., and Tripathi, R. (2019). Potential role of arteether on N-methyl-D-aspartate (NMDA) receptor expression in experimental cerebral malaria mice and extension of their survival. *Parasitology* 146, 1571–1577. doi:10.1017/S0031182019000878
- Sinha, S., Prakash, A., Medhi, B., Sehgal, A., Batovska, D. I., and Sehgal, R. (2021). Pharmacokinetic evaluation of Chalcone derivatives with antimalarial activity in New Zealand White Rabbits. *BMC Res. Notes* 14, 264. doi:10.1186/s13104-021-05684-8
- Smith, D. F., Whitesell, L., and Katsanis, E. (1998). Molecular chaperones: Biology and prospects for pharmacological intervention. *Pharmacol. Rev.* 50, 493–514.
- Smith, H. L., Li, W., and Cheetham, M. E. (2015). Molecular chaperones and neuronal proteostasis. *Semin. Cell Dev. Biol.* 40, 142–152. doi:10.1016/j.semcdb.2015.03.003
- Sowndhararajan, K., Deepa, P., Kim, M., Park, S. J., and Kim, S. (2018). Neuroprotective and cognitive enhancement potentials of baicalin: A review. *Brain Sci.* 8, 104. doi:10.3390/brainsci8060104
- Spielmann, T., and Gilberger, T.-W. (2010). Protein export in malaria parasites: Do multiple export motifs add up to multiple export pathways? *Trends Parasitol.* 26, 6–10. doi:10.1016/j.pt.2009.10.001
- Spycher, C., Rug, M., Pachlatko, E., Hanssen, E., Ferguson, D., Cowman, A. F., et al. (2008). The Maurer's cleft protein MAHRP1 is essential for trafficking of PfEMP1 to the surface of Plasmodium falciparum-infected erythrocytes. *Mol. Microbiol.* 68, 1300–1314. doi:10.1111/j.1365-2958.2008.06235.x
- Stetler, R. A., Gan, Y., Zhang, W., Liou, A. K., Gao, Y., Cao, G., et al. (2010). Heat shock proteins: Cellular and molecular mechanisms in the central nervous system. *Prog. Neurobiol.* 92, 184–211. doi:10.1016/j.pneurobio.2010.05.002
- Storm, J., and Craig, A. G. (2014a). Pathogenesis of cerebral malaria--inflammation and cytoadherence. *Front. Cell. Infect. Microbiol.* 4, 100. doi:10.3389/fcimb.2014.00100
- Storm, J., Jespersen, J. S., Seydel, K. B., Szelest, T., Mbewe, M., Chisala, N. V., et al. (2019). Cerebral malaria is associated with differential cytoadherence to brain endothelial cells. *EMBO Mol. Med.* 11, e9164–15. doi:10.15252/emmm.201809164
- Subedi, L., and Gaire, B. P. (2021). Neuroprotective effects of curcumin in cerebral ischemia: Cellular and molecular mechanisms. *ACS Chem. Neurosci.* 12, 2562–2572. doi:10.1021/acschemneuro.1c00153
- Suda, M., Honma, T., Miyagawa, M., and Wang, R.-S. (2008). Alteration of brain levels of neurotransmitters and amino acids in male F344 rats induced by three-week repeated inhalation exposure to 1-bromopropane. *Ind. Health* 46, 348–359. doi:10.2486/indhealth.46.348
- Talapko, J., Škrlec, I., Alebić, T., Jukić, M., and Včev, A. (2019). Malaria: The past and the present. *Microorganisms* 7 (6), 179(1–17). doi:10.3390/microorganisms7060179
- Tozzi, A., de Iure, A., Tantucci, M., Durante, V., Quiroga-Varela, A., Giampà, C., et al. (2015). Endogenous 17 $\beta$ -estradiol is required for activity-dependent long-term potentiation in the striatum: Interaction with the dopaminergic system. *Front. Cell. Neurosci.* 9, 192. doi:10.3389/fncel.2015.00192
- Tran, P. L. C. H. B., Kim, S. A., Choi, H. S., Yoon, J. H., and Ahn, S. G. (2010). Epigallocatechin-3-gallate suppresses the expression of HSP70 and HSP90 and exhibits anti-tumor activity *in vitro* and *in vivo*. *BMC Cancer* 10, 276. doi:10.1186/1471-2407-10-276
- Tripathi, A. K., Dwivedi, A., Pal, M. K., Rastogi, N., Gupta, P., Ali, S., et al. (2014). Attenuated neuroprotective effect of riboflavin under UV-B irradiation via miR-203/c-Jun signaling pathway *in vivo* and *in vitro*. *J. Biomed. Sci.* 21, 39. doi:10.1186/1423-0127-21-39
- Tripathi, A. K., Sha, W., Shulaev, V., Stins, M. F., and Sullivan, D. J. (2009). Plasmodium falciparum-infected erythrocytes induce NF-kappaB regulated inflammatory pathways in human cerebral endothelium. *Blood* 114, 4243–4252. doi:10.1182/blood-2009-06-226415
- Tzeng, Y.-M., and Lee, M.-J. (2015). Neuroprotective properties of kavalactones. *Neural Regen. Res.* 10, 875–877. doi:10.4103/1673-5374.158335
- van der Heyde, H. C., Nolan, J., Combes, V., Gramaglia, I., and Grau, G. E. (2006). A unified hypothesis for the Genesis of cerebral malaria: Sequestration, inflammation and hemostasis leading to microcirculatory dysfunction. *Trends Parasitol.* 22, 503–508. doi:10.1016/j.pt.2006.09.002
- van Holstein, M., Aarts, E., van der Schaaf, M. E., Geurts, D. E. M., Verkes, R. J., Franke, B., et al. (2011). Human cognitive flexibility depends on dopamine D2 receptor signaling. *Psychopharmacol. (Berl.)* 218, 567–578. doi:10.1007/s00213-011-2340-2
- Vauzour, D. (2012). Dietary polyphenols as modulators of brain functions: Biological actions and molecular mechanisms underpinning their beneficial effects. *Oxid. Med. Cell. Longev.* 2012, e914273. doi:10.1155/2012/914273
- Velaga, M. K., Basuri, C. K., Robinson Taylor, K. S., Yallapragada, P. R., Rajanna, S., and Rajanna, B. (2014). Ameliorative effects of Bacopa monniera on lead-induced oxidative stress in different regions of rat brain. *Drug Chem. Toxicol.* 37, 357–364. doi:10.3109/01480545.2013.866137
- Vijayan, V., Bhaskar, S., Kavitha, S. K., Ratheesh, M., Kripa, K., and Helen, A. (2010). Betulinic acid isolated from Bacopa monniera (L.) Wettst suppresses lipopolysaccharide stimulated interleukin-6 production through modulation of nuclear factor-kappaB in peripheral blood mononuclear cells. *Int. Immunopharmacol.* 10, 843–849. doi:10.1016/j.intimp.2010.04.013
- Walker, M. C., and van der Donk, W. A. (2016). The many roles of glutamate in metabolism. *J. Ind. Microbiol. Biotechnol.* 43, 419–430. doi:10.1007/s10295-015-1665-y
- Wang, C.-H., Chou, P.-C., Chung, F.-T., Lin, H.-C., Huang, K.-H., and Kuo, H.-P. (2017a). Heat shock protein70 is implicated in modulating NF- $\kappa$ B activation in alveolar macrophages of patients with active pulmonary tuberculosis. *Sci. Rep.* 7, 1214. doi:10.1038/s41598-017-01405-z
- Wang, G., Tang, W., and Bidigare, R. R. (2005). "Terpenoids as therapeutic drugs and pharmaceutical agents," in *Natural products: Drug discovery and therapeutic medicine*. Editors L. Zhang, and A. L. Demain (Totowa, NJ: Humana Press), 197–227. doi:10.1007/978-1-59259-976-9\_9
- Wang, H.-C., Wang, B.-D., Chen, M.-S., Chen, H., Sun, C.-F., Shen, G., et al. (2018). Neuroprotective effect of berberine against learning and memory deficits in diffuse axonal injury. *Exp. Ther. Med.* 15, 1129–1135. doi:10.3892/etm.2017.5496
- Wang, X.-S., Zhang, Z.-R., Zhang, M.-M., Sun, M.-X., Wang, W.-W., and Xie, C.-L. (2017b). Neuroprotective properties of curcumin in toxin-base animal models of Parkinson's disease: A systematic experiment literatures review. *BMC Complement. Altern. Med.* 17, 412. doi:10.1186/s12906-017-1922-x

- Webster, J. M., Darling, A. L., Uversky, V. N., and Blair, L. J. (2019). Small heat shock proteins, big impact on protein aggregation in neurodegenerative disease. *Front. Pharmacol.* 10, 1047. doi:10.3389/fphar.2019.01047
- Westerheide, S. D., Bosman, J. D., Mbadugha, B. N. A., Kawahara, T. L. A., Matsumoto, G., Kim, S., et al. (2004). Celastrols as inducers of the heat shock response and cytoprotection. *J. Biol. Chem.* 279, 56053–56060. doi:10.1074/jbc.M409267200
- White, N. J., Looareesuwan, S., Warrell, D. A., Warrell, M. J., Bunnag, D., and Harinasuta, T. (1982). Quinine pharmacokinetics and toxicity in cerebral and uncomplicated falciparum malaria. *Am. J. Med.* 73, 564–572. doi:10.1016/0002-9343(82)90337-0
- Who (2021). *World malaria report 2021*. Switzerland: WHO.
- Wickert, H., Wissing, F., Andrews, K. T., Stich, A., Krohne, G., and Lanzer, M. (2003). Evidence for trafficking of PfEMP1 to the surface of *P. falciparum*-infected erythrocytes via a complex membrane network. *Eur. J. Cell Biol.* 82, 271–284. doi:10.1078/0171-9335-00319
- Wu, W. C., Wu, M. H., Chang, Y. C., Hsieh, M. C., Wu, H. J., Cheng, K. C., et al. (2010). Geldanamycin and its analog induce cytotoxicity in cultured human retinal pigment epithelial cells. *Exp. Eye Res.* 91, 211–219. doi:10.1016/j.exer.2010.05.005
- Yamaguchi, T., Wang, H.-L., Li, X., Ng, T. H., and Morales, M. (2011). Mesocorticolimbic glutamatergic pathway. *J. Neurosci.* 31, 8476–8490. doi:10.1523/JNEUROSCI.1598-11.2011
- Ye, X., Rong, Z., Li, Y., Wang, X., Cheng, B., Cheng, Y., et al. (2018). Protective role of L-3-n-butylphthalide in cognitive function and dysthymic disorders in mouse with chronic epilepsy. *Front. Pharmacol.* 9, 734. doi:10.3389/fphar.2018.00734
- Yeo, T. W., Lampah, D. A., Kenangalem, E., Tjitra, E., Price, R. N., Weinberg, J. B., et al. (2015). Impaired systemic tetrahydrobiopterin bioavailability and increased dihydrobiopterin in adult falciparum malaria: Association with disease severity, impaired microvascular function and increased endothelial activation. *PLoS Pathog.* 11, e1004667. doi:10.1371/journal.ppat.1004667
- Youn, K., Ho, C.-T., and Jun, M. (2022). Multifaceted neuroprotective effects of (-)-epigallocatechin-3-gallate (EGCG) in alzheimer's disease: An overview of pre-clinical studies focused on  $\beta$ -amyloid peptide. *Food Sci. Hum. Wellness* 11, 483–493. doi:10.1016/j.fshw.2021.12.006
- Zeiler, F. A., Silvaggio, J., Kaufmann, A. M., Gillman, L. M., and West, M. (2014). Norepinephrine as a potential aggravator of symptomatic cerebral vasospasm: Two cases and argument for milrinone therapy. *Case Rep. Crit. Care* 2014, 630970. doi:10.1155/2014/630970
- Zhang, H. (2012). New insights into huperzine A for the treatment of Alzheimer's disease. *Acta Pharmacol. Sin.* 33, 1170–1175. doi:10.1038/aps.2012.128
- Zhang, S., Wang, R., and Wang, G. (2018). Impact of dopamine oxidation on dopaminergic neurodegeneration. *ACS Chem. Neurosci.* 10, 945–953. doi:10.1021/acscchemneuro.8b00454
- Zhang, T., Hamza, A., Cao, X., Wang, B., Yu, S., Zhan, C.-G., et al. (2008). A novel Hsp90 inhibitor to disrupt Hsp90/Cdc37 complex against pancreatic cancer cells. *Mol. Cancer Ther.* 7, 162–170. doi:10.1158/1535-7163.MCT-07-0484
- Zininga, T., Poee, O. J., Makhado, P. B., Ramatsui, L., Prinsloo, E., Achilonu, I., et al. (2017a). Polymyxin B inhibits the chaperone activity of Plasmodium falciparum Hsp70. *Cell Stress Chaperones* 22, 707–715. doi:10.1007/s12192-017-0797-6
- Zininga, T., Ramatsui, L., Makhado, P., Makumire, S., Achilinou, I., Hoppe, H., et al. (2017b). (-)-Epigallocatechin-3-Gallate inhibits the chaperone activity of Plasmodium falciparum Hsp70 chaperones and abrogates their association with functional partners. *Molecules* 22, 2139. doi:10.3390/molecules22122139



## OPEN ACCESS

## EDITED BY

Stanley Makumire,  
University of Cape Town, South Africa

## REVIEWED BY

Jude Przyborski,  
Justus-Liebig-University Gießen,  
Germany  
Dhanasekaran Shanmugam,  
National Chemical Laboratory (CSIR),  
India

## \*CORRESPONDENCE

Gregory L. Blatch,  
g.blatch@ru.ac.za

<sup>†</sup>These authors have contributed equally  
to this work

## SPECIALTY SECTION

This article was submitted to Molecular  
Diagnostics and Therapeutics,  
a section of the journal  
Frontiers in Molecular Biosciences

RECEIVED 26 June 2022

ACCEPTED 02 August 2022

PUBLISHED 31 August 2022

## CITATION

Almaazmi SY, Singh H, Dutta T and  
Blatch GL (2022), Exported J domain  
proteins of the human malaria parasite.  
*Front. Mol. Biosci.* 9:978663.  
doi: 10.3389/fmolb.2022.978663

## COPYRIGHT

© 2022 Almaazmi, Singh, Dutta and  
Blatch. This is an open-access article  
distributed under the terms of the  
Creative Commons Attribution License  
(CC BY). The use, distribution or  
reproduction in other forums is  
permitted, provided the original  
author(s) and the copyright owner(s) are  
credited and that the original  
publication in this journal is cited, in  
accordance with accepted academic  
practice. No use, distribution or  
reproduction is permitted which does  
not comply with these terms.

# Exported J domain proteins of the human malaria parasite

Shaikha Y. Almaazmi <sup>1†</sup>, Harpreet Singh <sup>2†</sup>,  
Tanima Dutta <sup>3,4,5†</sup> and Gregory L. Blatch <sup>1,3,4,6\*</sup>

<sup>1</sup>Biomedical Research and Drug Discovery Research Group, Faculty of Health Sciences, Higher Colleges of Technology, Sharjah, United Arab Emirates, <sup>2</sup>Department of Bioinformatics, Hans Raj Mahila Maha Vidyalaya, Jalandhar, India, <sup>3</sup>Vice Chancellery, The University of Notre Dame Australia, Fremantle, WA, Australia, <sup>4</sup>The Institute of Immunology and Infectious Diseases, Murdoch University, Perth, WA, Australia, <sup>5</sup>PathWest Nedlands, QEII Medical Centre, Nedlands, WA, Australia, <sup>6</sup>Biomedical Biotechnology Research Unit, Department of Biochemistry and Microbiology, Rhodes University, Grahamstown, South Africa

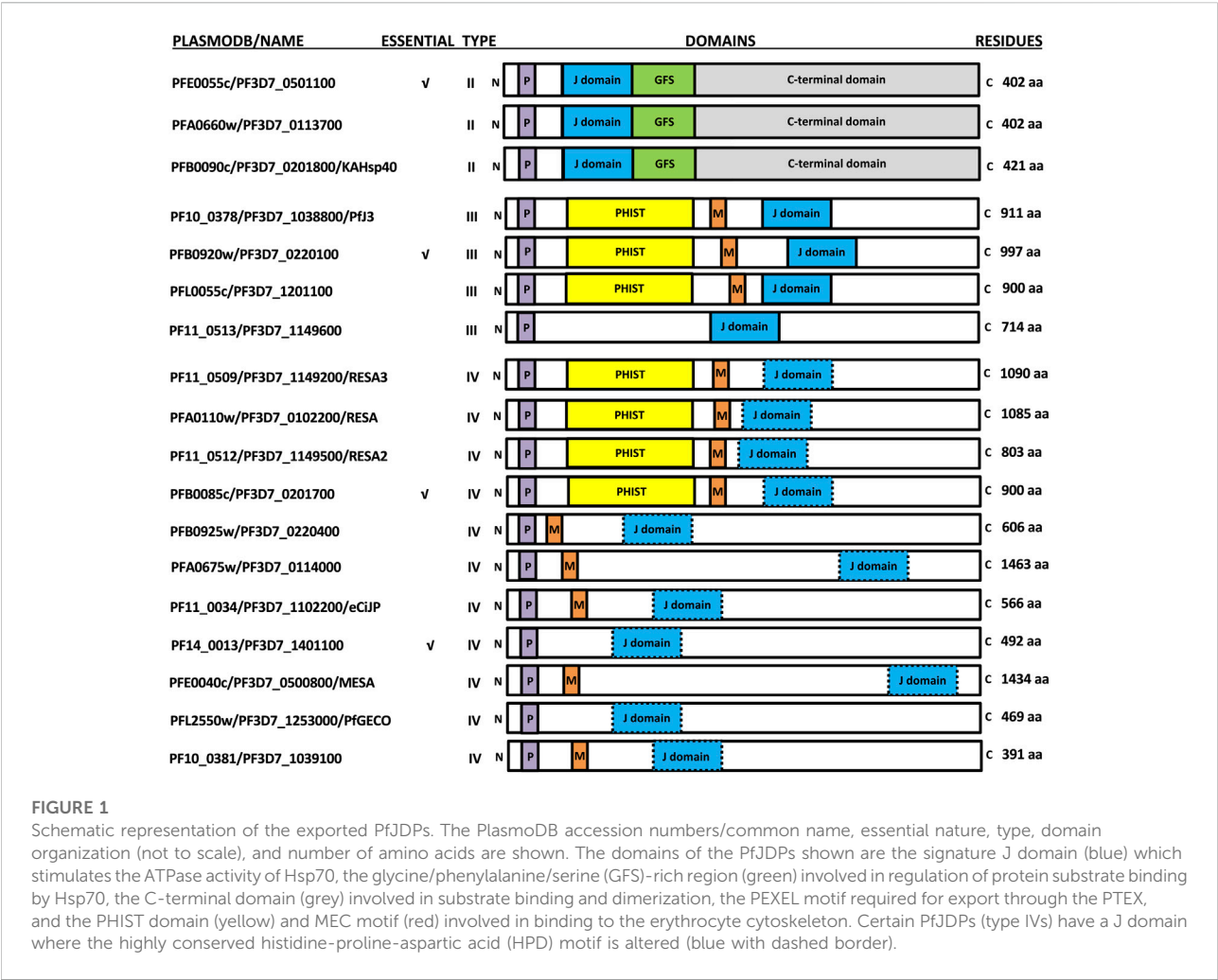
The heat shock protein 40 (Hsp40) family, also called J domain proteins (JDPs), regulate their Hsp70 partners by ensuring that they are engaging the right substrate at the right time and in the right location within the cell. A number of JDPs can serve as co-chaperone for a particular Hsp70, and so one generally finds many more JDPs than Hsp70s in the cell. In humans there are 13 Hsp70s and 49 JDPs. The human malaria parasite, *Plasmodium falciparum*, has dedicated an unusually large proportion of its genome to molecular chaperones, with a disproportionately high number of JDPs (PfJDPs) of 49 members. Interestingly, just under half of the PfJDPs are exported into the host cell during the asexual stage of the life cycle, when the malaria parasite invades mature red blood cells. Recent evidence suggests that these PfJDPs may be functionalizing both host and parasite Hsp70s within the infected red blood cell, and thereby driving the renovation of the host cell towards pathological ends. PfJDPs have been found to localize to the host cytosol, mobile structures within the host cytosol (so called “J Dots”), the host plasma membrane, and specialized structures associated with malaria pathology such as the knobs. A number of these exported PfJDPs are essential, and there is growing experimental evidence that they are important for the survival and pathogenesis of the malaria parasite. This review critiques our understanding of the important role these exported PfJDPs play at the host-parasite interface.

## KEYWORDS

heat shock proteins, J domain proteins, molecular chaperones and co-chaperones, *Plasmodium falciparum*, protein export, protein folding

## Introduction

The malaria parasite, *Plasmodium falciparum*, invades the cells of its human host, enabling it to evade the immune system and ultimately harness the cellular machinery to propagate itself and cause severe pathology. Surrounded by a self-created parasitophorous vacuole (PV) within human erythrocytes, the malaria parasite renovates the host cell by exporting over 400 parasite proteins,



including a number of heat shock proteins, which oversee protein folding as molecular chaperones and co-chaperones (Hiller et al., 2004; Marti et al., 2004; Jonsdottir et al., 2021). An important co-chaperone family, the *P. falciparum* J domain proteins (PfJDPs; also called heat shock protein 40 s, Hsp40s), are localized to almost every compartment of the infected erythrocyte, with arguably the greatest number of exported members of any protein family (Sargeant et al., 2006; Botha et al., 2007; Dutta et al., 2021a; Figure 1). Furthermore, many of the exported PfJDPs are expressed in the early stages of the asexual phase of the malaria parasite life cycle (Bozdech et al., 2003), consistent with their proposed critical role in the export of other malaria proteins and survival during febrile episodes (Dutta et al., 2021a). Indeed, there is growing evidence that these exported PfJDPs are key players in the survival and pathogenesis of the malaria parasite. The following sections of this review provide a critique of our understanding of the important role that these exported

PfJDPs play at the host-parasite interface of malaria pathology.

### The diversity, structure and function of PfJDPs

There are at least 49 PfJDPs encoded on the *P. falciparum* genome, far more than any other *Plasmodium* species (Njunge et al., 2013). All JDPs by definition contain a signature J domain (Kampinga et al., 2019), which contains a highly conserved histidine-proline-aspartic acid (HPD) motif, and is essential for regulation of the chaperone activity of partner heat shock protein 70 s (Hsp70s) (Hennessy et al., 2005). There are a number of other domains which have been used to categorize JDPs into four types (types I-IV; Botha et al., 2007). Interestingly, the HPD motif was thought to be invariant, until the discovery of the type IV JDPs containing a non-conserved HPD motif (Botha et al., 2007).



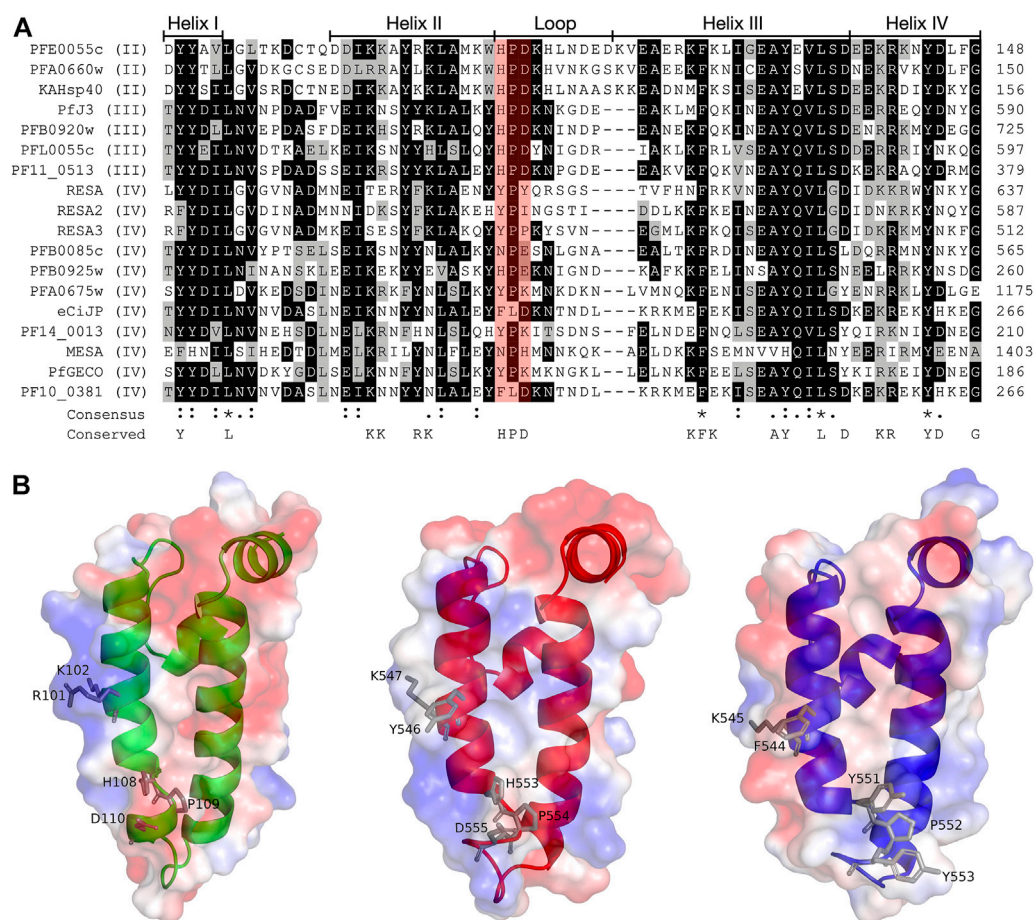


FIGURE 2

Multiple sequence alignment and molecular modelling of the J domains of exported PfJDPs. (A) Multiple sequence alignment of the J domains of the 18 exported PfJDPs proteins. The proteins are defined by either their PlasmoDB accession number or common name in the first column, and the roman numerals in brackets refer to the type of JDP. Colored in black are identical amino acids (in at least 50% of the aligned sequences), colored in light grey are similar amino acids (in at least 50% of the aligned sequences), and colored in white are the amino acids with no identity or similarity. The default categories for similar amino acids were applied to the multiple sequence alignment (ILV, FWY, KRH, DE, GAS, P, C and TNQM). The row titled "Consensus" are the common consensus symbols of the multiple sequence alignment: an \* (asterisk) indicates positions which have a single, fully conserved residue; a (colon) indicates conservation between groups of strongly similar properties; and a (period) indicates conservation between groups of weakly similar properties. The row titled "Conserved" refers to residues previously found to be highly conserved across J domains of different origins, with the residues defined at the bottom of the alignment (Hennessy et al., 2000; Hennessy et al., 2005). The protein helices and loop region are defined by bidirectional lines on top of the alignment. Highlighted in red shading is the HPD motif. The alignment was created using Clustal Omega (Sievers and Higgins, 2018) and rendered with box shading using Multiple Align Show (Stothard, 2000). (B) Three dimensional models of the J domains of PFE0055c type II (green), PfJ3 type III (red), and RESA type IV (blue) to illustrate the conserved HPD and RK motif (grey sticks). The positive charge is shown in blue colored surface, the negative charge is shown in red colored surface and the neutral potential are shown in white colored surface. The surface electrostatic potential was calculated by APBS. The models were prepared using SWISS-MODEL (Waterhouse et al., 2018; the template structures are listed in Supplementary Table S1) and graphically rendered using PyMol 2.5.2 (PyMOL Molecular Graphics System, Version 2.0 Schrödinger, LLC).

The *Plasmodium* export element (PEXEL; Hiller et al., 2004; Marti et al., 2004) has been shown to tag many *P. falciparum* proteins for export through the *Plasmodium* translocon of exported proteins (PTEx; de Koning-Ward et al., 2009; Beck et al., 2014; Elsworth et al., 2014; Elsworth et al., 2016). While the PEXEL was initially identified on 19 PfJDPs (Botha et al., 2007; Njunge et al., 2013; Pesce and Blatch 2014), recent revisions have indicated 18 PEXEL-containing PfJDPs (Dutta et al., 2021a). Therefore, at least 18 PfJDPs are proposed to be exported into the

infected erythrocyte based on the presence of a PEXEL; three type II, four type III and eleven type IV PfJDPs (Figure 1).

The exported PfJDPs appear to be critical for survival and pathogenesis of the malaria parasite, through their essential nature (4/18; Zhang et al., 2018; Figure 1), involvement in protein folding of exported virulence proteins (e.g., PFE0055c and PFA0660w associated with "J Dots"; Külzer et al., 2010; Külzer et al., 2012; Behl et al., 2019), requirement for growth or survival under febrile conditions (e.g., PFA0110w, the ring-

infected erythrocyte surface antigen protein, RESA; Silva et al., 2005; Diez-Silva et al., 2012) and involvement in pathogenesis (e.g., PF10\_0381; knockout causes loss of knobs; Maier et al., 2008). Of the 6 PfHsp70s expressed by the malaria parasite (Shonhai et al., 2007; Przyborski et al., 2015; Shonhai et al., 2021), PfHsp70-x appears to be the only member exported into the cytosol of the infected host erythrocyte (Külzer et al., 2010; Külzer et al., 2012; Grover et al., 2013), even though it lacks a PEXEL motif (Rhiel et al., 2016). Interestingly, the host cytosol appears to contain human chaperones and co-chaperones, including JDPs (which are likely to be non-functional remnants; Pasini et al., 2006; van Gestel et al., 2010) and significant levels of functional human Hsp70. (e.g., HSPA1A, also called Hsp72; referred to here as hHsp70), occurring free or in complex with Hsp90 and the Hsp70/Hsp90 organising protein, Hop (Banumathy et al., 2002). Furthermore, evidence is emerging that certain exported PfJDPs are capable of functionally interacting with PfHsp70-x, or hHsp70, or both Hsp70s (Dutta et al., 2021a; Diehl et al., 2021).

The structures of the ATPase (Day et al., 2019) and substrate binding (Schmidt and Vakonakis, 2020) domains of PfHsp70-x have been elucidated, as has the structure of the J domain of the exported PfJDP, PFA0660w (Day et al., 2019). In addition, molecular modelling revealed that helix II of the PFA0660w J domain makes a primary interface with the ATPase domain of PfHsp70-x (Day et al., 2019). Comparative molecular modelling suggested that the PFA0660w J domain-PfHsp70-x complex was less stable than that of another exported PfJDP (PFE0055c J domain-PfHsp70-x complex) (Dutta et al., 2021b). The functional differences between PFA0660w and PFE0055c were attributed to the J domain helix II of PFA0660w being less positively charged than the more typical J domain of PFE0055c. Interestingly, a multiple sequence alignment and surface electrostatic potential analysis of the J domains of all the exported PfJDs revealed that the positive nature of the J domain helix II appears to decrease going from type II to type IV, with the type IVs exhibiting significant negative charge or hydrophobicity (Figure 2; Supplementary Figure S1). These J domain surface differences together with the considerable variations in the HPD motifs for the type IVs, suggests that the structural and functional nature of the association, if any, between the different types of exported PfJDs and Hsp70 (PfHsp70-x or hHsp70) are likely to be considerably different.

## J Dots in the host cytosol contain PfJDs and PfHsp70-x

J Dots are highly mobile lipid-containing protein complexes found within the malaria parasite-infected erythrocyte cytosol (Külzer et al., 2010; Külzer et al., 2012; Petersen et al., 2016). Localization and immunoprecipitation studies have convincingly detected the exported type II PfJDs, PFA0660w and PFE0055c, and

PfHsp70-x in J Dots, which suggested that they formed a functional partnership in the host cytosol. However, these may not be the only J Dot chaperone partnerships, as an exported type IV PfJDP, called eCijP (PF11\_0034; a paralogue of PF10\_0381), has recently been reported to localize to J-Dots (Sahu et al., 2022). There is also evidence that J Dots associate with *P. falciparum* erythrocyte membrane protein 1 (PfEMP1), leading to the proposal that they may be involved in the trafficking of this major virulence factor (Külzer et al., 2012). These findings have been corroborated by biochemical studies on PFA0660w, PFE0055c and PfHsp70-x. PFA0660w was found to be highly effective at protein aggregation suppression, and both PFA0660w and PFE0055c were shown to be capable of specifically stimulating the basal ATPase activity of PfHsp70-x and not hHsp70 (Daniyan et al., 2016; Daniyan and Blatch 2017; Dutta et al., 2021b). These steady-state ATPase assays were conducted under saturating ATP concentrations which favour chaperone-co-chaperone over chaperone-substrate interactions, and in the case of PFE0055c could be inhibited by a J domain-specific inhibitor (chalcone C86), suggesting that PFA0660w and PFE0055c form specific co-chaperones partnerships with PfHsp70-x. PFE0055c stimulated the ATPase activity to a much greater extent than PFA0660w, and molecular modelling suggested that PFE0055c formed a more stable complex with PfHsp70-x than did PFA0660w (Dutta et al., 2021b). Furthermore, biochemical studies have shown that PfHsp70-x was capable of simultaneously associating with cholesterol-bound PFA0660w and PfEMP1 to form a stable complex (Behl et al., 2019). In contrast, biochemical studies using just the J domain of PFA0660w and PFE0055c (Day et al., 2019) or a PFA0660w J domain-substrate fusion construct (Diehl et al., 2021) have provided evidence that they may be capable of functional interaction with both PfHsp70-x and hHsp70. The inconsistency between the biochemical studies on full-length versus J domain proteins with respect to the hHsp70 findings, could be due to differences in the nature of the assays. However, it is also likely that the full-length PfJDs contain regions beyond the J domain that determine co-chaperone-chaperone specificity. This interpretation is consistent with structural analyses of the interaction between PFA0660w and PfHsp70-x, which indicated that they associated in a bipartite manner requiring both the J domain and the G/F region of PFA0660w (Behl and Mishra 2019).

## Exported PfJDs play a key role in malaria pathology

The third exported type II PfJDP (PFB0090c, also called knob-associated Hsp40, KAHsp40; Acharya et al., 2012), has not been reported to associate with PfHsp70-x or with J Dots, despite significant structural similarity to the other type II PfJDs. In contrast, PFB0090c has been shown to associate with PTEX and knobs, and is proposed to be involved in the trafficking, folding, and assembly of knob protein complexes (Acharya et al., 2012).

Knob complexes appear to contain human chaperones and co-chaperones in a highly complexed state (Hsp70, Hsp90 and Hop), and there is evidence that hHsp70 plays a role in assembly of knobs (Banumathy et al., 2002; Alampalli et al., 2018). It is tempting to speculate that PFB0090c is the co-chaperone recruiting hHsp70 to knobs. However, knock-out studies and associated genetic and biochemical analyses suggested that PFA0660w was also involved in knob formation and cytoadherence in collaboration with hHsp70 (Diehl et al., 2021). Interestingly, all of the exported type II PfJDPs (PFB0090c, PFA0660w, and PFE0055c) have been shown to functionally interact with hHsp70 using a heterologous yeast two-hybrid complementation assay (Jha et al., 2017). However, this assay did not test for functional association between PfJDPs and PfHsp70-x, and the biochemical and biophysical nature of the interactions were not investigated.

There are four exported type III PfJDPs (PFB0920w, PFL0055c, PF10\_0378/Pfj3 and PF11\_0513), three of which contain the *Plasmodium* helical interspersed sub-telomeric (PHIST) domain (Sargeant et al., 2006; Oakley et al., 2007; Oakley et al., 2011; Figure 1). Four exported type IV PfJDPs (PF11\_0509/RESA3, PF11\_0512/RESA2, PFA0110w/RESA and PFB0085c; Figure 1) also contain the PHIST domain (Figure 1). All of these PHIST-containing PfJDPs also contain the MEC (MESA erythrocyte cytoskeleton-binding) motif found in five other exported type IV PfJDPs (PFE0040c/mature parasite-infected erythrocyte surface antigen [MESA], PFA0675w, PFB0925w, PF10\_0381, PF11\_0034/eCijP; Bennett et al., 1997; Kilili and LaCount 2011; Njunge et al., 2013; Figure 1; Supplementary Figure S2). PHIST proteins are proposed to play an important role in trafficking of PfEMP1 proteins and the modulation of membrane rigidity and cytoadherence in parasite-infected erythrocytes (Kumar et al., 2019). Therefore, the presence of the MEC motif and the PHIST domain in these PfJDPs, is consistent with the proposed role of many of these proteins in remodelling at the cytoskeleton-membrane interface of the infected erythrocyte. RESA is arguably the most extensively studied exported PfJDP, and has been shown to play a key role in modulation of the rigidity of the infected erythrocyte membrane (Silva et al., 2005; Maier et al., 2008). RESA associates with spectrin and stabilizes its tertiary structure (Pei et al., 2007), and its effect on the cytoskeleton decreases the deformability of the infected erythrocyte, and protects the membrane during febrile episodes (Silva et al., 2005; Mills et al., 2007; Diez-Silva et al., 2012). The MEC motif enables MESA to bind to erythrocyte protein 4.1, thereby tethering it to the cytoskeleton (Coppel 1992; Bennett et al., 1997; Waller et al., 2003; Black et al., 2008); and MESA has been implicated in erythrocyte membrane modification (Coppel et al., 1988). However, the absence of MESA does not seem to have an influence on cytoadhesion (Petersen et al., 1989; Cooke et al., 2002). PF10\_0381 has been implicated in knob formation (Maier et al., 2008), while its paralogue, eCijP, has been shown to associate with the erythrocyte cytoskeleton, and potentially recruit hHsp70 to this location (Sahu et al., 2022; Figure 1). Apart from this report for

eCijP, there are virtually no reports on the interaction of type IV PfJDPs with Hsp70s (PfHsp70-x or hHsp70). Whether these proteins function as co-chaperones of Hsp70s remains to be determined.

## Exported PfJDPs as drug targets

Very few small molecule inhibitors have been identified that bind specifically to JDPs (e.g., phenoxy-N-arylamides; Cassel et al., 2012). In addition, the identification of inhibitors that can directly disrupt the interaction between JDPs and Hsp70s is challenging, as the interaction is transient and the binding sites are located on the surface of the protein as shallow exposed clefts which are recalcitrant to small molecule association (Pesce et al., 2016). Nevertheless, recent advances in our understanding of PfJDP-PfHsp70 interactions and their inhibition, suggests that they are a promising target for anti-malarial drug development (Daniyan and Blatch, 2017; Dutta et al., 2021a). Pyrimidinones have shown potential as protein-protein interaction inhibitors when tested on the parasite-resident PfJDP-PfHsp70 system (Botha et al., 2011). In contrast, naphthoquinones and prenylated alkaloids were identified that functionally disrupted the exported PfHsp70-x and its interaction with JDPs (Cockburn et al., 2014). The most promising inhibitor was the prenylated alkaloid, malonganenone A (MalA), where side-by-side inhibition assays conducted on JDP-PfHsp70-x and JDP-hHsp70 showed that MalA had no effect on the basal ATPase activity of both Hsp70s, and yet significantly inhibited the JDP-stimulated ATPase activity of PfHsp70-x but not that of hHsp70 (Cockburn et al., 2014). MalA has significant anti-malarial activity, but low cytotoxicity to human cell lines (Cockburn et al., 2011), suggesting that it is a promising small-molecule candidate for the development of specific inhibitors of the exported PfJDP-PfHsp70-x system. Chalcones represent another class of small molecules found to have anti-malarial activity (Sinha et al., 2019; Qin et al., 2020), and to inhibit JDP-hHsp70 interaction (Moses et al., 2018). Interestingly, chalcone C86 (3-nitro-2',4',6'-trimethoxychalcone) was found to bind to the J domain of JDP families A-C, indicating that it was a pan-inhibitor of JDPs (Moses et al., 2018). Recently, it was found that C86 also inhibited PfJDP-PfHsp70-x interaction (Dutta et al., 2021b). While C86 had no effect on the basal ATPase activity of PfHsp70-x, it significantly inhibited the PFE0055c-stimulated ATPase activity of PfHsp70-x (Dutta et al., 2021b). Notably, significant inhibition was only observed when C86 was pre-incubated with PFE0055c prior to the addition of PfHsp70-x. This finding is consistent with C86 binding specifically to the region of the J domain of PFE0055c that makes contact with PfHsp70-x (Dutta et al., 2021a). Molecular modelling of a predicted complex suggests that C86 makes major contacts with previously identified residues of helix II of the PFE0055c J domain involved in binding to the PfHsp70-x ATPase domain (Figure 3). This model provides a rationale for the development of C86 chemotypes, with the aim of identifying high affinity derivatives with specificity for PfJDPs. Given that the



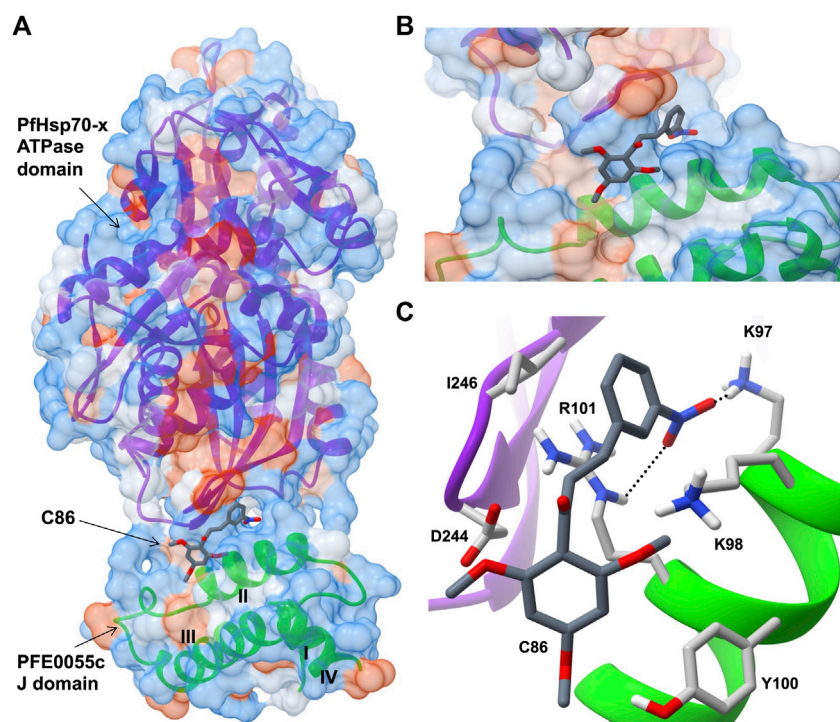


**FIGURE 3**

Predicted model of a complex of the small molecule inhibitor C86, PFE0055c J domain and PfHsp70-x ATPase domain. **(A)** Overall binding pose of C86 (middle) to the complex formed between the PfHsp70-x ATPase domain (top) and the PFE0055c J domain (bottom). **(B)** Focused view of C86 binding to the complex. **(C)** Detailed view of residues interacting with C86. The surface (set at 60% transparency) is colored according to amino acid hydrophobicity using the Kyte-Doolittle scale (with dodger blue representing more hydrophilic, to white, to orange red representing more hydrophobic residues). The cartoon representation underneath the surface depicts the secondary structure elements in the PfHsp70-x ATPase domain (purple) and PFE0055c J domain (green). The roman numerals (I to IV) mark the four helices of the PFE0055c J domain. C86 as well the interacting residues of the complex have been shown using the element color scheme (using red, blue and grey for oxygen, nitrogen and carbon, respectively). The carbons in C86 are depicted using dark grey while its interacting residues are colored in light grey. The residues are shown as sticks, and the numbering refers to their position in the full length protein. The predicted hydrogen bonds were identified using LigPlot + version 2.2.5 (<https://www.ebi.ac.uk/thornton-srv/software/LigPlus/>; Laskowski and Swindells, 2011), and have been rendered using FindHBond option in Chimera in relaxed mode and depicted using dotted lines (black). The lengths of the larger and the smaller hydrogen bonds are 2.74 Å and 2.32 Å, respectively. The PfHsp70-x ATPase domain-PFE0055c J domain complex was obtained using HADDOCK2.2 (Dutta et al., 2020a) while AutoDock Vina (<https://vina.scripps.edu/>; Trott and Olson, 2010) was used to dock C86 into this complex. Images for the 3D structures were rendered using UCSF Chimera 1.10.1 (<https://www.cgl.ucsf.edu/chimera/>), using one of the nine best binding conformations of C86.

exported PfJDP, PFE0055c, is essential (Zhang et al., 2018), the inhibition of its functional interaction with PfHsp70-x represents an important interface for anti-malarial drug development.

## Conclusion

There is solid evidence that certain exported type II PfJDs (PFA0660w and PFE0055c) functionally associate with PfHsp70-x (Daniyan et al., 2016; Dutta et al., 2021b), and are core components of J Dots potentially involved in the trafficking and folding of virulence factors (Külzer et al., 2010; Külzer et al., 2012; Petersen et al., 2016; Behl et al., 2019). However, there is also emerging evidence that these PfJDs play a role in knob formation (PFB0090c, Acharya et al., 2012), potentially in association with hHsp70 (PFA0660w, Diehl et al., 2021). Furthermore, a type IV

PfJDP (eCiJP) was recently reported to associate with both J Dots and the erythrocyte cytoskeleton, with the latter potentially involving interaction with hHsp70 (Sahu et al., 2022). Based on the presence of the PHIST domain and MEC motif, it would not be surprising if many of the exported type III and type IV PfJDs are found to associate at the cytoskeleton-membrane interface, and to be involved in recruitment of hHsp70 for remodeling purposes. Detailed mechanistic studies will no doubt shed light on this fascinating host-parasite interface, and elucidate the novel manner in which these exported PfJDs interact with their partner Hsp70s (PfHsp70-x or hHsp70) to trigger the assembly of erythrocyte cytoskeleton and knob-associated proteins. While there is a need to continue exploring the role of exported PfJDs in *P. falciparum*-infected erythrocytes, there is a pressing need to investigate their role in other stages of the parasite life cycle. For example, apart from studies on the type IV PfJDP, *P. falciparum*



gametocyte erythrocyte cytosolic protein (PfGECO/PFL2550w; Morahan et al., 2011; Figure 1), there have been limited studies on PfJDPs expressed in the gametocyte stage. Given the role of these exported PfJDPs in the pathogenesis of malaria, and the evidence indicating that their function can be inhibited, the elucidation of their protein networks across the entire parasite life cycle is needed to fully understand their biological role, and to reveal further novel anti-malarial drug targets.

## Author contributions

Conceptualization, GB; Figure 1, GB; bioinformatics analyses and Figure 2, SA; bioinformatics analyses and Figure 3, HS; writing—original draft preparation, GB; writing—review and editing, SA, TD, HS, and GB. All authors have read and agreed to the published version of the manuscript.

## Funding

GB acknowledges the financial support of Higher Colleges of Technology, UAE (Interdisciplinary Research Grant, IRG; grant number 213471), and Rhodes University, South Africa (Rated Researcher Grant, RRG; project number IFRR100006). HS acknowledges institutional funding from the Department of Science and Technology, Government of India, for the

development of computational resources (“Fund for Improvement of Science and Technology Infrastructure (FIST)” grant D. O. No. SR/FST/PG College/2009).

## Conflict of interest

The authors declare that the research was conducted in the absence of any commercial or financial relationships that could be construed as a potential conflict of interest.

## Publisher’s note

All claims expressed in this article are solely those of the authors and do not necessarily represent those of their affiliated organizations, or those of the publisher, the editors and the reviewers. Any product that may be evaluated in this article, or claim that may be made by its manufacturer, is not guaranteed or endorsed by the publisher.

## Supplementary material

The Supplementary Material for this article can be found online at: <https://www.frontiersin.org/articles/10.3389/fmolb.2022.978663/full#supplementary-material>

## References

- Acharya, P., Chaubey, S., Grover, M., and Tatu, U. (2012). An exported heat shock protein 40 associates with pathogenesis-related knobs in *Plasmodium falciparum* infected erythrocytes. *PLoS ONE* 7, e44605. doi:10.1371/journal.pone.0044605
- Alampalli, S. V., Grover, M., Chandran, S., Tatu, U., and Acharya, P. (2018). Proteome and structural organization of the knob complex on the surface of the *Plasmodium* infected red blood cell. *Proteomics. Clin. Appl.* 12, e1600177. doi:10.1002/prca.201600177
- Banumathy, G., Singh, V., and Tatu, U. (2002). Host chaperones are recruited in membrane-bound complexes by *Plasmodium falciparum*. *J. Biol. Chem.* 277, 3902–3912. doi:10.1074/jbc.M110513200
- Beck, J. R., Muralidharan, V., Oksman, A., and Goldberg, D. E. (2014). PTEX component HSP101 mediates export of diverse malaria effectors into host erythrocytes. *Nature* 511, 592–595. doi:10.1038/nature13574
- Behl, A., Kumar, V., Bisht, A., Panda, J. J., Hora, R., and Mishra, P. C. (2019). Cholesterol bound *Plasmodium falciparum* co-chaperone ‘PFA0660w’ complexes with major virulence factor ‘PfEMP1’ via chaperone ‘PfHsp70-x. *Sci. Rep.* 9, 2664–2667. doi:10.1038/s41598-019-39217-y
- Behl, A., and Mishra, P. C. (2019). Structural insights into the binding mechanism of *Plasmodium falciparum* exported Hsp40-Hsp70 chaperone pair. *Comput. Biol. Chem.* 83, 107099. doi:10.1016/j.compbiolchem.2019.107099
- Bennett, B. J., Mohandas, N., and Coppel, R. L. (1997). Defining the minimal domain of the *Plasmodium falciparum* protein MESA involved in the interaction with the red cell membrane skeletal protein 4.1. *J. Biol. Chem.* 272, 15299–15306. doi:10.1074/jbc.272.24.15299
- Black, C. G., Proellocks, N. I., Kats, L. M., Cooke, B. M., Mohandas, N., Coppel, R. L., et al. (2008). *In vivo* studies support the role of trafficking and cytoskeletal-binding motifs in the interaction of MESA with the membrane skeleton of *Plasmodium falciparum*-infected red blood cells. *Mol. Biochem. Parasitol.* 160, 143–147. doi:10.1016/j.molbiopara.2008.04.001
- Botha, M., Chiang, A. N., Needham, P. G., Stephens, L. L., Hoppe, H. C., Külzer, S., et al. (2011). *Plasmodium falciparum* encodes a single cytosolic type I Hsp40 that functionally interacts with Hsp70 and is upregulated by heat shock. *Cell Stress Chaperones* 16, 389–401. doi:10.1007/s12192-010-0250-6
- Botha, M., Pesce, E. R., and Blatch, G. L. (2007). The Hsp40 proteins of *Plasmodium falciparum* and other apicomplexa: Regulating chaperone power in the parasite and the host. *Int. J. Biochem. Cell Biol.* 39, 1781–1803. doi:10.1016/j.biocel.2007.02.011
- Bozdech, Z., Llinás, M., Pulliam, B. L., Wong, E. D., Zhu, J., and DeRisi, J. L. (2003). The transcriptome of the intraerythrocytic developmental cycle of *Plasmodium falciparum*. *PLoS Biol.* 1, E5. doi:10.1371/journal.pbio.0000005
- Cassel, J. A., Ilyin, S., McDonnell, M. E., and Reitz, A. B. (2012). Novel inhibitors of heat shock protein Hsp70-mediated luciferase refolding that bind to DnaJ. *Bioorg. Med. Chem.* 20, 3609–3614. doi:10.1016/j.bmc.2012.03.067
- Cockburn, I. L., Boshoff, A., Pesce, E. R., and Blatch, G. L. (2014). Selective modulation of plasmodial Hsp70s by small molecules with antimalarial activity. *Biol. Chem.* 395, 1353–1362. doi:10.1515/hsz-2014-0138
- Cockburn, I. L., Pesce, E. R., Pryzborski, J. M., Davies-Coleman, M. T., Clark, P. G., Keyzers, R. A., et al. (2011). Screening for small molecule modulators of Hsp70 chaperone activity using protein aggregation suppression assays: Inhibition of the plasmodial chaperone PfHsp70-1. *Biol. Chem.* 392, 431–438. doi:10.1515/BC.2011.040
- Cooke, B. M., Glenister, F. K., Mohandas, N., and Coppel, R. L. (2002). Assignment of functional roles to parasite proteins in malaria-infected red blood cells by competitive flow-based adhesion assay. *Br. J. Haematol.* 117, 203–211. doi:10.1046/j.1365-2141.2002.03404.x
- Coppel, R. L., Lustigman, S., Murray, L., and Anders, R. F. (1988). MESA is a *Plasmodium falciparum* phosphoprotein associated with the erythrocyte membrane skeleton. *Mol. Biochem. Parasitol.* 31, 223–231. doi:10.1016/0166-6851(88)90152-1

- Coppel, R. L. (1992). Repeat structures in a *Plasmodium falciparum* protein (MESA) that binds human erythrocyte protein 4.1. *Mol. Biochem. Parasitol.* 50, 335–347. doi:10.1016/0166-6851(92)90231-8
- Daniyan, M. O., and Blatch, G. L. (2017). Plasmodial Hsp40s: New avenues for antimalarial drug discovery. *Curr. Pharm. Des.* 23, 4555–4570. doi:10.2174/1381612823666170124142439
- Daniyan, M. O., Boshoff, A., Prinsloo, E., Pesce, E. R., and Blatch, G. L. (2016). The malarial exported PFA0660w is an Hsp40 co-chaperone of PfHsp70-x. *PLoS ONE* 11, e0148517. doi:10.1371/journal.pone.0148517
- Day, J., Passecker, A., Beck, H. P., and Vakonakis, I. (2019). The *Plasmodium falciparum* Hsp70-x chaperone assists the heat stress response of the malaria parasite. *FASEB J.* 33, 14611–14624. doi:10.1096/fj.201901741R
- de Koning-Ward, T. F., Gilson, P. R., Boddey, J. A., Rug, M., Smith, B. J., Papenfuss, A. T., et al. (2009). A newly discovered protein export machine in malaria parasites. *Nature* 459, 945–949. doi:10.1038/nature08104
- Diehl, M., Roling, L., Rohland, L., Weber, S., Cyrklaff, M., Sanchez, C. P., et al. (2021). Co-chaperone involvement in knob biogenesis implicates host-derived chaperones in malaria virulence. *PLoS Pathog.* 17, e1009969. doi:10.1371/journal.ppat.1009969
- Diez-Silva, M., Park, Y., Huang, S., Bow, H., Mercereau-Puijalon, O., Deplaine, G., et al. (2012). Pf155/RESA protein influences the dynamic microcirculatory behavior of ring-stage *Plasmodium falciparum* infected red blood cells. *Sci. Rep.* 2, 614. doi:10.1038/srep00614
- Dutta, T., Pesce, E. R., Maier, A. G., and Blatch, G. L. (2021a). Role of the J domain protein family in the survival and pathogenesis of *Plasmodium falciparum*. *Adv. Exp. Med. Biol.* 1340, 97–123. doi:10.1007/978-3-030-78397-6\_4
- Dutta, T., Singh, H., Gestwicki, J. E., and Blatch, G. L. (2021b). Exported plasmodial J domain protein, PFE0055c, and PfHsp70-x form a specific co-chaperone-chaperone partnership. *Cell Stress Chaperones* 26, 355–366. doi:10.1007/s12192-020-01181-2
- Elsworth, B., Matthews, K., Nie, C. Q., Kalanon, M., Charnaud, S. C., Sanders, P. R., et al. (2014). PTEX is an essential nexus for protein export in malaria parasites. *Nature* 511, 587–591. doi:10.1038/nature13555
- Elsworth, B., Sanders, P. R., Nebel, T., Batiniovic, S., Kalanon, M., Nie, C. Q., et al. (2016). Proteomic analysis reveals novel proteins associated with the *Plasmodium* protein exporter PTEX and a loss of complex stability upon truncation of the core PTEX component. *PTEX150. Cell. Microbiol.* 18, 1551–1569. doi:10.1111/cmi.12596
- Grover, M., Chaubey, S., Ranade, S., and Tatu, U. (2013). Identification of an exported heat shock protein 70 in *Plasmodium falciparum*. *Parasite* 20, 2. doi:10.1051/parasite/2012002
- Hennessy, F., Cheetham, M. E., Dirr, H. W., and Blatch, G. L. (2000). Analysis of the levels of conservation of the J domain among the various types of DnaJ-like proteins. *Cell Stress Chaperones* 5 (4), 347–358.
- Hennessy, F., Nicoll, W. S., Zimmermann, R., Cheetham, M. E., and Blatch, G. L. (2005). Not all J domains are created equal: Implications for the specificity of hsp40-hsp70 interactions. *Protein Sci.* 14, 1697–1709. doi:10.1110/ps.051406805
- Hiller, N. L., Bhattacharjee, S., van Ooij, C., Liolios, K., Harrison, T., Lopez-Estraño, C., et al. (2004). A host-targeting signal in virulence proteins reveals a secretome in malarial infection. *Science* 306, 1934–1937. doi:10.1126/science.1102737
- Jha, P., Laskar, S., Dubey, S., Bhattacharyya, M. K., and Bhattacharyya, S. (2017). *Plasmodium* Hsp40 and human Hsp70: A potential cochaperone-chaperone complex. *Mol. Biochem. Parasitol.* 214, 10–13. doi:10.1016/j.molbiopara.2017.03.003
- Jonsdottir, T. K., Gabriela, M., and Gilson, P. R. (2021). The role of malaria parasite heat shock proteins in protein trafficking and remodelling of red blood cells. *Adv. Exp. Med. Biol.* 1340, 141–167. doi:10.1007/978-3-030-78397-6\_6
- Kampinga, H. H., Andreasson, C., Barducci, A., Cheetham, M. E., Cyr, D., Emanuelsson, C., et al. (2019). Function, evolution, and structure of J-domain proteins. *Cell Stress Chaperones* 24, 7–15. doi:10.1007/s12192-018-0948-4
- Kilili, G. K., and LaCount, D. J. (2011). An erythrocyte cytoskeleton-binding motif in exported *Plasmodium falciparum* proteins. *Eukaryot. Cell* 10, 1439–1447. doi:10.1128/EC.05180-11
- Külzer, S., Charnaud, S., Dagan, T., Riedel, J., Mandal, P., Pesce, E. R., et al. (2012). *Plasmodium falciparum*-encoded exported hsp70/hsp40 chaperone/co-chaperone complexes within the host erythrocyte. *Cell. Microbiol.* 14, 1784–1795. doi:10.1111/j.1462-5822.2012.01840.x
- Külzer, S., Rug, M., Brinkmann, K., Cannon, P., Cowman, A., Lingelbach, K., et al. (2010). Parasite-encoded Hsp40 proteins define novel mobile structures in the cytosol of the *P. falciparum*-infected erythrocyte. *Cell. Microbiol.* 12, 1398–1420. doi:10.1111/j.1462-5822.2010.01477.x
- Kumar, V., Behl, A., Sharma, R., Sharma, A., and Hora, R. (2019). *Plasmodium* helical interspersed subtelomeric family—an enigmatic piece of the *Plasmodium* biology puzzle. *Parasitol. Res.* 118, 2753–2766. doi:10.1007/s00436-019-06420-9
- Laskowski, R. A., and Swindells, M. B. (2011). LigPlot+: Multiple ligand-protein interaction diagrams for drug discovery. *J. Chem. Inf. Model.* 51, 2778–2786. doi:10.1021/ci200227u
- Maier, A. G., Rug, M., O'Neill, M. T., Brown, M., Chakravorty, S., Szestak, T., et al. (2008). Exported proteins required for virulence and rigidity of *Plasmodium falciparum*-infected human erythrocytes. *Cell* 134, 48–61. doi:10.1016/j.cell.2008.04.051
- Marti, M., Good, R. T., Rug, M., Knuepfer, E., and Cowman, A. F. (2004). Targeting malaria virulence and remodeling proteins to the host erythrocyte. *Science* 306, 1930–1933. doi:10.1126/science.1102452
- Mills, J. P., Diez-Silva, M., Quinn, D. J., Dao, M., Lang, M. J., Tan, K. S., et al. (2007). Effect of plasmodial RESA protein on deformability of human red blood cells harboring *Plasmodium falciparum*. *Proc. Natl. Acad. Sci. U. S. A.* 104, 9213–9217. doi:10.1073/pnas.0703433104
- Morahan, B. J., Strobel, C., Hasan, U., Czesny, B., Mantel, P. Y., Marti, M., et al. (2011). Functional analysis of the exported type IV HSP40 protein PfGECO in *Plasmodium falciparum* gametocytes. *Eukaryot. Cell* 10, 1492–1503. doi:10.1128/EC.05155-11
- Moses, M. A., Kim, Y. S., Rivera-Marquez, G. M., Oshima, N., Watson, M. J., Beebe, K. E., et al. (2018). Targeting the Hsp40/Hsp70 chaperone axis as a novel strategy to treat castration-resistant prostate cancer. *Cancer Res.* 78, 4022–4035. doi:10.1158/0008-5472.CAN-17-3728
- Njunge, J. M., Ludwig, M. H., Boshoff, A., Pesce, E. R., and Blatch, G. L. (2013). Hsp70s and J proteins of *Plasmodium* parasites infecting rodents and primates: Structure, function, clinical relevance, and drug targets. *Curr. Pharm. Des.* 19, 387–403. doi:10.2174/138161213804143734
- Oakley, M. S., Gerald, N., McCutchan, T. F., Aravind, L., and Kumar, S. (2011). Clinical and molecular aspects of malaria fever. *Trends Parasitol.* 27, 442–449. doi:10.1016/j.pt.2011.06.004
- Oakley, M. S., Kumar, S., Anantharaman, V., Zheng, H., Mahajan, B., Haynes, J. D., et al. (2007). Molecular factors and biochemical pathways induced by febrile temperature in intraerythrocytic *Plasmodium falciparum* parasites. *Infect. Immun.* 75, 2012–2025. doi:10.1128/IAI.01236-06
- Pasini, E. M., Kirkegaard, M., Mortensen, P., Lutz, H. U., Thomas, A. W., and Mann, M. (2006). In-depth analysis of the membrane and cytosolic proteome of red blood cells. *Blood* 108, 791–801. doi:10.1182/blood-2005-11-007799
- Pei, X., Guo, X., Coppel, R., Bhattacharjee, S., Haldar, K., Gratzner, W., et al. (2007). The ring-infected erythrocyte surface antigen (RESA) of *Plasmodium falciparum* stabilizes spectrin tetramers and suppresses further invasion. *Blood* 110, 1036–1042. doi:10.1182/blood-2007-02-076919
- Pesce, E.-R., Blatch, G. L., and Edkins, A. L. (2016). Hsp40 co-chaperones as drug targets: Towards the development of specific inhibitors. *Top. Med. Chem.* 19, 163–196. doi:10.1007/7355\_2015\_92
- Pesce, E. R., and Blatch, G. L. (2014). Plasmodial Hsp40 and Hsp70 chaperones: Current and future perspectives. *Parasitology* 141, 1167–1176. doi:10.1017/S003118201300228X
- Petersen, C., Nelson, R., Magowan, C., Wollish, W., Jensen, J., and Leech, J. (1989). The mature erythrocyte surface antigen of *Plasmodium falciparum* is not required for knobs or cytoadherence. *Mol. Biochem. Parasitol.* 36, 61–65. doi:10.1016/0166-6851(89)90200-4
- Petersen, W., Külzer, S., Engels, S., Zhang, Q., Ingmundson, A., Rug, M., et al. (2016). J-dot targeting of an exported HSP40 in *Plasmodium falciparum*-infected erythrocytes. *Int. J. Parasitol.* 46, 519–525. doi:10.1016/j.ijpara.2016.03.005
- Przyborski, J. M., Diehl, M., and Blatch, G. L. (2015). Plasmodial HSP70s are functionally adapted to the malaria parasite life cycle. *Front. Mol. Biosci.* 2, 34. doi:10.3389/fmolb.2015.00034
- Qin, H. L., Zhang, Z. W., Lekkala, R., Alsulami, H., and Rakesh, K. P. (2020). Chalcone hybrids as privileged scaffolds in antimalarial drug discovery: A key review. *Eur. J. Med. Chem.* 193, 112215. doi:10.1016/j.ejmech.2020.112215
- Rhiel, M., Bittl, V., Tribensky, A., Charnaud, S. C., Strecker, M., Müller, S., et al. (2016). Trafficking of the exported *P. falciparum* chaperone PfHsp70x. *Sci. Rep.* 6, 36174. doi:10.1038/srep36174
- Sahu, W., Bai, T., Panda, P. K., Mazumder, A., Das, A., Ojha, D. K., et al. (2022). *Plasmodium falciparum* HSP40 protein eCijp traffics to the erythrocyte cytoskeleton and interacts with the human HSP70 chaperone HSPA1. *FEBS Lett.* 596, 95–111. doi:10.1002/1873-3468.14255
- Sargeant, T. J., Marti, M., Caler, E., Carlton, J. M., Simpson, K., Speed, T. P., et al. (2006). Lineage-specific expansion of proteins exported to erythrocytes in malaria parasites. *Genome Biol.* 7, R12. doi:10.1186/gb-2006-7-2-r12

- Schmidt, J., and Vakonakis, I. (2020). Structure of the substrate-binding domain of *Plasmodium falciparum* heat-shock protein 70-x. *Acta Crystallogr. F. Struct. Biol. Commun.* 76, 495–500. doi:10.1107/S2053230X2001208X
- Shonhai, A., and Blatch, G. L. (2021). Heat shock proteins of malaria: Highlights and future prospects. *Adv. Exp. Med. Biol.* 1340, 237–246. doi:10.1007/978-3-030-78397-6\_10
- Shonhai, A., Boshoff, A., and Blatch, G. L. (2007). The structural and functional diversity of Hsp70 proteins from *Plasmodium falciparum*. *Protein Sci.* 16, 1803–1818. doi:10.1110/ps.072918107
- Sievers, F., and Higgins, D. G. (2018). Clustal Omega for making accurate alignments of many protein sequences. *Protein Sci.* 27, 135–145. doi:10.1002/pro.3290
- Silva, M. D., Cooke, B. M., Guilloffe, M., Buckingham, D. W., Sauzet, J. P., Le Scanf, C., et al. (2005). A role for the *Plasmodium falciparum* RESA protein in resistance against heat shock demonstrated using gene disruption. *Mol. Microbiol.* 56, 990–1003. doi:10.1111/j.1365-2958.2005.04603.x
- Sinha, S., Batovska, D. I., Medhi, B., Radotra, B. D., Bhalla, A., Markova, N., et al. (2019). *In vitro* anti-malarial efficacy of chalcones: Cytotoxicity profile, mechanism of action and their effect on erythrocytes. *Malar. J.* 18, 421. doi:10.1186/s12936-019-3060-z
- Stothard, P. (2000). The sequence manipulation suite: JavaScript programs for analyzing and formatting protein and DNA sequences. *BioTechniques* 28, 1102–1104. doi:10.2144/00286ir01
- Trott, O., and Olson, A. J. (2010). AutoDock vina: Improving the speed and accuracy of docking with a new scoring function, efficient optimization and multithreading. *J. Comput. Chem.* 31, 455–461. doi:10.1002/jcc.21334
- van Gestel, R. A., van Solinge, W. W., van der Toorn, H. W., Rijksen, G., Hec, k. A. J., van Wijk, R., et al. (2010). Quantitative erythrocyte membrane proteome analysis with Blue-native/SDS PAGE. *J. Proteomics* 2010 73, 456–465. doi:10.1016/j.jprot.2009.08.010
- Waller, K. L., Nunomura, W., An, X., Cooke, B. M., Mohandas, N., and Coppel, R. L. (2003). Mature parasite-infected erythrocyte surface antigen (MESA) of *Plasmodium falciparum* binds to the 30-kDa domain of protein 4.1 in malaria-infected red blood cells. *Blood* 102, 1911–1914. doi:10.1182/blood-2002-11-3513
- Waterhouse, A., Bertoni, M., Bienert, S., Studer, G., Tauriello, G., Gumienny, R., et al. (2018). SWISS-MODEL: Homology modelling of protein structures and complexes. *Nucleic Acids Res.* 46, W296–W303. doi:10.1093/nar/gky427
- Zhang, M., Wang, C., Otto, T. D., Oberstaller, J., Liao, X., Adapa, S. R., et al. (2018). Uncovering the essential genes of the human malaria parasite *Plasmodium falciparum* by saturation mutagenesis. *Science* 360, eaap7847. doi:10.1126/science.aap7847



## OPEN ACCESS

EDITED BY  
Elias Georges,  
McGill University, Canada

REVIEWED BY  
Jyoti Chhibber-Goel,  
International Centre for Genetic  
Engineering and Biotechnology, India  
Rongguo Ren,  
University of Nebraska Medical Center,  
United States

\*CORRESPONDENCE  
Addmore Shonhai,  
addmore.shonhai@univen.ac.za

SPECIALTY SECTION  
This article was submitted to Molecular  
Diagnostics and Therapeutics,  
a section of the journal  
Frontiers in Molecular Biosciences

RECEIVED 18 May 2022  
ACCEPTED 29 August 2022  
PUBLISHED 13 September 2022

CITATION  
Muthelo T, Mulaudzi V, Netshishivhe M,  
Dongola TH, Kok M, Makumire S,  
de Villiers M, Burger A, Zininga T and  
Shonhai A (2022), Inhibition of  
*Plasmodium falciparum* Hsp70-Hop  
partnership by 2-  
phenylthynesulfonamide.  
*Front. Mol. Biosci.* 9:947203.  
doi: 10.3389/fmolb.2022.947203

COPYRIGHT  
© 2022 Muthelo, Mulaudzi,  
Netshishivhe, Dongola, Kok, Makumire,  
de Villiers, Burger, Zininga and Shonhai.  
This is an open-access article  
distributed under the terms of the  
Creative Commons Attribution License  
(CC BY). The use, distribution or  
reproduction in other forums is  
permitted, provided the original  
author(s) and the copyright owner(s) are  
credited and that the original  
publication in this journal is cited, in  
accordance with accepted academic  
practice. No use, distribution or  
reproduction is permitted which does  
not comply with these terms.

# Inhibition of *Plasmodium falciparum* Hsp70-Hop partnership by 2-phenylthynesulfonamide

Tshifhiwa Muthelo<sup>1</sup>, Vhahangwele Mulaudzi<sup>1</sup>,  
Munei Netshishivhe<sup>1</sup>, Tendamudzimu Harmfree Dongola<sup>1</sup>,  
Michelle Kok<sup>2</sup>, Stanley Makumire<sup>1,3</sup>, Marianne de Villiers<sup>2</sup>,  
Adèle Burger<sup>1</sup>, Tawanda Zininga<sup>1,2</sup> and Addmore Shonhai<sup>1\*</sup>

<sup>1</sup>Department of Biochemistry & Microbiology, University of Venda, Thohoyandou, South Africa,  
<sup>2</sup>Department of Biochemistry, Stellenbosch University, Matieland, South Africa, <sup>3</sup>Structural Biology  
Research Unit, Department of Integrative Biomedical Sciences, University of Cape Town, Cape Town,  
South Africa

*Plasmodium falciparum* Hsp70-1 (PfHsp70-1; PF3D7\_0818900) and PfHsp90 (PF3D7\_0708400) are essential cytosol localized chaperones of the malaria parasite. The two chaperones form a functional complex via the adaptor protein, Hsp90-Hsp70 organizing protein (PfHop [PF3D7\_1434300]), which modulates the interaction of PfHsp70-1 and PfHsp90 through its tetracoordinate repeat (TPR) domains in a nucleotide-dependent fashion. On the other hand, PfHsp70-1 and PfHsp90 possess C-terminal EEVD and MEEVD motifs, respectively, which are crucial for their interaction with PfHop. By coordinating the cooperation of these two chaperones, PfHop plays an important role in the survival of the malaria parasite. 2-Phenylthynesulfonamide (PES) is a known anti-cancer agent whose mode of action is to inhibit Hsp70 function. In the current study, we explored the antiparasitic activity of PES and investigated its capability to target the functions of PfHsp70-1 and its co-chaperone, PfHop. PES exhibited modest antiparasitic activity (IC<sub>50</sub> of 38.7 ± 0.7 μM). Furthermore, using surface plasmon resonance (SPR) analysis, we demonstrated that PES was capable of binding recombinant forms of both PfHsp70-1 and PfHop. Using limited proteolysis and intrinsic fluorescence-based analysis, we showed that PES induces conformational changes in PfHsp70-1 and PfHop. In addition, we demonstrated that PES inhibits the chaperone function of PfHsp70-1. Consequently, PES abrogated the association of the two proteins *in vitro*. Our study findings contribute to the growing efforts to expand the arsenal of potential antimalarial compounds in the wake of growing parasite resistance against currently used drugs.

## KEYWORDS

*Plasmodium falciparum*, molecular chaperone, PfHsp70-1, PfHop, inhibitor, PES, pifithrin μ



# 1 Introduction

It is estimated that malaria accounted for 627,000 deaths in 2020 (World Health Organisation, 2021). The latest data show that malaria deaths increased by over 200,000 deaths possibly on account of a lack of commitment to managing the disease in the wake of the COVID-19 pandemic. In addition, there are increasing reports of resistance against currently used antimalarial drugs. There is therefore urgent need to expand the arsenal of antimalarial compounds. The malaria parasite traverses between a cold-blooded mosquito vector and the

warm-blooded human host and thus undergoes multiple physiological changes during its complex life cycle. As part of its survival strategy, the parasite relies on its heat shock protein (Hsp) machinery to adapt to constant physiological changes and stress associated with its development (Pallavi et al., 2010; Shonhai, 2010). In addition, Hsps are implicated in antimalarial drug resistance (Witkowski et al., 2010).

Hsp70 is regarded as the most abundant molecular chaperone found in all major organelles (Saibil, 2013). Hsp70 is structurally divided into two major domains; a 45 kDa N-terminal nucleotide binding domain (NBD) that

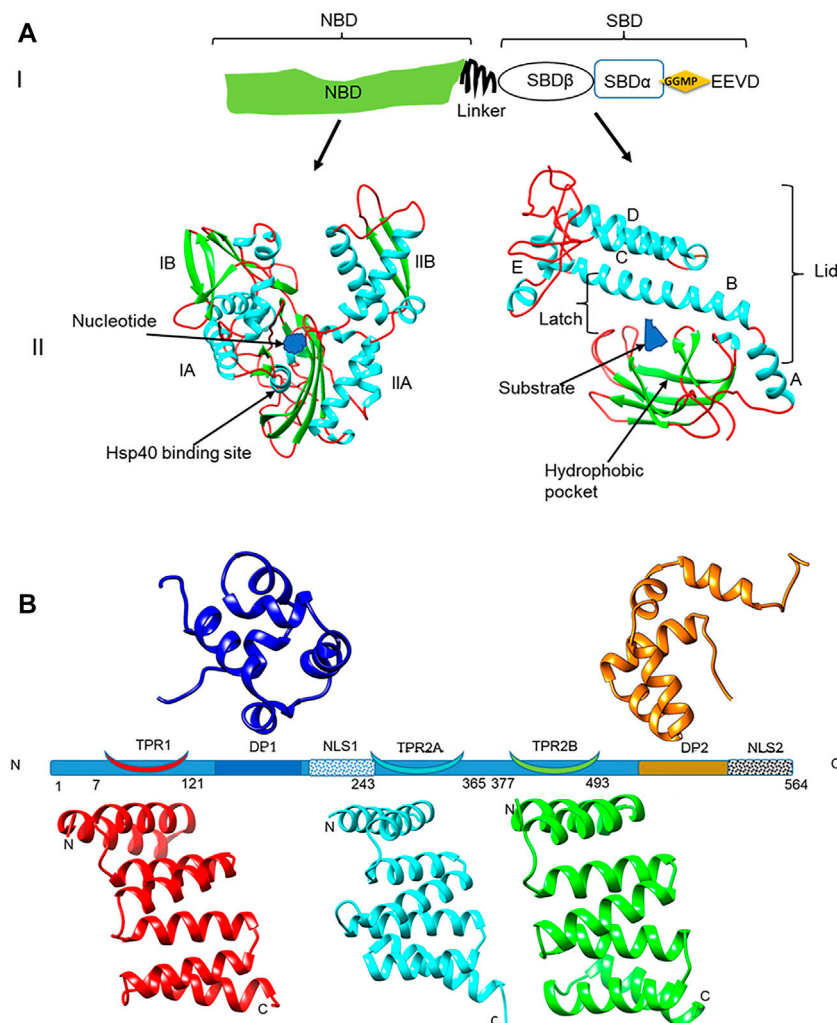


**FIGURE 1**

Domain representation of PfHsp70-1 and PfHop (A) (panel I): representation of the linear structural organization of PfHsp70-1 showing the NBD, a highly charged linker, and the-SBD. The C-terminal EEVD motif is illustrated. Panel II: Three-dimensional model of PfHsp70-1 domains. The N-terminal NBD which is subdivided into lobes IA, IB, IIA, and IIB, respectively, is shown. Also illustrated are the bound nucleotide (blue) and the Hsp40 co-chaperone binding site, respectively. The C-terminal SBD of the protein is shown on the right hand side. The hydrophobic pocket located in the SBD and a bound peptide substrate are also shown. The alpha-helical lid which is made up of helices A, B, C, D, and E is also depicted as adapted from Shonhai (2007). (B) Depiction of the structural organization of PfHop showing the relative positions of the three tetracopeptide repeat (TPR) regions, the two dipeptide domains (DP), and the two nuclear localization signals (NLS) of the protein. Ribbon representations of the three-dimensional models of TPR1, TPR2A, TPR2B, DP1, and DP2 domains are also shown. The models were generated using PHYRE<sup>2</sup> (<http://www.sbg.bio.ic.ac.uk/phyre2>; Kelley et al., 2015) and rendered using CHIMERA version 1.15rc (Pettersen et al., 2004).

exhibits ATPase activity and a 25 kDa substrate binding domain (SBD) that binds the target client protein (Mashaghi et al., 2016) (Figure 1A). *P. falciparum* Hsp70-1 (PfHsp70-1; PF3D7\_0818900) is an essential molecular chaperone that is resident within the parasite cytosol (Kappes et al., 1993; Shonhai, 2021). PfHsp90 (PF3D7\_0708400) co-localizes with PfHsp70-1 and the two proteins form a chaperone complex (Gitau et al., 2012) that is thought to coordinate the folding of select proteins that are important for the development of the parasite. In addition, the interaction of PfHsp70-1 and PfHsp90 is modulated by PfHop (PF3D7\_1434300; Gitau et al., 2012; Zininga et al., 2015) (Figure 1B), which serves as a module that facilitates substrate exchange between the two chaperones.

Both PfHsp70-1 and PfHsp90 are essential proteins (Banumathy et al., 2003; Lu et al., 2020), suggesting a possible essential role for PfHop. Due to their critical role in the development of the parasite, both PfHsp70-1 and PfHsp90 are deemed prospective antimalarial drug targets (reviewed in Zininga and Shonhai, 2019; Daniyan, 2021). However, targeting *P. falciparum* Hsps is a challenge, as these proteins are generally conserved (Pesce et al., 2010; Chakafana et al., 2019). Despite this, there is growing evidence that Hsp70s of parasitic origin, and in particular PfHsp70-1, exhibit distinct structure-function features that could make them amenable to selective targeting (Chakafana et al., 2019; Anas et al., 2020; Lebepe et al., 2020; Makumire et al., 2021). Promisingly, some antimalarial compounds demonstrating selective inhibition of parasite Hsp70 with minimum effects on the function of human Hsp70 have been described (Cockburn et al., 2014; reviewed in Zininga and Shonhai, 2019). One of the attractive features of targeting PfHsp70-1 is that its inhibition abrogates both its independent chaperone function as well as its association with co-chaperones (Zininga et al., 2017a, b). This, and growing evidence pointing to the role of Hsps in antimalarial drug resistance (Akide-Ndunge et al., 2009; Corey et al., 2016), justifies efforts to target them in antimalarial drug development efforts as they hold promise especially as co-targets in combination therapies.

2-Phenylthynylsulfonamide (PES), also known as pifithrin  $\mu$ , is a member of the benzene family. PES is an anticancer agent that is known to target human Hsp70 (Leu et al., 2009; Jiang and Xiao, 2020). However, the mechanism of action of PES on the Hsp70 function is not fully understood. It has been suggested that it binds to the NBD of Hsp70 (Zhou et al., 2017), and this contradicts earlier findings proposing that it binds to the C-terminal SBD (Leu et al., 2009). The antimalarial activity of PES and its effect on the function of PfHsp70-1 remains to be established. In the current study, we investigated the effect of PES on asexual blood-stage *P. falciparum* parasites and we established that it exhibits modest antiplasmodial activity. Furthermore, we observed that PES binds directly to both PfHsp70-1 and PfHop, inducing conformational changes in both proteins. Consequently, PES abrogated the chaperone activity of PfHsp70-1, and further inhibited its association with the co-chaperone, PfHop. We discuss the implications of our findings

with respect to both antimalarial drug discovery efforts and the possible mechanism of action of PES.

## 2 Experimental procedures

### 2.1 Materials

Unless otherwise stated, the materials used in this study were purchased from Sigma-Aldrich (Darmstadt, Germany), Merck Millipore (Darmstadt, Germany), and Melfords (Ipswich, United Kingdom). The following antibodies were used in the study:  $\alpha$ -PfHsp70-1 (Shonhai et al., 2008),  $\alpha$ -PfHop (Gitau et al., 2012), and  $\alpha$ -His (ThermoFisher, MA, United States).

### 2.2 *In silico* docking of PES onto PfHsp70-1 and PfHop

To predict the possible binding, as well as identify possible binding sites of PES on PfHop and PfHsp70-1, AutoDock Vina (Trott and Olson, 2010, <http://vina.scripps.edu>) was used. The structures used for the docking were obtained from homology modeling using AlphaFold's ColabFold (Mirdita et al., 2021). As templates, the crystal structures of the NBD (6S02 and 6RZQ, Day et al., 2019; 7P31, 7OOH, 7OOG, 7OOE, 7NQZ, 7NQU, 7NQS and 7NQR, Mohamad et al., 2021a–g) and SBD (6ZHI, Schmidt and Vakonakis, 2020) of PfHsp70-x bound to various ligands were used to predict the structure of PfHsp70-1. These were specified as custom templates. The structure of PfHop was predicted without any custom templates specified. Both the protein and ligand were prepared for docking using AutoDockTools4 (Morris et al., 2009). Default parameters were used with minor modifications. The active site was placed in a grid box with x, y, and z grid points set at 100 while the grid point spacing was 0.375 Å. The energy range was set at 4 and the exhaustiveness set at 100. Docking was initiated using command prompt. Upon completion of the docking, an output file with 9 binding modes was generated together with a log file scoring the modes in terms of binding affinity (in kcal/mol). The output files (in pdbqt format) were viewed in Pymol™ 2.4.1 (The PyMOL Molecular Graphics System, Schrodinger, LLC, NY, United States) and converted to PDB files. The receptor-ligand interactions were then performed in Discovery Studio Visualizer Version 20.1.0.19295; (BIOVIA, Sandiego, CA, United States) and images were generated using LigPlot+, version 2.2.4 (Wallace et al., 1995).

### 2.3 Expression and purification of recombinant proteins

Production and purification of recombinant forms of both PfHsp70-1 and PfHop protein was conducted as previously described (Makumire et al., 2020, 2021). Briefly, the plasmid

constructs for pQE30-PfHsp70-1 and pQE30-PfHop were transformed into *E. coli* XL1 Blue cells. An additional construct, pQE30-PfHsp70-1<sub>NBD</sub> encoding for the NBD of PfHsp70-1 was similarly used to express the truncated version of this chaperone (Zininga et al., 2016). The production of recombinant protein was induced by isopropylthiogalactoside (IPTG) and the protein was purified using sepharose nickel affinity chromatography (Makumire et al., 2020, 2021). The expression and purification of recombinant proteins were analyzed by SDS-PAGE and confirmed by Western blot analysis using  $\alpha$ -PfHsp70-1 (Shonhai et al., 2008),  $\alpha$ -PfHop (Gitau et al., 2012), and  $\alpha$ -His antibodies, respectively.

## 2.4 Investigation of the effect of PES on the conformation of PfHsp70-1 and PfHop using limited proteolysis

Limited proteolysis has previously been used to validate the nucleotide-dependent conformational alterations of PfHsp70-1 (Zininga et al., 2016). In the current study, we employed the same approach to explore the effects of PES on the fragmentation of the recombinant forms of PfHsp70-1 and PfHop. Fragmentation of PfHsp70-1 or PfHop in the presence of nucleotides served as controls. Briefly, recombinant PfHsp70-1 (4  $\mu$ M) or PfHop (4  $\mu$ M) was digested with 0.25 ng/ml of proteinase K at 37°C in the absence and presence of 25  $\mu$ M ADP/ATP or 20  $\mu$ M PES for 30 min. Proteolytic digestion of either PfHsp70-1 or PfHop was analyzed using SDS-PAGE analysis followed by silver staining using GE Healthcare PlusOne™ Silver Staining Kit (WI, United States).

## 2.5 Intrinsic fluorescence-based analysis of the effect of PES on the tertiary structures of PfHsp70-1 and PfHop

The effect of PES on the tertiary structural conformation of recombinant PfHsp70-1 and PfHop proteins relative to the nucleotide-dependent conformations were assessed by monitoring intrinsic fluorescence as previously described (Zininga et al., 2016; Lebepe et al., 2020). Briefly, recombinant PfHsp70-1 (4  $\mu$ M) or PfHop (4  $\mu$ M) was incubated in the absence or presence of 25  $\mu$ M ATP/ADP. The assay was repeated in the presence of 20  $\mu$ M PES. Fluorescence emission spectra were monitored at 300–400 nm after initial excitation at 295 nm. The spectra data collected from seven spectral scans were averaged and processed taking into account the baseline (effect of buffer in the absence of protein).

## 2.6 Analysis of the effect of PES on the chaperone activity of PfHsp70-1

The capability of PfHsp70-1 to prevent thermal aggregation of malate dehydrogenase (MDH) from porcine heart was previously

demonstrated (Shonhai et al., 2008). In the current study, we investigated the effect of PES on the holdase chaperone activity of PfHsp70-1. The assay was initiated by adding 1.25  $\mu$ M MDH and 0.75  $\mu$ M PfHsp70-1 to the assay buffer (50 mM Tris-HCl, 100 mM NaCl; pH 7.4) and heated to 51°C. Aggregation of MDH was monitored as a function of light scattering at 360 nm over 30 min at 51°C in a SpectraMax M3 (Molecular Devices, United States) microplate spectrometer. The assay was repeated at varying final concentrations (5, 15, 25, 50, 100 nM) of PES. The chaperone function of PfHsp70-1 under various experimental conditions was compared to the activity of the chaperone recorded in the absence of nucleotide. Statistical analysis was conducted using a student t-test and a  $p < 0.05$  represented functionally significant variation.

## 2.7 Determination of equilibrium binding kinetics of PES to either PfHop or PfHsp70-1

The steady-state equilibrium binding kinetics for the inhibitors on either PfHsp70-1 or PfHop were investigated using BioNavis Navi 420A ILVES multi-parametric surface plasmon resonance (MP-SPR) system (BioNavis, Finland) following a previously described method (Lebepe et al., 2020; Chakafana et al., 2021). Briefly, filter-sterilized degassed PBS (4.3 mM Na<sub>2</sub>HPO<sub>4</sub>, 1.4 mM KH<sub>2</sub>PO<sub>4</sub>, 137 mM NaCl, 3 mM KCl, 0.005% (v/v) Tween 20, and 20 mM EDTA; pH 7.4) was used as running buffer for the assay. The ligand (0.1  $\mu$ g/ml of PfHsp70-1/PfHop) was immobilized onto a carboxymethyl dextran (CMD 3-D) gold sensor chip through amine coupling. PES was injected (flow rate of 50  $\mu$ l/min) as analyte at varying final concentrations (0, 1.25, 2.5, 5, 10, 20 nM). Similarly, as controls nucleotides (5  $\mu$ M ATP/ADP) and a known *P. falciparum* Hsp70 inhibitor, (–)-Epigallocatechin-3-gallate (EGCG; Zininga et al., 2017b) were similarly injected at varying final concentrations (0, 1.25, 2.5, 5, 10, 20 nM) over the chip surface. Steady-state equilibrium was achieved after allowing the interaction to occur for 8 min at 25°C, followed by dissociation for 4 min at 25°C, respectively. The data generated were analyzed using Data Viewer (BioNavis, Finland) after subtraction of baseline (signals generated on the chip surface without protein immobilized and buffer without inhibitor). The resultant sensorgrams were analyzed to determine the equilibrium binding affinities using Trace Drawer software version 1.8 (Ridgeview Instruments; Sweden). A student t-test  $p < 0.05$  represented statistically significant differences in affinity recorded relative to the activity of the protein reported in the absence of nucleotide.

## 2.8 Analysis of the effect of PES on the association of PfHop and PfHsp70-1

### 2.8.1 Surface plasmon resonance assay

To determine the effect of inhibitors on the direct interaction of PfHsp70-1 with PfHop (Gitau et al., 2012; Zininga et al., 2015)

we conducted SPR analysis using the BioNavis Navi 420A ILVES MP-SPR system (BioNavis, Finland). PfHsp70-1 was immobilized as ligand and varying concentrations (0, 125, 250, 500, 1,000, and 2000 nM) of PfHop as analyte were injected on the chip surface at a flow rate of 20  $\mu$ l/min. To monitor the effects of the inhibitor, the analyte was suspended in PBS supplemented with 25  $\mu$ M PES and injected similarly. We previously established that EGCG abrogates PfHop-PfHsp70-1 interaction (Zininga et al., 2017b). As such, as control, the assay was repeated in the presence of 25  $\mu$ M of EGCG in place of the PES. Association was allowed to occur for 5 min, followed by dissociation for 10 min at 25°C. Data analysis was conducted taking baseline correction into account through double referencing [subtracting the signals recorded using both buffer blank (PBS supplemented with 25  $\mu$ M of inhibitor without the analyte protein) and the chip blank (channel with BSA as ligand protein immobilized)]. The generated sensorgrams were then analyzed as described in Section 2.7 above. The affinity values obtained under the various experimental conditions were compared to that observed for the assay conducted in the absence of nucleotide.

### 2.8.2 Enzyme-linked immunosorbent assay

An enzyme-linked immunosorbent assay (ELISA) was used to validate the effect of PES on the direct association of PfHsp70-1 and PfHop following a previously described protocol (Mabate et al., 2018). Briefly, ligand (5  $\mu$ g/ml of PfHsp70-1) suspended in 5 mM sodium bicarbonate ( $\text{NaHCO}_3$ ) at pH 9.5 was noncovalently immobilized onto a 96 well plate overnight at 4°C. BSA (5  $\mu$ g/ml) was used as a ligand for the negative control. The wells were washed with 150  $\mu$ l TBST which contains (Tris-buffered saline- Tween (TBST; 20 mM Tris HCl, pH 7.5, 500 mM NaCl supplemented with 0.1% Tween 20) prior to blocking with 5% fat-free milk in TBST and incubated at 25°C for 1 h. The wells were washed using TBST for a total of 10 min. Varying concentrations (0–1,000 nM) of analyte PfHop were added to the wells and incubated for 2 h at 25°C. To remove the unbound analyte, the plate was washed with 150  $\mu$ l TBST three times before the addition of rabbit-raised  $\alpha$ -PfHop antibody (1: 4,000) followed by incubation at 25°C for 1 h. Subsequently, the wells were washed with 150  $\mu$ l TBST three times before the addition of 100  $\mu$ l secondary HRP conjugated goat-raised  $\alpha$ -rabbit antibody (1: 4,000) and incubated for 45 min at 25°C. The substrate, 3,3',5,5'-tetramethylbenzidine (TMB) (Bio Scientific, United States) was added into the wells and incubated for 2 min at 25°C. Color development was monitored by recording absorbance readings at 370 nm at 5 min time intervals for 30 min using a SpectraMax M3 Microplate reader (Molecular Devices, United States). To determine the effect of the inhibitor, the assay was conducted in the presence of 25  $\mu$ M of PES. As controls, the assay was repeated in the presence of 25  $\mu$ M of ATP/ADP and EGCG (Zininga et al., 2015; Zininga et al., 2017b). Furthermore, the assay was repeated interchanging the

ligand and analyte to validate data reproducibility. The generated data were analyzed taking into account the background signal generated by BSA which served as the control protein. The absorbance values obtained at the highest concentration of each analyte were averaged to represent maximum (100%) binding. Titration curves were then generated using GraphPad Prism 9.3.1 (GraphPad Software, United States). The relative binding affinities of PES under each experimental setting were normalized relative to the affinity estimated for assay conducted in the absence of nucleotide at the highest concentration of PfHop. Statistical analysis was conducted to establish significant differences at  $p < 0.05$  using a student t-test.

## 2.9 Parasite growth inhibition studies

Asexual *P. falciparum* strain 3D7 parasites were cultured at 2–3% parasitemia in RBC (4% haematocrit) in RPMI complete media supplemented with 25 mM HEPES, 11 mM glucose, 200  $\mu$ M hypoxanthine (dissolved in 500 mM NaOH), 24  $\mu$ g/ml gentamycin and 0.6% m/v Albumax II serum. Growth inhibition assays were set up on synchronized ring-stage parasites using a 1% parasitemia and a 1% haematocrit suspension. The culture was exposed to increasing concentrations of PES (1.95–500  $\mu$ M) and incubated at 37°C in a continuous gas environment (93%  $\text{N}_2$ , 3%  $\text{O}_2$ , and 4%  $\text{CO}_2$ ) for 96 h. Chloroquine was used as the positive drug control at 1  $\mu$ M. Parasite growth without any drug present, which allowed the parasites to proliferate unrestricted, was used as negative drug control. SYBR<sup>TM</sup> Gold DNA stain (Invitrogen, ThermoFisher Scientific Inc., Germany) was used to measure the proliferation of the parasites compared to the controls as previously described (Smilkstein et al., 2004). Fluorescence was measured using a TECAN Spark<sup>®</sup> multimode microplate reader (Tecan Trading AG, Switzerland) and the data were analyzed using SigmaPlot, version 12 (Systat Software Inc., IL, United States).  $\text{IC}_{50}$  were generated based on dose-response curves obtained as technical triplicates for one biological test ( $n = 1$  for chloroquine) and three biological repeats ( $n = 3$  for PES).

## 3 Results

### 3.1 PES is predicted to directly bind to both PfHsp70-1 and PfHop

Molecular docking studies were conducted to assess the propensity of PES to bind to PfHsp70-1 and its co-chaperone, PfHop. PES was docked onto PfHsp70-1 and PfHop and the affinity was determined in each case (Figures 2, 3). Both PfHsp70-1 and PfHop bound to PES at notable predicted scores of -6.9 kcal/mol and 7.3 kcal/mol, respectively. The predicted binding of PfHop by PES came as a surprise since



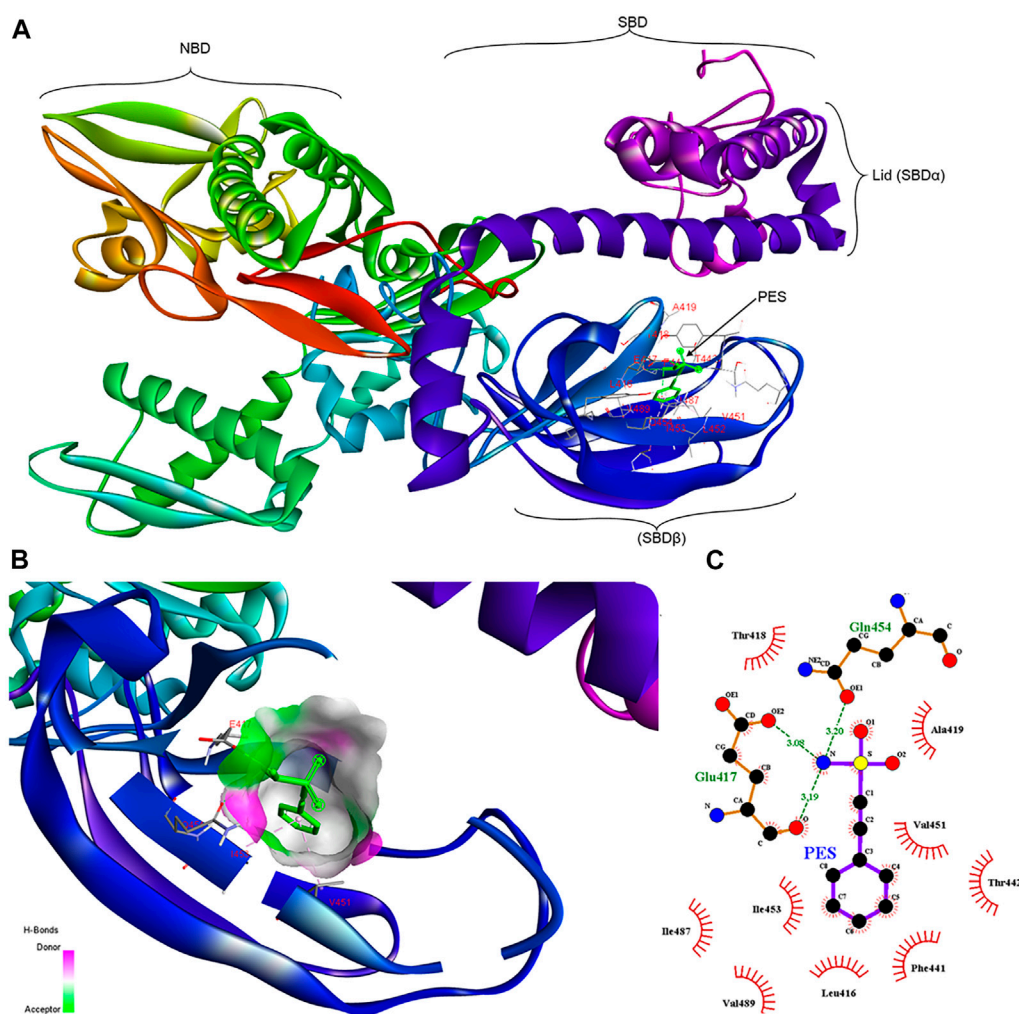


FIGURE 2

Schematic representing the interaction of PES with PfHsp70-1. (A) representation of a three-dimensional model with a ribbon structure of full-length PfHsp70-1 bound to PES through the SBD $\beta$ . The different domains of PfHsp70-1 are also shown. (B) Surface and ribbon views of the docked structures, showing the residues involved in the interaction, and (C) a 2D diagram showing receptor-ligand interface. PES makes H bond contacts with Glu417, Gln454 of PfHsp70-1. In addition, PES exhibits pi-alkyl contacts with Val451 and Ile453 of PfHsp70-1.

this compound is traditionally known to target Hsp70. Based on the docking model, PES is positioned within a binding pocket defined by residues Leu416, Glu417, Thr418, Ala419, Phe441, Thr442, Val451, Ile453, Gln454, Ile487, and Val489 located within the SBD of PfHsp70-1 (Figure 2). Our findings are thus in agreement with a previous study that proposed that PES binds to the SBD of human Hsp70 (Leu et al., 2009). It is thought that the substrate binding cavity of PfHsp70-1 is made up of residues Ala419, Tyr444, and Val451 (Shonhai et al., 2007; Shonhai et al., 2008). It is interesting to note that residues, Ala419 and Val451 that form part of the substrate binding cavity of PfHsp70-1 are predicted to make direct contact with PES. It is plausible that PES binding by PfHsp70-1 may abrogate substrate binding.

Furthermore, PES is predicted to interact with two residues, Met123 and Leu 124, located within the interface between the TPR1 and the dipeptide domain 1 (DP1) of PfHop (Figure 3). In addition, PES is thought to make direct contact with both Tyr372 and Ile373 which are located within the region joining TPR2A and TPR2B of PfHop. Residue Arg407, located within the TPR2B of PfHop seems to also make direct contact with PES (Figure 3). The predicted binding energies of PES for the two proteins are proportional to the estimated number of H-bond and the net number of interactions observed; 5 for PfHsp70-1 and 6 for PfHop, respectively (Figure 3; Table 1). The marginally higher binding affinity of PES for PfHop could be attributed to the distinct contacts it makes with this co-chaperone relative to PfHsp70-1 (Table 1).

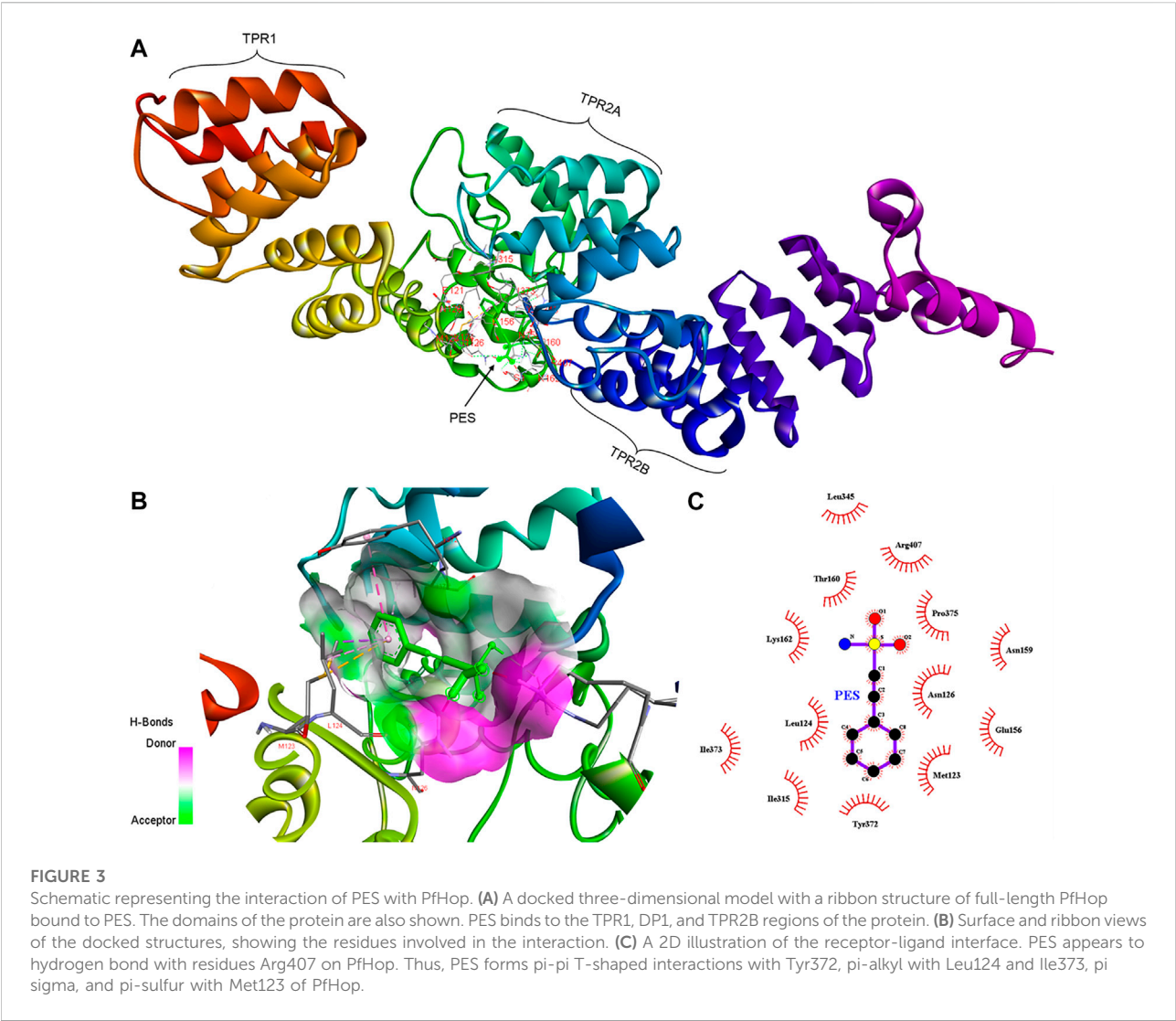


TABLE 1 Interaction of PES with *P. falciparum* Hsp70-1/PfHop as predicted *in silico*.

Protein	Compound	Binding energy (Kcal/mol)	Hydrogen bonding and residues involved	Hydrophobic interactions and residues involved
PfHop	PES	-7.3	Arg407	Met123, Leu124, Tyr 372, Ile373
PfHsp70-1		-6.9	Glu417, Gln454	Val451, Ile453

### 3.3 Experimental evidence for the direct binding of PES onto PfHsp70-1 and PfHop

We further experimentally investigated the direct interaction of PES with both PfHsp70-1 and PfHop. We employed SPR analysis to explore the association of PES with either of the two proteins. Recombinant forms of either PfHsp70-1 or PfHop were used as analytes while PES served as ligand. First, it was important to

validate the interaction of PfHsp70-1 with ATP (Table 2) as the latter is known to bind to PfHsp70-1 (Zininga et al., 2016). In addition, while human Hop binding to ATP has been reported (Yamamoto et al., 2014), the direct interaction of PfHop with nucleotides has not been established. As expected, PfHsp70-1 and its NBD both bound to ATP (Table 2). It is interesting to note that PfHop bound to ATP within affinity of the same order of magnitude as PfHsp70-1 (Table 2). This is the first report

TABLE 2 Equilibrium binding affinities of PES for PfHsp70-1/PfHsp70-1<sub>NBD</sub> and PfHop.

Ligand	Analyte	KD ( $\mu$ M)	$\chi^2$
PfHsp70-1	PES	$0.0692 \pm 0.02$	1.70
	ATP	$0.537 \pm 0.07$	1.73
PfHop	PES	$0.707 \pm 0.07$	7.31
	ATP	$0.861 \pm 0.01$	6.90
PfHsp70-1 <sub>NBD</sub>	PES	$7.39 \pm 0.09$	9.14
	ATP	$0.0223 \pm 0.03$	1.01

$K_D$ , equilibrium constant,  $\chi^2$  values indicate the goodness of fit for SPR, sensorgrams. Each parameter is the mean for three independent experiments, each performed in triplicate and standard errors of the mean are indicated.

TABLE 3 PES inhibits the direct association of PfHsp70-1 and PfHop.

Ligand	Analyte	Name of the inhibitor	IC <sub>50</sub> (nM)
PfHsp70-1	PfHop	EGCG	$13.90 \pm 1.2$
		PES	$32.43 \pm 2.1$
PfHop	PfHsp70-1	EGCG	$14.57 \pm 1.8$
		PES	$38.13 \pm 3.6$

Interaction of PfHsp70-1 and PfHop was investigated using ELISA, with analyte and ligand alternating. IC<sub>50</sub> values for the interaction of the proteins in the presence of PES and EGCG (control) are shown.

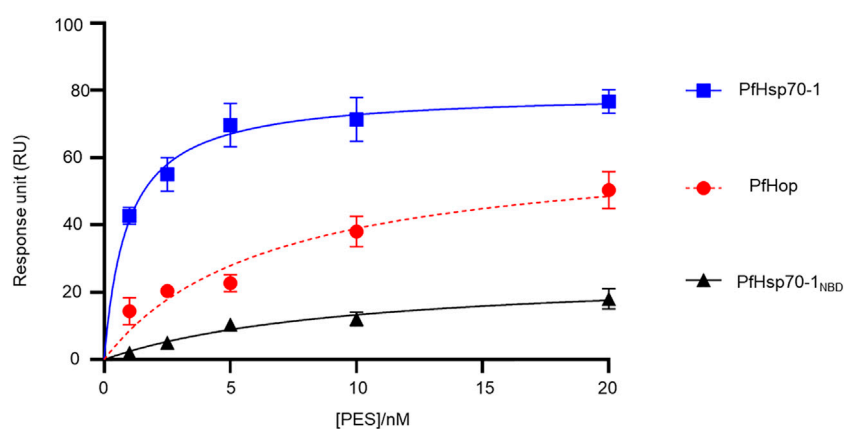


FIGURE 4

PES directly binds to both PfHsp70-1 and PfHop. As a ligand, each of PfHsp70-1 or PfHsp70-1<sub>NBD</sub> or PfHop was immobilized at a concentration of 0.1  $\mu$ g/ml. The assay was conducted in the presence of variable levels of PES. The interaction between ligand and analyte was determined at equilibrium. Each curve is the average determined for three independent experiments, each performed in triplicate. The error bars are indicated as standard error about the mean.

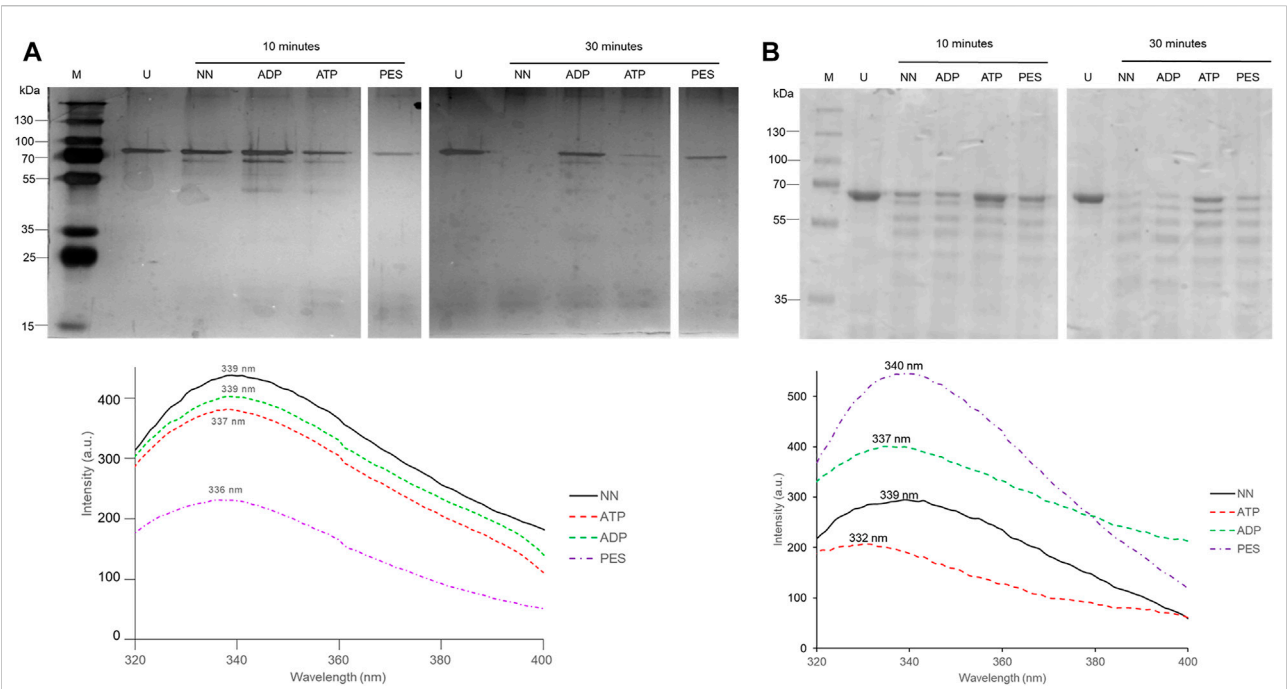
demonstrating that PfHop, like human Hop, is capable of binding ATP. *In silico* prediction suggests that PES binds primarily to the TPR2A subdomain of PfHop (Figure 3). However, this requires experimental validation. As expected, PfHsp70-1 bound to PES within the lower micromolar range (Table 2). On the other hand, the isolated NBD of PfHsp70-1 exhibited much less affinity (about two orders of magnitude lower) for PES, further confirming that PES binding is largely driven by residues located in the SBD (Figure 4). PfHop bound to PES with notable affinity, although its affinity for the ligand was one order of magnitude lower than PfHsp70-1.

Our SPR data (Figure 4; Table 2) is at variance with docking studies that suggested that PES exhibits a higher affinity for PfHop than PfHsp70-1 (Table 1). In addition, findings from the docking studies suggest that PES binds to Hsp70 via both the NBD and the SBD. While the minor discordances between *in silico* and experimental data were expected, both the *in silico* and experimental data strongly suggested that PfHop binds to PES.

While the recognition of PES by the SBD of Hsp70 has been established (Leu et al., 2009, 2011; Kaiser et al., 2011), evidence for its possible interaction with the N-terminal NBD of Hsp70 has been reported (Zhou et al., 2017). Thus, our findings suggest that PfHsp70-1 is capable of binding PES via both domains reconciling the previously contrasting reports.

### 3.2 PES induces conformational changes in PfHsp70-1 and PfHop

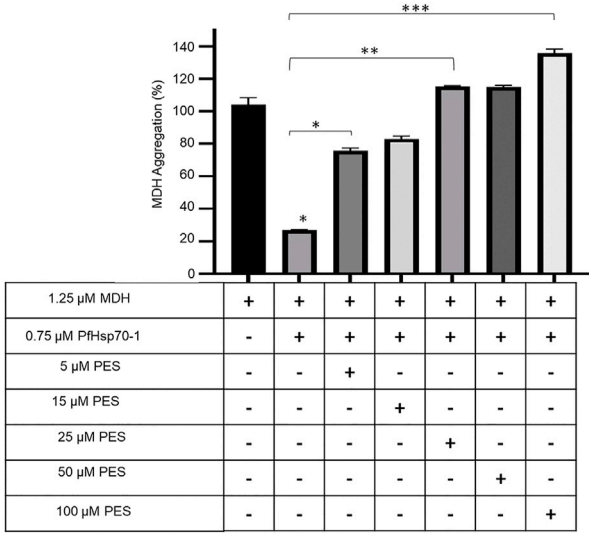
The capability of PES to induce conformational changes on PfHsp70-1 and PfHop was analyzed using limited proteolysis and intrinsic fluorescence analysis. The effect of ATP/ADP on the fragmentation of PfHsp70-1 or PfHop served as a control. The data generated through limited proteolysis and intrinsic fluorescence suggest that ATP and ADP each uniquely regulate



the conformations of either PfHsp70-1 (Figure 5A) or PfHop (Figure 5B). While it is well known that PfHsp70-1 is uniquely regulated by ATP and ADP (Zininga et al., 2016), this study constitutes the first report suggesting that the conformation of PfHop is regulated by nucleotides. We further explored the structural perturbations of both proteins in the presence of PES. Both PfHsp70-1 and PfHop digested in the presence of PES generated unique fragmentation patterns compared to protein digested in *apo* state (Figure 5A,B). This suggests that PES binds to PfHsp70-1 and PfHop to induce conformational changes. Similarly, intrinsic fluorescence data mirrored the same findings as we noted a blue shift (emission peak of 336 nm) registered by PfHsp70-1 in the presence of PES relative to the emission peak of 339 nm registered by protein in *apo* state (Figure 5A bottom panel). On the other hand, PfHop registered a marginal red shift (emission peak of 340 nm) in the presence of PES relative to the emission peak of 339 nm registered by the protein in *apo* state (Figure 5B bottom panel).

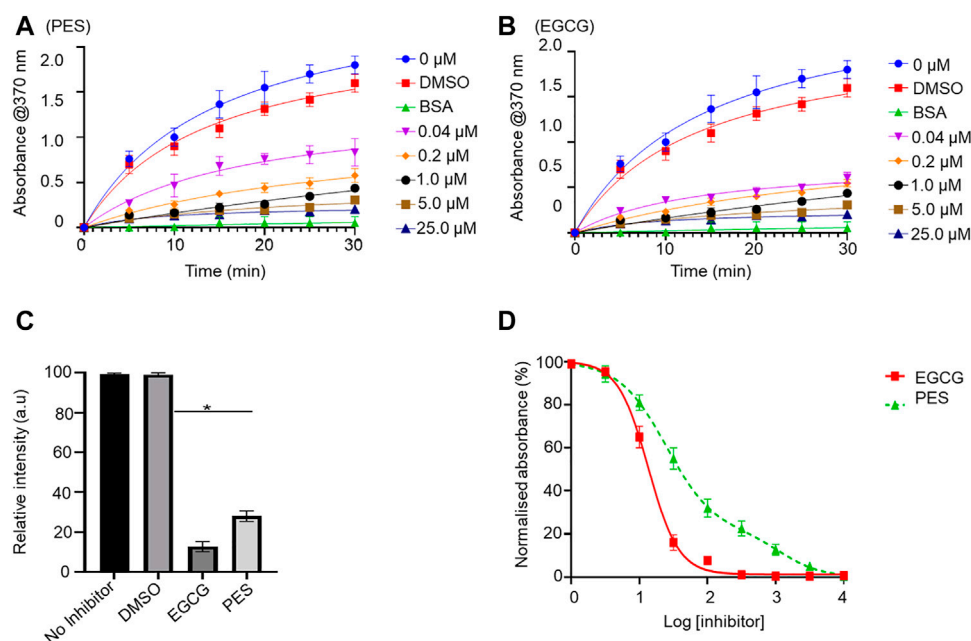
3.4 PES inhibits the holdase chaperone activity of PfHsp70-1

PfHsp70-1 is known to suppress the heat-induced aggregation of model substrate proteins such as MDH,



**FIGURE 6**  
PES inhibits the holdase chaperone activity of PfHsp70-1. The effect of PES on the heat-induced aggregation suppression activity of PfHsp70-1 was monitored by exposing aggregation-prone protein, MDH, to heat stress at 51 °C in the presence of PfHsp70-1 at equimolar levels and varying levels of PES. The heat-induced aggregation of MDH was monitored at 360 nm. Error bars indicate the mean generated from three assays conducted using independent PfHsp70-1 protein purifications. Statistical significance of differences was determined using one-way ANOVA and post-hoc test (\**p* < 0,05; \*\**p* < 0,01; \*\*\**p* < 0.001).



**FIGURE 7**

PES suppresses PfHsp70-1 association. PfHsp70-1 was immobilized onto the ELISA plate and PfHop (analyte) was suspended along with varying concentrations of PES. DMSO and BSA were used as controls. Representative binding curves obtained for the association of PfHsp70-1 and PfHop in the presence of (A) PES and EGCG (B) are shown. Bar graphs showing the comparative effects of the inhibitors on the interaction of PfHsp70-1 and PfHop are provided (C). The resultant dose-response curves for both PES and EGCG are shown (D). The error bars represent the standard deviations obtained from three independent assays conducted independently. Student t-test statistical significance of differences of inhibitor compared to the vehicle control, DMSO, are indicated by asterisks positioned above the bar graphs ( $p < 0.001^*$ ).

thereby exhibiting holdase chaperone activity (Shonhai et al., 2008; Makumire et al., 2021). We explored the effect of PES on the capability of PfHsp70-1 to suppress the heat-induced aggregation of MDH *in vitro*. The rationale of this assay is that inhibition of PfHsp70-1 would result in MDH aggregating in the presence of the chaperone. Our findings demonstrated that PES inhibited the chaperone activity of PfHsp70-1 in a concentration-dependent fashion (Figure 6).

### 3.5 PES inhibits the direct association of PfHsp70-1 and PfHop

The capability of PES to inhibit the direct association of PfHsp70-1 with PfHop was investigated using ELISA and SPR analyses as previously reported (Mabate et al., 2018). First, using ELISA, we established that PES inhibited the association of the two proteins in a concentration dependent fashion irrespective of which protein was used as a ligand (Supplementary Figure S1). BSA was used as a negative control protein as it does not interact with either PfHsp70-1 or PfHop (Supplementary Figure S1). The assay was repeated in the presence of 25 μM of either ATP or ADP (Supplementary Figure S1) or 25 μM inhibitor (Figure 7;

Table 3). The presence of ADP promoted the association, while ATP abrogated the association (Supplementary Figure S1). This observation was in line with our previous findings (Zininga et al., 2015; Zininga et al., 2017a; Zininga et al., 2017b), thus validating the assay. PES abrogated the interaction of PfHsp70-1 and PfHop in the same way as ATP (Figure 7A). The assay was further validated using EGCG (Figure 7B), a known inhibitor of PfHop-PfHsp70-1 interaction (Zininga et al., 2017b). This suggests that PES has an inhibitory effect on the association of PfHsp70-1 with PfHop as is the case for ATP or EGCG (Figure 7C). In addition, the ELISA-based data suggested that compared to EGCG, PES is marginally less effective at inhibiting PfHop-PfHsp70-1 interaction (Figure 7D).

We further validated the effect of PES on the PfHop-PfHsp70-1 association using SPR analysis. PfHsp70-1 was immobilized as ligand and varying concentrations of PfHop were injected as analyte. The assay was conducted in the absence or presence of 25 μM ATP/ADP, or PES (Figure 8). First, we confirmed that under the SPR-based experimental conditions PfHop and PfHsp70-1 associate in a nucleotide-dependent fashion (ADP promotes their association while ATP inhibits the association; Zininga et al., 2015; Figure 8). Our SPR-based data confirmed that PES significantly inhibited the interaction of PfHop with PfHsp70-1 (Figure 8). However, as

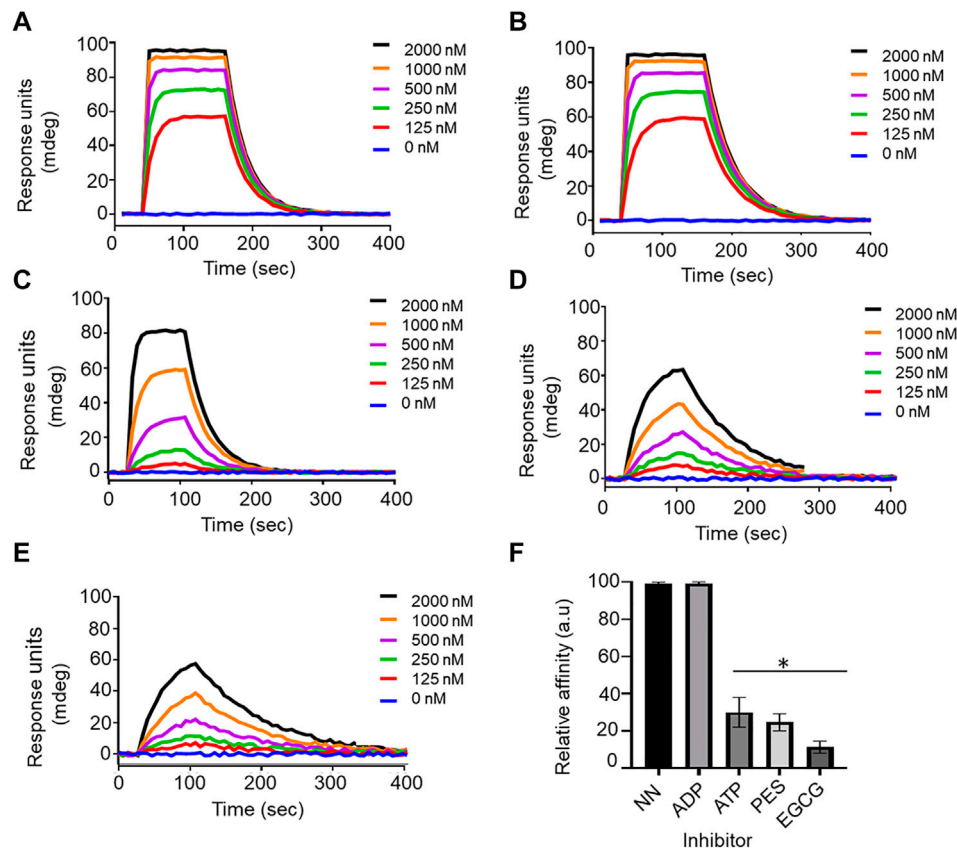


**FIGURE 8** Confirmation of the inhibitory function of PES on PfHop-PfHsp70-1 association. Representative sensorgrams generated from data obtained in absence of nucleotide (A), presence of ADP (B), ATP (C), and PES (D) and EGCG (E) are shown. The relative affinities of the association of PfHop with PfHsp70-1 in the absence (NN) of both nucleotides and inhibitors compared to interaction in the presence of nucleotides and inhibitors are shown in (F). Standard errors represent three independent assays conducted in triplicates using independent protein batches. A student t-test was used for statistical validation and statistically significant differences relative to data obtained in the absence of nucleotide state (NN) are indicated by asterisks above the bar graphs ( $p < 0.001^*$ ).

**TABLE 4** SPR based kinetics showing the effect of PES on the interaction of PfHsp70-1 with PfHop.

Ligand	Analyte	Nucleotide/Inhibitor	$k_a$ (1/Ms)	$k_d$ (1/s)	$K_D$ (nM)	$\chi^2$
PfHsp70-1	PfHop	NN	$7.67 (\pm 0.07) e^5$	$3.25 (\pm 0.05) e^{-3}$	$4.24 \pm 0.4$	0.91
		ADP	$7.81 (\pm 0.01) e^5$	$3.08 (\pm 0.08) e^{-3}$	$3.08 \pm 0.8$	0.75
		ATP	$2.59 (\pm 0.09) e^5$	$2.07 (\pm 0.07) e^{-2}$	$79.8 \pm 8.0^*$	2.12
		EGCG	$6.31 (\pm 0.01) e^3$	$1.30 (\pm 0.3) e^{-1}$	$20,700 \pm 700^*$	0.51
		PES	$1.25 (\pm 0.05) e^5$	$2.66 (\pm 0.06) e^{-2}$	$214 \pm 40^*$	0.13
PfHop	PfHsp70-1	NN	$7.60 (\pm 0.6) e^6$	$3.41 (\pm 0.01) e^{-2}$	$4.49 \pm 0.9$	0.19
		ADP	$8.07 (\pm 0.07) e^6$	$2.50 (\pm 0.5) e^{-2}$	$3.10 \pm 0.1$	0.10
		ATP	$2.66 (\pm 0.06) e^5$	$2.15 (\pm 0.05) e^{-2}$	$80.9 \pm 9.1^*$	1.67
		EGCG	$6.71 (\pm 0.01) e^3$	$9.14 (\pm 0.04) e^{-3}$	$1,360 \pm 60^*$	0.12
		PES	$3.50 (\pm 0.5) e^4$	$8.11 (\pm 0.01) e^{-3}$	$232 \pm 24^*$	0.28

$k_a$ , association rate constant;  $k_d$ , dissociation rate constant;  $K_D$ , equilibrium constant;  $\chi^2$  values indicate the goodness of fit for SPR, sensorgrams based on the bivalent fit model. Three independent analyses were conducted during the SPR, assay alternating ligand and analyte each time. Standard errors are shown in brackets. Statistical analysis was done using a student t-test ( $p < 0.05$ )<sup>\*</sup> represents statistically significant differences in affinities recorded in the absence of nucleotide (NN).

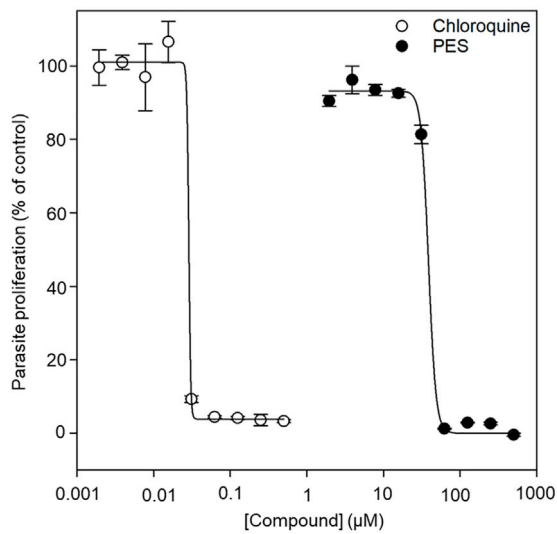


**FIGURE 9**

The normalized dose-response curve for the *in vitro* susceptibility of *P. falciparum* to PES. The *in vitro* antiparasmodial activity of PES was investigated using a SYBR<sup>TM</sup> Gold DNA stain to measure the proliferation of the parasites as compared to the controls. Fluorescence was measured using a TECAN Spark<sup>®</sup> multimode microplate reader and the data analysis was done using SigmaPlot, version 12 (Systat Software Inc., Chicago, IL, United States). IC<sub>50</sub> determinations were performed as technical triplicates for three biological repeats with standard error of the mean shown.

observed using the ELISA assay, PES was slightly less effective at this than EGCG (Figures 7, 8).

To further validate the inhibition of PfHsp70-1 and PfHop interaction, ligand and analyte were switched, and the assay was repeated (Table 4). As previously shown, a decrease in response was observed in the interaction of PfHsp70-1 with PfHop in the presence of PES. The binding affinities for PfHsp70-1 with PfHop in the presence of PES were within the same order of magnitude after swapping ligand and analyte (Table 4). Taken together, both our SPR and ELISA data suggest that PES abrogates the PfHop-PfHsp70-1 association.

### 3.6 The antiparasmodial activity of PES

We further explored the capability of PES to inhibit *P. falciparum* proliferation at the asexual blood stage. The antiparasmodial activity of PES was compared to that of chloroquine which is a known antimalarial (Zininga et al., 2017b). In the presence of PES, *P. falciparum* 3D7 parasite growth was inhibited in a concentration dependent manner with an IC<sub>50</sub> value of  $38.7 \pm 0.7 \mu\text{M}$  compared to chloroquine with an IC<sub>50</sub> value of  $29.1 \pm 1.3 \text{ nM}$  (Figure 9). The IC<sub>50</sub> of chloroquine compares well with published potencies ( $21 \pm 1.7 \text{ nM}$ , Smilkstein et al., 2004). On the other hand, PES exhibited mild antiparasmodial activity.

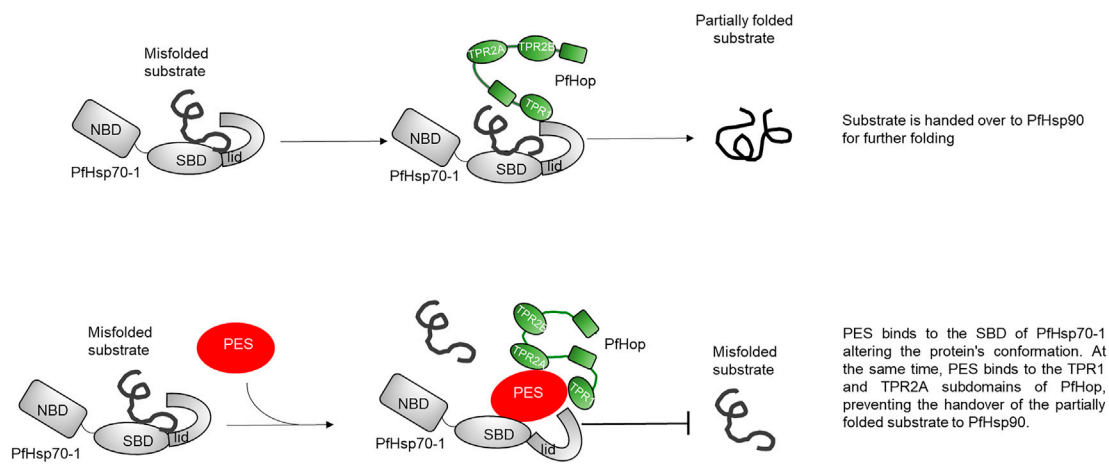


**FIGURE 10**

Proposed model of PES binding PfHsp70-1. The schematic represents a model for the mechanism of action of PES. The model suggests that PES binds to both PfHsp70-1 and PfHop thereby perturbing the conformations of the two proteins. Consequently, this abrogate the chaperone function of PfHsp70-1 and their interaction. The inhibition of the interaction of PfHsp70-1 and PfHop adversely impacts on the functional partnership between PfHsp70-1 and PfHsp90.

## 4 Discussion

*P. falciparum* causes the most severe form of malaria in humans. The effectiveness of antimalarial drugs has been reduced due to emerging drug-resistant parasite strains. As such, there is a need to explore novel drug targets for the treatment of malaria. PfHsp70-1 and PfHsp90 are two prominent and essential molecular chaperones of the parasite. The two chaperones functionally cooperate via PfHop mediation (Gitau et al., 2012; Zininga et al., 2015). PES has been reported to possess antitumour activity (Leu et al., 2009; Kaiser et al., 2011; Zhou et al., 2017) and offers promise toward repurposing as a potential agent to fight the growing threat of multidrug-resistant pathogens. It has been proposed that PES binds to the SBD of Hsp70 (reviewed in Moradhi-Marjaneh et al., 2019). This study is the first to show that PES binds to PfHsp70-1 to inhibit its chaperone function. Furthermore, PES inhibits the interaction of PfHsp70-1 with the co-chaperone, PfHop. Whereas the interaction of PES with Hsp70 has been established, this study for the first time demonstrated that PES binds to both PfHsp70-1 and PfHop.

First, we conducted *in silico* docking studies and observed that PES is predicted to bind to both proteins. It has been reported that PES binds to the SBD of human Hsp70 (Leu et al., 2009). We further demonstrated that the binding of PES onto PfHsp70-1 induces a conformational switch that is distinct compared to that of the protein in the *apo* state (Figure 5). Similarly, a conformational change was observed for PfHop in the presence of PES as compared to the protein in the *apo* state (Figure 5). In addition, the *in silico* data suggested that PES binds the co-chaperone, PfHop via contact residues located within the TPR1:DP1 and, TPR2A:TPR2B interfaces of the protein. We previously resolved the structure of PfHop using SAXS analysis. Our previous study demonstrated that the TPR domains of PfHop assemble like “beads on a string” (Makumire et al., 2020). This arrangement allows Hsp70 and Hsp90 to slide through the concave-shaped TPR domains to facilitate interaction. Thus, PES may abrogate the association of PfHop with PfHsp70-1 by perturbing the conformation of both PfHop and PfHsp70-1. Having established that PES forces PfHsp70-1 to assume a conformational switch, we further enquired if this would impact the chaperone activity of PfHsp70-1. PES abrogated the holdase chaperone activity of PfHsp70-1 (Figure 6). Apart from inducing a conformational switch, PES may also physically block substrate binding since our *in silico* data suggested that this compound interacts with residues located within the C-terminal substrate binding domain, including those constituting the hydrophobic pocket (Val451) and the arch (Ala419 and Tyr444) which are all crucial for substrate binding (Figure 10; Shonhai et al., 2008). Furthermore, our data demonstrated that PES binds to both proteins and hence we speculate that the dual binding role of PES may account for its capability to abrogate the interaction of the two proteins (Figure 10).

We further established that PES inhibited the growth of *P. falciparum* parasites maintained at the blood stage registering a modest IC<sub>50</sub> of 38.7 μM (Figure 9). The inhibition of the

PfHsp70-1-PfHop pathway may account for the observed antiparasitic activity. It has been suggested that about 24% of malarial proteins possess prion-like asparagine repeat-rich segments, thus, the parasite proteome may have propensity to aggregate under heat stress (Muralidharan et al., 2012; Pallarès et al., 2018). This makes the role of the molecular chaperone machinery of the parasite crucial for survival in the host.

Altogether, our findings demonstrate that PES binds both PfHsp70-1 and PfHop to disrupt their association as well as abrogate the chaperone function of PfHsp70-1. In addition, that PES is predicted to bind to TPR and DP1 subdomains of PfHop while possibly making contacts with several residues located in the SBC of PfHsp70-1 makes it an important scaffold for designing versatile chemical inhibitors targeting this pathway. Since PES has been shown to inhibit Hsp70 in cancer cells, its selectivity for parasites versus the human homolog may be in question. Hence, further work needs to be conducted to establish its utility in the fight against both malaria and cancer. Future efforts must focus on the crystallization of both PfHsp70-1 and PfHop in complex with PES. A thermal shift assay of the protein-ligand complexes would also serve as an appropriate precursor step to establish the prospects of successful crystallization of the complexes.

## Data availability statement

The raw data supporting the conclusions of this article will be made available by the authors, without undue reservation.

## Author contributions

Conceptualization, AS; TZ; writing-original draft preparation, TM; SM; TZ; AS, data acquisition and interpretation, TM; VM; MN; THD; SM; MK, writing-review and editing, VM, AB, MdV, TZ, AS, supervision, TZ; MdV, AS, funding acquisition, AS, MdV All authors have read and agreed to the published version of the manuscript.

## Funding

The study was supported through a Digital Cooperation Fellowship awarded to AS by the Alexander von Humboldt Foundation of Germany. This work is based on the research supported in part by the Department of Science and Technology/ National Research Foundation (NRF) of South Africa (Grant numbers, 75,464 & 92,598) awarded to AS; and (Grant numbers 129401 & 145,405) awarded to TZ. The authors would like to acknowledge the University of Cape Town, Faculty of Health Sciences for financial support to SM, University of Venda Research Grant (grant number SMNS/17/BCM/17) awarded to



AB and Stellenbosch University Sub-Committee B for financial support to TZ and MdV.

## Acknowledgments

We would also like to acknowledge the Western Cape Blood Service (WCBS) in South Africa for providing blood for malaria parasite culturing.

## Conflict of interest

The authors declare that the research was conducted in the absence of any commercial or financial relationships that could be construed as a potential conflict of interest.

## References

- Akide-Ndunge, O. B., Tambini, E., Giribaldi, G., McMillan, P. J., Müller, S., Arese, P., et al. (2009). Co-ordinated stage-dependent enhancement of *Plasmodium falciparum* antioxidant enzymes and heat shock protein expression in parasites growing in oxidatively stressed or G6PD-deficient red blood cells. *Malar. J.* 8 (1), 113–115. doi:10.1186/1475-2875-8-113
- Anas, M., Shukla, A., Tripathi, A., Kumari, V., Prakash, C., Nag, P., et al. (2020). Structural-functional diversity of malaria parasite's PfHSP70-1 and PfHSP40 chaperone pair gives an edge over human orthologs in chaperone-assisted protein folding. *Biochem. J.* 477 (18), 3625–3643. doi:10.1042/BCJ20200434
- Banumathy, G., Singh, V., Pavithra, S. R., and Tatu, U. (2003). Heat shock protein 90 function is essential for *Plasmodium falciparum* growth in human erythrocytes. *J. Biol. Chem.* 278 (20), 18336–18345. doi:10.1074/jbc.M211309200
- Chakafana, G., Mudau, P. T., Zininga, T., and Shonhai, A. (2021). Characterisation of a unique linker segment of the *Plasmodium falciparum* cytosol localised Hsp110 chaperone. *Int. J. Biol. Macromol.* 180, 272–285. doi:10.1016/j.ijbiomac.2021.03.056
- Chakafana, G., Zininga, T., and Shonhai, A. (2019). Comparative structure-function features of Hsp70s of *Plasmodium falciparum* and human origins. *Biophys. Rev.* 11 (4), 591–602. doi:10.1007/s12551-019-00563-w
- Cockburn, I. L., Boshoff, A., Pesce, E. R., and Blatch, G. L. (2014). Selective modulation of plasmodial Hsp70s by small molecules with antimalarial activity. *Biol. Chem.* 395 (11), 1353–1362. doi:10.1515/hsz-2014-0138
- Corey, V. C., Lukens, A. K., Istvan, E. S., Lee, M. C., Franco, V., Magistrado, P., et al. (2016). A broad analysis of resistance development in the malaria parasite. *Nat. Commun.* 7 (1), 11901–11909. doi:10.1038/ncomms11901
- Daniyan, M. O. (2021). “Heat shock proteins as targets for novel antimalarial drug discovery,” in *Heat shock proteins of malaria* (Cham: Springer), 205–236.
- Day, J., Passecker, A., Beck, H. P., and Vakonakis, I. (2019). The *Plasmodium falciparum* Hsp70-x chaperone assists the heat stress response of the malaria parasite. *FASEB J.* 33, 14611–14624. doi:10.1096/fj.201901741R
- Gitau, G. W., Mandal, P., Blatch, G. L., Przyborski, J., and Shonhai, A. (2012). Characterisation of the *Plasmodium falciparum* hsp70-hsp90 organising protein (PfHop). *Cell Stress Chaperones* 17 (2), 191–202. doi:10.1007/s12192-011-0299-x
- Jiang, L., and Xiao, J. (2020). 2-phenylethanesulfonamide inhibits growth of oral squamous cell carcinoma cells by blocking the function of heat shock protein 70. *Biosci. Rep.* 40 (3), BSR20200079. doi:10.1042/BSR20200079
- Kaiser, M., Kühnl, A., Reins, J., Fischer, S., Ortiz-Tanchez, J., Schlee, C., et al. (2011). Antileukemic activity of the HSP70 inhibitor pifithrin- $\mu$  in acute leukemia. *Blood Cancer J.* 1 (7), e28. doi:10.1038/bcj.2011.28
- Kappes, B., Suetterlin, B. W., Hofer-Warbinek, R., and Franklin, R. M. (1993). Two major phosphoproteins of *Plasmodium falciparum* are heat shock proteins. *Mol. Biochem. Parasitol.* 59 (1), 83–94. doi:10.1016/0166-6851(93)90009-m
- Kelley, L. A., Mezulis, S., Yates, C. M., Wass, M. N., and Sternberg, M. J. (2015). The Phyre2 web portal for protein modeling, prediction and analysis. *Nat. Protoc.* 10, 845–858. doi:10.1038/nprot.2015.053
- Lebepe, C. M., Matambanadzo, P. R., Makhoba, X. H., Achilonu, I., Zininga, T., and Shonhai, A. (2020). Comparative characterization of *Plasmodium falciparum* Hsp70-1 relative to *E. coli* DnaK reveals the functional specificity of the parasite chaperone. *Biomolecules* 10 (6), 856. doi:10.3390/biom10060856
- Leu, J. J., Pimkina, J., Frank, A., Murphy, M. E., and George, D. L. (2009). A small molecule inhibitor of inducible heat shock protein 70. *Mol. Cell* 36 (1), 15–27. doi:10.1016/j.molcel.2009.09.023
- Leu, J. J., Pimkina, J., Pandey, P., Murphy, M. E., and George, D. L. (2011). HSP70 inhibition by the small-molecule 2-phenylethanesulfonamide impairs protein clearance pathways in tumor cells. *Mol. Cancer Res.* 9 (7), 936–947. doi:10.1158/1541-7786.MCR-11-0019
- Lu, K. Y., Pasaje, C. F. A., Srivastava, T., Loisele, D. R., Niles, J. C., and Derbyshire, E. (2020). Phosphatidylinositol 3-phosphate and Hsp70 protect *Plasmodium falciparum* from heat-induced cell death. *Elife* 9, e56773. doi:10.7554/eLife.56773
- Mabate, B., Zininga, T., Ramatsui, L., Makumire, S., Achilonu, I., Dirr, H. W., et al. (2018). Structural and biochemical characterization of *Plasmodium falciparum* Hsp70-x reveals functional versatility of its C-terminal EEVN motif. *Proteins* 86 (11), 1189–1201. doi:10.1002/prot.25600
- Makumire, S., Dongola, T. H., Chakafana, G., Tshikonwane, L., Chauke, C. T., Maharaj, T., et al. (2021). Mutation of GGMP repeat segments of *Plasmodium falciparum* Hsp70-1 compromises chaperone function and Hop co-chaperone binding. *Int. J. Mol. Sci.* 22 (4), 2226. doi:10.3390/ijms22042226
- Makumire, S., Zininga, T., Vahokoski, J., Kursula, I., and Shonhai, A. (2020). Biophysical analysis of *Plasmodium falciparum* Hsp70-Hsp90 organising protein (PfHop) reveals a monomer that is characterised by folded segments connected by flexible linkers. *PLoS One* 15 (4), e0226657. doi:10.1371/journal.pone.0226657
- Mashaghi, A., Bezrukavnikov, S., Minde, D. P., Wentink, A. S., Kityk, R., Zachmann-Brand, B., et al. (2016). Alternative modes of client binding enable functional plasticity of Hsp70. *Nature* 539 (7629), 448–451. doi:10.1038/nature20137
- Mirdita, M., Ovchinnikov, S., Steinegger, M., and Heo, L. (2021). ColabFold - making protein folding accessible to all. *Nat. Methods* 19, 679–682. doi:10.1038/s41592-022-01488-1
- Mohamad, N., O'Donoghue, A., Kantsadi, A. L., and Vakonakis, I. (2021a). *Plasmodium falciparum* Hsp70-x chaperone nucleotide binding domain in complex with NCL-00023818. PDB DOI: doi:10.2210/pdb7P31/pdb
- Mohamad, N., O'Donoghue, A., Kantsadi, A. L., and Vakonakis, I. (2021b). *Plasmodium falciparum* Hsp70-x chaperone nucleotide binding domain in complex with NCL-00023823. doi:10.2210/pdb7OOG/pdb
- Mohamad, N., O'Donoghue, A., Kantsadi, A. L., and Vakonakis, I. (2021c). *Plasmodium falciparum* Hsp70-x chaperone nucleotide binding domain in complex with Z321318226. PDB DOI: doi:10.2210/pdb7OOE/pdb

## Publisher's note

All claims expressed in this article are solely those of the authors and do not necessarily represent those of their affiliated organizations, or those of the publisher, the editors and the reviewers. Any product that may be evaluated in this article, or claim that may be made by its manufacturer, is not guaranteed or endorsed by the publisher.

## Supplementary material

The Supplementary Material for this article can be found online at: <https://www.frontiersin.org/articles/10.3389/fmolb.2022.947203/full#supplementary-material>

- Mohamad, N., O'Donoghue, A., Kantsadi, A. L., and Vakonakis, I. (2021d). *Plasmodium falciparum* Hsp70-x chaperone nucleotide binding domain in complex with Z1827898537, PDB DOI: doi:10.2210/pdb7NQZ/pdb
- Mohamad, N., O'Donoghue, A., Kantsadi, A. L., and Vakonakis, I. (2021e). *Plasmodium falciparum* Hsp70-x chaperone nucleotide binding domain in complex with Z396380540, PDB DOI: doi:10.2210/pdb7NQU/pdb
- Mohamad, N., O'Donoghue, A., Kantsadi, A. L., and Vakonakis, I. (2021f). *Plasmodium falciparum* Hsp70-x chaperone nucleotide binding domain in complex with Z1203107138, doi:10.2210/pdb7NQS/pdb
- Mohamad, N., O'Donoghue, A., Kantsadi, A. L., and Vakonakis, I. (2021g). *Plasmodium falciparum* Hsp70-x chaperone nucleotide binding domain in complex with Z287256168, PDB DOI: doi:10.2210/pdb7NQR/pdb
- Moradi-Marjaneh, R., Paseban, M., and Moradi Marjaneh, M. (2019). Hsp70 inhibitors: Implications for the treatment of colorectal cancer. *IUBMB life* 71 (12), 1834–1845. doi:10.1002/iub.2157
- Morris, G. M., Huey, R., Lindstrom, W., Sanner, M. F., Belew, R. K., Goodsell, D. S., et al. (2009). AutoDock4 and AutoDockTools4: Automated docking with selective receptor flexibility. *J. Comput. Chem.* 30 (16), 2785–2791. doi:10.1002/jcc.21256
- Muralidharan, V., Oksman, A., Pal, P., Lindquist, S., and Goldberg, D. E. (2012). *Plasmodium falciparum* Hsp70-x chaperone nucleotide binding domain in complex with Z1827898537, PDB DOI: doi:10.2210/pdb7NQZ/pdb
- Pallares, I., de Groot, N. S., Iglesias, V., Sant'Anna, R., Biosca, A., Fernandez-Busquets, X., et al. (2018). Discovering putative prion-like proteins in *Plasmodium falciparum*: a computational and experimental analysis. *Front. Microbiol.* 9, 1737. doi:10.3389/fmicb.2018.01737
- Pallavi, R., Acharya, P., Chandran, S., Daily, J. P., and Tatu, U. (2010). Chaperone expression profiles correlate with distinct physiological states of *Plasmodium falciparum* in malaria patients. *Malar. J.* 9 (1), 236–312. doi:10.1186/1475-2875-9-236
- Pesce, E. R., Cockburn, I. L., Goble, J. L., Stephens, L. L., and Blatch, G. L. (2010). Malaria heat shock proteins: drug targets that chaperone other drug targets. *Infect. Disord. Drug Targets* 10 (3), 147–157. doi:10.2174/187152610791163417
- Petersen, E. F., Goddard, T. D., Huang, C. C., Couch, G. S., Greenblatt, D. M., Meng, E. C., et al. (2004). UCSF Chimera—a visualization system for exploratory research and analysis. *J. Comput. Chem.* 25, 1605–1612. doi:10.1002/jcc.20084
- Saibil, H. (2013). Chaperone machines for protein folding, unfolding and disaggregation. *Nat. Rev. Mol. Cell Biol.* 14 (10), 630–642. doi:10.1038/nrm3658
- Schmidt, J., and Vakonakis, I. (2020). Structure of the *Plasmodium falciparum* Hsp70-x substrate binding domain in complex with hydrophobic peptide. PDB DOI: doi:10.2210/pdb6ZHI/pdb
- Shonhai, A., Boshoff, A., and Blatch, G. L. (2007). The structural and functional diversity of Hsp70 proteins from *Plasmodium falciparum*. *Protein Sci.* 16 (9), 1803–1818. doi:10.1110/ps.072918107
- Shonhai, A. (2007). *Molecular characterisation of the chaperone properties of Plasmodium falciparum heat shock protein 70*. South Africa: Rhodes University. Available at: <https://core.ac.uk/download/pdf/145040463.pdf>.
- Shonhai, A. (2010). Plasmodial heat shock proteins: targets for chemotherapy. *FEMS Immunol. Med. Microbiol.* 58 (1), 61–74. doi:10.1111/j.1574-695X.2009.00639.x
- Shonhai, A. (2021). “The role of Hsp70s in the development and pathogenicity of *Plasmodium falciparum*,” in *Heat shock proteins of malaria* (Cham: Springer), 75–95.
- Smilkstein, M., Sriwilaijaroen, N., Kelly, J. X., Wilairat, P., and Riscoe, M. (2004). Simple and inexpensive fluorescence-based technique for high-throughput antimalarial drug screening. *Antimicrob. Agents Chemother.* 48 (5), 1803–1806. doi:10.1128/aac.48.5.1803-1806.2004
- Trott, O., and Olson, A. J. (2010). AutoDock Vina: improving the speed and accuracy of docking with a new scoring function, efficient optimization, and multithreading. *J. Comput. Chem.* 31 (2), 455–461. doi:10.1002/jcc.21334
- Wallace, A. C., Laskowski, R. A., and Thornton, J. M. (1995). LIGPLOT: a program to generate schematic diagrams of protein-ligand interactions. *Protein Eng.* 8 (2), 127–134. doi:10.1093/protein/8.2.127
- Witkowski, B., Lelièvre, J., López Barragán, M. J., Laurent, V., Su, X. Z., Berry, A., et al. (2010). Increased tolerance to artemisinin in *Plasmodium falciparum* is mediated by a quiescence mechanism. *Antimicrob. Agents Chemother.* 54 (5), 1872–1877. doi:10.1128/AAC.01636-09
- World Health Organisation (2021) World malaria report. Online. Available at: <https://www.who.int/teams/global-malaria-programme/reports/world-malaria-report-2021>
- Yamamoto, S., Subedi, G. P., Hanashima, S., Satoh, T., Otaka, M., Wakui, H., et al. (2014). ATPase activity and ATP-dependent conformational change in the co-chaperone HSP70/HSP90-organizing protein (HOP). *J. Biol. Chem.* 289 (14), 9880–9886. doi:10.1074/jbc.M114.553255
- Zhou, Y., Ma, J., Zhang, J., He, L., Gong, J., and Long, C. (2017). Pifithrin- $\mu$  is efficacious against non-small cell lung cancer via inhibition of heat shock protein 70. *Oncol. Rep.* 37 (1), 313–322. doi:10.3892/or.2016.5286
- Zininga, T., Achilonu, I., Hoppe, H., Prinsloo, E., Dirr, H. W., and Shonhai, A. (2016). *Plasmodium falciparum* Hsp70-z, an Hsp110 homologue, exhibits independent chaperone activity and interacts with Hsp70-1 in a nucleotide-dependent fashion. *Cell Stress Chaperones* 21 (3), 499–513. doi:10.1007/s12192-016-0678-4
- Zininga, T., Makumire, S., Gitau, G. W., Njunge, J. M., Poole, O. J., Klimek, H., et al. (2015). *Plasmodium falciparum* Hop (PfHop) interacts with the Hsp70 chaperone in a nucleotide-dependent fashion and exhibits ligand selectivity. *PLoS One* 10 (8), e0135326. doi:10.1371/journal.pone.0135326
- Zininga, T., Poole, O. J., Makhado, P. B., Ramatsui, L., Prinsloo, E., Achilonu, I., et al. (2017a). Polymyxin B inhibits the chaperone activity of *Plasmodium falciparum* Hsp70. *Cell Stress Chaperones* 22 (5), 707–715. doi:10.1007/s12192-017-0797-6
- Zininga, T., Ramatsui, L., Makhado, P. B., Makumire, S., Achilonu, I., Hoppe, H., et al. (2017b). (–)-Epigallocatechin-3-gallate inhibits the chaperone activity of *Plasmodium falciparum* Hsp70 chaperones and abrogates their association with functional partners. *Molecules* 22 (12), 2139. doi:10.3390/molecules22122139
- Zininga, T., and Shonhai, A. (2019). Small molecule inhibitors targeting the heat shock protein system of human obligate protozoan parasites. *Int. J. Mol. Sci.* 20 (23), 5930. doi:10.3390/ijms20235930



## OPEN ACCESS

## EDITED BY

Xolani Henry Makhoba,  
University of Fort Hare, South Africa

## REVIEWED BY

Michele M. Klingbeil,  
University of Massachusetts Amherst,  
United States  
Kirsten J. Meyer,  
University of Toronto, Canada

## \*CORRESPONDENCE

Aileen Boshoff,  
a.boshoff@ru.ac.za

<sup>†</sup>These authors have contributed equally  
to this work and share first authorship

## SPECIALTY SECTION

This article was submitted to Molecular  
Diagnostics and Therapeutics,  
a section of the journal  
Frontiers in Molecular Biosciences

RECEIVED 18 May 2022

ACCEPTED 24 August 2022

PUBLISHED 23 September 2022

## CITATION

Jamabo M, Bentley SJ,  
Macucule-Tinga P, Tembo P, Edkins AL  
and Boshoff A (2022), In silico analysis of  
the HSP90 chaperone system from the  
African trypanosome,  
*Trypanosoma brucei*.  
*Front. Mol. Biosci.* 9:947078.  
doi: 10.3389/fmolb.2022.947078

## COPYRIGHT

© 2022 Jamabo, Bentley, Macucule-Tinga, Tembo, Edkins and Boshoff. This is an open-access article distributed under the terms of the [Creative Commons Attribution License \(CC BY\)](#). The use, distribution or reproduction in other forums is permitted, provided the original author(s) and the copyright owner(s) are credited and that the original publication in this journal is cited, in accordance with accepted academic practice. No use, distribution or reproduction is permitted which does not comply with these terms.

# In silico analysis of the HSP90 chaperone system from the African trypanosome, *Trypanosoma brucei*

Miebaka Jamabo<sup>1†</sup>, Stephen John Bentley<sup>1†</sup>,  
Paula Macucule-Tinga<sup>1</sup>, Praise Tembo<sup>1</sup>, Adrienne Lesley Edkins<sup>2</sup>  
and Aileen Boshoff<sup>1\*</sup>

<sup>1</sup>Biotechnology Innovation Centre, Rhodes University, Grahamstown, South Africa, <sup>2</sup>Department of Biochemistry and Microbiology, Biomedical Biotechnology Research Unit (BioBRU), Rhodes University, Grahamstown, South Africa

African trypanosomiasis is a neglected tropical disease caused by *Trypanosoma brucei* (*T. brucei*) and spread by the tsetse fly in sub-Saharan Africa. The trypanosome relies on heat shock proteins for survival in the insect vector and mammalian host. Heat shock protein 90 (HSP90) plays a crucial role in the stress response at the cellular level. Inhibition of its interactions with chaperones and co-chaperones is being explored as a potential therapeutic target for numerous diseases. This study provides an *in silico* overview of HSP90 and its co-chaperones in both *T. brucei brucei* and *T. brucei gambiense* in relation to human and other trypanosomal species, including non-parasitic *Bodo saltans* and the insect infecting *Crithidia fasciculata*. A structural analysis of *T. brucei* HSP90 revealed differences in the orientation of the linker and C-terminal domain in comparison to human HSP90. Phylogenetic analysis displayed the *T. brucei* HSP90 proteins clustering into three distinct groups based on subcellular localizations, namely, cytosol, mitochondria, and endoplasmic reticulum. Syntenic analysis of cytosolic HSP90 genes revealed that *T. b. brucei* encoded for 10 tandem copies, while *T. b. gambiense* encoded for three tandem copies; *Leishmania major* (*L. major*) had the highest gene copy number with 17 tandem copies. The updated information on HSP90 from recently published proteomics on *T. brucei* was examined for different life cycle stages and subcellular localizations. The results show a difference between *T. b. brucei* and *T. b. gambiense* with *T. b. brucei* encoding a total of twelve putative HSP90 genes, while *T. b. gambiense* encodes five HSP90 genes. Eighteen putative co-chaperones were identified with one notable absence being cell division cycle 37 (Cdc37). These results provide an updated framework on approaching HSP90 and its interactions as drug targets in the African trypanosome.

## KEYWORDS

African trypanosomiasis, *Trypanosoma brucei*, HSP90, molecular chaperones, co-chaperone, heat shock proteins, HSP83

# 1 Introduction

*Trypanosoma brucei* (*T. brucei*), is an extracellular blood- and tissue-borne protozoan parasite transmitted by *Glossina* (tsetse) fly vectors, which causes devastating diseases in humans, wild animals, and domesticated livestock (Brun et al., 2010). Human African trypanosomiasis (HAT, also known as African sleeping sickness) is a potentially fatal tropical disease found in remote rural regions of sub-Saharan Africa and often coincides with insubstantial health care systems (Fèvre et al., 2008). HAT is caused by two subspecies of *T. brucei*; the chronic form of the disease, which is endemic to Central and Western Africa, is caused by *Trypanosoma brucei* (*T. b.*) *gambiense*, and the acute zoonotic form, which is endemic to Eastern and Southern Africa, is caused by *T. b. rhodesiense* (Simarro et al., 2010; Büscher et al., 2017). The livestock disease, nagana, is caused by *T. b. brucei* and has been shown, along with *T. congolense* and *T. vivax*, to have a crippling effect on socioeconomic development within sub-Saharan Africa (Alsan, 2015; Morrison et al., 2016). Recently, atypical human trypanosomiasis was reported to have emerged, with animal *Trypanosoma* species increasingly being detected in humans (Kumar et al., 2022). Despite the decreasing number of HAT cases and the first recently approved oral treatment called fexinidazole, which has now been added to the updated WHO guidelines as the recommended treatment for first and second stages *T. b. gambiense* HAT (Deeks, 2019; WHO, 2019; Lindner et al., 2020). There is still a need for the development of new and more effective drugs due to lack of a vaccine and increasing parasite resistance (Barrett and Croft, 2012). Molecular chaperones have been identified as an attractive target for drug development against protozoan parasites as this protein family plays essential roles in stress-induced stage differentiation and are vital for disease progression and transmission (Requena et al., 2015; Bentley et al., 2019; Zininga and Shonhai, 2019).

The 90-kDa heat shock protein (HSP90) family contains essential, highly conserved, and abundant molecular chaperones (Csermely et al., 1998; Chen et al., 2006; Johnson, 2012) that facilitate the proper folding and maturation of a large but specific group of substrates called client proteins (Jakob et al., 1995; Hartl et al., 2011; Hoter et al., 2018). More than 400 client proteins of human HSP90 have been identified to date (listed at <http://www.picard.ch/>), with many of them being implicated in protein folding and degradation, signaling pathways, cellular trafficking, cell cycle regulation, and differentiation (Echeverría et al., 2011; Samant et al., 2012; Taipale et al., 2012). In humans, the HSP90 family normally comprises four isoforms that are localized in various cellular compartments. Two HSP90 isoforms (the stress-inducible form HSP90 $\alpha$ /HSPC2 and the constitutive form HSP90 $\beta$ /HSPC3) are localized in the cytosol and in the nucleus (Subbarao Sreedhar et al., 2004; Kampinga et al., 2009; Li et al., 2012); GRP94/HSPC4 is present in the endoplasmic reticulum (ER) (Subbarao

Sreedhar et al., 2004; Kampinga et al., 2009; Marzec et al., 2012) and TRAP-1/HSPC5 is found in the mitochondrial matrix (Altieri et al., 2012). Some intracellular HSP90 isoforms are exported and functioned in the extracellular environment to regulate the immune response, cell migration, and invasion (Binder, 2014; Hance et al., 2014; Hunter et al., 2014; Baker-Williams et al., 2019).

HSP90 is a flexible dimeric protein with each monomer containing three domains: an N-terminal nucleotide-binding domain (NBD), a middle client protein-binding domain (MD), and a C-terminal domain (CTD) (Whitesell and Lindquist, 2005; Buchner and Li, 2013; Jackson, 2013). HSP90 is dependent on ATP hydrolysis, and a set of accessory proteins termed co-chaperones, which assist in the recruitment of client proteins and the regulation of the HSP90 reaction cycle (Prodromou, 2012; Röhl et al., 2013). The cytosolic HSP90 isoforms contain a conserved C-terminal MEEVD motif, which acts as a docking site for interaction with co-chaperones that possess the tetratricopeptide repeat (TPR-) domain (Blatch and Lässle, 1999; Prodromou, 1999). Other HSP90 co-chaperones interact with the molecular chaperone through its NBD or M domain (Röhl et al., 2013). Fifty co-chaperones have been identified in the mammalian HSP90 chaperone system to date (Dean and Johnson, 2021): 23 TPR co-chaperones have been characterized, 18 cysteine and histidine-rich domain (CHORD) or SGT1 (CS) domain co-chaperones, and eight co-chaperones without these two domains (Garcia-Ranea et al., 2002; Schopf et al., 2017; Dean and Johnson, 2021). However, the composition of the HSP90 chaperone system appears to vary across organisms, indicating that the role of some co-chaperones may be necessary for activating client proteins in a species-dependent manner, be replaceable with other co-chaperones, or be limited to a distinct subgroup of client proteins (Zuehlke and Johnson, 2010). HSP90 is also subject to post-translational modifications, including s-nitrosylation, phosphorylation, and acetylation, which may influence its activity, cellular localization, or its interaction with co-chaperones, nucleotides, or client proteins (Aoyagi and Archer, 2005; Duval et al., 2007; Rao et al., 2008; Yang et al., 2008). Some HSP90 isoforms are essential for viability, and maintenance of client proteins that are dependent on the chaperone (Citri et al., 2004), making it an attractive drug target for diseases including infectious diseases. Several HSP90 inhibitors, which have been well-studied in the laboratory and clinics for antitumor indications (Porter et al., 2010; Trepel et al., 2010), were also shown to arrest the growth of several kinetoplastids *in vitro* and have activity against *Trypanosoma evansi* and *T. brucei* in mice (Graefe et al., 2002; Pallavi et al., 2010; Meyer and Shapiro, 2013; Meyer et al., 2018). Thus, the repurposing of HSP90 inhibitors designed for cancer treatment is one strategy to evaluate new and effective antitrypanosomal agents (Kaiser et al., 2015).



In *Trypanosoma* and *Leishmania*, the HSP90 machinery plays a pivotal role in environmental sensing and life cycle control (Ploeg et al., 1985; Wiesgigl and Clos, 2001; Graefe et al., 2002). *In silico* analyses of the HSP90/HSPC family of intracellular kinetoplastid parasites has been published (Shonhai et al., 2011; Roy et al., 2012; Figueras et al., 2014; Urményi et al., 2014; Requena et al., 2015), and our study provides an updated and comprehensive analysis for the extracellular parasite, *T. brucei*. *T. brucei* exhibits a digenetic lifestyle, and therefore must adapt to fluctuating environmental conditions, such as change in temperature, pH, nutrients, and the pressure from the immune system, as it transitions from the gut of the tsetse fly to the body fluids of its mammalian host (Jones et al., 2008; Roy et al., 2012). A distinct molecular trait of trypanosomes is their dependence on polycistronic transcription akin to prokaryotes, their mRNAs are mainly generated by trans-splicing and there is a dependence on post-transcriptional mechanisms for gene regulation (Preußner et al., 2012). However, correlation studies comparing the previously reported RNA-seq data of transcript abundance and proteomic data from the procyclic form (PF) and bloodstream form (BSF) of the parasite shows that the differences observed between the PF and BSF are two-fold greater at the proteomic level when compared to the transcriptomic level (Urbaniak et al., 2012; Butter et al., 2013). Given the complexities of transcription, its incomplete representation of the life cycle stages of the parasite as well as its lack of control, trypanosome research has largely shifted to rely on proteomic data (Goos et al., 2017). Numerous proteomic studies have been conducted on the parasite, which have compared protein expression at the different life cycle stages (Gunasekera et al., 2012; Urbaniak et al., 2012; Butter et al., 2013), in the mitochondrion (Panigrahi et al., 2009), mitochondrial importome (Peikert et al., 2017), respiratome (Acestor et al., 2011), mitochondrial membranes (outer, intermembrane space, inner, and matrix) (Acestor et al., 2009), nucleus (Goos et al., 2017), nuclear pore (DeGrasse et al., 2008), glycosomes (Colasante et al., 2006; Güther et al., 2014), flagellum (Broadhead et al., 2006; Subota et al., 2014), and the cell surface (Shimogawa et al., 2015).

*T. brucei* and other trypanosomatids rely on post-translational modifications (PTMs) to increase their proteome diversity and complexity (Backe et al., 2020). Several studies exploring the phosphoproteome and acetylome of trypanosomes (Nett et al., 2009a, 2009b; Urbaniak et al., 2013; Moretti et al., 2018) have found that phosphorylation and acetylation are the most predominant modifications to occur in *T. brucei* proteins. Both PTMs are well known for impacting HSP90 intracellular localization in humans as well as their ability to bind co-chaperones, nucleotides, clients (Nett et al., 2009a; Backe et al., 2020), and even inhibitors (Zhang et al., 2020). However, the PTMs regulatory dynamic in the organellar TRAP-1 and GRP94 in humans are yet to be elucidated for a

global understanding of this critical chaperone activity regulator system.

The aim of this study was to provide a comprehensive depiction of the *T. brucei* HSP90 chaperone system based on structural, functional, and evolutionary analyses. *In silico* tools were used to evaluate the domain conservation, predicted subcellular localizations, syntenic, and phylogenetic analysis of the HSP90 chaperone system in *T. brucei* with respect to both *T. b. brucei* and *T. b. gambiense*. The HSP90 chaperone system was also comparatively analyzed in relation to those found in selected trypanosomatid parasites and *Homo sapiens* (*H. sapiens*). The proteomic findings on HSP90 and its co-chaperones from the numerous published proteomic data on *T. brucei* are presented, and we provide updated insights on the adaptability of the parasite from its stage-specific expressed proteins and provide an overall context for identifying new and potential drug targets for HAT.

## 2 Materials and methods

### 2.1 Database mining, sequence analyses, and the determination of the trypanosomatid and human orthologues

A BLASTP search using the amino acid sequences of the HSP90 isoforms from *T. b. brucei* obtained from previous *in silico* study (Folgueira and Requena, 2007), and the human HSP90AA1/HSPC1, HSPC2, HSP90AB1/HSPC3, HSP90B1/GRP94/HSPC4, and TRAP-1/HSPC5 isoforms were used as queries on the TriTrypDB (version 46) database (<http://tritrypdb.org/tritrypdb/>) (Aslett et al., 2010) and were conducted in order to determine the HSP90/HSPC complement encoded on the *T. b. gambiense* genome, as well as identify new *T. b. brucei* HSP90/HSPC protein members. The e-value was set at an intermediately stringent level of e-10 to identify HSP90/HSPC-related sequences for further analysis. In addition, a keyword search was performed to scan the genome of *T. b. gambiense* for HSP90/HSPC genes on the TriTrypDB database using the terms: “HSP90,” “HSP83,” “heat shock protein,” and “molecular chaperone.” The retrieved amino acid sequences from the various keyword searches were then screened using SMART 7 (Simple Modular Architecture Research Tool; <http://smart.embl-heidelberg.de/>) (Letunic et al., 2012) and PROSITE (<http://prosite.expasy.org/>) (Sigrist et al., 2010) for domains annotated by the online servers as “HSP90.” Incomplete sequences for each protein from TriTrypDB were omitted for construction of Table 1.

For identification of *T. brucei* orthologues of selected cytosolic HSP90 co-chaperones, the protein sequences of 50 human co-chaperones were used as queries in a BLASTP search on the TriTrypDB database. Reciprocal BLASTP was conducted to determine if the identified putative *T. brucei* co-

TABLE 1 HSP90/HSPC proteins from *Trypanosoma brucei* with putative orthologues in *T. cruzi*, *L. major*, *C. fasciculata*, *B. saltans*, and *H. sapiens*.

<i>H. sapiens</i>	<i>H. sapiens</i>	<i>T. brucei</i>	<i>T. cruzi</i> <sup>c</sup>	<i>L. major</i>	<i>C. fasciculata</i>	<i>B. saltans</i>			
Name <sup>a</sup>	Gene ID <sup>b</sup>	Gene ID <sup>b</sup>	Gene ID <sup>b</sup>	Gene ID <sup>b</sup>	Gene ID <sup>b</sup>	Gene ID <sup>b</sup>	Localization <sup>d</sup>	Reference	
HSP90-alpha/ HSPC2	3324	Tb927.10.10890 Tb927.10.10900				CFAC1_280011900 CFAC1_280012000	BSAL_87515	Gunasekera et al. (2012); Urbaniak et al. (2012); Subota et al. (2014); Shimogawa et al. (2015); Dean et al. (2017)	
		Tb927.10.10910	TcCLB.507713.30	LmjF.33.0312 LmjF.33.0314 LmjF.33.0316 LmjF.33.0318					
HSP90-beta/ HSPC3	3326	Tb927.10.10920	C4B63_113g25	LmjF.33.0320 LmjF.33.0323 LmjF.33.0326 LmjF.33.0330			CYT		
		Tb927.10.10930 Tb927.10.10940	C4B63_113g29	LmjF.33.0333 LmjF.33.0336 LmjF.33.0340 LmjF.33.0343			NUC		
		Tb927.10.10950 Tb927.10.10960 Tb927.10.10970 Tb927.10.10980	C4B63_113g30 C4B63_113g33 C4B63_84g87 C4B63_84g88 C4B63_84g89				FLAGELLAR		
		Tbg972.10.13260 Tbg972.10.13270 Tbg972.10.13280	Tc_MARK_3,581	LmjF.33.0346 LmjF.33.0350 LmjF.33.0355 LmjF.33.0360 LmjF.33.0365			CELL SURFACE		
GRP94/ HSPC4	7184	Tb927.3.3580 Tbg972.3.3850	C4B63_10g439 Tc_MARK_3058	LmjF.29.0760		CFAC1_1,00018800	BSAL_88715	ER NUC FLAGELLAR CELL SURFACE	Gunasekera et al. (2012); Urbaniak et al. (2012); Subota et al. (2014); Shimogawa et al. (2015)
TRAP-1/ HSPC5	10131	Tb927.11.2650 Tbg972.11.2900	TcCLB.504153.310 C4B63_2g430 Tc_MARK_6238	LmjF33.2390		CFAC1_230028300	BSAL_33145	MITO FLAGELLAR	Panigrahi et al. (2009); Subota et al. (2014); Dean et al. (2017)

<sup>a</sup>The nomenclature for the HSP90/HSPC, proteins from *T. b. brucei*, and *T. b. gambiense* were derived according to Folgueira and Requena (2007).

<sup>b</sup>The Gene IDs for the members of the *T. b. brucei* (Tb refers to Tbb), *T. b. gambiense*, *T. cruzi*, *C. fasciculata*, *B. saltans*, and *L. major* HSP90/HSPC protein family were retrieved from the TriTrypDB database (<http://tritrypdb.org/tritrypdb/>; Aslett et al., 2010). The Gene IDs for the members of the *H. sapiens* HSP90/HSPC protein family were retrieved from NCBI (<https://www.ncbi.nlm.nih.gov/>).

<sup>c</sup>The Gene IDs, for the orthologues, identified by reciprocal BLASTP, analysis, of three strains of *T. cruzi* are listed. *T. cruzi* CL, Brener Esmeraldo-like (TcCLB), *T. cruzi* Dm28c 2018 (C4B63), and *T. cruzi* marinkelli strain B7 (Tc\_MARK).

<sup>d</sup>Subcellular localizations for the *T. brucei* HSP90/HSPC proteins were either acquired from using the TrypTag database (<http://tryptag.org/>;Dean, Sunter, and Wheeler 2017) and/or predicted using various proteomic datasets and online prediction software listed in the materials and methods.

CYT-Cytosol and MITO- mitochondrion, CYT-Cytosol; MITO- mitochondrion; NUC- nucleus; ER- endoplasmic reticulum; GYLCO-glycosomes; FLAGELLAR- flagellar; CELL SURFACE- cell surface.

chaperone had the closest match to the desired human co-chaperone. The putative amino acid sequences of the co-chaperones from both *T. brucei* subspecies were used as queries in a BLASTP search on the National Centre for Biotechnology Information (NCBI) website ([www.ncbi.nlm.nih.gov](http://www.ncbi.nlm.nih.gov)), using the default parameters. If the most similar ortholog in the *T. brucei* subspecies was identical to the HSP90 co-chaperones sequence used as the first query, the sequence of the second query was selected as an ortholog. Reciprocal BLASTP was also conducted for the identification of human and selected trypanosomastid orthologues of the putative HSP90/HSPC and HSP90 co-chaperone proteins from both *T. brucei* subspecies.

## 2.2 Structural analysis of TbHSP83

The retrieved amino acid sequences for hHsp90 $\beta$  (NP\_001258899.1), TbHsp83 (Tb927.10.10890), and TbHsp83 (Tb972.10.13260) were analyzed using Jalview (Waterhouse et al., 2009). A multiple sequence alignment was conducted using Clustal with defaults via the Jalview web service. 3D prediction structures were retrieved from the AlphaFold database (<https://alphafold.ebi.ac.uk/>) by querying the database using the UniProt IDs of the respective proteins. The retrieved structures (TbHsp83- AF-Q389P1-F1; hHsp90 - AF-P08238-F1) were visualized and superimposed using PyMOL molecular graphics system, Version 2.0 Schrödinger, LLC. The FATCAT server (<https://fatcat.godziklab.org/>) was used to analyze the structural differences between the protein homologs (Li et al., 2020). The two structures were determined to be significantly similar with a *p*-value of 0.00 (raw FATCAT score 1931.78), 685 equivalent positions, and RMSD of 1.71 Å and two twists.

## 2.3 Phylogenetic and conserved syntenic analysis

The full-length amino acid sequences for the HSP90/HSPC family in the selected trypanosomastid parasites were obtained from the TriTrypDB database (Aslett et al., 2010), and the human protein sequences were obtained from the NCBI website ([www.ncbi.nlm.nih.gov](http://www.ncbi.nlm.nih.gov)). Accession numbers for the HSP90/HSPC amino acid sequences used in this study are provided in Table 1 and Supplementary Table S1. Multiple sequence alignments were performed using the inbuilt ClustalW program (Larkin et al., 2007) with default parameters in MEGA-X (Kumar et al., 2018) and are listed in Supplementary Figure S1. Maximum-likelihood (ML) was utilized to find the best model of evolution and was selected by the Bayesian information criterion (BIC) implemented in MEGA-X. The amino acid-based HSP90/

HSPC ML phylogeny was reconstructed using the JTT (Jones–Taylor–Thornton) model matrix (Jones et al., 1992), with gamma distribution shape parameter (G). The ML phylogenetic tree was constructed using MEGA-X (Kumar et al., 2018). The accuracy of the reconstructed tree was assessed using a bootstrap test using 1,000 replicates with a pairwise gap deletion mode. The phylogenetic tree for HSP90s was unrooted.

The putative HSP90 genes in the three *T. cruzi* strains homologous to HSP83 identified to be partial, and/or truncated genes were included in the syntenic analysis. Syntenic analysis was conducted to evaluate the conservation of the gene arrangement of the cytosolic HSP83 genes in *T. brucei* and selected trypanosomastid parasites. The conserved syntenic regions surrounding the selected HSP83 genes were searched by examining the conserved co-localization of neighboring genes on a scaffold of the *T. brucei* subspecies (*T. b. brucei* and *T. b. gambiense*) and selected trypanosomastid parasites for this study using genome information from the TriTrypDB database. The identities of unknown neighbor genes of the selected HSP83 genes were conducted using a BLASTP search on the NCBI database.

## 2.4 Physiochemical properties, protein expression, and the determination of the organelle distribution for the *T. brucei* HSP90/HSPC complement

The physiochemical properties, molecular weight (Da), and isoelectric point (pI) of each putative protein was determined using the compute pI/Mw tool from ExPASy ([https://web.expasy.org/compute\\_pi/](https://web.expasy.org/compute_pi/)) (Gasteiger et al., 2005). Data on the previously reported phenotypic RNAi knockdown screen (Alsford et al., 2011), for each member of the HSP90/HSPC complement and identified HSP83 co-chaperones, were retrieved from the TrypsNetDB database (<http://trypsinetdb.org/QueryPage.aspx>) (Gazestani et al., 2017). The organelle distribution for each putative protein was searched using the TrypTag microscopy project's online server (<http://tryptag.org/>) (Dean et al., 2017). This project aims at tagging every trypanosome protein with mNeonGreen (mNG) (Shaner et al., 2013) to determine the protein's localization within the parasite. Proteomic data from the mitochondrion (Panigrahi et al., 2009), mitochondrial importome (Peikert et al., 2017), respiratome (Acestor et al., 2009), mitochondrial membranes (outer, intermembrane space, inner, and matrix) (Acestor et al., 2009), nucleus (Goos et al., 2017), nuclear pore (DeGrasse et al., 2008), glycosomes (Colasante et al., 2006; Güther et al., 2014), flagellum (Broadhead et al., 2006; Subota et al., 2014), and cell surface (Shimogawa et al., 2015) were also used for the

prediction of the organelle distribution for the *T. brucei* HSP90 complements and HSP90/HSPC complements and HSP83 co-chaperones.

## 2.5 Identification of potential post-translational modification sites for the *T. brucei* HSP83 proteins

Data mining from a collection of relevant databases on *T. brucei* PTMs (Nett et al., 2009b; Urbaniak et al., 2013; Moretti et al., 2018; Zhang et al., 2020) for the relevant proteins was retrieved using the previously identified accession numbers. Information on the respective PTMs (modification sites, modification types, and modified residue) were obtained, and the modified residues were mapped onto [Supplementary Figure S2](#) for all HSP90 isoforms from *T. brucei* subspecies (*T. b. brucei* and *T. b. gambiense*) with orthologues from other trypanosomatids and from human, then analyzed for determination of conserved and specific PTMs among the *T. brucei* HSP90 complements.

## 3 Results and discussion

### 3.1 Determination of the *T. b. brucei* and *T. b. gambiense* HSP90/HSPC complements

The protozoan parasite *T. brucei* comprises three subspecies, with the genomes of *T. b. gambiense* and *T. b. brucei* already sequenced (Jackson et al., 2010; Gibson, 2012). Any information obtained from the genome of the non-human infective *T. brucei* subspecies, *T. b. brucei*, can be inferred for the human infective subspecies, *T. b. rhodesiense*, as the *T. b. brucei* TREU927 strain displays the full range of known *T. brucei* phenotypes and possesses similar biological and genetic characteristics (Gibson, 2012). However, the *T. b. gambiense* genome was sequenced due to the subspecies displaying profoundly different biological and genetic characteristics (Jackson et al., 2010). Genome-wide identification and *in silico* analyses of the HSP90/HSPC complement in both *T. brucei* subspecies was conducted to provide an overview of the *T. brucei* HSP90 family. The ortholog of the cytosolic HSP90 member in *T. brucei* is termed HSP83 (Mottram et al., 1989), while in this study we refer to the ER ortholog as GRP94 and the mitochondrial ortholog as TRAP-1. However, to underscore whether discussing a protein from *T. b. gambiense* or *T. b. brucei*, the abbreviations Tbg and Tbb were used in this study, respectively. The orthologous relationships of the HSP90 family from *T. b. brucei* and *T. b. gambiense* to the selected organisms in this study are presented in [Table 1](#), and a comprehensive domain organization of the predicted *T. brucei* HSP90 proteins is illustrated in [Supplementary Figure S3](#).

Twelve putative *HSP90* genes were identified to be encoded on the *T. b. brucei* genome ([Table 1](#)), which is consistent with previous findings (Mottram et al., 1989; Folgueira and Requena, 2007), while *T. b. gambiense* was identified in this study to only have five putative *HSP90* genes. The reduction in the *HSP90* gene numbers found in *T. b. gambiense* could be a consequence of the reduced genome size observed in the human infective subspecies (Dero et al., 1987). The intraspecific genomic variation is largely associated with tandem or segmental duplications observed in *T. b. brucei* (Jackson et al., 2010). This study also identified an unassigned putative *HSP90* gene (Tb11. v5.0543) in the animal infective subspecies, *T. b. brucei*, but this sequence could not be assembled into a chromosome and was part of a bin scaffold that was not considered during reannotation efforts. For the putative *HSP90* genes identified in this study for *T. b. brucei*, 10 of the 12 putative *HSP90* genes identified were found to be homologous to HSP83, whereas in *T. b. gambiense*, three of the five putative *HSP90* genes were homologous to HSP83 ([Table 1](#)). The remaining two *HSP90* genes found in both *T. b. brucei* (Tb927.3.3580 and Tbg972.3.3850) and *T. b. gambiense* (Tb927.11.2650 and Tbg972.11.2900) showed significant identity to the ER and mitochondrial resident paralogues of HSP90, GRP94, and TRAP-1, respectively ([Table 1](#)). This indicates that a single-gene copy for GRP94 and TRAP-1 is encoded on the genome in both *T. brucei* subspecies. Phylogenetic analysis shows that the *T. brucei* HSP90/HSPC family also comprises three distinct HSP90 groups (HSP83, GRP94, and TRAP-1), which cluster into clades according to protein sequence and subcellular localization ([Supplementary Figure S4](#)).

Previous literature reported that 11 *HSP90* genes are encoded on the *Trypanosoma cruzi* (*T. cruzi*) genome (Shonhai et al., 2011). In this study we included three different *T. cruzi* strains: CL Brener Esmeraldo-like (TcCLB), Dm28c 2018 (C4B63), and marinkelli strain B7 (Tc\_MARK) to determine the HSP90/HSPC complement in the American trypanosome. It was identified in this study that the *T. cruzi* CL Brener Esmeraldo-like strain has two *HSP90* genes, the Dm28c 2018 strain has nine *HSP90* genes, and the marinkelli strain B7 has three *HSP90* genes ([Table 1](#)). However, this study identified that many of the *HSP90* genes homologous to HSP83 in the three *T. cruzi* strains were found to be partial and/or truncated genes. In our syntenic analysis, these partial and/or truncated genes were included as they are probably a result of the methodology utilized to sequence the various *T. cruzi* strains, and it is very likely that the truncated sequences are full-length in the genome ([Figure 1](#)). The obvious discrepancy in numbers of genes among the *T. cruzi* strains, and its numerous partial and/or truncated HSP90 sequences has been recently reviewed. This review highlights the difficulties in *T. cruzi* genome analyses (Herrerros-Cabello et al., 2020); the first genome sequenced that is still widely accepted as the main reference has close to 50% repetitions in its sequence (El-Sayed et al., 2005a; 2005b) and though newer genomes have



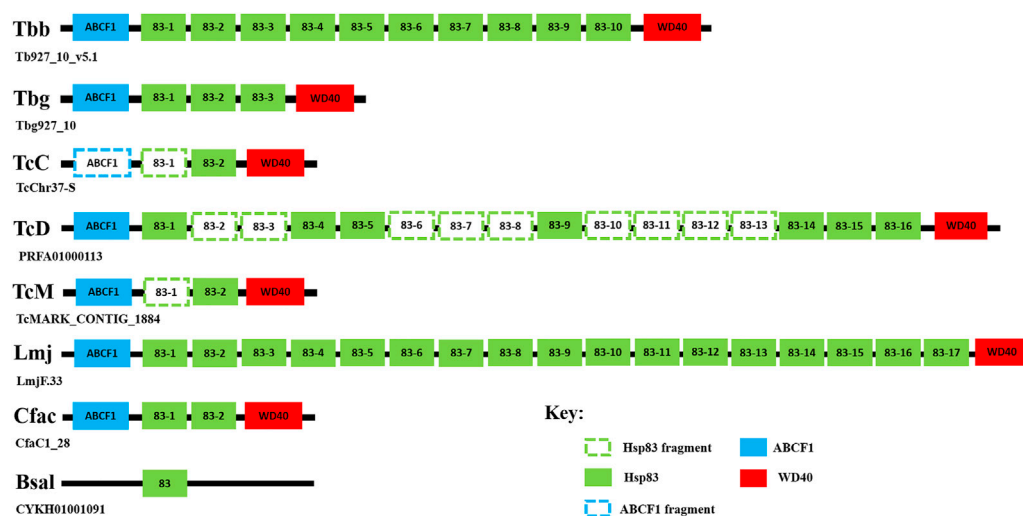


FIGURE 1

Syntenic analysis of the gene arrangement of the *HSP83* genes in *T. brucei* and selected trypanosomatids. The conserved syntenic regions surrounding the selected *HSP83* genes were searched by examining the conserved co-localization of neighboring genes on chromosome 10 on a scaffold of the *T. brucei* subspecies, *T. b. brucei* (Tbb), and *T. b. gambiense* (Tbg), and selected trypanosomatids: *T. cruzi* CL Brener Esmeraldo-like (TcC), *T. cruzi* Dm28c 2018 (TcD) strain, *T. cruzi* marinkelli strain B7 (TcM), *L. major* (Lmj), *B. saltans* (Bsal), and *C. fasciculata* (Cfac). The genome information used for this study was acquired from the TriTrypDB database (<http://tritrypdb.org/tritrypdb/>) (Aslett et al., 2010). The identities of unknown neighbor genes of the selected *HSP83* genes were conducted using a BLASTP search on the NCBI database. Abbreviations: ABCF1: ATP-binding cassette sub-family F member 1; WD40: WD40-repeat protein.

been sequenced using short-read sequencing methods as in the case of the *T. cruzi* marinkelli strain B7, these methods end up causing fragmented chromosomes due to their inability to create a complete chromosome from their short reads technique (Franzén et al., 2012; Herreros-Cabello et al., 2020). Other trypanosomatids included in this study were the non-parasitic *Bodo saltans* (*B. saltans*) (Deschamps et al., 2011) and the insect infecting *Crithidia fasciculata* (*C. fasciculata*) (Wallace, 1966), which were found to have three and four putative *HSP90* genes, respectively (Table 1). Both these trypanosomatids were found to possess genes encoding for all three *HSP90* isoforms, though *C. fasciculata* was identified to possess two *HSP83* genes (Table 1).

Early genomic studies suggested that the human genome contained 16 *HSP90* genes (five functional and 11 pseudogenes), which have been categorized, according to the proposed standardized guidelines for HSP nomenclature, into four isoforms under the superfamily name HSPC (Chen et al., 2006; Kampinga et al., 2009). In contrast to the trypanosomatids, humans have two isoforms of *HSP90* localized in the cytoplasm: the inducible form *HSP90α*/HSPC2 and the constitutive form *HSP90β*/HSPC3 (Subbarao Sreedhar et al., 2004). Phylogenetic analysis has suggested that the two cytosolic isoforms arose from gene duplication, and the organelle *HSP90s* (GRP94/HSPC4 and TRAP-1/HSPC5) developed from a common ancestor (Gupta, 1995; Emelyanov, 2002; Chen et al., 2005).

### 3.2 HSP83

The ortholog of the cytosolic *HSP90* member in trypanosomatids as mentioned previously is commonly referred to as *HSP83* and has been found to be an essential and highly abundant protein that is encoded by multiple gene copies organized in a head-to-tail tandem array (Folgueira and Requena, 2007). It has been identified in this study and previous studies (Mottram et al., 1989; Folgueira and Requena, 2007) that *T. b. brucei* has been shown to encode for 10 tandem copies of *HSP83* (Figure 1), whereas *T. b. gambiense* genome encodes for three tandem copies of *HSP83* (Figure 1). Syntenic analysis revealed that the *TbbHSP83* and *TbgHSP83* genes are both located on chromosome 10 in a head-to-tail orientation, with the same genomic organization being observed in both *T. brucei* subspecies (Figure 1). A discrepancy in *HSP83* gene copy numbers was observed for the three *T. cruzi* strains used in this study (Figure 1). Syntenic analysis revealed that the *T. cruzi* Dm28c 2018 (C4B63) strain has 16 tandem copies of *HSP83*, though nine were partial sequences (Figure 1), whereas both the CL Brener Esmeraldo-like (TcCLB) and marinkelli strain B7 (Tc\_MARK) encode for two *HSP83* genes, with one partial gene each (Figure 1). *Leishmania major* (Lmj) contained the largest *HSP90* family with a total of 19 *HSP90* genes (Table 1), 17 tandem copies were found to be homologous to *HSP83*, and these findings agree with previous studies (Folgueira and Requena, 2007; Shonhai et al., 2011;

Requena et al., 2015), also correlating with the high abundance of the protein being observed in *L. major* and several other *Leishmania* spp. (Brandau et al., 1995). Syntenic regions surrounding the *HSP83* genes were found to be virtually conserved across the selected trypanosomatids, with *B. saltans* being the exception (Figure 1). Thus, the discrepancy in gene copy number of *HSP83* in the two *T. brucei* subspecies and among the trypanosomatids may have arisen from the differences in their life cycles.

Data mining of transcriptomic and proteomic datasets revealed that all identified TbbHSP83 (TbbHSP83 1–10) proteins are constitutively expressed at all life cycle stages of the parasite, as well as expressed at all phases of the cell cycle (Gunasekera et al., 2012; Urbaniak et al., 2012). The protein expression of the TbbHSP83 proteins were all reported to be upregulated at the BSF stage (Urbaniak et al., 2012), despite gene regulation being unchanged in both the bloodstream and procyclic life cycle stages (Gunasekera et al., 2012). All TbbHSP83 proteins were also present in the cell surface proteome (Subota et al., 2014), though only TbbHSP83-10 (Tb927.10.10980) was found to be present in the flagellar proteome (Shimogawa et al., 2015).

The amplification of HSP genes in protozoan parasites has been reported previously (Urményi et al., 2014; Requena et al., 2015; Drini et al., 2016; Bentley et al., 2019) and is considered a means by which the parasites increase chaperone levels to maintain proteostasis under normal and stressful conditions (Wiesgigl and Clos, 2001). The heat shock response is a highly conserved transcriptional program that in most organisms involves increased heat shock gene transcription (de Nadal et al., 2011). However, in trypanosomatids, control of gene expression occurs almost exclusively at the post-transcriptional level, and that HSP synthesis during heat shock depends on regulation of mRNA turnover and translational control (Clayton and Shapira, 2007; Requena, 2011). In *T. brucei*, post-transcriptional regulation of chaperone mRNAs is facilitated by a zinc finger protein, ZC3H11 (Droll et al., 2013). The mRNA transcript levels of TbbHSP83 in BSF parasites increases >2-fold after heat shock (Ooi et al., 2020) and is stabilized by ZC3H11 to promote the survival of the parasite (Droll et al., 2013). Treatment of *T. brucei* BSF parasites with 17-AAG sensitized the parasites to heat shock, as well as caused severe morphological abnormalities and cell cycle disruption (Meyer and Shapiro, 2013). Pharmacological inhibition of HSP83 activity in several *Leishmania* spp. induced morphological and biochemical promastigote-to-amastigote differentiation (Wiesgigl and Clos, 2001; Bente et al., 2003; Hombach et al., 2013), which mimics environmental triggers such as heat shock and acidic milieu, indicating a pivotal role for HSP83 in trypanosomatid protists in environmental sensing and life cycle control. Interestingly, treatment of *T. cruzi* bloodstream trypomastigotes with geldanamycin, induced morphological changes in the parasites but not life cycle progression (Graefe

et al., 2002). Therefore, HSP90 cellular homeostasis as a key factor for the control of stage differentiation appears to be dependent on the tropism of the parasite and the different regulatory pathways for life cycle control. It would be interesting to investigate if the pharmacological inhibition of HSP83 affects cellular differentiation among the three *T. brucei* subspecies.

The monophyletic cluster of the cytosolic HSP83 proteins suggests a general conservation of function, structure, and sequence in the trypanosomatids HSP83 homologs (Supplementary Figure S4). In the amino acid sequences of TbbHSP83 and TbgHSP83 there was a single substitution at D461 to E in TbgHSP83 (Figure 2A). In comparison, hHSP90 was 63% identical in sequence to TbbHSP83 (Figure 2). The three HSP90 proteins displayed the characteristic domains (Figure 2A): the ATP-binding N-terminal domain (NTD); the middle domain (MD), which plays a role in ATPase activity and is responsible for interacting with client proteins and co-chaperones; and the C-terminal domain (CTD), which is responsible for HSP90 dimerization and interaction with the TPR domain-containing chaperones via a C-terminal (MEEVD) motif (Hoter et al., 2018). In addition, the NTD and MD are joined together via a charged linker (Jahn et al., 2014). This linker varies in size and is notably shorter in trypanosomatids compared to its human counterpart (Figure 2A) (Silva et al., 2013). Comparison of the hHSP90 to both TbbHSP83 and TbgHSP83 revealed that the amino acid sequence of the NBD was 68% identical, MD 69% identical, and CTD 60% identical (Figure 2). Conversely, the yeast HSP90 proteins (HSP82 and HSC82) were 97% identical in sequence (a difference of 16 amino acid residues) and yet the two proteins exhibit differences in stability, function, and chemical sensitivity (Girstmair et al., 2019). Residues D78 and E32 are conserved in humans and *T. brucei* HSP90 proteins (Figure 2A). Residue D79 (D78 in *T. brucei*) was previously described to be located deep in the inner region of the ATP-binding pocket of yeast HSP90 and determined to form a hydrogen bond with ATP and together with E33 (E32 in *T. brucei*) are important for ATP binding (Panaretou et al., 1998). Mutations of these two residues in yeast HSP90 led to a loss of viability (Panaretou et al., 1998). In comparison to humans, TbbHSP83 revealed a 50- to 60-fold higher sensitivity to the HSP90 ATPase inhibitor 17-AAG (Jones et al., 2008). The side chain of residue I171 in TbbHSP83 was found to be in contact with L33 and indirectly with I34 (Pizarro et al., 2013), the latter two residues have been implicated in radicicol resistance (Prodromou et al., 2012). Small sequence variations in HSP90 appear to result in large variations in chemical sensitivity between hHSP90 and TbbHSP83 (Jones et al., 2008; Prodromou et al., 2012; Pizarro et al., 2013).

The overall 3D structures of the TbbHSP83 and human HSP90 are similar (Figure 2B). The RMSD between the human and Tb structures is 1.71 Å for a Ca superposition of

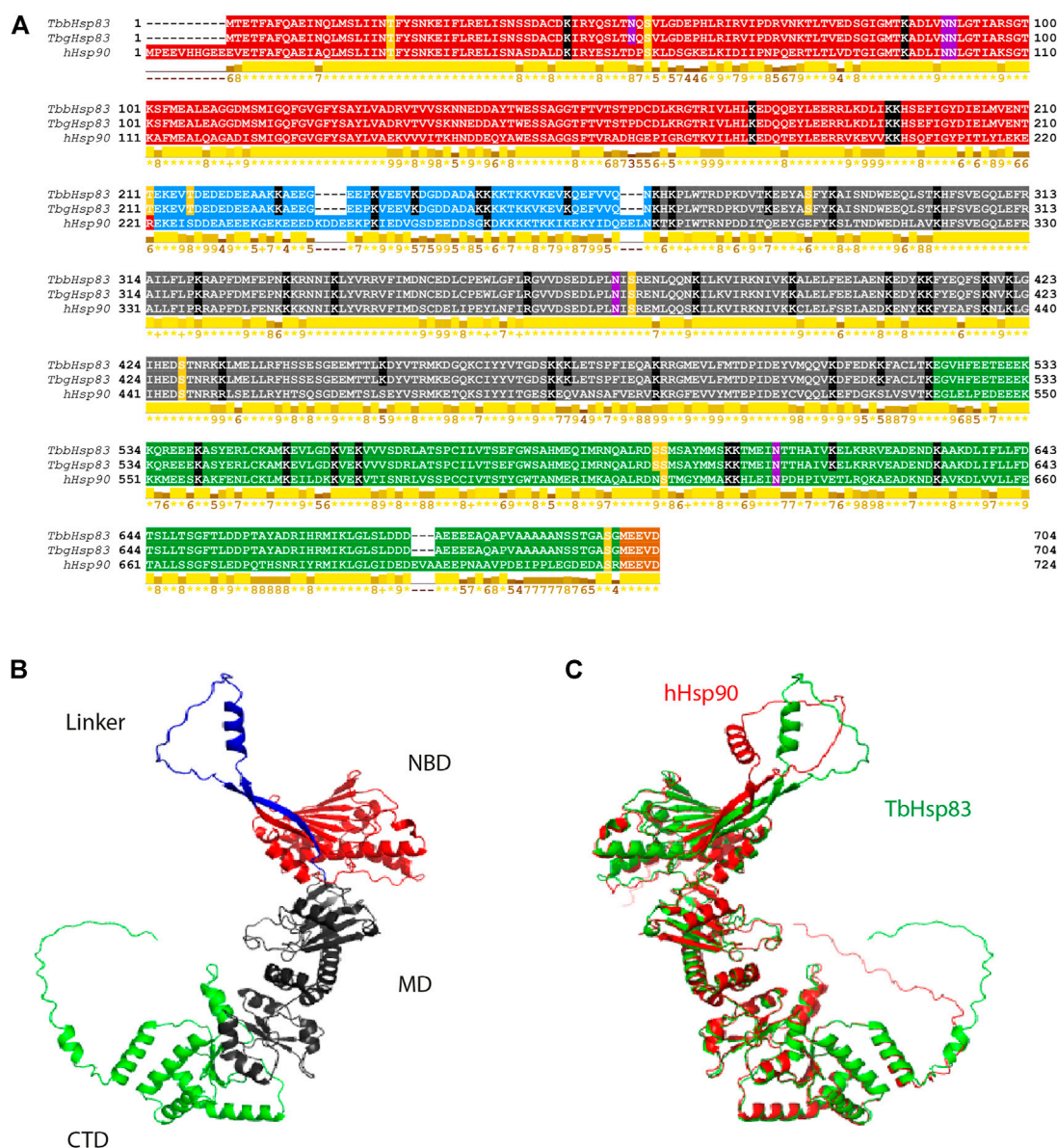


FIGURE 2

Sequence alignment and 3D structural analysis of TbHSP90. (A) Multiple sequence alignment of hHSP90, TbHSP83, and TbHSP90. The NTD is highlighted in red, the charged linker domain in blue, the MD in gray, the CTD in green, and the MEEVD motif in orange. The PTMs are highlighted: yellow—phosphorylation, black—acetylation, and pink—N-glycosylation. Conserved residues involved in ATP interaction are highlighted in brown. Conservation based on physico-chemical properties is shown as a numerical index at the bottom of the alignment: "\*" denotes score of 11 where amino acid residues are identical; "+" denotes score of 10 and indicates all properties are conserved. (B) Predicted 3D structure of the TbHSP83 monomer and (C) superimposed 3D structures of TbHSP83 (green) and hHSP90 (red).

the full-length proteins. The regions of sequence variation reveal themselves more evidently in the flexibility of the protein (Pizarro et al., 2013; López et al., 2021). The major differences that can be seen in the 3D structures are in the charged linker domain and the C-terminal domain (Figure 2B). The orientation of both regions differs to that of the human HSP90 protein. Furthermore, the C-terminal domain has an extension that contains a short helical structure present in TbHSP83 that is

absent in hHSP90 (residues 678–682, EEEEE). The CTD is responsible for dimerization and interaction with co-chaperones, and this may result in the possibility of unique interactors of the TbHSP83 protein. The spatial differences seen in the linker are a direct result of the differences in the length. The hHSP90 has a linker that is seven residues longer than that of TbHSP83 and has a higher overall negative formal charge (Figure 2A). The variation in length of the linker has been

noted across different species, the varying length could affect flexibility, and the varying charge could affect transient domain interactions that exist between the NTD and the linker (Jahn et al., 2014; López et al., 2021).

Post-translational modifications, and particularly phosphorylation of tyrosine, serine, and threonine residues, at multiple sites of cytosolic HSP90 is a well-known chaperone activity modulator mechanism in many organisms (Miyata and Yahara, 1992; Mollapour et al., 2011; Mollapour and Neckers, 2012; Hombach-Barrigah et al., 2019). HSP90 steady-state phosphorylation is species-specific relative to the different cellular environments (Mollapour and Neckers, 2012). Two phosphorylation sites, S53 and S286, were found to be unique to *T. brucei* HSP83 and conserved in all 10 cytosolic HSP83 proteins. The phosphorylation sites T211, T216, and S597 were conserved in all analyzed trypanomastids in this study, while S374 and S698 were found to be conserved in all proteins including humans (Supplementary Figure S2). The same phospho-modified residues were previously described for the cytosolic HSP83 ortholog from *L. donovani* (Hombach-Barrigah et al., 2019). Silencing mutations of *L. donovani* HSP90 T211 and T216 reduced parasite growth, while mutation of S594 reduced growth and infectivity (Hombach-Barrigah et al., 2019). The phosphorylation of *L. donovani* HSP90 at T21 plays a role in the binding of co-chaperones, and mutation of this residue irreversibly inhibited the growth of the promastigote stage (Hombach-Barrigah et al., 2019); however, this residue has not been detected as a *T. brucei* phospho-site (Cunningham et al., 2008; Mollapour et al., 2011; Hombach-Barrigah et al., 2019). The equivalent site in yeast HSP90 (T22) was found to be essential for dimerization and ATPase activity (Cunningham et al., 2008). Acetylation and ubiquitination sites were also predicted and mapped. The predicted N-glycosylation sites, N90, N372, and N612 were conserved in all cytosolic HSP90s analyzed in this study, while N51 was determined to be specific to *T. brucei* HSP83 (Supplementary Figure S2). Two ubiquitination sites identified in *T. brucei* HSP83 as K394 and K560 were found conserved in all analyzed cytosolic HSP90 isoforms in this study (Supplementary Figure S2).

### 3.3 TRAP-1

The mitochondrial isoform of the HSP90/HSPC family was first identified in association with the mammalian tumor necrosis factor 1 (TNF-1) protein, hence termed TRAP-1 (Song et al., 1995). It was promptly suggested as a member of the 90-kDa molecular chaperone family due to strong homology with other HSP90 members (Song et al., 1995). Since then, TRAP-1/HSPC5 orthologues have been identified in a variety of eukaryotic and prokaryotic organisms and was also recently referred to as HSP84 in *T. brucei* (Meyer and Shapiro, 2021). RNAi knockdown of HSP84 showed growth defects and led to

loss of kinetoplasts in bloodstream form trypanosomes (Meyer and Shapiro, 2021). Our study identified a single entry for a putative TRAP-1 gene annotated in the genomes of both *T. brucei* (Tb927.11.2650) and *T. b. gambiense* (Tbg972.11.2900) (Table 1). The selected kinetoplastids in this study were also identified to encode a single copy of TRAP-1 (Table 1), which are consistent with previous studies (Folgueira and Requena, 2007), except for *T. cruzi*, which was previously stated to encode for two TRAP-1 orthologues (Folgueira and Requena, 2007; Shonhai et al., 2011). Phylogenetic analysis indicates a general conservation in trypanosomatid TRAP-1 proteins (Supplementary Figure S4), though little experimental characterization of these genes has been conducted in kinetoplastids. It is predicted that the cellular role of the trypanosomatid TRAP-1 proteins will be orthologous to human TRAP-1, whose major functions is to maintain mitochondrial integrity, modulate mitochondrial metabolism, and protect against mitochondrial apoptosis (Altieri et al., 2012). Furthermore, human TRAP-1 counteracts protein aggregation inside the mitochondria and supports protein folding (Siegelin et al., 2011), leading to healthy, intact mitochondria.

Mammalian TRAP-1 orthologues are localized predominantly in the mitochondrial matrix, where it exists as at least six different protein variants, resulting from splicing patterns, amino acid additions and/or deletions (Cechetto and Gupta, 2000; Felts et al., 2000). The translation of the main TRAP-1 mRNA generates a precursor protein of 704 amino acids that contains a putative 59-amino acid, N-terminal mitochondrial import sequence, which is removed upon organelle import (Felts et al., 2000; Schleiff and Becker, 2011). It was predicted that both TbbTRAP-1 and TbgTRAP-1 localize in the mitochondria, as the proteins possess a positively charged N-terminal leader sequence (Supplementary Figure S1). Proteomic and localization studies confirmed that TbbTRAP-1 localizes to the mitochondria (Panigrahi et al., 2009; Dean et al., 2017), but interestingly the protein is also present in the flagella of *T. b. brucei* BSF parasites (Subota et al., 2014) (Table 1). The subcellular distribution of TbbTRAP-1 during the parasite's life cycle could be related to the shape and functional plasticity of the *T. brucei* single mitochondrion, which undergoes profound alterations to adapt to the different host environments (Osellame et al., 2012). Phenotypic knockdown of TbbTRAP-1 had a detrimental effect on the survival and fitness of the parasite at the procyclic stage of its life cycle and negatively affected parasite differentiation (Alsford et al., 2011). Thus, *T. brucei* TRAP-1 proteins may be an important modulator of mitochondrial bioenergetics at the procyclic stage, as well as play an integral role in parasite pathogenesis.

The phosphorylation sites, S363 and S453, were conserved in the middle domain of TRAP-1 for all trypanosome proteins, while S439 was conserved in TRAP-1 for all proteins studied including humans (Supplementary Figure S2). Several amino



acids were identified as potential targets for post-translational modifications in human TRAP-1, yet the phosphorylation mechanism remains to be revealed (Altieri et al., 2012). Acetylation sites found specific for TbbTRAP-1 include K109, K480, and K601 (Supplementary Figure S2). Most of the PTMs of HSP90 and other inferences stated are yet to be verified experimentally.

### 3.4 GRP94

The glucose-regulated 94 kDa protein (GRP94) is a HSP90 family member residing in the lumen of the endoplasmic reticulum (ER) (Argon and Simen, 1999), where it is involved in the maturation of membrane-resident and secreted protein clients (Marzec et al., 2012). GRP94 is present as a single gene in all metazoa, although the gene is not found in many unicellular organisms such as bacteria, archaea, yeast, and most fungi (Marzec et al., 2012). This study identified a single putative entry for the GRP94 gene in both *T. brucei* subspecies and the selected trypanosomatids in this study (Table 1). These findings are consistent with previous findings for *T. brucei* and *L. major* (Folgueira and Requena, 2007), though previous reports indicated that *T. cruzi* CL Brener Esmeraldo-like strain encodes three GRP94 orthologues (Folgueira and Requena, 2007; Shonhai et al., 2011). However, this study identified that only one GRP94 gene in *T. cruzi* CL Brener Esmeraldo-like strain (TcCLB.506,989.190) was found to encode for a full-length sequence. The genome of this *T. cruzi* strain needs to be further investigated to determine if these partial sequences of the GRP94 genes (TcCLB.506591.4 and TcCLB.503811.10) are due to sequencing errors.

Both TbbGRP94 and TbgGRP94 genes are present on chromosome III and are shown to encode for proteins considerably longer in amino acid sequence when compared to HSP83 (Supplementary Figure S1), which is characteristic of GRP94 protein members (Stechmann and Cavalier-Smith, 2003; Johnson, 2012). GRP94 proteins share structural similarity with cytosolic HSP90 proteins, though the N-terminus contains an ER signal peptide while the C-terminal MEEVD peptide is replaced with the KDEL motif that is required for retention in the ER (Argon and Simen, 1999). Sequence analysis of TbbGRP94 and TbgGRP94 indicates that the GRP94 protein shares domain architecture with typical GRP94 proteins including the possession of an N-terminal ER signal peptide (Supplementary Figure S1). However, a variation in the C-terminal ER retention motif, KDEL, is observed in all the trypanosomatid orthologues of GRP94; AGDL in *Trypanosoma* spp., KEEL in *B. saltans*, and EGDG in *C. fasciculata* and all *Leishmania* spp (Supplementary Figure S1). Transcriptomic and proteomic studies revealed that TbbGRP94 is expressed at all life cycles and throughout the phases of the cell cycle (Supplementary Table S2). Proteomic

studies confirm the presence of GRP94 in flagella and cell surface (Subota et al., 2014; Shimogawa et al., 2015).

In trypanosomatids, the first recognized and characterized GRP94 gene was in *Leishmania infantum* (*L. infantum*). The GRP94 ortholog in *L. infantum* was shown to localize in the ER and share many of the activities of GRP94s of other eukaryotes (Descoteaux, 2002). Unlike GRP94 in mammalian cells, LinGRP94 is not essential for cell viability, and LinGRP94 mRNA is induced developmentally rather than by canonical GRP94-inducing stresses (Descoteaux, 2002). The protein was highly immunogenic during *Leishmania* infection (Larreta et al., 2000, 2002), and essential for lipophosphoglycan (LPG) assembly (Descoteaux, 2002), an abundant surface glycolipid of *Leishmania* promastigotes that is critical to parasite virulence (Yao et al., 2003). Effectively, the critical role of GRP94 in *Leishmania* appears to be adapted to the synthesis of glycoconjugates and directing the host immune response implicating a pivotal role in parasite virulence (Descoteaux, 2002). Though whether this specialized role is conserved in *T. brucei* and other trypanosomatids will need to be elucidated. The function and cellular roles of TbGRP94 should be explored, given the immunogenic and antigenic properties shown by the *L. infantum* GRP94, as this protein could constitute a valuable molecule for diagnostic purposes, and quite possibly a potential candidate for studies of protective immunogenicity. N-glycosylation sites, N137, N370, and N639, were conserved across all species studies (Supplementary Figure S2). GRP94 phosphorylation sites, S63 and S372, were conserved for all species analyzed, while S625 was conserved in *T. brucei* and *T. cruzi* (Supplementary Figure S2). K472 and K504 acetylation sites were conserved in all the trypanosome species, while K515, K542, R587, and Q646 were unique to *T. brucei* (Supplementary Figure S2).

### 3.5 The *T. brucei* HSP90 co-chaperone system

In all organisms, HSP90 is a dynamic protein that undergoes a conformational cycle that is directionally determined, in large part by ATP binding/hydrolysis, and a cohort of proteins termed co-chaperones (Panaretou et al., 1998; Prodromou, 1999; Johnson and Brown, 2009). The HSP90 co-chaperone system in intracellular protozoan parasites has been explored in previous studies (Seraphim et al., 2013; Figueras et al., 2014). Thus, using the human and trypanosomatid systems, this study analyzed the composition of the *T. brucei* HSP83 co-chaperone system. It was determined in this study that *T. brucei* possesses a similar number of co-chaperones compared to humans (Table 2), with one notable absence being cell division cycle 37 (Cdc37). The absence of a gene encoding for Cdc37 has also been noted in several intracellular protozoan parasites (Chua et al., 2014; Figueras et al., 2014; Tatu and Neckers, 2014; Hombach-

TABLE 2 HSP83/HSPC co-chaperones from *Trypanosoma brucei* with their putative orthologues in *T. cruzi*, *L. major*, *C. fasciculata*, *B. saltans*, and *H. sapiens*.

<i>H. sapiens</i>	<i>H. sapiens</i>	<i>T. brucei</i>	<i>T. cruzi</i> <sup>3</sup>	<i>L. major</i>	<i>C. fasciculata</i>	<i>B. saltans</i>		
Name	Gene ID <sup>1</sup>	Gene ID <sup>1</sup>	Gene ID <sup>1</sup>	Gene ID <sup>1</sup>	Gene ID <sup>1</sup>	Gene ID <sup>1</sup>	Localization <sup>2</sup>	Reference
A: TPR-containing Hsp90 co-chaperones								
STI1/HOP	10963	Tb927.5.2940	Tc_MARK_9009	LmjF08.1110	CFAC1_020023900	BSAL_57725	CYTO	Gunasckera et al. (2012); Urbaniak et al. (2012); Butter et al. (2013); Shimogawa et al. (2015); Dean et al. (2017)
		Tbg972.5.4130	C4B63_59g115				NUC	
PP5	5536	Tb927.10.13670 Tbg972.10.16800	TcCLB.507.993.190	LmjF.18.0150	CFAC1_140007400	BSAL_15705	CYTO (BSF, PF)	Gunasckera et al. (2012); Urbaniak et al. (2012); Butter et al. (2013); Dean et al. (2017)
			C4B63_4g368					
Cyp40	5481	Tb927.9.9780 Tbg972.9.5630	TcCLB.506.885.400 Tc_MARK_4311	LmjF.35.4770	CFAC1_300099000	BSAL_06490	CYTO	Oberholzer et al. (2011); Dean et al. (2017)
DnaJC7	7266	Tb927.10.4900	TcCLB.504.203.60	LmjF.36.0500	CFAC1_250012000	BSAL_30720	CYTO	Urbaniak et al. (2012); Butter et al. (2013); Dean et al. (2017)
			Tc_MARK_8493					
FKBP5	2289	Tbg972.10.5950	C4B63_13g112				NUC (BSF, PF)	Gunasckera et al. (2012); Urbaniak et al. (2012); Butter et al. (2013); Subota et al. (2014); Shimogawa et al. (2015); Dean et al. (2017)
		Tb927.10.16100 Tbg972.10.19710	TcCLB.511.353.10 Tc_MARK_4665	LmjF.19.1530	CFAC1_210025000	BSAL_03610 BSAL_65235	CYTO	
			C4B63_157g28 C4B63_171g30				FLAGELLAR (BSF, PF)	
SGT	6449	Tb927.6.4000 Tbg972.6.3780	TcCLB.511.737.10 Tc_MARK_2022	LmjF.30.2740	CFAC1_260051600	BSAL_66445	CYTO	Gunasckera et al. (2012); Urbaniak et al. (2012); Butter et al. (2013); Subota et al. (2014); Shimogawa et al. (2015); Dean et al. (2017)
			C4B63_18g260				FLAGELLAR	
TPR domain protein	7268	Tb927.10.11380	TcCLB.507.709.70	LmjF.33.0700	CFAC1_280016100		CELL SURFACE (BSF, PF)	Urbaniak et al. (2012); Butter et al. (2013); Dean et al. (2017)
		Tbg972.10.13740	Tc_MARK_3620				CYTO	
			C4B63_84g34					
B: CS-containing Hsp90 co-chaperones								
p23	10728	Tb927.9.10230 Tb927.10.2620 Tbg972.9.5930 Tbg972.10.3260	TcCLB.509.551.70 TcCLB.506.407.60	LmjF.35.4470 LmjF.34.0210	CFAC1_300096200 CFAC1_290030000	BSAL_38665	CYTO	Dean et al. (2017)
			C4B63_2g235 C4B63_47g40				FLAGELLAR	
CHORD	26548	Tb927.1.3170	TcCLB.507.837.40	LmjF.20.1620	CFAC1_170031900	BSAL_00100	NUC	Gunasckera et al. (2012); Urbaniak et al. (2012); Butter et al. (2013); Dean et al. (2017)
		Tbg972.1.1930	Tc_MARK_7.282				CYTO (BSF, PF)	
Aarsd1	80755	Tb927.9.6650	TcCLB.504.883.50	LmjF.15.0690	CFAC1_240038900	BSAL_93700	CYTO	Dean et al. (2017)
			Tc_MARK_5844					
PIH1D1	55011	Tbg972.9.3510	C4B63_136g36					Dean et al. (2017)
		Tb927.9.10490 Tbg972.9.6100	TcCLB.506.147.150	LmjF.35.4330	CFAC1_300094700		CYTO	
PIH1D3	139212	Tb927.3.4410 Tbg972.3.4850	TcCLB.507.257.160	LmjF.29.1850	CFAC1_190042200	BSAL_07820	CYTO (BSF, PF)	Urbaniak et al. (2012); Butter et al. (2013); Dean et al. (2017)
			Tc_MARK_3.141					
Ubiquitin hydrolase	10869	Tb927.9.13430 Tbg972.9.8400	C4B63_10g277			BSAL_56185		Dean et al. (2017)
			TcCLB.510.749.40	LmjF.35.2410	CFAC1_300073100	BSAL_27670	CYTO	
			Tc_MARK_4527					
			C4B63_2g83					
CS domain/ TPR repeat	161582	Tb927.11.16050 Tbg972.11.17990	TcCLB.509.073.90	LmjF.32.2850	CFAC1_190042200	BSAL_62790	CYTO	Dean et al. (2017)
			Tc_MARK_3396					
NADH- cytochrome B5 reductase	51167	Tb927.11.3750 Tbg972.11.4290	C4B63_2g215					Dean et al. (2017)
			TcCLB.511.047.40	LmjF.13.1060	CFAC1_220039400	BSAL_93355	CYTO	
LRRC	23639	Tb927.11.3750 Tbg972.11.4290	Tc_MARK_6965					
			C4B63_46g107					
			TcCLB.503.671.30	LmjF.29.2210	CFAC1_200030000	BSAL_68670	CYTO	Butter et al. (2013); Dean et al. (2017)
			Tc_MARK_3.178					
			C4B63_23g85					
C: Non-TPR, non-CS-containing Hsp90 co-chaperones								
Aha1	10598	Tb927.10.13710 Tbg972.10.16840	TcCLB.507.993.150	LmjF.18.0210	CFAC1_140008400	BSAL_15670	CYTO	Gunasckera et al. (2012); Urbaniak et al. (2012); Butter et al. (2013); Dean et al. (2017)
			Tc_MARK_4860					
Phosphoducin	79031	Tb927.11.4930	C4B63_4g357	LmjF.24.0170	CFAC1_21006700	BSAL_83285	NUC (BSF, PF)	Dean et al. (2017)
			TcCLB.507.669.130				CYTO	
			Tc_MARK_6540					
		Tbg972.11.5550	C4B63_28g45					

<sup>a</sup>The Gene IDs for the *T. b. brucei* (Tb refers to Tbb), *T. b. gambiense*, *T. cruzi*, *C. fasciculata*, *B. saltans*, and *L. major* HSP83/HSPC co-chaperones were retrieved from the TriTrypDB database (<http://tritrypdb.org/tritrypdb/>; Aslett et al., 2010). The Gene IDs for the members of the *H. sapiens* HSP90/HSPC co-chaperones were retrieved from NCBI (<https://www.ncbi.nlm.nih.gov/>).

<sup>b</sup>The Gene IDs, for the orthologues, identified by reciprocal BLASTP analysis, of three strains of *T. cruzi* are listed. *T. cruzi* CL, Brener Esmeraldo-like (TcCLB), *T. cruzi* Dm28c 2018 (C4B63), and *T. cruzi* marinkelli strain B7 (Tc\_MARK).

<sup>c</sup>Subcellular localizations for the *T. brucei* HSP83/HSPC co-chaperone proteins were acquired from using the TrypTag database (<http://tryptag.org/>; Dean et al., 2017) and/or determined using various proteomic datasets listed in the materials and methods.

CYT-Cytosol; MITO- mitochondrion; NUC- nucleus; ER- endoplasmic reticulum; GYLCO-glycosomes; FLAGELLAR- flagellar; CELL SURFACE- cell surface.

Barrigah et al., 2019) and was not evident in 10 out of 19 divergent eukaryotic species examined in a study by Johnson and Brown (2009). Cdc37 is a co-chaperone that has a specialized and indispensable role in the maturation and/or stabilization of a large subset of protein kinases in mammalian cells (Smith and Workman, 2009). The absence of Cdc37 in some species is that clients that are dependent on a specific co-chaperone in one species may not require HSP90 for function in other species, thus the protein kinases in protozoan parasites may have evolved in such a way that the proteins bind a different co-chaperone or are independent of HSP90 for function. Since little is known about why a protein becomes dependent on HSP90 for activity or stability, it poses interesting questions on the mechanism by which the maturation and regulation of protein kinases in protozoan parasite is mediated dependent or independent of HSP83. Exploration of this mechanism may provide a potential avenue for chemotherapeutics since protein kinases are also an attractive drug target in infectious disease, such as African trypanosomiasis. The identified HSP83 co-chaperones in both *T. brucei* subspecies are listed in Table 2. In addition, the HSP90 co-chaperones were categorized in this study based on the presence of a TPR or CS (CHORD and SGT1) domain.

### 3.6 TPR-containing HSP83 co-chaperones

Seven putative TPR-containing co-chaperones were identified in this study.

#### 3.6.1 Stress-inducible protein 1 (STI1)

Stress-inducible protein 1 (STI1), also known as HSP70/HSP90-organizing protein (HOP or STIP1) in mammals, is one of the best studied co-chaperones in the HSP90 reaction cycle (Chang et al., 1997; Johnson et al., 1998) as it acts as an adapter protein, mediating the interaction between HSP70 and HSP90 through its TPR domains (Brinker et al., 2002; Odunuga et al., 2003; Baidur-Hudson et al., 2015). STI1/HOP is a widely conserved HSP90 co-chaperone and has been annotated and characterized across diverse organisms including several kinetoplastid protists. Initially thought to be an indispensable protein, recent discoveries in yeast and some eukaryotes show that direct interaction can take place *in vitro* between HSP70 and HSP90 in the absence of HOP (Kravats et al., 2018; Bhattacharya et al., 2020). A single *STI1/HOP* gene was found encoded in both *T. brucei* subspecies (Table 2). Nine TPR motifs arranged into three TPR domains (TPR1, TPR2A, and TPR2B) in addition to two domains rich in proline and aspartic acid (DP1 and DP2) were predicted (Scheufler et al., 2000; Nelson et al., 2003). Both STI1/HOP orthologues in *T. cruzi* and *L. major* were found to immunoprecipitate with HSP83 and HSP70 and co-localize with these chaperones in the cytoplasm and/or around nucleus (Webb et al., 1997; Schmidt et al., 2011). The expression of HOP isoforms was increased in response to different environmental

stresses (Webb et al., 1997; Schmidt et al., 2011), with LmjHOP being upregulated when the parasites are exposed under heat stress conditions (Webb et al., 1997), whereas only nutritional stress-induced expression of TcSTI1 in the late growth phase of epimastigotes (Schmidt et al., 2011). The HSP90-STI1 complex in *L. major* and *T. cruzi* has been shown to be pivotal to parasite differentiation (Webb et al., 1997; Hombach et al., 2013). Proteomic analysis in *T. brucei* indicates that TbbSTI1 is part of the cell surface (PF) proteome during the procyclic stage (Shimogawa et al., 2015). Though TbbSTI1 is present in both the BSF and PF stages of the parasite, it was more highly expressed in the bloodstream form (Gunasekera et al., 2012; Urbaniak et al., 2012; Butter et al., 2013). These data suggest that the STI1 ortholog in both *T. brucei* subspecies should function as an adapter protein for TbHSP83 and TbHSP70s, participating in the foldosome apparatus necessary for maintaining proteostasis, cytoprotection, and modulating parasite differentiation.

#### 3.6.2 Protein phosphatase 5 (PP5)

Protein phosphatase 5 (PP5) is a member of the PPP family of serine/threonine protein phosphatases and it associates with HSP90 in complexes during client protein maturation (Cohen, 1997; Chinkers, 2001; Golden et al., 2008). PP5 is characteristically unique from other PPP family members, in which it possesses an N-terminal TPR domain (Borthwick et al., 2001), which mediates interaction with HSP90 (Chen et al., 1996). This interaction enables PP5 to modify the phosphorylation status of HSP90 client proteins (Golden et al., 2008). The gene for PP5 in *T. brucei* (TbbPP5) has been extensively studied. TbbPP5 encodes a ~52-kDa protein that possesses the canonical N-terminal TPR domain and phosphatase catalytic domain (Anderson et al., 2006). TbbPP5 interacted with TbbHSP90 *in vivo* and co-localized with the chaperone in the cytosol of PRO parasites (Jones et al., 2008). Both TbbPP5 and TbbHSP90, upon heat shock and geldanamycin treatment, accumulated in the nucleus (Jones et al., 2008), indicating that both TbbPP5 and TbbHSP90 translocate to the nucleus when the parasites are exposed to proteotoxic stresses (Jones et al., 2008). TbbPP5 was detected in both BSF and PF stages of the parasite but upregulated in the procyclic form (Gunasekera et al., 2012; Urbaniak et al., 2012; Butter et al., 2013). Overexpression of TbbPP5 was found to partially negate the effect of geldanamycin treatment on cell growth, which indicates that the co-chaperone enhances the chaperoning function of TbbHSP90 and promotes the folding and maturation process of important regulatory molecules, which facilitate cell growth.

#### 3.6.3 Peptidyl-prolyl cis-trans-isomerases (PPIases)

The immunophilin superfamily consists of highly conserved proteins with rotamase or peptidyl-prolyl cis-trans-isomerase (PPIase) activity that accelerates protein folding by mediating the isomerization of X-Pro-peptide bonds (Galat, 2003; Pratt et al.,

2004). The best characterized PPIases belong to two families, the cyclophilin-type (Cyp) and the FKB-506 drug-binding protein type (FKBP) (Steiner and Haughey, 2010). Data mining of the *T. brucei* genome identified that Cyp40 and a putative FKB-506 binding like protein (FKBPL) are present in the extracellular parasite proteome (Table 2). Investigation of the domain structure and sequence conservation indicate that both Cyp40 and FKBPL in *T. brucei* were shown to display the characteristic two-domain structure of a N-terminal PPIase domain and a C-terminal TPR domain (data not shown). Though it must be noted that the C-terminal TPR domain in kinetoplastid Cyp40 underwent substantial evolutionary modification (Yau et al., 2010), thus potentially impacting Cyp40-HSP83 interactions. Future structure/function studies should explore the effect these modifications have on the isomerase and chaperone activities of the protein in comparison to its human counterpart.

Studies conducted on the Cyp40 ortholog in *L. donovani* have revealed that the protein functions in *Leishmania* stage-specific morphogenesis, motility, and the development of infectious-stage parasites (Yau et al., 2010, 2014). The study conducted by Yau et al. (2014) also suggested that LdCyp40 and LdFKBP2 functions in regulating *Leishmania* cytoskeletal dynamics. Given the capacity of Cyp40 and FKBPL to compete for molecular partners (Ratajczak et al., 2003), LdCyp40 may interact with microtubules to promote tubulin polymerization as a means of counteracting LdFKBP2-mediated depolymerization. RNAi-mediated knockdown of both Cyp40 and FKBPL in *T. brucei* parasites demonstrated that these proteins are essential at the BSF stage and are required for parasite differentiation (Alsford et al., 2011; Gunasekera et al., 2012; Urbaniak et al., 2012; Butter et al., 2013). Proteomic data predicted these proteins to reside in the cytosol and flagellar (Oberholzer et al., 2011; Subota et al., 2014). Together these data indicate that *T. brucei* Cyp40 and FKBPL may play essential roles in morphogenesis, motility, and the development of infectious-stage parasites.

### 3.6.4 J-protein 52

The J-protein family is a major subset of co-chaperones for the HSP70 chaperone machinery, and they are broadly classified into four subtypes (I–IV). The J-protein family from *T. brucei* has been explored previously (Bentley et al., 2019). It was shown in that study that J52 is one of six type III J proteins in *T. brucei* that possesses the TPR domain (others are J42, J51, J52, J53, J65, and J67) (Bentley et al., 2019). J52 is predicted to reside in the cytosol together with J51 and J42 (Bentley et al., 2019). DnaJC7/Trp2, the human ortholog of J52 was first identified as a cytosolic protein via a two-hybrid screen for interaction with a GAP-related segment (GRD) of neurofibromin. It was reported to encode seven TPR units and possess a domain of high similarity to the DnaJ family (Murthy et al., 1996). DnaJC7 also regulates the multichaperone system involving HSP70 and HSP90 but in a nucleotide-independent manner with HSP90. DnaJC7 is predominantly thought to be

involved in retrograde transport of client proteins from HSP90 to HSP70 (Brychzy et al., 2003; Moffatt et al., 2008). Proteomic analysis showed J52 to be upregulated in the procyclic form of the parasite (Urbaniak et al., 2012; Butter et al., 2013).

### 3.6.5 Small glutamine-rich TPR-containing protein (SGT)

The small glutamine-rich TPR-containing protein (SGT) is a co-chaperone involved in a specific branch of the global cellular quality control network that determines the fate of secretory and membrane proteins that mislocalize to the cytosol (Leznicki and High, 2012; Wunderley et al., 2014). Human SGT is a modular protein characterized by three characteristic sequence motifs, namely, an N-terminal dimerization domain, central TPR domain, and a glutamine-rich region at the C terminus (Roberts et al., 2015). The SGT orthologues in trypanosomatids are atypical (Table 2), as these proteins all lack the characteristic glutamine-rich region and contain a substituted region with charged amino acid residues (Ommen et al., 2010). Proteomic analysis identified TbbSGT to be upregulated in the procyclic form of the parasite and was found in the flagellar and cell surface proteome (Gunasekera et al., 2012; Urbaniak et al., 2012; Butter et al., 2013; Subota et al., 2014; Shimogawa et al., 2015). The SGT ortholog in *L. donovani* is an essential protein for *L. donovani* promastigote growth and viability (Ommen et al., 2010). LdSGT was shown to form large, stable complexes that included HSP83, HSP70, HIP, HOP, J-proteins, and HSP100 (Ommen et al., 2010), whereas recombinant *L. braziliensis* SGT was shown to interact with both LbHSP90 and HsHSP70-1A (Coto et al., 2018). Therefore, the orthologous proteins in *T. brucei* and *T. b. gambiense* may have developed the same activity and assist in the formation of the *T. brucei* HSP83 chaperone system. Though future studies should be conducted to elucidate SGT-HSP70/HSP83 interaction in *T. brucei*.

### 3.6.6 Tetratricopeptide repeat protein 4 (TTC4)

The co-chaperone TTC4 is the Tetratricopeptide repeat protein 4, a member of the TPR family that has been isolated and characterized in humans and is implicated in the pathogenesis of skin melanomas (Su et al., 1999; Poetsch et al., 2000). An ortholog of TTC4 has been characterized in *Drosophila* (Pit47) with both proteins shown to be nucleoplasmic; both contain three TPR motifs and are abundant in proliferating tissue (Crevel et al., 2008). A putative ortholog of TTC4 was found in *T. brucei* and other organisms in this study except in *B. saltans*. Proteomic analysis identified *T. brucei* TTC4 to be upregulated in the procyclic form of the parasite (Urbaniak et al., 2012; Butter et al., 2013).

## 3.7 CS-containing HSP83 co-chaperones

Nine putative CS-containing co-chaperones were identified in this study.



### 3.7.1 p23

The co-chaperone p23 is a small acidic protein that binds the HSP90 NBD to stabilize the closed conformation of HSP90, inhibiting ATPase activity and preventing client protein release from the complex (Young, 2000; McLaughlin et al., 2006). In addition to its HSP90 co-chaperone function, p23 has its own chaperoning activity *in vitro* and can suppress the aggregation of denatured proteins (Bose et al., 1996; Freeman et al., 1996). *In silico* analysis of the genomes of both *T. brucei* subspecies revealed that the parasite possesses two evolutionarily divergent p23 orthologues, and subsequently these orthologous proteins were named p23a and p23b (Table 2). The possession of two putative p23 proteins was found to be conserved in all the trypanosomatids in this study except *B. saltans* (Table 2). The Tbp23a and Tbp23b proteins share 28% identity to each other and share 33 and 26% identity, respectively, to human p23. In addition, RNAi knockdown of these proteins showed that each p23 protein is essential to parasite viability at specific stages of the life cycle (Alsford et al., 2011). The orthologues of these proteins have been explored in two *Leishmania* spp. (Batista et al., 2015). Both proteins in *L. braziliensis* possessed intrinsic chaperone activity, but they have different client protein specificities; they also inhibit LbrHSP83 ATPase activity to different extents (Batista et al., 2015). Such functional differences might be important in both HSP90 regulation and in their interactions with client proteins during the life stage transformations of kinetoplastid parasites. However, to support these assertions, more functional and *in vivo* studies of trypanosomatid p23a and p23b proteins are needed.

### 3.7.2 The cysteine- and histidine-rich domain-containing protein (CHORD)

The cysteine- and histidine-rich domain-containing protein (CHORD) is characterized by six cysteine and three histidine residues as well as a C-terminal CS domain as the characteristic domains of the CHORD-containing proteins (Wu et al., 2005). In humans there are two CHORD domains, CHORD-I was found to be dispensable toward the HSP90 interaction while CHORD-II is essential (Wu et al., 2005). CHORD was identified as an ADP-dependent HSP90 co-chaperone in humans as its interaction was shown to be stimulated by high ADP:ATP ratio in cell culture lysates (Gano and Simon, 2010). Data mining identified a single CHORD gene in *T. brucei* genome, and all other organisms were studied, and the CHORD protein was found upregulated in procyclic form of *T. brucei* parasite (Gunasekera et al., 2012; Urbaniak et al., 2012; Butter et al., 2013).

### 3.7.3 Alanyl-tRNA synthetase domain-containing 1 name (Aarsd1)

The mammalian *Aarsd1* gene is a complex gene with large number of exons. The gene gained its name—alanyl-tRNA synthetase domain-containing 1 name (*Aarsd1*) from the

shared homology of its 3' exons to the editing domain of tRNA synthetases (Echeverría et al., 2016). As a co-chaperone with 44% identity to p23 in its CS domain, it is primarily expressed in the heart and skeletal tissues and competes with p23 for binding to HSP90 (Taipale et al., 2014; Echeverría et al., 2016). Aarsd1 has previously been identified in *T. brucei* with its involvement in preventing misaminoacylation (Beebe, 2003; Cestari et al., 2013). Data mining revealed a single *Aarsd1* gene in all the organisms studied.

### 3.7.4 Protein interacting with HSP90 domain-containing protein 1 (PIH1D1/PIH1)

Protein interacting with HSP90 domain-containing protein 1 (PIH1D1/PIH1) also called Nop17 (Zhao et al., 2008) is involved in pre-RNA processing (Gonzales et al., 2005) and functions as an adapter protein that aids in recruiting clients (Henri et al., 2018). PIH1s a component of the R2TP (RUVBL1-RUVBL2-RPAP3-PIH1D1) complex, which has been found to be conserved in many species including yeast and humans (Henri et al., 2018; Martino et al., 2018). The human PIH1 contains an N-terminal domain with which it binds phosphorylated substrates and a C-terminal CS domain to bind other substrates of the R2TP complex (Hořejší et al., 2014). Data mining revealed the ortholog of PIH1 in *T. cruzi* and *L. major* and is the putative pre-RNA processing protein/Nop17 but the ortholog in *T. brucei* is alternatively named a component of motile flagella 56 (CMF56). This protein is absent in *B. saltans*.

### 3.7.5 PIH1D3

PIH1D3 in humans participates in axonemal dynein assembly in the testis and the respiratory system and mutations in *PIH1D3* have been shown to be a prominent cause of primary ciliary dyskinesia (Olcese et al., 2017). The ortholog of PIH1D3 in all organisms studied is the pre-RNA processing protein/NOP17. Proteomic analysis showed the presence of the PIH1D3 protein in both the bloodstream and procyclic forms of the parasite.

### 3.7.6 NADH cytochrome B5 reductase 4 (Ncb5or)

Ncb5or is a soluble flavohemoprotein with an N-terminal cytochrome b5-like domain and a C-terminal cytochrome b5 reductase domain (Zhu et al., 2004); it is present in a wide range of tissues in humans including some cancerous cell lines and supposedly functions as an oxygen sensor (Zhu et al., 1999). It contains the CS motif similar to p23 with which it mediates protein–protein interactions (Garcia-Ranea et al., 2002). Orthologues of Ncb5or are present in all organisms studied.

### 3.7.7 Leucine-rich repeat containing protein (LRRC)

Leucine-rich repeat containing proteins in eukaryotes share functional links with the co-chaperone SGT and together they are involved in the HSP90 chaperone machinery complex activation

(Stuttman et al., 2008). An ortholog of the LRRC protein was found in all organisms studied and it was upregulated in the procyclic form of *T. brucei* parasites (Butter et al., 2013).

### 3.7.8 Ubiquitin carboxyl-terminal hydrolase (Usp)

Ubiquitin carboxyl-terminal hydrolase 19 (Usp19) in humans has been implicated in various cancers and as a prognostic biomarker in renal cell carcinoma therapy (Shahriyari et al., 2019; Hu et al., 2020). A putative ortholog for ubiquitin carboxyl-terminal hydrolase was found in all organisms studied.

### 3.7.9 Dyslexia susceptibility 1 candidate gene 1 protein (DYX1C1)

Dyslexia susceptibility 1 candidate gene 1 protein (DYX1C1) in humans has been characterized to possess three TPR domains and is expressed in many tissues including the brain (Taipale et al., 2003). The ortholog in *T. brucei* is a putative CS domain/TPR repeat protein.

## 3.8 Non-TPR, non-CS-containing HSP83 co-chaperones

### 3.8.1 Activator of HSP90 ATPase homolog 1 (Aha1)

Aha1 has been identified as the primary activator of the ATPase activity of HSP90 and it acts independently of the other co-chaperones. Homologs of Aha1 have been identified across species from yeast to mammals; Aha1 binds with both its N- and C-terminal domain to the NBD and MD of HSP90 to facilitate the dimerization of the chaperone (Mayer et al., 2002; Koulov et al., 2010; Retzlaff et al., 2010). Data mining of the *T. brucei* genome identified that the parasite encodes for a single *Aha1* gene (Table 2). The Aha1 ortholog in *L. braziliensis* (LbrAha1) has been characterized, where it was shown to be a cognate protein that shared several structural and functional properties with the human and yeast orthologues. This suggested similar functional mechanism among these proteins despite the low degree of conservation in the amino acid sequence (Seraphim et al., 2013). Recombinant LbrAha1 stimulated the weak ATPase activity of recombinant LbrHSP83 by around 10-fold, exhibiting a cooperative behavior according to the model that two LbrAha1 molecules can act on one LbHSP83 dimer (Seraphim et al., 2013). Data from proteomic analysis in *T. brucei* revealed that TbbAha1 is upregulated in the BSF stage of the parasite (Gunasekera et al., 2012; Urbaniak et al., 2012; Butter et al., 2013) as well as being essential to parasite viability at this stage of life cycle (Alsford et al., 2011).

### 3.8.2 Phosphoducin (Pdc)

Phosphoducins in eukaryotes and other members of the phosphoducin family have been shown to function as chaperones/co-chaperones in the G-protein coupled receptors signal transduction pathways (Savage et al., 2000; Willardson and Howlett, 2007). Data mining revealed an ortholog of phosphoducin was found in all organisms studied.

## 4 Conclusion

The HSP90 family contains an abundant and essential group of proteins, which are highly conserved and implicated in a myriad of cellular functions. Due to their role in cellular proteostasis, they have been implicated in the pathology of many diseases which warrants their targeting as therapeutics (Samant et al., 2012). In this article, we report an *in silico* overview of HSP90 and its co-chaperones in both *T. b. brucei* and *T. b. gambiense* in relation to human and other trypanosomal species, including non-parasitic *Bodo saltans* and the insect infecting *Crithidia fasciculata*. *T. b. brucei* was found to have 12 putative HSP90 proteins, 10 of which are cytosolic (HSP83). Multiple copies of HSP83 may allow the parasite to reach a high synthesis level of the proteins in an organism that relies on post-transcriptional regulation, and this explains its high levels in the cell even under non-stress conditions (Requena et al., 2015). The expansion of the HSP90 chaperone complement also reiterates its importance in the biology and functioning of these protozoan parasites (Folgueira and Requena, 2007; Shonhai et al., 2011; Urményi et al., 2014). HSP83 was also found in both stages of the parasite but upregulated in the bloodstream form (BSF), this is similar to previous findings of much higher transcripts of HSP83 in bloodstream forms of *T. brucei* reflecting their temperature induced role of differentiation (Ploeg et al., 1985). The upregulation of HSP83 together with the co-chaperone Sti1 in the BSF may be a further indication of their heat inducibility and involvement in cell defiance, as seen in HSP70 (Urményi et al., 2014).

The protein sequence identities between human and *T. brucei* HSP90 proteins was the lowest in the linker and C-terminal domains; furthermore, the 3D structure revealed differences in the secondary structure and orientations of both regions. These differences may result in an altered mechanism of interacting with co-chaperones. This study identified 18 co-chaperones in the *T. brucei* HSP83 chaperone system, which is less than the current number of 50 co-chaperones in the human system, confirming that the HSP90 chaperone machinery is species-specific (Johnson and Brown, 2009; Dean and Johnson, 2021). We predict that additional co-chaperones of *T. brucei* will be uncovered, some of which

will be unique to trypanosomes and possibly *T. brucei*; and this will provide an interface for targeting chaperone/co-chaperone interactions as potential drug targets. Many of the recently discovered co-chaperones in humans are linked to human diseases including cancer (Dean and Johnson, 2021), and while orthologues have been found in *T. brucei* their roles remain to be elucidated. Many of these co-chaperones in *T. brucei* need to be further explored. So far, only the cytosolic HSP90 has been shown to require the function of co-chaperones, the other forms of HSP90 function in the absence of co-chaperones (Richter et al., 2007; Masgras et al., 2017). HSP90 partners with co-chaperones in order to maintain homeostasis; however, these partnerships appear to be dictated by the client protein being chaperoned (Radli and Rüdiger, 2017; Sahasrabudhe et al., 2017). A detailed report for clients in HSP90 is still largely absent (Roy et al., 2012). Previous studies have indicated that inhibitors targeting HSP83 have been shown to cure mice of *T. brucei* infection, although the toxicity of inhibitors to HSP90 in higher eukaryotes is attributed to a functional loss of client proteins and possible cell cycle arrest (Meyer and Shapiro, 2013). Most of the identified HSP90 client proteins in mammals are kinases (Taipale et al., 2012). Despite the fact that most clients for *T. brucei* HSP90 have not been identified, over 170 protein kinases (about 30% of the number present in their human host), have been recognized (Parsons et al., 2005; Nett et al., 2009b). In addition to being regulated by co-chaperones, HSP90 is also regulated by various post-translational modifications. Some of these PTM sites have been indicated as potential regulatory sites which affect the binding affinity of inhibitors in PfHSP90 (Pallavi et al., 2010). A number of unique PTM sites were identified in the TbHSP90 proteins and these could be targeted by inhibitors. The *T. brucei* HSP90, its co-chaperone network, post-translational modifications, and its regulatory mechanisms as well as the subtle structural differences compared to human HSP90 all provide a context for a HSP90-targeted therapy in *T. brucei*.

## Data availability statement

The original contributions presented in the study are included in the article/Supplementary Material; further inquiries can be directed to the corresponding author.

## References

- Acestor, N., Panigrahi, A. K., Ogata, Y., Anupama, A., and Stuart, K. D. (2009). Protein composition of *Trypanosoma brucei* mitochondrial membranes. *Proteomics* 9, 5497–5508. doi:10.1002/pmic.200900354
- Acestor, N., Ziková, A., Dalley, R. A., Anupama, A., Panigrahi, A. K., and Stuart, K. D. (2011). *Trypanosoma brucei* mitochondrial respirator: Composition and

## Author contributions

Conceptualization, SB and AB; methodology, SB, MJ, and PM-T; formal analysis, SB, MJ, and PM-T; writing—original draft preparation, SB, MJ, and PM-T; writing—review and editing, SB, MJ, PM-T, AE, and AB; supervision, AE and AB; and funding acquisition, AE and AB. All authors have read and agreed to the published version of the manuscript.

## Funding

MJ is a recipient of the 2018 DAAD In-Region Scholarship, PM-T is a recipient of the OWSD Scholarship. ALE is supported by the South African Research Chairs Initiative of the Department of Science and Technology (DST) and the National Research Foundation (NRF) (Grant No 98566), the NRF Competitive Programme for Rated Researchers (Grant No 129262) and Rhodes University (RGG). Open access publication fees were received from Rhodes University (grant no. PP85/2022 and Chair Support Grant - CHAIR03/2020).

## Conflict of interest

The authors declare that the research was conducted in the absence of any commercial or financial relationships that could be construed as a potential conflict of interest.

## Publisher's note

All claims expressed in this article are solely those of the authors and do not necessarily represent those of their affiliated organizations, or those of the publisher, the editors, and the reviewers. Any product that may be evaluated in this article, or claim that may be made by its manufacturer, is not guaranteed or endorsed by the publisher.

## Supplementary material

The Supplementary Material for this article can be found online at: <https://www.frontiersin.org/articles/10.3389/fmolb.2022.947078/full#supplementary-material>

organization in procyclic form. *Mol. Cell. Proteomics* 10, M110006908. doi:10.1074/mcp.M110.006908

Alsan, M. (2015). The effect of the TseTse fly on african development. *Am. Econ. Rev.* 105, 382–410. doi:10.1257/aer.20130604

- Alsford, S., Turner, D. J., Obado, S. O., Sanchez-Flores, A., Glover, L., Berriman, M., et al. (2011). High-throughput phenotyping using parallel sequencing of RNA interference targets in the African trypanosome. *Genome Res.* 21, 915–924. doi:10.1101/gr.115089.110
- Altieri, D. C., Stein, G. S., Lian, J. B., and Languino, L. R. (2012). TRAP-1, the mitochondrial Hsp90. *Biochim. Biophys. Acta* 1823, 767–773. doi:10.1016/j.bbamcr.2011.08.007
- Anderson, S., Jones, C., Saha, L., and Chaudhuri, M. (2006). Functional characterization of the serine/threonine protein phosphatase 5 from *Trypanosoma brucei*. *J. Parasitol.* 92, 1152–1161. doi:10.1645/GE-916R1.1
- Aoyagi, S., and Archer, T. K. (2005). Modulating molecular chaperone Hsp90 functions through reversible acetylation. *Trends Cell Biol.* 15, 565–567. doi:10.1016/j.tcb.2005.09.003
- Argon, Y., and Simen, B. B. (1999). GRP94, an ER chaperone with protein and peptide binding properties. *Semin. Cell Dev. Biol.* 10, 495–505. doi:10.1006/scdb.1999.0320
- Aslett, M., Aurrecochea, C., Berriman, M., Brestelli, J., Brunk, B. P., Carrington, M., et al. (2010). TriTrypDB: A functional genomic resource for the trypanosomatidae. *Nucleic Acids Res.* 38, D457–D462. doi:10.1093/nar/gkp851
- Backe, S. J., Sager, R. A., Woodford, M. R., Makedon, A. M., and Mollapour, M. (2020). Post-translational modifications of Hsp90 and translating the chaperone code. *J. Biol. Chem.* 295, 11099–11117. doi:10.1074/jbc.REV120.011833
- Baindur-Hudson, S., Edkins, A. L., and Blatch, G. L. (2015). Hsp70/Hsp90 organising protein (hop): Beyond interactions with chaperones and prion proteins. *Subcell. Biochem.* 78, 69–90. doi:10.1007/978-3-319-11731-7\_3
- Baker-Williams, A. J., Hashmi, F., Budzyński, M. A., Woodford, M. R., Gleicher, S., Himanen, S. V., et al. (2019). Co-Chaperones TIMP2 and AHA1 competitively regulate extracellular HSP90:client MMP2 activity and matrix proteolysis. *Cell Rep.* 28, 1894–1906. e6. doi:10.1016/j.celrep.2019.07.045
- Barrett, M. P., and Croft, S. L. (2012). Management of trypanosomiasis and leishmaniasis. *Br. Med. Bull.* 104, 175–196. doi:10.1093/bmb/lds031
- Batista, F. A. H., Almeida, G. S., Seraphim, T. V., Silva, K. P., Murta, S. M. F., Barbosa, L. R. S., et al. (2015). Identification of two p23 co-chaperone isoforms in *Leishmania braziliensis* exhibiting similar structures and Hsp90 interaction properties despite divergent stabilities. *FEBS J.* 282, 388–406. doi:10.1111/febs.13141
- Beebe, K., Ribas De Pouplana, L., and Schimmel, P. (2003). Elucidation of tRNA-dependent editing by a class II tRNA synthetase and significance for cell viability. *EMBO J.* 22, 668–675. doi:10.1093/emboj/cdg065
- Bente, M., Harder, S., Wiesgigl, M., Heukeshoven, J., Gelhaus, C., Krause, E., et al. (2003). Developmentally induced changes of the proteome in the protozoan parasite *Leishmania donovani*. *PROTEOMICS* 3, 1811–1829. doi:10.1002/pmic.200300462
- Bentley, S. J., Jamabo, M., and Boshoff, A. (2019). The Hsp70/J-protein machinery of the African trypanosome, *Trypanosoma brucei*. *Cell Stress Chaperones* 24, 125–148. doi:10.1007/s12192-018-0950-x
- Bhattacharya, K., Weidenauer, L., Luengo, T. M., Pieters, E. C., Echeverría, P. C., Bernasconi, L., et al. (2020). The Hsp70-Hsp90 co-chaperone Hop/Stip1 shifts the proteostatic balance from folding towards degradation. *Nat. Commun.* 11, 5975. doi:10.1038/s41467-020-19783-w
- Binder, R. J. (2014). Functions of heat shock proteins in pathways of the innate and adaptive immune system. *J. Immunol.* 193, 5765–5771. doi:10.4049/jimmunol.1401417
- Blatch, G. L., and Lässle, M. (1999). The tetratricopeptide repeat: A structural motif mediating protein-protein interactions. *BioEssays* 21, 932–939. doi:10.1002/(SICI)1521-1878(199911)21:11<932::AID-BIES5>3.0.CO;2-N
- Borthwick, E. B., Zeke, T., Prescott, A. R., and Cohen, P. T. W. (2001). Nuclear localization of protein phosphatase 5 is dependent on the carboxy-terminal region. *FEBS Lett.* 491, 279–284. doi:10.1016/S0014-5793(01)02177-9
- Bose, S., Weikl, T., Bugl, H., and Buchner, J. (1996). Chaperone function of hsp90-associated proteins. *Science* 274, 1715–1717. doi:10.1126/science.274.5293.1715
- Brandau, S., Dresel, A., and Clos, J. (1995). High constitutive levels of heat-shock proteins in human-pathogenic parasites of the genus *Leishmania*. *Biochem. J.* 310, 225–232. doi:10.1042/bj3100225
- Brinker, A., Scheufler, C., von der Mülbe, F., Fleckenstein, B., Herrmann, C., Jung, G., et al. (2002). Ligand discrimination by TPR domains: Relevance and selectivity of EEVD-RECOGNITION in Hsp70-Hop-Hsp90 complexes. *J. Biol. Chem.* 277, 19265–19275. doi:10.1074/jbc.M109002200
- Broadhead, R., Dawe, H. R., Farr, H., Griffiths, S., Hart, S. R., Portman, N., et al. (2006). Flagellar motility is required for the viability of the bloodstream trypanosome. *Nature* 440, 224–227. doi:10.1038/nature04541
- Brun, R., Blum, J., Chappuis, F., and Burri, C. (2010). Human african trypanosomiasis. *Lancet* 375, 148–159. doi:10.1016/S0140-6736(09)60829-1
- Brychzy, A., Rein, T., Winkhofer, K. F., Hartl, F. U., Young, J. C., and Obermann, W. M. J. (2003). Cofactor Tpr2 combines two TPR domains and a J domain to regulate the Hsp70/Hsp90 chaperone system. *EMBO J.* 22, 3613–3623. doi:10.1093/emboj/cdg362
- Buchner, J., and Li, J. (2013). Structure, function and regulation of the Hsp90 machinery. *Biomed. J.* 36, 106–117. doi:10.4103/2319-4170.113230
- Büscher, P., Cecchi, G., Jamonneau, V., and Priotto, G. (2017). Human african trypanosomiasis. *Lancet* 390, 2397–2409. doi:10.1016/S0140-6736(17)31510-6
- Butter, F., Bucerius, F., Michel, M., Cicova, Z., Mann, M., and Janzen, C. J. (2013). Comparative proteomics of two life cycle stages of stable isotope-labeled *Trypanosoma brucei* reveals novel components of the parasite's host adaptation machinery. *Mol. Cell. Proteomics* 12, 172–179. doi:10.1074/mcp.M112.019224
- Cechetto, J. D., and Gupta, R. S. (2000). Immunoelectron microscopy provides evidence that tumor necrosis factor receptor-associated protein 1 (TRAP-1) is a mitochondrial protein which also localizes at specific extramitochondrial sites. *Exp. Cell Res.* 260, 30–39. doi:10.1006/excr.2000.4983
- Cestari, I., Kalidas, S., Monnerat, S., Anupama, A., Phillips, M. A., and Stuart, K. (2013). A multiple aminoacyl-tRNA synthetase complex that enhances tRNA-aminoacylation in african trypanosomes. *Mol. Cell. Biol.* 33, 4872–4888. doi:10.1128/MCB.00711-13
- Chang, H. C., Nathan, D. F., and Lindquist, S. (1997). *In vivo* analysis of the Hsp90 cochaperone Sti1 (p60). *Mol. Cell. Biol.* 17, 318–325. doi:10.1128/MCB.17.1.318
- Chen, B., Piel, W. H., Gui, L., Bruford, E., and Monteiro, A. (2005). The HSP90 family of genes in the human genome: Insights into their divergence and evolution. *Genomics* 86, 627–637. doi:10.1016/j.ygeno.2005.08.012
- Chen, B., Zhong, D., and Monteiro, A. (2006). Comparative genomics and evolution of the HSP90 family of genes across all kingdoms of organisms. *BMC Genomics* 7, 156. doi:10.1186/1471-2164-7-156
- Chen, M.-S., Silverstein, A. M., Pratt, W. B., and Chinkers, M. (1996). The tetratricopeptide repeat domain of protein phosphatase 5 mediates binding to glucocorticoid receptor heterocomplexes and acts as a dominant negative mutant. *J. Biol. Chem.* 271, 32315–32320. doi:10.1074/jbc.271.50.32315
- Chinkers, M. (2001). Protein phosphatase 5 in signal transduction. *Trends Endocrinol. Metab.* 12, 28–32. doi:10.1016/S1043-2760(00)00335-0
- Chua, C.-S., Low, H., and Sim, T.-S. (2014). Co-chaperones of Hsp90 in *Plasmodium falciparum* and their concerted roles in cellular regulation. *Parasitology* 141, 1177–1191. doi:10.1017/S0031182013002084
- Citri, A., Kochupurakkal, B. S., and Yarden, Y. (2004). The achilles heel of ErbB-2/HER2: Regulation by the Hsp90 chaperone machine and potential for pharmacological intervention. *Cell Cycle* 3, 50–59. doi:10.4161/cc.3.1.607
- Clayton, C., and Shapira, M. (2007). Post-transcriptional regulation of gene expression in trypanosomes and leishmanias. *Mol. Biochem. Parasitol.* 156, 93–101. doi:10.1016/j.molbiopara.2007.07.007
- Cohen, P. T. W. (1997). Novel protein serine/threonine phosphatases: Variety is the spice of life. *Trends biochem. Sci.* 22, 245–251. doi:10.1016/S0968-0004(97)01060-8
- Colasante, C., Ellis, M., Ruppert, T., and Voncken, F. (2006). Comparative proteomics of glycosomes from bloodstream form and procyclic culture form *Trypanosoma brucei brucei*. *Proteomics* 6, 3275–3293. doi:10.1002/pmic.200500668
- Coto, A. L. S., Seraphim, T. V., Batista, F. A. H., Soares-Silva, P. R., Barranco, A. B. F., Teixeira, F. R., et al. (2018). Structural and functional studies of the *Leishmania braziliensis* SGT co-chaperone indicate that it shares structural features with HIP and can interact with both Hsp90 and Hsp70 with similar affinities. *Int. J. Biol. Macromol.* 118, 693–706. doi:10.1016/j.ijbiomac.2018.06.123
- Crevel, G., Bennett, D., and Cotterill, S. (2008). The human TPR protein TTC4 is a putative Hsp90 Co-chaperone which interacts with CDC6 and shows alterations in transformed cells. *PLoS ONE* 3, e0001737. doi:10.1371/journal.pone.0001737
- Csermely, P., Schnaider, T., So<sup>ti</sup>, C., Prohászka, Z., and Nardai, G. (1998). The 90-kDa molecular chaperone family: Structure, function, and clinical applications. A comprehensive review. *Pharmacol. Ther.* 79, 129–168. doi:10.1016/S0163-7258(98)00013-8
- Cunningham, C. N., Krukenberg, K. A., and Agard, D. A. (2008). Intra- and intermonomer interactions are required to synergistically facilitate ATP hydrolysis in Hsp90. *J. Biol. Chem.* 283, 21170–21178. doi:10.1074/jbc.M800046200



- de Nadal, E., Ammerer, G., and Posas, F. (2011). Controlling gene expression in response to stress. *Nat. Rev. Genet.* 12, 833–845. doi:10.1038/nrg3055
- Dean, M. E., and Johnson, J. L. (2021). Human Hsp90 cochaperones: Perspectives on tissue-specific expression and identification of cochaperones with similar *in vivo* functions. *Cell Stress Chaperones* 26, 3–13. doi:10.1007/s12192-020-01167-0
- Dean, S., Sunter, J. D., and Wheeler, R. J. (2017). TrypTag.org: A trypanosome genome-wide protein localisation resource. *Trends Parasitol.* 33, 80–82. doi:10.1016/j.pt.2016.10.009
- Deeks, E. D. (2019). Fexinidazole: First global approval. *Drugs* 79, 215–220. doi:10.1007/s40265-019-1051-6
- DeGrasse, J. A., Chait, B. T., Field, M. C., and Rout, M. P. (2008). High-yield isolation and subcellular proteomic characterization of nuclear and subnuclear structures from trypanosomes. *Methods Mol. Biol.* 463, 77–92. doi:10.1007/978-1-59745-406-3\_6
- Dero, B., Zampetti-Bosseler, F., Pays, E., and Steinert, M. (1987). The genome and the antigen gene repertoire of *Trypanosoma brucei gambiense* are smaller than those of *T. b. brucei*. *Mol. Biochem. Parasitol.* 26, 247–256. doi:10.1016/0166-6851(87)90077-6
- Deschamps, P., Lara, E., Marande, W., López-García, P., Ekelund, F., and Moreira, D. (2011). Phylogenomic analysis of kinetoplasts supports that trypanosomatids arose from within bodonids. *Mol. Biol. Evol.* 28, 53–58. doi:10.1093/molbev/msq289
- Descoteaux, A., Avila, H. A., Zhang, K., Turco, S. J., and Beverley, S. M. (2002). Leishmanial LPG3 encodes a GRP94 homolog required for phosphoglycan synthesis implicated in parasite virulence but not viability. *EMBO J.* 21, 4458–4469. doi:10.1093/emboj/cdf447
- Drini, S., Criscuolo, A., Lechat, P., Imamura, H., Skalický, T., Rachidi, N., et al. (2016). Species- and strain-specific adaptation of the HSP70 super family in pathogenic trypanosomatids. *Genome Biol. Evol.* 8, 1980–1995. doi:10.1093/gbe/evw140
- Droll, D., Minia, I., Fadda, A., Singh, A., Stewart, M., Queiroz, R., et al. (2013). Post-transcriptional regulation of the trypanosome heat shock response by a zinc finger protein. *PLoS Pathog.* 9, e1003286. doi:10.1371/journal.ppat.1003286
- Duval, M., Le Bœuf, F., Huot, J., and Gratton, J.-P. (2007). Src-mediated phosphorylation of Hsp90 in response to vascular endothelial growth factor (VEGF) is required for VEGF receptor-2 signaling to endothelial NO synthase. *Mol. Biol. Cell* 18, 4659–4668. doi:10.1091/mbc.e07-05-0467
- Echeverría, P. C., Bernthaler, A., Dupuis, P., Mayer, B., and Picard, D. (2011). An interaction network predicted from public data as a discovery tool: Application to the Hsp90 molecular chaperone machine. *PLOS ONE* 6, e26044. doi:10.1371/journal.pone.0026044
- Echeverría, P. C., Briand, P.-A., and Picard, D. (2016). A remodeled Hsp90 molecular chaperone ensemble with the novel cochaperone Aarsd1 is required for muscle differentiation. *Mol. Cell. Biol.* 36, 1310–1321. doi:10.1128/MCB.01099-15
- El-Sayed, N. M., Myler, P. J., Bartholomeu, D. C., Nilsson, D., Aggarwal, G., Tran, A.-N., et al. (2005a). The genome sequence of *Trypanosoma cruzi*, etiologic agent of Chagas disease. *Science* 309, 409–415. doi:10.1126/science.1112631
- El-Sayed, N. M., Myler, P. J., Blandin, G., Berriman, M., Crabtree, J., Aggarwal, G., et al. (2005b). Comparative genomics of trypanosomatid parasitic Protozoa. *Science* 309, 404–409. doi:10.1126/science.1112181
- Emelyanov, V. V. (2002). Phylogenetic relationships of organellar Hsp90 homologs reveal fundamental differences to organellar Hsp70 and Hsp60 evolution. *Gene* 299, 125–133. doi:10.1016/S0378-1119(02)01021-1
- Felts, S. J., Owen, B. A. L., Nguyen, P., Trepel, J., Donner, D. B., and Toft, D. O. (2000). The hsp90-related protein TRAP1 is a mitochondrial protein with distinct functional properties. *J. Biol. Chem.* 275, 3305–3312. doi:10.1074/jbc.275.5.3305
- Fèvre, E. M., Wissmann, B. v., Welburn, S. C., and Lutumba, P. (2008). The burden of human african trypanosomiasis. *PLoS Negl. Trop. Dis.* 2, e333. doi:10.1371/journal.pntd.0000333
- Figueras, M. J., Echeverría, P. C., and Angel, S. O. (2014). Protozoan HSP90-heterocomplex: Molecular interaction network and biological significance. *Curr. Protein Pept. Sci.* 15, 245–255. doi:10.2174/1389203715666140331114233
- Folgueira, C., and Requena, J. M. (2007). A postgenomic view of the heat shock proteins in kinetoplastids. *FEMS Microbiol. Rev.* 31, 359–377. doi:10.1111/j.1574-6976.2007.00069.x
- Fránzen, O., Talavera-López, C., Ochaya, S., Butler, C. E., Messenger, L. A., Lewis, M. D., et al. (2012). Comparative genomic analysis of human infective *Trypanosoma cruzi* lineages with the bat-restricted subspecies *T. cruzi marinkellei*. *BMC Genomics* 13, 531. doi:10.1186/1471-2164-13-531
- Freeman, B. C., Toft, D. O., and Morimoto, R. I. (1996). Molecular chaperone machines: Chaperone activities of the cyclophilin cyp-40 and the steroid aporeceptor-associated protein p23. *Science* 274, 1718–1720. doi:10.1126/science.274.5293.1718
- Galat, A. (2003). Peptidylprolyl cis/trans isomerases (immunophilins): Biological diversity - targets - functions. *Curr. Top. Med. Chem.* 3, 1315–1347. doi:10.2174/1568026033451862
- Gano, J. J., and Simon, J. A. (2010). A proteomic investigation of ligand-dependent HSP90 complexes reveals CHORDC1 as a novel ADP-dependent HSP90-interacting protein. *Mol. Cell. Proteomics* 9, 255–270. doi:10.1074/mcp.M900261-MCP200
- García-Ranea, J. A., Mirey, G., Camonis, J., and Valencia, A. (2002). p23 and HSP20/alpha-crystallin proteins define a conserved sequence domain present in other eukaryotic protein families. *FEBS Lett.* 529, 162–167. doi:10.1016/S0014-5793(02)03321-5
- Gasteiger, E., Hoogland, C., Gattiker, A., Duvaud, S., Wilkins, M. R., Appel, R. D., et al. (2005). "Protein identification and analysis tools on the ExPASy server," in *The proteomics protocols handbook* *springer protocols handbooks*. Editor J. M. Walker (Totowa, NJ: Humana Press), 571–607. doi:10.1385/1-59259-890-0:571
- Gazestani, V. H., Yip, C. W., Nikpour, N., Berghuis, N., and Salavati, R. (2017). TrypsNetDB: An integrated framework for the functional characterization of trypanosomatid proteins. *PLoS Negl. Trop. Dis.* 11, e0005368. doi:10.1371/journal.pntd.0005368
- Gibson, W. (2012). The origins of the trypanosome genome strains *Trypanosoma brucei brucei* TREU 927, *T. b. gambiense* DAL 972, *T. vivax* Y486 and *T. congolense* IL3000. *Parasit. Vectors* 5, 71. doi:10.1186/1756-3305-5-71
- Girstmaier, H., Tippel, F., Lopez, A., Tych, K., Stein, F., Haberkant, P., et al. (2019). The Hsp90 isoforms from *S. cerevisiae* differ in structure, function and client range. *Nat. Commun.* 10, 3626. doi:10.1038/s41467-019-11518-w
- Golden, T., Swingle, M., and Honkanen, R. E. (2008). The role of serine/threonine protein phosphatase type 5 (PP5) in the regulation of stress-induced signaling networks and cancer. *Cancer Metastasis Rev.* 27, 169–178. doi:10.1007/s10555-008-9125-z
- Gonzales, F. A., Zanchin, N. I. T., Luz, J. S., and Oliveira, C. C. (2005). Characterization of *Saccharomyces cerevisiae* Nop17p, a novel nop58p-interacting protein that is involved in pre-rRNA processing. *J. Mol. Biol.* 346, 437–455. doi:10.1016/j.jmb.2004.11.071
- Goos, C., Dejung, M., Janzen, C. J., Butter, F., and Kramer, S. (2017). The nuclear proteome of *Trypanosoma brucei*. *PLoS ONE* 12, e0181884. doi:10.1371/journal.pone.0181884
- Graefe, S. E. B., Wiesgigl, M., Gaworski, I., Macdonald, A., and Clos, J. (2002). Inhibition of HSP90 in *trypanosoma cruzi* induces a stress response but No stage differentiation. *Eukaryot. Cell* 1, 936–943. doi:10.1128/EC.1.6.936-943.2002
- Gunasekera, K., Wüthrich, D., Braga-Lagache, S., Heller, M., and Ochsenreiter, T. (2012). Proteome remodelling during development from blood to insect-form *Trypanosoma brucei* quantified by SILAC and mass spectrometry. *BMC Genomics* 13, 556. doi:10.1186/1471-2164-13-556
- Gupta, R. S. (1995). Phylogenetic analysis of the 90 kD heat shock family of protein sequences and an examination of the relationship among animals, plants, and fungi species. *Mol. Biol. Evol.* 12, 1063–1073. doi:10.1093/oxfordjournals.molbev.a040281
- Güther, M. L. S., Urbaniak, M. D., Tavendale, A., Prescott, A., and Ferguson, M. A. J. (2014). High-confidence glycosome proteome for procyclic form *Trypanosoma brucei* by epitope-tag organelle enrichment and SILAC proteomics. *J. Proteome Res.* 13, 2796–2806. doi:10.1021/pr401209w
- Hance, M. W., Nolan, K. D., and Isaacs, J. S. (2014). The double-edged sword: Conserved functions of extracellular hsp90 in wound healing and cancer. *Cancers (Basel)* 6, 1065–1097. doi:10.3390/cancers6021065
- Hartl, F. U., Bracher, A., and Hayer-Hartl, M. (2011). Molecular chaperones in protein folding and proteostasis. *Nature* 475, 324–332. doi:10.1038/nature10317
- Henri, J., Chagot, M.-E., Bourguet, M., Abel, Y., Terral, G., Maurizy, C., et al. (2018). Deep structural analysis of RPAP3 and PIH1D1, two components of the HSP90 Co-chaperone R2TP complex. *Structure* 26, 1196–1209. e8. doi:10.1016/j.str.2018.06.002
- Herreros-Cabello, A., Callejas-Hernández, F., Gironès, N., and Fresno, M. (2020). *Trypanosoma cruzi* genome: Organization, multi-gene families, transcription, and biological implications. *Genes* 11, 1196. doi:10.3390/genes11101196

- Hombach, A., Ommen, G., Chrobak, M., and Clos, J. (2013). The Hsp90-Sti1 interaction is critical for Leishmania donovani proliferation in both life cycle stages. *Cell. Microbiol.* 15, 585–600. doi:10.1111/cmi.12057
- Hombach-Barrigah, A., Bartsch, K., Smirlis, D., Rosenqvist, H., MacDonald, A., Dingli, F., et al. (2019). Leishmania donovani 90 kD heat shock protein – impact of phosphosites on parasite fitness, infectivity and casein kinase affinity. *Sci. Rep.* 9, 5074. doi:10.1038/s41598-019-41640-0
- Hořejší, Z., Stach, L., Flower, T. G., Joshi, D., Flynn, H., Skehel, J. M., et al. (2014). Phosphorylation-dependent PIH1D1 interactions define substrate specificity of the R2TP cochaperone complex. *Cell Rep.* 7, 19–26. doi:10.1016/j.celrep.2014.03.013
- Hoter, A., El-Sabban, M. E., and Naim, H. Y. (2018). The HSP90 family: Structure, regulation, function, and implications in health and disease. *Int. J. Mol. Sci.* 19, 2560. doi:10.3390/ijms19092560
- Hu, W., Su, Y., Fei, X., Wang, X., Zhang, G., Su, C., et al. (2020). Ubiquitin specific peptidase 19 is a prognostic biomarker and affect the proliferation and migration of clear cell renal cell carcinoma. *Oncol. Rep.* 43, 1964–1974. doi:10.3892/or.2020.7565
- Hunter, M. C., O'Hagan, K. L., Kenyon, A., Dhanani, K. C. H., Prinsloo, E., and Edkins, A. L. (2014). Hsp90 binds directly to fibronectin (FN) and inhibition reduces the extracellular fibronectin matrix in breast cancer cells. *PLoS One* 9, e86842. doi:10.1371/journal.pone.0086842
- Jackson, A. P., Sanders, M., Berry, A., McQuillan, J., Aslett, M. A., Quail, M. A., et al. (2010). The genome sequence of trypanosoma brucei gambiense, causative agent of chronic human african trypanosomiasis. *PLoS Negl. Trop. Dis.* 4, e658. doi:10.1371/journal.pntd.0000658
- Jackson, S. E. (2013). Hsp90: Structure and function. *Top. Curr. Chem.* 328, 155–240. doi:10.1007/128\_2012\_356
- Jahn, M., Rehn, A., Pelz, B., Hellenkamp, B., Richter, K., Rief, M., et al. (2014). The charged linker of the molecular chaperone Hsp90 modulates domain contacts and biological function. *Proc. Natl. Acad. Sci. U. S. A.* 111, 17881–17886. SAPP.PDF. doi:10.1073/pnas.1414073111
- Jakob, U., Meyer, I., Bügl, H., André, S., Bardwell, J. C. A., and Buchner, J. (1995). Structural organization of procaryotic and eucaryotic Hsp90. Influence of divalent cations on structure and function. *J. Biol. Chem.* 270, 14412–14419. doi:10.1074/jbc.270.24.14412
- Johnson, B. D., Schumacher, R. J., Ross, E. D., and Toft, D. O. (1998). Hop modulates hsp70/hsp90 interactions in protein folding. *J. Biol. Chem.* 273, 3679–3686. doi:10.1074/jbc.273.6.3679
- Johnson, J. L., and Brown, C. (2009). Plasticity of the Hsp90 chaperone machine in divergent eukaryotic organisms. *Cell Stress Chaperones* 14, 83–94. doi:10.1007/s12192-008-0058-9
- Johnson, J. L. (2012). Evolution and function of diverse Hsp90 homologs and cochaperone proteins. *Biochim. Biophys. Acta* 1823, 607–613. doi:10.1016/j.bbamcr.2011.09.020
- Jones, C., Anderson, S., Singha, U. K., and Chaudhuri, M. (2008). Protein phosphatase 5 is required for Hsp90 function during proteotoxic stresses in Trypanosoma brucei. *Parasitol. Res.* 102, 835–844. doi:10.1007/s00436-007-0817-z
- Jones, D. T., Taylor, W. R., and Thornton, J. M. (1992). The rapid generation of mutation data matrices from protein sequences. *Comput. Appl. Biosci.* 8, 275–282. doi:10.1093/bioinformatics/8.3.275
- Kaiser, M., Maes, L., Tadoori, L. P., Spangenberg, T., and Ioset, J.-R. (2015). Repurposing of the open access malaria box for kinetoplastid diseases identifies novel active scaffolds against trypanosomatids. *J. Biomol. Screen.* 20, 634–645. doi:10.1177/1087057115569155
- Kampinga, H. H., Hageman, J., Vos, M. J., Kubota, H., Tanguay, R. M., Bruford, E. A., et al. (2009). Guidelines for the nomenclature of the human heat shock proteins. *Cell Stress Chaperones* 14, 105–111. doi:10.1007/s12192-008-0068-7
- Koulov, A. V., LaPointe, P., Lu, B., Razvi, A., Coppinger, J., Dong, M.-Q., et al. (2010). Biological and structural basis for Aha1 regulation of Hsp90 ATPase activity in maintaining proteostasis in the human disease cystic fibrosis. *Mol. Biol. Cell* 21, 871–884. doi:10.1091/mbc.e09-12-1017
- Kravats, A. N., Hoskins, J. R., Reidy, M., Johnson, J. L., Doyle, S. M., Genest, O., et al. (2018). Functional and physical interaction between yeast Hsp90 and Hsp70. *Proc. Natl. Acad. Sci. U. S. A.* 115, E2210–E2219. doi:10.1073/pnas.1719969115
- Kumar, R., Gupta, S., Bhutia, W. D., Vaid, R. K., and Kumar, S. (2022). Atypical human trypanosomiasis: Potentially emerging disease with lack of understanding. *Zoonoses Public Health* 69, 259–276. doi:10.1111/zph.12945
- Kumar, S., Stecher, G., Li, M., Knyaz, C., and Tamura, K. (2018). Mega X: Molecular evolutionary genetics analysis across computing platforms. *Mol. Biol. Evol.* 35, 1547–1549. doi:10.1093/molbev/msy096
- Larkin, M. A., Blackshields, G., Brown, N. P., Chenna, R., McGettigan, P. A., McWilliam, H., et al. (2007). Clustal W and clustal X version 2.0. *Bioinformatics* 23, 2947–2948. doi:10.1093/bioinformatics/btm404
- Larreta, R., Guzman, F., Patarroyo, M. E., Alonso, C., and Requena, J. M. (2002). Antigenic properties of the Leishmania infantum GRP94 and mapping of linear B-cell epitopes. *Immunol. Lett.* 80, 199–205. doi:10.1016/S0165-2478(01)00331-5
- Larreta, R., Soto, M., Alonso, C., and Requena, J. M. (2000). Leishmania infantum: Gene cloning of the GRP94 homologue, its expression as recombinant protein, and analysis of antigenicity. *Exp. Parasitol.* 96, 108–115. doi:10.1006/expr.2000.4553
- Letunic, I., Doerks, T., and Bork, P. (2012). Smart 7: Recent updates to the protein domain annotation resource. *Nucleic Acids Res.* 40, D302–D305. doi:10.1093/nar/gkr931
- Leznicki, P., and High, S. (2012). SGTA antagonizes BAG6-mediated protein triage. *Proc. Natl. Acad. Sci. U. S. A.* 109, 19214–19219. doi:10.1073/pnas.1209997109
- Li, J., Soroka, J., and Buchner, J. (2012). The Hsp90 chaperone machinery: Conformational dynamics and regulation by co-chaperones. *Biochim. Biophys. Acta* 1823, 624–635. doi:10.1016/j.bbamcr.2011.09.003
- Li, Z., Jaroszewski, L., Iyer, M., Sedova, M., and Godzik, A. (2020). Fatcat 2.0: Towards a better understanding of the structural diversity of proteins. *Nucleic Acids Res.* 48, W60–W64. doi:10.1093/NAR/GKAA443
- Lindner, A. K., Lejon, V., Chappuis, F., Seixas, J., Kazumba, L., Barrett, M. P., et al. (2020). New WHO guidelines for treatment of gambiense human african trypanosomiasis including fexinidazole: Substantial changes for clinical practice. *Lancet. Infect. Dis.* 20, e38–e46. doi:10.1016/S1473-3099(19)30612-7
- López, A., Elimelech, A. R., Klimm, K., and Sattler, M. (2021). The charged linker modulates the conformations and molecular interactions of Hsp90. *Chembiochem.* 22, 1084–1092. doi:10.1002/CBIC.202000699
- Martino, F., Pal, M., Muñoz-Hernández, H., Rodríguez, C. F., Núñez-Ramírez, R., Gil-Carton, D., et al. (2018). RPAP3 provides a flexible scaffold for coupling HSP90 to the human R2TP co-chaperone complex. *Nat. Commun.* 9, 1501. doi:10.1038/s41467-018-03942-1
- Marzec, M., Eletto, D., and Argon, Y. (2012). GRP94: An HSP90-like protein specialized for protein folding and quality control in the endoplasmic reticulum. *Biochim. Biophys. Acta* 1823, 774–787. doi:10.1016/j.bbamcr.2011.10.013
- Masgras, I., Sanchez-Martin, C., Colombo, G., and Rasola, A. (2017). The chaperone TRAP1 as a modulator of the mitochondrial adaptations in cancer cells. *Front. Oncol.* 7, 58. doi:10.3389/fonc.2017.00058
- Mayer, M. P., Nikolay, R., and Bukau, B. (2002). Aha, another regulator for Hsp90 chaperones. *Mol. Cell* 10, 1255–1256. doi:10.1016/S1097-2765(02)00793-1
- McLaughlin, S. H., Sobott, F., Yao, Z., Zhang, W., Nielsen, P. R., Grossmann, J. G., et al. (2006). The Co-chaperone p23 arrests the Hsp90 ATPase cycle to trap client proteins. *J. Mol. Biol.* 356, 746–758. doi:10.1016/j.jmb.2005.11.085
- Meyer, K. J., Caton, E., and Shapiro, T. A. (2018). Model system identifies kinetic driver of Hsp90 inhibitor activity against african trypanosomes and plasmodium falciparum. *Antimicrob. Agents Chemother.* 62, e00056. doi:10.1128/AAC.00056-18
- Meyer, K. J., and Shapiro, T. A. (2021). Cytosolic and mitochondrial Hsp90 in cytokinesis, mitochondrial DNA replication, and drug action in trypanosoma brucei. *Antimicrob. Agents Chemother.* 65, e0063221–21. doi:10.1128/AAC.00632-21
- Meyer, K. J., and Shapiro, T. A. (2013). Potent antitrypanosomal activities of heat shock protein 90 inhibitors in vitro and in vivo. *J. Infect. Dis.* 208, 489–499. doi:10.1093/infdis/jit179
- Miyata, Y., and Yahara, I. (1992). The 90-kDa heat shock protein, Hsp90, binds and protects casein kinase II from self-aggregation and enhances its kinase activity. *J. Biol. Chem.* 267, 7042–7047. doi:10.1016/S0021-9258(19)50533-6
- Moffatt, N. S. C., Bruinsma, E., Uhl, C., Obermann, W. M. J., and Toft, D. (2008). Role of the cochaperone Tpr2 in Hsp90 chaperoning. *Biochemistry* 47, 8203–8213. doi:10.1021/bi800770g
- Mollapour, M., and Neckers, L. (2012). Post-translational modifications of Hsp90 and their contributions to chaperone regulation. *Biochim. Biophys. Acta* 1823, 648–655. doi:10.1016/j.bbamcr.2011.07.018
- Mollapour, M., Tsutsumi, S., Truman, A. W., Xu, W., Vaughan, C. K., Beebe, K., et al. (2011). Threonine 22 phosphorylation attenuates Hsp90 interaction with cochaperones and affects its chaperone activity. *Mol. Cell* 41, 672–681. doi:10.1016/j.molcel.2011.02.011
- Moretti, N. S., Cestari, I., Anupama, A., Stuart, K., and Schenkman, S. (2018). Comparative proteomic analysis of lysine acetylation in trypanosomes. *J. Proteome Res.* 17, 374–385. doi:10.1021/acs.jproteome.7b00603

- Morrison, L. J., Vezza, L., Rowan, T., and Hope, J. C. (2016). Animal african trypanosomiasis: Time to increase focus on clinically relevant parasite and host species. *Trends Parasitol.* 32, 599–607. doi:10.1016/j.pt.2016.04.012
- Mottram, J. C., Murphy, W. J., and Agabian, N. (1989). A transcriptional analysis of the *Trypanosoma brucei* hsp83 gene cluster. *Mol. Biochem. Parasitol.* 37, 115–127. doi:10.1016/0166-6851(89)90108-4
- Murthy, A. E., Bernards, A., Church, D., Wasmuth, J., and Gusella, J. F. (1996). Identification and characterization of two novel tetratricopeptide repeat-containing genes. *DNA Cell Biol.* 15, 727–735. doi:10.1089/dna.1996.15.727
- Nelson, G. M., Huffman, H., and Smith, D. F. (2003). Comparison of the carboxy-terminal DP-repeat region in the co-chaperones Hop and Hip. *Cell Stress Chaperones* 8, 125–133. doi:10.1379/1466-1268(2003)008<0125:cotcdr>2.0.co;2
- Nett, I. R. E., Davidson, L., Lamont, D., and Ferguson, M. A. J. (2009a). Identification and specific localization of tyrosine-phosphorylated proteins in *trypanosoma brucei*. *Eukaryot. Cell* 8, 617–626. doi:10.1128/EC.00366-08
- Nett, I. R. E., Martin, D. M. A., Miranda-Saavedra, D., Lamont, D., Barber, J. D., Mehler, A., et al. (2009b). The phosphoproteome of bloodstream form *Trypanosoma brucei*, causative agent of African sleeping sickness. *Mol. Cell. Proteomics* 8, 1527–1538. doi:10.1074/mcp.M800556-MCP200
- Oberholzer, M., Langousis, G., Nguyen, H. T., Saada, E. A., Shimogawa, M. M., Jonsson, Z. O., et al. (2011). Independent analysis of the flagellum surface and matrix proteomes provides insight into flagellum signaling in mammalian-infectious *trypanosoma brucei*. *Mol. Cell. Proteomics* 10, M111010538. doi:10.1074/mcp.M111.010538
- Oduaga, O. O., Hornby, J. A., Bies, C., Zimmermann, R., Pugh, D. J., and Blatch, G. L. (2003). Tetratricopeptide repeat motif-mediated hsc70-mST11 interaction: Molecular characterization of the critical contacts for successful binding and specificity. *J. Biol. Chem.* 278, 6896–6904. doi:10.1074/jbc.M206867200
- Olcese, C., Patel, M. P., Shoemark, A., Kiviluoto, S., Legendre, M., Williams, H. J., et al. (2017). X-linked primary ciliary dyskinesia due to mutations in the cytoplasmic axonemal dynein assembly factor PIH1D3. *Nat. Commun.* 8, 14279. doi:10.1038/ncomms14279
- Ommen, G., Chrobak, M., and Clos, J. (2010). The co-chaperone SGT of *Leishmania donovani* is essential for the parasite's viability. *Cell Stress Chaperones* 15, 443–455. doi:10.1007/s12192-009-0160-7
- Ooi, C. P., Benz, C., and Urbaniak, M. D. (2020). Phosphoproteomic analysis of mammalian infective *Trypanosoma brucei* subjected to heat shock suggests atypical mechanisms for thermotolerance. *J. Proteomics* 219, 103735. doi:10.1016/j.jprot.2020.103735
- Osellame, L. D., Blacker, T. S., and Duchon, M. R. (2012). Cellular and molecular mechanisms of mitochondrial function. *Best. Pract. Res. Clin. Endocrinol. Metab.* 26, 711–723. doi:10.1016/j.beem.2012.05.003
- Pallavi, R., Roy, N., Nageshan, R. K., Talukdar, P., Pavithra, S. R., Reddy, R., et al. (2010). Heat shock protein 90 as a drug target against Protozoan infections BIOCHEMICAL characterization of hsp90 from plasmodium falciparum and *trypanosoma evansi* and evaluation of its inhibitor as a candidate drug. *J. Biol. Chem.* 285, 37964–37975. doi:10.1074/jbc.M110.155317
- Panaretou, B., Prodromou, C., Roe, S. M., O'Brien, R., Ladbury, J. E., Piper, P. W., et al. (1998). ATP binding and hydrolysis are essential to the function of the Hsp90 molecular chaperone *in vivo*. *EMBO J.* 17, 4829–4836. doi:10.1093/emboj/17.16.4829
- Panigrahi, A. K., Ogata, Y., Zíková, A., Anupama, A., Dalley, R. A., Acestor, N., et al. (2009). A comprehensive analysis of *Trypanosoma brucei* mitochondrial proteome. *Proteomics* 9, 434–450. doi:10.1002/pmic.200800477
- Parsons, M., Worthey, E. A., Ward, P. N., and Mottram, J. C. (2005). Comparative analysis of the kinomes of three pathogenic trypanosomatids: *Leishmania major*, *Trypanosoma brucei* and *Trypanosoma cruzi*. *BMC Genomics* 6, 127. doi:10.1186/1471-2164-6-127
- Peikert, C. D., Mani, J., Morgenstern, M., Käser, S., Knapp, B., Wenger, C., et al. (2017). Charting organellar importers by quantitative mass spectrometry. *Nat. Commun.* 8, 15272. doi:10.1038/ncomms15272
- Pizarro, J. C., Hills, T., Senisterra, G., Wernimont, A. K., Mackenzie, C., Norcross, N. R., et al. (2013). Exploring the *Trypanosoma brucei* Hsp83 potential as a target for structure guided drug design. *PLoS Negl. Trop. Dis.* 7, e2492. doi:10.1371/JOURNAL.PNTD.0002492
- Ploeg, L. V. der, Giannini, S. H., and Cantor, C. R. (1985). Heat shock genes: Regulatory role for differentiation in parasitic protozoa. *Science* 228, 1443–1446. doi:10.1126/science.4012301
- Poetsch, M., Dittberner, T., Cowell, J. K., and Woenckhaus, C. (2000). TTC4, a novel candidate tumor suppressor gene at 1p31 is often mutated in malignant melanoma of the skin. *Oncogene* 19, 5817–5820. doi:10.1038/sj.onc.1203961
- Porter, J. R., Fritz, C. C., and Depew, K. M. (2010). Discovery and development of Hsp90 inhibitors: A promising pathway for cancer therapy. *Curr. Opin. Chem. Biol.* 14, 412–420. doi:10.1016/j.cbpa.2010.03.019
- Pratt, W. B., Galigniana, M. D., Harrell, J. M., and DeFranco, D. B. (2004). Role of hsp90 and the hsp90-binding immunophilins in signalling protein movement. *Cell. Signal.* 16, 857–872. doi:10.1016/j.cellsig.2004.02.004
- Preußer, C., Jaé, N., and Bindereif, A. (2012). mRNA splicing in trypanosomes. *Int. J. Med. Microbiol.* 302, 221–224. doi:10.1016/j.ijmm.2012.07.004
- Prodromou, C., SiliGardi, G., O'Brien, R., Woolfson, D. N., Regan, L., Panaretou, B., et al. (1999). Regulation of Hsp90 ATPase activity by tetratricopeptide repeat (TPR)-domain co-chaperones. *EMBO J.* 18, 754–762. doi:10.1093/emboj/18.3.754
- Prodromou, C. (2012). The 'active life' of Hsp90 complexes. *Biochim. Biophys. Acta* 1823, 614–623. doi:10.1016/j.bbamcr.2011.07.020
- Radli, M., and Rüdiger, S. G. D. (2017). Picky hsp90—every game with another mate. *Mol. Cell* 67, 899–900. doi:10.1016/j.molcel.2017.09.013
- Rao, R., Fiskus, W., Yang, Y., Lee, P., Joshi, R., Fernandez, P., et al. (2008). HDAC6 inhibition enhances 17-AAG-mediated abrogation of hsp90 chaperone function in human leukemia cells. *Blood* 112, 1886–1893. doi:10.1182/blood-2008-03-143644
- Ratajczak, T., Ward, B., and Minchin, R. (2003). Immunophilin chaperones in steroid receptor signalling. *Curr. Top. Med. Chem.* 3, 1348–1357. doi:10.2174/1568026033451934
- Requena, J. M. (2011). Lights and shadows on gene organization and regulation of gene expression in *Leishmania*. *Front. Biosci.* 16, 2069–2085. doi:10.2741/3840
- Requena, J. M., Montalvo, A. M., and Fraga, J. (2015). Molecular chaperones of *Leishmania*: Central players in many stress-related and -unrelated physiological processes. *Biomed. Res. Int.* 2015, e301326. doi:10.1155/2015/301326
- Retzlaff, M., Hagn, F., Mitschke, L., Hessling, M., Gugel, F., Kessler, H., et al. (2010). Asymmetric activation of the Hsp90 dimer by its cochaperone Aha1. *Mol. Cell* 37, 344–354. doi:10.1016/j.molcel.2010.01.006
- Richter, K., Reinstein, J., and Buchner, J. (2007). A grp on the Hsp90 mechanism. *Mol. Cell* 28, 177–179. doi:10.1016/j.molcel.2007.10.007
- Roberts, J. D., Thapaliya, A., Martínez-Lumbreras, S., Krysztofinska, E. M., and Isaacson, R. L. (2015). Structural and functional insights into small, glutamine-rich, tetratricopeptide repeat protein alpha. *Front. Mol. Biosci.* 2, 71. doi:10.3389/fmolb.2015.00071
- Röhl, A., Rohrberg, J., and Buchner, J. (2013). The chaperone Hsp90: Changing partners for demanding clients. *Trends biochem. Sci.* 38, 253–262. doi:10.1016/j.tibs.2013.02.003
- Roy, N., Nageshan, R. K., Ranade, S., and Tatu, U. (2012). Heat shock protein 90 from neglected protozoan parasites. *Biochim. Biophys. Acta* 1823, 707–711. doi:10.1016/j.bbamcr.2011.12.003
- Sahasrabudhe, P., Rohrberg, J., Biebl, M. M., Rutz, D. A., and Buchner, J. (2017). The plasticity of the Hsp90 Co-chaperone system. *Mol. Cell* 67, 947–961. e5. doi:10.1016/j.molcel.2017.08.004
- Samant, R. S., Clarke, P. A., and Workman, P. (2012). The expanding proteome of the molecular chaperone HSP90. *Cell Cycle* 11, 1301–1308. doi:10.4161/cc.19722
- Savage, J. R., McLaughlin, J. N., Skiba, N. P., Hamm, H. E., and Willardson, B. M. (2000). Functional roles of the two domains of phosphatidylcholine transferase protein. *J. Biol. Chem.* 275, 30399–30407. doi:10.1074/jbc.M005120200
- Scheufler, C., Brinker, A., Bourenkov, G., Pegoraro, S., Moroder, L., Bartunik, H., et al. (2000). Structure of TPR domain-peptide complexes: Critical elements in the assembly of the hsp70-hsp90 multichaperone machine. *Cell* 101, 199–210. doi:10.1016/S0092-8674(00)80830-2
- Schleiff, E., and Becker, T. (2011). Common ground for protein translocation: Access control for mitochondria and chloroplasts. *Nat. Rev. Mol. Cell Biol.* 12, 48–59. doi:10.1038/nrm3027
- Schmidt, J. C., Soares, M. J., Goldenberg, S., Pavoni, D. P., and Krieger, M. A. (2011). Characterization of TcSTI-1, a homologue of stress-induced protein-1, in *Trypanosoma cruzi*. *Mem. Inst. Oswaldo Cruz* 106, 70–77. doi:10.1590/s0074-02762011000100012
- Schopf, F. H., Biebl, M. M., and Buchner, J. (2017). The HSP90 chaperone machinery. *Nat. Rev. Mol. Cell Biol.* 18, 345–360. doi:10.1038/nrm.2017.20
- Seraphim, T. V., Alves, M. M., Silva, I. M., Gomes, F. E. R., Silva, K. P., Murta, S. M. F., et al. (2013). Low resolution structural studies indicate that the activator of Hsp90 ATPase 1 (Aha1) of *Leishmania braziliensis* has an elongated shape which allows its interaction with both N- and M-domains of Hsp90. *PLoS One* 8, e66822. doi:10.1371/journal.pone.0066822
- Shahriyari, L., Abdel-Rahman, M., and Cebulla, C. (2019). BAP1 expression is prognostic in breast and uveal melanoma but not colon cancer and is highly positively correlated with RBM15B and USP19. *PLoS One* 14, e0211507. doi:10.1371/journal.pone.0211507



- Shaner, N. C., Lambert, G. G., Chammas, A., Ni, Y., Cranfill, P. J., Baird, M. A., et al. (2013). A bright monomeric green fluorescent protein derived from *Branchiostoma lanceolatum*. *Nat. Methods* 10, 407–409. doi:10.1038/nmeth.2413
- Shimogawa, M. M., Saada, E. A., Vashisht, A. A., Barshop, W. D., Wohlschlegel, J. A., and Hill, K. L. (2015). Cell surface proteomics provides insight into stage-specific remodeling of the host-parasite interface in trypanosoma brucei. *Mol. Cell. Proteomics* 14, 1977–1988. doi:10.1074/mcp.M114.045146
- Shonhai, A., Maier, G., Przyborski, A. M., and Blatch, L. (2011). Intracellular Protozoan parasites of humans: The role of molecular chaperones in development and pathogenesis. *Protein Pept. Lett.* 18, 143–157. doi:10.2174/092986611794475002
- Siegelin, M. D., Dohi, T., Raskett, C. M., Orlowski, G. M., Powers, C. M., Gilbert, C. A., et al. (2011). Exploiting the mitochondrial unfolded protein response for cancer therapy in mice and human cells. *J. Clin. Invest.* 121, 1349–1360. doi:10.1172/JCI44855
- Sigrist, C. J. A., Cerutti, L., de Castro, E., Langendijk-Genevaux, P. S., Bulliard, V., Bairoch, A., et al. (2010). PROSITE, a protein domain database for functional characterization and annotation. *Nucleic Acids Res.* 38, D161–D166. doi:10.1093/nar/gkp885
- Silva, K. P., Seraphim, T. V., and Borges, J. C. (2013). Structural and functional studies of Leishmania braziliensis Hsp90. *Biochim. Biophys. Acta* 1834, 351–361. doi:10.1016/j.bbapap.2012.08.004
- Simarro, P. P., Cecchi, G., Paone, M., Franco, J. R., Diarra, A., Ruiz, J. A., et al. (2010). The atlas of human african trypanosomiasis: A contribution to global mapping of neglected tropical diseases. *Int. J. Health Geogr.* 9, 57. doi:10.1186/1476-072X-9-57
- Smith, J. R., and Workman, P. (2009). Targeting CDC37: An alternative, kinase-directed strategy for disruption of oncogenic chaperoning. *Cell Cycle* 8, 362–372. doi:10.4161/cc.8.3.7531
- Song, H. Y., Dunbar, J. D., Zhang, Y. X., Guo, D., and Donner, D. B. (1995). Identification of a protein with homology to hsp90 that binds the type 1 tumor necrosis factor receptor. *J. Biol. Chem.* 270, 3574–3581. doi:10.1074/jbc.270.8.3574
- Stechmann, A., and Cavalier-Smith, T. (2003). Phylogenetic analysis of eukaryotes using heat-shock protein Hsp90. *J. Mol. Evol.* 57, 408–419. doi:10.1007/s00239-003-2490-x
- Steiner, J. P., and Haughey, N. J. (2010). “Immunophilin ligands,” in *Encyclopedia of movement disorders*. Editors V. Leo and K. Katie (Amsterdam, Netherland: Elsevier), 66–68. doi:10.1016/B978-0-12-374105-9.00254-9
- Stuttman, J., Parker, J. E., and Noël, L. D. (2008). Staying in the fold: The SGT1/chaperone machinery in maintenance and evolution of leucine-rich repeat proteins. *Plant Signal. Behav.* 3, 283–285. doi:10.4161/psb.3.5.5576
- Su, G., Roberts, T., and Cowell, J. K. (1999). TTC4, a novel human gene containing the tetratricopeptide repeat and mapping to the region of chromosome 1p31 that is frequently deleted in sporadic breast cancer. *Genomics* 55, 157–163. doi:10.1006/geno.1998.5633
- Subbarao Sreedhar, A., Kalmár, É., Csermely, P., and Shen, Y.-F. (2004). Hsp90 isoforms: Functions, expression and clinical importance. *FEBS Lett.* 562, 11–15. doi:10.1016/S0014-5793(04)00229-7
- Subota, I., Julkowska, D., Vincensini, L., Reeg, N., Buisson, J., Blisnick, T., et al. (2014). Proteomic analysis of intact flagella of procyclic Trypanosoma brucei cells identifies novel flagellar proteins with unique sub-localization and dynamics. *Mol. Cell. Proteomics* 13, 1769–1786. doi:10.1074/mcp.M113.033357
- Taipale, M., Kaminen, N., Nopola-Hemmi, J., Haltia, T., Myllyluoma, B., Lyytinen, H., et al. (2003). A candidate gene for developmental dyslexia encodes a nuclear tetratricopeptide repeat domain protein dynamically regulated in brain. *Proc. Natl. Acad. Sci. U. S. A.* 100, 11553–11558. doi:10.1073/pnas.1833911100
- Taipale, M., Krykbaeva, I., Koeva, M., Kayatekin, C., Westover, K. D., Karras, G. I., et al. (2012). Quantitative analysis of HSP90-client interactions reveals principles of substrate recognition. *Cell* 150, 987–1001. doi:10.1016/j.cell.2012.06.047
- Taipale, M., Tucker, G., Peng, J., Krykbaeva, I., Lin, Z.-Y., Larsen, B., et al. (2014). A quantitative chaperone interaction network reveals the architecture of cellular protein homeostasis pathways. *Cell* 158, 434–448. doi:10.1016/j.cell.2014.05.039
- Tatu, U., and Neckers, L. (2014). Chaperoning parasitism: The importance of molecular chaperones in pathogen virulence. *Parasitology* 141, 1123–1126. doi:10.1017/S0031182014000778
- Trepel, J., Mollapour, M., Giaccone, G., and Neckers, L. (2010). Targeting the dynamic HSP90 complex in cancer. *Nat. Rev. Cancer* 10, 537–549. doi:10.1038/nrc2887
- Urbaniak, M. D., Guthrie, M. L. S., and Ferguson, M. A. J. (2012). Comparative SILAC proteomic analysis of Trypanosoma brucei bloodstream and procyclic lifecycle stages. *PLoS ONE* 7, e36619. doi:10.1371/journal.pone.0036619
- Urbaniak, M. D., Martin, D. M. A., and Ferguson, M. A. J. (2013). Global quantitative SILAC phosphoproteomics reveals differential phosphorylation is widespread between the procyclic and bloodstream form lifecycle stages of Trypanosoma brucei. *J. Proteome Res.* 12, 2233–2244. doi:10.1021/pr400086y
- Urményi, T. P., Silva, R., and Rondinelli, E. (2014). The heat shock proteins of Trypanosoma cruzi. *Subcell. Biochem.* 74, 119–135. doi:10.1007/978-94-007-7305-9\_5
- Wallace, F. G. (1966). The trypanosomatid parasites of insects and arachnids. *Exp. Parasitol.* 18, 124–193. doi:10.1016/0014-4894(66)90015-4
- Waterhouse, A. M., Procter, J. B., Martin, D. M. A., Clamp, M., and Barton, G. J. (2009). Jalview version 2—A multiple sequence alignment editor and analysis workbench. *Bioinformatics* 25, 1189–1191. doi:10.1093/BIOINFORMATICS/BTP033
- Webb, J. R., Campos-Neto, A., Skeiky, Y. A., and Reed, S. G. (1997). Molecular characterization of the heat-inducible LmSTT1 protein of Leishmania major. *Mol. Biochem. Parasitol.* 89, 179–193. doi:10.1016/s0166-6851(97)00115-1
- Whitesell, L., and Lindquist, S. L. (2005). HSP90 and the chaperoning of cancer. *Nat. Rev. Cancer* 5, 761–772. doi:10.1038/nrc1716
- WHO (2019). WHO interim guidelines for the treatment of gambiense human African trypanosomiasis. Geneva: World Health Organization. Available at: <http://www.ncbi.nlm.nih.gov/books/NBK545514/> (Accessed August 7, 2022).
- Wiesig, M., and Clos, J. (2001). The heat shock protein 90 of Leishmania donovani. *Med. Microbiol. Immunol.* 190, 27–31. doi:10.1007/s004300100074
- Willardson, B. M., and Howlett, A. C. (2007). Function of phosphatidylcholine-like proteins in G protein signaling and chaperone-assisted protein folding. *Cell. Signal.* 19, 2417–2427. doi:10.1016/j.cellsig.2007.06.013
- Wu, J., Luo, S., Jiang, H., and Li, H. (2005). Mammalian CHORD-containing protein 1 is a novel heat shock protein 90-interacting protein. *FEBS Lett.* 579, 421–426. doi:10.1016/j.febslet.2004.12.005
- Wunderley, L., Leznicki, P., Payapilly, A., and High, S. (2014). SGTA regulates the cytosolic quality control of hydrophobic substrates. *J. Cell Sci.* 127, 4728–4739. doi:10.1242/jcs.155648
- Yang, Y., Rao, R., Shen, J., Tang, Y., Fiskus, W., Nechtman, J., et al. (2008). Role of acetylation and extracellular location of heat shock protein 90alpha in tumor cell invasion. *Cancer Res.* 68, 4833–4842. doi:10.1158/0008-5472.CAN-08-0644
- Yao, C., Donelson, J. E., and Wilson, M. E. (2003). The major surface protease (MSP or GP63) of Leishmania sp. Biosynthesis, regulation of expression, and function. *Mol. Biochem. Parasitol.* 132, 1–16. doi:10.1016/S0166-6851(03)00211-1
- Yau, W.-L., Blisnick, T., Taly, J.-F., Helmer-Citterich, M., Schiene-Fischer, C., Leclercq, O., et al. (2010). Cyclosporin A treatment of Leishmania donovani reveals stage-specific functions of cyclophilins in parasite proliferation and viability. *PLoS Negl. Trop. Dis.* 4, e729. doi:10.1371/journal.pntd.0000729
- Yau, W.-L., Pescher, P., MacDonald, A., Hem, S., Zander, D., Retzlaff, S., et al. (2014). The *L. eishmania donovani* chaperone cyclophilin 40 is essential for intracellular infection independent of its stage-specific phosphorylation status: LdCyP40 null mutant analysis. *Mol. Microbiol.* 93, 80–97. doi:10.1111/mmi.12639
- Young, J. C., and Hartl, F. U. (2000). Polypeptide release by Hsp90 involves ATP hydrolysis and is enhanced by the co-chaperone p23. *EMBO J.* 19, 5930–5940. doi:10.1093/emboj/19.21.5930
- Zhang, N., Jiang, N., Zhang, K., Zheng, L., Zhang, D., Sang, X., et al. (2020). Landscapes of protein posttranslational modifications of african trypanosoma parasites. *iScience* 23, 101074. doi:10.1016/j.isci.2020.101074
- Zhao, R., Kakiyama, Y., Gribun, A., Huen, J., Yang, G., Khanna, M., et al. (2008). Molecular chaperone Hsp90 stabilizes Pih1/Nop17 to maintain R2TP complex activity that regulates snoRNA accumulation. *J. Cell Biol.* 180, 563–578. doi:10.1083/jcb.200709061
- Zhu, H., Larade, K., Jackson, T. A., Xie, J., Ladoux, A., Acker, H., et al. (2004). NCB5OR is a novel soluble NAD(P)H reductase localized in the endoplasmic reticulum. *J. Biol. Chem.* 279, 30316–30325. doi:10.1074/jbc.M402664200
- Zhu, H., Qiu, H., Yoon, H.-W. P., Huang, S., and Bunn, H. F. (1999). Identification of a cytochrome b<sub>5</sub>-type NAD(P)H oxidoreductase ubiquitously expressed in human cells. *Proc. Natl. Acad. Sci. U. S. A.* 96, 14742–14747. doi:10.1073/pnas.96.26.14742
- Zininga, T., and Shonhai, A. (2019). Small molecule inhibitors targeting the heat shock protein system of human obligate Protozoan parasites. *Int. J. Mol. Sci.* 20, 5930. doi:10.3390/ijms20235930
- Zuehlke, A., and Johnson, J. L. (2010). Hsp90 and co-chaperones twist the functions of diverse client proteins. *Biopolymers* 93, 211–217. doi:10.1002/bip.21292





## OPEN ACCESS

## EDITED BY

Graham Chakafana,  
Stanford University, United States

## REVIEWED BY

Keda Zhou,  
The University of Hong Kong, Hong  
Kong SAR, China  
Yong Xue,  
Jiangsu Ocean University, China

## \*CORRESPONDENCE

Adrian Arrieta,  
aarrieta1335@gmail.com

## SPECIALTY SECTION

This article was submitted to Protein  
Folding, Misfolding and Degradation,  
a section of the journal  
Frontiers in Molecular Biosciences

RECEIVED 11 July 2022

ACCEPTED 12 September 2022

PUBLISHED 30 September 2022

## CITATION

Arrieta A and Vondriska TM (2022),  
Nucleosome proteostasis and  
histone turnover.  
*Front. Mol. Biosci.* 9:990006.  
doi: 10.3389/fmolb.2022.990006

## COPYRIGHT

© 2022 Arrieta and Vondriska. This is an  
open-access article distributed under  
the terms of the [Creative Commons  
Attribution License \(CC BY\)](#). The use,  
distribution or reproduction in other  
forums is permitted, provided the  
original author(s) and the copyright  
owner(s) are credited and that the  
original publication in this journal is  
cited, in accordance with accepted  
academic practice. No use, distribution  
or reproduction is permitted which does  
not comply with these terms.

# Nucleosome proteostasis and histone turnover

Adrian Arrieta<sup>1\*</sup> and Thomas M. Vondriska<sup>1,2,3</sup>

<sup>1</sup>Departments of Anesthesiology and Perioperative Medicine, David Geffen School of Medicine, University of California, Los Angeles, Los Angeles, CA, United States, <sup>2</sup>Departments of Medicine/Cardiology, David Geffen School of Medicine, University of California, Los Angeles, Los Angeles, CA, United States, <sup>3</sup>Departments of Physiology, David Geffen School of Medicine, University of California, Los Angeles, Los Angeles, CA, United States

Maintenance of protein folding homeostasis, or proteostasis is critical for cell survival as well as for execution of cell type specific biological processes such as muscle cell contractility, neuronal synapse and memory formation, and cell transition from a mitotic to post-mitotic cell type. Cell type specification is driven largely by chromatin organization, which dictates which genes are turned off or on, depending on cell needs and function. Loss of chromatin organization can have catastrophic consequences either on cell survival or cell type specific function. Chromatin organization is highly dependent on organization of nucleosomes, spatiotemporal nucleosome assembly and disassembly, and histone turnover. In this review our goal is to highlight why nucleosome proteostasis is critical for chromatin organization, how this process is mediated by histone chaperones and ATP-dependent chromatin remodelers and outline potential and established mechanisms of disrupted nucleosome proteostasis during disease. Finally, we highlight how these mechanisms of histone turnover and nucleosome proteostasis may conspire with unfolded protein response programs to drive histone turnover in cell growth and development.

## KEYWORDS

chaperone, histone, folding, disease, development, chromatin, nucleosome

## Maintaining nucleosome proteostasis

Across all domains of life, protein quality control is critical for organismal survival. Within organelles such as the mitochondria and endoplasmic reticulum, there is a balance between the proteins that reside within these compartments that give them their function e.g., the electron transport chain proteins that generate ATP in the mitochondria, and the protein folding chaperones that catalyze folding of the organelle's polypeptides into their final 3D structure, ensuring proper function. During the folding process, chaperones sequester unstable proteins to prevent them from detrimentally interacting with other proteins or other macromolecules, and modulate the kinetics i.e., speed, of folding, and often across several folding cycles, until a stable *and* functional structure is reached (Balchin et al., 2016). Chaperones not only serve to fold newly synthesized proteins and maintain the folding of longer-lived proteins, they also serve to usher “terminally misfolded proteins”, proteins that have gone through several folding cycles without

reaching a functional folded state (Balchin et al., 2016), towards dedicated subcellular protein degradation machinery such as the proteasome. Together these chaperone functions stave off accumulation of cytotoxic misfolded protein aggregates; however, when there are more unfolded proteins than there are chaperones to fold them in compartments such as the ER, mitochondria, and cytosol, these compartments increase the activity of their respective unfolded protein responses (UPRs) (Ron and Walter, 2007; Ankar and Sistonen, 2011; Arrieta et al., 2019). Activation of these UPR pathways results in increased expression of the resident protein folding and protein degradation networks. If protein folding homeostasis (also known as proteostasis) is not restored, these same UPRs will then engage in cell death signaling (Doroudgar and Glembotski, 2013). Just as there are dedicated chaperones and protein degradation machinery that co-evolved with the client polypeptides that traverse the ER or power the mitochondria, there is dedicated machinery that has evolved to meet the protein complex assembly and genome folding demands of chromatin (Hammond et al., 2017; Alvarez-Ponce et al., 2019).

The main organizational subunit of chromatin, the nucleosome, is composed of 147 base pairs of DNA wrapped around a protein octamer of two subunits each of histone H2A, H2B, H3 and H4 (Zhou et al., 2019). These histone proteins are extensively post-translationally modified—by some counts, individual cells can have hundreds of distinct modifications on their nucleosomes (Zhao and Garcia, 2015). Several of these modifications have been shown to operate (alone or in combination) to regulate the binding of other proteins, local chromatin accessibility, transcription, DNA repair and other processes. The role of histone modifications in chromatin biology and gene expression is an active area of research that has been reviewed elsewhere (Henikoff and Smith, 2015). Additionally, nucleosome stability is modulated by co-occupancy with linker histones, which influence formation of higher order chromatin structure, as well as by replacement of core histones with variants of histone H2A, H2B, and H3 (Henikoff and Smith, 2015; Hergeth and Schneider, 2015; Martire and Banaszynski, 2020). Maintaining chromatin organization is a formidable task, given that chromatin must participate in process such as genome duplication, mitosis, and cellular differentiation, all while maintaining cell type identity and the ability to respond to physiological and pathophysiological stimuli (Palozola et al., 2019). In this review, our goals are to highlight the specific protein complex assembly challenges associated with maintenance of chromatin, to examine how chromatin function changes during disease and development through the lens of nucleosome and histone turnover, and to shed light on potentially druggable interactions between other protein quality control pathways and the histone chaperone and chromatin remodeling network. The mechanisms by which histone chaperones engage in the folding of histones

and nucleosome assembly has been described elsewhere (Hammond et al., 2017).

## The histone chaperone network and ATP-dependent chromatin remodelers in replication-dependent and independent histone turnover

The histone chaperone network is the group of chaperones that mediate the various aspects of histone turnover which include histone synthesis, histone deposition onto and ejection from chromatin, histone sequestration and recycling, histone degradation, histone post-translational modification, and nucleosome assembly and disassembly (Hammond et al., 2017). Much like “typical chaperones”, histone chaperones are defined by their ability to shield and sequester histones from forming dysfunctional interactions with other proteins as well as nucleic acids. However, whereas other chaperones are thought to operate at least in part by shielding aggregation-prone hydrophobic protein topologies, histone chaperones must contend with preventing improper electrostatic interactions driven by the net positive charge characteristic of histone proteins (Hammond et al., 2017). Histone chaperones execute these various processes of histone metabolism during DNA replication, termed replication-dependent histone turnover (Figure 1A) and outside of DNA replication, termed replication-independent histone turnover (Figure 1B). Additionally, similar to how other protein quality control processes are ATP-dependent (Stein et al., 2014; Balchin et al., 2016), we will also discuss how the histone chaperone network operates in concert with ATP-dependent chromatin remodelers to mediate various aspects of nucleosome assembly and disassembly during replication-dependent and independent histone turnover.

During replication-dependent histone turnover, newly synthesized histone variants—in conjunction with “old histones” that are thought to contribute to maintenance of epigenetically repressed states (Escobar et al., 2022)—are deposited behind the replisome by histone chaperones onto chromatin during DNA synthesis, resulting in the formation of pre-nucleosomes. Pre-nucleosomes, composed of approximately 80 base pairs loosely wrapped around the histone octamer, are converted into mature nucleosomes *via* DNA translocation by ATP-dependent chromatin remodelers like ACF or CHD1 (Figure 1A) (Lusser et al., 2005; Fei et al., 2015). As DNA is replicated, newly synthesized H3.1/H3.2 and H4 are imported via the nuclear pore localized importin 4 (Soniati et al., 2016) (IPO4), and this histone heterodimer is bound by the histone chaperone anti-silencing factor 1 (Asf1) before being transferred to the chromatin assembly factor (CAF-1) histone chaperone complex that is associated with the DNA replisome (Groth et al., 2005; Groth et al., 2007; Gunesdogan et al., 2014)

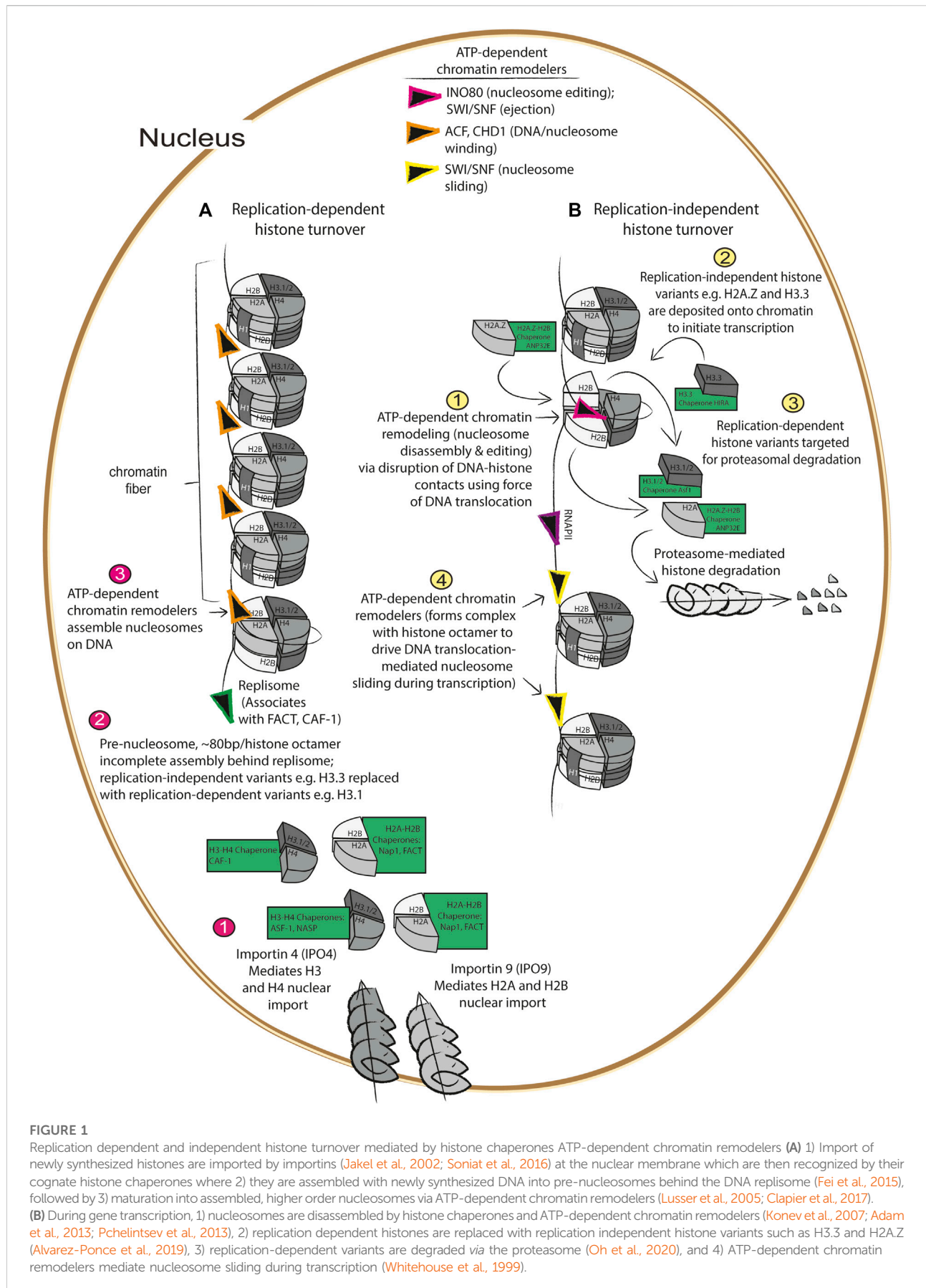


(Figure 1A). Concurrently, nucleosome assembly protein 1 (Nap1) and/or the facilitates chromatin transaction (FACT) complex mediates nuclear import of H2A/H2B via importin 9 (IPO9) (Jakel et al., 2002), and mediates nucleosome assembly at sites of DNA replication (Aguilar-Gurrieri et al., 2016). While these processes are the essential components of replication-dependent histone turnover, they also interface with various aspects of replication-independent histone turnover (Figure 1B).

Replication-independent histone turnover refers to histone turnover events that occur outside of DNA replication, which include centromere formation, DNA repair, and initiation of transcription (Figure 1B). As part of the cell cycle, centromeres are formed which are critical for mitotic spindle assembly; centromeres are formed when H3 variants are replaced by the centrosome-specific H3 variant, Histone H3-like centromeric protein A (CENPA) which is deposited onto highly repetitive DNA sequences by the CENPA-specific chaperone, Holliday junction recognition protein (HJURP), during the G1 phase of the cell cycle (Dunleavy et al., 2009; Dunleavy et al., 2011). In addition to the role of histone turnover in centromere formation, histone turnover is also a critical aspect of the DNA damage response, as nucleosomes must be disassembled by the histone chaperones and ATP-dependent chromatin remodelers working in concert to allow the DNA to be accessible to the repair machinery (Rogakou et al., 1998). As will be discussed in further detail below, the process of nucleosome disassembly and histone degradation following DNA damage is driven by deposition and phosphorylation of the histone variant H2AX, and this phosphorylated form is referred to as  $\gamma$ H2AX (Rogakou et al., 1998; Hauer et al., 2017; Piquet et al., 2018). Deposition of H2AX is mediated by the Facilitator of Chromatin Transactions (FACT) complex, and phosphorylation of H2AX by the kinase known as ataxia-telangiectasia-mutated and Rad3-related (ATR) initiates nucleosome disassembly and recruitment of the DNA damage response machinery, including the ATP-dependent chromatin remodeler and nucleosome editor INO80 [this family of proteins uses DNA translocation to disrupt DNA-histone interaction to mediate histone eviction and replacement (Rogakou et al., 1998; Clapier et al., 2017; Hauer et al., 2017; Piquet et al., 2018)]. Interestingly, H2AX deposition occurs at sites where the histone chaperone ANP32E, together with INO80, mediates eviction of the pro-transcription H2A.Z/H2B heterodimer (Piquet et al., 2018). Following DNA repair, H3.3 is deposited onto newly repaired DNA by the H3.3 histone chaperone histone cell cycle regulator (HIRA) complex, composed of HIRA, ASF-1, and CABIN-1, in conjunction with the ATP-dependent chromatin remodeler CHD1 (Konev et al., 2007) to drive re-initiation of transcription following DNA damage (Adam et al., 2013). These studies are consistent with the notion that deposition of H2A.Z and H3.3 at

transcription start sites drives gene transcription. In the following section, we will discuss how various aspects of replication-dependent and independent histone turnover cooperate to ensure fidelity in re-establishment of epigenetic states following mitosis.

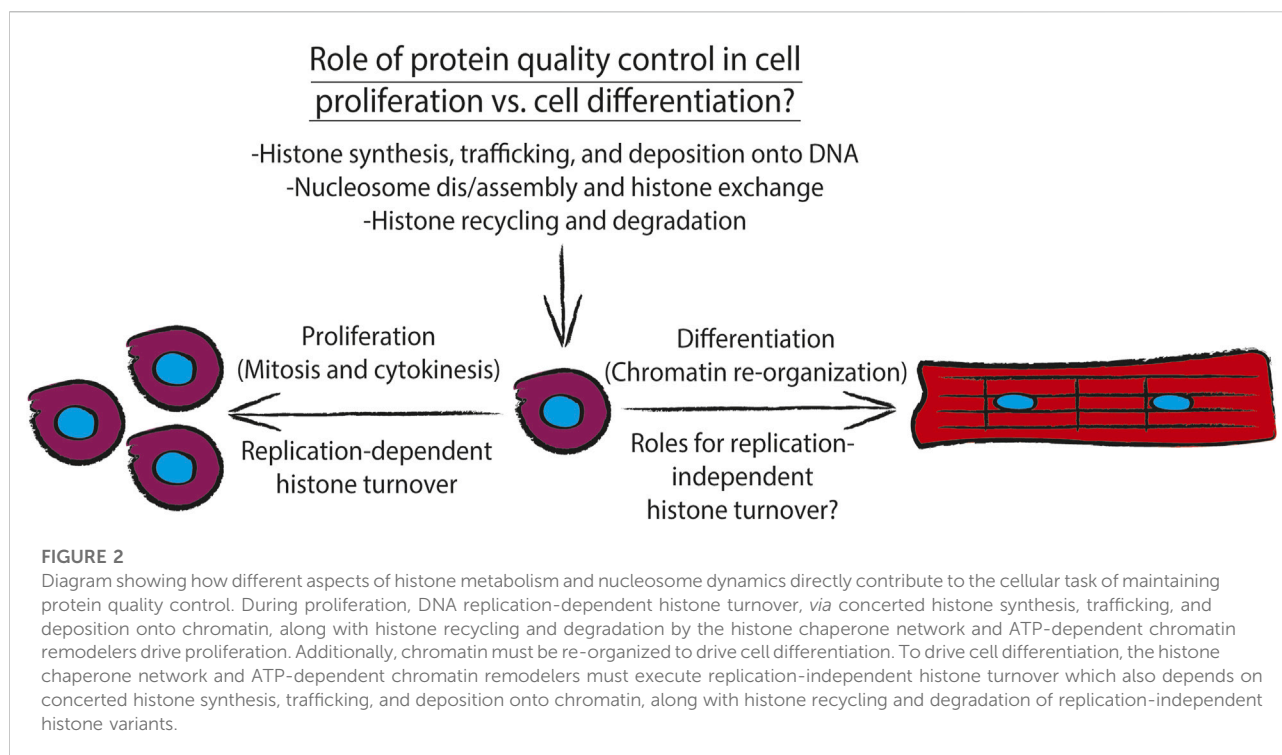
## Replication-dependent and independent histone turnover in proliferating cells

During DNA replication (i.e., S phase of the cell cycle), cells must duplicate the entire genome, and as a result must contain approximately twice the number of histone proteins present in a non-dividing cell (Gunesdogan et al., 2014). As discussed above, uncontrolled interactions of histones with DNA or other proteins can be geno- and proteotoxic and can result in genomic instability (Gunjan and Verreault, 2003; Singh et al., 2010). Such catastrophic interactions are avoided during DNA replication by an orchestrated balance between histone synthesis, histone degradation, and histone chaperone activity, which cooperate to maintain nucleosome dynamics (Figure 2). These concerted activities contribute to “epigenetic memory” (Palozola et al., 2019)- the concept that cells are able to remember what gene programs to keep on or off following cell division or other events that force a loss of interphase chromatin territories such as repair of DNA double stranded breaks.

Cellular histone levels are tightly controlled via regulation of their synthesis as well as their degradation during cell proliferation, specifically, during DNA synthesis (Figure 2). It has been demonstrated that in proliferating cultures of the yeast *Saccharomyces cerevisiae*, histone synthesis undergoes sub scaling during cell growth i.e., synthesis of histones is matched to DNA content and phase of the cell cycle, rather than cell size (Marzluff et al., 2008; Swaffer et al., 2021). At the post-transcriptional level, the transcripts encoding replication-dependent histones exhibit a short half-life due to the lack of a stabilizing poly-A tail. However, they are stabilized and trafficked to the translational machinery during S phase by histone stem-loop-binding protein (SLBP), which binds to the 3' untranslated region of these transcripts and is degraded at the end of S phase in the cell cycle (Zheng et al., 2003).

Following mitosis, during which gene transcription is mostly silent due to a combination of chromatin inaccessibility to transcription machinery and removal of pro-transcriptional histone variants e.g. H2A.Z and H3.3 (Figures 1A,B), the cell must re-initiate gene transcription which is thought to require turnover of replication-dependent histone variants for replication-independent histone variants (discussed further below). Recently, it has been demonstrated in embryonic stem cells that the anaphase promoting complex (APC), which canonically ubiquitylates securin and cyclin B to initiate their proteasome-mediated degradation to drive anaphase (King et al.,





1995; Cohen-Fix et al., 1996), also mediates ubiquitylation and proteasome-mediated degradation of histones present at transcription start sites of genes critical to mRNA translation and ribosome function (Oh et al., 2020). This task of extracting histones from chromatin is performed by a AAA-ATPase that is associated with the APC, valosin-containing protein (p97/VCP); VCP-mediated extraction of histones from chromatin is similar to the process of endoplasmic reticulum-associated degradation (ERAD), during which VCP hydrolyzes ATP to extract misfolded ER luminal and transmembrane proteins from the endoplasmic reticulum to allow for their ubiquitylation by the ER transmembrane E3 ubiquitin ligase Hrd1 (Ye et al., 2005). This study (Oh et al., 2020) went on to show that the chromatin associated factor, WDR5, which binds to H3K4 trimethylated histones (H3K4Me3; a mark that is associated with active interphase promoters) recruits the APC along with transcription initiation factors TF-IIID and TBP, and the ATP-dependent chromatin remodelers INO80 which mediates nucleosome editing (Figure 1B). These results support the notion that pathways of protein quality control, cell cycle control, and chromatin remodeling cooperate to mediate histone turnover and thus maintenance of cellular identity in dividing cells (Figure 2).

There are several pieces of evidence that members of the histone chaperone network work with ATP-dependent chromatin remodelers to contribute to the maintenance of cellular identity in dividing cells. HIRA, which exists in a complex with chromatin remodelers ISWI, SNF, and Brg1

(Hang et al., 2010; Pchelintsev et al., 2013), is required for the maintenance of cellular identity of C2C12 myoblasts, yet also drives myoblast differentiation into myotubes (Yang et al., 2016; Esteves de Lima et al., 2021). With regard to maintenance of cellular identity in proliferating cells, knockout of HIRA results in loss of satellite muscle stem cell identity as indicated by decreased expression of Pax7, an established marker of satellite muscle stem cells, and of myogenic transcription factor MyoD, along with impaired capacity to differentiate into myotubes. Knockout of *Hira* also increased expression of different lineage markers unrelated to muscle function (e.g., neuronal development and synapse organization) (Esteves de Lima et al., 2021). Consistent with a role for HIRA in driving replication-independent turnover, knockout of *Hira* resulted in decreased levels of H3.3 and H3K27Ac at the promoters of genes encoding skeletal muscle-specific genes. Additionally, there was an increase in H3K4Me3 at gene promoters, along with increased transcript expression, of genes encoding proteins found in other cell and tissue types (Esteves de Lima et al., 2021). The ability of HIRA to engage in depositing and turnover of histone H3.3 is dictated by a phosphorylation switch (Yang et al., 2016). In proliferating C2C12 myoblasts, HIRA was shown to be phosphorylated by Akt1/2, and upon differentiation into myotubes HIRA is dephosphorylated, which was followed by a concomitant increase in expression of myogenic genes e.g. myogenin and myosin heavy chain. Expression of human HIRA containing a non-phosphorylatable S650A point mutation (HIRA<sub>S650A</sub>) was sufficient to drive myoblast differentiation

into myotubes and resulted in increased deposition of H3.3 at active gene promoters, as determined by H3.3 ChIP-qPCR for the MyoD promoter. Furthermore, expression of the phosphomimetic mutant, HIRA<sub>S650D</sub>, prevented accumulation of H3.3 at the MyoD promoter. As for how Hira knockout might contribute to increased expression of genes associated with alternative cellular identities, it is possible that loss of this histone chaperone disrupts the Hira complex which, as discussed above, is formed in part by UBN1 and HIRA. Together these two chaperones have been shown to mediate formation of senescence-associated heterochromatin foci i.e. transcriptionally repressed chromatin, which include cell cycle control genes e.g. Cyclin A2 (Banumathy et al., 2009).

Together these studies support the idea that maintenance of epigenetic memory and concomitant chromatin remodeling in proliferating cells is reliant on coordinated activities between post-transcriptional regulation of histone synthesis, protein quality control and cell cycle control pathways, and activities of the histone chaperone network that can be modulated by post-translational modifications (Figure 2).

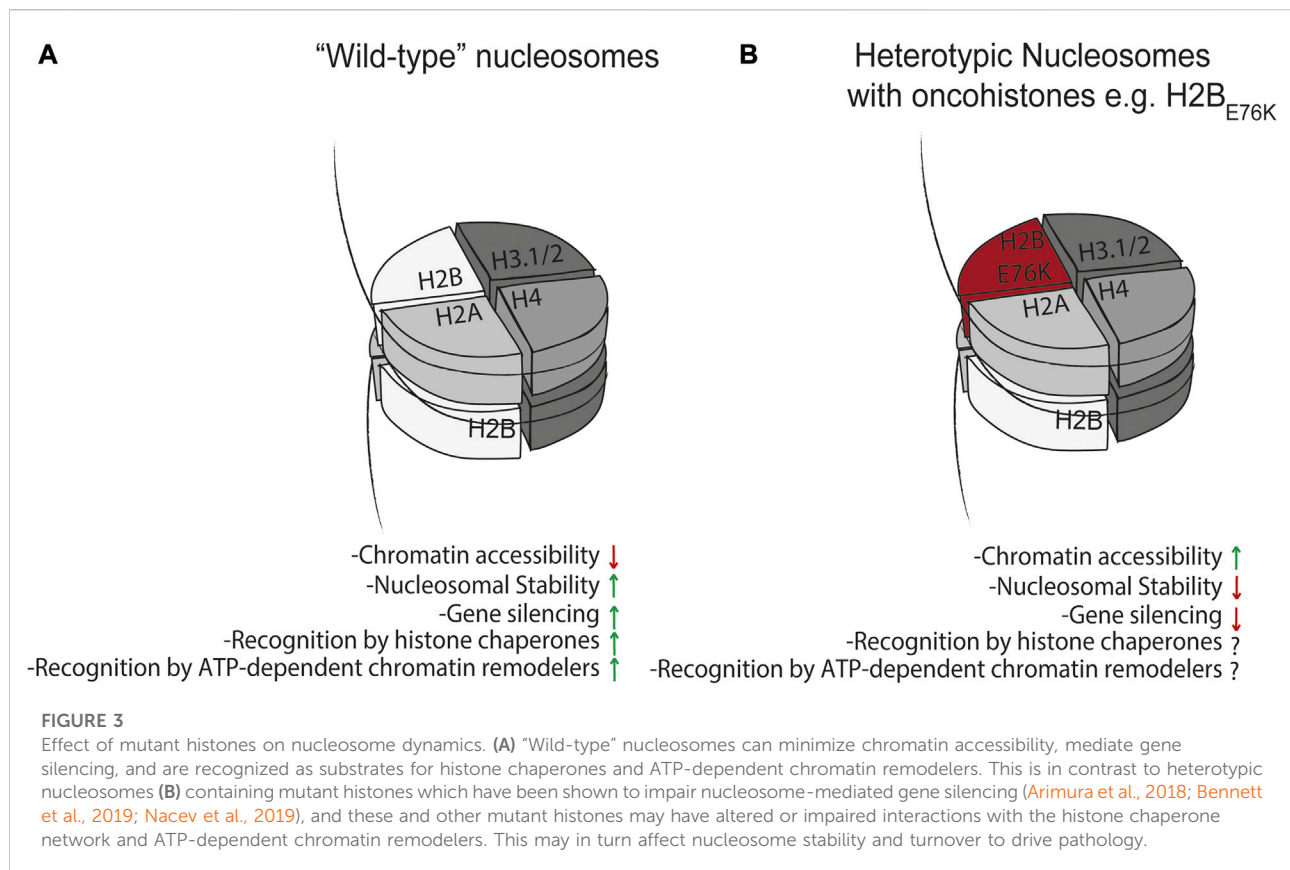
## Onco-histones and the histone chaperone network

Cancer, as a disease characterized by uncontrolled cell proliferation due in part to gain-of-function mutations in proto-oncogenes and loss-of-function mutations in tumor suppressor genes, heavily relies on robust function of protein quality control networks in order for tumor cells to survive within the tumor microenvironment. For example, inconsistent and low tumor perfusion, due to a mismatch between the rate of tumor growth and tumor-mediated angiogenesis, results in low oxygen and nutrient concentration, thus putting a strain on the energy-dependent aspects of maintaining proteostasis e.g., ATP-mediated protein folding in the endoplasmic reticulum (Tu et al., 2000). In this section, we aim to discuss how mutated histone proteins, known as “onco-histones” (Nacev et al., 2019) drive aggressive tumor proliferation via chromatin remodeling.

There is mounting evidence that cancer cells acquire mutations in histone genes that can result in genome-wide changes in chromatin organization or destabilize interactions of histones within the nucleosome, in turn disrupting gene regulatory mechanisms (Nacev et al., 2019). Mutations can occur within the dimerization interface of histones resulting in nucleosome instability, perhaps resulting in disruption of higher order chromatin structures that are critical in maintenance of cellular identity, or in the histone tails which can alter the affinity post-translational modifiers have for these mutant histones. The poster child of onco-histone mutations is exemplified by a Lys27Met mutation in histone H3.3 (H3.3<sub>K27M</sub>) (Lewis et al., 2013) in pediatric glioblastoma.

Additionally, human diffuse intrinsic pontine gliomas (DIPGs) containing this K27M mutation display significantly lower overall amounts of the gene-silencing histone modification H3 lysine 27 trimethylation (H3K27me3) and higher amounts of the gene activating mark H3K27Ac, the former of which the authors demonstrated was due to the H3.3<sub>K27M</sub> mutant histone directly inhibiting PRC2 methyltransferase activity (Lewis et al., 2013). A critical observation made in this study with the regard to the effects of H3.3<sub>K27M</sub> on the epigenome is that even though H3.3<sub>K27M</sub> itself cannot be methylated or acetylated due to the methionine substitution, H3.3<sub>K27M</sub> only needs to make up a fraction of the total H3 pool (thereby resulting in heterotypic nucleosomes containing a wild-type H3 and mutant H3.3<sub>K27M</sub>) to drive genome wide decreases in H3K27Me3 and increases in H3K27Ac on the remaining wild-type H3 expressed in the cell. In a subsequent study (Nacev et al., 2019) in which onco-histones are defined and catalogued across various tumor contexts, two standout example of how mutations in present in onco-histones are very likely to alter their folding are glycine or proline substitutions at R29 in histone H2A and R39 in histone H4, which is predicted to disrupt the stability of their  $\alpha$ -helical folds. These putative onco-histones could theoretically require longer-lived interactions with their cognate chaperones and form highly unstable nucleosomes, although to the best of our knowledge the former has not been formally tested. In support of the argument that mutations in histone proteins result in nucleosome instability, ATAC-seq was used in MCF10A cells expressing wild type histone H2B or H2B<sub>E76K</sub> (Bennett et al., 2019) to demonstrate that accessible regions in both WT or H2B<sub>E76K</sub> cells tended to be *more* accessible in the latter. Furthermore, expression of H2B<sub>E76K</sub> in yeast impaired the ability of cells to execute nucleosome-mediated gene silencing (Figure 3). Additionally, this study demonstrated, via nucleosome thermal stability assay, that nucleosomes containing H2B<sub>E76K</sub> displayed lower stability. These results, along with a separate study (Arimura et al., 2018) showing the relative instability of nucleosomes containing mutant forms of H3.1, H2A.Z, or H2B, are consistent with the notion that onco-histones do indeed alter the stability of nucleosomes (Figure 3). Whether onco-histones, and the nucleosomes they are incorporated into, are more dependent on the histone chaperone network and ATP-dependent chromatin remodelers to achieve their structure, stability, and incorporation into nucleosomes is unknown (Figure 3), but could be addressed experimentally by directly measuring differential turnover and deposition of onco-histones *in vivo*.

We discussed above the finding that the H3.3<sub>K27M</sub> onco-histone only needs to make up a fraction of the total H3.3 pool to drive genome-wide decreases in placement of H3K27Me3 (Lewis et al., 2013). This observation suggests that increased concentration of mutation-containing histones via alternative



mechanisms like translational infidelity (Kapur and Ackerman, 2018) or somatic cell mutation mosaicism (Frank, 2014) can drive other disease pathologies; like onco-histones, these mutant histones may have altered interactions with the histone chaperone network and ATP-dependent chromatin remodelers for their deposition onto chromatin where they might mediate disease progression via disruption of chromatin organization (Figure 3).

## Histone turnover in the neonatal and post-natal heart

The mammalian heart maintains a certain proliferative myocyte capacity after birth, which is critical to cardiac development and function, that is lost as the organism ages (Porrello et al., 2011; Serpooshan et al., 2017; Bogush et al., 2020). In addition to this proliferative switch, cardiac myocytes undergo a metabolic switch where ATP is generated via glycolysis in the neonatal heart versus fatty acid  $\beta$ -oxidation and oxidative phosphorylation in the adult heart (Lopaschuk et al., 1992). This metabolic switch is thought to be driven by a combination of increased blood oxygen tension, increased circulating fatty acids from the mother's milk, and increased

circulating catecholamine levels (Faxelius et al., 1983; Lopaschuk and Jaswal, 2010), all together enforcing the said switch to oxidative phosphorylation which provides enough ATP to power cardiac contractility. The increased rate of oxidative phosphorylation comes with increased production of reactive oxygen species, which can result in DNA damage and result in myocyte death in cases of cardiac ischemia/reperfusion injury. This series of events provides a unique chromatin remodeling challenge in cardiac myocytes as they must maintain a proliferative capacity after birth, contend with changes in oxygen tension after birth which is thought to mediate mitochondrial ROS generation and ensuing DNA damage, and also engage in transcriptomic reprogramming to allow for hypertrophic rather than hyperplastic myocyte growth as the heart develops (Nakada et al., 2017). The first studies to examine histone stoichiometry at the protein level in the diseased heart revealed a decrease in the core to linker ratio during the compensatory hypertrophic growth phase (as measured by H1:H4), concomitant with temporal reprogramming of abundance, and DNA association by, other non-nucleosomal chromatin structural proteins (including HMGs and nucleolin) as the heart transitions from hypertrophy to failure (Franklin et al., 2011; Franklin et al., 2012; Monte et al., 2013; Monte et al., 2016). More recent studies

have assessed roles for ATP-dependent chromatin remodelers of the SWI/SNF family in driving maturation of the neonatal heart (Hang et al., 2010), and histone turnover in the adult heart, shedding light on mechanisms that may drive this process.

Since the frequency of adult myocyte proliferation is vanishingly low and inadequate for repair after injury (Eschenhagen et al., 2017), myocytes likely engage primarily in replication-independent histone turnover for maintenance of chromatin structure. To our knowledge, the first study (Li et al., 2019) to examine histone turnover in the heart employed the following approach: Col1a1<sup>tetO-H2B-GFP</sup> x Rosa26<sup>M2rtTA</sup> transgenic mice were administered doxycycline-containing water to induce expression of GFP-H2B (i.e., a GFP-H2B pulse), followed by removal of doxycycline-containing water resulting in decreased transgene expression (i.e., an unlabeled H2B chase). Isolated myocytes were then subjected to GFP-H2B ChIP-Seq at various chase times, and the resulting sequencing data was used to calculate rates of genome-wide GFP-H2B turnover. Promoters of genes highly transcribed in cardiac myocytes (i.e., striated-muscle specific gene promoters), and cardiac-specific enhancers containing activating histone marks such as H3K27Ac, demonstrated higher rates of GFP-H2B turnover, as compared to genes with silencing marks or pluripotency enhancers. Two considerations for this study are the use of GFP-tagged H2B and the use of an isoform of H2B (*HIST1H2Bj*) that is normally encoded as a replication-dependent histone variant. With regard to the first point, protein tagging has been shown to alter the stability and/or folding kinetics of the protein it is fused to (Sokolowski et al., 2015), suggesting that turnover of GFP-H2B may not perfectly reflect endogenous H2B turnover due to differences in their stability. With regard to the second point, the replication-dependent and independent forms of H2B rely on different members of the histone chaperone network to mediate their folding, trafficking, and deposition onto chromatin (Hammond et al., 2017) (Figures 1A,B), and thus may reflect different rates of turnover depending on whether they are expressed in a dividing versus a non-dividing cell (Hammond et al., 2017). Interestingly, an orthogonal approach used metabolic labeling with deuterated H<sub>2</sub>O to assess rates of protein turnover in adult hearts treated with isoproterenol (Lam et al., 2014). In this study, only histone H4 showed detectable turnover, although technical considerations with the mass spectrometry-based detection of histones prevents a direct comparison of these studies. Consistent with the notion that cardiac remodeling events drive histone turnover, a recent study employed cardiomyocyte specific Ribo-Seq to identify transcripts engaged with polysomal ribosomes in response to pressure-overload mediated cardiac hypertrophy (Doroudgar et al., 2019). Ribosomes containing a myocyte specific HA-tagged ribosome subunit were purified from transgenic mouse hearts, and ribosome footprints from hypertrophic mouse hearts

displayed increased histone H4 as well as histone H2AX transcripts, but no increase in replication-dependent histone variants such as *HIST1H2Bj* and histone H3.1 and H3.2. As will be discussed further below, increased expression of H2AX is consistent with the notion that replication-independent turnover occurs in the adult mammalian heart and is due at least in part to the activities of  $\gamma$ H2Ax and the DNA damage response. Knockout of *Hira*, a histone chaperone, in cardiac myocytes resulted in cardiac hypertrophy concomitant with impaired contractility, re-expression of fetal genes, and cardiac fibrosis (Valenzuela et al., 2016). Importantly, the ATP-dependent chromatin remodeler BRG1 which interacts with HIRA, is required for cardiac hypertrophy, and was required for GFP-H2B turnover in the study described above (Hang et al., 2010). Together these studies suggest that replication-independent histone turnover occurs in the adult mammalian heart in response to pathological insult.

As discussed above, the high metabolic capacity of cardiac myocytes i.e., ROS generation as a byproduct of oxidative phosphorylation, suggests that cardiomyocytes constantly engage in a higher level of DNA repair activity, particularly in the days and weeks after birth. If this were the case, activity of the DNA damage response in the neonatal heart would be concomitant with the histone turnover that occurs as a result of DNA damage-mediated nucleosome disassembly, and H3.3/H2A.Z-mediated re-initiation of transcription (Adam et al., 2013; Hauer et al., 2017). This is supported by studies demonstrating that 1) myocyte cell cycle exit and indicators of DNA damage in mice can be reversed with exposure to decreased oxygen tension (Nakada et al., 2017) and 2) that pathological growth of the heart in response to pressure overload is associated with increased expression and nuclear localization of  $\gamma$ H2Ax (Nakada et al., 2019), which as described above is an orchestrator of nucleosome disassembly (Rogakou et al., 1998; Hauer et al., 2017; Piquet et al., 2018). Together these studies suggest that ROS is a driver of both cardiac development and disease, and that the histone chaperone network is critical for postnatal growth of cardiac myocytes and maintained function of the heart in the disease state.

Recent studies have demonstrated that the potent ER stress response transcription factor ATF6, which is activated in response to accumulation of misfolded proteins in the ER, is responsible for maintaining protein quality and quantity control mechanisms in other subcellular compartments (Blackwood et al., 2020). Specifically, during ischemia/reperfusion injury ATF6 was shown to transcriptionally upregulate critical members of the oxidative stress response, for example catalase, demonstrating that ATF6 prevents cardiomyocytes from accumulating ROS during ischemia/reperfusion injury (Jin et al., 2017). These results support the notion that perhaps ATF6-mediated induction of catalase can also mitigate oxidative stress in the days after birth where neonates adjust to life with atmospheric versus *in utero* oxygen



tension. Additionally, an examination of microarray (Martindale et al., 2006) and RNA-Seq (Blackwood et al., 2019) data sets from mouse hearts expressing the transcriptionally active fragment of ATF6 fused to the mutated estrogen receptor demonstrates a significant upregulation of VCP, which as discussed above is critical for histone turnover in proliferating cells. In considering how and why the ER stress response and the histone chaperone network may conspire to drive histone turnover and therefore development of the heart, it has been recently reported that myocyte binucleation after birth is critical for functional maturation of the heart, and that impairment of this process results in non-compaction cardiomyopathy (Gan et al., 2022). Along with postnatal myocyte proliferation that is critical for development and function of the heart (Serpooshan et al., 2017; Bogush et al., 2020), these bouts of mitotic activity—associated or not with cytokinesis—are likely to require histone turnover and re-initiation of transcription following mitosis or DNA damage, in order to maintain myocyte epigenetic memory following mitosis. Given that mitosis and binucleation have been observed in postnatal rat cardiomyocytes (Li et al., 1997), there is the possibility that the replication- and APC/VCP complex-dependent mechanisms of histone turnover described above (Oh et al., 2020) are at play in the postnatal heart. Consistent with ATP-dependent chromatin remodeler activity (i.e. nucleosome remodeling) in response to injury and cardiac development, the SWI/SNF ATP-dependent nucleosome remodeler BRG1 has been shown to be critical for neonatal cardiac development and pathological cardiac hypertrophy (Hang et al., 2010). Together these observations support the notion, which will ultimately need to be supported with future studies, that upon physiological reperfusion that occurs with mammalian birth, ATF6 transcriptionally induces ER targeted chaperones to protect against ER protein misfolding during myocyte growth, induces catalase to protect against excessive ROS-mediated DNA damage after birth (Figure 2), and induces VCP to mediate re-initiation of genes critical to hypertrophic myocyte growth following myocyte mitosis.

## Conclusions and future directions

In summary, histone quality control and the histone chaperone network and ATP-dependent chromatin remodelers that mediate this process are drivers of organism development and disease, representing potential

targets in the treatment of pathologies such as cardiovascular disease and cancer. However, some level of caution must be levied in considering these approaches as much remains to be learned about how, over what time course, and for what cellular function histones are turned over by their cognate chaperones (Figure 2). What is the threshold of what is recognized as a damaged or misfolded histone, and does it change in the context of disease or aging? And do misfolded or alternatively folded histones represent as yet an unexplored “epigenetic mark” that signals for chromatin remodeling by histone chaperones and downstream gene expression? As much as it is important to answer these questions in the context of disease, there is much to be gleaned by returning to the basic science of understanding what drives histone turnover at the molecular level.

## Author contributions

All authors listed have made a substantial, direct, and intellectual contribution to the work and approved it for publication.

## Funding

This work was supported by NIH grants R01HL105699 and R01HL150225 (TV); AA was supported by NIH T32 HL144449 (UCLA/Caltech Integrated Cardiometabolic Medicine for Bioengineers).

## Conflict of interest

The authors declare that the research was conducted in the absence of any commercial or financial relationships that could be construed as a potential conflict of interest.

## Publisher's note

All claims expressed in this article are solely those of the authors and do not necessarily represent those of their affiliated organizations, or those of the publisher, the editors and the reviewers. Any product that may be evaluated in this article, or claim that may be made by its manufacturer, is not guaranteed or endorsed by the publisher.

## References

Adam, S., Polo, S. E., and Almouzni, G. (2013). Transcription recovery after DNA damage requires chromatin priming by the H3.3 histone chaperone HIRA. *Cell* 155 (1), 94–106. doi:10.1016/j.cell.2013.08.029

Aguilar-Gurrieri, C., Larabi, A., Vinayachandran, V., Patel, N. A., Yen, K., Reja, R., et al. (2016). Structural evidence for Nap1-dependent H2A-H2B deposition and nucleosome assembly. *EMBO J.* 35 (13), 1465–1482. doi:10.15252/embj.201694105

- Alvarez-Ponce, D., Aguilar-Rodriguez, J., and Fares, M. A. (2019). Molecular chaperones accelerate the evolution of their protein clients in yeast. *Genome Biol. Evol.* 11 (8), 2360–2375. doi:10.1093/gbe/evz147
- Anckar, J., and Sistonen, L. (2011). Regulation of HSF1 function in the heat stress response: Implications in aging and disease. *Annu. Rev. Biochem.* 80, 1089–1115. doi:10.1146/annurev-biochem-060809-095203
- Arimura, Y., Ikura, M., Fujita, R., Noda, M., Kobayashi, W., Horikoshi, N., et al. (2018). Cancer-associated mutations of histones H2B, H3.1 and H2A.Z.1 affect the structure and stability of the nucleosome. *Nucleic Acids Res.* 46 (19), 10007–10018. doi:10.1093/nar/gky661
- Arrieta, A., Blackwood, E. A., Stauffer, W. T., and Glembofski, C. C. (2019). Integrating ER and mitochondrial proteostasis in the healthy and diseased heart. *Front. Cardiovasc. Med.* 6, 193. doi:10.3389/fcvm.2019.00193
- Balchin, D., Hayer-Hartl, M., and Hartl, F. U. (2016). *In vivo* aspects of protein folding and quality control. *Science* 353 (6294), aac4354. doi:10.1126/science.aac4354
- Banumathy, G., Somaiah, N., Zhang, R., Tang, Y., Hoffmann, J., Andrade, M., et al. (2009). Human UBN1 is an ortholog of yeast Hpc2p and has an essential role in the HIRA/ASF1a chromatin-remodeling pathway in senescent cells. *Mol. Cell. Biol.* 29 (3), 758–770. doi:10.1128/MCB.01047-08
- Bennett, R. L., Bele, A., Small, E. C., Will, C. M., Nabet, B., Oyer, J. A., et al. (2019). A mutation in histone H2B represents a new class of oncogenic driver. *Cancer Discov.* 9 (10), 1438–1451. doi:10.1158/2159-8290.CD-19-0393
- Blackwood, E. A., Bilal, A. S., Stauffer, W. T., Arrieta, A., and Glembofski, C. C. (2020). Designing novel therapies to mend broken hearts: ATF6 and cardiac proteostasis. *Cells* 9 (3), E602. doi:10.3390/cells9030602
- Blackwood, E. A., Hofmann, C., Santo Domingo, M., Bilal, A. S., Sarakki, A., Stauffer, W., et al. (2019). ATF6 regulates cardiac hypertrophy by transcriptional induction of the mTORC1 activator, rheb. *Rheb. Circ. Res.* 124 (1), 79–93. doi:10.1161/CIRCRESAHA.118.313854
- Bogush, N., Tan, L., Naib, H., Faizullahoy, E., Calvert, J. W., Iismaa, S. E., et al. (2020). DUSP5 expression in left ventricular cardiomyocytes of young hearts regulates thyroid hormone (T3)-induced proliferative ERK1/2 signaling. *Sci. Rep.* 10 (1), 21918. doi:10.1038/s41598-020-78825-x
- Clapier, C. R., Iwasa, J., Cairns, R. B., and Peterson, C. L. (2017). Mechanisms of action and regulation of ATP-dependent chromatin-remodelling complexes. *Nat. Rev. Mol. Cell Biol.* 18 (7), 407–422. doi:10.1038/nrm.2017.26
- Cohen-Fix, O., Peters, J. M., Kirschner, M. W., and Koshland, D. (1996). Anaphase initiation in *Saccharomyces cerevisiae* is controlled by the APC-dependent degradation of the anaphase inhibitor Pds1p. *Genes Dev.* 10 (24), 3081–3093. doi:10.1101/gad.10.24.3081
- Doroudgar, S., and Glembofski, C. C. (2013). New concepts of endoplasmic reticulum function in the heart: Programmed to conserve. *J. Mol. Cell. Cardiol.* 55, 85–91. doi:10.1016/j.jmcc.2012.10.006
- Doroudgar, S., Hofmann, C., Boileau, E., Malone, B., Riechert, E., Gorska, A. A., et al. (2019). Monitoring cell-type-specific gene expression using ribosome profiling *in vivo* during cardiac hemodynamic stress. *Circ. Res.* 125 (4), 431–448. doi:10.1161/CIRCRESAHA.119.314817
- Dunleavy, E. M., Almouzni, G., and Karpen, G. H. (2011). H3.3 is deposited at centromeres in S phase as a placeholder for newly assembled CENP-A in G<sub>1</sub> phase. *Nucleus* 2 (2), 146–157. doi:10.4161/nucl.2.2.15211
- Dunleavy, E. M., Roche, D., Tagami, H., Lacoste, N., Ray-Gallet, D., Nakamura, Y., et al. (2009). HJURP is a cell-cycle-dependent maintenance and deposition factor of CENP-A at centromeres. *Cell* 137 (3), 485–497. doi:10.1016/j.cell.2009.02.040
- Eschenhagen, T., Bolli, R., Braun, T., Field, L. J., Fleischmann, B. K., Frisen, J., et al. (2017). Cardiomyocyte regeneration: A consensus statement. *Circulation* 136 (7), 680–686. doi:10.1161/CIRCULATIONAHA.117.029343
- Escobar, T. M., Yu, J. R., Liu, S., Lucero, K., Vasilyev, N., Nudler, E., et al. (2022). Inheritance of repressed chromatin domains during S phase requires the histone chaperone NPM1. *Sci. Adv.* 8 (17), eabm3945. doi:10.1126/sciadv.abm3945
- Esteves de Lima, J., Bou Akar, R., Machado, L., Li, Y., Drayton-Libotte, B., Dilworth, F. J., et al. (2021). HIRA stabilizes skeletal muscle lineage identity. *Nat. Commun.* 12 (1), 3450. doi:10.1038/s41467-021-23775-9
- Faxelius, G., Hagnevik, K., Lagercrantz, H., Lundell, B., and Irestedt, L. (1983). Catecholamine surge and lung function after delivery. *Arch. Dis. Child.* 58 (4), 262–266. doi:10.1136/adc.58.4.262
- Fei, J., Torigoe, S. E., Brown, C. R., Khuong, M. T., Kassavets, G. A., Boeger, H., et al. (2015). The prenucleosome, a stable conformational isomer of the nucleosome. *Genes Dev.* 29 (24), 2563–2575. doi:10.1101/gad.272633.115
- Frank, S. A. (2014). Somatic mosaicism and disease. *Curr. Biol.* 24 (12), R577–R581. doi:10.1016/j.cub.2014.05.021
- Franklin, S., Chen, H., Mitchell-Jordan, S., Ren, S., Wang, Y., and Vondriska, T. M. (2012). Quantitative analysis of the chromatin proteome in disease reveals remodeling principles and identifies high mobility group protein B2 as a regulator of hypertrophic growth. *Mol. Cell. Proteomics* 11 (6), M111.014258. doi:10.1074/mcp.M111.014258
- Franklin, S., Zhang, M. J., Chen, H., Paulsson, A. K., Mitchell-Jordan, S. A., Li, Y., et al. (2011). Specialized compartments of cardiac nuclei exhibit distinct proteomic anatomy. *Mol. Cell. Proteomics* 10 (1), M110.000703. doi:10.1074/mcp.M110.000703
- Gan, P., Wang, Z., Morales, M. G., Zhang, Y., Bassel-Duby, R., Liu, N., et al. (2022). RBPMS is an RNA-binding protein that mediates cardiomyocyte binucleation and cardiovascular development. *Dev. Cell* 57 (8), 959–973. doi:10.1016/j.devcel.2022.03.017
- Groth, A., Corpet, A., Cook, A. J., Roche, D., Bartek, J., Lukas, J., et al. (2007). Regulation of replication fork progression through histone supply and demand. *Science* 318 (5858), 1928–1931. doi:10.1126/science.1148992
- Groth, A., Ray-Gallet, D., Quivy, J. P., Lukas, J., Bartek, J., and Almouzni, G. (2005). Human Asf1 regulates the flow of S phase histones during replicational stress. *Mol. Cell* 17 (2), 301–311. doi:10.1016/j.molcel.2004.12.018
- Gunesdogan, U., Jackle, H., and Herzig, A. (2014). Histone supply regulates S phase timing and cell cycle progression. *Elife* 3, e02443. doi:10.7554/eLife.02443
- Gunjan, A., and Verreault, A. (2003). A Rad53 kinase-dependent surveillance mechanism that regulates histone protein levels in *S. cerevisiae*. *Cell* 115 (5), 537–549. doi:10.1016/s0092-8674(03)00896-1
- Hammond, C. M., Stromme, C. B., Huang, H., Patel, D. J., and Groth, A. (2017). Histone chaperone networks shaping chromatin function. *Nat. Rev. Mol. Cell Biol.* 18 (3), 141–158. doi:10.1038/nrm.2016.159
- Hang, C. T., Yang, J., Han, P., Cheng, H. L., Shang, C., Ashley, E., et al. (2010). Chromatin regulation by Brg1 underlies heart muscle development and disease. *Nature* 466 (7302), 62–67. doi:10.1038/nature09130
- Hauer, M. H., Seeber, A., Singh, V., Thierry, R., Sack, R., Amitai, A., et al. (2017). Histone degradation in response to DNA damage enhances chromatin dynamics and recombination rates. *Nat. Struct. Mol. Biol.* 24 (2), 99–107. doi:10.1038/nsmb.3347
- Henikoff, S., and Smith, M. M. (2015). Histone variants and epigenetics. *Cold Spring Harb. Perspect. Biol.* 7 (1), a019364. doi:10.1101/cshperspect.a019364
- Hergeth, S. P., and Schneider, R. (2015). The H1 linker histones: Multifunctional proteins beyond the nucleosomal core particle. *EMBO Rep.* 16 (11), 1439–1453. doi:10.15252/embr.201540749
- Jakel, S., Mingot, J. M., Schwarzmaier, P., Hartmann, E., and Gorlich, D. (2002). Importins fulfil a dual function as nuclear import receptors and cytoplasmic chaperones for exposed basic domains. *EMBO J.* 21 (3), 377–386. doi:10.1093/emboj/21.3.377
- Jin, J. K., Blackwood, E. A., Azizi, K., Thuerauf, D. J., Fahem, A. G., Hofmann, C., et al. (2017). ATF6 decreases myocardial ischemia/reperfusion damage and links ER stress and oxidative stress signaling pathways in the heart. *Circ. Res.* 120 (5), 862–875. doi:10.1161/CIRCRESAHA.116.310266
- Kapur, M., and Ackerman, S. L. (2018). mRNA translation gone awry: Translation fidelity and neurological disease. *Trends Genet.* 34 (3), 218–231. doi:10.1016/j.tig.2017.12.007
- King, R. W., Peters, J. M., Tugendreich, S., Rolfe, M., Hieter, P., and Kirschner, M. W. (1995). A 20S complex containing CDC27 and CDC16 catalyzes the mitosis-specific conjugation of ubiquitin to cyclin B. *Cell* 81 (2), 279–288. doi:10.1016/0092-8674(95)90338-0
- Konev, A. Y., Tribus, M., Park, S. Y., Podhraski, V., Lim, C. Y., Emelyanov, A. V., et al. (2007). CHD1 motor protein is required for deposition of histone variant H3.3 into chromatin *in vivo*. *Science* 317 (5841), 1087–1090. doi:10.1126/science.1145339
- Lam, M. P., Wang, D., Lau, E., Liem, D. A., Kim, A. K., Ng, D. C., et al. (2014). Protein kinetic signatures of the remodeling heart following isoproterenol stimulation. *J. Clin. Invest.* 124 (4), 1734–1744. doi:10.1172/JCI73787
- Lewis, P. W., Muller, M. M., Koletsky, M. S., Cordero, F., Lin, S., Banaszynski, L. A., et al. (2013). Inhibition of PRC2 activity by a gain-of-function H3 mutation found in pediatric glioblastoma. *Science* 340 (6134), 857–861. doi:10.1126/science.1232245
- Li, F., Wang, X., Bunger, P. C., and Gerdes, A. M. (1997). formation of binucleated cardiac myocytes in rat heart: I. Role of actin-myosin contractile ring. *J. Mol. Cell. Cardiol.* 29 (6), 1541–1551. doi:10.1006/jmcc.1997.0381
- Li, Y., Ai, S., Yu, X., Li, C., Li, X., Yue, Y., et al. (2019). Replication-independent histone turnover underlines the epigenetic homeostasis in adult heart. *Circ. Res.* 125 (2), 198–208. doi:10.1161/CIRCRESAHA.118.314366
- Lopaschuk, G. D., Collins-Nakai, R. L., and Itoi, T. (1992). Developmental changes in energy substrate use by the heart. *Cardiovasc. Res.* 26 (12), 1172–1180. doi:10.1093/cvr/26.12.1172

- Lopaschuk, G. D., and Jaswal, J. S. (2010). Energy metabolic phenotype of the cardiomyocyte during development, differentiation, and postnatal maturation. *J. Cardiovasc. Pharmacol.* 56 (2), 130–140. doi:10.1097/FJC.0b013e3181e74a14
- Lusser, A., Urwin, D. L., and Kadonaga, J. T. (2005). Distinct activities of CHD1 and ACF in ATP-dependent chromatin assembly. *Nat. Struct. Mol. Biol.* 12 (2), 160–166. doi:10.1038/nsmb884
- Martindale, J. J., Fernandez, R., Thuermer, D., Whittaker, R., Gude, N., Sussman, M. A., et al. (2006). Endoplasmic reticulum stress gene induction and protection from ischemia/reperfusion injury in the hearts of transgenic mice with a tamoxifen-regulated form of ATF6. *Circ. Res.* 98 (9), 1186–1193. doi:10.1161/01.RES.0000220643.65941.8d
- Martire, S., and Banaszynski, L. A. (2020). The roles of histone variants in fine-tuning chromatin organization and function. *Nat. Rev. Mol. Cell Biol.* 21 (9), 522–541. doi:10.1038/s41580-020-0262-8
- Marzluff, W. F., Wagner, E. J., and Duronio, R. J. (2008). Metabolism and regulation of canonical histone mRNAs: Life without a poly(A) tail. *Nat. Rev. Genet.* 9 (11), 843–854. doi:10.1038/nrg2438
- Monte, E., Mouillesseaux, K., Chen, H., Kimball, T., Ren, S., Wang, Y., et al. (2013). Systems proteomics of cardiac chromatin identifies nucleolin as a regulator of growth and cellular plasticity in cardiomyocytes. *Am. J. Physiol. Heart Circ. Physiol.* 305 (11), H1624–H1638. doi:10.1152/ajpheart.00529.2013
- Monte, E., Rosa-Garrido, M., Karbassi, E., Chen, H., Lopez, R., Rau, C. D., et al. (2016). Reciprocal regulation of the cardiac epigenome by chromatin structural proteins hmg and ctf: Implications for transcriptional regulation. *J. Biol. Chem.* 291 (30), 15428–15446. doi:10.1074/jbc.M116.719633
- Nacev, B. A., Feng, L., Bagert, J. D., Lemiesz, A. E., Gao, J., Soshnev, A. A., et al. (2019). The expanding landscape of 'oncohistone' mutations in human cancers. *Nature* 567 (7749), 473–478. doi:10.1038/s41586-019-1038-1
- Nakada, Y., Canseco, D. C., Thet, S., Abdulsalam, S., Asaithamby, A., Santos, C. X., et al. (2017). Hypoxia induces heart regeneration in adult mice. *Nature* 541 (7636), 222–227. doi:10.1038/nature20173
- Nakada, Y., Nhi Nguyen, N. U., Xiao, F., Savla, J. J., Lam, N. T., Abdulsalam, S., et al. (2019). DNA damage response mediates pressure overload-induced cardiomyocyte hypertrophy. *Circulation* 139 (9), 1237–1239. doi:10.1161/CIRCULATIONAHA.118.034822
- Oh, E., Mark, K. G., Mocciaro, A., Watson, E. R., Prabu, J. R., Cha, D. D., et al. (2020). Gene expression and cell identity controlled by anaphase-promoting complex. *Nature* 579 (7797), 136–140. doi:10.1038/s41586-020-2034-1
- Palozola, K. C., Lerner, J., and Zaret, K. S. (2019). A changing paradigm of transcriptional memory propagation through mitosis. *Nat. Rev. Mol. Cell Biol.* 20 (1), 55–64. doi:10.1038/s41580-018-0077-z
- Pchelintsev, N. A., McBryan, T., Rai, T. S., van Tuyn, J., Ray-Gallet, D., Almouzni, G., et al. (2013). Placing the HIRA histone chaperone complex in the chromatin landscape. *Cell Rep.* 3 (4), 1012–1019. doi:10.1016/j.celrep.2013.03.026
- Piquet, S., Le Parc, F., Bai, S. K., Chevallier, O., Adam, S., and Polo, S. E. (2018). The histone chaperone FACT coordinates H2A.x-dependent signaling and repair of DNA damage. *Mol. Cell* 72 (5), 888–901. doi:10.1016/j.molcel.2018.09.010
- Porrello, E. R., Mahmoud, A. I., Simpson, E., Hill, J. A., Richardson, J. A., Olson, E. N., et al. (2011). Transient regenerative potential of the neonatal mouse heart. *Science* 331 (6020), 1078–1080. doi:10.1126/science.1200708
- Rogakou, E. P., Pilch, D. R., Orr, A. H., Ivanova, V. S., and Bonner, W. M. (1998). DNA double-stranded breaks induce histone H2AX phosphorylation on serine 139. *J. Biol. Chem.* 273 (10), 5858–5868. doi:10.1074/jbc.273.10.5858
- Ron, D., and Walter, P. (2007). Signal integration in the endoplasmic reticulum unfolded protein response. *Nat. Rev. Mol. Cell Biol.* 8 (7), 519–529. doi:10.1038/nrm2199
- Serpooshan, V., Liu, Y. H., Buikema, J. W., Galdos, F. X., Chirikian, O., Paige, S., et al. (2017). Nkx2.5+ cardiomyoblasts contribute to cardiomyogenesis in the neonatal heart. *Sci. Rep.* 7 (1), 12590. doi:10.1038/s41598-017-12869-4
- Singh, R. K., Liang, D., Gajjalaiahvari, U. R., Kabbaj, M. H., Paik, J., and Gunjan, A. (2010). Excess histone levels mediate cytotoxicity via multiple mechanisms. *Cell Cycle* 9 (20), 4236–4244. doi:10.4161/cc.9.20.13636
- Sokolovski, M., Bhattacharjee, A., Kessler, N., Levy, Y., and Horovitz, A. (2015). Thermodynamic protein destabilization by GFP tagging: A case of interdomain allosteric. *Biophys. J.* 109 (6), 1157–1162. doi:10.1016/j.bpj.2015.04.032
- Soniati, M., Cagatay, T., and Chook, Y. M. (2016). Recognition elements in the histone H3 and H4 tails for seven different importins. *J. Biol. Chem.* 291 (40), 21171–21183. doi:10.1074/jbc.M116.730218
- Stein, A., Ruggiano, A., Carvalho, P., and Rapoport, T. A. (2014). Key steps in ERAD of luminal ER proteins reconstituted with purified components. *Cell* 158 (6), 1375–1388. doi:10.1016/j.cell.2014.07.050
- Swaffer, M. P., Kim, J., Chandler-Brown, D., Langhinrichs, M., Marinov, G. K., Greenleaf, W. J., et al. (2021). Transcriptional and chromatin-based partitioning mechanisms uncouple protein scaling from cell size. *Mol. Cell* 81 (23), 4861–4875. doi:10.1016/j.molcel.2021.10.007
- Tu, B. P., Ho-Schleyer, S. C., Travers, K. J., and Weissman, J. S. (2000). Biochemical basis of oxidative protein folding in the endoplasmic reticulum. *Science* 290 (5496), 1571–1574. doi:10.1126/science.290.5496.1571
- Valenzuela, N., Fan, Q., Fa'ak, F., Soibam, B., Nagandla, H., Liu, Y., et al. (2016). Cardiomyocyte-specific conditional knockout of the histone chaperone HIRA in mice results in hypertrophy, sarcolemmal damage and focal replacement fibrosis. *Dis. Model. Mech.* 9 (3), 335–345. doi:10.1242/dmm.022889
- Whitehouse, I., Flaus, A., Cairns, B. R., White, M. F., Workman, J. L., and Owen-Hughes, T. (1999). Nucleosome mobilization catalysed by the yeast SWI/SNF complex. *Nature* 400 (6746), 784–787. doi:10.1038/23506
- Yang, J. H., Song, T. Y., Jo, C., Park, J., Lee, H. Y., Song, I., et al. (2016). Differential regulation of the histone chaperone HIRA during muscle cell differentiation by a phosphorylation switch. *Exp. Mol. Med.* 48, e252. doi:10.1038/emm.2016.68
- Ye, Y., Shibata, Y., Kikkert, M., van Voorden, S., Wiertz, E., and Rapoport, T. A. (2005). Recruitment of the p97 ATPase and ubiquitin ligases to the site of retrotranslocation at the endoplasmic reticulum membrane. *Proc. Natl. Acad. Sci. U. S. A.* 102 (40), 14132–14138. doi:10.1073/pnas.0505006102
- Zhao, Y., and Garcia, B. A. (2015). Comprehensive catalog of currently documented histone modifications. *Cold Spring Harb. Perspect. Biol.* 7 (9), a025064. doi:10.1101/cshperspect.a025064
- Zheng, L., Dominski, Z., Yang, X. C., Elms, P., Raska, C. S., Borchers, C. H., et al. (2003). Phosphorylation of stem-loop binding protein (SLBP) on two threonines triggers degradation of SLBP, the sole cell cycle-regulated factor required for regulation of histone mRNA processing, at the end of S phase. *Mol. Cell. Biol.* 23 (5), 1590–1601. doi:10.1128/mcb.23.5.1590-1601.2003
- Zhou, K., Gaullier, G., and Luger, K. (2019). Nucleosome structure and dynamics are coming of age. *Nat. Struct. Mol. Biol.* 26 (1), 3–13. doi:10.1038/s41594-018-0166-x



## OPEN ACCESS

## EDITED BY

Xolani Henry Makhoba,  
University of Fort Hare, South Africa

## REVIEWED BY

Tawanda Zininga,  
Stellenbosch University, South Africa  
Andani Mulelu,  
University of Cape Town, South Africa  
Matodzi Portia Makhubu,  
Rhodes University, South Africa

## \*CORRESPONDENCE

Hee-Won Park,  
hpark1@tulane.edu

## SPECIALTY SECTION

This article was submitted to Molecular  
Diagnostics and Therapeutics,  
a section of the journal  
Frontiers in Molecular Biosciences

RECEIVED 29 May 2022

ACCEPTED 03 August 2022

PUBLISHED 07 October 2022

## CITATION

Mrozek A, Antoshchenko T, Chen Y,  
Zepeda-Velázquez C, Smil D, Kumar N,  
Lu H and Park H-W (2022), A non-  
traditional crystal-based compound  
screening method targeting the ATP  
binding site of *Plasmodium falciparum*  
GRP78 for identification of novel  
nucleoside analogues.  
*Front. Mol. Biosci.* 9:956095.  
doi: 10.3389/fmolb.2022.956095

## COPYRIGHT

© 2022 Mrozek, Antoshchenko, Chen,  
Zepeda-Velázquez, Smil, Kumar, Lu and  
Park. This is an open-access article  
distributed under the terms of the  
[Creative Commons Attribution License](#)  
(CC BY). The use, distribution or  
reproduction in other forums is  
permitted, provided the original  
author(s) and the copyright owner(s) are  
credited and that the original  
publication in this journal is cited, in  
accordance with accepted academic  
practice. No use, distribution or  
reproduction is permitted which does  
not comply with these terms.

# A non-traditional crystal-based compound screening method targeting the ATP binding site of *Plasmodium falciparum* GRP78 for identification of novel nucleoside analogues

Alexander Mrozek<sup>1</sup>, Tetyana Antoshchenko<sup>1</sup>, Yun Chen<sup>1</sup>,  
Carlos Zepeda-Velázquez<sup>2</sup>, David Smil<sup>2</sup>, Nirbhay Kumar<sup>3</sup>,  
Hua Lu<sup>1</sup> and Hee-Won Park<sup>1\*</sup>

<sup>1</sup>Department of Biochemistry & Molecular Biology, Tulane University School of Medicine, New Orleans, LA, United States, <sup>2</sup>Drug Discovery Program, Ontario Institute for Cancer Research, Toronto, ON, Canada, <sup>3</sup>Department of Global Health, George Washington University Milken Institute of Public Health, Washington, D.C., DC, United States

Drug resistance to front-line malarial treatments represents an ongoing threat to control malaria, a vector borne infectious disease. The malarial parasite, *Plasmodium falciparum* has developed genetic variants, conferring resistance to the current standard therapeutic artemisinin and its derivatives commonly referred to as artemisinin-combination therapies (ACTs). Emergence of multi-drug resistance parasite genotypes is a warning of potential treatment failure, reaffirming the urgent and critical need to find and validate alternate drug targets to prevent the spread of disease. An attractive and novel drug target includes glucose-regulated protein 78 kDa (GRP78, or BiP), an essential molecular chaperone protein involved in the unfolded protein response that is upregulated in ACT treated *P. falciparum* parasites. We have shown that both sequence and structure are closely related to human GRP78 (hGRP78), a chaperone belonging to the HSP70 class of ATPase proteins, which is often upregulated in cellular stress responses and cancer. By screening a library of nucleoside analogues, we identified eight 'hit' compounds binding at the active site of the ATP binding domain of *P. falciparum* GRP78 using a high-throughput ligand soaking screen using x-ray crystallography. These compounds were further evaluated using protein thermal shift assays to assess target binding activity. The nucleoside analogues identified from our screen provide a starting point for the development of more potent and selective antimalarial inhibitors. In addition, we have established a well-defined, high-throughput crystal-based screening approach that can be applied to many crystallizable *P. falciparum* proteins for generating anti-*Plasmodium* specific compounds.

## KEYWORDS

*Plasmodium falciparum*, malaria, GRP78, chaperone, unfolded protein response, nucleoside analogues, drug discovery & development



## Introduction

Malaria is a vector borne infectious disease caused by the protozoan parasite of the *Plasmodium* genus, infecting both the host liver and blood cells causing an estimated 627,000 deaths annually (World Health Organization, 2021). There are five species known to infect humans: *P. falciparum*, *P. vivax*, *P. ovalae*, *P. malariae* and *P. knowlesi*, however *P. falciparum* is by far the most dangerous resulting in the highest associated mortality and morbidity (World Health Organization, 2021). Despite numerous therapeutic and preventative efforts leading to an overall reduction in death and disease over the past decade, the spread of partial resistance to front-line malarial therapeutics such as artemisinin and related artemisinin combination therapies (ACTs) has emerged and continues to spread (Visser et al., 2014; Suresh and Haldar, 2018). Malaria multidrug resistance highlights the critical and urgent need to discover new targets and chemical scaffolds.

One class of druggable targets is the endoplasmic reticulum (ER) resident molecular heat shock chaperone GRP78, which is also referred to as Immunoglobulin Binding Protein (BiP), an HSP70-like stress response protein implicated in the cellular unfolded protein response (UPR). GRP78 is essential in the maintenance of ER homeostasis, where it facilitates proper protein folding, mitigating physiological and pathological damages that may cause an accumulation of misfolded proteins and ER stress (Ibrahim et al., 2019). Moreover, it has been shown that GRP78 from *P. falciparum* (*pf*GRP78) is associated with numerous protein families such as: transcriptional and translational machinery, the proteasome and proteolytic enzymes, as well as proteins involved in physiological and metabolic pathways (Gardner et al., 2013). There is growing evidence *pf*GRP78 is cytoprotective, aiding in adaptation between physiological and environmental changes occurring during transmission from the host vector to the infected cell (Kumar et al., 1988; Przyborski et al., 2015; Day et al., 2019). We hypothesize that up-regulated expression of *pf*GRP78 allows *P. falciparum* infected cells to withstand and adapt to host conditions and have improved rates of survival.

The presence of the ER stress-response chaperone *pf*GRP78 in the malaria parasite suggest that this protein could be used as a rational therapeutic target, and various studies including the previous work from our group have explored small molecule inhibitors against *P. falciparum* and human HSP70-like chaperones (Frame et al., 2015; Jones et al., 2016; Chen et al., 2018). *pf*GRP78 shares an 84.4% sequence identity to the human orthologue of GRP78 and this value increased to 87.8% when evaluating the nucleotide-binding domain (NBD) only (Chen et al., 2018). GRP78 is structurally divided into two distinct domains: the nucleotide-binding domain at the amino terminus followed by a flexible linker to the substrate-binding domain at the carboxyl-terminus (Chakafana et al., 2019). ATP hydrolysis and ADP/ATP

exchange within the NBD of GRP78 play an essential role in the chaperone activity (Pobre et al., 2019). Therefore, the disruption of the interaction of *pf*GRP78-NBD with ATP using nucleoside analogues with varying structural modifications could inhibit *pf*GRP78 functions requiring ATP hydrolysis.

In this present study, we expressed and purified recombinant *pf*GRP78-NBD and the human orthologue hGRP78-NBD from bacteria. We then grew crystals of *pf*GRP78-NBD to perform a novel compound screening assay using adenine-based nucleoside analogues with distinct modifications to interrogate the active site of *pf*GRP78-NBD in effort to identify compounds that bind the *Plasmodium* protein with enhanced selectivity when compared to the human ortholog hGRP78-NBD. Our crystal-based assay identified eight distinct nucleoside analogues present at the active site of *pf*GRP78-NBD in the complex crystal structures. We then used a protein Thermal Shift Assay (TSA) to further characterize and identify potential differences between the malaria and human chaperone ATP binding sites.

## Materials and methods

### Reagents

All reagents, materials and nucleoside analogues were purchased from commercial suppliers and were used as received unless otherwise noted. HP1, HP2, HP3, HP4, HP5, HP13, HP14 were purchased from Carbosynth. HP18 was purchased from Acros Organics. HP19, HP20, HP21, HP22, HP23, HP24, HP25, HP26, HP27 were purchased from TargetMol. HP28, HP31, HP32 and HP33 were purchased from Selleck Chemicals. HP9, HP10, HP11 and HP12 were synthesized as detailed below.

### DNA cloning, protein expression and purification

The plasmids used in this study have been described previously (Chen et al., 2018). Briefly, the gene encoding for *pf*GRP78-NBD (residues 26-404) and hGRP78-NBD (residues 26-407) were amplified from full-length *pf*GRP78 (residues 26-652) and hGRP78 (residues 1-654) by PCR and ligated into a pET28-MHL vector containing an N-terminal His<sub>6</sub>-tag (GenBank accession EF456735) and expressed in *E. coli* BL21 (DE3) competent cells (Thermo Scientific). Bacterial starter cultures were grown in LB medium containing 50 µg/ml kanamycin for 16 h at 37°C and then transferred to Terrific Broth containing 50 µg/ml kanamycin. The cells were further grown until the OD<sub>600nm</sub> reached ~2.0 and expression was induced with 0.2 mM isopropyl β-D-1-thiogalactopyranoside at 17°C. Eighteen hours post-induction, the cells were harvested by centrifugation at 10,000 rpm for 20 min at 4°C,

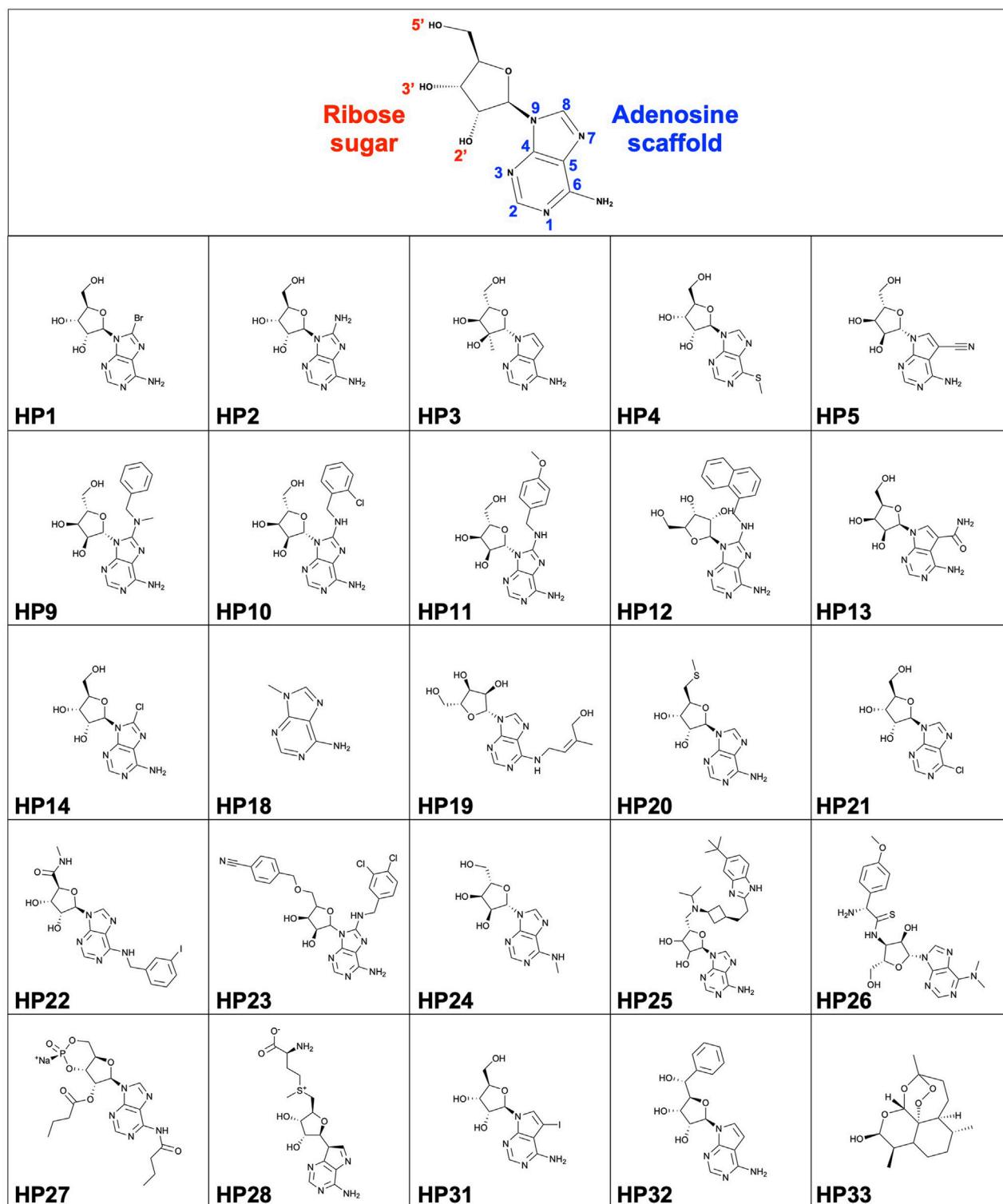


FIGURE 1

Structure of nucleoside scaffold and HP compound library (HP1-HP33).

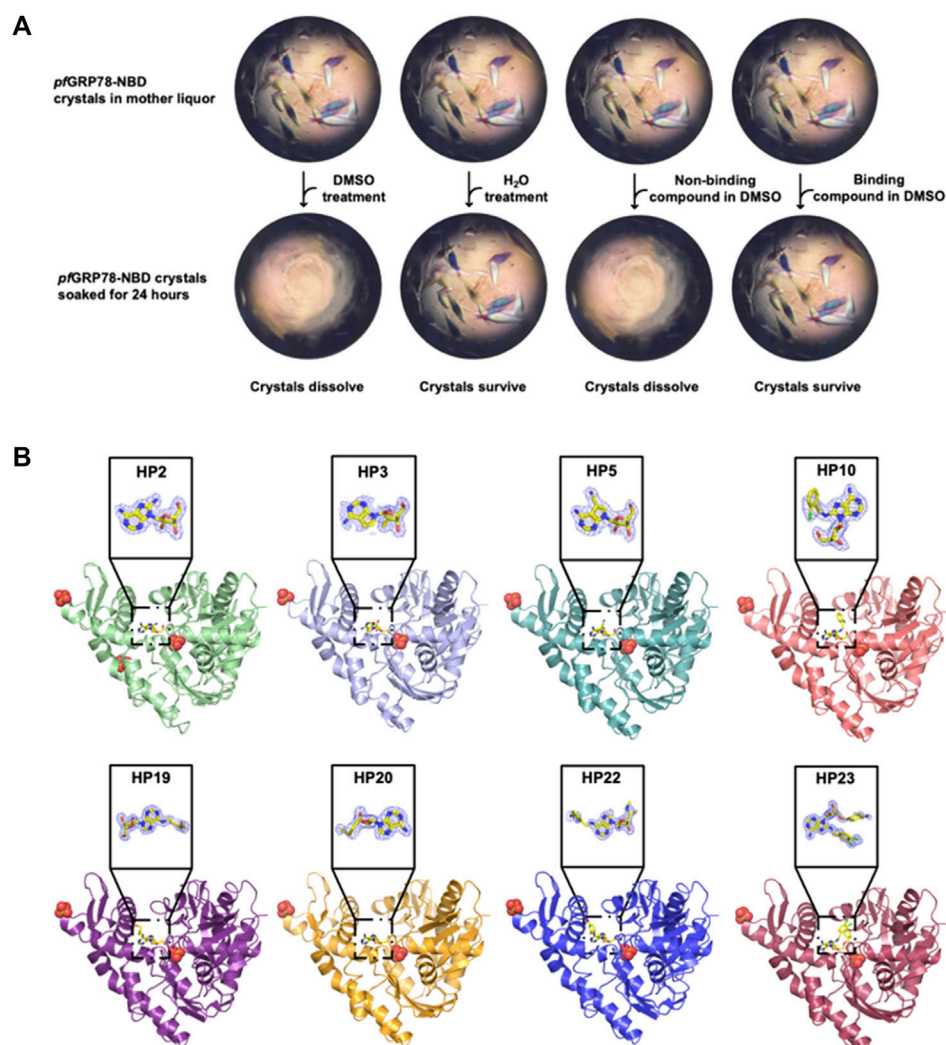


FIGURE 2

Crystal structures of *pfGRP78-NBD* bound with eight nucleoside analogues. (A) DMSO-driven Crystal-ligand replacement assay schematic. (B) Protein-ligand complex structures of *pfGRP78-NBD* with nucleoside analogues (HP2, HP3, HP5, HP10, HP19, HP20, HP22 and HP23) and corresponding electron density maps contoured to  $2F_o - F_c$  at the  $1\sigma$  level showing molecular replacement of 8-bromoadenosine at the active site of *pfGRP78-NBD*.

resuspended in a binding buffer (20 mM TRIS-HCl pH 7.5, 200 mM NaCl, 1 mM  $\beta$ -mercaptoethanol) supplemented with (1 mM PMSF, 1 mM Benzamidine, 0.1% IGEPAL CA-630) and lysed by sonification. Lysates were clarified by centrifugation at 10,000 rpm for 20 min at 4°C and the supernatant was loaded on to 5 ml column of Ni-NTA agarose beads (Thermo Scientific) pre-equilibrated with the binding buffer. The matrix was washed in a stepwise manner using the binding buffer containing increasing concentrations of imidazole (5 mM, 20 mM, 50 mM) and the protein was eluted with the same buffer containing 250 mM imidazole. The eluate was loaded on to a HiLoad 26/600 Superdex 200 pg column (Cytiva) pre-equilibrated with the binding buffer. Target protein-containing fractions were pooled and concentrated using 10 kDa MWCO centrifugal filters (Amicon),

flash frozen and stored at  $-80^\circ\text{C}$ . Expression and purification of *pfGRP78* was identical to hGRP78. The N-terminal His<sub>6</sub>-tag was cleaved using a 1:50 ratio of TEV protease at 4°C overnight. TEV-cut *pfGRP78-NBD* was mixed with a 10-fold molar excess of 8-bromoadenosine and was concentrated to  $\sim 30$  mg/ml for crystallization.

### Crystallization, DMSO-driven crystal-ligand replacement screening, data collection and structure determination

Initial crystallization trials were conducted using the sitting-drop, vapor diffusion method using in-house crystallization

screening kits, with each drop containing a solution of the complex of *p*fGRP78-NBD with 8-bromoadenosine and a reservoir solution by high throughput crystallization robot Mosquito Xtal3 (SPT Labtech). Drops were set in 96-well Intelliplates (Art Robbins Instruments). Crystals appeared within a week in the reservoir solution containing 0.7 M  $(\text{NH}_4)_2\text{SO}_4$ , 1.2 M  $\text{Li}_2\text{SO}_4$ , 0.1 M NaCitrate, pH 5.6 at a room temperature. These crystals were then used for crystal-ligand replacement screening using DMSO. Crystals were first subjected to a DMSO soaking test by titrating them with various concentrations of DMSO to determine a critical threshold between surviving and dissolving (5% addition of DMSO to the drop volume dissolved crystals completely, but 4% DMSO kept crystals intact without change in morphology). Subsequent experiments added 5% of DMSO and 5 mM of each nucleoside analogue into the crystal-containing drop for DMSO-driven crystal-ligand replacement screening. Survived crystals for eight different nucleoside analogues were cryoprotected using paratone-N and flash-frozen in liquid nitrogen until data collection. These survived crystals come from bound 8-bromoadenosine being replaced by the added nucleoside analog, resulting in stabilization of proteins in the crystal lattice. The diffraction data were collected at the Canadian Light Source 08B1-1 beamline in Saskatoon, Canada, as well as the Advanced Photon Source 19-ID-D and 23-ID-D beamlines at the Argonne National Laboratory in Chicago, Illinois. Data were processed using XDS (Kabsch, 2010) and all structures were solved by molecular replacement using MOLREP (Vagin and Teplyakov, 2010) in the CCP4 crystallographic suite (Winn et al., 2011). Structures were solved using the ADP bound *p*fGRP78-NBD structure excluding ADP (PDB ID: 5UMB) as a search model. After molecular replacement, each model was subjected to multiple rounds of model building and refinement using COOT (Emsley and Cowtan, 2004) and REFMAC (Murshudov et al., 2011), respectively. Coordinate files for all eight *p*fGRP78-NBD structures have been deposited in the Protein Data Bank with accession codes: 8DIQ (HP2), 8DIP (HP3), 8DIS (HP5), 8D1W (HP10), 8DIY (HP19), 8D20 (HP20), 8D22 (HP22) AND 8D24 (HP23). Structural figures were generated using PyMOL Molecular Graphics System (Version 2.5.0 Schrödinger, LLC) as well as LIGPLOT (Laskowski and Swindells, 2011).

## Thermal shift assay

Thermal shift assay measurements were performed on a QuantStudio 6 Flex Real-Time PCR instrument (Applied Biosystems) in 96-well plates (Axygen) sealed with transparent adhesive film (BioRad). *p*fGRP78-NBD and hGRP78-NBD were diluted to a final concentration of 5  $\mu\text{M}$  in DSF assay buffer (25 mM HEPES pH 7.5, 250 mM NaCl, 1 mM  $\beta$ -mercaptoethanol) and nucleoside analogues were added at a

final concentration of 0.5 mM (5% DMSO final concentration). Protein-compound samples were aliquoted in four replicates followed by the addition of the fluorescent probe bis-ANS (Invitrogen) diluted to 50  $\mu\text{M}$  in a 20  $\mu\text{L}$  total reaction volume. Temperature was continuously increased from 10°C to 95°C at an increment of 1°C/min. Melting curves were analyzed using the software Thermal Shift Assay—Curve Rapid and Automatic Fitting Tool (Lee et al., 2019).  $T_m$  was defined as the temperature corresponding to the maximum value of the first derivative of fluorescence. Error bars shown in Figure 4 represent standard error of the mean and were calculated using GraphPad Prism (version 9.3.1) for macOS (GraphPad Software, San Diego, California, United States, [www.graphpad.com/](http://www.graphpad.com/)).

## Synthesis of nucleoside analogues HP9, HP10, HP11 and HP12

A series of nucleoside analogues (HP9, HP10, HP11, HP12) with modifications at the C8 position of the adenine moiety were synthesized from a previously described method (Tatani et al., 2015) and all characterizations by LRMS and  $^1\text{H}$  NMR were consistent with reported values.

### Preparation of HP9 ((2R,3R,4S,5R)-2-(6-amino-8-(benzyl(methyl)amino)-9H-purin-9-yl)-5-(hydroxymethyl)tetrahydrofuran-3,4-diol)

HP9 was synthesized according to the synthesis procedure above from a mixture of 8-bromoadenosine (100 mg, 0.289 mmol, 1 eq.), *N*-methyl-1-phenylmethanamine (0.867 mmol, 3 eq.), and *N,N*-diisopropylethylamine (1.73 mmol, 0.302 ml, 6 eq.) was heated to 140°C under microwave irradiation for 10 h. The reaction mixture was then concentrated under reduced pressure, and the residue purified by column chromatography on silica gel (Biotage SNAP 10 g column, 0–40% MeOH/EtOAc as the eluent, 28 CV) to afford the desired product in 56% yield (64 mg). LRMS ( $M + H$ ) $^+$ : 387.5 Purity: 98% (UV/254 nm).

### Preparation of HP10 ((2R,3R,4S,5R)-2-(6-amino-8-((2-chlorobenzyl)amino)-9H-purin-9-yl)-5-(hydroxymethyl)tetrahydrofuran-3,4-diol)

HP10 was synthesized according to the synthesis procedure above from a mixture of 8-bromoadenosine (100 mg, 0.289 mmol, 1 eq.), (2-chlorophenyl)methanamine (0.867 mmol, 3 eq.), and *N,N*-diisopropylethylamine (1.73 mmol, 0.302 ml, 6 eq.) was heated to 140°C under microwave irradiation for 10 h. The reaction mixture was then concentrated under reduced pressure,



and the residue purified by column chromatography on silica gel (Biotage SNAP 10 g column, 0–40% MeOH/EtOAc as the eluent, 28 CV) to afford the desired product in 59% yield (71 mg). LRMS ( $M + H$ )<sup>+</sup>: 407.4. Purity: 98% (UV/254 nm).

### Preparation of HP11 ((2*R*,3*R*,4*S*,5*R*)-2-(6-amino-8-((4-methoxybenzyl)amino)-9*H*-purin-9-yl)-5-(hydroxymethyl)tetrahydrofuran-3,4-diol)

HP11 was synthesized according to the synthesis procedure above from a mixture of 8-bromoadenosine (100 mg, 0.289 mmol, 1 eq.), (4-methoxyphenyl)methanamine (0.867 mmol, 3 eq.), and *N,N*-diisopropylethylamine (1.73 mmol, 0.302 ml, 6 eq.) was heated to 140°C under microwave irradiation for 10 h. The reaction mixture was then concentrated under reduced pressure, and the residue purified by column chromatography on silica gel (Biotage SNAP 10 g column, 0–40% MeOH/EtOAc as the eluent, 28 CV) to afford the desired product in 67% yield (78 mg). LRMS ( $M + H$ )<sup>+</sup>: 403.5. Purity: 100% (UV/254 nm).

### Preparation of HP12 ((2*R*,3*R*,4*S*,5*R*)-2-(6-amino-8-((naphthalen-1-yl)methyl)amino)-9*H*-purin-9-yl)-5-(hydroxymethyl)tetrahydrofuran-3,4-diol)

HP12 was synthesized according to the synthesis procedure above from a mixture of 8-bromoadenosine (100 mg, 0.289 mmol, 1 eq.), naphthalen-1-ylmethanamine (0.867 mmol, 3 eq.), and *N,N*-diisopropylethylamine (1.73 mmol, 0.302 ml, 6 eq.) was heated to 140°C under microwave irradiation for 10 h. The reaction mixture was then concentrated under reduced pressure, and the residue purified by column chromatography on silica gel (Biotage SNAP 10 g column, 0–40% MeOH/EtOAc as the eluent, 28 CV) to afford the desired product in 61% yield (74 mg). LRMS ( $M + H$ )<sup>+</sup>: 423.4. Purity: 96% (UV/254 nm).

## Results and discussion

### Crystal-based screening and identification of *pf*GRP78-NBD bound with eight nucleoside analogues

In order to structurally characterize nucleoside analogue as potential anti-*plasmodium* chemical scaffolds in complexes with *pf*GRP78-NBD, we crystallized *pf*GRP78-NBD in complex with HP1 (8-bromoadenosine). We then soaked crystals with nucleoside analogues (Figure 1) using our novel DMSO-driven crystal-ligand replacement screening method. Certain

compounds stabilized proteins in the crystal lattice, leading to the survival of the soaked crystals, resulting in the identification of protein-binding compounds later confirmed by x-ray crystallography. On the other hand, crystals soaked with non-binding compounds were dissolved within 24 h (Figure 2A). These results demonstrate our novel crystal-ligand DMSO soaking assay reduces the total number of crystal samples sent out for data collection and can be used for potential drug discovery efforts at large. Synchrotron beam time is a rate-limiting step in compound screening by conventional soaking approaches, thus the reduced number of samples sent out for data collection leads to a reduction in false-positives and expedited data analysis, representing a significant improvement in throughput. Using this approach, we successfully identified eight *pf*GRP78-NBD inhibitor complex structures to high resolutions. PDB entries for these *pf*GRP78-NBD nucleoside analogue complex structures are summarized in Table 1. These hit nucleoside analogs are HP2: 8-Aminoadenosine, HP3: 7-Deaza-2'-C-methyladenosine, HP5: Toyocamycin, HP10: (2*R*,3*R*,4*S*,5*R*)-2-(6-amino-8-((2-chlorobenzyl)amino)-9*H*-purin-9-yl)-5-(hydroxymethyl)tetrahydrofuran-3,4-diol, HP19: Trans-Zeatin Riboside, HP20: 5'-Methylthioadenosine, HP22: Piclidenoson and HP23: VER155008. In the active sites of all *pf*GRP78-NBD and nucleoside analogue complexes, electron density is well shaped for unambiguous modeling of eight hit compounds that replaced the 8-bromoadenosine compound (Figure 2B).

### X-ray crystallographic analysis of *pf*GRP78-NBD: Ligand interactions at the ATP binding site

To identify specific modifications of adenosine advantageous for designing plasmodium specific compounds, we analyzed the complex structures of *pf*GRP78-NBD with the eight hit compounds identified through the crystal-ligand replacement screening method and compared the interactions to those present in hGRP78-NBD. Here we discuss the relevance of chemical modifications of the eight hit nucleoside analogues at the C8, C6, N7, 2' and 5' positions.

In Figure 3A, HP2 (8-Aminoadenosine) forms several hydrogen bonds with *pf*GRP78-NBD active site residues. HP2 forms direct hydrogen bonds with Lys293, Ser297 and Arg364. Four water molecules provide water-mediated hydrogen bonding with Asp256, Glu290, Arg294 and Ser362, further stabilizing HP2 to *pf*GRP78-NBD. Hydrophobic contacts are present with Gly224, Gly252, Gly361 and Ile365. The amino substituent at the C8 position directly interacts with Asp388, forming a hydrogen bond and has minimal hydrophobic interactions with Arg294. In comparison, the HP2-bound structure of hGRP78-NBD shows the conservation of most residues involved in HP2 binding (e.g., *pf*Lys293 and hLys296,

TABLE 1 X-ray data collection, refinement and validation statistics.

Ligand	HP2	HP3	HP5	HP10	HP19	HP20	HP22	HP23
PDB ID	8DIQ	8DIP	8DIS	8D1W	8DIY	8D20	8D22	8D24
Beamline	CLS 08B1-1	APS 19-ID	APS 19-ID	APS 19-ID	CLS 08B1-1	CLS 08B1-1	CLS 08B1-1	APS 23-ID-D
<b>Data Collection</b>								
Wavelength (Å)	1.5212	0.97918	0.97918	0.97918	1.5212	1.5212	1.5212	1.03322
Resolution (Å)	50.0–2.15	50.0–1.88	50.0–2.25	50.0–2.10	50.0–1.90	50.0–1.95	50.0–2.00	50.0–1.75
Space Group	P6 <sub>5</sub> 22	P6 <sub>5</sub> 22	P6 <sub>5</sub> 22	P6 <sub>5</sub> 22	P6 <sub>5</sub> 22	P6 <sub>5</sub> 22	P6 <sub>5</sub> 22	P6 <sub>5</sub> 22
No. of molecules in ASU	1	1	1	1	1	1	1	1
Unit cell parameters (Å)	a = 85.11, c = 292.07	a = 84.26, c = 291.78	a = 84.38, c = 292.49	a = 84.29, c = 292.22	a = 83.88, c = 291.23	a = 84.32, c = 291.75	a = 84.28, c = 292.20	a = 84.00, c = 292.60
No. of unique reflections <sup>a</sup>	34,525 (5360)	51,027 (8063)	30,364 (4774)	36,996 (5825)	49,029 (7724)	44,948 (6955)	42,527 (6624)	62,702 (9890)
Wilson B-Factor (Å <sup>2</sup> )	40.5	33.4	34.5	35.1	28.3	27.6	33.1	29.4
Redundancy <sup>a</sup>	19.1 (19.6)	18.9 (19.6)	18.9 (19.2)	18.9 (19.8)	18.5 (17.4)	19.2 (19.6)	18.7 (18.9)	19.0 (19.6)
R <sub>sym</sub> (%) <sup>a,b</sup>	8.1 (60.9)	6.2 (46.4)	11.2 (52.8)	9.3 (49.5)	8.6 (51.3)	8.2 (50.7)	7.5 (50.4)	6.4 (51.2)
Average I/σ <sup>a</sup>	27.30 (5.55)	35.23 (6.36)	27.10 (8.99)	28.90 (8.26)	26.44 (5.67)	37.96 (9.25)	30.55 (6.13)	32.2 (6.01)
<b>Refinement</b>								
Resolution (Å)	48.73–2.15	45.62–1.88	48.80–2.25	45.66–2.10	48.58–1.90	45.63–1.95	48.75–2.00	48.81–1.75
Completeness (%)	97.8	99.9	99.9	99.9	99.9	97.3	99.2	99.9
R <sub>work</sub> /R <sub>free</sub> (%) <sup>c</sup>	20.1/24.0	18.9/21.6	18.3/22.6	19.1/22.1	19.3/22.2	19.6/22.7	19.9/23.1	20.1/21.7
<b>No. of atoms</b>								
Protein	3003	3069	2987	2973	3005	3010	2982	3076
Ligand/ion	34	49	30	37	29	29	38	47
Water	239	277	236	265	310	321	302	301
RMSD bond length (Å)	0.011	0.013	0.012	0.012	0.014	0.013	0.014	0.013
RMSD bond angle (°)	1.712	1.781	1.729	1.780	1.816	1.800	1.835	1.860
<b>Ramachandran Analysis</b>								
Favored (%)	96.1	97.3	96.9	97.3	96.9	97.5	96.1	96.7
Outliers (%)	0.8	0.3	0.3	0.6	0.3	0.3	0.6	0.0

<sup>a</sup>Values in parentheses denote the highest-resolution shell.

<sup>b</sup>R<sub>sym</sub> = Σ[(I − <I>)]/Σ(I), where I is the observed intensity and <I> is the average intensity.

<sup>c</sup>R<sub>work</sub> = Σ[|F<sub>obs</sub> − F<sub>calc</sub>|]/Σ|F<sub>obs</sub>|, where |F<sub>obs</sub>| and |F<sub>calc</sub>| are magnitudes of observed and calculated structure factors. R<sub>free</sub> was calculated as R<sub>work</sub> using 5.0% of the data, which was set aside for an unbiased test of the progress of refinement.

*pf*Gly252 and hGly255). Specifically, a hydrogen bond and hydrophobic interactions with equivalent residues of hGRP78-NBD (hAsp391 and hArg297, respectively) are conserved, although the hydrogen bond is water-mediated in hGRP78-NBD. This suggests that the C8 amino substituent may not enhance specificity for *pf*GRP78-NBD, despite the improved stabilization this modification provides.

As depicted in Figure 3B, HP3 (7-Deaza-2'-C-methyladenosine) was used to assess how chemical modification at the 2' hydroxyl group of the ribose sugar and the deaza-modified adenine moiety

(i.e., N7 to C5) affect protein-ligand interactions at the ATP binding site of *pf*GRP78-NBD. It is evident that HP3 interacts with *pf*GRP78-NBD, but lacks hydrogen bonding with Arg364 due to the deaza substitution. Similarly, the HP3-bound structure of hGRP78-NBD shows no hydrogen bonding between hArg367 and HP3 either. In other nucleoside analogue-bound *pf*GRP78-NBD structures, a hydrogen bond is clear present between N7 and Arg364 (Table 2). The 2' methyl substituent directs the 2' hydroxyl group to form a hydrogen bond with Lys293, but it itself is involved in hydrophobic interactions with Glu290. In the HP3-bound structure of hGRP78-NBD, the N7 deaza

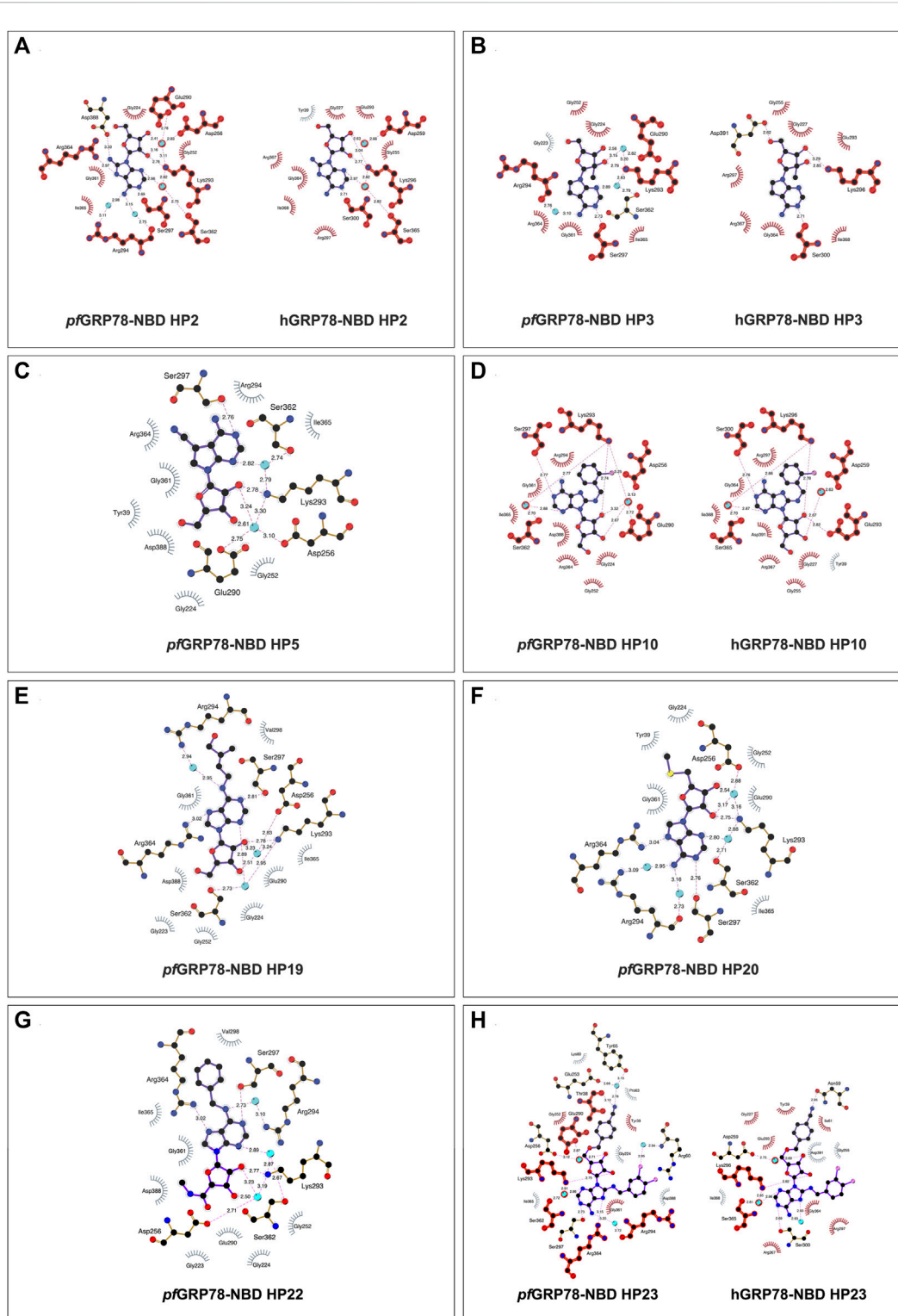


FIGURE 3

2D representation of protein-ligand interactions of hit nucleoside analogues identified from crystal-ligand soaking. (A) HP2, (B) HP3, (C) HP5, (D) HP10, (E) HP19, (F) HP20, (G) HP22 and (H) HP23. Ligand bonds are shown in purple, non-ligand bonds are shown in brown. C, N, O, S and Cl atoms are represented in black, blue, red, yellow and pink, respectively. Water atoms are represented in turquoise. Hydrophobic interactions are represented by grey spokes radiating towards the contacting ligand atoms and hydrogen bonds are represented by pink dashed lines with bond-lengths in Å. Red highlight represents amino acid equivalence between *pfGRP78-NBD* and *hGRP78-NBD* structure.

TABLE 2 *pf*GRP78-NBD & hGRP78-NBD Ligand Interaction Profile with Hit Nucleoside Analogues.

Compound	Hydrogen bond forming residues		Hydrophobic interaction forming residues	
	<i>pf</i> GRP78-NBD	hGRP78-NBD	<i>pf</i> GRP78-NBD	hGRP78-NBD
HP2	Asp256, Glu290, Lys293, Arg294, Ser297, Ser362, Arg364, Asp388	Asp259, Lys296, Ser300, Ser365	Gly224, Gly252, Gly361, Ile365	Tyr39, Gly227, Gly255, Glu293, Arg297, Gly364, Arg367, Ile368
HP3	Glu290, Lys293, Arg294, Ser297, Ser362	Lys296, Ser300, Asp391	Gly223, Gly224, Gly252, Gly361, Arg364, Ile365	Gly227, Gly255, Glu293, Arg297, Gly364, Arg367, Ile368
HP5	Asp256, Glu290, Lys293, Ser297, Ser362	—	Tyr39, Gly224, Gly252, Arg294, Gly361, Arg364, Ile365, Asp388	—
HP10	Asp256, Glu290, Lys293, Ser297, Ser362	Asp259, Glu293, Lys296, Ser300, Ser365	Gly224, Gly252, Arg294, Gly361, Arg364, Ile365, Asp388	Tyr39, Gly227, Gly255, Arg297, Gly364, Arg367, Ile368, Asp391
HP19	Asp256, Lys293, Arg294, Ser297, Ser362, Arg364	—	Gly223, Gly224, Gly252, Glu290, Val298, Gly361, Ile365, Asp388	—
HP20	Asp256, Lys293, Arg294, Ser297, Ser362, Arg364	—	Tyr39, Gly224, Gly252, Glu290, Gly361, Ile365	—
HP22	Asp256, Lys293, Arg294, Ser297, Ser362, Arg364	—	Gly223, Gly224, Gly252, Glu290, Val298, Gly361, Ile365, Asp388	—
HP23	Thr38, Arg60, Tyr65, Glu253, Asp256, Glu290, Lys293, Arg294, Ser297, Ser362, Arg364	Asn59, Asp259, Lys296, Ser300, Ser365	Tyr39, Pro63, Lys80, Gly224, Gly252, Gly361, Ile365, Asp388	Tyr39, Ile61, Gly227, Gly255, Glu293, Arg297, Gly364, Arg367, Ile368, Asp391

substituent of HP3 is not involved in hydrogen binding, similar to that of *pf*GRP78-NBD. In addition, the 2' methyl substituent of HP3 helps orient the 2' hydroxyl group to form a hydrogen bond with hLys296 and has hydrophobic interactions with hGlu293 conserved in *pf*GRP78-NBD. The finding that the hydrogen bonding and hydrophobic contacts are conserved and indistinguishable between the *P. falciparum* and the human orthologue suggest that neither the deaza modification at the N7 position nor the 2' methylation enhance selectivity for *pf*GRP78-NBD.

The active site architecture of *pf*GRP78-NBD with HP5 (Toyocamycin) is shown in Figure 3C. The HP5 compound also has deaza modification at the N7 position, which becomes C5. In addition, a cyano substituent is attached at the C5 position. Direct hydrogen bonds are made between Lys293 and the 2' hydroxyl on the ribose moiety as well as Ser297 and the N1 position on the adenine moiety. Two water molecules provide water-mediated hydrogen bonds with Asp256, Glu290 and Ser362. Eight hydrophobic interactions are observed with Tyr39, Gly224, Gly252, Arg294, Gly361, Arg364, Ile365 and Asp388. The cyano substituent at the C5 position does not form direct hydrogen bonding with *pf*GRP78-NBD, but forms hydrophobic interactions with the aliphatic side chain of Arg294. Direct structural comparison with hGRP78-NBD cannot be made at this time due to the lack of structural data for the human orthologue in complex with HP5. However, most of the residues of *pf*GRP78-NBD interacting with HP5 are conserved in hGRP78-NBD, (e.g., hArg297, hSer300, hLys296) suggesting a similar binding mode for HP5, which involves no direct hydrogen bonding of the cyano substituent of HP5 with hGRP78-NBD.

The structure of HP10 ((2R,3R,4S,5R)-2-(6-amino-8-((2-chlorobenzyl)amino)-9H-purin-9-yl)-5-(hydroxymethyl) tetrahydrofuran-3,4-diol) in complex with *pf*GRP78-NBD is shown in Figure 3D. This compound has a modification at the C8 position, by adding an amino group followed by a chlorobenzyl moiety. Direct hydrogen bonding is observed with Lys293 and Ser297. Water-mediated hydrogen bonding is shown with Asp256, Glu290 and Ser362. Hydrophobic interactions are found with Gly224, Gly252, Arg294, Gly361, Arg364, Ile365 and Asp388. The C8 substituent shows minimal hydrophobic interactions with the hydrocarbon side chain of Arg294, although multiple hydrophobic interactions at the C8 substituent are observed in hGRP78-NBD involving Glu293, Lys296 and Ser300 (Figure 3D). This loose hydrophobic interactions at the active site of *pf*GRP78-NBD can be tightened by additional chemical modifications at this position to further occupy the open active site pocket, allowing for the development of more potent inhibitors specific to the *P. falciparum* protein.

Interactions of HP19 (Trans-Zeatin Riboside) with *pf*GRP78-NBD is shown in Figure 3E. This compound has a methylbutenol substituent at the C6 position. Direct hydrogen bonding of HP19 occurs with Lys293, Ser297 and Arg364. Three water molecules provide indirect hydrogen bonding with Asp256, Ser362 and Arg294. Hydrophobic interactions are also shown with Gly223, Gly224, Gly252, Glu290, Val298, Gly361, Ile365 and Asp388. The C6 substituent does not have any direct hydrogen bonding interactions with *pf*GRP78-NBD, although there is a water-mediated hydrogen bond that may provide additional stability. The C6 substituent forms hydrophobic interactions with Arg294 and Val298. Although



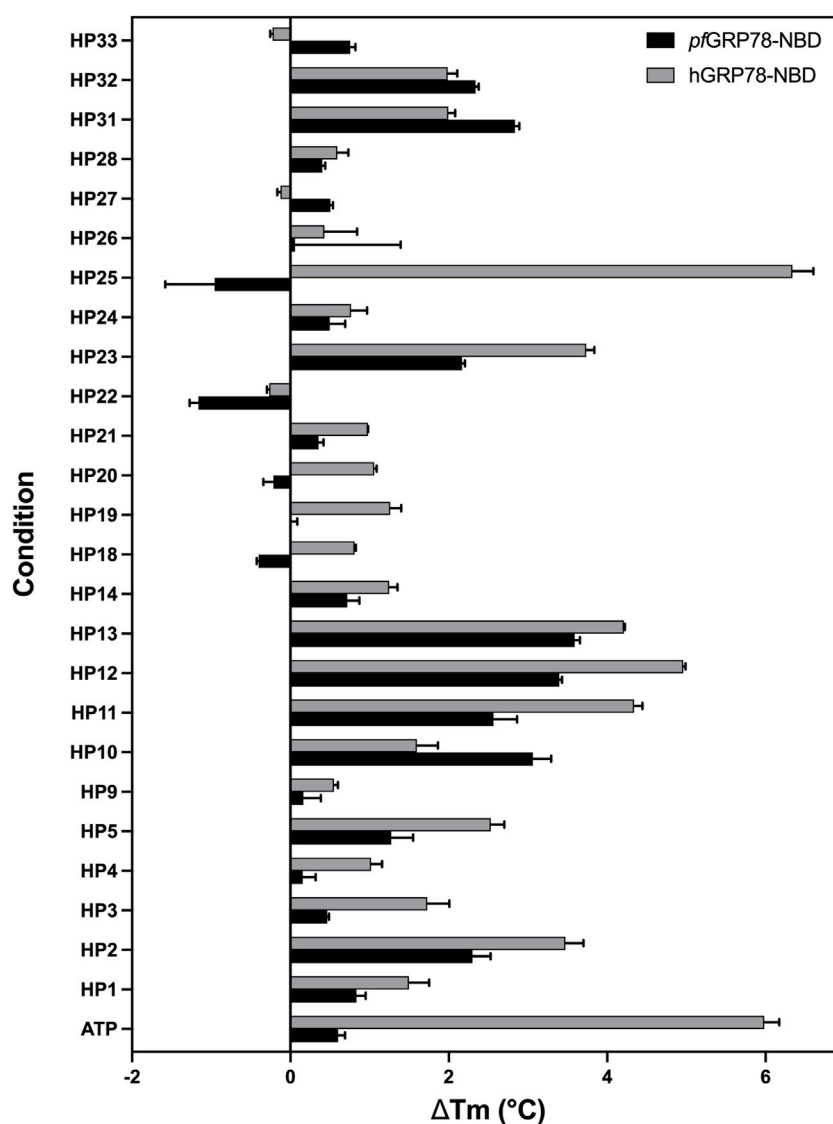


FIGURE 4

Interaction of nucleoside analogues on thermal stability of *pf*GRP78-NBD and hGRP78-NBD.  $\Delta T_m$  is defined as the difference in  $T_m$  between protein with ligand minus the  $T_m$  of protein without ligand. Error bars represent standard error of the mean of four repeats.

the HP19-bound structure of hGRP78-NBD is not available, many active site residues of *pf*GRP78-NBD involved in HP19 interactions are conserved in hGRP78-NBD (e.g., hArg297, hArg367, hSer365). Interestingly, the C6 substituent forms hydrophobic interactions with *pf*Val298, which may not occur in hGRP78-NBD since *pf*Val298 is not conserved in hGRP78-NBD (hGln301). This difference can therefore be further probed for the development of compounds specific to *pf*GRP78-NBD.

Figure 3F shows the interactions between HP20 (5'-Methylthioadenosine) and *pf*GRP78-NBD. This compound has a modification at the 5' position of the ribose sugar, with the

deletion of the 5' hydroxyl group and the addition of a methylated sulfur moiety. It is clear that no direct hydrogen bonding is observed at this modified 5' position. Direct hydrogen bonding is however shown at other sites on HP20, which interact with Lys293, Ser297 and Arg364. Four water molecules provide water-mediated hydrogen bonding with Asp256, Arg294 and Ser362. There are six hydrophobic interactions shown with Try39, Gly224, Gly252, Glu290, Gly361 and Ile365. In *pf*GRP78-NBD, there are hydrophobic interactions of the 5' substituent with Tyr39. Without the HP20-bound structure of hGRP78-NBD, we predict a similar binding mode of *P. falciparum* and human GRP78 for HP20 because of the

conservation of HP20 binding residues between the two species including *pf*Tyr39 and hTyr39.

HP22 (Piclidenoson) interacts with the active site residues of *pf*GRP78-NBD in [Figure 3G](#). This compound has modifications at both the 5' position and the C6 position. Direct hydrogen bonds of HP22 are formed with Ser297, Lys293 and Arg364. Three water molecules provide water-mediated hydrogen bonds with Asp256, Arg294 and Ser362. Neither the 5' modified group nor C6 modified group form direct hydrogen bonds with *pf*GRP78-NBD active site residues. However, there is a water-mediated hydrogen bond between the nitrogen atom of the C6 substituent and Arg294. There are eight hydrophobic interactions which include Gly223, Gly224, Gly252, Glu290, Val298, Gly361, Ile365 and Asp388. The 5' modified substituent has hydrophobic interactions with Asp388 and Gly223 and the ring structure of the C6 substituent forms hydrophobic interactions with Val298. In the absence of the HP22-bound structure of hGRP78-NBD, we still can predict the binding mode of hGRP78-NBD for HP22. The 5' substituent of HP22 can form hydrophobic interactions with hAsp391, equivalent to *pf*Asp388. However, the C6 substituent may not form hydrophobic interactions with the *pf*Val298-equivalent residue of hGRP78-NBD (hGln301). This suggests that further modification at the C6 position could be used in the development of the next generation of C6-modified nucleoside analogues that are more selective to *pf*GRP78-NBD.

The structure of *pf*GRP78-NBD with HP23 (VER155008) is shown in [Figure 3H](#). This compound has modifications at the C8 and 5' positions. Direct hydrogen bonding of HP23 is shown with Thr38, Lys293, Ser297 and Arg364. Five water molecules provide water-mediated hydrogen bonds with Tyr65, Arg60, Glu253, Asp256, Arg294, Ser362. Hydrophobic interactions are shown with Tyr39, Pro63, Lys80, Gly224, Gly252, Gly361, Asp388 and Ile365. Especially, the 5' substituent makes direct interactions with Thr38 and water-mediated contacts with Glu253 and Tyr65. Moreover, a chlorine atom of the C8 substituent makes water-mediated hydrogen bonding with Arg60. In hGRP78-NBD, HP23 has direct hydrogen bonding with Asn59 and Lys296. Three water molecules mediate hydrogen bonds are present between N7 with Asp259, Lys296 and Ser365. When comparing *pf*GRP78-NBD and hGRP78-NBD, many interactions at the active site are conserved (e.g., *pf*Lys293 and hLys296, *pf*Ser362 to hSer365). These findings suggest HP23 binds to both *pf*GRP78 and hGRP78 indistinguishably. Different modification will be required to generate nucleoside analogues specific for *pf*GRP78-NBD.

## Identification of nucleoside analogues that thermally stabilize the *pf*GRP78-NBD

To further evaluate the interaction of *pf*GRP78-NBD with the hit nucleoside analogues, we performed thermal shift assays

to measure the stability of protein-ligand complexes. Recombinant *pf*GRP78-NBD and hGRP78-NBD were used to evaluate potential preferential binding differences between the parasite versus host chaperone. We speculated that the limited structural variation between the highly conserved *P. falciparum* and human NBD of GRP78 may be an obstacle to developing selective antimalarial drugs, however discernable differences were noted between the thermal melting profiles. In this assay, the melting temperature ( $T_m$ ; temperature at which protein denaturation = 50%) is monitored by a fluorescent molecular probe binding to exposed hydrophobic regions on the protein and protein-ligand interactions are characterized by an observed shift in the melting temperature ( $\Delta T_m$ ; difference in  $T_m$  between a sample treated with ligand minus the  $T_m$  of a sample in the absence of ligand). Thermal shifts values above 2°C were considered significant and are indicative of protein-compound interaction.

The extent of thermal stabilization of *pf*GRP78-NBD and hGRP78-NBD in the presence of various nucleoside analogues to determine their binding to GRP78-NBDs ([Figure 4](#)). As a positive control, we used ATP as a model binding substrate. Both *pf*GRP78-NBD and hGRP78-NBD showed a positive thermal shift in the presence of ATP, compared to protein only. Although, the increase in melting temperature was more noticeable for hGRP78-NBD with a thermal shift of 5.6°C compared to only 0.5°C for *pf*GRP78-NBD. It is evident that numerous compounds interact with *pf*GRP78-NBD with different  $\Delta T_m$  values, generating a unique chemical fingerprint. Eight out of the twenty-five screened compounds showed a significant effect on the *pf*GRP78-NBD thermal stability, these include: HP2, HP10, HP11, HP12, HP13, HP23, HP31 and HP32. Three of the eight compounds that showed a notable difference in the thermal stability were also identified using our DMSO crystal-ligand replacement screening, those being HP2, HP10 and HP23. Relative to the ATP control, the TSA data demonstrated stabilizing effects for many of the nucleoside analogues, with changes in melting temperature higher than ATP. These results are consistent with our hypothesis that the adenosine structural moiety common among compounds in this library would elevate the overall melting temperature and provides justification for further investigation.

In addition, screening the human homologue of GRP78-NBD generated different fingerprints indicative of differences in chemical sensitivity between the *P. falciparum* and human GRP78 chaperones that might be exploited in the design of selective inhibitors. Most notably, this can be seen in the case of HP25, which had a more noticeable ( $\Delta T_m > 2^\circ\text{C}$ ) shift for hGRP78, whereas the plasmodium chaperone was destabilized by HP25. These findings suggest the potential for designing inhibitors specific for *pf*GRP78. Interestingly, HP22 destabilized both *pf*GRP78-NBD and hGRP78-NBD in TSA, however our DMSO crystal-ligand replacement assay

results clearly provide the crystal structure of *pf*GRP78-NBD with this nucleoside analogue bound at the active site. This result stresses the importance of performing orthogonal approaches to validate putative hit compounds.

## Conclusion

In summary, we purified recombinantly expressed *pf*GRP78-NBD and hGRP78-NBD and performed biophysical assays such as TSA to identify chemical moieties that could be used to generate more specific therapeutics to *P. falciparum*. We further characterized the active site of the NBD by providing new crystal structures of the *P. falciparum* GRP78 in complex with eight different nucleoside analogues using our innovative, high-throughput DMSO crystal-ligand replacement screening method. The results from the TSA and DMSO crystal-ligand replacement screening are in agreement and provide further validation of the hit compounds we identified in this study. Moreover, we provided proof of concept that protein crystals can tolerate DMSO soaking and stabilizing compounds remain intact, whereas non-binding compounds dissolve. Taken together, this study established an excellent platform for a rapid, stream-lined approach to compound screening, data collection and identification of protein-ligand complexes using x-ray crystallography. It is our belief that the development of our DMSO crystal-ligand screening approach can be applied in the larger context of drug discovery by minimizing time, cost and hours spent working to obtain protein-ligand co-crystal structures and will complement existing drug discovery approaches to identify and validate candidate drug targets. The research outcomes presented here will play a fundamental role in future studies to generate a refined adenosine chemotype containing structure-driven modifications on the adenosine scaffold specific and selective to *pf*GRP78.

## Data availability statement

The datasets presented in this study can be found in online repositories. The names of the repository/repositories and accession number(s) can be found in the article/supplementary material.

## Author contributions

Conceived and designed the experiments: AM and H-WP. Performed the experiments: AM, TA, YC, CZ-V and DS. Analyzed

the data: AM, H-WP and HL. Contributed reagents and analysis tools: H-WP, HL, DS, NK. Wrote the paper: AM and H-WP.

## Funding

Research described in this paper used resources of the Advanced Photon Source, a U.S. Department of Energy (DOE) Office of Science user facility operated for the DOE Office of Science by Argonne National Laboratory under Contract No. DE-AC02-06CH11357 (APS Beamlines 19-ID-D & 23-ID-D). Part of the research described in this paper was performed using beamline CMCF-ID at the Canadian Light Source, a national research facility of the University of Saskatchewan, which is supported by the Canada Foundation for Innovation (CFI), the Natural Sciences and Engineering Research Council (NSERC), the National Research Council (NRC), the Canadian Institutes of Health Research (CIHR), the Government of Saskatchewan, and the University of Saskatchewan (CLS Beamlines 08B1-1). HL was supported by NIH-NCI grant R01 CA234605.

## Acknowledgments

We kindly thank the following current and previous lab members for their work and support on this project including: Claire Pierce, Yuhua Huang and Matthew Moreida for help with diffraction data collection. We also thank Jia Fan for mass spectrometry validation of synthesized HP compounds.

## Conflict of interest

The authors declare that the research was conducted in the absence of any commercial or financial relationships that could be construed as a potential conflict of interest.

## Publisher's note

All claims expressed in this article are solely those of the authors and do not necessarily represent those of their affiliated organizations, or those of the publisher, the editors and the reviewers. Any product that may be evaluated in this article, or claim that may be made by its manufacturer, is not guaranteed or endorsed by the publisher.

## References

- Chakafana, G., Zininga, T., and Shonhai, A. (2019). Comparative structure-function features of Hsp70s of *Plasmodium falciparum* and human origins. *Biophys. Rev.* 11, 591–602. doi:10.1007/s12551-019-00563-w
- Chen, Y., Murillo-Solano, C., Kirkpatrick, M. G., Antoshchenko, T., Park, H.-W., and Pizarro, J. C. (2018). Repurposing drugs to target the malaria parasite unfolding protein response. *Sci. Rep.* 8 (1), 10333. doi:10.1038/s41598-018-28608-2
- Day, J., Passecker, A., Beck, H. P., and Vakonakis, I. (2019). The *Plasmodium falciparum* Hsp70-x chaperone assists the heat stress response of the malaria parasite. *FASEB J.* 33 (12), 14611–14624. doi:10.1096/fj.201901741R
- Emsley, P., and Cowtan, K. (2004). Coot: Model-building tools for molecular graphics. *Acta Crystallogr. D. Biol. Crystallogr.* 60 (12), 2126–2132. doi:10.1107/S0907444904019158
- Frame, I. J., Deniskin, R., Arora, A., and Akabas, M. H. (2015). Purine import into malaria parasites as a target for antimalarial drug development. *Ann. N. Y. Acad. Sci.* 1342, 19–28. doi:10.1111/nyas.12568
- Gardner, B. M., Pincus, D., Gotthardt, K., Gallagher, C. M., and Walter, P. (2013). Endoplasmic reticulum stress sensing in the unfolded protein response. *Cold Spring Harb. Perspect. Biol.* 5 (3), a013169. doi:10.1101/cshperspect.a013169
- Ibrahim, I. M., Abdelmalek, D. H., and Elfiky, A. A. (2019). GRP78: A cell's response to stress. *Life Sci.* 226, 156–163. doi:10.1016/j.lfs.2019.04.022
- Jones, A. M., Westwood, I. M., Osborne, J. D., Matthews, T. P., Cheeseman, M. D., Rowlands, M. G., et al. (2016). A fragment-based approach applied to a highly flexible target: Insights and challenges towards the inhibition of HSP70 isoforms. *Sci. Rep.* 6, 34701. doi:10.1038/srep34701
- Kabsch, W. (2010). Integration, scaling, space-group assignment and post-refinement. *Acta Crystallogr. D. Biol. Crystallogr.* 66 (2), 133–144. doi:10.1107/S0907444909047374
- Kumar, N., Syin, C., Carter, R., Quakyi, I., and Miller, L. H. (1988). *Plasmodium falciparum* gene encoding a protein similar to the 78-kDa rat glucose-regulated stress protein. *Proc. Natl. Acad. Sci. U. S. A.* 85, 6277–6281. doi:10.1073/pnas.85.17.6277
- Laskowski, R. A., and Swindells, M. B. (2011). LigPlot+: Multiple ligand-protein interaction diagrams for drug discovery. *J. Chem. Inf. Model.* 51 (10), 2778–2786. doi:10.1021/ci200227u
- Lee, P. H., Huang, X. X., Teh, B. T., and Ng, L. M. (2019). TSA-CRAFT: A free software for automatic and robust thermal shift assay data analysis. *SLAS Discov.* 24 (5), 606–612. doi:10.1177/2472555218823547
- Murshudov, G. N., Skubak, P., Lebedev, A. A., Pannu, N. S., Steiner, R. A., Nicholls, R. A., et al. (2011). REFMAC5 for the refinement of macromolecular crystal structures. *Acta Crystallogr. D. Biol. Crystallogr.* 67 (4), 355–367. doi:10.1107/S0907444911001314
- Pobre, K. F. R., Poet, G. J., and Hendershot, L. M. (2019). The endoplasmic reticulum (ER) chaperone BiP is a master regulator of ER functions: Getting by with a little help from ERdj friends. *J. Biol. Chem.* 294 (6), 2098–2108. doi:10.1074/jbc.REV118.002804
- Przyborski, J. M., Diehl, M., and Blatch, G. L. (2015). Plasmodial HSP70s are functionally adapted to the malaria parasite life cycle. *Front. Mol. Biosci.* 2, 34. doi:10.3389/fmolb.2015.00034
- Suresh, N., and Haldar, K. (2018). Mechanisms of artemisinin resistance in *Plasmodium falciparum* malaria. *Curr. Opin. Pharmacol.* 42, 46–54. doi:10.1016/j.coph.2018.06.003
- Tatani, K., Hiratochi, M., Nonaka, Y., Isaji, M., and Shuto, S. (2015). Identification of 8-aminoadenosine derivatives as a new class of human concentrative nucleoside transporter 2 inhibitors. *ACS Med. Chem. Lett.* 6 (3), 244–248. doi:10.1021/ml500343r
- Vagin, A., and Teplyakov, A. (2010). Molecular replacement with MOLREP. *Acta Crystallogr. D. Biol. Crystallogr.* 66 (1), 22–25. doi:10.1107/S0907444909042589
- Visser, B. J., van Vugt, M., and Grobusch, M. P. (2014). Malaria: An update on current chemotherapy. *Expert Opin. Pharmacother.* 15 (15), 2219–2254. doi:10.1517/14656566.2014.944499
- Winn, M. D., Ballard, C. C., Cowtan, K. D., Dodson, E. J., Emsley, P., Evans, P. R., et al. (2011). Overview of the CCP4 suite and current developments. *Acta Crystallogr. D. Biol. Crystallogr.* 67 (4), 235–242. doi:10.1107/S0907444910045749
- World Health Organization (2021). *World malaria report 2021*. Geneva, Switzerland: WHO.



# Frontiers in Molecular Biosciences

Explores biological processes in living organisms  
on a molecular scale

Focuses on the molecular mechanisms  
underpinning and regulating biological processes  
in organisms across all branches of life.

## Discover the latest Research Topics

[See more](#) →

### Frontiers

Avenue du Tribunal-Fédéral 34  
1005 Lausanne, Switzerland  
[frontiersin.org](https://frontiersin.org)

### Contact us

+41 (0)21 510 17 00  
[frontiersin.org/about/contact](https://frontiersin.org/about/contact)



### Frontiers in Molecular Biosciences

